EARLY SIGNALING IN THE RHIZOBIUM-LEGUME SYMBIOSIS

EDITED BY: Maria Jose Soto, Jose María Vinardell, Luis Cardenas, Benjamin Gourion and Christian Staehelin

PUBLISHED IN: Frontiers in Plant Science

frontiers Research Topics

frontiers

ISSN 1664-8714
ISBN 978-2-83250-675-2
DOI 10.3389/978-2-83250-675-2

About Frontiers

Frontiers is more than just an open-access publisher of scholarly articles: it is a pioneering approach to the world of academia, radically improving the way scholarly research is managed. The grand vision of Frontiers is a world where all people have an equal opportunity to seek, share and generate knowledge. Frontiers provides immediate and permanent online open access to all its publications, but this alone is not enough to realize our grand goals.

Frontiers Journal Series

The Frontiers Journal Series is a multi-tier and interdisciplinary set of open-access, online journals, promising a paradigm shift from the current review, selection and dissemination processes in academic publishing. All Frontiers journals are driven by researchers for researchers; therefore, they constitute a service to the scholarly community. At the same time, the Frontiers Journal Series operates on a revolutionary invention, the tiered publishing system, initially addressing specific communities of scholars, and gradually climbing up to broader public understanding, thus serving the interests of the lay society, too.

Dedication to Quality

Each Frontiers article is a landmark of the highest quality, thanks to genuinely collaborative interactions between authors and review editors, who include some of the world's best academicians. Research must be certified by peers before entering a stream of knowledge that may eventually reach the public - and shape society; therefore, Frontiers only applies the most rigorous and unbiased reviews.
Frontiers revolutionizes research publishing by freely delivering the most outstanding research, evaluated with no bias from both the academic and social point of view. By applying the most advanced information technologies, Frontiers is catapulting scholarly publishing into a new generation.

What are Frontiers Research Topics?

Frontiers Research Topics are very popular trademarks of the Frontiers Journals Series: they are collections of at least ten articles, all centered on a particular subject. With their unique mix of varied contributions from Original Research to Review Articles, Frontiers Research Topics unify the most influential researchers, the latest key findings and historical advances in a hot research area! Find out more on how to host your own Frontiers Research Topic or contribute to one as an author by contacting the Frontiers Editorial Office: frontiersin.org/about/contact

EARLY SIGNALING IN THE RHIZOBIUM-LEGUME SYMBIOSIS

Topic Editors:
Maria Jose Soto, Experimental Station of Zaidín, Spanish National Research Council (CSIC), Spain
Jose María Vinardell, Sevilla University, Spain
Luis Cardenas, National Autonomous University of Mexico, Mexico
Benjamin Gourion, UMR2594 Laboratoire Interactions Plantes-Microorganismes (LIPM), France
Christian Staehelin, Sun Yat-sen University, China

Citation: Soto, M. J., Vinardell, J. M., Cardenas, L., Gourion, B., Staehelin, C., eds. (2022). Early Signaling in the Rhizobium-legume Symbiosis.
Lausanne: Frontiers Media SA. doi: 10.3389/978-2-83250-675-2

Table of Contents

frontiers | Frontiers in Plant Science

TYPE Editorial
PUBLISHED 19 October 2022
DOI 10.3389/fpls.2022.1056830

OPEN ACCESS

EDITED AND REVIEWED BY
Katharina Pawlowski,
Stockholm University, Sweden

*CORRESPONDENCE
María J. Soto
mariajose.soto@eez.csic.es

SPECIALTY SECTION
This article was submitted to Plant Symbiotic Interactions, a section of the journal Frontiers in Plant Science

RECEIVED 29 September 2022
ACCEPTED 06 October 2022
PUBLISHED 19 October 2022

CITATION
Soto MJ, Staehelin C, Gourion B, Cárdenas L and Vinardell JM (2022) Editorial: Early signaling in the rhizobium-legume symbiosis. *Front. Plant Sci.* 13:1056830. doi: 10.3389/fpls.2022.1056830

Editorial: Early signaling in the rhizobium-legume symbiosis

María J. Soto[1]*, Christian Staehelin[2], Benjamin Gourion[3], Luis Cárdenas[4] and José M. Vinardell[5]

[1]Genetics of Phytobacterial Infections, Estación Experimental del Zaidín, Department of Biotechnology and Environmental Protection, CSIC, Granada, Spain, [2]State Key Laboratory of Biocontrol and Guangdong Key Laboratory of Plant Resources, School of Life Sciences, Sun Yat-sen University, Guangzhou, China, [3]LIPME, INRAE, CNRS, Université de Toulouse, Castanet-Tolosan, France, [4]Instituto de Biotecnología, Universidad Nacional Autónoma de México, Morelos, Mexico, [5]Department of Microbiology, University of Sevilla, Sevilla, Spain

KEYWORDS

rhizosphere, chemotaxis, plant nodulation genes, exopolysaccharides, effectors, volatiles

Editorial on the Research Topic
Early signaling in the rhizobium-legume symbiosis

The rhizobium-legume symbiosis is a beneficial plant-bacteria association between soil bacteria collectively known as rhizobia and leguminous plants (Poole et al., 2018). To establish symbiosis, the rhizobia invade roots of host plants and trigger the formation of a new organ, the nodule. The rhizobia differentiate then into bacteroids and reduce atmospheric nitrogen into ammonia that will be used by the plant. The formation of nitrogen-fixing nodules is a complex process in which bacterial infection needs to be co-ordinated with the nodule organogenesis program. This is achieved through a continuous molecular dialogue between the host plant and rhizobia, which leads to a high degree of specificity in the interaction with even strain- and host cultivar-dependent effects (Cangioli et al., 2022). Much of that specificity is conferred by an exchange of signals that take place in the rhizosphere during the early stages of the association (Roy et al., 2020). The 10 articles hosted in the Research Topic "Early signaling in the rhizobium-legume symbiosis", increase our knowledge on the molecular bases underlying the mutual recognition of plants and rhizobia during early stages of the interaction, i.e., before the onset of nitrogen fixation.

The initiation of the rhizobium-legume symbiosis requires localization of the bacteria to potential infection sites on host roots. In this process, rhizobial chemotaxis and motility play a relevant role. The reviews by Aroney et al. and Compton and Scharf revised some important concepts related to motility and chemotaxis and the preferred attractants of several model rhizobia. Aroney et al. highlighted the importance of understanding chemotaxis and motility in legume symbionts, especially under the

environmental conditions found in the field. This, together with the identification of different compounds sensed through the chemotaxis systems in each rhizobial species, might predict symbiotic performance based on specific environmental conditions and root exudate composition, making the selection of elite inoculants more accurate.

The role of (iso)flavonoids as chemoattractants in rhizobia is not clear. However, they are crucial in the initiation of the symbiosis by triggering production of specific lipochitooligosaccharidic Nod-factors (NFs) in the rhizobial partner. Perception of NFs by specific plant receptors activates the symbiosis signaling pathway required for rhizobial infection and nodule formation. Three studies of the article collection provide insights on early plant symbiotic genes. Solovev et al. have addressed the difference in symbiotic specificity between Afghanistan and European pea landraces, in which the former can interact only with *Rhizobium leguminosarum* bv. *viciae* strains that have the *nodX* gene and produce NFs with an additional acetyl group at the reducing end while European pea lines can also be nodulated by strains lacking *nodX*. By using molecular modelling of putative receptor heterodimers with different NFs, the authors identified the *LykX* receptor gene as a possible determinant of pea specificity toward *nodX*-containing strains. Kovacs et al. have investigated the protein complex formed by NSP1 and NSP2, two transcriptional regulators of *Medicago truncatula* required for the activation of several early nodulation genes. Specifically, the authors addressed amino acid polymorphisms in the VHIID motif of NSP2. Characterization of a mutant allele unveiled the importance of a conserved Asp residue in NSP2, which is essential for the formation of a functional NSP1-NSP2 signaling module. Root hair deformation and infection thread formation require an important cell reorganization during which Rho GTPases called ROPs (for Rho of plants) play key roles. García-Soto et al. reported on ROP3, a novel Rho-GTPase of *Lotus japonicus*. The study shows that, in response to rhizobial inoculation, *rop3* mutant plants exhibit altered root hair deformation and expression of nodulation-related genes, and form fewer nodules than wild-type plants, indicating that ROP3 is a positive regulator of rhizobial infection thread formation.

In addition to NFs, rhizobial surface polysaccharides and effector proteins delivered by specialised secretion systems play important roles in the success of the interaction, very often in a host-specific manner (Acosta-Jurado et al., 2021; Jiménez-Guerrero et al., 2022). A good example of that has been provided by Castellani et al. who analysed the symbiotic relevance of the exopolysaccharide (EPS) of *Rhizobium favelukesii* LPU83, a strain which like *Sinorhizobium meliloti* is able to nodulate alfalfa. Interestingly, although both strains produce the same EPS, this polysaccharide is essential for a successful interaction of alfalfa with *S. meliloti*, but not with *R. favelukesii*. The production of symbiotically important EPSs is under the control of different regulatory systems, which are also relevant for the symbiosis. In *S. meliloti*, one of them is the ExoS/ChvI two-component regulatory system, which is normally activated in rhizobial cells during the transition from a free-living to a symbiotic life style. Mutations that increase or decrease activity of the system lead to symbiotic defects. Geiger et al. demonstrated that the lack of the phospholipid phosphatidylcholine (PC) in the sinorhizobial membrane leads to permanent activation of ExoS/ChvI, which might explain the inability of a PC-deficient mutant to form nodules on alfalfa roots.

The type 3 secretion system (T3SS) is the main protein secretion apparatus known to have an impact in the symbiosis. Ratu et al. showed that the T3SS effector protein Bel2-5 of *Bradyrhizobium elkanii* USDA61 possesses multiple domains that might interact and modify host targets and provoke opposite roles on symbiosis with soybean depending on the plant genotype: Bel2-5 promotes NF-independent symbiosis with a *nfr1* soybean mutant but blocks nodulation with soybean plants carrying the *Rj4* allele. Besides the most relevant T3SS, recent studies have shown the participation of additional rhizobial protein secretion systems in the symbiotic association. Hug et al. studied type 6 secretion systems (T6SSs) of *Paraburkholderia phymatum* STM815. This strain is able to nodulate a broad range of legumes and its T6SS-b appears to play a role in bacterial motility. T6SS-b gene expression was found to be activated in the presence of citrate and germinated seeds of host legumes.

The inter-kingdom signaling between rhizobia and legumes is complex and additional players, which might not be essential for nodulation but could contribute to fine-tune some aspects of the symbiosis, could be added to the chemical dialogue. Based on the recognized role played by microbial volatiles in inter-kingdom signaling with plants (Weisskopf et al., 2021), Soto et al. have raised the possibility that rhizobial volatiles might play a signaling role in their interaction with legumes, whose precise role in symbiosis requires further investigation.

Author contributions

MS wrote the article with contributions from JV, CS, BG, and LC. All authors contributed to the article and approved the submitted version.

Funding

MS was supported by grants PGC2018-096477-B-I00 and PID2021-123540NB-I00 funded by MCIN/AEI/10.13039/

501100011033 and by "ERDF A way of making Europe" and by grant P20_00225 funded by the Junta de Andalucía PAIDI/FEDER/EU. CS was supported by grants 31670241 and 32161133026 funded by the National Natural Science Foundation of China. JV was supported by the Spanish Ministry of Science and Innovation, grant number PID2019-107634RB-I00, and by Junta de Andalucía PAIDI/FEDER/EU, grant number P20_00185.

Acknowledgments

The editors would like to thank all the authors and expert reviewers who have participated in the preparation and evaluation of manuscripts hosted in this Research Topic.

Conflict of interest

The authors declare that the research was conducted in the absence of any commercial or financial relationships that could be construed as a potential conflict of interest.

Publisher's note

References

Acosta-Jurado, S., Fuentes-Romero, F., Ruíz-Saínz, J.-E., Janczarek, M., and Vinardell, J.-M. (2021). Rhizobial exopolysaccharides: Genetic regulation of their synthesis and relevance in symbiosis with legumes. *Int. J. Mol. Sci.* 22, 6233. doi: 10.3390/ijms22126233

Cangioli, L., Vaccaro, F., Fini, M., Mengoni, A., and Fagorzi, C. (2022). Scent of a symbiont: The personalized genetic relationships of rhizobium-plant interaction. *Int. J. Mol. Sci.* 23, 3358. doi: 10.3390/ijms23063358

Jiménez-Guerrero, I., Medina, C., Vinardell, J. M., Ollero, F. J., and López-Baena, F. J. (2022). The rhizobial type 3 secretion system: The Dr. Jekyll and Mr. Hyde in the rhizobium-legume symbiosis. *Int. J. Mol. Sci.* 23, 11089. doi: 10.3390/ijms231911089

Poole, P., Ramachandran, V., and Terpolilli, J. (2018). Rhizobia: from saprophytes to endosymbionts. *Nat. Rev. Microbiol.* 16, 291–303. doi: 10.1038/nrmicro.2017.171

Roy, S., Liu, W., Nandety, R. S., Crook, A., Mysore, K. S., Pislariu, C. I., et al. (2020). Celebrating 20 years of genetic discoveries in legume nodulation and symbiotic nitrogen fixation. *Plant Cell* 32, 15–41. doi: 10.1105/tpc.19.00279

Weisskopf, L., Schulz, S., and Garbeva, P. (2021). Microbial volatile organic compounds in intra-kingdom and inter-kingdom interactions. *Nat. Rev. Microbiol.* 19, 391–404. doi: 10.1038/s41579-020-00508-1

frontiers in Plant Science

ORIGINAL RESEARCH
published: 10 February 2021
doi: 10.3389/fpls.2021.642576

Exopolysaccharide Characterization of *Rhizobium favelukesii* LPU83 and Its Role in the Symbiosis With Alfalfa

*Lucas G. Castellani[1†], Abril Luchetti[1†], Juliet F. Nilsson[1], Julieta Pérez-Giménez[1], Caren Wegener[2], Andreas Schlüter[2], Alfred Pühler[2], Antonio Lagares[1], Susana Brom[3], Mariano Pistorio[1], Karsten Niehaus[2] and Gonzalo A. Torres Tejerizo[1]**

[1] Instituto de Biotecnología y Biología Molecular (IBBM), CCT-La Plata, CONICET, Departamento de Ciencias Biológicas, Facultad de Ciencias Exactas, Universidad Nacional de La Plata, La Plata, Argentina, [2] CeBiTec, Bielefeld University, Bielefeld, Germany, [3] Programa de Ingeniería Genómica, Centro de Ciencias Genómicas, Universidad Nacional Autónoma de México, Cuernavaca, Mexico

OPEN ACCESS

Edited by:
Jose Maria Vinardell,
University of Seville, Spain

Reviewed by:
Monika Janczarek,
Maria Curie-Skłodowska University, Poland
Sebastián Acosta Jurado,
University of Seville, Spain

***Correspondence:**
Gonzalo A. Torres Tejerizo
gatt@biol.unlp.edu.ar

[†] These authors have contributed equally to this work and share first authorship

Specialty section:
This article was submitted to Plant Symbiotic Interactions, a section of the journal Frontiers in Plant Science

Received: 16 December 2020
Accepted: 20 January 2021
Published: 10 February 2021

Citation:
Castellani LG, Luchetti A, Nilsson JF, Pérez-Giménez J, Wegener C, Schlüter A, Pühler A, Lagares A, Brom S, Pistorio M, Niehaus K and Torres Tejerizo GA (2021) Exopolysaccharide Characterization of Rhizobium favelukesii LPU83 and Its Role in the Symbiosis With Alfalfa. Front. Plant Sci. 12:642576. doi: 10.3389/fpls.2021.642576

One of the greatest inputs of available nitrogen into the biosphere occurs through the biological N_2-fixation to ammonium as result of the symbiosis between rhizobia and leguminous plants. These interactions allow increased crop yields on nitrogen-poor soils. Exopolysaccharides (EPS) are key components for the establishment of an effective symbiosis between alfalfa and *Ensifer meliloti*, as bacteria that lack EPS are unable to infect the host plants. *Rhizobium favelukesii* LPU83 is an acid-tolerant rhizobia strain capable of nodulating alfalfa but inefficient to fix nitrogen. Aiming to identify the molecular determinants that allow *R. favelukesii* to infect plants, we studied its EPS biosynthesis. LPU83 produces an EPS I identical to the one present in *E. meliloti*, but the organization of the genes involved in its synthesis is different. The main gene cluster needed for the synthesis of EPS I in *E. meliloti*, is split into three different sections in *R. favelukesii*, which probably arose by a recent event of horizontal gene transfer. A *R. favelukesii* strain devoided of all the genes needed for the synthesis of EPS I is still able to infect and nodulate alfalfa, suggesting that attention should be directed to other molecules involved in the development of the symbiosis.

Keywords: rhizobia, exopolysaccharide, alfalfa, symbiosis, nitrogen fixation

INTRODUCTION

Alfalfa (*Medicago sativa*), is a widely cultivated legume used worldwide for feeding cattle mainly due to its high nutritional value, but also because its cultivation does not cause a high soil erosion (Li et al., 2011; Li and Brummer, 2012). This legume establishes a highly specific symbiosis with rhizobia, in which the model symbiont is *Ensifer* (*Sinorhizobium*) *meliloti*. This symbiosis allows the biological reduction of atmospheric N_2 to plant-usable forms of nitrogen (Roy et al., 2020). The interaction between rhizobia and leguminous plants is a complex process, and needs the production of specific compounds from both organisms. A successful symbiosis requires a sophisticated exchange of signals between bacteria and plant (Oldroyd, 2013). This communication involves molecules of the plant, as flavonoids present in exudates or proteins such as lectins, and molecules produced by rhizobia: Nod factors or surface polysaccharides (Niehaus and Becker, 1998). The plant secretes a set of different flavonoids for which rhizobia have a specific receptor, the NodD

protein (Peck et al., 2006). The recognition of flavonoids induces expression of Nod factors (NFs) in bacteria (Peters et al., 1986; Peters and Long, 1988), which are responsible for root hair curling and induction of cell division in the root cortex (Oldroyd et al., 2011). Bacteria proliferate within the infection thread and achieve invasion and colonization of the root interior (Jones et al., 2007).

Rhizobia can produce different types of surface polysaccharides relevant for the symbiosis establishment, such as exopolysaccharides (EPS), lipopolysaccharides (LPS), capsular polysaccharides (KPS), and cyclic β-glucans (CG) (Niehaus and Becker, 1998; Fraysse et al., 2003). The surface polysaccharides are required for a successful invasion (Fraysse et al., 2003; Kawaharada et al., 2015). Rhizobial mutants defective in the production of distinct polysaccharides show deficiencies in symbiosis establishment (Diebold and Noel, 1989; Hotter and Scott, 1991; Cheng and Walker, 1998; Fraysse et al., 2003; Hozbor et al., 2004). As examples, in *E. meliloti* 2011, a mutation of *exoB* (which encodes an UDP-glucose epimerase) leads to non-infected nodules on alfalfa (Buendia et al., 1991) and, also in *E. meliloti* 2011, mutants of *exoY* (encoding an undecaprenyl-phosphate galactose phosphotransferase) are not able to elongate infection threads (Reuber and Walker, 1993; Jones, 2012). Nevertheless, each symbiotic relationship has to be carefully evaluated, as it has been reported that a mutant of *Sinorhizobium fredii* HH103 that lacks EPS, shows an increase in the competitive capacity and forms N_2-fixing nodules on *Vigna unguiculata* (Rodriguez-Navarro et al., 2014).

The relevance of each polysaccharide is specific for each rhizobia-leguminous plant interaction (Niehaus and Becker, 1998). Different strains of *E. meliloti* can produce more than one symbiotically active polysaccharide (**Table 1**). *E. meliloti* 1021 (henceforth, *Eme*1021) produces an exopolysaccharide called EPS I or succinoglycan, which is necessary for infection initiation and extension of the infection thread (Cheng and Walker, 1998). *E. meliloti* Rm41 (*Eme*Rm41) produces succinoglycan and KPS active forms, also required for infection initiation (Pellock et al., 2000). An *exoB* mutant of *Eme*Rm41 (*Eme*AK631) is defective in EPS I production but still produces KPS and shows a similar symbiotic phenotype as its parental strain, *Eme*Rm41 (Pellock et al., 2000). A derivative of *Eme*1021 with a mutation in *expR101*, acquires the capacity to produce EPS II, which differs in composition to that of EPS I. This strain showed a less effective invasion compared to the strain producing succinoglycan, but still showed induction of effective nodules (Pellock et al., 2000). Although the different surface polysaccharides can partially restore the nodulation capacity of mutants defective in EPS production, efficiency in the different steps of the nodulation process vary depending on the structure of the polysaccharide produced. Succinoglycan consists of octasaccharide repeating units of one galactose and seven glucose residues, but the repeating units can be associated with additional acetyl, pyruvyl, and succinyl groups. Cheng and Walker (1998) described that the acetyl modification is not critical for the symbiotic function of succinoglycan in *E. meliloti*, but the lack of this modification reduces the efficiency of infection thread formation. At the same time, they visualized that a deficiency in succinylation is associated with the formation of aborted infection threads. Microarrays assays of *Medicago truncatula* showed that succinylation of EPS changes the transcriptomic response during infection, especially the lack of succinoglycan enhances the transcription of plant defense genes (Jones and Walker, 2008; Jones et al., 2008). EPS can be produced in a high-molecular-weight (HMW) and a low-molecular-weight (LMW), and succinylation of EPS is necessary for the cleavage that generates the LMW (York and Walker, 1998). A mutant in *exoH* of *Eme*1021, which produces EPS I of HMW without the succinyl modification, is not able to extend infection threads and cannot perform a fruitful symbiosis (Cheng and Walker, 1998). It was recently confirmed that the succinyl modification is the essential feature, rather than the production of EPS I of LMW (Mendis et al., 2016).

Alfalfa can also be nodulated by other rhizobia, such as the acid tolerant *Rhizobium favelukesii* (Torres Tejerizo et al., 2016). This bacterium has the ability to nodulate different *Medicago* species, *Phaseolus vulgaris* and *Leucaena leucocephala*, but this interaction leads to inefficient nitrogen fixation nodules (Eardly et al., 1985; Wegener et al., 2001). The nodules developed in alfalfa by *R. favelukesii* are white, small and contain fewer bacteroids than those developed by *E. meliloti* (Wegener et al., 2001). Nevertheless, *R. favelukesii* is very competitive for the nodulation of alfalfa in acid soils (Segundo et al., 1999). During the symbiosis between *M. sativa* and *R. favelukesii* LPU83, it was shown that this bacterium does not require sulfated forms of the NFs (Torres Tejerizo et al., 2011). This is a remarkable difference in comparison with the symbiosis of alfalfa and *E. meliloti*, which absolutely needs sulfated NFs to nodulate (Schultze et al., 1995). Moreover, in alfalfa nodules developed by *E. meliloti*, only one bacteroid is found within the peribacteroidal membrane (Vasse et al., 1990), while in *R. favelukesii* it was shown that up to six bacteroids were found within a single peribacteroidal membrane, separated by matrix material (Wegener et al., 2001). Up to now, nodulation of alfalfa by *R. favelukesii* has shown differences during nodule development, nitrogen fixation and requirement of decorations on the NFs. In this work, we aimed to analyze another of the molecules necessary for infection: the EPS, which are involved in the development of the symbiosis between alfalfa and *E. meliloti*.

MATERIALS AND METHODS

Bacterial Strains and Plasmids

The strains and plasmids used in this work are listed in **Supplementary Table 5**. *Escherichia coli* was grown on Luria–Bertani (LB) (Miller, 1972) medium at 37°C. *Rhizobium* and *Ensifer* strains were grown on Tryptone–Yeast extract (TY) (Beringer, 1974),Yeast extract–Mannitol (YEM) (Vincent, 1970), or Vincent Minimal Medium (VMM) (Vincent, 1970) at 28°C. For solid media 15 g of agar per liter of medium were added. When needed, Congo Red was added at 0.25% (w/v) and Calcofluor was added at 0.02% (w/v). The final concentration of antibiotics used was (in $\mu g\ ml^{-1}$): gentamicin (Gm) 10,

TABLE 1 | Relevant characteristics of different *E. meliloti* strains with different polysaccharides [Data obtained from Pellock et al. (2000)].

Name	Genotype	EPS I	EPS II	KPS	Efficiency in infection thread initiation	Efficiency in infection thread extension	Nodulation on alfalfa
E. meliloti 1021 / 2011	Wild-type	+	–	–	100%	100%	+
E. meliloti Rm41	Wild-type	+	–	+	100%	100%	+
E. meliloti AK631 (*exoB*)	*Eme*Rm41 *exoB*631	–	–	+	80%	30%	+
E. meliloti 9000	*Eme*1021 *expR*101 *exoY*210::Tn*5*	–	+	–	50%	20%	+
E. meliloti 7210	*Eme*1021 *exoY*210::Tn*5*	–	–	–	10%	0%	–

kanamycin (Km) 25, and tetracycline (Tc) 10 for *E. coli*. For *Rhizobium* and *Ensifer*: streptomycin (Sm) 400, nalidixic acid (Nal) 20, neomycin (Nm) 60, rifampicin (Rif) 100, spectinomycin (Sp) 100, Gm 30, and Tc 5.

EPS and Total Proteins Quantification

Ensifer meliloti and *R. favelukesii* were cultivated in YEM medium. Cultures were centrifuged 45 min at 10,000 × *g*. The EPS in the supernatant was precipitated with three volumes of ethanol overnight at −20°C and stored until processed. Then, the samples were centrifuged for 45 min at 10,000 × *g* and the pellets were resuspended in water. The quantification was performed by the anthrone method (Loewus, 1952). Amounts of EPS were normalized per mg of total proteins, which was determined by Bradford assay with Coomassie brilliant blue (Bradford, 1976).

EPS Composition and Structure

Bacteria were grown in shaker flasks containing 200 ml of VMM at 30°C for 7 days. The precipitation and purification of EPS were done according to Müller et al. (1988). For monosaccharide analysis, the EPS was hydrolysed in 2 M trifluoroacetic acid for 2 h at 120°C in sealed glass vials. The hydrolysate was subsequently dried using a rotary evaporator. Remaining amounts of trifluoracetic acid were removed by the addition of isopropanol and dried again using the rotary evaporator. This treatment was carried out twice. Samples were dissolved in water and the sugars were analyzed by high-performance anion-exchange chromatography with pulsed amperometric detection on a Carbo Pac PA1 column (250 by 4 mm; Dionex, Sunnyvale, Calif.) and isocratic elution (1 ml/min) with 16 mM NaOH.

The EPS was analyzed by proton nuclear magnetic resonance (^{1}H-NMR) spectroscopy. For ^{1}H-NMR analysis, purified EPS was dissolved in deuterium oxide (99.7%), lyophilized, redissolved, and again lyophilized. Finally, 10 mg/ml of EPS was dissolved in deuterium oxide (99.99%), and sonicated for 5 min at room temperature. Spectra were recorded at 600 MHz and 80°C (Bruker Avance III–600).

Bacterial Matings

Bacterial matings were performed as described by Simon et al. (1983). The visualization of plasmids in the transconjugants (plasmid profiles) was evaluated on Eckhardt-gels (Eckhardt, 1978) as modified by Hynes and McGregor (1990).

DNA Manipulation and Genetic Constructs

Total DNA and plasmid preparations, restriction-enzyme analysis, cloning procedures, and *E. coli* transformation were performed according to previously established techniques (Sambrook et al., 1989). PCR amplification was carried out with recombinant *Taq* DNA polymerase or Pfu DNA polymerase as specified by the manufacturers. Primers are listed in **Supplementary Table 6**.

Plasmid Constructions and Mutagenesis

The deletion of the *exo* cluster located in the plasmid, yielding strain LPU83 Δplasmid, was generated as follows. Firstly, a fragment of 414 bp of the *exoV* gene was amplified with *Taq* polymerase and primers *exoV-BamHI-del-LEFT/exoV-XbaI-del-RIGHT* and cloned into the commercial vector pCR 2.1-TOPO (Invitrogen), obtaining pTOPO-*exoV* (4365 bp). Plasmid pHP45 Sp allows the release of the Sp resistance gene as blunt *SmaI* fragment of 2066 bp. This *SmaI* fragment of pHP45 Sp was introduced into the *EcoRV* site of pTOPO-*exoV*, selecting the construction with Km^r Sp^r Amp^r (pTOPO-*exoV*-Sp, 6431 bp). In parallel, a fragment of 382 bp of the *exoP* gene was amplified with *taq* polymerase and primers *exoP-BamHI-del-LEFT/exoP-XbaI-del-RIGHT* and cloned into the commercial vector pCR 2.1-TOPO, obtaining pTOPO-*exoPp* (4313 bp). Digestion of pTOPO-*exoPp* with *EcoRI* allows the release of the *exoPp* fragment (400 bp). The *EcoRI* fragment of pTOPO-*exoPp* was cloned into the *EcoRI* site of pK18mobSacB. The vector with the desired orientation was called pK18mobSacB-*exoPp* (6121 bp). This construction was digested with *NheI* and *SalI*, and ligated with the *SpeI*/*XhoI* product of TOPO-*exoV*-Sp (2576 bp), which contains both the *exoV* fragment and the Sp resistance gene, generating pK18mobSacB *exoV*-Sp-*exoPp* (8505 bp). To introduce the pK18mobSacB-*exoV*-Sp-*exoPp* into *R. favelukesii* LPU83, firstly pK18mobSacB-*exoV*-Sp-*exoPp* was transformed in *E. coli* S17-1 and then matings were carried out. Double recombinants were selected as Nm^s, and Sp^r. To corroborate the insertion, PCRs were carried out with primer *Sm-Sp* and *L_exoV-out-LEFT* (682 bp) and *Sm-Sp* and *L_exoP-out-RIGHT* (626 bp).

For the construction of strain LPU83 Δchromo, fragments of *exoZ* and *exoP* genes were amplified (185 and 210 bp, respectively), using *Phusion* polymerase (Thermo Scientific) and primers *exoZ_Fw_cro83_Eco/exoZ_Rv_cro83_Sma* and *exoP_Fw_cro83_Bam/exoP_Rv_cro83_Hin*, respectively. The

fragments were cloned into the *SmaI* site of pK18mob. pK18mob-*exoPc* (4027 bp) was digested with *BamHI* and *HindIII*, and the released fragment (216 bp) was cloned into pK18mobSacB, obtaining pK18mobSacB-*exoPc* (5907 bp). Then, an *EcoRI*/*SmaI* fragment from pK18mob-*exoZ* (193 bp) containing the *exoZ* fragment was cloned into the *EcoRI*/*SmaI* sites of pK18mobSacB-*exoPc*, obtaining pK18mobSacB-*exoZ-exoPc* (6082 bp). To add the Tc resistance gene, the *SmaI* fragment of pHP45 Tc (2160 bp) containing the Tc resistance gene was cloned into the *SmaI* site of pK18mobSacB-*exoZ-exoPc*, selecting the Km^r Tc^r vector, called pK18mobSacB-*exoZ*-Tc-*exoPc*. This vector was introduced by conjugation into *R. favelukesii* LPU83. Double recombinants were selected as Km^s, and Tc^r. To corroborate the insertion, PCRs were carried out with primer *side_exoZ_out* and *Tc-out-Nter* (774 bp) and *side_exoP_out* and *Tc-out-Cter* (983 bp). The result is a LPU83 derivative with a deletion on the chromosome *exo* cluster.

The LPU83 mutant in the *exoB* gene was carried out by a simple crossing over. For this, a fragment of 295 bp of the *exoB* gene was amplified using *Phusion* polymerase and primers *exoB-Fw-int*/*exoB-Rv-int*. The product was cloned into the *SmaI* site of pK18mob, obtaining pK18mob-*exoB* (4088 bp). This vector was introduced by conjugation into *R. favelukesii* LPU83. Simple recombinants mutants were selected as Nm^r. To corroborate the insertion, PCRs were carried out with primer *M13-Fw-40* and *exoB-Rv-comp* (1072 bp) and *M13-Rv-40* and *exoB-Fw-comp* (726 bp). The result is a LPU83 derivative with an insertion on the *exoB* gene.

The vector for the *exoB* complementation assay was constructed as follows. A fragment containing the full *exoB* gene was amplified (1372 bp) with *Phusion* polymerase and primers *exoB-Fw-comp*/*exoB-Rv-comp*. The fragment was cloned into the *SmaI* site of the broad host range vector pBBR1MCS-5. The orientation of the gene was evaluated to make sure that the Lac promoter that is present in the vector would express the *exoB* gene. The resulting vector was called pBBR1MCS5-*exoB* (6140 bp).

Bioinformatics Approaches and Phylogenetic Analyses

For comparative genomics studies, the genes were searched for by means of BLASTp on the NCBI webpage. To examine genetic neighborhood, https://img.jgi.doe.gov/ was also used.

For the construction of the phylogenetic trees, the proteins were aligned with the module of Clustal implemented in MEGAX (Kumar et al., 2018). Prottest2.4 was used to determine the models of protein evolution (Abascal et al., 2005). The best model was LG+I+G for ExoB, LG+G+F for ExoH, LG+G for ExoV and LG+G for ExoY. Maximum likelihood (ML) trees were inferred under the selected model using PhyML v3.1 (Guindon and Gascuel, 2003). The robustness of the ML topologies was evaluated using a Shimodaira-Hasegawa-like test for branches implemented in PhyML v3.1 (values display in the nodes are multiplied by 100). We employed the best of NNIs and SPRs algorithms to search the tree topology and 100 random trees as initial trees. The accession numbers for the proteins selected for the phylogeny are display in each tree.

Plant Assays

Medicago sativa (Alfalfa Sardi ten) seeds where surface-sterilized for 5 min in a 70% (v/v) ethanol solution, then washed with sterile distilled water. Subsequently, seeds were immersed in a solution of sodium hypochlorite (11 g l^{-1}) for 15 min and washed six times with sterile distilled water. Seeds where placed on water agar (0.8% w/v) overnight. Afterward, seeds were placed on ethylene-oxide-sterilized plastic growth pouches containing 10 ml of Rolfe medium (Rolfe et al., 1980), with modifications (Barsch et al., 2006). Germination occurred in the pouches, and the roots developed through the hole in the paper. Seeds that did not germinate or did not grown through the hole were discarded. Three days post-germination, plants were inoculated with 10^6 colony-forming units of each strain used in this work (at least 25 plants per strain). Plants were cultured in a growth chamber at 22°C with a 16-h photoperiod, watered with modified Rolfe medium and water. The CFU that each inocula contained were estimated by plate counts. Plant assays were repeated at least twice.

Plants were harvested 4 weeks after inoculation. Nodules were counted, weighted and conserved at 4°C. The shoot dry matter weight was measured. For nodule occupancy, nodules were sterilized and treated as previously described (Torres Tejerizo et al., 2010; Montiel et al., 2016). Briefly, the nodules that previously were weighted and counted, were surface-sterilized with H_2O_2 (30 volume) for 10 min, washed with sterile distilled water and then crushed in 200 ul of sterile isotonic solution followed by plating serial dilutions on TY with the corresponding antibiotics. 2–3 days after, CFU were counted.

For microscopy, nodules were embedded in 6% (w/v) agarose. Nodule sections of 60 μm were obtained using a Leica VT1000 S Vibratome. Fresh sections were then stained with Live/Dead BacLight bacterial Viability Kit (Thermo Fisher). The staining solutions were then removed and nodule sections were resuspended in PBS buffer. Images were acquired with a Leica TCS SP5 confocal microscope.

RESULTS AND DISCUSSION

Localization and Gene Arrangement of Exopolysaccharide-Related Genes in *R. favelukesii* LPU83

During the symbiotic interaction between *E. meliloti* and alfalfa, different polysaccharides play relevant roles. Among them, EPS I (succinoglycan) is critical (Niehaus and Becker, 1998), but in some strains, the lack of EPS I may be overcome by EPS II (galactoglucan) or KPS (capsular polysaccharide, also referred as K antigen) (Pellock et al., 2000). As *R. favelukesii* LPU83 is able to infect alfalfa with some particular features (as mentioned in the introduction), the orthologs to the genes known to be involved in polysaccharides synthesis were searched for using BLAST. In addition to establishing a minimum of 35% identity as a cut-off

to define orthologs (Rost, 1999), query coverage (>70%) and synteny were also considered in the analyses.

Capsular Polysaccharide

As mentioned in the Introduction, *Eme*AK631 only produces KPS (Putnoky et al., 1988; Putnoky et al., 1990; Reuhs et al., 1995) and, despite the lack of EPS I and EPS II, it is able to infect alfalfa (Putnoky et al., 1990; Pellock et al., 2000). Three clusters involved in KPS synthesis were described in *Eme*AK631 (**Supplementary Figure 1**): *rkp-1*, formed by *rkpABCDEFGHIJ* (Petrovics et al., 1993; Kiss et al., 1997), *rkp-2* which harbors *lpsL* and *rkpK* (Kereszt et al., 1998) and *rkp-3*, constituted by *rkpLMNOPQRSTZ* (Kiss et al., 2001). Later on, *rkpU* was found to be located upstream of *rkpA* in *Eme*AK631 and in *S. fredii* HH103 (Parada et al., 2006; Hidalgo et al., 2010). Recently, the parental strain of *Eme*AK631, *Eme*Rm41, was completely sequenced (Weidner et al., 2013). Surprisingly, in the annotation of the genome of *Eme*Rm41 a very large *rkpA* gene was detected, which comprises the *rkpABCDEF* genes from *Eme*AK631 (**Supplementary Figure 1**). A similar gene-fusion was observed in *Eme*1021 and *S. fredii* HH103 (Parada et al., 2006). By means of BLASTp, orthologs for the genes involved in KPS synthesis were searched for in LPU83. *rkpA* was not found as a large ORF in LPU83. We compared the genes of both, *Eme*AK631 and *Eme*2011. Some orthologs were found, but with low identity at the amino acid sequence (*ca.* 25–45%) and low coverage (**Supplementary Tables 1, 2**). In addition, none of the genes found were distributed in clusters.

For the *rkp-2* cluster, proteins with high similarity were found (for *lpsL*, LPU83_3231 and for *rkpK*, LPU83_3230). These genes showed *ca.* 70% identity and almost a full coverage in comparison to *Eme*2011 (**Supplementary Figure 1**). It is notable that in LPU83 *lpsL* is located downstream of *rkpK*, while in the *E. meliloti* strains the order of the genes is inverted, with *rkpK* situated downstream of *lpsL* (**Supplementary Figure 1B**).

For the genes that formed *rkp-3* cluster, again, differences were observed between *Eme*AK631 and *Eme*Rm41 (**Supplementary Figure 1**). Furthermore, it was observed that in *Eme*2011 the *rkp-3* cluster was not complete (**Supplementary Figure 1**), lacking *rkpLMNOPQ*. A similar lack of genes is observed in *Eme*1021 (not shown). In LPU83, only some orthologs were found, and they are not organized in clusters (**Supplementary Table 3**). The structure of KPS has been described in *Eme*AK631 (and also in other rhizobia) as repetitive units of hexose linked with 3-deoxy-D-*manno*-2-octulosonic acid (Kdo) or related 1-carboxy-2-keto-3-deoxy sugars (Reuhs et al., 1993; Reuhs et al., 1998; Fraysse et al., 2003). The KPS of *Eme*1021 is composed solely by Kdo and a phospholipid anchor (Pellock et al., 2000). *Eme*1021 has been shown to produce KPS, but it is biologically inefficient (Fraysse et al., 2005) and cannot support the symbiosis with alfalfa (Pellock et al., 2000).

The lack of orthologs in *Eme*2011 (and in *Eme*1021) to some of the genes involved in the biosynthesis of KPS (**Supplementary Figure 1**) could be related to the particular inefficient KPS described by Fraysse et al. (2005). Likewise, as LPU83 lacks almost all the orthologs for KPS synthesis, the probabilities of producing an efficient KPS should be very low.

Galactoglucan

Ensifer meliloti is able to synthetize, under specific environmental conditions or certain mutations, a galactoglucan called EPS II, which was described as a non-Calcofluor-binding exopolysaccharide that reacts with anthrone (Glazebrook and Walker, 1989). EPS II is composed of glucose and galactose residues in a 1:1 ratio. The proteins needed for its production are encoded in the *exp* gene cluster located in the pSymB (organized in five transcriptional units, see **Supplementary Figure 2**) (Becker et al., 2002). It has been demonstrated that strains producing EPS II, but neither EPS I nor KPS, are able to infect alfalfa, reinforcing a relevant role in the symbiosis (Pellock et al., 2000). Despite this infection being less efficient than that of strains expressing EPS I alone, EPS II is able to restore the nodule development and nitrogen fixation that is lacking in EPS I mutants (Glazebrook and Walker, 1989). For the production of EPS II, the transcriptional regulator ExpR must be expressed to activate the transcription of the genes in the *exp* cluster. ExpR is a homolog of the LuxR family regulators (Pellock et al., 2002). ExpR homologs were searched for in LPU83. Three hits were found, LPU83_4100 (65% identity and 97% coverage), LPU83_pLPU83b_0215 (41% identity and 47% coverage), and LPU83_pLPU83d_1676 (46% identity and 14% coverage), suggesting that some of them could play a similar role as that of ExpR in *E. meliloti*. Thus, the orthologs to the 21 genes that form the *exp* cluster of *Eme*2011 were searched in LPU83 (**Supplementary Table 4**). The results showed no hits for six genes (*expE8*, *expE5*, *expC*, *expA4*, *expA5*, and *expA6*) but for the remaining genes, some hits were found mainly dispersed among the chromosome and plasmids of LPU83. In most of the cases with low identity scores (*ca.* 30–40% of identity) and without synteny, with exception of the genes LPU83_pLPU83d_1427, LPU83_pLPU83d_1428, and LPU83_pLPU83d_1429 that are similar to *expD1*, *expD2*, and *expE1*, respectively. Altogether, and as will be shown below, the results suggest that no galactoglucan should be produced by LPU83.

Together with the already mentioned ExpR master regulator, *E. meliloti* possesses another master regulator of EPS biosynthesis, namely MucR representing a homolog of the RosR protein from *Agrobacterium tumefaciens* (Keller et al., 1995). Mutation of *mucR* increases EPS II production and reduces EPS I synthesis (Becker et al., 2002). It was also shown that MucR increases nod factor production (Mueller and Gonzalez, 2011). We found a homolog to MucR from *Eme*1021 (P55323.1) in LPU83, namely LPU83_1234 (81% identity and 99% coverage), which is actually annotated as *rosR* and is located on the chromosome. This suggests that EPS biosynthesis and nod factor production might be regulated by LPU83_1234, the MucR/RosR homolog.

Succinoglycan

Succinoglycan, also namely EPS I, is an acidic Calcofluor-binding exopolysaccharide that has been extensively studied and demonstrated as a key molecule for the proper symbiosis of *Eme*2011 with alfalfa (Leigh et al., 1985; Leigh et al., 1987; Niehaus and Becker, 1998; Jones et al., 2007; Marczak et al., 2017). EPS I

is composed of repeating octasaccharidic subunits with glucose and galactose in a 7:1 ratio and different substituents (succinyl, acetyl, and pyruvyl) (Becker and Pühler, 1998; Fraysse et al., 2003). The synthesis of the EPS I is carried out by several proteins encoded in the gene cluster (*exoBZQFYXUVWTIHKLAMONP*) located in the pSymB (**Figure 1**). Mutants in *exoZ*, *exoX*, *exoI*, *exoK*, *exoO*, and *exoN* have been described as able to infect alfalfa [reviewed by Niehaus and Becker (1998)]. The genes involved in EPS I synthesis were searched for in the LPU83 genome using *E. meliloti* as query (**Figure 1**). Orthologs to *E. meliloti* genes were found distributed among a cluster in the chromosome (*exoZQFYXUWHKAMOP*), the smallest of the plasmids present in LPU83, pLPU83a (*exoVWTHKLAMO1O3P*) and elsewhere, but not clustered, in the chromosome (*exoB*, *exoI*–LPU83_RS49150 Id 33% Qc 92% and *exoN*–LPU83_RS55945 Id 65% Qc 92%) (**Figure 1**). In this case, the scores were higher in comparison to similar genes involved in EPS II or KPS biosynthesis. Remarkably, some genes are duplicated between the plasmid and chromosome clusters. *exoV* and *exoT* are only present in pLPU83a, while *exoZQFYXU* are only present in the chromosome of LPU83. *exoV* encodes for a glycosyltransferase that is necessary for the addition of the pyruvyl substituent (Glucksmann et al., 1993; Reuber and Walker, 1993). *exoT* encodes for a transmembrane protein needed for the polymerization and/or export of the EPS I (Becker et al., 1993; Glucksmann et al., 1993; Reuber and Walker, 1993). Both genes were early recognized as indispensable for the production of EPS I and for the infection of alfalfa by *E. meliloti* (Becker et al., 1993). Thus, the *exo* gene cluster present in pLPU83a could be essential for a proper EPS I production.

Arabinose-Containing Polysaccharide

It was recently shown that *Eme*2011 is also able to produce a Congo Red-binding extracellular polysaccharide (Schäper et al., 2017). This polysaccharide is an arabinose-containing polysaccharide (APS), whose production is enhanced when cyclic di-GMP levels are elevated. Through an over-expression of *pleD*, encoding a diguanylate cyclase, and *cuxR* encoding a c-di-GMP responsive transcriptional activator of the APS operon, Schäper et al. (2019) were able to study the regulation of genes involved in the synthesis of the APS operon: the operon *uxs1-uxe-apsS-apsH1-apsE-apsH2* (**Figure 1**). Strains that produce APS generate wrinkled red-colored macro-colonies on Congo Red containing medium (Schäper et al., 2019), but at this time there is no evidence of its role in symbiosis. A gene cluster of APS genes was found in pLPU83d, the largest plasmid of LPU83. Most of the APS-like genes showed identity values higher than 50%, with exception of *apsH1* and *apsH2* (**Figure 1**). Nevertheless, as it will be shown below, wrinkled macro-colonies were not observed in LPU83 nor in the mutants made in this work.

Cyclic β-Glucans (CG) and Mixed-Linkage β-Glucans (MLG)

Cyclic ß-glucans in *E. meliloti* consist of 17–25 glucose residues linked by ß-1,2 bonds [CGs bonds may be different in other rhizobia (Breedveld and Miller, 1994)]. CGs synthesis in *E. meliloti* is directed by the translated products of the genes *ndvA* and *ndvB*, and mutants in any of these genes are impaired in the symbiosis with alfalfa (Dylan et al., 1986; Dickstein et al., 1988; Stanfield et al., 1988; Jones et al., 2007). Homologs to *Eme*1021 NdvA (CAC47862.1) and NdvB (P20471.2) are present in strain LPU83, namely LPU83_4101 (CDM59736.1,

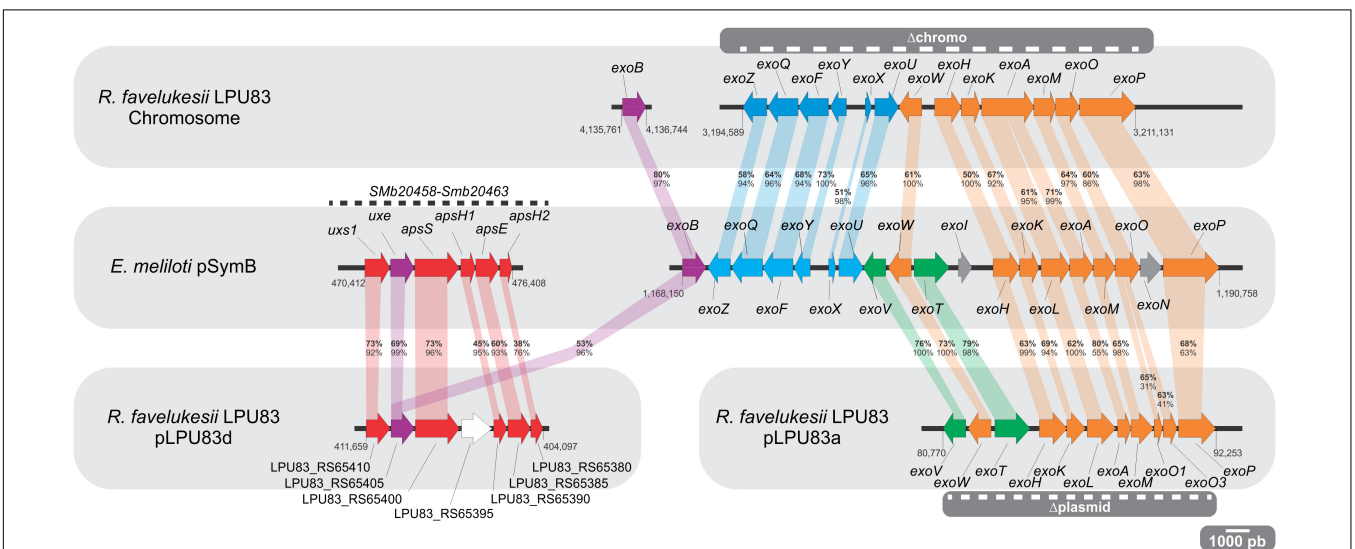

FIGURE 1 | Genetic organization of the EPS I and APS genes. The *E. meliloti* pSymB figure (middle) shows the organization of the cluster of genes involved in APS (left) and EPS I (right) synthesis. The upper box shows the distribution of orthologs to EPS I production genes, distributed among *R. favelukesii* LPU83 chromosome. The bottom box shows the distribution of orthologs to APS (left) and EPS I (right) production genes, distributed among plasmids pLPU83d and pLPU83a, respectively. Numbers at the beginning and at the end of each cluster indicate the position of each gene. Orthologs are marked and connected with similar colors. Percentages in bold stand for amino acidic identity of the proteins. Percentages below bold-numbers stand for query coverage. All the comparisons were made using *E. meliloti* 2011 *exo* genes as query. The striped lines within gray boxes indicate the deletions made in the *exo* cluster of the chromosome and the plasmid.

76% identity and 94% coverage when compared with NdvA) and LPU83_4179 (CDM59813.1 and 69% identity and 99% coverage when compared with NdvB). Despite such sequence similarity, *ndvA* and *ndvB* are not syntenic in *E. meliloti* and *R. favelukesii*. While in *Em*e1021 the *ndv* genes are separated by 3 Kbp, in *R. favelukesii* LPU83 the same genes are separated by more than 70 Kbp. Currently available data demonstrate that *ndvA* and *ndvB* are strongly transcribed at low extracellular pH in *R. favelukesii* LPU83 (Nilsson et al., 2020), a result that suggests a possible role of the CGs during the response of the bacteria to an increased concentration of extracellular hydrogen ions. Nonetheless, further biochemical analyses are necessary to investigate whether there is or not CGs production in *R. favelukesii* LPU83.

Under artificial increments of cyclic di-GMP levels it has been shown that *E. meliloti* 8530 is able to produce a different polysaccharide named mixed-linkage ß-glucans (MLGs). MLGs are linear (1→3) (1→4)-ß-D-glucans that are relevant for adhesion and colonization of alfalfa roots but not for nodule development (Pérez-Mendoza et al., 2015). Rhizobial colonies that produce MLGs bind both Calcofluor and Congo Red. The synthesis of MLGs in *E. meliloti* 8530 is mediated by BgsA (GT-2 protein, CAC48777.1) and BgsB (a membrane fusion protein, CAC48776.1). Homologs to *E. meliloti* BgsA and BgsB were found in *R. favelukesii* LPU83 (i.e., LPU83_pLPU83c_0651, CDM61213.1, 80% identity and 99% coverage; and LPU83_pLPU83c_0650, CDM61212.1, 68% identity and 100% coverage; respectively). Despite the synteny between the *bgs* genes in *E. meliloti* and *R. favelukesii*, we do not have yet evidence of MLGs production in strain LPU83.

The data presented suggests that LPU83 has the potential to produce EPS I and, under specific conditions, as increments of cyclic di-GMP levels, APS as stated by Schäper et al. (2017, 2019) or MLG as suggested by Pérez-Mendoza et al. (2015). Morphological observations of LPU83 show mucoid macro-colonies which predict the production of polysaccharides (Torres Tejerizo et al., 2016). The particular genetic organization that we found for the EPS I gene cluster raises some questions: which is the evolutionary relationship of the genes present in the plasmids? Are both genetic clusters essential for EPS synthesis? Is the EPS produced by LPU83 similar to the one produced by *E. meliloti*? Finally, how relevant is the EPS of LPU83 for the infection of alfalfa?

Phylogenetic Analyses of EPS I Genes in *Rhizobium favelukesii* LPU83

The presence of two main clusters of *exo* genes in LPU83, one in the chromosome and another in plasmid pLPU83a point out that an event of horizontal gene transfer (HGT) could have occurred during the evolution of LPU83, where the strain acquired the *exo* genes from other bacteria. It is worth mentioning that previous work from our group has shown that pLPU83a is able to perform conjugative transfer (Torres Tejerizo et al., 2010), and the regulation of this phenomena depends on their genomic background and environmental conditions (Torres Tejerizo et al., 2014). Moreover, the plasmid gene cluster could be complementing the chromosomal genes to get a fully functional EPS I production.

To understand if such event of HGT occurred, phylogenetic analyses were made employing four genes. One only present in the chromosomal gene cluster (*exoY*), one present only in the plasmid gene cluster (*exoV*), one present in both clusters (*exoH*) and the *bonafide exoB*, that was present in the chromosome but not in the *exo* gene cluster. For the phylogenetic inference, the translated products of the genes were used. The ExoB phylogenetic tree showed that it was related to *Rhizobium tibeticum* CCBAU85039 and *Rhizobium grahamii* CCGE 502 (**Figure 2**), strains with which it shares a close chromosomal relationship (Torres Tejerizo et al., 2016). In a similar way, ExoY (also harbored in the chromosome) clusters with the same strains. Meanwhile, ExoV, which is present in pLPU83a, groups with *E. meliloti* and *Ensifer medicae* strains. No orthologs to ExoV were found in *R. tibeticum* CCBAU85039 and *R. grahamii* CCGE 502. Finally, the phylogenetic tree of ExoH, locates the chromosomal-encoded copy near to *R. tibeticum* CCBAU85039 and *R. grahamii* CCGE 502 while the plasmid-encoded copy is closer to *E. meliloti* and *E. medicae*. These results support the hypothesis that the plasmid *exo* cluster arose from an HGT event, probably from an *Ensifer*-related strain. It was previously shown that the *exo* cluster present in the plasmid is flanked by two inverted repeats, which encode a Tn*3*-like transposase and recombinase (Castellani et al., 2019). These structures could be a reminiscence of an insertion/excision of foreign DNA.

Evidence of HGT events toward new-symbiotic strains has been shown previously, although the efficiency of the resulting symbioses may be low. Sullivan et al. (1995) and Sullivan and Ronson (1998) showed the lateral transfer of a symbiotic island from *Mesorhizobium loti* to non-symbiotic mesorhizobia allowing the evolution of the latter into symbiotic rhizobia. A similar event was observed in soils of the Brazilian Cerrados (Batista et al., 2007), where evidence of HGT from inoculated *Bradyrhizobium* strains to soil bacteria was detected. Recently, it was shown that the symbiotic plasmid of *Rhizobium etli* CFN42, or at least fragments of it, can be transferred to bean-endophytic bacteria, generating new strains with the ability to nodulate and fix nitrogen (Bañuelos-Vazquez et al., 2020). In our group, we showed that the gene cluster involved in the synthesis of the nodulation factors (NFs) of LPU83 has a structure similar to that of *E. meliloti*, with whom it also shares a close phylogenetic relationship (Del Papa et al., 2007; Torres Tejerizo et al., 2011). Thus, not only genes involved in NFs synthesis could have been recruited by HGT, but also a gene cluster involved in EPS biosynthesis, during the evolution of LPU83.

The Exopolysaccharide Produced by *R. favelukesii* LPU83 Is Similar to the Succinoglycan of *E. meliloti*

Several determinants, including EPS, play essential roles during the complex molecular crosstalk before and during the interaction between rhizobia and plants (Jones et al., 2007). Rhizobial EPS varies among strains and species, harboring different substitutions (Skorupska et al., 2006). Due to the

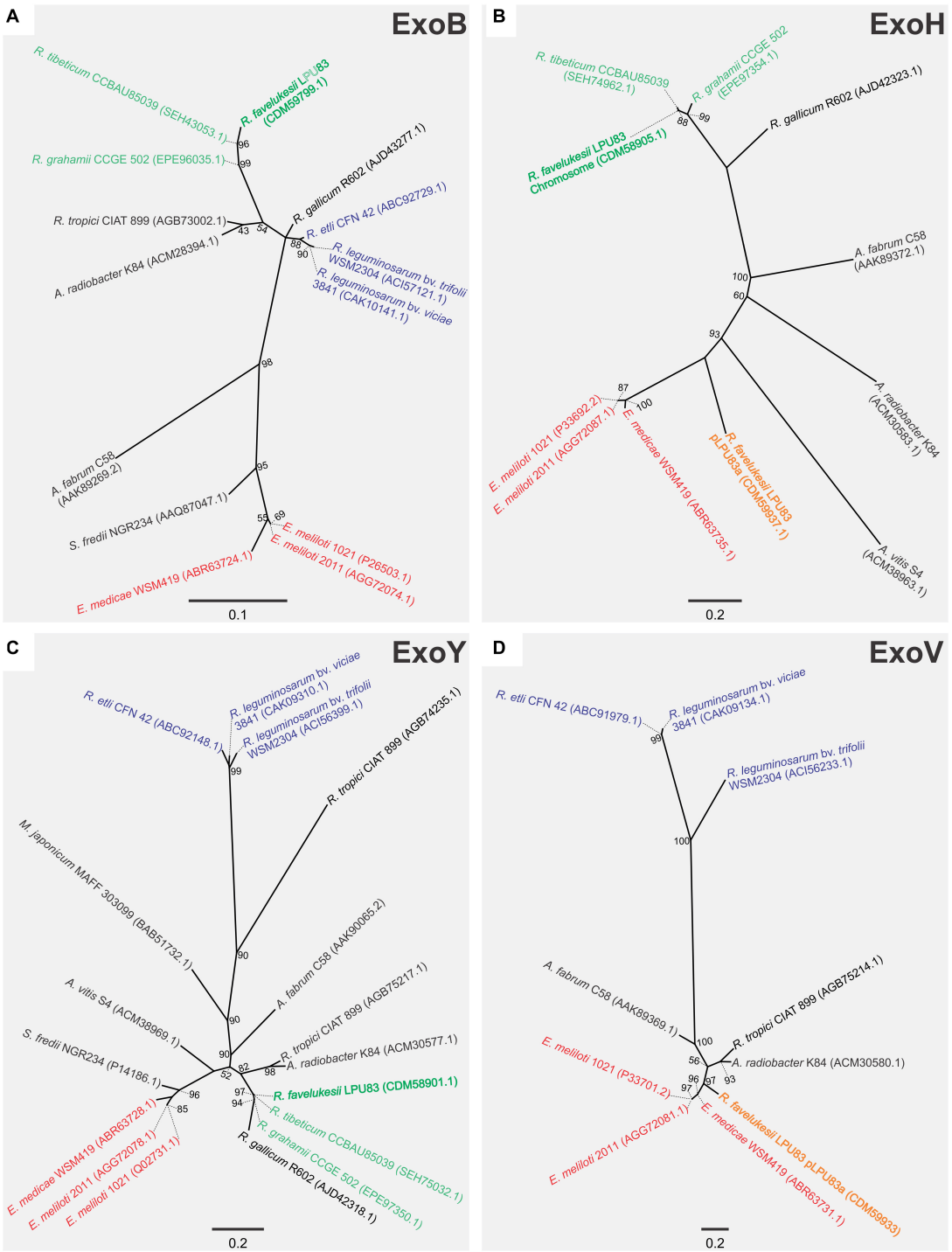

FIGURE 2 | Phylogenetic analyses of EPS I genes of LPU83. Phylogenetic tree based on **(A)** ExoB (only in the chromosome of LPU83), **(B)** ExoH (in the chromosome of LPU83 and pLPU83a), **(C)** ExoY (only in the chromosome of LPU83), and **(D)** ExoV (only in the plasmid pLPU83a). Analyses were conducted by means of the Maximum Likelihood method. Support values (SH like × 100) greater than 50 are indicated at the nodes. Bars indicate substitution/site.

relevant role of EPS during the symbiosis between rhizobia and *Medicago* spp. and the ability of LPU83 to nodulate *Medicago* spp. and other legumes (Wegener et al., 2001), the structure of the EPS produced by LPU83 was analyzed. EPS was precipitated from culture supernatants. Monosaccharide analysis of the hydrolyzed EPS of LPU83 indicated that the strain produces an EPS that consists of glucose and galactose in a ratio of 7 to 1, similar to EPS I of *Eme*2011 (**Figure 3**).

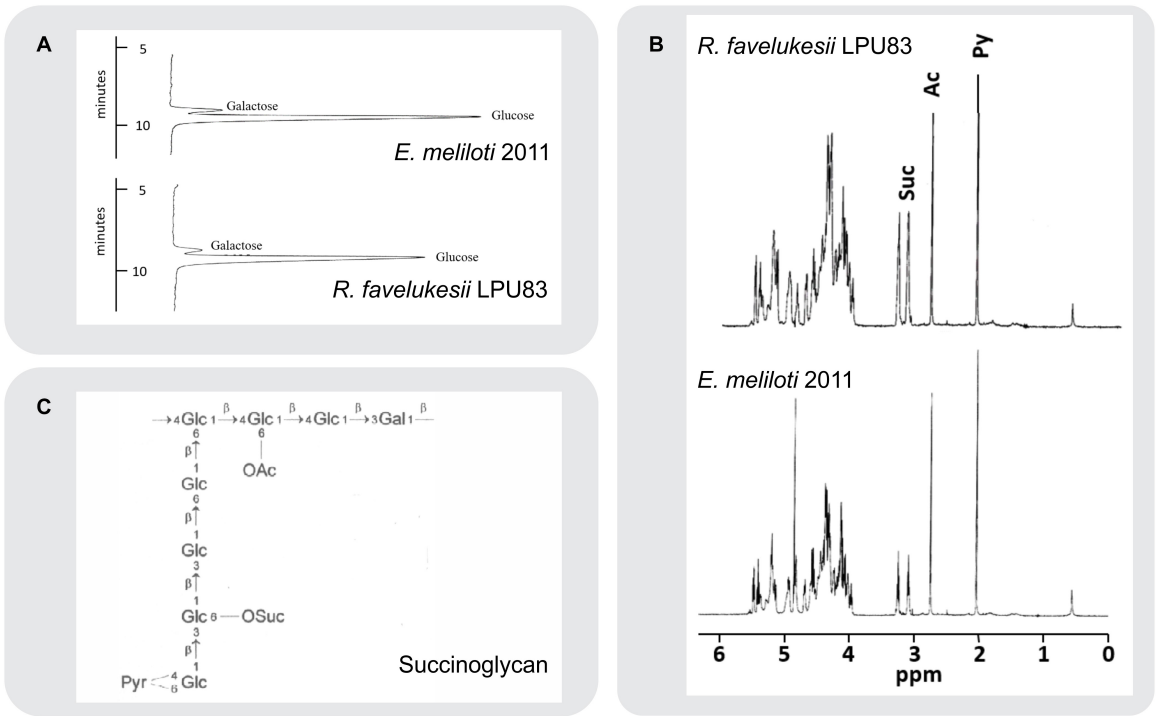

FIGURE 3 | Composition and structural analyses of EPS. **(A)** Separation of monosaccharides obtained by acid hydrolysis of cetylpyridinium chloride (CPC) and ethanol precipitated culture supernatant of *E. meliloti* 2011 and *R. favelukesii* LPU83. The monosaccharides were separated by high-performance anion-exchange chromatography with pulsed amperometric detection on a Carbo Pac PA1 column. Only the relevant parts of the chromatograms are shown. **(B)** ^{1}H-NMR spectra of isolated acidic exopolysaccharides (EPS) from *R. favelukesii* LPU83 and *E. meliloti* 2011. The singlets at 2.1 and 2.7 ppm represent the methyl protons from pyruvate and acetyl groups, respectively. The triplets at 3.1 and 3.25 ppm arise from the methylene protons of the succinyl group, while the complex region between 3.9 and 5.5 ppm represents signals from the ring protons of the carbohydrate constituents. **(C)** Structure of *E. meliloti* EPS I (succinoglycan). Diagram showing the octasaccharide repeating unit of succinoglycan (*OAc*, acyl group; *Pyr*, pyruvyl group; *OSuc*, succinyl group).

The EPS of LPU83 was further analyzed by ^{1}H-NMR and gas chromatography/mass spectrometry (GC/MS) studies. A ^{1}H-NMR spectrum of EPS I isolated from *Eme*2011 was recorded as a control (**Figure 3B**). This spectrum was in accordance with data already published for this EPS I (Leigh et al., 1987; Keller et al., 1995). The proton resonances between 3.8 and 5.4 ppm were assigned to glycosyl components arising from ring protons, and the singlet resonances at 2.1 and 2.8 ppm were assigned to methyl protons of the 1-carboxyethylidene (pyruvate) and acetyl groups, respectively. The characteristic triplets at 3.1 and 3.25 ppm represent the methylene protons of the succinyl groups. The EPS isolated from LPU83 gave rise to virtually the same proton NMR spectrum, indicating that the main polysaccharide secreted by this strain is identical to succinoglycan from *Eme*2011.

At first glance, it may have been proposed that the different substitution/modifications of the EPS could be related to the failure in the nodule development and differentiation observed in *R. favelukesii* (Eardly et al., 1985; Del Papa et al., 1999; Wegener et al., 2001). Our results demonstrate that despite the different organization of EPS I genes, whose localization is not restricted to one cluster and that the evolution of both clusters seems to integrate genes from different rhizobial linages, the EPS 1 produced is identical to that of *E. meliloti*. The question that remains is whether these clusters are essential for this EPS production and plant infection or not.

Genomic Regions Required for EPS Production of LPU83

We showed that LPU83 produces a succinoglycan identical to the one produced by *E. meliloti* and that the genes involved in the synthesis are distributed between the chromosome of LPU83 and plasmid pLPU83a. This particular organization leads to the question whether both gene clusters are relevant for the production of EPS I. To determine this, a genetic approach was used. The chromosome cluster was deleted by double crossing-over and inserting a resistance to Tc, generating strain LPU83 Δchromo (the region is indicated in **Figure 1**), as indicated in section "Materials and Methods". The cluster located in pLPU83a was deleted in a similar way, but a Sp resistance was used instead, generating strain LPU83 Δplasmid (also indicated in **Figure 1**). ExoB has been recognized as a UDP-glucose 4-epimerase which provides the UDP-galactose in *E. meliloti* (Buendia et al., 1991). Mutants in *exoB* of *E. meliloti* fail to produce proper EPS I and EPS II due to the lack of galactose (Putnoky et al., 1990; Buendia et al., 1991; Reuhs et al., 1995). Due to the relevance of *exoB*, a

mutant was also made. In this case, by single recombination through the integration of pK18mob-*exoB* plasmid (LPU83-*exoB*$^{-}$). Afterward, the mutations were combined to generate a double deletion mutant (LPU83 Δchromo Δplasmid) and a triple mutant (LPU83-*exoB*$^{-}$ Δchromo Δplasmid). Finally, LPU83-*exoB*$^{-}$ was complemented in *trans* with a full copy of *exoB* (pBBR1MCS5-*exoB*). Wild type *Eme*2011 and *Eme*2011 Δ*exo* [which harbors a markerless deletion of the *exo* gene cluster from *exoP* to *exoZ* (Schäper et al., 2019)] were used as controls. EPS production was quantified with the anthrone method (**Figure 4A**) and EPS I was visualized due to its fluorescence in medium containing calcofluor (**Figure 4B**). The calcofluor assays demonstrated that only wild type strains (*Eme*2011 and LPU83) or the LPU83-*exoB*$^{-}$ complemented in *trans* were able to produce EPS I. In agreement with this result, anthrone assays also showed EPS production by the same strains. The levels of EPS of the *exoB* mutant complemented were slightly lower than the wild type (**Figure 4A**), but the calcofluor fluorescence phenotype was clearly observed (**Figure 4B**).

Schäper et al. (2016, 2017) have shown that in *Eme*2011 EPS production is enhanced when cyclic di-GMP levels are elevated. Also, a new polysaccharide was described: an arabinose-containing polysaccharide (APS) (Schäper et al., 2019). The ectopical overexpression of *pleD* (diguanylate cyclase) and *cuxR* (c-di-GMP responsive transcriptional activator) leads to high di-GMP levels and, consequently, to an APS overproduction, generating wrinkled red-colored macro-colonies on medium containing Congo red (CR). Moreover, Pérez-Mendoza et al. (2015) showed that when cyclic di-GMP levels increase, MLGs can be produced. MLGs also bind Calcofluor and CR. The morphology of LPU83 and its mutants was evaluated in medium with CR, to determine binding of this dye. Neither LPU83 nor the mutants showed wrinkled macro-colonies nor red staining. Mutants of LPU83 did not show Calcofluor fluorescence (**Figure 4**). These results indicate that under our experimental conditions, APS and MLGs are not synthetized.

Exopolysaccharides production depends on many genes (Niehaus and Becker, 1998). In LPU83, the genes needed for the production of EPS I are distributed among different replicons. As shown above, both clusters and the *exoB* gene are needed for EPS production. In addition to the lack of orthologs of the genes needed for the synthesis of EPS II, the lack of glucose in the mutants suggest that galactoglucan is not produced in LPU83. The lack of CR staining suggests that also APS is not produced under our laboratory conditions. Altogether, LPU83 seems to be producing only EPS I, requiring both *exo* clusters and *exoB*.

Symbiotic Phenotype of the LPU83 EPS Mutants

As mentioned earlier, KPS and EPS II may replace, at least partially, the lack of EPS I in the effective nodulation of alfalfa by *E. meliloti* (Pellock et al., 2000). But when only EPS I is

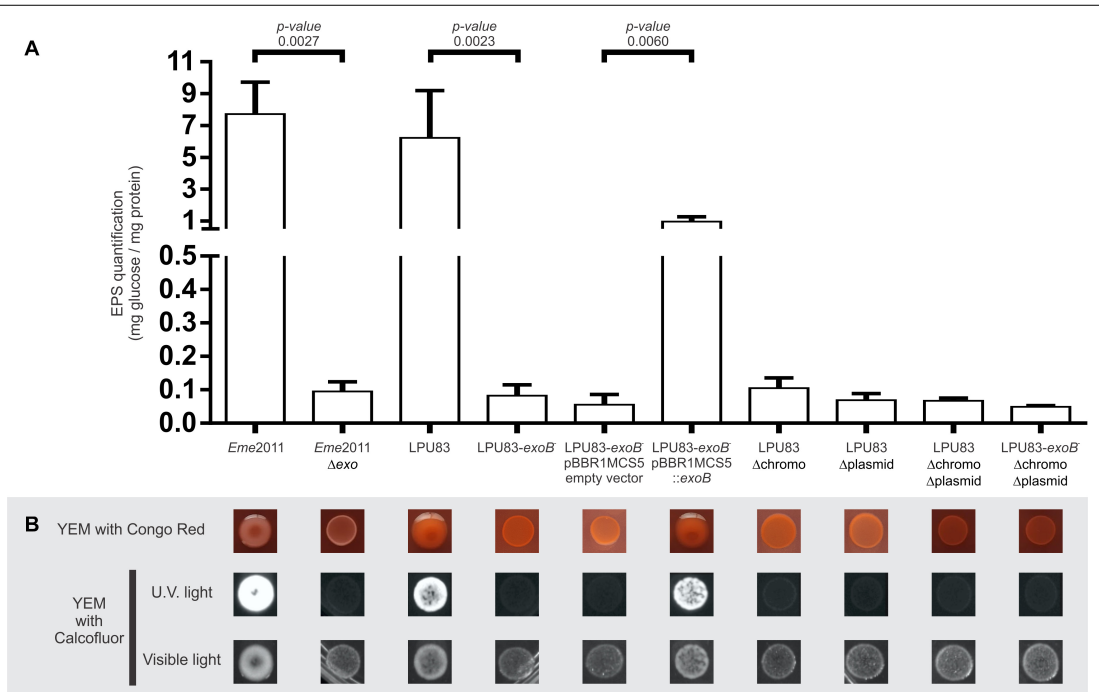

FIGURE 4 | Characterization of EPS production of LPU83 mutants. **(A)** EPS quantification by the anthrone method. The EPS amount normalized per mg of total proteins is shown for each evaluated strain of *E. meliloti* and *R. favelukesii*. **(B)** Phenotypic analyses of the LPU83 mutants. EPS production was evaluated in YEM with Congo Red (first line) and in YEM with calcofluor under visible light and under UV light (lines below). The presence of EPS I is evidenced in the last condition due to its fluorescence. The statistical analysis was done by a *t*-test using three independent biological replicates. Representative pictures of at least three different experiments are shown.

produced, mutants in its biosynthesis fail to nodulate (Cheng and Walker, 1998; Niehaus and Becker, 1998; Mendis et al., 2016). Also in *Eme*2011, mutants in the genes involved in the sulfation of NFs are not able to nodulate (Roche et al., 1991; Schultze et al., 1995). LPU83 has the particular capacity to nodulate alfalfa even in absence of sulfated NFs (Torres Tejerizo et al., 2011). This peculiarity encouraged us to evaluate the nodulation of alfalfa using all the constructed strains. As control, we included *Eme*2011 and *Eme*2011 Δ*exo* strains. *Eme*2011 Δ*exo* is a deletion mutant that lacks the *exo* gene cluster from *exoP* to *exoZ*, but retains the *exoB* gene. *Eme*2011 Δ*exo* lacks the same genes as LPU83 Δchromo Δplasmid. Nodules induced by *Eme*2011 exhibited the typical cylindrical shape of alfalfa nodules with pink coloration. In contrast, *Eme*2011 Δ*exo* showed small white round nodules (**Figure 5**). Some of the nodules induced by wild-type LPU83 showed the typical cylindrical shape, however they were mostly white instead of pink. Similar to the nodules observed for the *Eme*2011 *exoB*

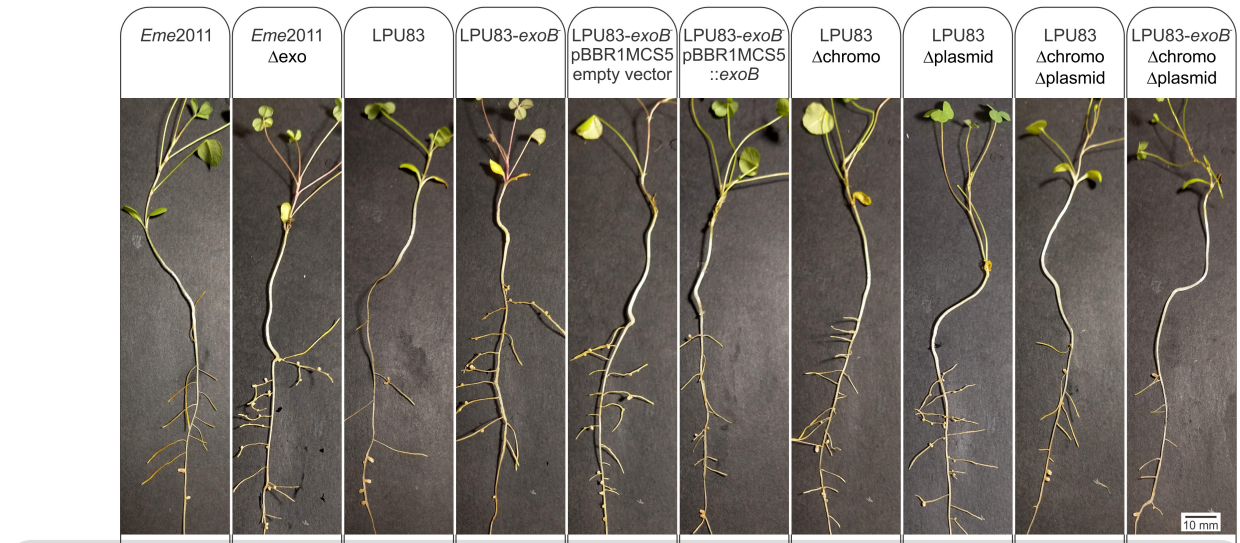

	*Eme*2011	*Eme*2011 Δexo	LPU83	LPU83-*exoB*	LPU83-*exoB* pBBR1MCS5 empty vector	LPU83-*exoB* pBBR1MCS5 ::*exoB*	LPU83 Δchromo	LPU83 Δplasmid	LPU83 Δchromo Δplasmid	LPU83-*exoB* Δchromo Δplasmid
Fresh nodule weight ± SD (mg / nodule)	1.21 ± 0.12^{a}	0.86 ± 0.01^{bcde}	0.98 ± 0.23^{abc}	0.58 ± 0.17^{e}	0.65 ± 0.17^{de}	0.77 ± 0.06^{cde}	0.87 ± 0.09^{bcd}	1.05 ± 0.13^{abc}	1.12 ± 0.07^{ab}	0.95 ± 0.01^{abc}
Number of Nodules per plant ± SD	2.86 ± 0.94^{a}	6.59 ± 3.74^{bcd}	5.49 ± 3.63^{abc}	10.32 ± 6.17^{d}	7.95 ± 4.77^{cd}	4.86 ± 3.07^{abc}	6.60 ± 6.14^{bc}	7.22 ± 4.16^{cd}	7.42 ± 4.01^{cd}	3.68 ± 3.21^{ab}
CFU ($x10^{5}$) per nodule ± SD	7.22 ± 0.56^{bcd}	not detected	18.54 ± 3.16^{a}	6.45 ± 0.50^{cd}	1.76 ± 1.54^{e}	4.17 ± 2.05^{de}	6.34 ± 2.54^{cde}	11.08 ± 0.60^{bc}	9.45 ± 0.59^{b}	10.57 ± 3.34^{bc}
Dry weight per plant ± SD (mg)	7.35 ± 0.94^{a}	3.27 ± 1.25^{b}	3.37 ± 0.98^{b}	3.54 ± 0.70^{b}	3.82 ± 1.38^{b}	3.95 ± 1.68^{b}	3.33 ± 0.92^{b}	3.95 ± 0.76^{b}	4.12 ± 1.23^{b}	3.13 ± 1.17^{b}

FIGURE 5 | Analysis of the nodulation of LPU83 EPS I mutant strains. *M. sativa* plants infected by the indicated strains were harvested at 4 weeks post-inoculation. In the top panel, a representative plant was photographed. In second panel, zoom on the nodules of each plant was made. The number of nodules per plant were counted and weighted. Nodules were surfaced-sterilized, then crushed in sterile isotonic solution followed by plating on TY with the corresponding antibiotics and after 2 days CFU were counted. The shoot dry weight per plant was measured. Non-inoculated roots did not show nodules and the dry weight per plant was 3.98 ± 0.78^{b}. Results were statistically analyzed by the ANOVA and least significant difference tests (Box et al., 1978). Values followed by different letters differed significantly with $p < 0.05$.

mutant (Schäper et al., 2019), the nodules induced by LPU83-*exoB*$^{-}$ and by LPU83-*exoB*$^{-}$ (pBBR1MCS5 empty vector) were tiny and round, while the complemented mutant, LPU83-*exoB*$^{-}$ (pBBR1MCS5-*exoB*), showed bigger nodules than LPU83-*exoB*$^{-}$. The nodules induced by LPU83 Δplasmid were mainly round, but some of them were cylindrical. In contrast, the ones induced by LPU83 Δchromo were mainly cylindrical, but some were round. Unexpectedly, most of the nodules induced by the double and triple mutant were cylindrical. Nodules from all the derivatives of LPU83 were mostly white (**Figure 5**).

In the double and triple mutants, many nodules appeared with brown necrotic areas, while in the wild-type LPU83, these brown necrotic areas were observed in only a few nodules. These brown necrotic areas have been previously reported and related to plant defense symptoms, in nodules induced by EPS-deficient rhizobial mutants (Niehaus et al., 1993; Parniske et al., 1994; Fraysse et al., 2003; Berrabah et al., 2015). This led to the assumption that rhizobial EPS could act as suppressor of the plant defense response (Niehaus and Becker, 1998; Jones and Walker, 2008; Jones et al., 2008). This could cause the presence of the brown necrotic areas in nodules developed by LPU83 mutants, but it cannot explain their presence in the wild-type LPU83. One possibility is that the wild-type LPU83 triggers, at low levels, a plant defense mechanism. Studies with transcriptional fusions demonstrated that *exo* genes of *Eme*1021 were highly expressed in free-living cells but their expression decreased in later stages of symbiosis (Reuber et al., 1991). These observations were confirmed with recent high-throughput transcriptome studies (Capela et al., 2006; Roux et al., 2014). The expression of these genes might be fine-tuned by nodule signals, to allow a proper modulation of the plant defense. It cannot be disregarded that, despite the identical structure of EPS I of *Eme*2011 and LPU83, the spatial and temporal expression pattern of the *exo* genes could differ, causing a different response of the plant inside the nodules induced by LPU83.

Fresh nodules were counted, weighted and the number of CFU per nodule was evaluated (**Figure 5**). As expected, the comparison between *Eme*2011 and *Eme*2011 Δ*exo* showed statistical significant differences in fresh nodule numbers and weight. Among the LPU83 derivatives, wild-type LPU83, double and triple mutants and LPU83 Δplasmid showed similar fresh weight, while the LPU83-*exoB*$^{-}$ showed lower fresh weight. LPU83-*exoB*$^{-}$ and LPU83-*exoB*$^{-}$ (pBBR1MCS5 empty vector) showed the highest numbers of nodules per plant, but harbored less bacteria inside. The complemented mutant, LPU83-*exoB*$^{-}$ (pBBR1MCS5-*exoB*), generates similar numbers of nodules as LPU83, but less than the LPU83-*exoB*$^{-}$ mutant. No CFU were detected in *Eme*2011 Δ*exo* nodules, indicating the lack of a proper infection. The absence of bacteria in mutants in EPS I production of *Eme*2011 was previously shown (Cheng and Walker, 1998; Niehaus and Becker, 1998). Nodules occupied by LPU83 showed the highest number of CFU per nodule. Unexpectedly, bacteria could be recovered from the nodules induced by all LPU83 mutants. LPU83 Δplasmid and the double and triple mutants showed CFU per nodule values similar to those of *Eme*2011. The estimation of nitrogen-fixing ability was evaluated by comparisons of the shoot-dry weights. As expected, *Eme*2011 showed nitrogen fixation, while *Eme*2011 Δ*exo* did not. LPU83 and its mutants showed a poor nitrogen fixation and the constructed mutations did not change the behavior of the wild-type strain (**Figure 5**).

As the recovery of bacteria from the nodules induced by all LPU83 mutants was unexpected, nodule histology was evaluated by confocal microscopy. Nodules were cut and

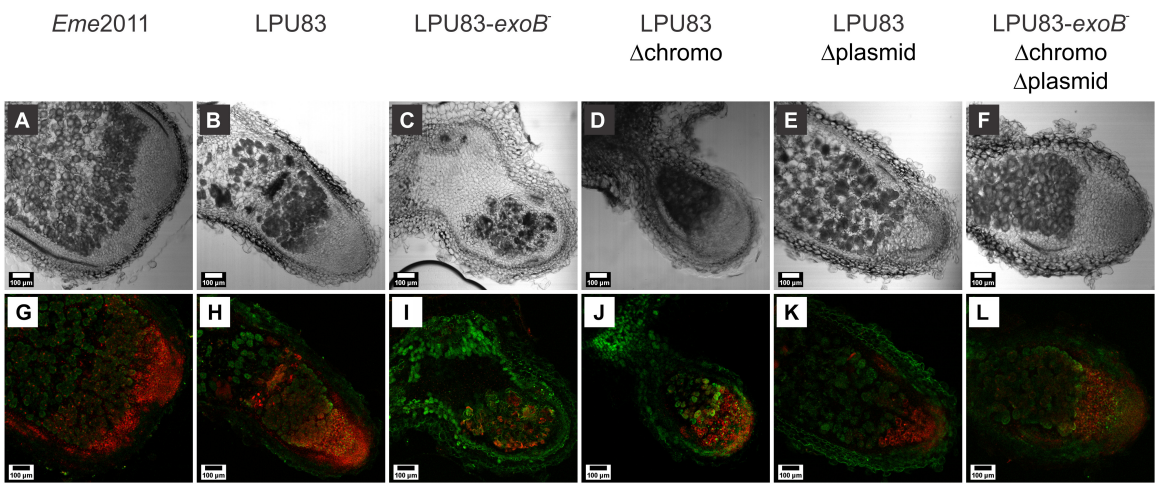

FIGURE 6 | Morphology and occupancy of *M. sativa* nodules generated by EPS-I mutants of LPU83. Plants infected by *E. meliloti* 2011 and the indicated EPS I mutant strains of *R. favelukesii* LPU83 were harvested at 4 weeks post-inoculation. Nodule sections of 60 μm were obtained by means of a vibratome, and then stained with Syto 9 (green fluorescence that indicates living cells) and Propidium Iodide (red fluorescence that indicates cells with a damage in the membrane, i.e., dead). Light **(A–F)** and fluorescence **(G–L)** micrographs of full nodule slices were acquired with a confocal microscope. The photographs are representative of nodules of different plants experiments.

stained with Live-Dead BacLight. As a control, *Eme*2011 showed the typical tissue organization, where zones delimitation and living bacteria stained by SYTO9 were clearly visible (green fluorescence) and distributed in the nodule after the meristem (zone I) (**Figures 6A,G**). Nodules infected with LPU83 showed a similar pattern, but red-stained bacteria (indicative of dead bacteria) were observed. Moreover, less plant cells seem to be occupied by LPU83 than by *Eme*2011 (**Figures 6B,H**). The triple mutant, LPU83 Δplasmid and LPU83 Δchromo showed a similar pattern to the one observed in LPU83, but more cells seem to be alive. Also, more plant cells appear to be occupied by the mentioned mutants (**Figures 6D–F,J–L**). The LPU83-*exoB*$^{-}$ strain showed smaller nodules, with an unclear definition of the zones and a large portion of the nodule was empty. Nevertheless, bacteria were observed inside these nodules but many of them were red-stained bacteria (**Figures 6C,I**). The size and shape of the nodules, the CFU per nodule obtained and the observed histology in nodules from LPU83-*exoB*$^{-}$, show that the alteration in *exoB* severely impairs the nodulation of LPU83 but, contrary to *E. meliloti exoB* mutant (Schäper et al., 2019), LPU83-*exoB*$^{-}$ is still able to infect. Remarkably, LPU83-*exoB*$^{-}$ Δchromo Δplasmid, which lacks all *exo* genes, presents number of nodules, size, occupation and histology more similar to LPU83 than to the mutant LPU83-*exoB*$^{-}$.

Overall, our results indicate that *R. favelukesii* LPU83 shows a lack of differentiation inside the nodules, which could explain the low nitrogen fixing rate. During the last years, nodule-specific cysteine-rich (NCRs) peptides have been intensively studied due to their role in the differentiation of the rhizobia inside the nodules (Van de Velde et al., 2010). Despite that NCRs show toxicity for the rhizobia *in vitro*, they are needed for the proper differentiation of the bacteria into bacteroids (Kondorosi et al., 2013; Pan and Wang, 2017). Furthermore, the membrane, the EPS and the LPS have been suggested as key components in the resistance to the NCRs (Montiel et al., 2017; Lima et al., 2020). It could be hypothesized that some other difference in the LPU83 cell envelope does not allow a correct perception of NCRs or that the expression of NCRs differs between the infection of *E. meliloti* and LPU83, resulting in non-proper symbiotic nodules in the case of infection by LPU83.

CONCLUDING REMARKS

Legumes are of growing importance to reduce the global carbon dioxide footprint, since they do not need nitrogen fertilizers. The symbiosis between bacteria and leguminous plants has been therefore widely studied due its agronomical importance and also for providing the opportunity to understand the biochemical process involved in the communication between both partners (Jones et al., 2007). This communication includes several determinants from both organisms. One of them, the EPS, has been demonstrated as a key feature in different bacteria, with a role in recognition and signaling (Fraysse et al., 2003; Kawaharada et al., 2015). *E. meliloti* (especially the isogenic strains *Eme*1021 and *Eme* 2011) is considered as the model bacterium to study the symbiotic interaction between rhizobia and alfalfa. Nevertheless, *R. favelukesii* is a species that is also able to infect alfalfa, but its symbiosis is deficient. This failure seems to be related with the differentiation of the bacteria inside the nodules. Many determinants are involved in the differentiation, not only expressed in the late stages, but also during an early recognition. The synthesis of different EPS involves many genes, and their production could change according to different environmental conditions. The results presented here show that *R. favelukesii* produces an identical EPS I to the one produced by *E. meliloti*, whose synthesis is directed by genes located within a chromosomal cluster and a plasmid cluster. Both clusters have a different evolutionary origin and both of them are essential for the EPS I synthesis.

Remarkably, *R. favelukesii* does not need EPS I production to infect alfalfa. We observed that the mutants defective in EPS synthesis are able to generate nodules, with high titers of bacteria recovered from them. Noteworthy, a mutation affecting only *exoB* seems to be more severe than the lack of the whole *exo* genes. This could suggest that a punctual change in EPS I composition, as the lack of galactose, may be more harmful than the complete lack of it. In terms of specific determinants for the infection of alfalfa, *R. favelukesii* is a special species that differs from *E. meliloti*, since it is able to infect alfalfa, but with NFs that are somewhat different and with no EPS. Indeed, discerning the mechanism and determinants employed by *R. favelukesii* will lead us to a better understanding of the molecular pathway for a proper symbiosis and probably to alternative pathways or molecules for invasion that have yet to be described.

DATA AVAILABILITY STATEMENT

The original contributions presented in the study are included in the article/**Supplementary Material**, further inquiries can be directed to the corresponding author/s.

AUTHOR CONTRIBUTIONS

LC, ALu, JN, JPG, CW, MP, KN, and GTT did the experiments. AS, AP, ALa, SB, MP, KN, and GTT performed the data analysis and interpretation. LC, ALu, JN, and GTT wrote the manuscript. JPG, AS, AP, ALa, SB, MP, KN, and GTT manage the project and the fundings. All authors contributed to the discussion, provided comments on the manuscript, revised the manuscript, and have given approval to the final version of the manuscript.

FUNDING

This work was partially supported by grants PICT2016-0210 to GTT, PICT2017-2833 to MP, and PICT2016-0604 to JPG. LC, ALu, and JN are fellows of CONICET. JPG, ALa, MP, and GTT are members of the Research Career of CONICET.

GTT has received a fellowship from the Alexander von Humboldt Foundation.

ACKNOWLEDGMENTS

The authors are grateful to Claudio Mazo, Paula Giménez, and Silvana Tongiani (members of CPA CONICET at IBBM). We acknowledge the financial support of the German Research Foundation (DFG) and the Open Access Publication Fund of Bielefeld University for the article processing charge.

SUPPLEMENTARY MATERIAL

The Supplementary Material for this article can be found online at: https://www.frontiersin.org/articles/10.3389/fpls.2021.642576/full#supplementary-material

REFERENCES

Abascal, F., Zardoya, R., and Posada, D. (2005). ProtTest: selection of best-fit models of protein evolution. *Bioinformatics* 21, 2104–2105. doi: 10.1093/bioinformatics/bti263

Bañuelos-Vazquez, L. A., Cazares, D., Rodríguez, S., Cervantes-De, La Luz, L., Sánchez-López, R., et al. (2020). Transfer of the symbiotic plasmid of *Rhizobium etli* CFN42 to endophytic bacteria inside nodules. *Front. Microbiol.* 11:1752. doi: 10.3389/fmicb.2020.01752

Barsch, A., Tellstrom, V., Patschkowski, T., Kuster, H., and Niehaus, K. (2006). Metabolite profiles of nodulated alfalfa plants indicate that distinct stages of nodule organogenesis are accompanied by global physiological adaptations. *Mol. Plant Microbe Interact.* 19, 998–1013. doi: 10.1094/MPMI-19-0998

Batista, J. S., Hungria, M., Barcellos, F. G., Ferreira, M. C., and Mendes, I. C. (2007). Variability in *Bradyrhizobium japonicum* and *B. elkanii* seven years after introduction of both the exotic microsymbiont and the soybean host in a cerrados soil. *Microb. Ecol.* 53, 270–284. doi: 10.1007/s00248-006-9149-2

Becker, A., Kleickmann, A., Kuster, H., Keller, M., Arnold, W., and Puhler, A. (1993). Analysis of the *Rhizobium meliloti* genes *exoU*, *exoV*, *exoW*, *exoT*, and *exoI* involved in exopolysaccharide biosynthesis and nodule invasion: *exoU* and *exoW* probably encode glucosyltransferases. *Mol. Plant Microbe Interact.* 6, 735–744. doi: 10.1094/mpmi-6-735

Becker, A., and Pühler, A. (1998). "Production of exopolysaccharides," in *The Rhizobiaceae: Molecular Biology of Model Plant-Associated Bacteria*, eds H. P. Spaink, A. Kondorosi, and P. J. J. Hooykaas (Dordrecht: Springer), 97–118.

Becker, A., Ruberg, S., Baumgarth, B., Bertram-Drogatz, P. A., Quester, I., and Puhler, A. (2002). Regulation of succinoglycan and galactoglucan biosynthesis in *Sinorhizobium meliloti*. *J. Mol. Microbiol. Biotechnol.* 4, 187–190.

Beringer, J. E. (1974). R factor transfer in *Rhizobium leguminosarum*. *J. Gen. Microbiol.* 84, 188–198. doi: 10.1099/00221287-84-1-188

Berrabah, F., Ratet, P., and Gourion, B. (2015). Multiple steps control immunity during the intracellular accommodation of rhizobia. *J. Exp. Bot.* 66, 1977–1985. doi: 10.1093/jxb/eru545

Box, G., Hunter, W., and Hunter, J. (1978). *Statistics for Experimenters*. New York, NY: Wiley.

Bradford, M. M. (1976). A rapid and sensitive method for the quantitation of microgram quantities of protein utilizing the principle of protein-dye binding. *Anal. Biochem.* 72, 248–254. doi: 10.1006/abio.1976.9999

Breedveld, M. W., and Miller, K. J. (1994). Cyclic beta-glucans of members of the family *Rhizobiaceae*. *Microbiol. Rev.* 58, 145–161.

Buendia, A. M., Enenkel, B., Koplin, R., Niehaus, K., Arnold, W., and Puhler, A. (1991). The *Rhizobium meliloti exoZl exoB* fragment of megaplasmid 2: ExoB functions as a UDP-glucose 4-epimerase and ExoZ shows homology to NodX of *Rhizobium leguminosarum* biovar *viciae* strain TOM. *Mol. Microbiol.* 5, 1519–1530. doi: 10.1111/j.1365-2958.1991.tb00799.x

Capela, D., Filipe, C., Bobik, C., Batut, J., and Bruand, C. (2006). *Sinorhizobium meliloti* differentiation during symbiosis with alfalfa: a transcriptomic dissection. *Mol. Plant Microbe Interact.* 19, 363–372. doi: 10.1094/MPMI-19-0363

Castellani, L. G., Nilsson, J. F., Wibberg, D., Schluter, A., Puhler, A., Brom, S., et al. (2019). Insight into the structure, function and conjugative transfer of pLPU83a, an accessory plasmid of *Rhizobium favelukesii* LPU83. *Plasmid* 103, 9–16. doi: 10.1016/j.plasmid.2019.03.004

Cheng, H. P., and Walker, G. C. (1998). Succinoglycan is required for initiation and elongation of infection threads during nodulation of alfalfa by *Rhizobium meliloti*. *J. Bacteriol.* 180, 5183–5191. doi: 10.1128/JB.180.19.5183-5191.1998

Del Papa, M. F., Balagué, L. J., Sowinski, S. C., Wegener, C., Segundo, E., Abarca, F. M., et al. (1999). Isolation and characterization of alfalfa-nodulating rhizobia present in acidic soils of central argentina and uruguay. *Appl. Environ. Microbiol.* 65, 1420–1427. doi: 10.1128/AEM.65.4.1420-1427.1999

Del Papa, M. F., Pistorio, M., Draghi, W. O., Lozano, M. J., Giusti, M. A., Medina, C., et al. (2007). Identification and characterization of a *nodH* ortholog from the alfalfa-nodulating Or191-like rhizobia. *Mol. Plant Microbe Interact.* 20, 138–145. doi: 10.1094/MPMI-20-2-0138

Dickstein, R., Bisseling, T., Reinhold, V. N., and Ausubel, F. M. (1988). Expression of nodule-specific genes in alfalfa root nodules blocked at an early stage of development. *Genes Dev.* 2, 677–687. doi: 10.1101/gad.2.6.677

Diebold, R., and Noel, K. D. (1989). Rhizobium leguminosarum exopolysaccharide mutants: biochemical and genetic analyses and symbiotic behavior on three hosts. *J. Bacteriol.* 171, 4821–4830. doi: 10.1128/jb.171.9.4821-4830.1989

Dylan, T., Ielpi, L., Stanfield, S., Kashyap, L., Douglas, C., Yanofsky, M., et al. (1986). Rhizobium meliloti genes required for nodule development are related to chromosomal virulence genes in *Agrobacterium tumefaciens*. *Proc. Natl. Acad. Sci. U.S.A.* 83, 4403–4407. doi: 10.1073/pnas.83.12.4403

Eardly, B. D., Hannaway, D. B., and Bottomley, P. J. (1985). Characterization of rhizobia from ineffective alfalfa nodules: ability to nodulate bean plants [*Phaseolus vulgaris* (L.) Savi.]. *Appl. Environ. Microbiol.* 50, 1422–1427. doi: 10.1128/AEM.50.6.1422-1427.1985

Eckhardt, T. (1978). A rapid method for the identification of plasmid desoxyribonucleic acid in bacteria. *Plasmid* 1, 584–588. doi: 10.1016/0147-619x(78)90016-1

Fraysse, N., Couderc, F., and Poinsot, V. (2003). Surface polysaccharide involvement in establishing the rhizobium-legume symbiosis. *Eur. J. Biochem.* 270, 1365–1380. doi: 10.1046/j.1432-1033.2003.03492.x

Fraysse, N., Lindner, B., Kaczynski, Z., Sharypova, L., Holst, O., Niehaus, K., et al. (2005). *Sinorhizobium meliloti* strain 1021 produces a low-molecular-mass capsular polysaccharide that is a homopolymer of 3-deoxy-D-manno-oct-2-ulosonic acid harboring a phospholipid anchor. *Glycobiology* 15, 101–108. doi: 10.1093/glycob/cwh142

Glazebrook, J., and Walker, G. C. (1989). A novel exopolysaccharide can function in place of the calcofluor-binding exopolysaccharide in nodulation of alfalfa by *Rhizobium meliloti*. *Cell* 56, 661–672.

Glucksmann, M. A., Reuber, T. L., and Walker, G. C. (1993). Genes needed for the modification, polymerization, export, and processing of succinoglycan by *Rhizobium meliloti*: a model for succinoglycan biosynthesis. *J. Bacteriol.* 175, 7045–7055. doi: 10.1128/jb.175.21.7045-7055.1993

Guindon, S., and Gascuel, O. (2003). A simple, fast, and accurate algorithm to estimate large phylogenies by maximum likelihood. *Syst. Biol.* 52, 696–704. doi: 10.1080/10635150390235520

Hidalgo, A., Margaret, I., Crespo-Rivas, J. C., Parada, M., Murdoch Pdel, S., Lopez, A., et al. (2010). The *rkpU* gene of *Sinorhizobium fredii* HH103 is required for bacterial K-antigen polysaccharide production and for efficient nodulation with soybean but not with cowpea. *Microbiology* 156, 3398–3411. doi: 10.1099/mic.0.042499-0

Hotter, G. S., and Scott, D. B. (1991). Exopolysaccharide mutants of *Rhizobium loti* are fully effective on a determinate nodulating host but are ineffective on an

indeterminate nodulating host. *J. Bacteriol.* 173, 851–859. doi: 10.1128/jb.173.2.851-859.1991

Hozbor, D. F., Pich Otero, A. J., Lodeiro, A. R., Del Papa, M. F., Pistorio, M., and Lagares, A. (2004). The symbiotic defect in a *Sinorhizobium meliloti* lipopolysaccharide mutant can be overcome by expression of other surface polysaccharides. *Res. Microbiol.* 155, 855–860. doi: 10.1016/j.resmic.2004.06.012

Hynes, M. F., and McGregor, N. F. (1990). Two plasmids other than the nodulation plasmid are necessary for formation of nitrogen-fixing nodules by *Rhizobium leguminosarum*. *Mol. Microbiol.* 4, 567–574. doi: 10.1111/j.1365-2958.1990.tb00625.x

Jones, K. M. (2012). Increased production of the exopolysaccharide succinoglycan enhances *Sinorhizobium meliloti* 1021 symbiosis with the host plant *Medicago truncatula*. *J. Bacteriol.* 194, 4322–4331. doi: 10.1128/JB.00751-12

Jones, K. M., Kobayashi, H., Davies, B. W., Taga, M. E., and Walker, G. C. (2007). How rhizobial symbionts invade plants: the *Sinorhizobium-Medicago* model. *Nat. Rev. Microbiol.* 5, 619–633. doi: 10.1038/nrmicro1705

Jones, K. M., Sharopova, N., Lohar, D. P., Zhang, J. Q., Vandenbosch, K. A., and Walker, G. C. (2008). Differential response of the plant *Medicago truncatula* to its symbiont *Sinorhizobium meliloti* or an exopolysaccharide-deficient mutant. *Proc. Natl. Acad. Sci. U.S.A.* 105, 704–709. doi: 10.1073/pnas.0709338105

Jones, K. M., and Walker, G. C. (2008). Responses of the model legume *Medicago truncatula* to the rhizobial exopolysaccharide succinoglycan. *Plant Signal Behav.* 3, 888–890. doi: 10.4161/psb.3.10.6512

Kawaharada, Y., Kelly, S., Nielsen, M. W., Hjuler, C. T., Gysel, K., Muszynski, A., et al. (2015). Receptor-mediated exopolysaccharide perception controls bacterial infection. *Nature* 523, 308–312. doi: 10.1038/nature14611

Keller, M., Roxlau, A., Weng, W. M., Schmidt, M., Quandt, J., Niehaus, K., et al. (1995). Molecular analysis of the *Rhizobium meliloti mucR* gene regulating the biosynthesis of the exopolysaccharides succinoglycan and galactoglucan. *Mol. Plant Microbe Interact.* 8, 267–277. doi: 10.1094/mpmi-8-0267

Kereszt, A., Kiss, E., Reuhs, B. L., Carlson, R. W., Kondorosi, A., and Putnoky, P. (1998). Novel *rkp* gene clusters of *Sinorhizobium meliloti* involved in capsular polysaccharide production and invasion of the symbiotic nodule: the *rkpK* gene encodes a UDP-glucose dehydrogenase. *J. Bacterio.l* 180, 5426–5431. doi: 10.1128/JB.180.20.5426-5431.1998

Kiss, E., Kereszt, A., Barta, F., Stephens, S., Reuhs, B. L., Kondorosi, A., et al. (2001). The *rkp-3* gene region of *Sinorhizobium meliloti* Rm41 contains strain-specific genes that determine K antigen structure. *Mol. Plant Microbe Interact.* 14, 1395–1403. doi: 10.1094/MPMI.2001.14.12.1395

Kiss, E., Reuhs, B. L., Kim, J. S., Kereszt, A., Petrovics, G., Putnoky, P., et al. (1997). The *rkpGHI* and *-J* genes are involved in capsular polysaccharide production by *Rhizobium meliloti*. *J. Bacteriol.* 179, 2132–2140. doi: 10.1128/jb.179.7.2132-2140.1997

Kondorosi, E., Mergaert, P., and Kereszt, A. (2013). A paradigm for endosymbiotic life: cell differentiation of *Rhizobium* bacteria provoked by host plant factors. *Annu. Rev. Microbiol.* 67, 611–628. doi: 10.1146/annurev-micro-092412-155630

Kumar, S., Stecher, G., Li, M., Knyaz, C., and Tamura, K. (2018). MEGA X: molecular evolutionary genetics analysis across computing platforms. *Mol. Biol. Evol.* 35, 1547–1549. doi: 10.1093/molbev/msy096

Leigh, J. A., Reed, J. W., Hanks, J. F., Hirsch, A. M., and Walker, G. C. (1987). *Rhizobium meliloti* mutants that fail to succinylate their calcofluor-binding exopolysaccharide are defective in nodule invasion. *Cell* 51, 579–587. doi: 10.1016/0092-8674(87)90127-9

Leigh, J. A., Signer, E. R., and Walker, G. C. (1985). Exopolysaccharide-deficient mutants of *Rhizobium meliloti* that form ineffective nodules. *Proc. Natl. Acad. Sci. U.S.A.* 82, 6231–6235. doi: 10.1073/pnas.82.18.6231

Li, X., and Brummer, E. C. (2012). Applied genetics and genomics in alfalfa breeding. *Agronomy* 2, 40–61. doi: 10.3390/agronomy2010040

Li, X., Wei, Y., Moore, K. J., Michaud, R., Viands, D. R., Hansen, J. L., et al. (2011). Association mapping of biomass yield and stem composition in a tetraploid alfalfa breeding population. *Plant Genome* 4, 24–35. doi: 10.3835/plantgenome2010.09.0022

Lima, R. M., Kylarova, S., Mergaert, P., and Kondorosi, E. (2020). Unexplored arsenals of legume peptides with potential for their applications in medicine and agriculture. *Front. Microbiol.* 11:1307. doi: 10.3389/fmicb.2020.01307

Loewus, F. A. (1952). Improvement in anthrone method for determination of carbohydrates. *Anal. Chem.* 24, 219–219. doi: 10.1021/ac60061a050

Marczak, M., Mazur, A., Koper, P., Zebracki, K., and Skorupska, A. (2017). Synthesis of rhizobial exopolysaccharides and their importance for symbiosis with legume plants. *Genes* 8, 360. doi: 10.3390/genes8120360

Mendis, H. C., Madzima, T. F., Queiroux, C., and Jones, K. M. (2016). Function of succinoglycan polysaccharide in *Sinorhizobium meliloti* host plant invasion depends on succinylation, not molecular weight. *mBio* 7:e00606-16. doi: 10.1128/mBio.00606-16

Miller, J. H. (1972). *Experiments in Molecular Genetics*. Cold Spring Harbor, NY: Cold Spring Harbor Laboratory.

Montiel, J., Downie, J. A., Farkas, A., Bihari, P., Herczeg, R., Bálint, B., et al. (2017). Morphotype of bacteroids in different legumes correlates with the number and type of symbiotic NCR peptides. *Proc. Natl. Acad. Sci. U.S.A.* 114, 5041–5046. doi: 10.1073/pnas.1704217114

Montiel, J., Szucs, A., Boboescu, I. Z., Gherman, V. D., Kondorosi, E., and Kereszt, A. (2016). Terminal bacteroid differentiation is associated with variable morphological changes in legume species belonging to the inverted repeat-lacking clade. *Mol. Plant Microbe Interact.* 29, 210–219. doi: 10.1094/MPMI-09-15-0213-R

Mueller, K., and Gonzalez, J. E. (2011). Complex regulation of symbiotic functions is coordinated by MucR and quorum sensing in *Sinorhizobium meliloti*. *J. Bacteriol.* 193, 485–496. doi: 10.1128/JB.01129-10

Müller, P., Hynes, M., Kapp, D., Niehaus, K., and Pühler, A. (1988). Two classes of *Rhizobium meliloti* infection mutants differ in exopolysaccharide production and in coinoculation properties with nodulation mutants. *Mol. Gen. Genet.* 211, 17–26. doi: 10.1007/bf00338388

Niehaus, K., and Becker, A. (1998). The role of microbial surface polysaccharides in the *Rhizobium*-legume interaction. *Subcell Biochem.* 29, 73–116. doi: 10.1007/978-1-4899-1707-2_3

Niehaus, K., Kapp, D., and Pühler, A. (1993). Plant defence and delayed infection of alfalfa pseudonodules induced by an exopolysaccharide (EPS I)-deficient *Rhizobium meliloti* mutant. *Planta* 190, 415–425. doi: 10.1007/BF00196971

Nilsson, J. F., Castellani, L. G., Draghi, W. O., Mogro, E. G., Wibberg, D., Winkler, A., et al. (2020). Global transcriptome analysis of *Rhizobium favelukesii* LPU83 in response to acid stress. *FEMS Microbiol. Ecol.* 97:fiaa235. doi: 10.1093/femsec/fiaa235

Oldroyd, G. E. (2013). Speak, friend, and enter: signalling systems that promote beneficial symbiotic associations in plants. *Nat. Rev. Microbiol.* 11, 252–263. doi: 10.1038/nrmicro2990

Oldroyd, G. E., Murray, J. D., Poole, P. S., and Downie, J. A. (2011). The rules of engagement in the legume-rhizobial symbiosis. *Annu. Rev. Genet.* 45, 119–144. doi: 10.1146/annurev-genet-110410-132549

Pan, H., and Wang, D. (2017). Nodule cysteine-rich peptides maintain a working balance during nitrogen-fixing symbiosis. *Nat. Plants* 3:17048. doi: 10.1038/nplants.2017.48

Parada, M., Vinardell, J. M., Ollero, F. J., Hidalgo, A., Gutierrez, R., Buendia-Claveria, A. M., et al. (2006). Sinorhizobium fredii HH103 mutants affected in capsular polysaccharide (KPS) are impaired for nodulation with soybean and *Cajanus cajan*. *Mol. Plant Microbe Interact.* 19, 43–52. doi: 10.1094/MPMI-19-0043

Parniske, M., Schmidt, P. E., Kosch, K., and Muller, P. (1994). Plant defense responses of host plants with determinate nodules induced by EPS-defective exoB mutants of *Bradyrhizobium japonicum*. *Mol. Plant Microbe Interact.* 7, 631–638. doi: 10.1094/MPMI-7-0631

Peck, M. C., Fisher, R. F., and Long, S. R. (2006). Diverse flavonoids stimulate NodD1 binding to nod gene promoters in *Sinorhizobium meliloti*. *J. Bacteriol.* 188, 5417–5427. doi: 10.1128/JB.00376-06

Pellock, B. J., Cheng, H. P., and Walker, G. C. (2000). Alfalfa root nodule invasion efficiency is dependent on *Sinorhizobium meliloti* polysaccharides. *J. Bacteriol.* 182, 4310–4318. doi: 10.1128/jb.182.15.4310-4318.2000

Pellock, B. J., Teplitski, M., Boinay, R. P., Bauer, W. D., and Walker, G. C. (2002). A LuxR homolog controls production of symbiotically active extracellular polysaccharide II by *Sinorhizobium meliloti*. *J. Bacteriol.* 184, 5067–5076. doi: 10.1128/jb.184.18.5067-5076.2002

Pérez-Mendoza, D., Rodriguez-Carvajal, M. A., Romero-Jimenez, L., Farias Gde, A., Lloret, J., Gallegos, M. T., et al. (2015). Novel mixed-linkage beta-glucan activated by c-di-GMP in *Sinorhizobium meliloti*. *Proc. Natl. Acad. Sci. U.S.A.* 112, E757–E765. doi: 10.1073/pnas.1421748112

Peters, N. K., Frost, J. W., and Long, S. R. (1986). A plant flavone, luteolin, induces expression of *Rhizobium meliloti* nodulation genes. *Science* 233, 977–980. doi: 10.1126/science.3738520

Peters, N. K., and Long, S. R. (1988). Alfalfa root exudates and compounds which promote or inhibit induction of *Rhizobium meliloti* nodulation genes. *Plant Physiol.* 88, 396–400. doi: 10.1104/pp.88.2.396

Petrovics, G., Putnoky, P., Reuhs, B., Kim, J., Thorp, T. A., Noel, K. D., et al. (1993). The presence of a novel type of surface polysaccharide in *Rhizobium meliloti* requires a new fatty acid synthase-like gene cluster involved in symbiotic nodule development. *Mol. Microbiol.* 8, 1083–1094. doi: 10.1111/j.1365-2958.1993.tb01653.x

Putnoky, P., Grosskopf, E., Ha, D. T., Kiss, G. B., and Kondorosi, A. (1988). *Rhizobium fix* genes mediate at least two communication steps in symbiotic nodule development. *J. Cell Biol.* 106, 597–607. doi: 10.1083/jcb.106.3.597

Putnoky, P., Petrovics, G., Kereszt, A., Grosskopf, E., Ha, D. T., Banfalvi, Z., et al. (1990). *Rhizobium meliloti* lipopolysaccharide and exopolysaccharide can have the same function in the plant-bacterium interaction. *J. Bacteriol.* 172, 5450–5458. doi: 10.1128/jb.172.9.5450-5458.1990

Reuber, T. L., Long, S., and Walker, G. C. (1991). Regulation of *Rhizobium meliloti* exo genes in free-living cells and in planta examined by using TnphoA fusions. *J. Bacteriol.* 173, 426–434. doi: 10.1128/jb.173.2.426-434.1991

Reuber, T. L., and Walker, G. C. (1993). Biosynthesis of succinoglycan, a symbiotically important exopolysaccharide of *Rhizobium meliloti*. *Cell* 74, 269–280. doi: 10.1016/0092-8674(93)90418-p

Reuhs, B. L., Carlson, R. W., and Kim, J. S. (1993). *Rhizobium fredii* and *Rhizobium meliloti* produce 3-deoxy-D-manno-2-octulosonic acid-containing polysaccharides that are structurally analogous to group II K antigens (capsular polysaccharides) found in *Escherichia coli*. J. Bacteriol. 175, 3570–3580. doi: 10.1128/jb.175.11.3570-3580.1993

Reuhs, B. L., Geller, D. P., Kim, J. S., Fox, J. E., Kolli, V. S., and Pueppke, S. G. (1998). *Sinorhizobium fredii* and *Sinorhizobium meliloti* produce structurally conserved lipopolysaccharides and strain-specific K antigens. *Appl. Environ. Microbiol.* 64, 4930–4938. doi: 10.1128/AEM.64.12.4930-4938.1998

Reuhs, B. L., Williams, M. N., Kim, J. S., Carlson, R. W., and Cote, F. (1995). Suppression of the Fix- phenotype of *Rhizobium meliloti exoB* mutants by *lpsZ* is correlated to a modified expression of the K polysaccharide. *J. Bacteriol.* 177, 4289–4296. doi: 10.1128/jb.177.15.4289-4296.1995

Roche, P., Debellé, F., Maillet, F., Lerouge, P., Faucher, C., Truchet, G., et al. (1991). Molecular basis of symbiotic host specificity in *rhizobium meliloti*: *nodH* and *nodPQ* genes encode the sulfation of lipo-oligosaccharide signals. *Cell* 67, 1131–1143. doi: 10.1016/0092-8674(91)90290-f

Rodriguez-Navarro, D. N., Rodriguez-Carvajal, M. A., Acosta-Jurado, S., Soto, M. J., Margaret, I., Crespo-Rivas, J. C., et al. (2014). Structure and biological roles of *Sinorhizobium fredii* HH103 exopolysaccharide. *PLoS One* 9:e115391. doi: 10.1371/journal.pone.0115391

Rolfe, B. G., Gresshoff, P. M., and Shine, J. (1980). Rapid screening for symbiotic mutants of Rhizobium and white clover. *Plant Sci. Lett.* 19, 277–284. doi: 10.1016/0304-4211(80)90082-6

Rost, B. (1999). Twilight zone of protein sequence alignments. *Protein Eng.* 12, 85–94. doi: 10.1093/protein/12.2.85

Roux, B., Rodde, N., Jardinaud, M. F., Timmers, T., Sauviac, L., Cottret, L., et al. (2014). An integrated analysis of plant and bacterial gene expression in symbiotic root nodules using laser-capture microdissection coupled to RNA sequencing. *Plant J.* 77, 817–837. doi: 10.1111/tpj.12442

Roy, S., Liu, W., Nandety, R. S., Crook, A., Mysore, K. S., Pislariu, C. I., et al. (2020). Celebrating 20 years of genetic discoveries in legume nodulation and symbiotic nitrogen fixation. *Plant Cell* 32, 15–41. doi: 10.1105/tpc.19.00279

Sambrook, J., Fritsch, E. F., and Maniatis, T. (1989). *Molecular Cloning: A Laboratory Manual*, 2nd Edn. Cold Spring Harbor, NY: Cold Spring Harbor Laboratory Press.

Schäper, S., Krol, E., Skotnicka, D., Kaever, V., Hilker, R., Søgaard-Andersen, L., et al. (2016). Cyclic Di-GMP regulates multiple cellular functions in the symbiotic alphaproteobacterium *Sinorhizobium meliloti*. *J. Bacteriol.* 198, 521–535. doi: 10.1128/jb.00795-15

Schäper, S., Steinchen, W., Krol, E., Altegoer, F., Skotnicka, D., Søgaard-Andersen, L., et al. (2017). AraC-like transcriptional activator CuxR binds c-di-GMP by a PilZ-like mechanism to regulate extracellular polysaccharide production. *Proc. Natl. Acad. Sci. U.S.A.* 114, E4822–E4831. doi: 10.1073/pnas.1702435114

Schäper, S., Wendt, H., Bamberger, J., Sieber, V., Schmid, J., and Becker, A. (2019). A bifunctional UDP-Sugar 4-Epimerase supports biosynthesis of multiple cell surface polysaccharides in *Sinorhizobium meliloti*. *J. Bacteriol.* 201::e00801-18. doi: 10.1128/JB.00801-18

Schultze, M., Staehelin, C., Röhrig, H., John, M., Schmidt, J., Kondorosi, E., et al. (1995). In vitro sulfotransferase activity of *Rhizobium meliloti* NodH protein: lipochitooligosaccharide nodulation signals are sulfated after synthesis of the core structure. *Proc. Natl. Acad. Sci. U.S.A.* 92, 2706–2709. doi: 10.1073/pnas.92.7.2706

Segundo, E., Martinez-Abarca, F., Dillewijn, P., Fernández-López, M., Lagares, A., Martinez-Drets, G., et al. (1999). Characterisation of symbiotically efficient alfalfa-nodulating rhizobia isolated from acid soils of Argentina and Uruguay. *FEMS Microbiol. Ecol.* 28, 169–176. doi: 10.1111/j.1574-6941.1999.tb00572.x

Simon, R., Priefer, U., and Pühler, A. (1983). A broad host range mobilization system for in vivo genetic engineering: transposon mutagenesis in gram negative bacteria. *Bio/Technology* 1, 784–791. doi: 10.1128/jb.177.1.52-58.1995

Skorupska, A., Janczarek, M., Marczak, M., Mazur, A., and Krol, J. (2006). Rhizobial exopolysaccharides: genetic control and symbiotic functions. *Microb. Cell Fact.* 5:7. doi: 10.1186/1475-2859-5-7

Stanfield, S. W., Ielpi, L., O'brochta, D., Helinski, D. R., and Ditta, G. S. (1988). The ndvA gene product of *Rhizobium meliloti* is required for beta-(1—-2)glucan production and has homology to the ATP-binding export protein HlyB. *J. Bacteriol.* 170, 3523–3530. doi: 10.1128/jb.170.8.3523-3530.1988

Sullivan, J. T., Patrick, H. N., Lowther, W. L., Scott, D. B., and Ronson, C. W. (1995). Nodulating strains of *Rhizobium loti* arise through chromosomal symbiotic gene transfer in the environment. *Proc. Natl. Acad. Sci. U.S.A.* 92, 8985–8989. doi: 10.1073/pnas.92.19.8985

Sullivan, J. T., and Ronson, C. W. (1998). Evolution of rhizobia by acquisition of a 500-kb symbiosis island that integrates into a phe-tRNA gene. *Proc. Natl. Acad. Sci. U.S.A.* 95, 5145–5149. doi: 10.1073/pnas.95.9.5145

Torres Tejerizo, G., Del Papa, M. F., Giusti, M. A., Draghi, W., Lozano, M., Lagares, A., et al. (2010). Characterization of extrachromosomal replicons present in the extended host range *Rhizobium* sp. LPU83. *Plasmid* 64, 177–185. doi: 10.1016/j.plasmid.2010.07.004

Torres Tejerizo, G., Del Papa, M. F., Soria-Diaz, M. E., Draghi, W., Lozano, M., Giusti, M. A., et al. (2011). The nodulation of alfalfa by the acid tolerant *Rhizobium* sp. strain LPU83 does not require sulfated forms of lipo-chitooligosaccharide nodulation signals. *J. Bacteriol.* 193, 30–39. doi: 10.1128/JB.01009-10

Torres Tejerizo, G., Pistorio, M., Althabegoiti, M. J., Cervantes, L., Wibberg, D., Schlüter, A., et al. (2014). Rhizobial plasmid pLPU83a is able to switch between different transfer machineries depending on its genomic background. *FEMS Microbiol. Ecol.* 88, 565–578. doi: 10.1111/1574-6941.12325

Torres Tejerizo, G., Rogel, M. A., Ormeño-Orrillo, E., Althabegoiti, M. J., Nilsson, J. F., Niehaus, K., et al. (2016). *Rhizobium favelukesii* sp. nov., isolated from the root nodules of alfalfa (*Medicago sativa* L). Int. J. Syst. Evol. Microbiol. 66, 4451–4457. doi: 10.1099/ijsem.0.001373

Van de Velde, W., Zehirov, G., Szatmari, A., Debreczeny, M., Ishihara, H., Kevei, Z., et al. (2010). Plant peptides govern terminal differentiation of bacteria in symbiosis. *Science* 327, 1122–1126. doi: 10.1126/science.1184057

Vasse, J., De Billy, F., Camut, S., and Truchet, G. (1990). Correlation between ultrastructural differentiation of bacteroids and nitrogen fixation in alfalfa nodules. *J. Bacteriol.* 172, 4295–4306. doi: 10.1128/jb.172.8.4295-4306.1990

Vincent, J. M. (1970). *A Manual for the Practical Study of the Root-Nodule Bacteria.: IBP Handbook No.* 15. Oxford: Blackwell Scientific.

Wegener, C., Schröder, S., Kapp, D., Pühler, A., Lopez, E. S., Martinez-Abarca, F., et al. (2001). Genetic uniformity and symbiotic properties of acid-tolerant alfalfa-nodulating rhizobia isolated from dispersed locations throughout Argentina. *Symbiosis* 30, 141–162.

Weidner, S., Baumgarth, B., Gottfert, M., Jaenicke, S., Puhler, A., Schneiker-Bekel, S., et al. (2013). Genome Sequence of *Sinorhizobium meliloti* Rm41. *Genome Announc.* 1:e00013-12. doi: 10.1128/genomeA.00013-12

York, G. M., and Walker, G. C. (1998). The succinyl and acetyl modifications of succinoglycan influence susceptibility of succinoglycan to cleavage by the *Rhizobium meliloti* glycanases ExoK and ExsH. *J. Bacteriol.* 180, 4184–4191. doi: 10.1128/JB.180.16.4184-4191.1998

Conflict of Interest: The authors declare that the research was conducted in the absence of any commercial or financial relationships that could be construed as a potential conflict of interest.

frontiers in Plant Science

MINI REVIEW
published: 04 May 2021
doi: 10.3389/fpls.2021.686465

Rhizobial Chemoattractants, the Taste and Preferences of Legume Symbionts

*K. Karl Compton and Birgit E. Scharf**

Department of Biological Sciences, Life Sciences I, Virginia Tech, Blacksburg, VA, United States

The development of host-microbe interactions between legumes and their cognate rhizobia requires localization of the bacteria to productive sites of initiation on the plant roots. This end is achieved by the motility apparatus that propels the bacterium and the chemotaxis system that guides it. Motility and chemotaxis aid rhizobia in their competitiveness for space, resources, and nodulation opportunities. Here, we examine studies on chemotaxis of three major model rhizobia, namely *Sinorhizobium meliloti*, *Rhizobium leguminosarum*, and *Bradyrhizobium japonicum*, cataloging their range of attractant molecules and correlating this in the context of root and seed exudate compositions. Current research areas will be summarized, gaps in knowledge discussed, and future directions described.

Keywords: bacterial survival, flagellar motility, plant-host exudate, plant-microbe signaling, rhizosphere, symbiosis

OPEN ACCESS

Edited by:
Maria Jose Soto,
Consejo Superior de Investigaciones Científicas (CSIC), Spain

Reviewed by:
Gladys Alexandre,
The University of Tennessee, Knoxville, United States
Tino Krell,
Consejo Superior de Investigaciones Científicas (CSIC), Spain

***Correspondence:**
Birgit E. Scharf
bscharf@vt.edu

Specialty section:
This article was submitted to Plant Symbiotic Interactions, a section of the journal Frontiers in Plant Science

Received: *26 March 2021*
Accepted: *12 April 2021*
Published: *04 May 2021*

Citation:
Compton KK and Scharf BE (2021) Rhizobial Chemoattractants, the Taste and Preferences of Legume Symbionts. Front. Plant Sci. 12:686465. doi: 10.3389/fpls.2021.686465

INTRODUCTION

The endosymbiosis between leguminous plants and rhizobia benefits both parties whereby the bacteria, sheltered and supplied nutrients from the plant, fix nitrogen into ammonia for their host. Several rhizobium-legume combinations have stood out as the model systems for this symbiosis, namely *Sinorhizobium* (*Ensifer*) *meliloti* – *Medicago truncatula*, *Bradyrhizobium japonicum* – *Glycine max*, and *Rhizobium leguminosarum*, the latter able to nodulate clovers, pea, common bean, or others depending on the biovar. These organisms have been used to build our knowledge on the genetics, biochemistry, development, and ecology of the many facets of this interaction. The initiation step of the symbiosis occurs at the tips of young root hairs, which curl and pinch in on a population of rhizobia, allowing access inside the plant cells. Prior to this, the rhizobia must localize themselves to the root hairs and outcomplete other bacteria for this niche (Ames et al., 1980; Ames and Bergman, 1981; Pinochet et al., 1993). This is achieved with chemotaxis and motility, the phenomenon by which bacteria move up a gradient of attractant or down a gradient of repellent. Attractant and repellent signals are many and diverse, as bacteria can respond to carbon sources, heavy metals, osmolytes, pH, light, and temperature (Tso and Adler, 1974; Hazelbauer, 1975; Croxen et al., 2006; Jekely, 2009; Paulick et al., 2017; Webb et al., 2017a). The typical mechanism of chemotactic sensing starts with transmembrane sensor proteins called methyl-accepting chemotaxis proteins (MCPs or receptors), which sense multiple and highly different signals such as single molecules, chemical classes, and physical stimuli (Paulick et al., 2017). MCP-ligand binding modulates the autokinase activity of the internal chemotaxis protein CheA. Phosphorylated CheA transfers its phosphoryl group to the response regulator CheY, which interacts with the flagellar motor to affect a change in its

rotation. This two-component system thus controls the movement of the bacterium toward an attractant or away from a repellent by sensing increasing or decreasing ligand binding (Parkinson et al., 2015; Salah Ud-Din and Roujeinikova, 2017).

To study chemotaxis, numerous assays have been used to quantify bacterial behavior, but Adler's capillary assay remains the gold standard (Adler, 1966, 1973). In short, the method involves filling glass capillaries with a putative attractant solution and placing the capillary into a suspension of bacteria. During incubation, the attractant solution forms a gradient which the bacteria follow inside the capillary. The result is typically measured with colony counts of the capillary contents. A reference capillary containing only buffer is included to account for diffusion of cells, acting as an internal negative control. Chemotaxis values are either reported by subtracting reference counts from test counts or as a coefficient with test counts being divided by the reference. Unfortunately, variations in growth conditions, technical procedures, and bacterial strains make comparing studies between lab groups difficult. For example, one study might define a few thousand cells above background as significant, while another might require $>10^5$ cells as a significant response (Aguilar et al., 1988; Barbour et al., 1991; Kape et al., 1991; Meier et al., 2007; Webb et al., 2014).

Here, we review studies that used the capillary assay to derive information about the attractants of *B. japonicum*, *R. leguminosarum*, and *S. meliloti* (**Table 1**). Other methods such as swim plates are available, but do not offer comparable resolution and so will be excluded (Sampedro et al., 2015). A discussion will focus on chemical classes that have been tested for chemotaxis and their prevalence in plant exudates.

ATTRACTANTS CLASSES OF MODEL RHIZOBIA

When comparing results from different behavioral chemotaxis assays, one should bear in mind that attractant profiles of different species and strains will vary. Growth conditions (such as variations in media, temperature, aeration, and growth phase) can cause variances in receptor expression, altering the sensory capability of the bacterium (Lopez-Farfan et al., 2017). In addition, the literature is biased because some compounds have been tested more frequently than others and not to the same extent in different rhizobial species. However, it is naive to expect every source to standardize the array of compounds tested since most studies have a focus on a

TABLE 1 | A catalog of the attractants identified in quantitative chemotaxis assays.

Species	Strain	Attractants found	Weak/not attracants	References
Sinorhizobium meliloti	MVII-1	All amino acids	Sugars	Götz et al. (1982)
	Ve 26	Some amino acids such as aspartate, lysine; gluconate	Hydrophobic amino acids; sugars	Burg et al. (1982)
	RCR2011 (SU47)	Luteolin		Caetanoanollés et al. (1988)*
	L5.30	Certain amino acids; sugars, especially sucrose	Glutamine; xylose	Malek (1989)
	2011	4',7-Dihydroxyflavone; 4',7-dihydroxyflavanone; 4,4'-dihydroxy-2'-methoxychalcone; luteolin		Dharmatilake and Bauer (1992)*
	RU11/001	Non-acidic amino acids; monocarboxylates; quaternary ammonium compounds	Aspartate, glutamate; butyrate, formate; flavonoids	Webb et al. (2017a,b), Compton et al. (2018, 2020)
Rhizobium leguminosarum biovar. *Phaseoli*	RP8002	Raffinose, sucrose, xylose; apigenin, luteolin, p-hydroxybenzoic acid, 3,4-dihydroxybenzoic acid	Glucose, maltose; vanillyl alcohol; naringenin	Aguilar et al. (1988)
	WU163	L-arabinose, cellobiose, D-glucose, D-ribose, D-xylose	Sucrose; trehalose	Bowra and Dilworth (1981)
Rhizobium leguminosarum biovar. *Viciae*	N5	Amino acids; organic acids; sugars such as arabinose, maltose, glucose, xylose	Fucose, sucrose, trehalose	Gaworzewska and Carlile, 1982
	8,401	Small amino acids; sucrose, mannitol, maltose; succinate; apigenin, naringenin, kaempferol	Galactose, ribose; propionate; hesperitin	Armitage et al., 1988
Bradyrhizobium japonicum	110spc4	Hydroxycinnamic acids; succinate	Coniferyl alcohol, chlorogenic acid, coumestrol, daidzein, genistein	Kape et al., 1991
	USDA 110	Aspartate, glutamate; organic acids	Non-acidic amino acids; citrate; daidzein, genistein, luteolin; sugars	Barbour et al. (1991)
	10 K	Alanine, glutamate, phenylalanine, threonine; arabinose, mannitol; citrate	Other amino acids; organic acids; sugars	Chuiko et al., 2002
	LP 3008	Aspartate, glycine, lysine; mannitol		Althabegoiti et al. (2008)

Note that information may conflict between reports. *Results are disputed. See Compton et al. (2020).

particular compound or component of plant exudates. As it stands, comparative analyses are restricted.

Amino Acids

One of the most frequently tested compounds is amino acids because they are ubiquitous in exudates (Moe, 2013). *Rhizobium leguminosarum* biovar *viciae* is similarly attracted to all amino acids; only glutamate and proline stand out as stronger attractants (Gaworzewska and Carlile, 1982; Armitage et al., 1988). In contrast, *B. japonicum* was weakly attracted to non-acidic amino acids, while aspartate and glutamate were potent attractants (Barbour et al., 1991; Chuiko et al., 2002; Althabegoiti et al., 2008). *S. meliloti* senses all amino acids as attractants. Two groups presented aspartate or leucine as the strongest (Burg et al., 1982; Götz et al., 1982, respectively). However, these findings are in contrast with more recent reports that described the molecular mechanism for amino acid sensing, showing that arginine, phenylalanine, proline, and tryptophan are the strongest attractants of this class (Webb et al., 2017b). The chemoreceptor McpU directly binds all amino acids except for glutamate and aspartate, which do not serve as chemoattractants for *S. meliloti* RU11/001 (Webb et al., 2014, 2017b). The chemical nature of the R-group appears to be important for the bias of different bacterial species toward acidic or non-acidic amino acids.

Carboxylates

Carboxylates, also referred to as organic acids, are carbon sources commonly found in plant exudates, the rhizosphere, and bulk soil. Citrate, malate, and succinate are attractants for *R. leguminosarum*, but are generally weaker than the amino acids (Gaworzewska and Carlile, 1982; Armitage et al., 1988). In *B. japonicum*, malonate and succinate elicit a strong attractant response, equivalent to aspartate and glutamate. In addition, other 4-carbon carboxylates are also attractants, although citrate is not (Barbour et al., 1991; Kape et al., 1991). *Sinorhizobium meliloti* has a dedicated 2–3 carbon monocarboxylate sensor, McpV, and a sensor for small dicarboxylates, McpT (Baaziz et al., in review; Compton et al., 2018). The mono- and di-carboxylates are weak attractants compared to the amino acids (Webb et al., 2014).

Flavonoids

Flavonoids belong to a plant-borne compound group that are of interest because they induce the expression of symbiotic genes in their cognate rhizobia (Abdel-Lateif et al., 2012).

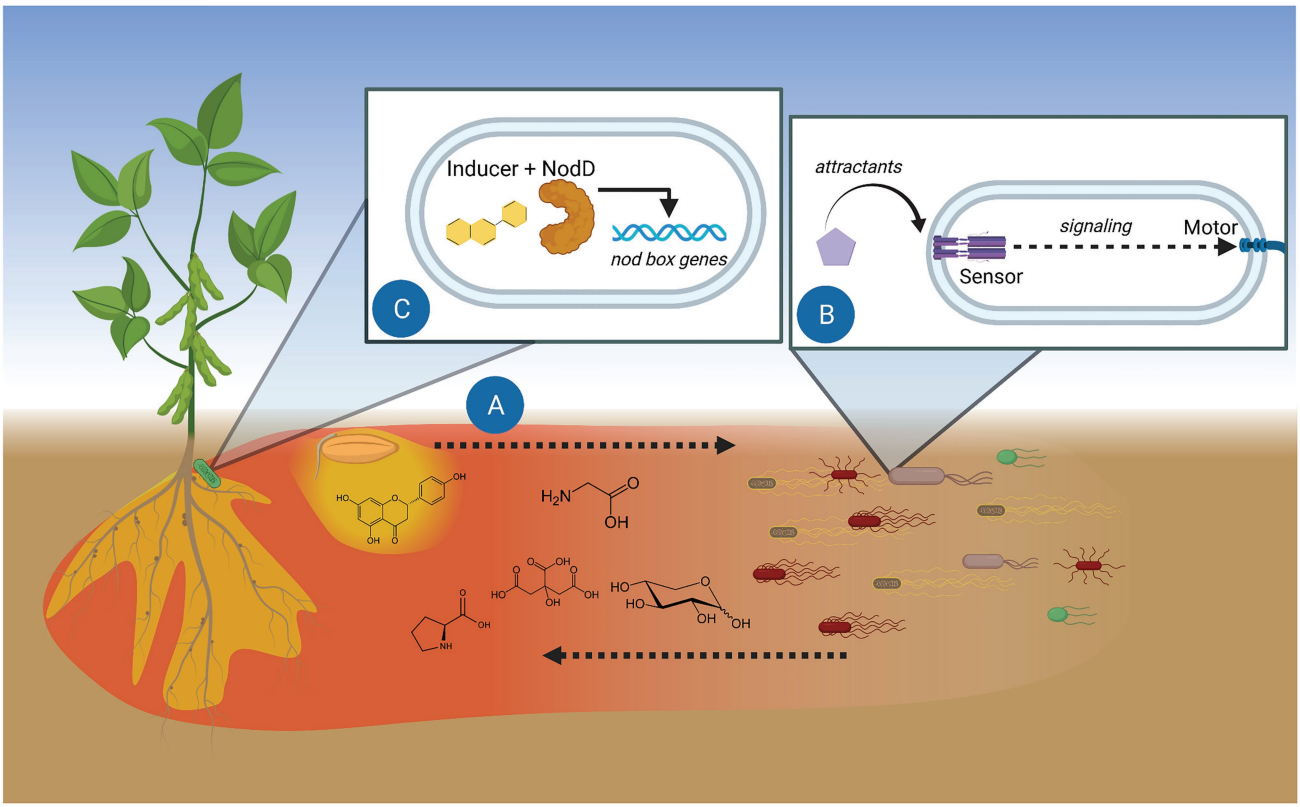

FIGURE 1 | Model of chemotaxis function in the initiation of rhizobium-legume symbiosis. **(A)** Root and seed exudates diffuse and create chemical trails. Gradients of soluble exudates (red) travel furthest and act as chemoattractants. Hydrophobic exudate components (yellow) stay closer to the source. **(B)** Specific exuded compounds are detected by bacterial methyl-accepting chemotaxis proteins (MCPs), the dedicated sensors of attractants. Signaling between the chemosensory system and the motor guides the bacterium toward the attractant source. **(C)** Perception of plant flavonoids by rhizobial NodD initiates transcription of genes involved in infecting the proper host. Figure created with BioRender.

Although apigenin and luteolin do not induce *nod* gene expression in *R. leguminosarum*, they are attractants in this organism. In contrast, naringenin is a *nod* gene inducer but not an attractant (Aguilar et al., 1988). Two reports on *B. japonicum* chemotaxis showed that all flavonoids tested have no attractant function (Barbour et al., 1991; Kape et al., 1991). Studies of *S. meliloti* chemotaxis reported that the *nod* gene inducers dihydroxyflavone and luteolin are attractants, but that responses were very low. The studies did not test any other compounds for comparison and, therefore, lack context (Caetanoanollés et al., 1988; Dharmatilake and Bauer, 1992). The conclusion that flavonoids are attractants was not replicated and recently disputed (Compton et al., 2020). Taken together, the evidence for flavonoid chemotaxis as a general phenomenon in rhizobia is debatable.

Phenolics

The phenolics comprise a class of compounds that include phenylpropanoid derivatives of aromatic acids, which are common plant metabolites and precursors to flavonoids. *Bradyrhizobium japonicum* senses several phenylpropanoid acids and coniferyl alcohol as attractants, but not chlorogenic acid (Kape et al., 1991). Benzoic alcohols are attractants for *R. leguminosarum* with acetosyringone being one of the strongest attractants reported, while umbelliferone and vanillyl alcohol are weak to moderate attractants (Aguilar et al., 1988).

Saccharides

Saccharides or sugars and their subclasses such as sugar alcohols and sugar acids are some of the most readily available carbon sources (Geddes and Oresnik, 2014). Common energy sources like gluconate and glucose as well as structural components of pectins such as arabinose and xylose are logical candidates to serve as attractants for rhizobia. Multiple reports investigated the taxis of *R. leguminosarum* to sugars, but these gave conflicting results. Glucose, maltose, ribose, and sucrose were reported as attractants in certain studies, but the evidence in other references suggests that they are not (Bowra and Dilworth, 1981; Gaworzewska and Carlile, 1982; Aguilar et al., 1988; Armitage et al., 1988). However, arabinose and xylose were identified as attractants in all studies, although they were not necessarily the strongest chemoattractants (Bowra and Dilworth, 1981; Gaworzewska and Carlile, 1982; Aguilar et al., 1988). Information on *B. japonicum* and *S. meliloti* taxis to sugars is sparse. Mannitol, a sugar alcohol, is the only member of this class that was presented as an attractant for *B. japonicum*, while common sugars such as arabinose and glucose do not appear to serve as attractants (Barbour et al., 1991; Chuiko et al., 2002). In *S. meliloti*, gluconate and sucrose were reported to be the best attractants among the sugars over arabinose, fructose, and glucose (Malek, 1989). Currently, it is difficult to make conclusions on the prevalence of sugars as chemoattractants in rhizobia. Most compounds were only tested in a single study and at one concentration (**Table 1**). Sugars are a large, complex class because of the numerous structural and stereoisomers, which further complicates analysis. Currently, there is too little information to make a clear statement about the role of sugars as attractants.

PREFERRED ATTRACTANTS FOR RHIZOBIA

A prominent aim in chemotaxis research is identifying dominant or preferred attractants for a given organism because it is indicative of its role in the ecosystem. The clearest body of information available for this conclusion comes from work done on *S. meliloti* strain RU11/001. All studies examining different classes of chemoattractants included comparative experiments with the chemoattractant proline and used similar techniques – thus creating a standard for comparison. This body of work allows the conclusion that amino acids are of similar attractant strength to quaternary ammonium compounds (QACs) such as betaines or choline (another class of attractants that was only recently recognized), and 5- to 10-fold stronger attractants than carboxylates (Webb et al., 2014, 2017a,b; Compton et al., 2018).

Work on the chemosensing of *B. japonicum*, albeit from a single study, revealed that glutamate, malonate, and succinate are the most potent attractants. It is noteworthy that glutamate was used as a nitrogen source in the growth medium, raising the possibility that chemotaxis responses are inducible in this organism (Barbour et al., 1991).

Acetosyringone is the strongest attractant reported for *R. leguminosarum*, followed by the flavonoids apigenin and luteolin. The evidence for rhizobial chemotaxis to flavonoids is strongest in *R. leguminosarum*, even though the bacterium only appears to be attracted to non-*nod* gene inducing flavonoid species (Aguilar et al., 1988). Arabinose and xylose are not the strongest attractants but have been consistently reported to attract multiple strains of *R. leguminosarum* (Bowra and Dilworth, 1981; Gaworzewska and Carlile, 1982; Aguilar et al., 1988).

WHERE ARE ATTRACTANTS FOUND?

Seed Exudates

The compounds released from germinating seeds are a great source of attractants for rhizobia, readily available for study, and consistent between samples. When seeds are formed, the seed coat is impregnated with numerous chemicals from the mother plant (Radchuk and Borisjuk, 2014). Upon imbibition, these chemicals are leeched out as an exudate into the surrounding medium forming what is called the spermosphere (Nelson, 2004). Amino acids and carboxylates are some of the most sampled constituents of seed exudates and these compounds have the clearest link to known bacterial chemosensory systems (Götz et al., 1982; Rozan et al., 2001; Kuo et al., 2004; Kamilova et al., 2006; Lambers et al., 2013; Webb et al., 2016). However, there is great chemical diversity in exudates that include QACs such as betaines, saccharides, fatty acids, phenolics, and alcohols (Silva et al., 2013; Schiltz et al., 2015; Webb et al., 2017a; Mildaziene et al., 2020; Zuluaga et al., 2020). The gradients these chemicals form serve to recruit microorganisms to the surface of the nascent plant.

Root Exudates

Exudates from roots share the chemical diversity of seed exudates, but their specific composition will vary according

to biotic and abiotic factors and the state of the plant. Changes in exudate profiles are strongly driven by environmental factors (Herz et al., 2018; Dietz et al., 2019). Conditions lacking mineral nutrients induce the release of organic acids to solubilize phosphorus and chelate iron (Shen et al., 2005; Preece and Penuelas, 2020; Vives-Peris et al., 2020). Young or immature plants tend to release more sugars, while the exudates of older plants are biased toward amino acids and phenolics (Chaparro et al., 2013). In another example, a biocontrol organism induces the release of a plant metabolite that is toxic to a pathogen, but not to the biocontrol agent (Wang et al., 2019). In fact, and at the risk of overgeneralizing, it appears that nearly any environmental or physiological perturbation influences the composition or quantity of root exudates (Canarini et al., 2019; Vives-Peris et al., 2020). It would follow that chemotactic recruitment of soil bacteria is, in many cases, a byproduct of plant activity. In support of this, the saprotrophic soil bacterium *Pseudomonas putida* possesses a chemoreceptor that preferentially senses citrate-magnesium complex compared to free citrate, possibly sourced from efforts of a plant to acquire magnesium or other chelated cations (Martin-Mora et al., 2016). However, plants are not indifferent to their rhizosphere neighbors. Recruitment of soil symbionts is a definite priority for plants because of the benefits their microbiota provide. Furthermore, stressed plants release additional carbon compounds to recruit symbionts and other beneficial bacteria in times of need (Ames and Bergman, 1981; Gulash et al., 1984; Badri and Vivanco, 2009; Canarini et al., 2019; O'Neal et al., 2020; Vives-Peris et al., 2020).

Other Attractant Sources

The vast majority of research focuses on rhizobial activities in the rhizosphere and nodule (Poole et al., 2018). Few studies examine rhizobial survival in the bulk soil. This is nonetheless an important topic, because effective inoculants and symbionts must persist in the soil to infect the next generation of hosts (Pinochet et al., 1993; Hirsch and Spokes, 1994; Da and Deng, 2003). In the absence of hosts, rhizobia can subsist on soil organic carbon, an amalgam containing energy and nutrient sources from detritus and decaying matter, which take the form of aromatics, alkyl compounds, carboxylates, and nitrogenous molecules such as proteins (Beyer et al., 1995; Chiu et al., 2002; Spielvogel et al., 2004). Rhizobia are adapted to saprophytic lifestyles, and chemotaxis to the carbon and nitrogen sources available is critical to survival in the bulk soil (Kennedy and Lawless, 1985; Turnbull et al., 2001; diCenzo et al., 2016; Poole et al., 2018).

Attractant signals need not be chemical compounds. Chemoreceptors can sense oxygen gradients or the cellular redox state as an indicator of the surrounding milieu, a strategy termed energy taxis. In the nitrogen fixing *Azospirilum brasilense*, metabolism mediates and is necessary for chemotaxis to attractants. This behavior is also critical to the colonization of host plants (Alexandre et al., 2000; Greer-Phillips et al., 2004). Utilizing a generalized strategy such as energy taxis allows a bacterium to seek areas suitable to its needs, regardless of the identity of the attractant source.

CONCLUSION AND FUTURE DIRECTIONS

Chemotaxis is a major survival strategy for bacteria and greatly aids in seeking hosts (Raina et al., 2019). The rhizobia sense a wide array of chemical cues that are concomitantly found in the exudates of respective host plants but differ in their physiological role (**Figure 1**). Many of these attractants are primary metabolites and do not signify the identity of the source plant. A single chemical that is specific to a host would be difficult to pinpoint. Among semi polar metabolites, very few compounds are exclusively found in a particular plant species (Dietz et al., 2019). At best, specific metabolites might be characteristic of a genus or family (Rosenthal and Nkomo, 2000; Kidd et al., 2018). Rhizobia, therefore, have numerous chemoreceptors that may detect any of the thousands of compounds found in plant exudates, although in some cases, only a few chemoreceptors have any impact on host colonization (Feng et al., 2019). As each rhizobial species or strain analyzed seems to have different preferred attractants, the question remains how these preferences are formed. Since chemotactic preferences must be shaped by selection, perhaps each rhizobium specializes in obtaining particular types of nutrients. In effect, this is akin to a broad survival strategy that expands upon the phenomenon of catabolite repression, where a specific carbon source takes priority in the organism's metabolism (Georgi and Ettinger, 1941; Bruckner and Titgemeyer, 2002; Iyer et al., 2016).

Every species or strain of rhizobia harbors numerous chemoreceptors that bestow perception of a particular signal. The number of MCPs per rhizobium varies greatly from less than 10 in *Sinorhizobium* and *Ensifer* spp. to over 30 in *R. leguminosarum* and *B. japonicum* isolates (for more information on chemoreceptor distributions, see Scharf et al., 2016). Currently, only four MCPs in *S. meliloti* have been assigned functions (Baaziz et al., in review; Webb et al., 2014, 2017b; Compton et al., 2018). The remainder of our knowledge on rhizobial chemotaxis is limited to dated behavioral studies. A complete understanding of rhizobium chemotaxis is an important goal for the following reasons: (1) total knowledge of a rhizobium's chemotaxis system permits the modeling of its behavior in the environment and the prediction of its performance in host nodulation based on its exudate composition (Edgington and Tindall, 2018); (2) inoculant strains can be optimized to more efficiently nodulate crops, outcompete symbiotically inefficient native strains, and better survive in the soil, which increases the longevity of their application; and (3) chemoreceptors are often conserved among plant and animal pathogens, making information on MCPs translational to numerous fields (Brewster et al., 2016; Compton et al., 2018).

The way forward is, therefore, to increase the output of studies on MCP function that address the following goals: (1) identification of attractant classes and their relative strengths; (2) determination of sensors responsible for detecting attractants and the molecular mechanism of sensing; and (3) evaluation of the purpose of attractants in the survival or symbiosis of rhizobia. These aims can be easily initiated by revisiting known attractants and identifying their respective sensors.

Two approaches are effective in characterizing MCP-ligand relationships. The first approach involves defining an attractant class and identifying a corresponding sensor, as exemplified by McpX in *S. meliloti* and the QACs (Webb et al., 2017a). The second approach identifies the ligand profile of an MCP using high-throughput screens followed by behavioral assays (McKellar et al., 2015). These pursuits will eventually illuminate each rhizobium's attractome, the total range of compounds sensed through its chemotaxis systems. These findings will be a great boon to the economical, technical, and ecological challenges facing modern agriculture.

AUTHOR CONTRIBUTIONS

KC and BS contributed to conception of the study. KC wrote the first draft of the manuscript. Both the authors contributed to manuscript revision, read, and approved the submitted version.

FUNDING

This work was supported by NSF grants MCB-1253234 and MCB-1817652 to BS.

REFERENCES

Abdel-Lateif, K., Bogusz, D., and Hocher, V. (2012). The role of flavonoids in the establishment of plant roots endosymbioses with arbuscular mycorrhiza fungi, rhizobia and *Frankia* bacteria. *Plant Signal. Behav.* 7, 636–641. doi: 10.4161/psb.20039

Adler, J. (1966). Chemotaxis in bacteria. *Science* 153, 708–716. doi: 10.1126/science.153.3737.708

Adler, J. (1973). A method for measuring chemotaxis and use of the method to determine optimum conditions for chemotaxis by *Escherichia coli*. *J. Gen. Microbiol.* 74, 77–91. doi: 10.1099/00221287-74-1-77

Aguilar, J. M. M., Ashby, A. M., Richards, A. J. M., Loake, G. J., Watson, M. D., and Shaw, C. H. (1988). Chemotaxis of *Rhizobium leguminosarum* biovar phaseoli towards flavonoid inducers of the symbiotic nodulation genes. *J. Gen. Microbiol.* 134, 2741–2746. doi: 10.1099/00221287-134-10-2741

Alexandre, G., Greer, S. E., and Zhulin, I. B. (2000). Energy taxis is the dominant behavior in *Azospirillum brasilense*. *J. Bacteriol.* 182, 6042–6048. doi: 10.1128/JB.182.21.6042-6048.2000

Althabegoiti, M. J., Lopez-Garcia, S. L., Piccinetti, C., Mongiardini, E. J., Perez-Gimenez, J., Quelas, J. I., et al. (2008). Strain selection for improvement of *Bradyrhizobium japonicum* competitiveness for nodulation of soybean. *FEMS Microbiol. Lett.* 282, 115–123. doi: 10.1111/j.1574-6968.2008.01114.x

Ames, P., and Bergman, K. (1981). Competitive advantage provided by bacterial motility in the formation of nodules by *Rhizobium meliloti*. *J. Bacteriol.* 148, 728–729. doi: 10.1128/JB.148.2.728-729.1981

Ames, P., Schluederberg, S. A., and Bergman, K. (1980). Behavioral mutants of *Rhizobium meliloti*. *J. Bacteriol.* 141, 722–727. doi: 10.1128/JB.141.2.722-727.1980

Armitage, J. P., Gallagher, A., and Johnston, A. W. (1988). Comparison of the chemotactic behaviour of *Rhizobium leguminosarum* with and without the nodulation plasmid. *Mol. Microbiol.* 2, 743–748. doi: 10.1111/j.1365-2958.1988.tb00085.x

Badri, D. V., and Vivanco, J. M. (2009). Regulation and function of root exudates. *Plant Cell Environ.* 32, 666–681. doi: 10.1111/j.1365-3040.2009.01926.x

Barbour, W. M., Hattermann, D. R., and Stacey, G. (1991). Chemotaxis of *Bradyrhizobium japonicum* to soybean exudates. *Appl. Environ. Microbiol.* 57, 2635–2639. doi: 10.1128/AEM.57.9.2635-2639.1991

Beyer, L., Blume, H. P., Elsner, D. C., and Willnow, A. (1995). Soil organic-matter composition and microbial activity in urban soils. *Sci. Total Environ.* 168, 267–278. doi: 10.1016/0048-9697(95)04704-5

Bowra, B. J., and Dilworth, M. J. (1981). Motility and chemotaxis towards sugars in *Rhizobium-leguminosarum*. *J. Gen. Microbiol.* 126, 231–235. doi: 10.1099/00221287-126-1-231

Brewster, J. L., McKellar, J. L., Finn, T. J., Newman, J., Peat, T. S., and Gerth, M. L. (2016). Structural basis for ligand recognition by a cache chemosensory domain that mediates carboxylate sensing in *Pseudomonas syringae*. *Sci. Rep.* 6:35198. doi: 10.1038/srep35198

Bruckner, R., and Titgemeyer, F. (2002). Carbon catabolite repression in bacteria: choice of the carbon source and autoregulatory limitation of sugar utilization. *FEMS Microbiol. Lett.* 209, 141–148. doi: 10.1016/S0378-1097(02)00559-1

Burg, D., Guillaume, J., and Tailliez, R. (1982). Chemotaxis by *Rhizobium meliloti*. *Arch. Microbiol.* 133, 162–163. doi: 10.1007/BF00413532

Caetanoanollés, G., Cristestes, D. K., and Bauer, W. D. (1988). Chemotaxis of *Rhizobium meliloti* to the plant flavone luteolin requires functional nodulation genes. *J. Bacteriol.* 170, 3164–3169. doi: 10.1128/JB.170.7.3164-3169.1988

Canarini, A., Kaiser, C., Merchant, A., Richter, A., and Wanek, W. (2019). Root exudation of primary metabolites: mechanisms and their roles in plant responses to environmental stimuli. *Front. Plant Sci.* 10:157. doi: 10.3389/fpls.2019.00157

Chaparro, J. M., Badri, D. V., Bakker, M. G., Sugiyama, A., Manter, D. K., and Vivanco, J. M. (2013). Root exudation of phytochemicals in *Arabidopsis* follows specific patterns that are developmentally programmed and correlate with soil microbial functions. *PLoS One* 8:e55731. doi: 10.1371/journal.pone.0055731

Chiu, C. Y., Wang, M. K., Hwong, J. L., and King, H. B. (2002). Physical and chemical properties in rhizosphere and bulk soils of Tsuga and Yushania in a temperate rain forest. *Commun. Soil Sci. Plant Anal.* 33, 1723–1735. doi: 10.1081/Css-120004818

Chuiko, N. V., Antonyuk, T. S., and Kurdish, I. K. (2002). The chemotactic response of *Bradyrhizobium japonicum* to various organic compounds. *Microbiology* 71, 391–396. doi: 10.1023/A:1019881124077

Compton, K. K., Hildreth, S. B., Helm, R. F., and Scharf, B. E. (2018). *Sinorhizobium meliloti* chemoreceptor McpV senses short-chain carboxylates via direct binding. *J. Bacteriol.* 200:e00519–18. doi: 10.1128/JB.00519-18

Compton, K. K., Hildreth, S. B., Helm, R. F., and Scharf, B. E. (2020). An updated perspective on *Sinorhizobium meliloti* chemotaxis to alfalfa flavonoids. *Front. Microbiol.* 11:581482. doi: 10.3389/fmicb.2020.581482

Croxen, M. A., Sisson, G., Melano, R., and Hoffman, P. S. (2006). The *Helicobacter pylori* chemotaxis receptor TlpB (HP0103) is required for pH taxis and for colonization of the gastric mucosa. *J. Bacteriol.* 188, 2656–2665. doi: 10.1128/JB.188.7.2656-2665.2006

Da, H. N., and Deng, S. P. (2003). Survival and persistence of genetically modified *Sinorhizobium meliloti* in soil. *Appl. Soil Ecol.* 22, 1–14. doi: 10.1016/S0929-1393(02)00127-0

Dharmatilake, A. J., and Bauer, W. D. (1992). Chemotaxis of *Rhizobium-meliloti* towards todulation gene-inducing bompounds from alfalfa roots. *Appl. Environ. Microbiol.* 58, 1153–1158. doi: 10.1128/AEM.58.4.1153-1158.1992

diCenzo, G. C., Checcucci, A., Bazzicalupo, M., Mengoni, A., Viti, C., Dziewit, L., et al. (2016). Metabolic modelling reveals the specialization of secondary replicons for niche adaptation in *Sinorhizobium meliloti*. *Nat. Commun.* 7:12219. doi: 10.1038/ncomms12219

Dietz, S., Herz, K., Doll, S., Haider, S., Jandt, U., Bruelheide, H., et al. (2019). Semi-polar root exudates in natural grassland communities. *Ecol. Evol.* 9, 5526–5541. doi: 10.1002/ece3.5043

Edgington, M. P., and Tindall, M. J. (2018). Mathematical analysis of the *Escherichia coli* chemotaxis signalling pathway. *Bull. Math. Biol.* 80, 758–787. doi: 10.1007/s11538-018-0400-z

Feng, H., Zhang, N., Fu, R., Liu, Y., Krell, T., Du, W., et al. (2019). Recognition of dominant attractants by key chemoreceptors mediates recruitment of plant growth-promoting rhizobacteria. *Environ. Microbiol.* 21, 402–415. doi: 10.1111/1462-2920.14472

Gaworzewska, E. T., and Carlile, M. J. (1982). Positive chemotaxis of *Rhizobium leguminosarum* and other bacteria towards root exudates from legumes and other plants. *Microbiology* 128, 1179–1188. doi: 10.1099/00221287-128-6-1179

Geddes, B. A., and Oresnik, I. J. (2014). Physiology, genetics, and biochemistry of carbon metabolism in the alphaproteobacterium *Sinorhizobium meliloti*. *Can. J. Microbiol.* 60, 491–507. doi: 10.1139/cjm-2014-0306

Georgi, C. E., and Ettinger, J. M. (1941). Utilization of carbohydrates and sugar acids by the rhizobia. *J. Bacteriol.* 41, 323–340. doi: 10.1128/JB.41.3.323-340.1941

Götz, R., Limmer, N., Ober, K., and Schmitt, R. (1982). Motility and chemotaxis in 2 strains of rhizobium with complex flagella. *J. Gen. Microbiol.* 128, 789–798. doi: 10.1099/00221287-128-4-789

Greer-Phillips, S. E., Stephens, B. B., and Alexandre, G. (2004). An energy taxis transducer promotes root colonization by *Azospirillum brasilense*. *J. Bacteriol.* 186, 6595–6604. doi: 10.1128/JB.186.19.6595-6604.2004

Gulash, M., Ames, P., Larosiliere, R. C., and Bergman, K. (1984). Rhizobia are attracted to localized sites on legume roots. *Appl. Environ. Microbiol.* 48, 149–152. doi: 10.1128/AEM.48.1.149-152.1984

Hazelbauer, G. L. (1975). Maltose chemoreceptor of *Escherichia coli*. *J. Bacteriol.* 122, 206–214. doi: 10.1128/JB.122.1.206-214.1975

Herz, K., Dietz, S., Gorzolka, K., Haider, S., Jandt, U., Scheel, D., et al. (2018). Linking root exudates to functional plant traits. *PLoS One* 13:e0204128. doi: 10.1371/journal.pone.0204128

Hirsch, P. R., and Spokes, J. D. (1994). Survival and dispersion of genetically modified rhizobia in the field and genetic interactions with native strains. *FEMS Microbiol. Ecol.* 15, 147–159. doi: 10.1111/j.1574-6941.1994.tb00239.x

Iyer, B., Rajput, M. S., Jog, R., Joshi, E., Bharwad, K., and Rajkumar, S. (2016). Organic acid mediated repression of sugar utilization in rhizobia. *Microbiol. Res.* 192, 211–220. doi: 10.1016/j.micres.2016.07.006

Jekely, G. (2009). Evolution of phototaxis. *Philos. Trans. R. Soc. Lond. Ser. B Biol. Sci.* 364, 2795–2808. doi: 10.1098/rstb.2009.0072

Kamilova, F., Kravchenko, L. V., Shaposhnikov, A. I., Azarova, T., Makarova, N., and Lugtenberg, B. (2006). Organic acids, sugars, and L-tryptophane in exudates of vegetables growing on stonewool and their effects on activities of rhizosphere bacteria. *Mol. Plant-Microbe Interact.* 19, 250–256. doi: 10.1094/MPMI-19-0250

Kape, R., Parniske, M., and Werner, D. (1991). Chemotaxis and nod gene activity of *Bradyrhizobium japonicum* in response to hydroxycinnamic acids and isoflavonoids. *Appl. Environ. Microbiol.* 57, 316–319. doi: 10.1128/AEM.57.1.316-319.1991

Kennedy, M. J., and Lawless, J. G. (1985). Role of chemotaxis in the ecology of denitrifiers. *Appl. Environ. Microbiol.* 49, 109–114. doi: 10.1128/AEM.49.1.109-114.1985

Kidd, D. R., Ryan, M. H., Hahne, D., Haling, R. E., Lambers, H., Sandral, G. A., et al. (2018). The carboxylate composition of rhizosheath and root exudates from twelve species of grassland and crop legumes with special reference to the occurrence of citramalate. *Plant Soil* 424, 389–403. doi: 10.1007/s11104-017-3534-0

Kuo, Y. H., Rozan, P., Lambein, F., Frias, J., and Vidal-Valverde, C. (2004). Effects of different germination conditions on the contents of free protein and non-protein amino acids of commercial legumes. *Food Chem.* 86, 537–545. doi: 10.1016/j.foodchem.2003.09.042

Lambers, H., Clements, J. C., and Nelson, M. N. (2013). How a phosphorus-acquisition strategy based on carboxylate exudation powers the success and agronomic potential of lupines (*Lupinus*, *Fabaceae*). *Am. J. Bot.* 100, 263–288. doi: 10.3732/ajb.1200474

Lopez-Farfan, D., Reyes-Darias, J. A., and Krell, T. (2017). The expression of many chemoreceptor genes depends on the cognate chemoeffector as well as on the growth medium and phase. *Curr. Genet.* 63, 457–470. doi: 10.1007/s00294-016-0646-7

Malek, W. (1989). Chemotaxis in *Rhizobium meliloti* strain L5.30. *Arch. Microbiol.* 152, 611–612. doi: 10.1007/BF00425496

Martin-Mora, D., Reyes-Darias, J. A., Ortega, A., Corral-Lugo, A., Matilla, M. A., and Krell, T. (2016). McpQ is a specific citrate chemoreceptor that responds preferentially to citrate/metal ion complexes. *Environ. Microbiol.* 18, 3284–3295. doi: 10.1111/1462-2920.13030

McKellar, J. L. O., Minnell, J. J., and Gerth, M. L. (2015). A high-throughput screen for ligand binding reveals the specificities of three amino acid chemoreceptors from *Pseudomonas syringae* pv. *actinidiae*. *Mol. Microbiol.* 96, 694–707. doi: 10.1111/mmi.12964

Meier, V. M., Muschler, P., and Scharf, B. E. (2007). Functional analysis of nine putative chemoreceptor proteins in *Sinorhizobium meliloti*. *J. Bacteriol.* 189, 1816–1826. doi: 10.1128/JB.00883-06

Mildaziene, V., Ivankov, A., Pauzaite, G., Nauciene, Z., Zukiene, R., Degutyte-Fomins, L., et al. (2020). Seed treatment with cold plasma and electromagnetic field induces changes in red clover root growth dynamics, flavonoid exudation, and activates nodulation. *Plasma Process. Polym.* 18:2000160. doi: 10.1002/ppap.202000160

Moe, L. A. (2013). Amino acids in the rhizosphere: from plants to microbes. *Am. J. Bot.* 100, 1692–1705. doi: 10.3732/ajb.1300033

Nelson, E. B. (2004). Microbial dynamics and interactions in the spermosphere. *Annu. Rev. Phytopathol.* 42, 271–309. doi: 10.1146/annurev.phyto.42.121603.131041

O'Neal, L., Vo, L., and Alexandre, G. (2020). Specific root exudate compounds sensed by dedicated chemoreceptors shape *Azospirillum brasilense* chemotaxis in the rhizosphere. *Appl. Environ. Microbiol.* 86:e01026–20. doi: 10.1128/AEM.01026-20

Parkinson, J. S., Hazelbauer, G. L., and Falke, J. J. (2015). Signaling and sensory adaptation in *Escherichia coli* chemoreceptors: 2015 update. *Trends Microbiol.* 23, 257–266. doi: 10.1016/j.tim.2015.03.003

Paulick, A., Jakovljevic, V., Zhang, S., Erickstad, M., Groisman, A., Meir, Y., et al. (2017). Mechanism of bidirectional thermotaxis in *Escherichia coli*. *elife* 6:e26607. doi: 10.7554/eLife.26607

Pinochet, X., Arnaud, F., and Cleyetmarel, J. C. (1993). Competition for nodule occupancy of introduced *Bradyrhizobium japonicum* strain Smgs1 in french soils already containing *Bradyrhizobium japonicum* strain G49. *Can. J. Microbiol.* 39, 1022–1028. doi: 10.1139/m93-155

Poole, P., Ramachandran, V., and Terpolilli, J. (2018). Rhizobia: from saprophytes to endosymbionts. *Nat. Rev. Microbiol.* 16, 291–303. doi: 10.1038/nrmicro.2017.171

Preece, C., and Penuelas, J. (2020). A return to the wild: root exudates and food security. *Trends Plant Sci.* 25, 14–21. doi: 10.1016/j.tplants.2019.09.010

Radchuk, V., and Borisjuk, L. (2014). Physical, metabolic and developmental functions of the seed coat. *Front. Plant Sci.* 5:510. doi: 10.3389/fpls.2014.00510

Raina, J. B., Fernandez, V., Lambert, B., Stocker, R., and Seymour, J. R. (2019). The role of microbial motility and chemotaxis in symbiosis. *Nat. Rev. Microbiol.* 17, 284–294. doi: 10.1038/s41579-019-0182-9

Rosenthal, G. A., and Nkomo, P. (2000). The natural abundance of L-canavanine, an active anticancer agent, in alfalfa, *Medicago sativa* (L.). *Pharm. Biol.* 38, 1–6. doi: 10.1076/1388-0209(200001)3811-BFT001

Rozan, P., Kuo, Y. H., and Lambein, F. (2001). Amino acids in seeds and seedlings of the genus *Lens*. *Phytochemistry* 58, 281–289. doi: 10.1016/S0031-9422(01)00200-X

Salah Ud-Din, A. I. M., and Roujeinikova, A. (2017). Methyl-accepting chemotaxis proteins: a core sensing element in prokaryotes and archaea. *Cell. Mol. Life Sci.* 74, 3293–3303. doi: 10.1007/s00018-017-2514-0

Sampedro, I., Parales, R. E., Krell, T., and Hill, J. E. (2015). Pseudomonas chemotaxis. *FEMS Microbiol. Rev.* 39, 17–46. doi: 10.1111/1574-6976.12081

Scharf, B. E., Hynes, M. F., and Alexandre, G. M. (2016). Chemotaxis signaling systems in model beneficial plant-bacteria associations. *Plant Mol. Biol.* 90, 549–559. doi: 10.1007/s11103-016-0432-4

Schiltz, S., Gaillard, I., Pawlicki-Jullian, N., Thiombiano, B., Mesnard, F., and Gontier, E. (2015). A review: what is the spermosphere and how can it be studied? *J. Appl. Microbiol.* 119, 1467–1481. doi: 10.1111/jam.12946

Shen, H., He, L. F., Sasaki, T., Yamamoto, Y., Zheng, S. J., Ligaba, A., et al. (2005). Citrate secretion coupled with the modulation of soybean root tip under aluminum stress. Up-regulation of transcription, translation, and threonine-oriented phosphorylation of plasma membrane H+-ATPase. *Plant Physiol.* 138, 287–296. doi: 10.1104/pp.104.058065

Silva, L. R., Pereira, M. J., Azevedo, J., Mulas, R., Velazquez, E., Gonzalez-Andres, F., et al. (2013). Inoculation with *Bradyrhizobium japonicum* enhances the organic and fatty acids content of soybean (*Glycine max* (L.) Merrill) seeds. *Food Chem.* 141, 3636–3648. doi: 10.1016/j.foodchem.2013.06.045

Spielvogel, S., Knicker, H., and Kogel-Knabner, I. (2004). Soil organic matter composition and soil lightness. *J. Plant Nutr. Soil Sci.* 167, 545–555. doi: 10.1002/jpln.200421424

Tso, W. W., and Adler, J. (1974). Negative chemotaxis in *Escherichia coli*. *J. Bacteriol.* 118, 560–576. doi: 10.1128/JB.118.2.560-576.1974

Turnbull, G. A., Morgan, J. A. W., Whipps, J. M., and Saunders, J. R. (2001). The role of bacterial motility in the survival and spread of *Pseudomonas fluorescens* in soil and in the attachment and colonisation of wheat roots. *FEMS Microbiol. Ecol.* 36, 21–31. doi: 10.1111/j.1574-6941.2001.tb00822.x

Vives-Peris, V., de Ollas, C., Gomez-Cadenas, A., and Perez-Clemente, R. M. (2020). Root exudates: from plant to rhizosphere and beyond. *Plant Cell Rep.* 39, 3–17. doi: 10.1007/s00299-019-02447-5

Wang, N., Wang, L. Y., Zhu, K., Hou, S. S., Chen, L., Mi, D. D., et al. (2019). Plant root exudates are involved in *Bacillus cereus* AR156 mediated biocontrol against *Ralstonia solanacearum*. *Front. Microbiol.* 10:98. doi: 10.3389/fmicb.2019.00098

Webb, B. A., Compton, K. K., Castañeda Saldaña, R., Arapov, T., Ray, W. K., Helm, R. F., et al. (2017a). *Sinorhizobium meliloti* chemotaxis to quaternary ammonium compounds is mediated by the chemoreceptor McpX. *Mol. Microbiol.* 103, 333–346. doi: 10.1111/mmi.13561

Webb, B. A., Compton, K. K., del Campo, J. S. M., Taylor, D., Sobrado, P., and Scharf, B. E. (2017b). *Sinorhizobium meliloti* chemotaxis to multiple amino acids is mediated by the chemoreceptor McpU. *Mol. Plant-Microbe Interact.* 30, 770–777. doi: 10.1094/MPMI-04-17-0096-R

Webb, B. A., Helm, R. F., and Scharf, B. E. (2016). Contribution of individual chemoreceptors to *Sinorhizobium meliloti* chemotaxis towards amino acids of host and nonhost seed exudates. *Mol. Plant-Microbe Interact.* 29, 231–239. doi: 10.1094/MPMI-12-15-0264-R

Webb, B. A., Hildreth, S., Helm, R. F., and Scharf, B. E. (2014). *Sinorhizobium meliloti* chemoreceptor McpU mediates chemotaxis toward host plant exudates through direct proline sensing. *Appl. Environ. Microbiol.* 80, 3404–3415. doi: 10.1128/AEM.00115-14

Zuluaga, A. M., Mena-Garcia, A., Monzon, A. C. S., Rada-Mendoza, M., Chito, D. M., Ruiz-Matute, A. I., et al. (2020). Microwave assisted extraction of inositols for the valorization of legume by-products. *LWT* 133:109971. doi: 10.1016/j.lwt.2020.109971

Conflict of Interest: The authors declare that the research was conducted in the absence of any commercial or financial relationships that could be construed as a potential conflict of interest.

frontiers in Plant Science

ORIGINAL RESEARCH
published: 07 May 2021
doi: 10.3389/fpls.2021.642591

Towards Understanding Afghanistan Pea Symbiotic Phenotype Through the Molecular Modeling of the Interaction Between LykX-Sym10 Receptor Heterodimer and Nod Factors

Yaroslav V. Solovev[1,2†], Anna A. Igolkina[3†], Pavel O. Kuliaev[2], Anton S. Sulima[3], Vladimir A. Zhukov[3,4,5], Yuri B. Porozov[6,5], Evgeny A. Pidko[7,2] and Evgeny E. Andronov[3,4,8]*

[1]Shemyakin-Ovchinnikov Institute of Bioorganic Chemistry, Russian Academy of Sciences, Moscow, Russia, [2]TheoMAT Research Group, ITMO University, Saint Petersburg, Russia, [3]All-Russia Research Institute for Agricultural Microbiology (ARRIAM), Saint-Petersburg, Russia, [4]Department of Genetics and Biotechnology, Saint-Petersburg State University, Saint-Petersburg, Russia, [5]Sirius University of Science and Technology, Sochi, Russia, [6]World-Class Research Center "Digital Biodesign and Personalized Healthcare", I.M. Sechenov First Moscow State Medical University, Moscow, Russia, [7]Inorganic Systems Engineering Group, Department of Chemical Engineering, Faculty of Applied Sciences, Delft University of Technology, Delft, Netherlands, [8]V.V. Dokuchaev Soil Institute, Moscow, Russia

The difference in symbiotic specificity between peas of Afghanistan and European phenotypes was investigated using molecular modeling. Considering segregating amino acid polymorphism, we examined interactions of pea LykX-Sym10 receptor heterodimers with four forms of Nodulation factor (NF) that varied in natural decorations (acetylation and length of the glucosamine chain). First, we showed the stability of the LykX-Sym10 dimer during molecular dynamics (MD) in solvent and in the presence of a membrane. Then, four NFs were separately docked to one European and two Afghanistan dimers, and the results of these interactions were in line with corresponding pea symbiotic phenotypes. The European variant of the LykX-Sym10 dimer effectively interacts with both acetylated and non-acetylated forms of NF, while the Afghanistan variants successfully interact with the acetylated form only. We additionally demonstrated that the length of the NF glucosamine chain contributes to controlling the effectiveness of the symbiotic interaction. The obtained results support a recent hypothesis that the *LykX* gene is a suitable candidate for the unidentified *Sym2* allele, the determinant of pea specificity toward *Rhizobium leguminosarum bv. viciae* strains producing NFs with or without an acetylation decoration. The developed modeling methodology demonstrated its power in multiple searches for genetic determinants, when experimental detection of such determinants has proven extremely difficult.

Keywords: Pea, plant-rhizobia symbiosis, LykX, Sym2, nod factor, molecular dynamics, COSMO-RS model

OPEN ACCESS

Edited by:
Benjamin Gourion, UMR2594 Laboratoire Interactions Plantes-Microorganismes (LIPM), France

Reviewed by:
Cheng-Wu Liu, University of Science and Technology of China, China
Giovanna Frugis, National Research Council, Consiglio Nazionale delle Ricerche (CNR), Italy

***Correspondence:**
Anna A. Igolkina
igolkinaanna11@gmail.com

†These authors share first authorship

Specialty section:
This article was submitted to Plant Symbiotic Interactions, a section of the journal Frontiers in Plant Science

Received: *16 December 2020*
Accepted: *13 April 2021*
Published: *07 May 2021*

Citation:
Solovev YV, Igolkina AA, Kuliaev PO, Sulima AS, Zhukov VA, Porozov YB, Pidko EA and Andronov EE (2021) Towards Understanding Afghanistan Pea Symbiotic Phenotype Through the Molecular Modeling of the Interaction Between LykX-Sym10 Receptor Heterodimer and Nod Factors. Front. Plant Sci. 12:642591. doi: 10.3389/fpls.2021.642591

INTRODUCTION

The symbiosis between leguminous plants (*Fabaceae*) and nodule bacteria (collectively called *rhizobia*) demonstrates an extremely high specificity. When the host plant interacts with a large number of soil microorganisms looking for an appropriate partner, it should be selective enough to avoid penetration of any pathogens, discriminate between different types of *rhizobia*, and allow symbiotic interaction with the most effective partner. Interactions between partners are carried out by a complicated interplay of signaling; however, several essential details of these molecular mechanisms are still under question (Denarie, 1996; Oldroyd, 2013; Walker et al., 2020).

The molecular crosstalk between partners starts at the early stages of the plant-rhizobia interaction and results in root nodule formation (**Figure 1A**, photos). Bacteria secrete molecules called Nodulation factors (Nod factors, NFs), which serve as the primary recognition "key" signal for a plant "lock." The structure of NFs was discovered more than 30 years ago; this molecule generally consists of 3, 4, or 5 N-acelylglucosamines linearly oligomerized through (1,4)-β-linkages and decorated with a fatty acid residue and various small substitutions that play a crucial role in partner recognition (Denarie, 1996; Ritsema et al., 1996). All these decorations are genetically controlled and determine NF shapes, which are distinctive for different *rhizobia* species (or strains). Each rhizobial strain produces several slightly different NF molecules that may allow the strain to extend the spectrum of its potential hosts (Mergaert and Van Montagu, 1997). In contrast, the beneficial strategy for plants is to narrow their symbiotic specificity and interact with reliable symbiotic partners only. The co-evolution of these strategies results in cross-inoculation groups (CIGs; Baldwin et al., 1927; Sears and Carroll, 1927). This concept describes distinct groups, each containing both legumes and *rhizobia* strains, so that all plant-bacteria combinations within a group form effective and highly specific symbiotic relationships. Originally, CIGs were thought to be non-overlapped; each legume species and *rhizobia* strain was considered to belong to only one group

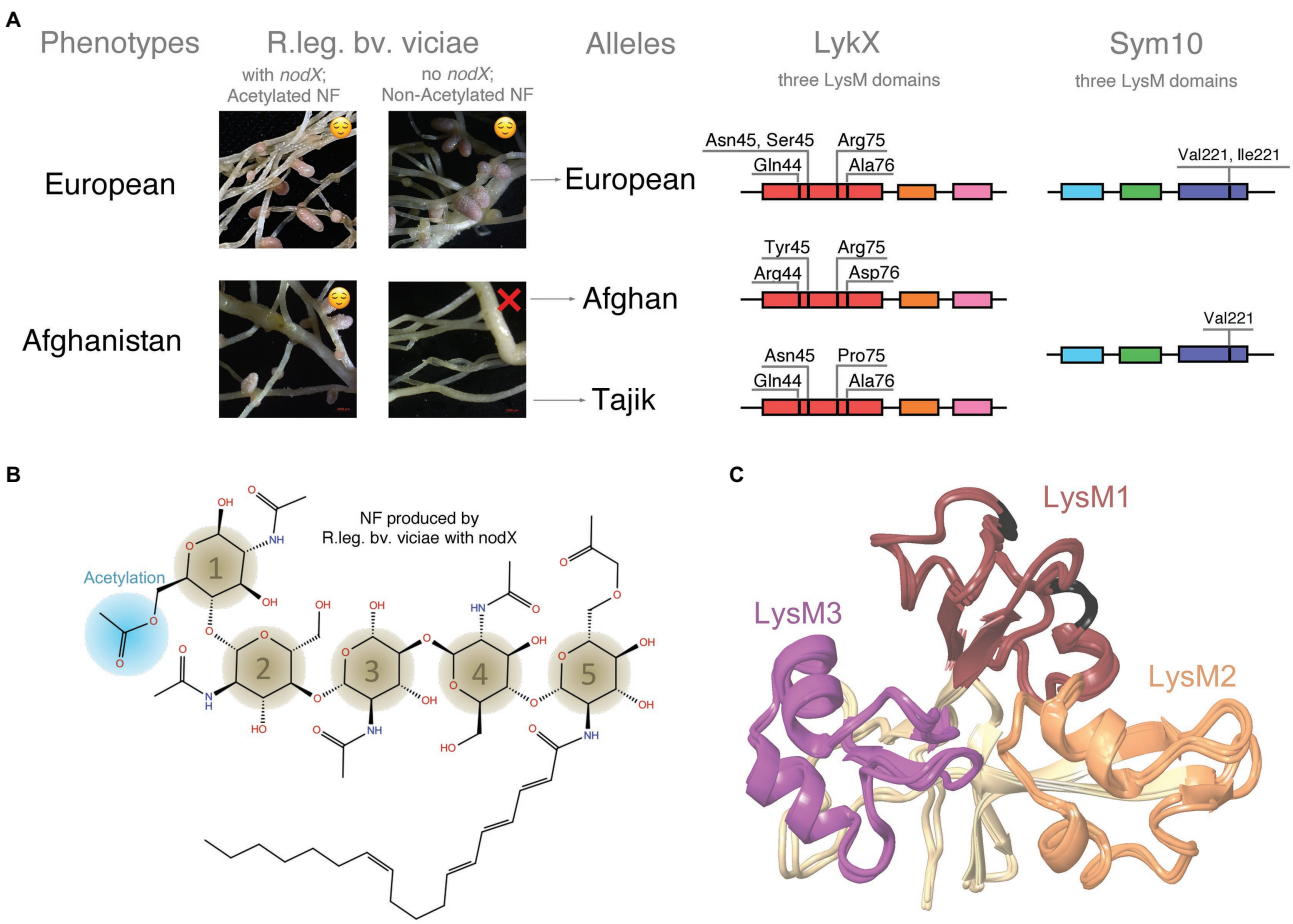

FIGURE 1 | (A) Phenotypes and alleles of garden pea (*Pisum sativum* L.). Garden pea has two symbiotic phenotypes (European and Afghanistan) differing in symbiosis with R.leg.bv.vicia, which have no *nodX* gene and produce non-acetylated nodulation factors (NFs). At the molecular level, two alleles of *LykX* gene were found for Afghanistan phenotype (Afghan and Tajik). Three LysM domains and amino acid polymorphisms for LykX and Sym10 are shown. **(B)** Structure of a NF. **(C)** Structural alignment of the Afghan, Tajik, and European LykX proteins. LysM1 domains are colored in dark red (variable amino acids are highlighted with black), LysM2 – in faded orange, and LysM3 – in dark purple.

(Baldwin et al., 1927; Sears and Carroll, 1927). However, further studies demonstrated that real boundaries between CIGs are blurred, and many cases of non-canonical interactions between legumes and *rhizobia* from different groups exist (Provorov, 1994; Viprey et al., 2000). Even within a particular CIG, one can find variations in the symbiotic efficiency (Provorov, 1994).

This variation within a CIG was demonstrated for the garden pea (*Pisum sativum* L.); Afghanistan and European pea landraces show different symbiotic success with *Rhizobium leguminosarum bv. viciae* depending on presence of the *nodX* gene in *rhizobia* (Firmin et al., 1993; Ovtsyna et al., 1999). This gene encodes an acetyltransferase that attaches a small acetylation decoration to NF (**Figure 1B**) (Lie, 1978; Davis et al., 1988; Ovtsyna et al., 1999). The Afghanistan pea landraces can interact only with *R. leguminosarum bv. viciae* strains, which have the *nod*X gene, while European pea lines display relaxed specificity and can also be nodulated by strains lacking this gene (**Figure 1A**). The reason for this variation relates to the difference in the NF receptors of pea subtypes. However, the particular pea receptors that interact with NFs are not known.

Plant receptors for NF perception belong to a family of LysM domain-containing receptor-like kinases (LysM-RLKs), and contain three LysM domains in the extracellular part of the protein, a transmembrane domain, and an intracellular kinase domain (Bensmihen et al., 2011; Buendia et al., 2018). All plant LysM-RLKs fall into two classes: LYK (with active kinase) and LYR (with non-active pseudo-kinase; Arrighi, 2006). A heterodimeric receptor of two LysM-RLKs from different classes is required for NF perception (Radutoiu et al., 2003; Arrighi, 2006; Zipfel and Oldroyd, 2017). The differences in receptor protein sequences, in theory, should reflect the difference in NF structure. However, in practice, different leguminous species with a relatively high level of between-species amino acid polymorphism in receptor genes effectively interact with the same rhizobial strains. Interestingly, a single amino acid variation in a particular LysM domain of the LysM-RLK NFR5 (Nod-factor receptor 5) has been shown to dramatically change the recognition of NFs by Lotus species (Radutoiu et al., 2007). The latter example resembles the case of Afghanistan and European pea cultivars demonstrating a relatively low level of genetic divergence and, at the same time, clearly different symbiotic phenotypes (**Figure 1A**). To understand the molecular mechanisms of these different interactions, one needs to study NF-receptor interaction and the meaning of amino acid substitutions in this process. It is first necessary to investigate what is known about the interactions between pea receptors and NF. Expectedly, NF receptors should be homologs of the previously identified legume LysM-RLKs, but in practice, it is almost impossible to match known pea LysM-RLKs with their homologs in other leguminous plants, as LysM-RLKs families consist of a number of closely related receptors.

The existence of the specific pea receptor for acetylated NF was shown with a classic genetic approach more than 20 years ago. It was well-proven that the difference in interaction exhibited by acetylated and non-acetylated NF is controlled by a single plant gene called *Sym2* (Kozik et al., 1995, 1996). Despite being described long ago, *Sym2* has not yet been cloned, and the position of this gene in the pea genome ("the Sym2 region") was determined only in genetic mapping experiments (Kozik et al., 1996). The main candidates for *Sym2* are *Sym37*, *K1*, and *LykX* genes that are located in the Sym2 region (Sulima et al., 2017). However, based on sequence differences between Afghanistan and European pea subtypes, *LykX* has amino acid segregating polymorphism, while *Sym37* and *K1* were identical between subtypes (Zhukov et al., 2008). Therefore, only *LykX* out of three candidates has the potential to be responsible for the phenotypic difference between Afghanistan and European peas. Since NF perception requires a heterodimeric receptor with LYR and LYK subunits, we considered the *LykX* gene as encoding the LYR subunit, and the conventional Sym10 gene as encoding the LYK subunit. The Sym10 gene was demonstrated to be required for the legume-rhizobia symbiosis development, and the possibility of Sym10-Sym37 and Sym10-K1 complexes formation was also shown (Kirienko et al., 2019).

The most obvious way to prove the action of LykX as the NF receptor is by investigating the direct binding of the isolated receptor with NF. However, the evidence for direct binding of acetylated and non-acetylated NFs to LykX protein is still lacking. Only several attempts to show such binding have been successful to date (Broghammer et al., 2012; Kirienko et al., 2018). The difficulty of this detection may be caused by the fact that legume NF receptors work in heterodimers (Xiao et al., 2014; Igolkina et al., 2018; Kirienko et al., 2019), whereas modern technologies are aimed to test the "one receptor-one ligand" model. Additionally, NF isolation and purification are very time- and resource-consuming procedures, while the chemical synthesis of NF is extremely difficult due to the high complexity of its structure.

Therefore, as long as the demonstration of the physical interaction between receptor heterodimers and NFs remains challenging, molecular modeling is a suitable and appealing alternative to direct experimental approaches. Recently, based on this method, probable complexes of plant heterodimeric receptors with NF have been proposed, and the overlap between population polymorphisms in the contact zone between receptors in the complex has been analyzed (Igolkina et al., 2018). To date, molecular modeling provides the opportunity for the *in silico* mass-testing of interactions between NFs and plant receptors to highlight and support further targeted validation in experiments.

In this study, we exploited the merits of molecular modeling to analyze the effect of specific chemical modifications in NF produced by *R. leguminosarum bv. viciae* on its interaction with the LykX-Sym10 receptor. For all possible LykX-Sym10-NF complexes, we performed two independent *in silico* validations – canonical MD and an original thermochemical-based pipeline – and obtained stable configurations in line with the observed pea phenotypes. The modeling analysis supported the *LykX* gene as a suitable determinant for *Sym2*.

MATERIALS AND METHODS

Sequence Analysis

We analyzed 95 amino acid sequences of *Ps*LykX receptor (MF155382–MF155469; MN187362–MN187364, and MN200353–MN200358; Sulima et al., 2017, 2019) and eight

amino acid sequences of *Ps*Sym10 receptor (MN727808, MN727809, MN727810, and MN727811 – this work; AJ575250, AJ575251, AJ575252, and AJ575253 – Madsen et al., 2003). Among the LykX sequences used in this study, seven represented the Afghanistan pea phenotype and 85 represented the European pea phenotype. According to the Sulima et al. (2019), the Afghanistan pea phenotype has two alleles, Afghan and Tajik, which were present in our dataset in five and two variants, respectively. Therefore, we separately analyzed three subsets of *Ps*LykX sequences based on the following pea alleles: Afghan, Tajik, and European. It should be noted that the names of alleles do not reflect the geographical origin of the corresponding pea samples. Within eight sequences of the *PsSym10* receptor gene, three belonged to Afghanistan phenotype, and five to the European phenotype (**Supplementary Table 1**).

Most of the analyzed sequences were obtained from previous studies, but four alleles of *PsSym10* (MN727808, MN727809, MN727810, and MN727811) were sequenced in the current study. DNA was extracted from young leaves (top or second-from-top node). Extraction was conducted according to the previously described CTAB protocol (Rogers and Bendich, 1985; Sulima et al., 2017). PCR was performed in 0.5 ml eppendorf-type microcentrifuge tubes on an iCycler (Bio-Rad, Hercules, CA, United States) or Dyad (Bio-Rad) thermocycler using the ScreenMix-HS kit (Evrogen, Moscow, Russia). The PCR cycling conditions were as follows: 95°C (5 min), 35 cycles [95°C (30 s), Tm (varying depending on primers; 30 s), 72°C (1 min)], and 72°C (5 min). The PCR fragments were sequenced using the ABI Prism 3500xL system (Applied Biosystems, Palo Alto, CA, United States) at the Genomic Technologies, Proteomics, and Cell Biology Core Center of the ARRIAM (St. Petersburg, Russia). PCR primer sequences are listed in **Supplementary Table 2**. The resulting sequences have been deposited into the NCBI database (see accession in **Supplementary Table 1**).

Extra-membrane domains of LykX and Sym10 receptors contain 212 and 226 amino acids, respectively. Sequences for LykX and Sym10 were aligned separately in Mega X using the MUSCLE algorithm (Kumar et al., 2018). In each alignment, we analyzed polymorphic positions within and between allele subsets and focused only on polymorphic positions found between subsets. We hypothesized that the polymorphisms found between subsets are responsible for the difference in pea phenotypes.

Protein Homology Modeling

Three LysM-containing kinase crystals were used as templates for the homology modeling of extracellular domains of the receptors: 5JCD of the *Oryza sativa* OsCEBiP chitin receptor (Liu et al., 2016), 4EBZ of the *Arabidopsis thaliana* AtCERK1 chitin elicitor receptor kinase (Liu et al., 2012), and 5LS2 of the *Lotus japonicus* LysM-containing protein (Bozsoki et al., 2017).

For European and Afghan alleles of the LykX and Sym10 proteins, the extracellular and transmembrane domains were predicted with three separate methods: SWISS-MODEL (Waterhouse et al., 2018), Iterative Threading ASSEmbly Refinement (I-Tasser) (Zhang, 2009), and Phyre2 (Kelley et al., 2015) algorithms. The structure of the Tajik allele of LykX was obtained by a single amino acid mutation (ARG75PRO) in the European model and then relaxed using the MM approach. For all five obtained models (3 for LykX and 2 for Sym10), we analyzed Ramachandran plots and RMSD deviations from the corresponding template geometry, and filtered out models with defective secondary structures of the LysM domains. Final models were prepared using Protein Preparation Wizard (Sastry et al., 2013; Schrödinger, 2021) and minimized in Maestro using OPLS3ext force field (Roos et al., 2019).

Protein-Protein Docking and Clustering of Dimers

For LykX-Sym10 pairs, we performed the protein-protein docking assay in the Piper package (Kozakov et al., 2006) and obtained 30 docking poses of dimers for each of the three pea alleles (European, Afghan, and Tajik).

Then, we clustered 90 obtained dimers (30 × 3) in the following way: using the Procrustes analysis (rotation and shift, without scaling; Rudemo, 2000), we placed all dimers into the comparable coordinates, so that LykX subunits of all dimers were matched in 3D. Positions of the remaining Sym10 subunits were different from each other, and we utilized this difference for clustering. For each pair of dimers, we calculated two measures of dissimilarity. For two dimers, the first measure was the angle formed by two lines drawn from the center of LykX toward two centers of Sym10. The second measure was the minimal correlation between X, Y, and Z coordinates of two Sym10 subunits. For each measure, we introduced a threshold: dimers were considered similar if the angle was lower than 45 and the minimal correlation was higher than 0.5. Then, we performed clustering based on the binary similarity matrix and found groups containing at least four pairwise similar dimers. Some of these groups had a non-empty intersection; hence, we merged them until the independent clusters were obtained. As was expected, several dimers were not clustered. For each cluster, we randomly chose a typical dimer and checked whether the mutual orientation of LykX and Sym10 domains and possible orientation of dimers to the cytoplasmic membrane were biologically justified.

Typical dimers for clusters were relaxed in an orthorhombic box for 50 ns in a TIP4P solvent by use of MD, Desmond-v5.4 package (Bowers et al., 2006) of Schrödinger 2018-2. The minimal initial distance between protein and simulation box border was 20 Å. Protein dimer poses obtained after trajectory clustering were employed for ligand docking assays. To identify binding energy between LykX and Sym10 proteins, the MM-GBSA approach was applied (Schrodinger, 2013).

Molecular Dynamics Parameters

Molecular dynamics was carried out in the Desmond-v5.4 package of Schrödinger 2018-2, using the TIP4P water solvent model; systems were neutralized by adding single-charged ions (Na^+ or Cl^-). In addition, 0.15 M of NaCl was added to emulate standard cytoplasmic ion concentration. MD properties were the following: ensemble class: NPT, thermostat method Nose-Hoover chain, barostat method Martyna-Tobias-Klein, relaxation

time 5 ps, temperature 300 K, pressure 1,013 bar, and interaction cutoff radius 9 Å. MD trajectories were clustered by the Desmond Trajectory Clustering package.

Stability of the Protein Dimers in the Cytoplasmic Membrane Model

As all three LykX-Sym10 dimers were stable in the solvent, we randomly selected one (the Afghan variant) to test its conformation stability in solvent together with the membrane. To assemble the membrane, transmembrane domains, and dimer into one complex, we performed the following steps. First, we modeled hydrophobic α-helices of LykX and Sym10 transmembrane domains and docked them to imitate the interaction between transmembrane domains in the LykX-Sym10 heterodimer. Second, we sewed subunits of LykX-Sym10 dimer to corresponding transmembrane domains *via* native peptide linkers through peptide bonds. Lastly, we applied MD in the solvent with the presence of the 1,2-dimyristoyl-sn-glycero-3-phosphorylcholine (DMPC) full-atom membrane model for 100 ns. The protein-lipid complex was placed in an orthorhombic box with the minimal distance between protein and simulation box borders equal to 30 Å.

Ligand Structure Preparation

We considered four types of NF structures according to the possible repertoire produced by *R. leguminosarum bv. viciae*. The analysis of NF conformer structures and their stability was carried out hierarchically. First, molecular mechanics (MM) was employed to perform the initial screening of NF conformers using the MMFF94 force field (Halgren, 1996) as implemented in the Frog2 program package (Miteva et al., 2010), and the 100 lowest-energy conformers were selected for each type of NF molecule. Second, an initial assessment of each conformer's stability in aqueous medium was carried out using the primitive implicit solvent model (COSMO). Third, based on the assessments, each NF conformer was refined by semi-empirical electronic structure calculations at the PM6-DH2X level (Řezáč and Hobza, 2011) using the MOPAC2016 program package (Stewart, 2016). For each NF, the 15 most stable conformers were then used in the docking procedure and in thermochemical analysis.

Ligand Docking

For ligand docking, the Glide-v7.9 package of Schrödinger 2018-2 was applied (Friesner et al., 2004). We ran two flexible XP dockings for each previously obtained typical dimer; grid boxes were centered on #44 and #76 polymorphic amino acids of the LykX protein. The internal size of each grid box was 30x30x30 Å, and the external size was 50x50x50 Å. Intramolecular hydrogen bonds were rewarded, and stereochemical transitions in ligand rings were strictly forbidden. Docking results contained the 10 best docking poses for each ligand. Docking poses were clusterized using the interaction fingerprints method, and the best pose for each ligand was selected by Glide Emodel criteria. Protein-ligand complexes with the best docking energy (Glide E) were chosen for each protein dimer pose.

Relaxation and Analysis of Protein-Ligand Complexes

Sym10-LykX-NF complexes were placed in an orthorhombic box and relaxed for 300 ns using the MD approach. The minimal distance between protein and simulation box borders was 20 Å. Obtained MD trajectories were clusterized by the Desmond Trajectory Clustering method. The MM-GBSA method was applied before and after MD to identify binding energy between (i) LykX and Sym10 proteins and (ii) Sym10-LykX dimers and NF ligands.

Quantum Mechanical Parameters

Quantum mechanical gas-phase calculations were carried out using the ORCA program package (ver. 4.0.1; Neese, 2018). All structures were re-optimized using the higher-level composite RI-B97-3c method (Brandenburg et al., 2018). The energies of solvated structures were estimated by applying the hybrid COSMO-RS solvation model (Klamt and Eckert, 2004) using the CosmoTherm 16 program (Grimme, 2012) The COSMO-RS correction was applied to the DFT results obtained at the BP86/TZVP level of theory (Becke, 1988; Weigend and Ahlrichs, 2005) as a recommended procedure for the COSMO-RS calculations (Hellweg and Eckert, 2017).

RESULTS

Sequence Analysis

Ninety-five sequences of *P. sativum LykX* gene contained 23 polymorphic sites; the difference between two sequences was 4.7 amino acid positions on average. Among 23 sites, only four demonstrated polymorphisms between pea alleles: amino acids #44, #45, #75, and #76 (**Figure 1A**). Some of these four positions may potentially be responsible for the difference in European and Afghan pea phenotypes. It should be noted that European and Tajik *LykX* alleles are more similar to each other than to the Afghan allele variant. For modeling, we took the most frequent *LykX* sequence within each of the three groups of alleles.

Analysis of *Sym10* sequences revealed only one valine-isoleucine polymorphism at #221 position, which was not specific for any pea allele, and valine-isoleucine substitution that was almost insignificant at both structural and chemical levels. This allowed us to conclude that the Sym10 gene sequence is universal for Afghan, Tajik, and European alleles, and guided us to use one Sym10 protein model in all further experiments.

A comparative table of polymorphisms in *LykX* and *Sym10* amino acid sequences is presented in **Supplementary Table S3**.

Protein Model Reconstruction

As templates for modeling, we utilized three crystal structures of three plant chitin receptors from the PDB database: 5JCD, 4EBZ, and 5LS2. The similarity values between target protein sequences (LykX or Sym10) and all templates were higher than 18% (**Supplementary Table 4**), but the highest values

were observed for the 5LS2 template in all cases. Therefore, we used this template to model both LykX and Sym10.

We performed modeling by three different servers: the I-Tasser method (threading), the SWISS-MODEL pipeline (homology modeling), and the Phyre2 algorithm (homology modeling and threading). Analysis of Ramachandran plots and βααβ motifs of LysM domains revealed that the I-Tasser server predicted the most appropriate structures of both LykX and Sym10 receptors. After fold recognition, all models were relaxed by the energy minimization approach in Schrödinger using the implicit GB/SA water solvent model.

We constructed LykX models of European, Afghan, and Tajik alleles separately and observed that amino acids polymorphisms in the variants had no significant impact on both secondary and 3D structures of LysM domains (**Figure 1C**).

LykX-Sym10 Dimer Assembly

We performed protein-protein docking of LykX and Sym10 proteins for each of three *P. sativum* alleles; in each case, we obtained 30 configurations of LykX-Sym10 complexes. Then, 90 models (3 × 30) were clustered and four distinct clusters consisting of 39 dimers in total were found (**Supplementary Figure 1**). After that, clusters with biologically inadequate dimer subunit orientations were filtered out. Only one cluster (**Supplementary Figure 1**) had dimers that met all necessary conditions. This cluster contained dimers of all three pea alleles.

From the remaining cluster, we randomly chose dimers corresponding to each pea subpopulation (IDs: A01, T00, and E25 in **Supplementary Data 1**) and relaxed these variants in water using MD for 50 ns. Analysis of trajectories and Gibbs energy demonstrated the stability of the dimer that allowed us to consider this dimer as potentially existing in the solvent.

Membrane Model Emulation

The simulation trajectory contained two clusters. For both clusters, the RMSD from the initial geometry was around 6 Å, with flexible linker fragments providing the main contribution. The closest distance between transmembrane domains was 10.8 Å, which corresponds to the semi-bounded condition for transmembrane domains (Polyansky et al., 2012). The structure of the dimer was stable during the simulation, and moved closer to the membrane after the relaxation of linker fragments (**Figure 2B**). Therefore, we can conclude that the obtained orientation of subunits in the LykX-Sym10 dimer may exist.

Protein-Ligand Docking

To determine the mechanism of NF reception, all four NF types were separately docked into three dimers corresponding to three *P. sativum* alleles. We considered a dimer to recognize a NF if the fatty acid was caught in the hydrophobic pocket (cave) between the LykX and Sym10 proteins. Otherwise, plant root cells could not distinguish NFs from chitin and chitosan oligomers and trigger the early symbiotic cascades instead of an immune response. We propose that the hydrophobic recognition of the NF fatty tail by the pocket occurs at the structural level. Therefore, any structural variability in the NF tail (i.e., chain length or double bond positions) can potentially have an impact on NF-dimer specificity. This conclusion is in line with previous results, where the correspondence between population diversities of the rhizobial nodA gene (coding for the acyltransferase involved in the fatty acid tail decoration of the NF) and plant heterodimeric receptor genes was demonstrated (Igolkina et al., 2019). Plausible mechanisms of this linkage, namely coordinated variability of amino acids in contact with the surface of the receptor dimer adjacent to the NF fatty tail, were proposed (Igolkina et al., 2018). Other earlier works (Debellé et al., 1996; Ritsema et al., 1996; Moulin et al., 2004; Wu et al., 2011) also showed that nodA gene variability relates to the bacterial host range specificity. Summarizing the above, we can assume that coordinated variability of the fatty tail structure and receptor regions interacting with the fatty tail is one of the possible ways to fine-tune host specificity in legume-rhizobial symbiosis.

Based on protein-ligand docking results, NF5Ac and NF4Ac were recognized by all three dimers; NF5NonAc and NF4NonAc were recognized only by Tajik and European dimers, respectively, while Afghan dimers did not recognize any non-acetylated NFs (**Figures 2A,C**). The total number of successful NF binding is eight. In each of these complexes, at least four NF-protein hydrogen bonds were formed, except T-NF5NonAc, in which only three bonds were detected (**Supplementary Figure 2**). LykX protein played the primary role in NF recognition, while Sym10 was involved in ligand reception only in T-NF(4,5)Ac and E-NF4NonAc complexes and seemed to act as a supporter kinase. We analyzed common amino acid residues contacting the NF and observed that Asn48 of the LykX protein was involved in NF recognition in at least five out of eight poses. At the same time, between-allele polymorphic positions in LykX – #44 and #45 – interacted with NF in the most poses. Polymorphic LykX residue #75 partly interacted with NF5Ac in Afghan and European dimers. This residue was also located in a close proximity to NFs in all other docking poses, influencing NF recognition indirectly. Some LykX amino acids were principal for the interaction with specific NF types, e.g., Asn59 took part in NF5Ac reception by both Afghan and Tajik dimers, and Thr47 was essential for NF4Ac recognition by European and Afghan dimers. The hydrophobic pocket for NF fatty tail perception was found to be formed mostly by Val37, Met38, Pro39, Ala40, Phe41, Leu42, Leu43, Tyr119, and Ala121 residues of LykX and Val217 and Phe218 residues of the Sym10 protein.

MD Relaxation of Protein-Ligand Complexes

Along the MD trajectories, all NF-LykX-Sym10 complexes stably interacted with NF in the following manner: the NF fatty acyl tail was located in a hydrophobic pocket between dimer subunits (except T-NF5NonAc), and the NF chitin core was abundantly hydrated, forming many water bridges to dimer residues (**Figure 2D**).

The principal residues involved in NF reception before and after MD were similar (**Supplementary Table 5**). The Asn48 of the LykX protein was principal for NF recognition in all

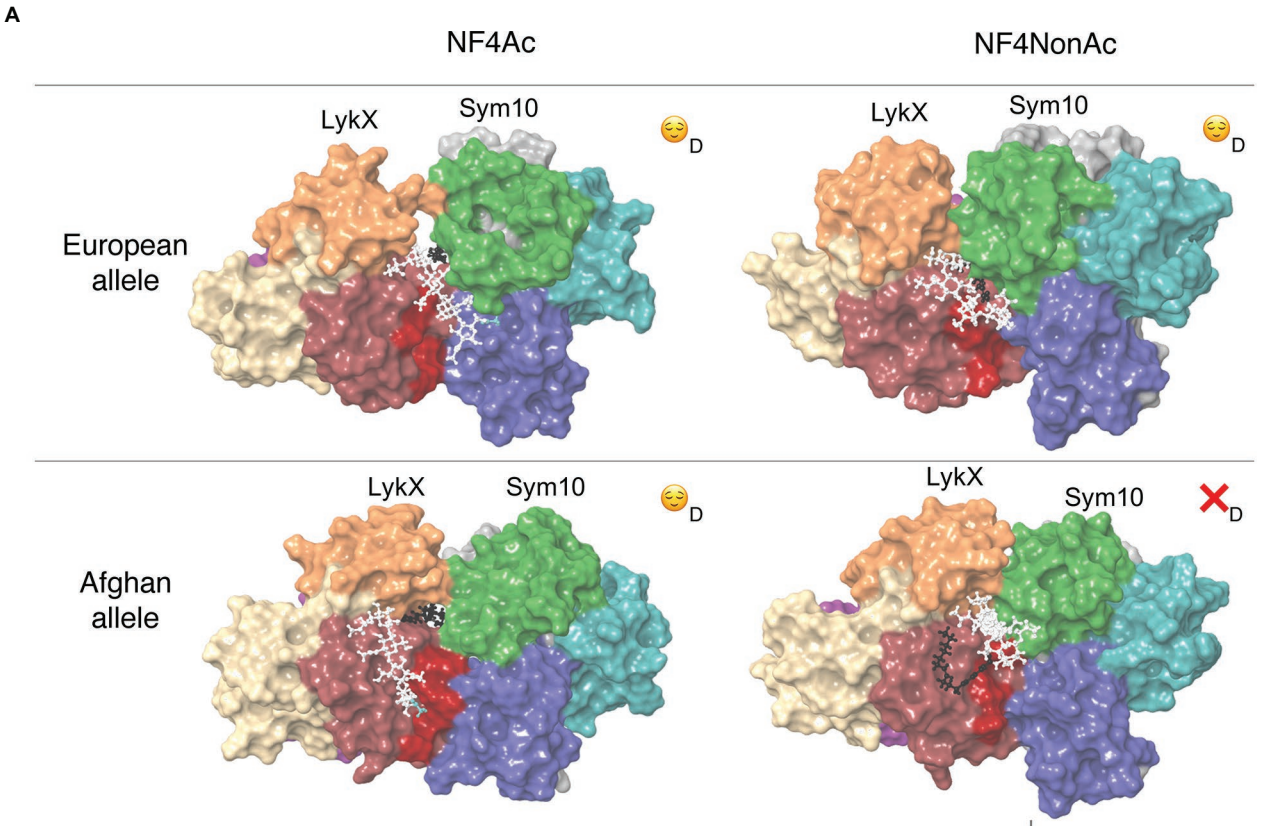

FIGURE 2 | (A) Four docking poses after docking. NFs core is colored with white, fatty tail – with black, and acetylation – with blue. **(B)** LykX-Sym10 dimer with transmembrane domains and membrane after 100 ns molecular dynamics (MD); **(C)** Table with successful and unfavorable NF-LykX-Sym10 complexes; **(D)** QR-code to the video with the MD simulation of the NF5Ac-LykX-Sym10 complex (Tajik alleles); NPT ensemble, 300 K, 500 ns, TIP4P water molecules are hidden.

performed MD, hence we can consider it as one of the key residues in NF reception, along with #44 and #45 polymorphic residues. The role of #75 and #76 polymorphic residues in the LykX protein is less evident; they do not form contacts with NFs during MD, but could be critical in early stages of NF recognition, forming the steric landscape on the dimer surface. The Phe41 residue of LykX interacted with the fatty acyl group in all MD. The contribution of other amino acids

(Tyr35, Met38, and Leu42) from the hydrophobic pocket was less pronounced and could vary.

To additionally prove the relevance of predicted NF-dimer complexes, we examined the possible mechanism of NF reception directly from the solvent. As previously demonstrated, the NF-dimer contact zone is composed of two different parts: hydrophilic contact with the NF core and hydrophobic contact with a fatty tail. However, the question remained as to what occurs first. We supposed that the primary contacts between NF and dimer are hydrophilic contacts, as they are (i) more probable in solvent and (ii) localized on the dimer surface. After the hydrophilic contacts are established, the NF fatty tail penetrates the hydrophobic pocket if their structures fit together. For this experiment, we placed NF5Ac close to the Tajik dimer surface at the previously discovered docking site nearby and MD was performed for 500 ns. We observed T-NF5Ac complex formation within 20 ns. During the first stage, the NF hydrophilic core was caught by a few separate non-stable hydrogen bonds and the fatty acid was pushed by the water molecules into the hydrophobic cave formed between both proteins. This led to the small rearrangement of LykX-Sym10 complex geometry and the effective recognition of the NF hydrophilic region by protein dimer (**Supplementary Video**). Thus, the principal role of LykX-Sym10 amino acid interface and the fatty acid in NF reception was proven.

Thermochemical Verification of Ligand-Receptor Complex Formation

During the formation of a ligand-receptor complex, NF changes its conformation in solvent from the free state into the binding pose. To estimate the thermodynamic benefit and principal opportunity of this transition, we computed the lowest energies of NF geometries in several states using the quantum mechanical calculations (**Figure 3**). The "stable" state describes the lowest energy NF conformation in gas (vacuum). The "active" NF state is obtained after docking with a dimer with further re-optimization in vacuum. For both states, we added solvent corrections, re-optimized NF conformations, and obtained "stable solvated" and "active solvated" states, respectively. We also introduced "bonded" energy, representing "active solvated" energy accounting for the docking energy (**Figure 3**). For each state, we calculated ΔG energy, set the "stable solvated" state as the reference point, and compared all other states with this reference point. As a result, we obtained ΔΔG energies reflecting energies of states subtracting ΔG ("stable solvated"). We then applied the following filtration criteria: negative "bonded" energy corresponds to potentially active NF molecules, while its positive value indicates impossible states. Based on these criteria, six out of eight successful docking poses were considered to be thermodynamically advantageous for forming ligand-receptor complexes. Two complexes containing acetylated NF with four

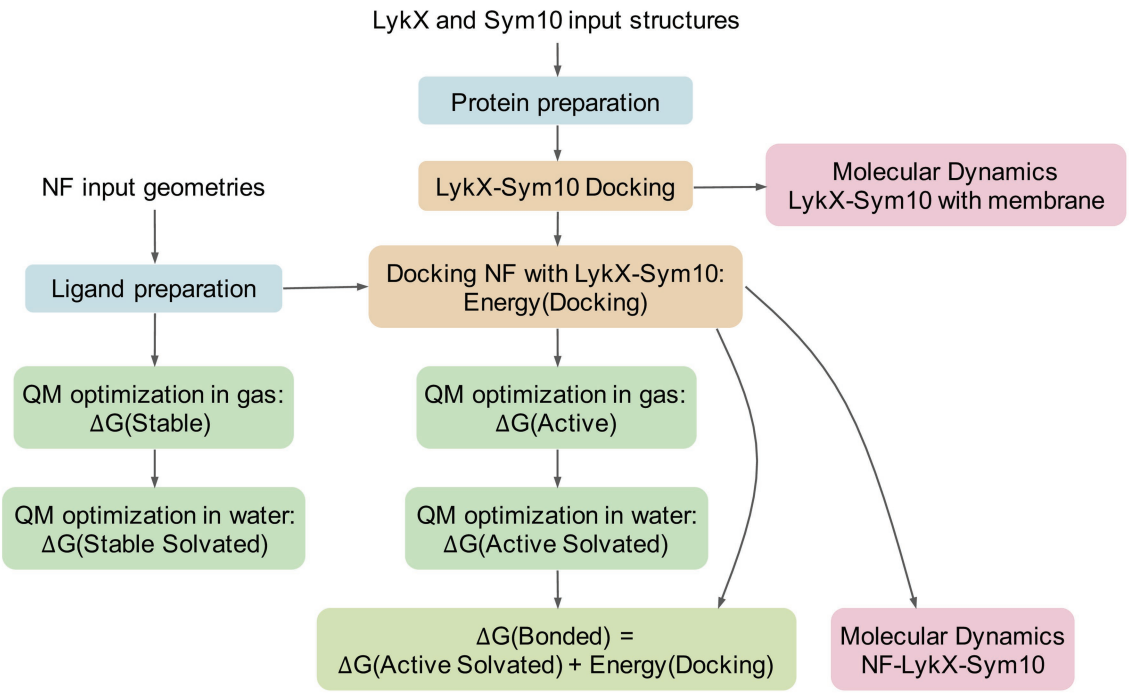

FIGURE 3 | Pipeline of the analysis. Same colors highlight technically or logically similar steps. The pipeline has two inputs: receptors and NFs. At the first stage, all molecules pass the special preparation procedures (blue boxes). Then, the LykX-NF-Sym10 complex is successively assembled: first, docking of LykX and Sym10, and then, docking of the NF to the LykX-Sym10 heterodimer (yellow boxes). To evaluate the stability of the LykX-NF-Sym10 complex and the LykX-Sym10 complex in the presence of membrane, molecular dynamics is applied (pink boxes). To assess thermodynamically advantageous LykX-NF-Sym10 complexes in water, quantum mechanical methods (QM) are used in different modes (green boxes). The comparison of obtained energies results in ΔG(Bonded) energy, which means the NF's energy in the optimized docking pose in the presence of water accounting for the heterodimer docking energy. The negative ΔG(Bonded) corresponds to the thermodynamic benefit of the LykX-NF-Sym10 complex over the LykX-Sym10 complex.

chitins in the backbone – E-NF4Ac and A-NF4Ac – were filtered out (**Supplementary Figure 3**).

DISCUSSION

We studied a possible source of variability in pea symbiotic phenotypes while interacting with *rhizobia*. In brief, (i) in addition to the European phenotype, the non-classical Afghanistan symbiotic pea phenotype was identified in 1978 (Lie, 1978); (ii) in 2003, it was first shown that legume receptors recognize rhizobial NFs working in pairs (Radutoiu et al., 2003), and (iii) after a relatively long lag, a putative pair of NF receptors in pea – LykX and Sym10 – was suggested based on sequence comparative analysis (Sulima et al., 2017).

The proposed pair of receptors requires experimental confirmation, for example, by studying mutants of LykX (currently in progress by Zhukov V.) in interactions with Sym10 in the yeast two-hybrid system. However, this approach may only justify the involvement of the target gene in controlling the Afghanistan phenotype, but may not validate the direct interaction between the mutant LykX-Sym10 receptor and NFs. Experimental detection of the NF-LykX-Sym10 interaction is difficult because of challenges in isolating the receptor heterodimer in its natural form.

Due to the complexity of the system under study, molecular modeling is a promising way to test whether the LykX-Sym10 heterodimer is the NF receptor responsible for European/Afghanistan symbiotic phenotypes. We considered four stages in the assembly of the NF-LykX-Sym10 complex and performed molecular modeling of each of them (**Figure 3**):

1. Stability of the LykX-Sym10 heterodimer in solvent in the presence of a membrane by MD.
2. Successful docking of NF to LykX-Sym10.
3. Stability of the NF-LykX-Sym10 complex in solvent during MD.
4. Possibility of NF-LykX-Sym10 complex formation in terms of thermodynamic benefits.

We not only demonstrated that LykX-Sym10 is stable in solvent in the presence of a membrane, but also found that LykX-Sym10 heterodimers of both European and Afghanistan phenotypes have the same 3D configuration. The natural and non-deleterious amino acid polymorphisms in receptors should not significantly impact their mutual disposition in a correctly working dimer. Therefore, the observed match in dimer structures likely indicates that the obtained LykX-Sym10 configuration is correct. Moreover, this configuration corresponds to the previously proposed stable "sandwich-like" configuration (Igolkina et al., 2018), where a LysM domain of one subunit binds between LysM2 and LysM3 domains of another subunit. This 3D conservatism of the LykX-Sym10 structure could be a criterion for filtering legume receptor dimers in other modeling studies.

Analysis of NF docking poses in LykX-Sym10 revealed that in most cases (8 out of 12); the NF fatty acid tail was located in the hydrophobic pocket formed by the contact zone of two receptor subunits. This result is also in line with the previously elucidated stable configuration (Igolkina et al., 2018). Therefore, we considered these eight poses to be biologically justified. It should be noted that only non-acetylated NFs were involved in four unsuccessful docking poses.

For each of eight NF-LykX-Sym10 complexes we applied both MD and thermodynamic analysis, each playing the filtration role. It is important to emphasize that these steps are independent and answer different questions: (i) whether the complex is stable and (ii) whether the complex is possible, respectively. Sets of NF-LykX-Sym10 complexes, which were filtered out by each procedure, were not overlapped, which demonstrates that MD and thermodynamic calculations cannot be interchangeable steps.

During the thermodynamic calculations, we compared ΔG energies of NF in different states assuming that biologically active NF geometries correspond to stable states. The chemical structure of NF makes it very flexible, which leads to the plurality of conformations. We assumed that NF stable states could be biologically active if their free energies allow them to interact with the dimer. This assumption is in line with our observation about the conservatism of LykX-Sym10 configurations. Summarizing all together, we can speculate that the conservatism or stability of molecular structures is the important property for biological functioning, and should be taken into account during filtration of biologically justifying models.

Only five out of 12 NF-LykX-Sym10 complexes successfully passed all steps of the analysis (**Figure 2C**), and they precisely match the known pea symbiotic differences: peas of European phenotype can form a symbiosis with *R. leguminosarum bv. viciae*, producing both acetylated and non-acetylated NFs, while peas of Afghanistan phenotype react on only acetylated NFs. It is important to note that all the LykX-Sym10 heterodimer complexes considered here formed successful complexes with NF5Ac. Based on our analysis and match between estimated and observed pea phenotypes, we can conclude that the *LykX* gene is a suitable candidate gene for *Sym2*.

Our results are in line with the recent experimental study demonstrating the LysM1 domain in plant LysM-RLKs as a determinant in specific recognition and discrimination of NFs and chitin ligands (Bozsoki et al., 2017). Authors constructed chimeric Lotus receptors combining segments of NFR1 and CERK6 genes and tested nodulation activity of *nfr1* loss-of-function mutants transformed with chimeric vectors. The presence of NFR1 LysM1 domain in a chimeric receptor induced nodule formation, and, additionally, the point mutations in the II and IV regions of the LysM1 domain caused the absence of symbiotic signaling both in native and chimeric proteins. In our study, all mutations in the LykX receptor segregating Afghanistan and European peas are also located in the II and in the IV regions of LysM1 domain (44, 45 and 75, 76 positions, correspondingly). Based on the modeling, the LysM1 domain of LykX receptor plays a premier role in the NF perception.

Our molecular modeling indicated some properties of the NF-LykX-Sym10 complex that allow us to hypothesize a reasonable idea of NF's role in initiating intracellular

phosphorylation cascade. LykX and Sym10 receptors belong to LysM-RLKs, which have three extracellular LysM domains, a transmembrane domain, an intracellular protein kinase domain, and, what is often without due attention, a linker sequence connecting LysMs and the transmembrane domain. Linkers in pea LYK and LYR receptors are unstructured (i.e., flexible) and quite long, and LykX and Sym10 are no exception. We performed the molecular dynamics (MD) of LykX and Sym10 with membrane and demonstrated that, due to of the linkers' structure, trajectories of the extracellular parts faintly relate to movements of transmembrane domains. Hence, a signal from the extracellular domains to intracellular ones is likely not transmitted mechanically. Therefore, initiation of the intracellular phosphorylation cascade probably occurs after the convergence and subsequent interaction of kinase domains. However, the LysM-RLKs receptors work in pairs and form dimers before NFs perception, as was demonstrated both experimentally (Kirienko et al., 2018) and *in silico* (Igolkina et al., 2018). The lifetime of dimers should be long enough to catch NFs, but short enough to prevent the false initiation. Thus, we hypothesize that the role of NFs is to specifically stabilize receptor dimers, providing enough time for interaction of kinase domains to run the downstream phosphorylation cascade. To extend this assumption to other legume species, we considered candidate genes to form the NF receptor heterodimer in *Medicago truncatula* (*MtLYK3* and *MtNFP* genes) and *L. japonicus* (*LjNFR1* and *LjNFR5* genes). Then, we estimated their secondary structure with Jpred (Drozdetskiy et al., 2015) and assess the structure of linkers between LysM3 domains and transmembrane domains. The average length was 20aa, and in all cases, it was unstructured, which makes our proposal extendable to other species (the estimated secondary structures are in **Supplementary Data**).

In sum, molecular modeling has shown itself to be an effective way of functional analysis complementary to traditional approaches, and its results provide appealing directions for further studies in this area, such as determining functional meaning of minor components of NF mixtures produced by *rhizobia*, or reconstruction of the evolutionary history of signal systems in plant-microbe interactions.

DATA AVAILABILITY STATEMENT

The datasets presented in this study can be found in online repositories. The names of the repository/repositories and accession number(s) can be found in the article/**Supplementary Material**.

AUTHOR CONTRIBUTIONS

YS and AI contributed equally. The methodology was developed by EP, YS, AI, and YP. Data analysis was performed by YS, AI, and PK. Visualization was performed by YS and AI. 3D modeling and QM calculations were performed by YS and PK. Initial writing and draft preparation were done by YS and AI. Review and editing were made by all authors. Data are curated by AS and VZ. Software is provided by YP and EP. All authors contributed to the article and approved the submitted version.

FUNDING

This work has been supported by the Russian Science Foundation # 19-16-00081.

ACKNOWLEDGMENTS

Quantum chemical calculations were carried out using SurfSara supercomputer facilities with a support from NWO.

SUPPLEMENTARY MATERIAL

The Supplementary Material for this article can be found online at: https://www.frontiersin.org/articles/10.3389/fpls.2021.642591/full#supplementary-material

REFERENCES

Arrighi, J.-F. (2006). The *Medicago truncatula* lysine motif-receptor-Like kinase gene family includes NFP and new nodule-expressed genes. *Plant Physiol.* 142, 265–279. doi: 10.1104/pp.106.084657

Baldwin, I. L., Fred, E. B., and Hastings, E. G. (1927). Grouping of legumes according to biological reactions of their seed proteins. Possible explanation of phenomenon of cross inoculation. *Bot. Gaz.* 83, 217–243. doi: 10.1086/333728

Becke, A. D. (1988). Density-functional exchange-energy approximation with correct asymptotic behavior. *Phys. Rev. A* 38:3098. doi: 10.1103/PhysRevA.38.3098

Bensmihen, S., de Billy, F., and Gough, C. (2011). Contribution of NFP LysM domains to the recognition of Nod factors during the *Medicago truncatula*/*Sinorhizobium meliloti* Symbiosis. *PLoS One* 6:e26114. doi: 10.1371/journal.pone.0026114

Bowers, K. J., Sacerdoti, F. D., Salmon, J. K., Shan, Y., Shaw, D. E., Chow, E., et al. (2006). "Molecular dynamics – scalable algorithms for molecular dynamics simulations on commodity clusters." in *Proceedings of the 2006 ACM/IEEE conference on Supercomputing - SC'06;* November 11-17, 2006.

Bozsoki, Z., Cheng, J., Feng, F., Gysel, K., Vinther, M., Andersen, K. R., et al. (2017). Receptor-mediated chitin perception in legume roots is functionally separable from Nod factor perception. *Proc. Natl. Acad. Sci. U. S. A.* 114, E8118–E8127. doi: 10.1073/pnas.1706795114

Brandenburg, J. G., Bannwarth, C., Hansen, A., and Grimme, S. (2018). B97-3c: a revised low-cost variant of the B97-D density functional method. *J. Chem. Phys.* 148:064104. doi: 10.1063/1.5012601

Broghammer, A., Krusell, L., Blaise, M., Sauer, J., Sullivan, J. T., Maolanon, N., et al. (2012). Legume receptors perceive the rhizobial lipochitin oligosaccharide signal molecules by direct binding. *Proc. Natl. Acad. Sci. U. S. A.* 109, 13859–13864. doi: 10.1073/pnas.1205171109

Buendia, L., Girardin, A., Wang, T., Cottret, L., and Lefebvre, B. (2018). LysM receptor-like kinase and LysM receptor-Like protein families: an update on phylogeny and functional characterization. *Front. Plant Sci.* 9:1531. doi: 10.3389/fpls.2018.01531

Davis, E. O., Evans, I. J., and Johnston, A. W. B. (1988). Identification of nodX, a gene that allows *Rhizobium leguminosarum* biovar viciae strain TOM to nodulate Afghanistan peas. *Mol. Gen. Genet.* 212, 531–535. doi: 10.1007/BF00330860

Debellé, F., Plazanet, C., Roche, P., Pujol, C., Savagnac, A., Rosenberg, C., et al. (1996). The NodA proteins of *Rhizobium meliloti* and *Rhizobium tropici* specify the N-acylation of Nod factors by different fatty acids. *Mol. Microbiol.* 22, 303–314. doi: 10.1046/j.1365-2958.1996.00069.x

Denarie, J. (1996). *Rhizobium* lipo-chitooligosaccharide nodulation factors: signaling molecules mediating recognition and morphogenesis. *Annu. Rev. Biochem.* 65, 503–535. doi: 10.1146/annurev.bi.65.070196.002443

Drozdetskiy, A., Cole, C., Procter, J., and Barton, G. J. (2015). JPred4: a protein secondary structure prediction server. *Nucleic Acids Res.* 43, W389–W394. doi: 10.1093/nar/gkv332

Firmin, J. L., Wilson, K. E., Carlson, R. W., Davies, A. E., and Downie, J. A. (1993). Resistance to nodulation of cv. Afghanistan peas is overcome by nodX, which mediates an O-acetylation of the *Rhizobium leguminosarum* lipo-oligosaccharide nodulation factor. *Mol. Microbiol.* 10, 351–360. doi: 10.1111/j.1365-2958.1993.tb01961.x

Friesner, R. A., Banks, J. L., Murphy, R. B., Halgren, T. A., Klicic, J. J., Mainz, D. T., et al. (2004). Glide: a new approach for rapid, accurate docking and scoring. 1. Method and assessment of docking accuracy. *J. Med. Chem.* 47, 1739–1749. doi: 10.1021/jm0306430

Grimme, S. (2012). Supramolecular binding thermodynamics by dispersion-corrected density functional theory. *Chem. Eur. J.* 18, 9955–9964. doi: 10.1002/chem.201200497

Halgren, T. A. (1996). Merck molecular force field. I. Basis, form, scope, parameterization, and performance of MMFF94. *J. Comput. Chem.* 17, 490–519. doi: 10.1002/(SICI)1096-987X(199604)17:5/6<490::AID-JCC1>3.0.CO;2-P

Hellweg, A., and Eckert, F. (2017). Brick by brick computation of the gibbs free energy of reaction in solution using quantum chemistry and COSMO-RS. *AICHE J.* 63, 3944–3954. doi: 10.1002/aic.15716

Igolkina, A. A., Bazykin, G. A., Chizhevskaya, E. P., Provorov, N. A., and Andronov, E. E. (2019). Matching population diversity of rhizobial nodA and legume NFR5 genes in plant–microbe symbiosis. *Ecol. Evol.* 9, 10377–10386. doi: 10.1002/ece3.5556

Igolkina, A. A., Porozov, Y. B., Chizhevskaya, E. P., and Andronov, E. E. (2018). Structural insight into the role of mutual polymorphism and conservatism in the contact zone of the NFR5–K1 heterodimer with the nod factor. *Front. Plant Sci.* 9:344. doi: 10.3389/fpls.2018.00344

Kelley, L. A., Mezulis, S., Yates, C. M., Wass, M. N., and Sternberg, M. J. E. (2015). The Phyre2 web portal for protein modeling, prediction and analysis. *Nat. Protoc.* 10, 845–858. doi: 10.1038/nprot.2015.053

Kirienko, A. N., Porozov, Y. B., Malkov, N. V., Akhtemova, G. A., Le Signor, C., Thompson, R., et al. (2018). Role of a receptor-like kinase K1 in pea *Rhizobium symbiosis* development. *Planta* 248, 1101–1120. doi: 10.1007/s00425-018-2944-4

Kirienko, A. N., Vishnevskaya, N. A., Kitaeva, A. B., Shtark, O. Y., Kozyulina, P. Y., Thompson, R., et al. (2019). Structural variations in LysM domains of LysM-RLK psK1 may result in a different effect on Pea–Rhizobial symbiosis development. *Int. J. Mol. Sci.* 20:1624. doi: 10.3390/ijms20071624

Klamt, A., and Eckert, F. (2004). Prediction of vapor liquid equilibria using COSMOtherm. *Fluid Phase Equilib.* 217, 53–57. doi: 10.1016/j.fluid.2003.08.018

Kozakov, D., Brenke, R., Comeau, S. R., and Vajda, S. (2006). PIPER: An FFT-based protein docking program with pairwise potentials. *Proteins* 65, 392–406. doi: 10.1002/prot.21117

Kozik, A., Heidstra, R., Horvath, B., Kulikova, O., Tikhonovich, I., Ellis, T. H. N., et al. (1995). Pea lines carrying syml or sym2 can be nodulated by *Rhizobium* strains containing nodX; sym1 and sym2 are allelic. *Plant Sci.* 108, 41–49. doi: 10.1016/0168-9452(95)04123-C

Kozik, A., Matvienko, M., Scheres, B., Paruvangada, V. G., Bisseling, T., van Kammen, A., et al. (1996). The pea early nodulin gene PsENOD7 maps in the region of linkage group I containing sym2 and leghaemoglobin. *Plant Mol. Biol.* 31, 149–156. doi: 10.1007/BF00020614

Kumar, S., Stecher, G., Li, M., Knyaz, C., and Tamura, K. (2018). MEGA X: molecular evolutionary genetics analysis across computing platforms. *Mol. Biol. Evol.* 35, 1547–1549. doi: 10.1093/molbev/msy096

Lie, T. A. (1978). Symbiotic specialisation in pea plants: the requirement of specific *Rhizobium* strains for peas from Afghanistan. *Ann. Appl. Biol.* 88, 462–465. doi: 10.1111/j.1744-7348.1978.tb00743.x

Liu, T., Liu, Z., Song, C., Hu, Y., Han, Z., She, J., et al. (2012). Chitin-induced dimerization activates a plant immune receptor. *Science* 336, 1160–1164. doi: 10.1126/science.1218867

Liu, S., Wang, J., Han, Z., Gong, X., Zhang, H., and Chai, J. (2016). Molecular mechanism for fungal cell wall recognition by rice chitin receptor OsCEBiP. *Structure* 24, 1192–1200. doi: 10.1016/j.str.2016.04.014

Madsen, E. B., Madsen, L. H., Radutoiu, S., Olbryt, M., Rakwalska, M., Szczyglowski, K., et al. (2003). A receptor kinase gene of the LysM type is involved in legumeperception of rhizobial signals. *Nature* 425, 637–640. doi: 10.1038/nature02045

Mergaert, P, and Van Montagu, M. (1997). Molecular mechanisms of Nod factor diversity. *Mol. Microbiol.* 25, 811–817.

Miteva, M. A., Guyon, F., and Tufféry, P. (2010). Frog2: efficient 3D conformation ensemble generator for small compounds. *Nucleic Acids Res.* 38, W622–W627. doi: 10.1093/nar/gkq325

Moulin, L., Béna, G., Boivin-Masson, C., and Stępkowski, T. (2004). Phylogenetic analyses of symbiotic nodulation genes support vertical and lateral gene co-transfer within the *Bradyrhizobium* genus. *Mol. Phylogenet. Evol.* 30, 720–732. doi: 10.1016/S1055-7903(03)00255-0

Neese, F. (2018). Software update: the ORCA program system, version 4.0. Wiley Interdisciplinary Reviews: Computational Molecular Science.

Oldroyd, G. E. D. (2013). Speak, friend, and enter: signalling systems that promote beneficial symbiotic associations in plants. *Nat. Rev. Microbiol.* 11, 252–263. doi: 10.1038/nrmicro2990

Ovtsyna, A. O., Rademaker, G. J., Esser, E., Weinman, J., Rolfe, B. G., Tikhonovich, I. A., et al. (1999). Comparison of characteristics of the nodX genes from various *Rhizobium leguminosarum* strains. *Mol. Plant-Microbe Interact.* 12, 252–258. doi: 10.1094/MPMI.1999.12.3.252

Polyansky, A. A., Volynsky, P. E., and Efremov, R. G. (2012). Multistate organization of transmembrane helical protein dimers governed by the host membrane. *J. Am. Chem. Soc.* 134, 14390–14400. doi: 10.1021/ja303483k

Provorov, N. A.. (1994). The interdependence between taxonomy of legumes and specificity of their interaction with rhizobia in relation to evolution of the symbiosis. *Symbiosis.* 17, 183–200.

Radutoiu, S., Madsen, L. H., Madsen, E. B., Felle, H. H., Umehara, Y., Grønlund, M., et al. (2003). Plant recognition of symbiotic bacteria requires two LysM receptor-like kinases. *Nature* 425, 585–592. doi: 10.1038/nature02039

Radutoiu, S., Madsen, L. H., Madsen, E. B., Jurkiewicz, A., Fukai, E., Quistgaard, E. M. H., et al. (2007). LysM domains mediate lipochitin – oligosaccharide recognition and Nfr genes extend the symbiotic host range. *EMBO J.* 26, 3923–3935. doi: 10.1038/sj.emboj.7601826

Řezáč, J., and Hobza, P. (2011). A halogen-bonding correction for the semiempirical PM6 method. *Chem. Phys. Lett.* 506, 286–289. doi: 10.1016/j.cplett.2011.03.009

Ritsema, T., Wijfjes, A. H. M., Lugtenberg, B. J. J., and Spaink, H. P. (1996). Rhizobium nodulation protein NodA is a host-specific determinant of the transfer of fatty acids in Nod factor biosynthesis. *Mol. Gen. Genet.* 251, 44–51. doi: 10.1007/BF02174343

Rogers, S. O., and Bendich, A. J. (1985). Extraction of DNA from milligram amounts of fresh, herbarium and mummified plant tissues. *Plant Mol. Biol.* 5, 69–76. doi: 10.1007/BF00020088

Roos, K., Wu, C., Damm, W., Reboul, M., Stevenson, J. M., Lu, C., et al. (2019). OPLS3e: extending force field coverage for drug-Like small molecules. *J. Chem. Theory Comput.* 15, 1863–1874. doi: 10.1021/acs.jctc.8b01026

Rudemo, M.. (2000). Statistical Shape Analysis. I. L. Dryden and K. V. Mardia, Wiley, Chichester (1998). No. of pages: xvii+347. Price: £60.00.ISBN 0-471-95816-6. *Statistics in Medicine.* 19, 2716–2717.

Sastry, G. M., Adzhigirey, M., Day, T., Ramakrishna, A., and Sherman, W. (2013). Protein and ligand preparation: parameters, protocols, and influence on virtual screening enrichments. *J. Comput. Aided Mol. Des.* 27, 221–234. doi: 10.1007/s10822-013-9644-8

Schrodinger, LLC (2013). MacroModel, Version 10.2. New York (NY).

Schrödinger (2021). Protein Preparation Wizard | Schrödinger. Schrödinger Release 2021-1.

Sears, O. H., and Carroll, W. R. (1927). Cross inoculation with cowpea and soybean nodule bacteria. *Soil Sci.* 24, 413–420. doi: 10.1097/00010694-192712000-00003

Stewart, JJP. (2016). MOPAC2016. Impact, Schrödinger, LLC, New York, NY; Prime, Schrödinger, LLC, New York, NY, 2021.

Sulima, A. S., Zhukov, V. A., Afonin, A. A., Zhernakov, A. I., Tikhonovich, I. A., and Lutova, L. A. (2017). Selection signatures in the first exon of paralogous receptor kinase genes from the Sym2 region of the *Pisum sativum* L. genome. *Front. Plant Sci.* 8:1957. doi: 10.3389/fpls.2017.01957

Sulima, A. S., Zhukov, V. A., Kulaeva, O. A., Vasileva, E. N., Borisov, A. Y., and Tikhonovich, I. A. (2019). New sources of Sym2A allele in the pea

(*Pisum sativum* L.) carry the unique variant of candidate LysM-RLK gene LykX. *PeerJ* 7:e8070. doi: 10.7717/peerj.8070

Viprey, V., Rosenthal, A., Broughton, W. J., and Perret, X. (2000). Genetic snapshots of the rhizobium species NGR234 genome. *Genome Biol.* 1:RESEARCH0014. doi: 10.1186/gb-2000-1-6-research0014

Walker, L., Lagunas, B., and Gifford, M. L. (2020). Determinants of host range specificity in legume-rhizobia Symbiosis. *Front. Microbiol.* 11:585749. doi: 10.3389/fmicb.2020.585749

Waterhouse, A., Bertoni, M., Bienert, S., Studer, G., Tauriello, G., Gumienny, R., et al. (2018). SWISS-MODEL: homology modeling of protein structures and complexes. *Nucleic Acids Res.* 46, W296–W303. doi: 10.1093/nar/gky427

Weigend, F., and Ahlrichs, R. (2005). Balanced basis sets of split valence, triple zeta valence and quadruple zeta valence quality for H to Rn: design and assessment of accuracy. *Phys. Chem. Chem. Phys.* 7, 3297–3305. doi: 10.1039/b508541a

Wu, L. J., Wang, H. Q., Wang, E. T., Chen, W. X., and Tian, C. F. (2011). Genetic diversity of nodulating and non-nodulating rhizobia associated with wild soybean (*Glycine soja* Sieb. & Zucc.) in different ecoregions of China. *FEMS Microbiol. Ecol.* 76, 439–450. doi: 10.1111/j.1574-6941.2011.01064.x

Xiao, T. T., Schilderink, S., Moling, S., Deinum, E. E., Kondorosi, E., Franssen, H., et al. (2014). Fate map of *Medicago truncatula* root nodules. *Development* 141, 3517–3528. doi: 10.1242/dev.110775

Zhang, Y. (2009). I-TASSER: fully automated protein structure prediction in CASP8. *Proteins* 77 (Suppl. 9), 100–113. doi: 10.1002/prot.22588

Zhukov, V., Radutoiu, S., Madsen, L. H., Rychagova, T., Ovchinnikova, E., Borisov, A., et al. (2008). The pea Sym37 receptor kinase gene controls infection-thread initiation and nodule development. *Mol. Plant-Microbe Interact.* 21, 1600–1608. doi: 10.1094/MPMI-21-12-1600

Zipfel, C., and Oldroyd, G. E. D. (2017). Plant signalling in symbiosis and immunity. *Nature* 543, 328–336. doi: 10.1038/nature22009

Conflict of Interest: The authors declare that the research was conducted in the absence of any commercial or financial relationships that could be construed as a potential conflict of interest.

frontiers in Plant Science

ORIGINAL RESEARCH
published: 07 June 2021
doi: 10.3389/fpls.2021.689064

Multiple Domains in the Rhizobial Type III Effector Bel2-5 Determine Symbiotic Efficiency With Soybean

*Safirah Tasa Nerves Ratu[1], Atsushi Hirata[2], Christian Oliver Kalaw[3], Michiko Yasuda[3], Mitsuaki Tabuchi[2] and Shin Okazaki[1,3]**

[1] United Graduate School of Agricultural Science, Tokyo University of Agriculture and Technology, Fuchu, Japan, [2] Department of Applied Biological Science, Faculty of Agriculture, Kagawa University, Kagawa, Japan, [3] Graduate School of Agriculture, Tokyo University of Agriculture and Technology, Fuchu, Japan

Bradyrhizobium elkanii utilizes the type III effector Bel2-5 for nodulation in host plants in the absence of Nod factors (NFs). In soybean plants carrying the *Rj4* allele, however, Bel2-5 causes restriction of nodulation by triggering immune responses. Bel2-5 shows similarity with XopD of the phytopathogen *Xanthomonas campestris* pv. *vesicatoria* and possesses two internal repeat sequences, two ethylene (ET)-responsive element-binding factor-associated amphiphilic repression (EAR) motifs, a nuclear localization signal (NLS), and a ubiquitin-like protease (ULP) domain, which are all conserved in XopD except for the repeat domains. By mutational analysis, we revealed that most of the putative domains/motifs in Bel2-5 were essential for both NF-independent nodulation and nodulation restriction in *Rj4* soybean. The expression of soybean symbiosis- and defense-related genes was also significantly altered by inoculation with the *bel2-5* domain/motif mutants compared with the expression upon inoculation with wild-type *B. elkanii*, which was mostly consistent with the phenotypic changes of nodulation in host plants. Notably, the functionality of Bel2-5 was mostly correlated with the growth inhibition effect of Bel2-5 expressed in yeast cells. The nodulation phenotypes of the domain-swapped mutants of Bel2-5 and XopD indicated that both the C-terminal ULP domain and upstream region are required for the Bel2-5-dependent nodulation phenotypes. These results suggest that Bel2-5 interacts with and modifies host targets via these multiple domains to execute both NF-independent symbiosis and nodulation restriction in *Rj4* soybean.

Keywords: symbiosis, nodulation, rhizobia, type III secretion system, effector, soybean

OPEN ACCESS

Edited by:
Jose María Vinardell, Seville University, Spain

Reviewed by:
Michael Göttfert, Technische Universität Dresden, Germany
Francisco Javier López-Baena, Seville University, Spain

***Correspondence:**
Shin Okazaki
sokazaki@cc.tuat.ac.jp

Specialty section:
This article was submitted to Plant Symbiotic Interactions, a section of the journal Frontiers in Plant Science

Received: *31 March 2021*
Accepted: *10 May 2021*
Published: *07 June 2021*

Citation:
Ratu STN, Hirata A, Kalaw CO, Yasuda M, Tabuchi M and Okazaki S (2021) Multiple Domains in the Rhizobial Type III Effector Bel2-5 Determine Symbiotic Efficiency With Soybean. Front. Plant Sci. 12:689064. doi: 10.3389/fpls.2021.689064

Abbreviations: NFs, Nod factors; T3SS, type III secretion system; T3Es, type III-secreted effectors; MAPK, mitogen-activated protein kinase; ETI, effector triggered-immunity; RD, repeat domain; EAR, ethylene-responsive element-binding-factor-associated amphiphilic repression; NLS, nuclear localization signal; ULP, ubiquitin-like protease; SA, salicylic acid; JA, jasmonic acid; *NIN*, nodule inception; *ENOD40*, early nodulin 40; *ACO1*, 1-amino-cyclopropane-1-carboxylate (ACC) oxidase; *ERF1b*, ethylene response factor 1b; *PR1*, pathogenesis-related protein 1; dai, days after inoculation; USDA61, *Bradyrhizobium elkanii* wild-type; Δ*bel2-5*, *bel2-5* knockout mutant; ΔRD1, repeat domain I deletion mutant; BERD1; EAR1, amino acid substitution mutant of the EAR1; BEEAR1; NLS, amino acid substitution mutant of the NLS; BENLS; ΔRD2, repeat domain 2 deletion mutant; BERD2; C1286A, amino acid substitution mutant of the ULP domain; BEC1286A; and EAR2, amino acid substitution mutant of the EAR2; BEEAR2, Δ*bel2-5:xopD*, *bel2-5* knockout mutant complemented with *xopD*; Δ*bel2-5:bel2-5_xopDULP*, *bel2-5* knockout mutant complemented with *bel2-5* harboring the ULP domain of *xopD*; Δ*bel2-5:xopD_bel2-5ULP*, *bel2-5* knockout mutant complemented with *xopD* harboring the ULP domain of *bel2-5*.

INTRODUCTION

Legume plants cope with nitrogen-deficient soils by establishing symbiosis with nitrogen-fixing bacteria, called rhizobia. This symbiosis results in the formation of a unique organ, the root nodule, where rhizobia provide ammonia for plants in exchange for carbon sources and other nutrients essential for their growth (Oldroyd et al., 2011). This symbiosis is of agronomic importance, as it reduces the need for chemical fertilizers in the production of legume crops such as soybean (Soumare et al., 2020).

Root nodule symbiosis is a highly specific interaction, as each rhizobium defines its host legumes via molecular dialogs with the host. In the first step, the bacteria recognize root-derived flavonoids secreted by legumes. The host-derived flavonoids induce the expression of rhizobial nodulation (*nod*) genes, which leads to the biosynthesis and secretion of lipochitooligosaccharides, called Nod factors (NFs). Nod factors are perceived by host lysin-motif receptors (Nod factor receptors, NFRs), and the perception activates the nodulation signaling cascade, leading to bacterial infection and nodule organogenesis (Madsen et al., 2003; Radutoiu et al., 2003). In addition to NFs, rhizobia have evolved several strategies to promote their infection of plants, including the use of surface polysaccharides such as extracellular polysaccharides, capsular polysaccharides, and lipopolysaccharides (Becker et al., 2005; Simsek et al., 2007; Kawaharada et al., 2015). However, most remarkably, numerous rhizobia utilize a type III secretion system (T3SS), which in pathogenic bacteria is known for its delivery of virulence factors, to promote symbiosis with host legumes (Deakin and Broughton, 2009).

Some gram-negative bacteria can deliver effector proteins from the bacterial cytoplasm into a eukaryotic host cell through a syringe-like multi-protein apparatus, the T3SS (Diepold and Wagner, 2014). Plant pathogens often use the T3SS to inject effector proteins (T3Es) into host cells to suppress the host immune response and promote infection (Coburn et al., 2007). To counteract these threats, plants have evolved to produce resistance (R) proteins that perceive the presence or action of effector proteins and allow them to elicit resistance responses called effector-triggered immunity (ETI), which halts pathogen invasion and disease (Jones and Dangl, 2006). Thus, bacterial T3Es and the plant immune system both contribute to shaping plant-pathogen interactions. Similarly, rhizobial T3Es often act as determinants of host specificity. Depending on the host cultivar (genotype), they might affect symbiosis either positively or negatively. Some rhizobia utilize T3Es to enhance nodule formation by suppressing host defense responses by modulating the MAPK cascade (Miwa and Okazaki, 2017). In soybean cultivars carrying *Rj* genes, recognition of particular rhizobial T3SS (and thus T3Es) restricts bacterial infection and nodule organogenesis (Okazaki et al., 2009; Faruque et al., 2015; Sugawara et al., 2018; Shobudani et al., 2020). This commonality between pathogenic bacteria and rhizobia suggests that they utilize similar genetic traits to invade and establish compatible association with plant hosts.

Recently, a distinct role of the rhizobial T3SS has been discovered in two different legume-rhizobium interactions: between *Bradyrhizobium elkanii* and soybean and between *Bradyrhizobium* sp. ORS3257 and an aquatic legume of the genus *Aeschynomene* (Okazaki et al., 2013, 2016). In these interactions, *Bradyrhizobium* strains utilize the T3SS to induce nodule formation in the absence of NF signals, which have been considered essential for nodule formation (Okazaki et al., 2013, 2016; Teulet et al., 2019). The T3Es responsible for the NF-independent pathway have also been identified; effector required for nodulation-A (ErnA) of *Bradyrhizobium* sp. ORS3257 (Teulet et al., 2019) and Bel2-5 of *B. elkanii* (Ratu et al., 2021). *Aeschynomene indica*, a host plant of *Bradyrhizobium* sp. ORS3257, is known for its nodulation, which does not require NFs. However, in ORS3257 a mutation of T3SS or *ernA* led to a Nod- phenotype (Teulet et al., 2019). Furthermore, ectopic expression of ErnA triggered cell division, resulting in the formation of nodule-like structures (Teulet et al., 2019). Bel2-5 of *B. elkanii* has been identified as a T3E that enables nodulation on the non-nodulating soybean En1282 (an *nfr1* mutant) (Ratu et al., 2021). In soybean roots, Bel2-5 could upregulate symbiosis-related genes and downregulate defense-related genes (Ratu et al., 2021). To our knowledge, Bel2-5 and ErnA have only a limited level of sequence similarity and are capable of inducing nodules only in their host legumes (e.g., soybean and *Aeschynomene*, respectively). These results suggest that rhizobia possibly customized specific T3SS and T3Es to reflect on the particular symbiotic partners.

Bel2-5 of *B. elkanii* resembles the XopD effector of the phytopathogen *Xanthomonas campestris* (*Xcv.*). While Bel2-5 can trigger nodulation signaling in the soybean *nfr1* mutant, the presence of Bel2-5 causes restriction of nodulation on soybean carrying the *Rj4* allele (Faruque et al., 2015; Ratu et al., 2021). *In silico* analysis showed that Bel2-5 possesses two internal repeat domains, two ethylene (ET)-responsive element-binding factor-associated amphiphilic repression (EAR) motifs, a nuclear localization signal (NLS), and a ubiquitin-like protease (ULP) domain (Ratu et al., 2021). Intriguingly, XopD also possesses all of these domains except for the repeat domains, and which play pivotal roles in pathogenicity in host plants (Hotson et al., 2003; Kim et al., 2008, 2013). However, the functions of these domains/motifs of Bel2-5 in symbiotic interactions remain unclear. In this study, we investigated the importance of the domains/motifs of the Bel2-5 effector in symbiosis in the context of both NF-independent nodulation in *nfr1* soybean and nodulation restriction in *Rj4* soybean.

MATERIALS AND METHODS

Bacterial and Yeast Strains and Their Growth Conditions

The bacterial strains and plasmids used in this study are listed in **Supplementary Table S1**. *B. elkanii* strains were grown at 28°C in arabinose-gluconate (AG) (Sadowsky et al., 1987) medium supplemented with appropriate antibiotics (50 μg/mL polymyxin, 200 μg/mL kanamycin, 200 μg/mL

streptomycin, and 200 μg/mL spectinomycin). *Escherichia coli* strains were grown at 37°C in Luria-Bertani medium (Green and Sambrook, 2012) supplemented with appropriate antibiotics (50 μg/mL kanamycin, 50 μg/mL streptomycin, and 50 μg/mL spectinomycin). Yeast strains were grown in yeast extract, peptone and dextrose (YPD) medium, synthetic dextrose (SD) medium (2% glucose, 0.67% yeast nitrogen base without amino acids) or synthetic galactose (SGal) medium (2% galactose, 0.67% yeast nitrogen base without amino acids). Appropriate amino acids and bases were added to the SD or SGal medium as necessary. Yeast cells were cultured at 26°C unless otherwise stated. All conjugation processes for *B. elkanii* mutant construction were performed on peptone-salts-yeast extract (PSY) medium (Regensburger and Hennecke, 1983).

Plasmid Construction and Mutagenesis of *Bradyrhizobium elkanii*

All the constructs prepared in this study are listed in **Supplementary Table S1**, which includes the primers and cloning strategies. The construction of *B. elkanii* strains carrying mutated *bel2-5* derivatives (substitution or deletion) was performed using a QuikChange Lightning Site-Directed Mutagenesis Kit (Agilent Technologies, CA, United States). First, a ∼4.5-kb DNA fragment containing *bel2-5* with its promoter sequence (**Supplementary Data S1**) was synthesized (GENEWIZ, NJ, United States) and cloned into the carrier plasmid pUC57, which was then used as the template for generating plasmids carrying a substitution or deletion of targeted sequences using specific primer sets (**Supplementary Table S1**). The constructed substitution or deletion plasmids were confirmed by Sanger sequencing. Next, the *bel2-5* sequence with desired point mutations was excised from the carrier plasmid (pUC57) by digestion at the *Eco*RI/*Xba*I sites or further amplified to create *Sac*I/*Kpn*I sites for cloning. The resultant DNA fragments were transferred into the plasmid pK18mob or pBjGroEL4:dsRED and integrated into the *bel2-5* deletion mutant (Δ*bel2-5*) through single-crossover recombination. The constructed *B. elkanii* mutant strains were screened by antibiotic resistance testing and confirmed by PCR and sequence analysis.

For swapping the ULP-like domain region between the Bel2-5 and XopD effectors, artificial sequences were synthesized as detailed in **Supplementary Data S2** (GENEWIZ, NJ, United States) and cloned into the carrier plasmid pUC57. The synthetic sequences were then used as the template for PCR amplification using specific primer sets for cloning into the plasmid pBjGroEL4:dsRED at the *Sac*I/*Kpn*I sites. The constructed plasmids were confirmed using Sanger sequencing, then integrated into the *bel2-5* deletion mutant (Δ*bel2-5*) through a single homologous recombination. The constructed *B. elkanii* mutant strains were screened by antibiotic resistance and confirmed by PCR.

Nodulation Tests

The soybean cultivars used in this study were *Glycine max* (L.) Merr. En1282 (an *nfr1* mutant) and BARC-2 (*Rj4/Rj4*). Soybean seeds were surface-sterilized and germinated as previously described (Krause et al., 2002); 2-day-old germinated seedlings were transferred into a plant box (CUL-JAR300; Iwaki, Japan) containing sterilized vermiculite and inoculated with 1×10^7 cells/mL *B. elkanii* strains or sterilized water (mock treatment). Plants were cultivated in a plant growth chamber at 25°C and 70% humidity under a 16/8-h day/night regimen; an appropriate amount of B&D nitrogen-free solution (Broughton and Dilworth, 1971) was added to water the plants. Nodule numbers were determined at 30 days after inoculation (dai).

Expression of Bel2-5 and Its Mutated Derivatives in Yeast Cells

The full-length *bel2-5* sequence without a stop codon (∼4.0-kb) was amplified using a specific primer set according to the Gateway Technology Kit instruction manual (Invitrogen, CA, United States). The amplified PCR product was then used to generate a yeast-inducible expression plasmid as described previously (Tabuchi et al., 2009). Briefly, further PCR amplification was performed using *attB* adaptor primers to obtain the *att*B-flanked PCR product, which was cloned into the donor vector pDONR207 by the BP reaction. The entry clone was screened for antibiotic resistance and confirmed by PCR and sequence analysis. Next, the constructed entry clone of Bel2-5 was subcloned into the Gateway vector pMT751 via the LR reaction and then transformed into the yeast MTY914 (*smt3*Δ:*KanMX4* carrying pRS415-HA-*SMT3*). Yeast carrying the *bel2-5* sequence was used for localization and spot assays to check yeast growth inhibition. Partial deletion or substitution of *bel2-5* was performed by inverse PCR with specific primer sets using KOD-Plus-Neo DNA polymerase (Toyobo, Osaka, Japan). Inserts were sequenced to ensure that no mutations were introduced due to manipulation. For yeast growth inhibition assay, yeast cells carrying plasmids expressing Bel2-5 or its derivatives were suspended in sterilized water and the cell suspensions were measured and adjusted to $OD_{600\,nm} = 1.0$. The cell suspensions were spotted into 10-fold serial dilution on SD (-ura) and SGal (-ura) plates and grown at 26℃ for 2–3 days.

Fluorescence Microscopy

Localization of Bel2-5 in yeast cells was performed as described previously (Tabuchi et al., 2009). Briefly, GFP fluorescence in non-fixed yeast cells was observed using an Olympus BX51 microscope (Olympus, Japan) with a GFP filter. Images were captured with a Hamamatsu C11440-10C Orca-Flash 2.8 CMOS camera (Hamamatsu Photonics, Japan) using Metamorph software (Molecular Devices, Japan).

Soybean RNA Extraction and qRT-PCR Analysis

RNA Extraction

En1282 (*nfr1* mutant) and BARC-2 (*Rj4/Rj4*) soybean seeds were surface sterilized, germinated at 25°C for 2 days, and then transferred to a seed pack (Daiki Rika Co., Ltd., Japan) with B&D nitrogen-free solution. On the following day (the third day of germination), seeds were inoculated with 2×10^7

cells/mL (for En1282 soybean) or 1×10^7 cells/mL (for BARC-2 soybean) bacterial cultures. Then, at three or four dai, the soybean roots were immediately frozen in liquid nitrogen and then ground to a fine powder; 100 mg of the powder was used for total RNA extraction using an RNeasy Plant Mini Kit (Qiagen, Hilden, Germany) and treated with DNase I (Qiagen, Hilden, Germany) according to the manufacturer's instructions. RNA quality and concentration were evaluated using a NanoDrop 2000/200c (Thermo Fisher, MA, United States).

qRT-PCR Analysis

The extracted RNA samples were used as the template for cDNA synthesis in a final volume of 20 μL (containing 400 ng of total RNA) by using the SuperScript III First-Strand Synthesis System for RT-PCR (Invitrogen, CA, United States). The RT-qPCR mixture and thermal cycling conditions were set as previously described (Yasuda et al., 2016). qRT-PCR was performed using a StepOne real-time PCR system (Applied Biosystems, MA, United States) with the primer set listed in **Supplementary Table S1**. Transcript levels of soybean genes were normalized to those of the housekeeping gene *SUBI-2* (Brechenmacher et al., 2008), which were measured in the same samples.

Statistical Analysis

Data were analyzed using Student's *t*-test and Tukey's honestly significant difference (HSD) test, performed using IBM SPSS Statistics 22.0 software.

RESULTS

Nodulation Phenotype of Soybean Infected With *bel2-5* Mutants

Bel2-5 shares similarity with the rhizobial T3E NopD (Xiang et al., 2020) and with XopD (Noël et al., 2002), from the plant pathogen *Xcv*. (Ratu et al., 2021). *In silico* analysis revealed that Bel2-5 possesses two repeat sequences (designated repeat domains 1 and 2), two EAR motifs, an NLS, and a ULP domain (Ratu et al., 2021, **Figure 1**).

To elucidate the function of each domain/motif in Bel2-5 during symbiosis with soybean, we deleted or substituted the region or critical amino acids in the predicted domain/motif (**Figure 1A**). The constructed mutants as well as the wild type (WT) and the *bel2-5* deletion mutant (Δ*bel2-5*) of *B. elkanii* strains were inoculated on the soybean cultivars En1282 (*nfr1* mutant) and BARC-2 (*Rj4/Rj4*). In En1282, nodulation was observed in roots inoculated with USDA61, whereas nodulation was completely abolished following inoculation with the *bel2-5* deletion mutant (**Figures 1B,C**). The nodule numbers observed with the other mutants, namely, BERD1, BERD2, BEC1286A, and BEEAR2, were also decreased to similar levels as those observed upon inoculation with the *bel2-5* deletion mutant. Moreover, En1282 formed nodules when inoculated with the BEEAR1 and BENLS mutants (**Figures 1B,C**). These results demonstrate that some domains/motifs (RD1, RD2, C1286A, and EAR2) play pivotal roles in Bel2-5 during nodulation of the *nfr1* mutant soybean, while EAR1 and NLS are less important.

BARC-2 plants inoculated with *B. elkanii* USDA61 formed only a few nodules, whereas those inoculated with the *bel2-5* deletion mutant formed numerous nodules (**Figures 1B,C**). The nodule numbers derived by BEC1286A also increased to similar levels as those observed for BERD2 and the *bel2-5* deletion mutant, followed by those observed for BERD1, BENLS, and BEEAR2, while plants inoculated with BEEAR1 formed few nodules, similar to those inoculated with WT USDA61 (**Figures 1B,C**). Together, these results suggest that each domain/motif plays a vital role in the nodulation phenotypes of both En1282 and BARC-2, except for EAR1, which exhibited less importance than the other domains/motifs.

Differential Expression of Soybean Symbiosis and Defense-Related Genes After Infection With *bel2-5* Mutants

A previous study revealed that Bel2-5 regulates the expression of symbiosis- and defense-related genes in soybean (Ratu et al., 2021). Additionally, in the incompatible interaction between BARC-2 (*Rj4/Rj4*) and *B. elkanii*, the T3SS of *B. elkanii* induced the expression of the soybean defense-related genes *PR-1* and *PDF1.2*, which are known to participate in salicylic acid (SA) and jasmonic acid (JA) signaling to restrict rhizobial infection (Yasuda et al., 2016). To further investigate the importance of each domain/motif of Bel2-5 in the expression of these soybean genes, we compared their expression in the roots of En1282 and BARC-2 inoculated with WT USDA61 and the *bel2-5* deletion mutant and its derivatives using quantitative RT-PCR.

In the roots of En1282, the relative expression levels of *NIN* and *ENOD40*, two well-characterized symbiosis genes, were significantly increased by inoculation with USDA61 (**Figure 2A**). The induction of *NIN* was diminished in the roots inoculated with the *bel2-5* deletion mutant and other mutants. Moreover, the induction of *ENOD40* was diminished only by inoculation with the *bel2-5* deletion mutant and BERD2 (repeat domain 2 deletion mutant) compared with USDA61. Upon inoculation with the other mutants, the expression of *ENOD40* was similar to that upon inoculation with USDA61 and was higher than that in the mock treatment (**Figure 2A**).

The defense-related genes *WRKY33*, *ACO1*, and *ERF1b* were previously reported to be suppressed by the Bel2-5 effector in the roots of En1282 (Ratu et al., 2021). Suppression was observed for the expression of *WRKY33* and *ACO1,* as inoculation with the *bel2-5* deletion mutant significantly increased the expression of these genes. The suppression of *WRKY33* was not diminished by mutation of each domain/motif. Moreover, for *ACO1* and *ERF1b*, only mutations in the NLS motif significantly increased the expression of these genes compared with that observed with USDA61 (**Figure 2A**), suggesting that the nuclear localization of Bel2-5 is critical for the suppression of these defense-related genes.

In BARC-2 roots, the expression of the symbiosis-related genes *NIN* and *ENOD40* was significantly induced by inoculation with all the tested strains (**Figure 2B**). Notably, USDA61 and the BEEAR1 mutant, which formed few nodules on BARC-2 plants,

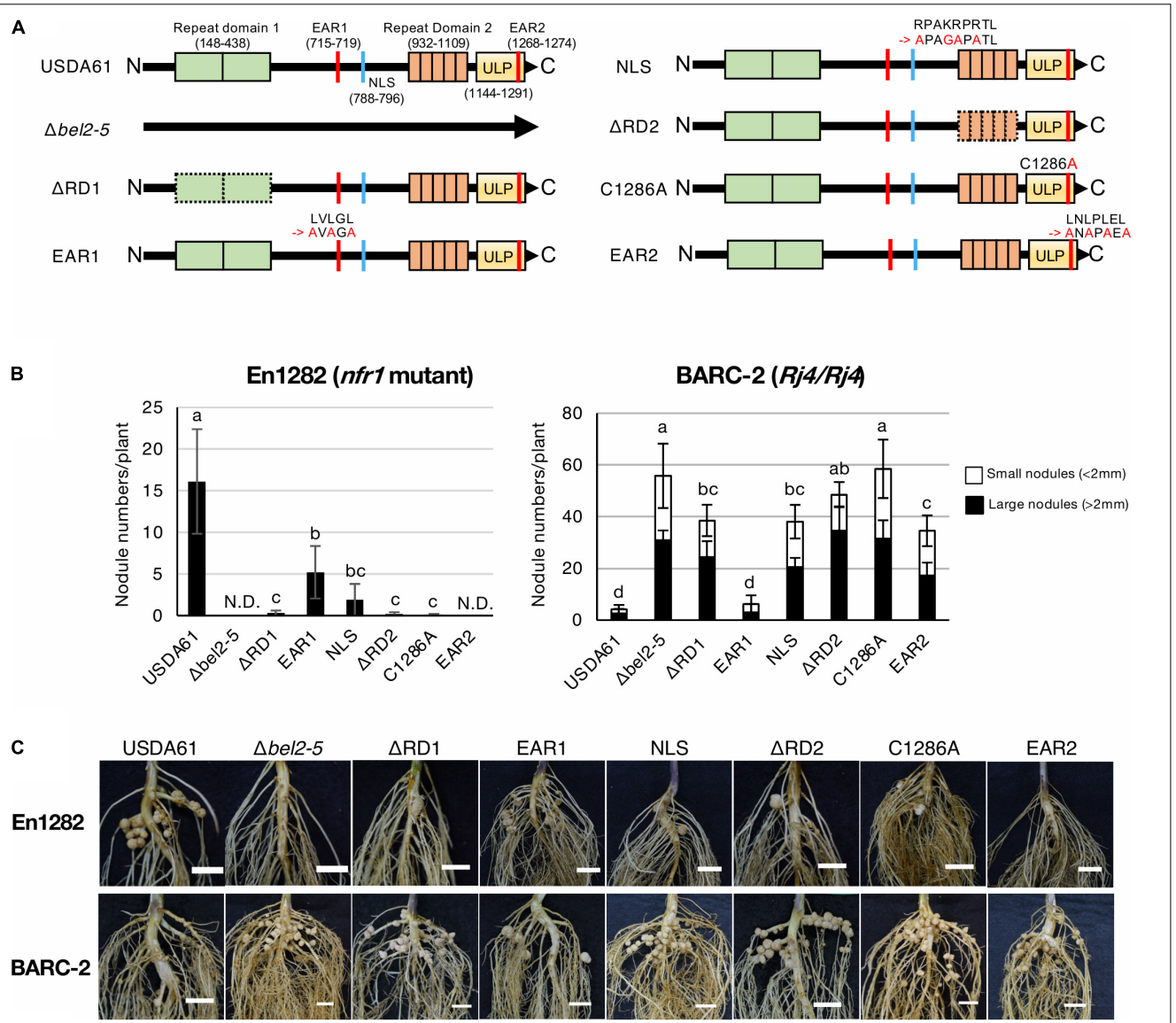

FIGURE 1 | Nodulation phenotypes of *B. elkanii* USDA61 wild-type and the *bel2-5* deletion mutant and its derivatives (substitutions or deletions) on En1282 (*nfr1* mutant) and BARC-2 (*Rj4*/*Rj4*) soybean plants. **(A)** Schematic representation of Bel2-5 and its mutant derivatives in USDA61 and mutant strains. Bel2-5 possesses two internal repeat domains, two ethylene-responsive element-binding factor-associated amphiphilic repression (EAR) motifs, a nuclear localization signal (NLS), and a ubiquitin-like protease (ULP) domain. **(B)** Nodulation of *G. max* cv. En1282 and BARC-2 inoculated with wild-type and *bel2-5* mutant strains of *B. elkanii* USDA61. Nodule numbers were counted at 30 days after inoculation (dai). The values represent the mean ± SD (*n* = at least 10 plants, from two independent inoculation tests). N.D., not detected. Means followed by different letters are significantly different at the 0.05 level by Tukey's test. **(C)** Roots of En1282 and BARC-2 inoculated with wild-type and mutant strains of *B. elkanii* USDA61. Roots were photographed at 30 dai. Scale bars, 1 cm. USDA61, *Bradyrhizobium elkanii* wild-type; Δ*bel2-5*, *bel2-5* knockout mutant; ΔRD1, repeat domain I deletion mutant; BERD1; EAR1, amino acid substitution mutant of the EAR1; BEEAR1; NLS, amino acid substitution mutant of the NLS; BENLS; ΔRD2, repeat domain 2 deletion mutant; BERD2; C1286A, amino acid substitution mutant of the ULP domain; BEC1286A; and EAR2, amino acid substitution mutant of the EAR2; BEEAR2.

also induced the expression of genes, suggesting that these strains were able to trigger NF signaling but failed to induce nodulation at the later stage. The expression of the *PR1* and *Rj4* genes that were reported to be induced by the *B. elkanii* T3SS (Yasuda et al., 2016) was diminished by mutation of each domain/motif of *bel2-5* to the same level as that observed with the *bel2-5* deletion, while the USDA61 strain triggered their expression (**Figure 2B**). These results suggest that each domain/motif of the Bel2-5 effector plays pivotal roles in the induction of the expression of the *PR1* and *Rj4* genes.

Expression of Bel2-5 in Yeast Causes Growth Inhibition

Effector proteins have been observed to confer a growth inhibition phenotype when heterologously expressed in the yeast

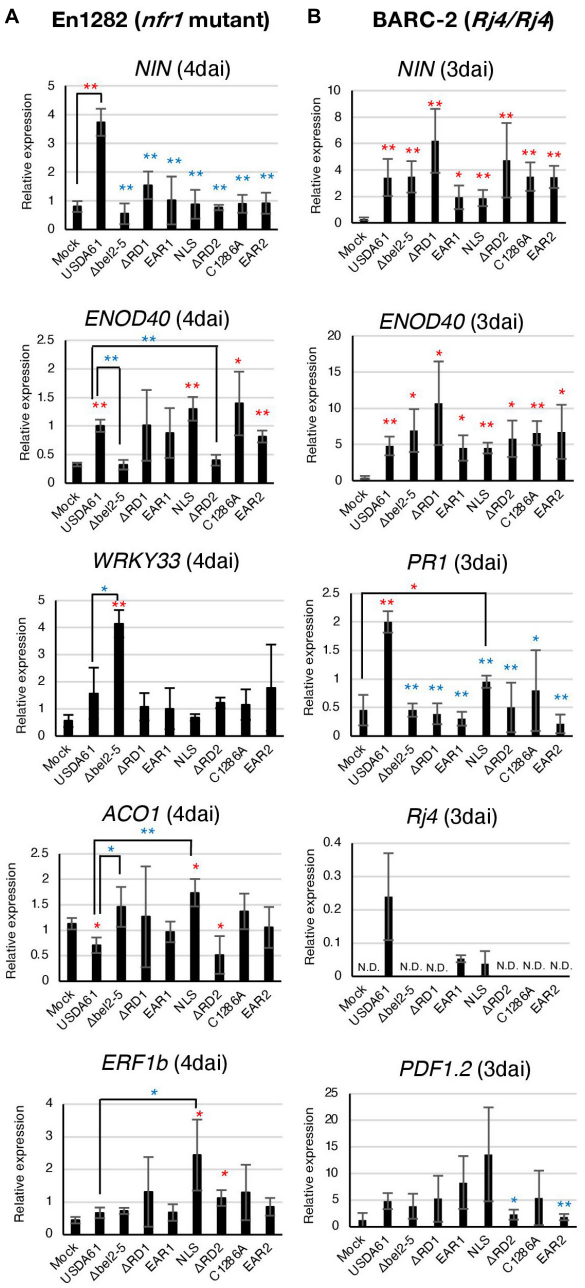

FIGURE 2 | qRT-PCR analysis of soybean defence- and symbiosis-related genes in roots of En1282 **(A)** and BARC-2 **(B)** inoculated with the *B. elkanii* USDA61 wild-type and the *bel2-5* deletion mutant and its derivatives (substitutions or deletions). RNA was isolated from the roots of En1282 and BARC-2 at 4 and 3 days after inoculation (dai), respectively. The expression level of each gene was normalized to that of the *SUBI2-2* gene. The values represent the mean ± SD (n = 3–4 independent soybean roots) **(A,B)**. Statistical analyses (Student's t-test) were performed for comparison of each inoculation with the mock control (water) (red asterisk) or wild-type USDA61 (blue asterisk). $^{*}P < 0.05$; $^{**}P < 0.01$ **(A,B)**. USDA61, *Bradyrhizobium elkanii* wild-type; Δ*bel2-5*, *bel2-5* knockout mutant; ΔRD1, repeat domain I deletion mutant; BERD1; EAR1, amino acid substitution mutant of the EAR1; BEEAR1; NLS, amino acid substitution mutant of the NLS; BENLS; ΔRD2, repeat domain 2 deletion mutant; BERD2; C1286A, amino acid substitution mutant of the ULP domain; BEC1286A; and EAR2, amino acid substitution mutant of the EAR2; BEEAR2.

Saccharomyces cerevisiae (Siggers and Lesser, 2008; Popa et al., 2016). This growth inhibition is thought to be the consequence of the effector-induced compromise of cellular processes conserved between yeast and higher eukaryotes. To investigate the function of the Bel2-5 effector, we expressed Bel2-5 in yeast cells under the control of the *GAL1* promoter and evaluated its effect on yeast growth. As shown in **Figure 3C**, the expression of WT Bel2-5 caused yeast growth inhibition at a level similar to that of Ulp1, which is a yeast deSUMOylation enzyme. We confirmed that GFP-tagging at the C-terminus of Bel2-5 did not affect its yeast growth inhibitory activity (**Supplementary Figure S1**). To clarify the determinant domain/motif for the yeast growth inhibitory activity of Bel2-5, a set of mutant derivatives of *bel2-5* was created and analyzed in yeast (**Figure 3A**). Bel2-5 was localized in the nucleus in yeast, as confirmed by co-staining the nucleus with Hoechst 33342 (**Figure 3B**, left panels: WT). We confirmed that this nuclear localization was partly dependent on the NLS sequence of Bel2-5 (**Figure 3B**) and appeared to be partly responsible for the yeast growth inhibitory activity (**Figure 3C**, lower panel).

Next, we analyzed the N- or C-terminus truncation mutants of *bel2-5* in yeast. The N-terminus truncation mutants Δ2-725 and Δ2-796 exhibited reduced yeast growth inhibitory activity compared with WT, whereas the Δ2-1109 mutant, with the ULP domain only, exhibited yeast growth inhibitory activity similar to that of WT (**Figure 3C**). Interestingly, the C-terminal truncation mutant, the 1-1143 mutant, which lacked the ULP domain, exhibited even stronger yeast growth inhibitory activity than WT, and the 1-931 mutant showed the same level of growth inhibitory activity as WT (**Figure 3C**). Furthermore, the C-terminal truncation mutants 1-787 and 1-714, which lacked NLS sequences, lost their yeast growth inhibitory activity, indicating that nuclear localization is important for the yeast growth inhibitory activity of the N-terminal domain.

We further focused on the ULP domain of Bel2-5 and examined the growth of the yeast C1286A mutants, harboring a substitution of a cysteine residue by an alanine residue in the putative active site of the ULP domain (**Figures 3A,D**). Yeast growth inhibitory activity is still conferred from the full-length Bel2-5 carrying C1286A mutation, while Δ2-1109 truncation with the C1286A mutation exhibited complete loss of the growth inhibitory activity (**Figure 3D**), indicating that the yeast growth inhibitory activity of Bel2-5 is partly dependent on ULP activity.

Together, these results confirm that Bel2-5 possesses independent functional activities in the N-terminal domain containing the NLS sequence and the C-terminal domain containing the ULP domain.

Domain Swapping Between *B. elkanii* Bel2-5 and *Xcv*. Effector XopD

Both *B. elkanii* Bel2-5 and *Xcv*. XopD carry EAR, NLS, and ULP domains/motifs, and each of them plays an important role in symbiosis and pathogenicity in the interaction with the respective hosts (**Figures 1–3**, Hotson et al., 2003; Kim et al., 2008, 2013). To clarify whether Bel2-5 and XopD possess unique features to perform their symbiotic/pathogenic functions in the respective

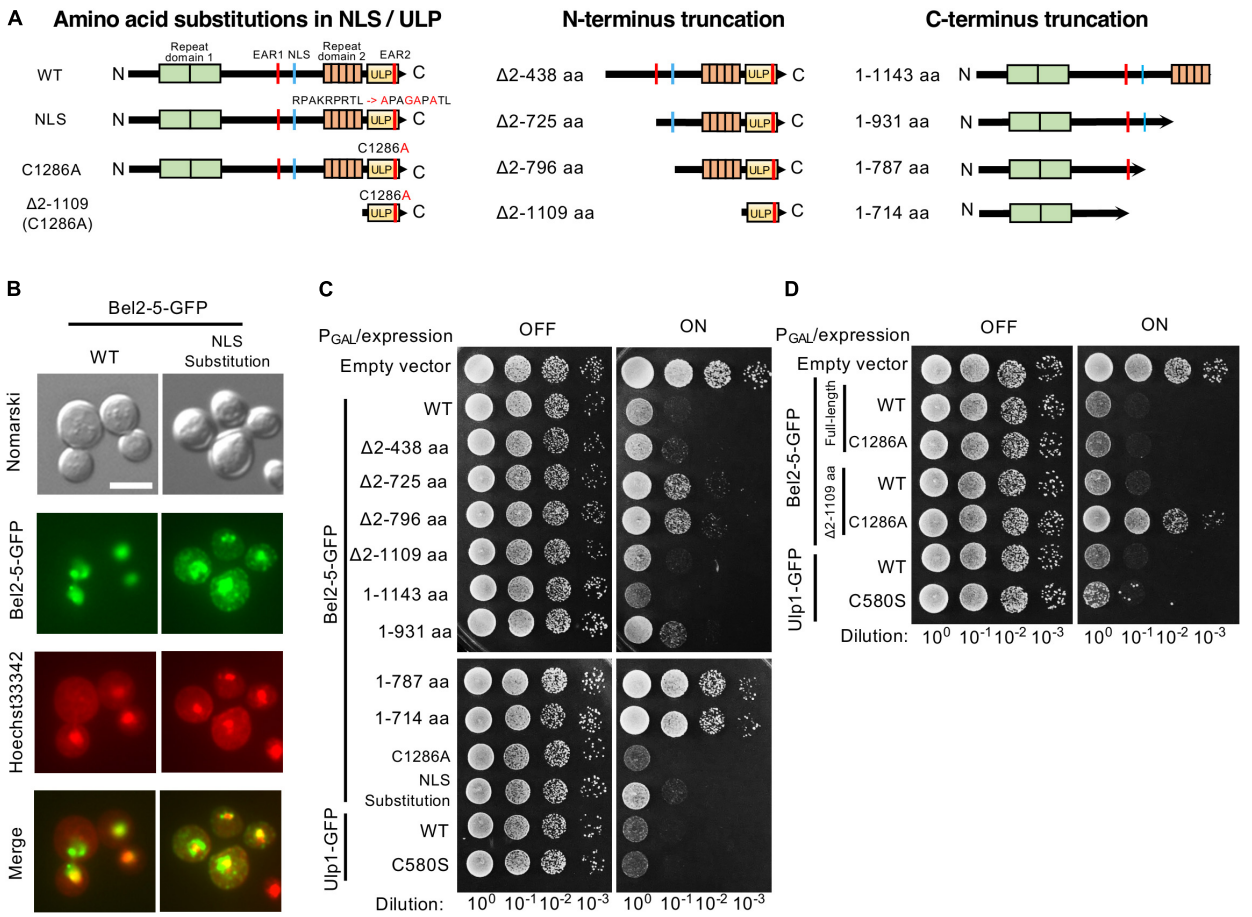

FIGURE 3 | Expression of Bel2-5 and its derivatives in yeast cells. **(A)** Schematic representation of Bel2-5 and its derivatives used for heterologous expression in yeast cells. Amino acid substitutions in the nuclear localization signal (NLS) and catalytic core of the ubiquitin-like protease (ULP) domain of Bel2-5. The Bel2-5 N- or C-terminal truncated constructs. **(B)** Subcellular localization of wild-type Bel2-5 and its mutant on the predicted NLS motif in yeast cells. *Bel2-5* was tagged with a GFP reporter. Yeast cells were stained with Hoechst dye solution as a counterstain for Bel2-5 localization. From top to bottom: unstained yeast cells (Nomarski), the GFP-labeled Bel2-5 effector, yeast cells stained with Hoechst 3342 dye, and combined GFP-tagged Bel2-5 and Hoechst 3342 dye staining. Scale bars: 5 μm. **(C, D)** Expression of the GFP-tagged Bel2-5 effector and its derivative mutants in yeast cells. Bel2-5 expression was under the control of the inducible promoter *GAL1*. The GFP-tagged wild-type yeast Ulp1 and its catalytic core mutant, with a cysteine to serine (C580S) mutation, was used as a control to compare the activity of Bel2-5 in yeast cells.

hosts or can function as interchangeable effectors, we performed domain swapping between Bel2-5 and XopD (**Figure 4A** and **Supplementary Data S2**). Domain-swapped chimaeras were constructed and introduced into the *bel2-5* deletion mutant strain, which was then used for nodulation assays on En1282 and BARC-2 soybean plants. In En1282, the full-length *Xcv.* XopD (Δ*bel2-5:xopD*) did not complement the nodulation capability of the *bel2-5* deletion mutant. Intriguingly, when the ULP domain of XopD was replaced with that of Bel2-5 (Δ*bel2-5:xopD_bel2-5ULP*), nodule formation was observed, although the number of nodules was very small (**Figures 4B,C**). Moreover, when the ULP domain of Bel2-5 was replaced with that of XopD (Δ*bel2-5:bel2-5_xopDULP*), the nodule numbers were drastically decreased compared with those of WT Bel2-5 (USDA61) (**Figures 4B,C**).

On the other hand, no significant effect was observed among the nodule numbers of the domain-swapped construct on BARC-2 soybean (**Figures 4B,C**). These results suggest that the ULP domains of these effectors are partially exchangeable and function similarly during nodulation events, while other parts of Bel2-5 also contain unique features that are involved in the differentiation of species-specific functions in the respective host plants.

DISCUSSION

In this study, we analyzed the functional domains/motifs of the *B. elkanii* Bel2-5 effector in controlling NF-independent symbiosis with En1282 and incompatible symbiosis with BARC-2 (*Rj4/Rj4*). Bel2-5 possesses two repeat sequences (RD1 and RD2), two EAR motifs (EAR1 and 2), an NLS, and a ULP domain (Ratu et al., 2021, **Figure 1**). By mutational analysis, we revealed that the Bel2-5-dependent nodulation phenotype requires most of the domains/motifs, as the mutation of any

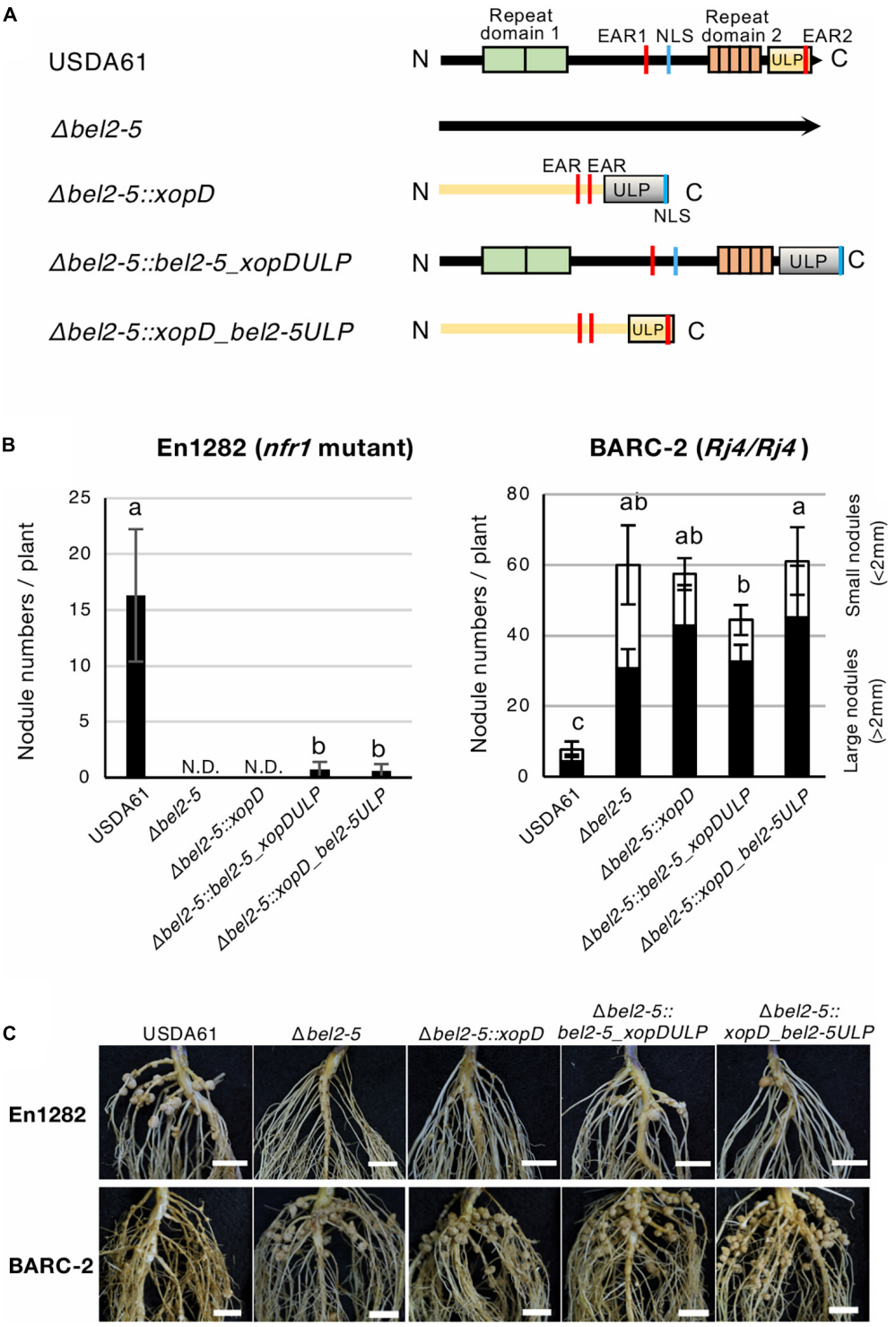

FIGURE 4 | Nodulation phenotypes of *B. elkanii* USDA61 wild-type and the *bel2-5* deletion mutant and its derivatives carrying swapped regions of the ULP-like domain on soybean En1282 (*nfr1* mutant) and BARC-2 (*Rj4*/*Rj4*). **(A)** Schematic representation of swapping of the ULP-like domain between *B. elkanii* Bel2-5 and *Xcv.* XopD. **(B)** Nodulation of *G. max* cv. En1282 and BARC-2 inoculated with wild-type and mutant strains of *B. elkanii* USDA61. Nodule numbers were counted at 30 days after inoculation (dai). The values represent the mean ± SD (n = 10 plants, from two independent inoculation tests). N.D., not detected. Means followed by different letters are significantly different at the 0.05 level by Tukey's test. **(C)** Roots of En1282 and BARC-2 inoculated with wild-type and mutant strains of *B. elkanii* USDA61. Roots were photographed at 30 dai. Scale bars, 1 cm. USDA61, *Bradyrhizobium elkanii* wild-type; Δ*bel2-5*, *bel2-5* knockout mutant; Δ*bel2-5:xopD*, *bel2-5* knockout mutant complemented with *xopD*; Δ*bel2-5:bel2-5_xopDULP*, *bel2-5* knockout mutant complemented with *bel2-5* harboring the ULP domain of *xopD*; Δ*bel2-5:xopD_bel2-5ULP*, *bel2-5* knockout mutant complemented with *xopD* harboring the ULP domain of *bel2-5*.

of these domains/motifs caused significant changes in the nodulation phenotype, similar to the *bel2-5* deletion mutant (**Figure 1**). Notably, the functionality of Bel2-5 was mostly correlated with the growth inhibition effect of Bel2-5 expressed in yeast cells; yeast carrying the Bel2-5 WT sequence and mostly, truncated mutants of *bel2-5* exhibited significant growth inhibition (**Figure 3**).

Among the domains, the EAR1 motif seems to be less important than the others, as the strain carrying a mutation in EAR1 still induced nodulation on En1282 and exhibited incompatibility with BARC-2 plants (**Figure 1**). The differential impact of each domain was observed only for the EAR2 motif; the BEEAR2 mutant exhibited complete loss of nodulation capability on En1282, while the inhibition of nodulation in BARC-2 was still present, albeit weakened (**Figure 1**). This may suggest that Bel2-5 interacts with different host targets in En1282 and BARC-2 via EAR2, leading to differential effects in each host. Except for EAR2, most of the domains/motifs exhibited similar levels of impact on both NF-dependent nodulation in En1282 and nodulation restriction in BARC-2 (**Figure 1**). This may also suggest that in both En1282 and BARC-2 plants, Bel2-5 targets nucleus via NLS, then binds to the same host target proteins (via EAR1, RD1, RD2) and ULP domain mediates the interaction with host target via deSUMOylation activity. In compatible hosts, this modification of the host target may lead to activation of symbiosis signals, including *NIN* and *ENOD40* genes, ultimately leading to nodule formation. On the other hand, in incompatible hosts such as BARC-2, modification of the host target may be recognized by the host surveillance system and activate ETI, which halts rhizobial infection and nodule development. Identification of host targets that interact with Bel2-5 and are deSUMOylated by Bel2-5 would provide clues to elucidate the molecular mechanism underlying the Bel2-5-dependent nodulation phenotypes.

The expression of Bel2-5 in yeast cells revealed that Bel2-5 possesses independent functional activities in the N-terminal domain containing the NLS sequence and the C-terminal domain containing the ULP domain. Yeast growth was significantly inhibited when the N-terminal domain containing the NLS sequence was expressed (aa 1-1143 and aa 1-931) but not when the NLS was absent (aa 1-787 and aa 1-714) (**Figure 3**). These results suggest that the N-terminal domain modulates cellular function only in the nucleus, probably by binding with nuclear proteins via repeat domain 1 or the EAR1 motif. Moreover, the C-terminal domain containing the ULP domain (Δ2-1109) exhibited inhibitory activity only when the ULP catalytic domain was intact. In yeast cells, Ulp1 is involved in the SUMO modification pathway and has dual functions, processing the SUMO precursor to mature SUMO and deconjugating SUMO from its substrate protein (Li and Hochstrasser, 1999). Similar to Bel2-5, yeast Ulp1 contains an NLS motif on its NH_2-terminus, which is necessary and sufficient to concentrate the enzyme into nuclear bodies (Li and Hochstrasser, 2003). Interestingly, a previous study on the function of yeast Ulp1 in the cell cycle showed that its activity was separated from nucleocytoplasmic transport; only the catalytic domain of yeast Ulp1 was sufficient to recognize certain substrates and cleave Smt3 conjugates, although localization into the nuclear pore could increase its ability to process SUMO conjugates efficiently (Li and Hochstrasser, 2003). Intriguingly, when only the non-catalytic domain of yeast Ulp1 (without a protease region) was expressed at high levels, it also caused growth impairment due to excessive accumulation of SUMOylated proteins inside yeast cells (Li and Hochstrasser, 2003). Accordingly, we speculate that the ULP domain of Bel2-5 (Δ2-1109) may act similarly to yeast Ulp1 and modulate the cell cycle progression of yeast, not only in the nucleus but also in the cytoplasm, resulting in yeast growth inhibition.

Subcellular localization of Bel2-5 in yeast cells showed that disruption of the NLS caused nucleocytoplasmic distribution, but Bel2-5 was still partially concentrated in the nucleus (**Figure 3B**). This passive diffusion may contribute to partial changes in the nodulation phenotypes of the mutant (**Figure 1**). Expression analysis of soybean genes showed that suppression of *ACO1* and *ERF1b* in the roots of the *nfr1* mutant required a functional NLS, while *NIN* was expressed at a significantly lower level when the NLS was mutated (**Figure 2A**). In BARC-2, the expression of at least the *PR1* and *Rj4* genes was induced by infection with the BENLS mutant strain but not by the other mutants (**Figure 2B**). To date, some rhizobial T3Es have been shown to localize to the nucleus, including NopL of *Sinorhizobium* sp. NGR234 (Ge et al., 2016), ErnA of *Bradyrhizobium* sp. ORS3257 (Teulet et al., 2019), and NopD of *Bradyrhizobium* sp. XS1150 (Xiang et al., 2020). However, whether their cellular/symbiotic activities depend on nuclear localization remains unknown. Furthermore, the role of the NLS sequence in some pathogenic effectors has been demonstrated. For example, the avirulence activity of the *Xcv*. AvrBs3 effector in plant cells was confirmed to be dependent on an active NLS (Van den Ackerveken et al., 1996). Similarly, *Xcv*. HpaA-mediated disease development requires the two functional NLSs of this protein (Huguet et al., 1998). Non-canonical nuclear signals of the gall-forming HsvG, a T3E of the phytopathogen *Pantoea agglomerans* pv. *gypsophilae*, could bind with importin-α proteins of *Arabidopsis*, and NLS deletion abolished the pathogenicity of HsvG (Weinthal et al., 2011). Overall, it is likely that the nuclear localization of Bel2-5 via its NLS motif is critical for Bel2-5-dependent soybean gene regulation and alters nodulation efficiency.

A homology search revealed that Bel2-5 shares high similarity with at least three putative T3 effectors, namely, Blr1693, Blr1705, and Bll8244, of *Bradyrhizobium diazoefficiens* USDA110 (Ratu et al., 2021). Intriguingly, unlike USDA61, USDA110 is unable to form nodules in En1282 and nodulates well in *Rj4* soybean (Okazaki et al., 2013; Hayashi et al., 2014). Structural analysis indicated that these homologs lack repeat domain 1 (RD1, aa 148-438) and the EAR1 motif (aa 715-719) within their sequences. Similarly, repeat domain 2 (RD2, aa 932-1109) of Bel2-5 exists among USDA110 homologs; however, it has low sequence conservation and differs in the number of repetitions (**Supplementary Data S3**, Ratu et al., 2021). The function of repeat domains in rhizobia remains unknown; however, our phenotypic test showed that mutations in repeat domains of Bel2-5 significantly affected the nodulation phenotype (**Figure 1**). The pathogenic T3 effector HsvG possesses 71-aa and 75-aa tandem repeats that function as transcriptional activators and are involved in host specificity (Nissan et al., 2006). The T3 effector

transcriptional activator-like (TAL) of *Xanthomonas* spp. carries a unique tandem 34-aa repeat domain that determines DNA binding specificity. DNA-binding effector proteins induce the expression of host susceptibility genes to promote *Xanthomonas* colonization (Richter et al., 2014). The repeat sequence was also found in the *Ralstonia solanacearum* T3 effector RipTAL1, which activates transcription of host susceptibility genes (de Lange et al., 2013). Furthermore, it has been reported that diverse variations in the sequence composition and number of protein domain repeats allow flexible binding to multiple binding partners (Björklund et al., 2006; Boch et al., 2009). Together, the repeat domains of Bel2-5 and USDA110 effector homologs may be involved in the recognition of specific host proteins, resulting in different symbiotic phenotypes.

Of particular interest is the species-specific function of the *B. elkanii* Bel2-5 and *Xcv.* XopD effectors. Bel2-5 shares a high degree of homology with XopD, and both effectors contain ULP domain with a catalytic triad (H, D, and C), which is well conserved (Ratu et al., 2021). A nodulation test using ULP domain-swapped *bel2-5* and *xopD* mutants revealed that both Bel2-5 carrying ULP of XopD and XopD carrying ULP of Bel2-5 were capable of inducing the formation of only a limited number of nodules on En1282 (**Figure 4**). These results indicated that both the ULP domain and upstream region of the Bel2-5 effector are required for triggering NF-independent nodulation signaling in soybean cells. Similarly, in BARC-2 soybean, domain-swapped mutants induced the formation of numerous nodules, similar to the effect of Δ*bel2-5*, indicating that both the ULP domain and upstream region of Bel2-5 are required for the induction of ETI-like responses leading to nodulation restriction. These results may imply that both the ULP domain and upstream region of Bel2-5 work together, e.g., the upstream region recruits and interacts with the host target, and the ULP domain deSUMOylates it to trigger signaling, leading to Bel2-5-dependent nodulation. In addition to the conserved ULP domain, Bel2-5 and XopD also share some features, including EAR motifs and their ability to accumulate in the plant nucleus via the NLS motif. Thus, other parts, such as the DNA-binding domain (DBD) in XopD and repeat domains in Bel2-5, are likely involved in the interaction with their respective target in host cells and are thus responsible for species specificity.

A previous study reported that the *Xcv.* strain colonizes tomato plants by suppressing ET production via XopD-mediated deSUMOylation of the SIERF4 transcription factor (Kim et al., 2013). Structural and functional study of the XopD effector revealed that the DBD and EAR motifs were involved in the critical step for the substrate specificity or enzyme kinetics of its SUMO protease activity (Kim et al., 2013). Intriguingly, our present study revealed that the EAR motifs in Bel2-5 were essential for its symbiotic functions, with EAR1 playing a less important role than EAR2 (**Figure 1**). When expressed in yeast cells, the EAR1-deleted mutant (Δ2-725 aa) showed weaker inhibitory activity than that carrying EAR1 (Δ2-438 aa) (**Figure 3**). To our knowledge, Bel2-5 is the only rhizobial effector reported to have functional EARs that determine the interaction with host plants. The EAR motifs were found to be highly conserved, at least within Bel2-5 rhizobial homologs (Ratu et al., 2021). Notably, the pattern of EARs in Bel2-5 was different from that in *Xcv.* XopD but similar to that in PopP2, a T3 effector of *R. solanacearum* that causes bacterial wilt in a wide range of host plants (Genin and Denny, 2012). In plant cells, PopP2 is recognized by the RPS4/RRS1 protein complex via direct binding with the WRKY domain on the RRS1 C-terminus, resulting in the activation of defense responses (Le Roux et al., 2015; Sarris et al., 2015). Mutation in the EAR motif of PopP2 impaired not only the avirulence activity of *R. solanacearum* but also bacterial virulence and stability in plant cells (Segonzac et al., 2017). The expression of marker genes, such as *PR1*, *FMO1*, *PBS3*, and *SARD1*, was induced by T3S-derived PopP2, but their expression was diminished by the *R. solanacearum* EAR-mutated strain (Segonzac et al., 2017). Notably, we also found that Bel2-5 EAR motifs determine the transcriptional level of soybean defense genes, including *WRKY33*, *PR1*, *Rj4*, and *PDF1.2* (**Figure 2**). How these EAR motifs modulate the expression of soybean genes and control nodulation remains unclear. As EAR motifs are known to facilitate protein-protein interactions in transcriptional complexes and function in transcriptional repression (Kazan, 2006), it is likely that the Bel2-5 effector interacts with plant transcription complexes via EAR motifs and controls host stress and defense responses in the nuclear membrane, as reported in pathogenic effectors (Kim et al., 2008; Segonzac et al., 2017).

In conclusion, we identified the functional domains/motifs of Bel2-5 responsible for NF-independent symbiosis in the *nfr* soybean mutant and nodulation restriction in *Rj4* soybean. Bel2-5-dependent symbiosis requires most of the predicted domains/motifs, as the mutation of each domain/motif significantly affected the symbiotic phenotypes, as well as the expression levels of symbiosis- and defense-related genes in soybean roots. Nodulation phenotypes of the domain-swapped mutants of *bel2-5* and *xopD* indicated that both the ULP domain and upstream region are required for Bel2-5-dependent symbiotic phenotypes (**Figure 4**). While XopD suppresses the defensive response (Kim et al., 2008), Bel2-5 has the dual function of triggering the symbiotic signal and suppressing the defensive response, suggesting that Bel2-5 has evolved to perform a symbiotic function during coevolution with host legumes. Identification of the Bel2-5 host target and its modification by the effector would provide clues to elucidate the mechanism of Bel2-5-dependent symbiotic signaling and shed light on the evolution of this effector from pathogenicity to symbiotic utilization.

DATA AVAILABILITY STATEMENT

The original contributions presented in the study are included in the article/**Supplementary Material**, further inquiries can be directed to the corresponding author.

AUTHOR CONTRIBUTIONS

SR, AH, MT, and SO designed the research. SR, AH, and CK performed the research and analyzed data. MY contributed

new reagents and analytic tools. SR, MT, and SO wrote the manuscript. All authors contributed to the article and approved the submitted version.

FUNDING

This study was supported by the JSPS Kakenhi (19H02860 and 19K22303) and the Tojuro Iijima Foundation for Food Science and Technology. This paper is based on results obtained from a project, JPNP18016, commissioned by the New Energy and Industrial Technology Development Organization (NEDO).

ACKNOWLEDGMENTS

We acknowledge the technical expertise of the DNA core facility of the Gene Research Center, Kagawa University.

SUPPLEMENTARY MATERIAL

The Supplementary Material for this article can be found online at: https://www.frontiersin.org/articles/10.3389/fpls.2021.689064/full#supplementary-material

REFERENCES

Becker, A., Fraysse, N., and Sharypova, L. (2005). Recent advances in studies on structure and symbiosis-related function of rhizobial K-antigens and lipopolysaccharides. *Mol. Plant-Microbe Interact.* 18, 899–905. doi: 10.1094/mpmi-18-0899

Björklund, A. K., Ekman, D., and Elofsson, A. (2006). Expansion of protein domain repeats. *PLoS Comput. Biol.* 2:e114. doi: 10.1371/journal.pcbi.0020114

Boch, J., Scholze, H., Schornack, S., Landgraf, A., Hahn, S., Kay, S., et al. (2009). Breaking the code of DNA binding specificity of TAL-type III effectors. *Science* 326, 1509–1512. doi: 10.1126/science.1178811

Brechenmacher, L., Kim, M. Y., Benitez, M., Li, M., Joshi, T., Calla, B., et al. (2008). Transcription profiling of soybean nodulation by *Bradyrhizobium japonicum*. *Mol. Plant-Microbe Interact.* 21, 631–645. doi: 10.1094/mpmi-21-5-0631

Broughton, W. J., and Dilworth, M. J. (1971). Control of leghaemoglobin synthesis in snake beans. *Biochem. J.* 125, 1075–1080. doi: 10.1042/bj1251075

Coburn, B., Sekirov, I., and Finlay, B. B. (2007). Type III secretion systems and disease. *Clin. Microbiol. Rev.* 20, 535–549. doi: 10.1128/CMR.00013-07

de Lange, O., Schreiber, T., Schandry, N., Radeck, J., Braun, K. H., Koszinowski, J., et al. (2013). Breaking the DNA-binding code of *Ralstonia solanacearum* TAL effectors provides new possibilities to generate plant resistance genes against bacterial wilt disease. *New Phytol.* 199, 773–786. doi: 10.1111/nph.12324

Deakin, W. J., and Broughton, W. J. (2009). Symbiotic use of pathogenic strategies: rhizobial protein secretion systems. *Nat. Rev. Microbiol.* 7, 312–320. doi: 10.1038/nrmicro2091

Diepold, A., and Wagner, S. (2014). Assembly of the bacterial type III secretion machinery. *FEMS Microbiol. Rev.* 38, 802–822. doi: 10.1111/1574-6976.12061

Faruque, O. M., Miwa, H., Yasuda, M., Fujii, Y., Kaneko, T., Sato, S., et al. (2015). Identification of Bradyrhizobium elkanii genes involved in incompatibility with soybean plants carrying the Rj4 allele. *Appl. Environ. Microbiol.* 81, 6710–6717. doi: 10.1128/AEM.01942-15

Ge, Y. Y., Xiang, Q. W., Wagner, C., Zhang, D., Xie, Z. P., and Staehelin, C. (2016). The type 3 effector NopL of *Sinorhizobium sp*. strain NGR234 is a mitogen-activated protein kinase substrate. *J. Exp. Bot.* 67, 2483–2494. doi: 10.1093/jxb/erw065

Genin, S., and Denny, T. P. (2012). Pathogenomics of the *Ralstonia solanacearum* species complex. *Annu. Rev. Phytopathol.* 50, 67–89. doi: 10.1146/annurev-phyto-081211-173000

Green, M. R., and Sambrook, J. (2012). *Molecular Cloning A Laboratory Manual. Cold Spring Harbor*. New York, NY: Cold Spring Harbor Laboratory Press.

Hayashi, M., Shiro, S., Kanamori, H., Mori-Hosokawa, S., Sasaki-Yamagata, H., Sayama, T., et al. (2014). A thaumatin-like protein, Rj4, controls nodule symbiotic specificity in soybean. *Plant Cell Physiol.* 55, 1679–1689. doi: 10.1093/pcp/pcu099

Hotson, A., Chosed, R., Shu, H., Orth, K., and Mudgett, M. B. (2003). Xanthomonas type III effector XopD targets SUMO-conjugated proteins in planta. *Mol. Microbiol.* 50, 377–389. doi: 10.1046/j.1365-2958.2003.03730.x

Huguet, E., Hahn, K., Wengelnik, K., and Bonas, U. (1998). hpaA mutants of *Xanthomonas campestris* pv. vesicatoria are affected in pathogenicity but retain the ability to induce host-specific hypersensitive reaction. *Mol. Microbiol.* 29, 1379–1390. doi: 10.1046/j.1365-2958.1998.01019.x

Jones, J. D. G., and Dangl, J. L. (2006). The plant immune system. *Nature* 444, 323–329. doi: 10.1038/nature05286

Kawaharada, Y., Kelly, S., Nielsen, M. W., Hjuler, C. T., Gysel, K., Muszyński, A., et al. (2015). Receptor-mediated exopolysaccharide perception controls bacterial infection. *Nature* 523, 308–312. doi: 10.1038/nature14611

Kazan, K. (2006). Negative regulation of defence and stress genes by EAR-motif-containing repressors. *Trends Plant Sci.* 11, 109–112. doi: 10.1016/j.tplants.2006.01.004

Kim, J. G., Stork, W., and Mudgett, M. B. (2013). Xanthomonas type III effector XopD desumoylates tomato transcription factor SlERF4 to suppress ethylene responses and promote pathogen growth. *Cell Host Microbe* 13, 143–154. doi: 10.1016/j.chom.2013.01.006

Kim, J. G., Taylor, K. W., Hotson, A., Keegan, M., Schmelz, E. A., and Mudgett, M. B. (2008). XopD SUMO protease affects host transcription, promotes pathogen growth, and delays symptom development in Xanthomonas-infected tomato leaves. *Plant Cell* 20, 1915–1929. doi: 10.1105/tpc.108.058529

Krause, A., Doerfel, A., and Göttfert, M. (2002). Mutational and transcriptional analysis of the type III secretion system of *Bradyrhizobium japonicum*. *Mol. Plant-Microbe Interact.* 15, 1228–1235. doi: 10.1094/mpmi.2002.15.12.1228

Le Roux, C., Huet, G., Jauneau, A., Camborde, L., Trémousaygue, D., Kraut, A., et al. (2015). A receptor pair with an integrated decoy converts pathogen disabling of transcription factors to immunity. *Cell* 161, 1074–1088. doi: 10.1016/j.cell.2015.04.025

Li, S. J., and Hochstrasser, M. (1999). A new protease required for cell-cycle progression in yeast. *Nature* 398, 246–251. doi: 10.1038/18457

Li, S. J., and Hochstrasser, M. (2003). The ULP1 SUMO isopeptidase: distinct domains required for viability, nuclear envelope localization, and substrate specificity. *J. Cell Biol.* 160, 1069–1081. doi: 10.1083/jcb.200212052

Madsen, E. B., Madsen, L. H., Radutoiu, S., Olbryt, M., Rakwalska, M., Szczyglowski, K., et al. (2003). A receptor kinase gene of the LysM type is involved in legume perception of rhizobial signals. *Nature* 425, 637–640. doi: 10.1038/nature02045

Miwa, H., and Okazaki, S. (2017). How effectors promote beneficial interactions. *Curr. Opin. Plant Biol.* 38, 148–154. doi: 10.1016/j.pbi.2017.05.011

Nissan, G., Manulis-Sasson, S., Weinthal, D., Mor, H., Sessa, G., and Barash, I. (2006). The type III effectors HsvG and HsvB of gall-forming *Pantoea agglomerans* determine host specificity and function as transcriptional activators. *Mol. Microbiol.* 61, 1118–1131. doi: 10.1111/j.1365-2958.2006.05301.x

Noël, L., Thieme, F., Nennstiel, D., and Bonas, U. (2002). Two novel type-III-secreted proteins of *Xanthomonas campestris* pv. vesicatoria are encoded within the hrp pathogenicity island. *J. Bacteriol.* 184, 1340–1348. doi: 10.1128/JB.184.5.1340-1348.2002

Okazaki, S., Kaneko, T., Sato, S., and Saeki, K. (2013). Hijacking of leguminous nodulation signaling by the rhizobial type III secretion system. *Proc. Natl. Acad. Sci. U S A.* 110, 17131–17136. doi: 10.1073/pnas.1302360110

Okazaki, S., Tittabutr, P., Teulet, A., Thouin, J., Fardoux, J., Chaintreuil, C., et al. (2016). Rhizobium-legume symbiosis in the absence of Nod factors: two possible scenarios with or without the T3SS. *ISME J.* 10, 64–74. doi: 10.1038/ismej.2015.103

Okazaki, S., Zehner, S., Hempel, J., Lang, K., and Göttfert, M. (2009). Genetic organization and functional analysis of the type III secretion system of

Bradyrhizobium elkanii. *FEMS Microbiol. Lett.* 295, 88–95. doi: 10.1111/j.1574-6968.2009.01593.x

Oldroyd, G. E. D., Murray, J. D., Poolw, P. S., and Downie, J. A. (2011). The rules of engagement in legume-rhizobial symbiosis. *Annu. Rev. Genet.* 45, 119–144. doi: 10.1146/annurev-genet-110410-132549

Popa, C., Coll, N. S., Valls, M., and Sessa, G. (2016). Yeast as a heterologous model system to uncover type III effector function. *PLoS Pathog* 12:e1005360. doi: 10.1371/journal.ppat.1005360

Radutoiu, S., Madsen, L. H., Madsen, E. B., Felle, H. H., Umehara, Y., Grønlund, M., et al. (2003). Plant recognition of symbiotic bacteria requires two LysM receptor-like kinases. *Nature* 425, 585–592. doi: 10.1038/nature02039

Ratu, S. T. N., Teulet, A., Miwa, H., Masuda, S., Nguyen, H. P., Yasuda, M., et al. (2021). Rhizobia use a pathogenic-like effector to hijack leguminous nodulation signalling. *Sci. Rep.* 11:2034. doi: 10.1038/s41598-021-81598-6

Regensburger, B., and Hennecke, H. (1983). RNA polymerase from *Rhizobium japonicum*. *Arch. Microbiol.* 135, 103–109. doi: 10.1007/bf00408017

Richter, A., Streubel, J., Blücher, C., Szurek, B., Reschke, M., Grau, J., et al. (2014). A TAL effector repeat architecture for frameshift binding. *Nat. Commun.* 5:3447. doi: 10.1038/ncomms4447

Sadowsky, M. J., Tully, R. E., Cregan, P. B., and Keyser, H. H. (1987). Genetic diversity in *Bradyrhizobium japonicum* serogroup 123 and its relation to genotype-specific nodulation of soybean. *Appl. Environ. Microbiol.* 53, 2624–2630. doi: 10.1128/aem.53.11.2624-2630.1987

Sarris, P. F., Duxbury, Z., Huh, S. U., Ma, Y., Segonzac, C., Sklenar, J., et al. (2015). A plant immune receptor detects pathogen effectors that target WRKY transcription factors. *Cell* 161, 1089–1100. doi: 10.1016/j.cell.2015.04.024

Segonzac, C., Newman, T. E., Choi, S., Jayaraman, J., Choi, D. S., Jung, G. Y., et al. (2017). A conserved EAR motif is required for avirulence and stability of the *Ralstonia solanacearum* effector PopP2 in planta. *Front. Plant Sci.* 8:1330. doi: 10.3389/fpls.2017.01330

Shobudani, M., Htwe, A. Z., Yamakawa, T., Ishibashi, M., and Tsurumaru, H. (2020). Mutants disrupted in the type III secretion system of *Bradyrhizobium elkanii* BLY3-8 overcome nodulation restriction by Rj3-genotype soybean. *Microbes Environ.* 35:2. doi: 10.1264/jsme2.ME19151

Siggers, K. A., and Lesser, C. F. (2008). The yeast *Saccharomyces cerevisiae*: a versatile model system for the identification and characterization of bacterial virulence proteins. *Cell Host Microbe* 4, 8–15. doi: 10.1016/j.chom.2008.06.004

Simsek, S., Ojanen-Reuhs, T., Stephens, S. B., and Reuhs, B. L. (2007). Strain-ecotype specificity in Sinorhizobium meliloti-Medicago truncatula symbiosis is correlated to succinoglycan oligosaccharide structure. *J. Bacteriol.* 189, 7733–7740. doi: 10.1128/JB.00739-07

Soumare, A., Diedhiou, A. G., Thuita, M., Hafidi, M., Ouhdouch, Y., et al. (2020). Exploiting biological nitrogen fixation: a route towards a sustainable agriculture. *MDPI Plants Rev.* 9:1011. doi: 10.3390/plants9081011

Sugawara, M., Takahashi, S., Umehara, Y., Iwano, H., Tsurumaru, H., Odake, H., et al. (2018). Variation in bradyrhizobial NopP effector determines symbiotic incompatibility with Rj2-soybeans via effector-triggered immunity. *Nat. Commun.* 9:3139. doi: 10.1038/s41467-018-05663-x

Tabuchi, M., Kawai, Y., Nishie-Fujita, M., Akada, R., Izumi, T., Yanatori, I., et al. (2009). Development of a novel functional high-throughput screening system for pathogen effectors in the yeast *Saccharomyces cerevisiae*. *Biosci. Biotechnol. Biochem.* 73, 2261–2267. doi: 10.1271/bbb.90360

Teulet, A., Busset, N., Fardoux, J., Gully, D., Chaintreuil, C., Cartieaux, F., et al. (2019). The rhizobial type III effector ErnA confers the ability to form nodules in legumes. *Proc. Natl. Acad. Sci. U S A.* 116, 21758–21768. doi: 10.1073/pnas.1904456116

Van den Ackerveken, G., Marois, E., and Bonas, U. (1996). Recognition of the bacterial avirulence protein AvrBs3 occurs inside the host plant cell. *Cell* 87, 1307–1316. doi: 10.1016/s0092-8674(00)81825-5

Weinthal, D. M., Barash, I., Tzfira, T., Gaba, V., Teper, D., Sessa, G., et al. (2011). Characterization of nuclear localization signals in the type III effectors HsvG and HsvB of the gall-forming bacterium *Pantoea agglomerans*. *Microbiology* 157, 1500–1508. doi: 10.1099/mic.0.047118-0

Xiang, Q. W., Bai, J., Cai, J., Huang, Q. Y., Wang, Y., Liang, Y., et al. (2020). NopD of Bradyrhizobium sp. XS1150 possesses SUMO protease activity. *Front. Microbiol.* 11:386. doi: 10.3389/fmicb.2020.00386

Yasuda, M., Miwa, H., Masuda, S., Takebayashi, Y., Sakakibara, H., and Okazaki, S. (2016). Effector-triggered immunity determines host genotype-specific incompatibility in legume–*Rhizobium symbiosis*. *Plant Cell Physiol.* 57, 1791–1800. doi: 10.1093/pcp/pcw104

Conflict of Interest: The authors declare that the research was conducted in the absence of any commercial or financial relationships that could be construed as a potential conflict of interest.

frontiers in Plant Science

PERSPECTIVE
published: 22 June 2021
doi: 10.3389/fpls.2021.698912

Rhizobial Volatiles: Potential New Players in the Complex Interkingdom Signaling With Legumes

María J. Soto[1], Isabel M. López-Lara[2], Otto Geiger[2], María C. Romero-Puertas[1] and Pieter van Dillewijn[1]*

[1]Estación Experimental del Zaidín, CSIC, Granada, Spain, [2]Centro de Ciencias Genómicas, Universidad Nacional Autónoma de México, Cuernavaca, Mexico

Bacteria release a wide range of volatile compounds that play important roles in intermicrobial and interkingdom communication. Volatile metabolites emitted by rhizobacteria can promote plant growth and increase plant resistance to both biotic and abiotic stresses. Rhizobia establish beneficial nitrogen-fixing symbiosis with legume plants in a process starting with a chemical dialog in the rhizosphere involving various diffusible compounds. Despite being one of the most studied plant-interacting microorganisms, very little is known about volatile compounds produced by rhizobia and their biological/ecological role. Evidence indicates that plants can perceive and respond to volatiles emitted by rhizobia. In this perspective, we present recent data that open the possibility that rhizobial volatile compounds have a role in symbiotic interactions with legumes and discuss future directions that could shed light onto this area of investigation.

Keywords: *Rhizobium*, volatile compounds, signaling, symbiosis, plant defense, iron uptake, interkingdom communication

OPEN ACCESS

Edited by:
Katharina Pawlowski, Stockholm University, Sweden

Reviewed by:
Cecile Vriet, UMR7267 Ecologie et Biologie des Interactions (EBI), France
Xavier Perret, Université de Genève, Switzerland

****Correspondence:***
María J. Soto
mariajose.soto@eez.csic.es

Specialty section:
This article was submitted to Plant Symbiotic Interactions, a section of the journal Frontiers in Plant Science

Received: *22 April 2021*
Accepted: *27 May 2021*
Published: *22 June 2021*

Citation:
Soto MJ, López-Lara IM, Geiger O, Romero-Puertas MC and van Dillewijn P (2021) Rhizobial Volatiles: Potential New Players in the Complex Interkingdom Signaling With Legumes. Front. Plant Sci. 12:698912. doi: 10.3389/fpls.2021.698912

INTRODUCTION

Microorganisms can produce a broad variety of chemical signals, many of which play important roles in communication with neighboring organisms. In addition to the better-studied small diffusible chemical signals, in the last decades microbial volatile compounds (VCs) are receiving increased attention. Accumulating evidence indicates that VCs are not just by-products of microbial metabolism but also exhibit relevant biological activities with important roles in intermicrobial communication and interkingdom interactions with eukaryotic hosts (Weisskopf et al., 2021). Microbial volatiles are characterized by their low molecular mass (<300 Daltons) and high vapor pressure, properties that facilitate their dispersal in air and water over long distances (Schulz and Dickschat 2007). Volatiles emitted by bacteria exhibit diverse chemical structures, comprising inorganic (CO_2, CO, NO, H_2S, NH_3, or HCN) and organic compounds, with the latter belonging to various chemical classes, such as terpenes, aromatic compounds, hydrocarbons, ketones, alcohols, aldehydes, acids, or nitrogen- and sulfur-containing metabolites (Schulz and Dickschat 2007; Audrain et al., 2015; Lemfack et al., 2018). The amount and profile of species-specific and generic volatiles produced by a microorganism (i.e., volatilome) vary in response to numerous factors including the availability of nutrients and oxygen, humidity,

pH, temperature, growth phase, and even the presence of other organisms (Schmidt et al., 2015, 2017; Misztal et al., 2018).

Bacterial volatile metabolites can influence important physiological processes in numerous bacteria, fungi, and plants. Some of them negatively influence the growth and virulence of microorganisms, characteristics that could be harnessed in the design of new strategies to fight against the rise of antibiotic resistance in pathogens (Avalos et al., 2018). Bacterial volatiles are especially well known for their capacity to increase plant growth and resistance against both biotic and abiotic stresses. These properties could be exploited for the development of eco-friendly solutions in the form of biofertilizers and biopesticides to improve plant health and productivity (Kanchiswamy et al., 2015; Chung et al., 2016; Sharifi and Ryu, 2018; Garbeva and Weisskopf, 2020; Thomas et al., 2020).

Considering the relevant effects of bacterial volatiles in intermicrobial and interkingdom communication, it is surprising that very little is known about the production and ecological role of volatile compounds emitted by soil bacteria that establish nitrogen-fixing symbiosis with legumes, collectively referred to as rhizobia. Paradoxically, rhizobia are among the best-known plant-interacting microorganisms and they have frequently been used as inoculants to improve N fertilization of legume plants. Perhaps, efforts focused on the nodulation and nitrogen fixation processes, which are the most relevant attributes of these plant endosymbionts, have contributed that some other properties of these rhizobacteria have been overlooked. In this perspective, we present recent data that open the possibility that rhizobial volatiles have a role in the interkingdom communication with plants that could impact the outcome of symbiotic interactions with legumes as well as other plant-microbe interactions.

OVERVIEW OF THE ROLE OF BACTERIAL VOLATILE COMPOUNDS IN INTERMICROBIAL AND INTERKINGDOM INTERACTIONS

The effects of bacterial volatile compounds (BVCs) in microbe-microbe interactions are diverse and have been described in several reviews (Audrain et al., 2015; Schmidt et al., 2015; Schulz-Bohm et al., 2017; Tyc et al., 2017; Weisskopf et al., 2021). These bacterial airborne metabolites can either positively or negatively influence the physiology of different microorganisms. Some have strong antimicrobial effects, inhibiting the growth of fungi and/or bacteria. Others act as infochemical molecules that, at a distance, are capable of altering gene expression and important behaviors, such as motility, biofilm formation, virulence, development, or stress and antibiotic resistance. The same volatile can elicit different or even opposing responses depending on the interacting organism, highlighting the importance of deciphering the mechanism of action of these compounds. Up to now, very little is known about how microorganisms perceive and respond to the wide spectrum of BVCs, and this represents an intense research area. Alteration of membrane permeability, induction of pH changes in the medium, oxidative stress mitigation, or interference with quorum sensing regulation are some of the mechanisms that have been shown to play a role in the microbial responses to different volatiles (reviewed in Weisskopf et al., 2021).

While the role of BVCs in intermicrobial interactions has only recently been acknowledged, their functions in interkingdom interactions with plants have been known for almost 20 years (reviewed in Sharifi and Ryu, 2018; Garbeva and Weisskopf, 2020; Thomas et al., 2020; Weisskopf et al., 2021). Since the seminal contribution by Ryu et al. (2003) reporting that volatile blends emitted by two *Bacillus* species were able to promote growth of *Arabidopsis*, numerous studies have described the different and relevant effects of BVCs on plants. Plant growth promotion is a common property of volatile mixtures emitted by rhizosphere bacteria (Blom et al., 2011). However, the molecular bases responsible for this effect are still poorly understood. Stimulation of photosynthesis, root growth, and the uptake of specific nutrients, such as iron and sulfur, are some of the mechanisms known to contribute to the BVC-mediated plant growth promotion (Ryu et al., 2003; Zhang et al., 2008, 2009; Meldau et al., 2013). Interestingly, BVCs can also help plants to cope with abiotic and biotic stresses. BVC-mediated plant tolerance to abiotic stresses (drought, salinization, and heavy metal toxicity) is achieved by increasing osmoprotectants, antioxidant activities, Na^+ homeostasis, or sulfur-containing metabolites (reviewed in Sharifi and Ryu, 2018). An important property of some BVCs is their ability to protect plants from pathogenic microorganisms, an effect that could be the result of both direct inhibition of pathogen growth/virulence and the activation of plant immunity (i.e., induced systemic resistance), although the latter seems to play a more important role (Bailly and Weisskopf, 2017). Interestingly, rhizobacteria produce volatiles that can facilitate mutualistic associations between plants and beneficial bacteria without compromising resistance against phytopathogens in a process dependent on phosphorus availability for the plant (Morcillo et al., 2020).

In the different plant responses triggered by BVCs, signaling molecules, such as reactive oxygen species and NO and the modulation of the biosynthesis, perception, and homeostasis of different phytohormones, play a pivotal role (Sharifi and Ryu, 2018; Tyagi et al., 2018). Ethylene, auxin, cytokinin, abscisic acid, and gibberellin are involved in BVC-mediated plant growth promotion, while ethylene, jasmonic acid, and salicylic acid are crucial for BVC-induced plant defense responses.

RHIZOBIUM-LEGUME SYMBOSIS: COMPLEX SIGNAL EXCHANGE IN THE RHIZOSPHERE

The development of nitrogen-fixing root nodules characteristic of the *Rhizobium*-legume symbiosis is the outcome of a process that involves a complex signal exchange between the host plant and rhizobia (Oldroyd, 2013; Poole et al., 2018; Roy et al., 2020). This interkingdom signaling initiates in the rhizosphere, i.e., the region of soil under the influence of plant roots

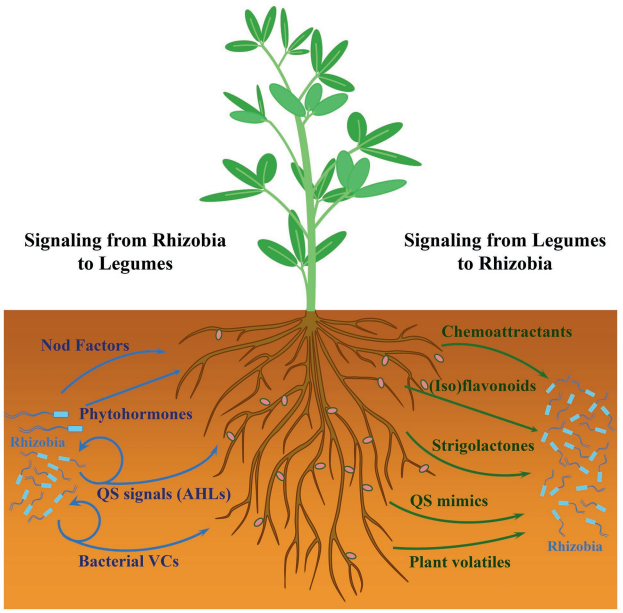

FIGURE 1 | Interkingdom signaling in the rhizosphere between rhizobia and legumes. The effects of bacteria- and plant-derived signals are shown with blue and green arrows, respectively. Bacterial quorum sensing (QS) signals (i.e., *N*-acyl-homoserine lactones, AHLs) and volatile compounds (VCs) also play a role in intermicrobial communication.

(Bakker et al., 2013). In this niche, several plant- and bacteria-derived diffusible compounds have been shown to participate in the early dialog established between the two organisms (**Figure 1**). Some of the signaling compounds are crucial for root nodulation. This is the case of plant root-exuded (iso) flavonoids, which induce bacterial *nod* genes, leading to the synthesis and secretion of lipochitooligosaccharides, also known as Nod factors. This key bacterial signal is perceived by the plant *via* specific receptors to activate the symbiosis signaling pathway required for rhizobial infection and nodule formation while, at the same time, overriding host defense reactions triggered during rhizobial invasion (Zipfel and Oldroyd, 2017; Roy et al., 2020). Besides the well-known (iso)flavonoids and Nod factors, additional legume- and rhizobia-produced diffusible molecules described below participate in an interkingdom communication that is not essential for nodule organogenesis but contribute to fine-tune some aspects of the symbiosis.

Compounds present in legume root exudates, such as amino acids, quaternary ammonium compounds, and organic acids function as chemoattractants for rhizobia. Upon perception by specific bacterial chemoreceptors, they promote bacterial movement toward plant roots facilitating root colonization and the possibility of finding proper sites for infection (Scharf et al., 2016; Compton et al., 2020; Compton and Scharf, 2021). Root exudates can also contain various low molecular weight compounds that mimic bacterial signals and affect quorum sensing (QS) regulation in rhizobia, thereby enhancing or inhibiting the phenotypes controlled by this cell density-dependent regulatory mechanism (Gao et al., 2003; Mathesius et al., 2003; Bauer and Mathesius, 2004). In rhizobia, QS usually relies on the production and perception of *N*-acyl-homoserine lactones (AHLs) that control important functions, some of which are relevant for the interaction with the legume host (Calatrava-Morales et al., 2018). Strigolactones (SLs), a group of carotenoid-derived plant hormones exuded by roots, participate in the interaction of plants with beneficial soil microorganisms (López-Ráez et al., 2017). SLs have a positive influence on nodulation by promoting infection thread formation, in a process in which they may act as a signal for the bacterial partner (Soto et al., 2010; McAdam et al., 2017). In fact, a synthetic SL promotes bacterial surface motility in the alfalfa symbiont *Sinorhizobium* (*Ensifer*) *meliloti* (Peláez-Vico et al., 2016). Plant roots also produce a plethora of volatile compounds that participate in different trophic interactions belowground, including the attraction of beneficial bacteria (Schulz-Bohm et al., 2018). The role of these plant-derived chemical signals in communication with rhizobia deserves attention but is not discussed in this perspective.

Besides Nod factors, phytohormones and AHLs produced by rhizobia are the main diffusible signals participating in the interkingdom signaling with legumes to impact the establishment of symbiosis (**Figure 1**). The ability to synthesize all major phytohormones (auxin, cytokinin, abscisic acid, and gibberellins) has been described among rhizobial species (Ferguson and Mathesius, 2014). The production of these signals by the microbial partner affects the establishment of the symbiosis by controlling nodulation and nitrogen fixation (Ferguson and Mathesius, 2014). AHL-type QS signals for intra- and interspecies communication are also perceived by legumes, leading to different responses, such as changes in root protein content and secretion of signal-mimic compounds, that can influence the outcome of the symbiosis (Mathesius et al., 2003; Veliz-Vallejos et al., 2014, 2020). Although less well studied than in other rhizobacteria, volatile compounds (VCs) are also produced by symbiotic rhizobia. Recent reports have shown that these rhizobial metabolites can trigger plant responses and interfere with the establishment of plant-bacteria interactions (Orozco-Mosqueda et al., 2013; Sánchez-López et al., 2016; Hernández-Calderón et al., 2018; López-Lara et al., 2018). These findings support the notion that rhizobial volatiles might be additional players in the interkingdom signaling with legumes and whose precise role in symbiosis requires further investigation.

BIOACTIVITIES ASSIGNED TO RHIZOBIAL VOLATILES

The production of VCs by rhizobia and its effects on plants have been little investigated. One of the first studies analyzed the VCs produced by *S. meliloti* in the absence or the presence of volatiles emitted by *Medicago truncatula* seedlings (Orozco-Mosqueda et al., 2013). Some of the *S. meliloti* VCs detected like 2-methyl-1-propanol and dimethyl-disulfide were previously described in the volatilomes of different rhizobacteria. Particularly noteworthy was the identification of five compounds that were detected only when the plant and bacteria were co-cultivated in the same Petri dish without physical contact,

thereby suggesting the existence of an interkingdom communication whereby the plant, the bacterium, or both were able to detect and respond to the volatiles produced by the other interacting organism.

Interestingly, two studies have shown that VCs emitted by two different rhizobial species, *S. meliloti* and *Sinorhizobium fredii*, were capable of promoting growth of the non-legume plants *Sorghum bicolor* and *Arabidopsis* (Sánchez-López et al., 2016; Hernández-Calderón et al., 2018). Moreover, exposure to VCs emitted by *S. meliloti* activated iron-uptake mechanisms, namely rhizosphere acidification and increased root ferric reductase, in *M. truncatula* (Orozco-Mosqueda et al., 2013), and increased chlorophyll content and transcriptional activity of iron-uptake genes in *S. bicolor* (Hernández-Calderón et al., 2018). These observations led the authors to suggest that the rhizobial VC-mediated phytostimulatory effect could be caused by improving the plants' iron content, as has been shown for other beneficial rhizobacteria (Zhang et al., 2009). However, this possibility still needs to be experimentally tested. This is an important issue because accumulating evidence indicates that the plant iron-deficiency response is linked to the activation of defense responses (Koen et al., 2014; Romera et al., 2019). Indeed, volatile blends emitted by beneficial rhizobacteria are able to trigger both plant defense and Fe deficiency responses (Zamioudis et al., 2015). In agreement with this, exposure of *S. bicolor* to *S. meliloti* VCs not only induced the expression of Fe-uptake genes but also that of plant-defense genes (Hernández-Calderón et al., 2018). The coordinated activation of the iron-deficiency and defense responses in plants has also been shown in legumes exposed to pure volatiles. Medium supplemented with *N,N*-dimethylhexadecylamine (DMHDA), a volatile produced during the co-cultivation of *S. meliloti* and *M. truncatula* (Orozco-Mosqueda et al., 2013), has been shown to promote plant growth and induce iron-deficiency and defense response genes in *M. truncatula* (Montejano-Ramírez et al., 2020). However, effects of either DMHDA or volatile blends of rhizobia in the establishment of the *Rhizobium*-legume symbiosis have not been reported yet.

To the best of our knowledge, only one study associates the effect of a rhizobial VC with the *Rhizobium*-legume symbiosis. The methylketone 2-tridecanone (2-TDC) was identified as the volatile responsible for the pleiotropic phenotype shown by a *S. meliloti* mutant impaired in alfalfa root colonization and exhibiting increased surface motility and defects in biofilm formation (López-Lara et al., 2018). 2-TDC is known as a natural insecticide produced by wild varieties of tomato plants (Williams et al., 1980), and its production was reported in several bacterial species, including different rhizobacteria (Blom et al., 2011; Lemfack et al., 2018). The results described by López-Lara et al. (2018) indicate that 2-TDC is an infochemical able to affect important bacterial traits, such as surface motility and biofilm formation. Moreover, 2-TDC negatively interfered with different plant–bacteria associations, hampering alfalfa nodulation by *S. meliloti* and also the development of tomato bacterial speck disease by *Pseudomonas syringae* pv *tomato* (López-Lara et al., 2018). It was also shown that 2-TDC hinders the bacterial ability to efficiently colonize plant tissues. However, it remains unknown whether this is the result of 2-TDC altering bacterial behaviors required for plant colonization, and/or that the ketone elicits plant responses that have a negative effect on the interacting bacteria.

FUTURE PERSPECTIVES

Evidence clearly indicates that plants can perceive and respond to volatile blends emitted by rhizobia. Plant growth promotion, activation of iron-uptake mechanisms, and increased transcription of defense genes are some of the responses detected in plants exposed to rhizobial VCs. However, many questions remain concerning the effects of rhizobial VCs on their host plants, and specifically on the establishment of efficient symbiosis (**Figure 2**).

The ability of bacterial volatiles to trigger plant defense responses led to the suggestion that these airborne metabolites could be considered as Microbe-Associated Molecular Patterns (MAMPs; Sharifi and Ryu, 2018). MAMPs are usually conserved microbial molecules, which are perceived by plant cell surface transmembrane receptors and activate a basal defense known as the MAMP-triggered immunity (Jones and Dangl, 2006). Up to now, rhizobial VC-mediated activation of plant defense responses has only been reported in a non-host monocotyledonous plant (Hernández-Calderón et al., 2018). Since the development of nitrogen-fixing nodules requires the strict and continuous control of plant immunity (Cao et al., 2017; Berrabah et al., 2019; Benezech et al., 2020), evaluation of defense responses in legumes exposed to rhizobial VCs deserves special attention and could give clues about the contribution of these metabolites to the *Rhizobium*-legume symbiosis. Moreover, the finding that a rhizobial produced volatile (2-TDC) can protect plants against bacterial phytopathogens through an as yet unknown mechanism (López-Lara et al., 2018) opens the possibility of using rhizobia and their volatilomes as new biocontrol solutions and sources for new biopesticides.

Interestingly, bacterial volatiles can also facilitate mutualistic associations with beneficial rhizobacteria without compromising disease resistance (Morcillo et al., 2020). Whether rhizobial VCs can also facilitate symbiosis with their legume hosts by triggering plant-specific responses to attract the microsymbiont and/or by activating the symbiosis signaling pathway are aspects worth investigating.

The activation of root iron-uptake mechanisms has been detected in both legumes and non-legumes exposed to rhizobial VCs. This effect could be linked to the activation of plant defense responses as has been shown for VCs of other beneficial rhizobacteria (Zamioudis et al., 2015; Romera et al., 2019). The molecular bases responsible for the coordinated regulation of the plant iron-deficiency response and plant immunity have been investigated mainly in *Arabidopsis* where several phytohormones, signaling molecules as well as a transcription factor have been shown to be involved in regulating both processes (Romera et al., 2019). Whether similar regulatory mechanisms participate in rhizobial VC-mediated effects in

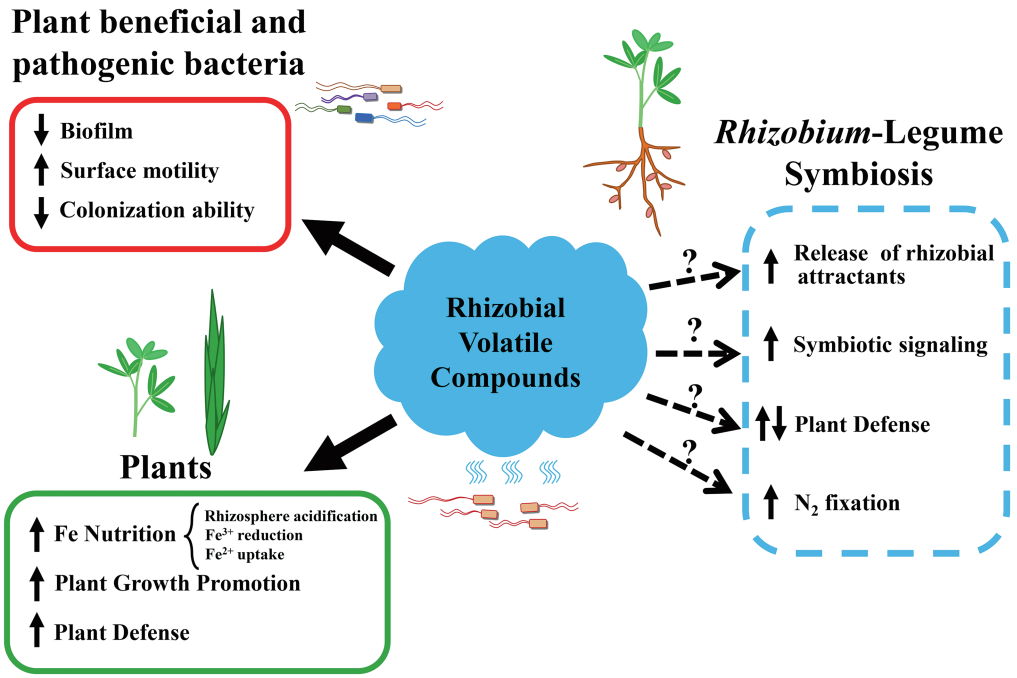

FIGURE 2 | Recognized and putative biological activities of volatile compounds emitted by rhizobia. Bioactivities associated with rhizobial volatile compounds in the literature are shown on the left side of the figure and indicated with solid arrows. Effects on plant beneficial and pathogenic bacteria caused by the discrete application of a rhizobial volatile are shown in a red box. Effects on legume and non-legume plants triggered by rhizobial volatilomes are shown in a green box. Putative effects of rhizobial volatiles, as either volatile blends or discrete compounds, with an impact on the *Rhizobium*-legume symbiosis are shown on the right side of the figure and indicated with dashed arrows and question marks as hypotheses that need to be evaluated.

legumes awaits further investigation. Moreover, considering that symbiotic nitrogen fixation is a Fe-demanding process, the VC-mediated activation of iron-uptake mechanisms in legume roots could contribute to the efficiency of the symbiosis.

Nitrogen availability in the soil is the major factor determining whether the plant will establish nitrogen-fixing symbiosis with rhizobia (Streeter and Wong, 1988). The molecular bases underlying this regulatory mechanism are starting to be deciphered (Chaulagain and Frugoli, 2021). Recently, it has been shown that the availability of a nutrient, namely phosphate, determines the plant's response to a bacterial volatile to result in either mutualism or increased defense responses (Morcillo et al., 2020). Therefore, to assess whether soil nitrogen conditions modulate the legume response to rhizobial VC is another interesting area of research.

Microbial VCs are considered early signaling molecules whose effects in plants depend on the compound's concentration and the plant developmental stage, but the plant receptors and regulatory pathways involved in their recognition are still largely unknown (Weisskopf et al., 2021). The biological activities associated with rhizobial VCs suggest that they could be additional players in the early signaling with legumes and impact the establishment of symbiosis. Further investigation of legume responses to rhizobial VCs, both as volatile blends and as discrete compounds, and ideally using experimental setups that better simulate complex rhizosphere conditions (Kai et al., 2016) will help to elucidate their specific roles in symbiosis and shed light on how plants perceive these signals.

DATA AVAILABILITY STATEMENT

The original contributions presented in the study are included in the article/supplementary material, and further inquiries can be directed to the corresponding author.

AUTHOR CONTRIBUTIONS

MS conceived and wrote most of the sections. PD made all the drawings. PD, IL-L, OG, and MR-P contributed to the writing and editing of the manuscript. All authors read and approved the manuscript.

FUNDING

This work was supported by grants from the Spanish Ministerio de Ciencia, Innovación y Universidades (MCIU), Agencia Estatal de Investigación (AEI) and European Regional Development Funds (FEDER; grant numbers PGC2018-096477-B-I00 and PGC2018-098372-B-I00), from Dirección General de Asuntos de Personal Académico-Universidad Nacional Autónoma de México (DGAPA/UNAM; PAPIIT IN200819), and the Consejo Nacional de Ciencia y Tecnología (CONACyT; 253549). We acknowledge funding by MCIU/AEI/FEDER, DGAPA/UNAM and CONACyT.

REFERENCES

Audrain, B., Farag, M. A., Ryu, C. M., and Ghigo, J. M. (2015). Role of bacterial volatile compounds in bacterial biology. *FEMS Microbiol. Rev.* 39, 222–233. doi: 10.1093/femsre/fuu013

Avalos, M., van Wezel, G. P., Raaijmakers, J. M., and Garbeva, P. (2018). Healthy scents: microbial volatiles as new frontier in antibiotic research? *Curr. Opin. Microbiol.* 45, 84–91. doi: 10.1016/j.mib.2018.02.011

Bailly, A. L., and Weisskopf, L. (2017). Mining the volatilomes of plant-associated microbiota for new biocontrol solutions. *Front. Microbiol.* 8:1638. doi: 10.3389/fmicb.2017.01638

Bakker, P. A., Berendsen, R. L., Doornbos, R. F., Wintermans, P. C., and Pieterse, C. M. (2013). The rhizosphere revisited: root microbiomics. *Front. Plant Sci.* 4:165. doi: 10.3389/fpls.2013.00165

Bauer, W. D., and Mathesius, U. (2004). Plant responses to bacterial quorum sensing signals. *Curr. Opin. Plant Biol.* 7, 429–433. doi: 10.1016/j.pbi.2004.05.008

Benezech, C., Doudement, M., and Gourion, B. (2020). Legumes tolerance to rhizobia is not always observed and not always deserved. *Cell. Microbiol.* 22:e13124. doi: 10.1111/cmi.13124

Berrabah, F., Ratet, P., and Gourion, B. (2019). Legume nodules: massive infection in the absence of defense induction. *Mol. Plant-Microbe Interact.* 32, 35–44. doi: 10.1094/MPMI-07-18-0205-FI

Blom, D., Fabbri, C., Connor, E. C., Schiestl, F. P., Klauser, D. R., Boller, T., et al. (2011). Production of plant growth modulating volatiles is widespread among rhizosphere bacteria and strongly depends on culture conditions. *Environ. Microbiol.* 13, 3047–3058. doi: 10.1111/j.1462-2920.2011.02582.x

Calatrava-Morales, N., McIntosh, M., and Soto, M. J. (2018). Regulation mediated by *N*-acyl homoserine lactone quorum sensing signals in the *Rhizobium*-legume symbiosis. *Genes* 9:263. doi: 10.3390/genes9050263

Cao, Y., Halane, M. K., Gassmann, W., and Stacey, G. (2017). The role of plant innate immunity in the legume-*Rhizobium* symbiosis. *Annu. Rev. Plant Biol.* 68, 535–561. doi: 10.1146/annurev-arplant-042916-041030

Compton, K. K., Hildreth, S. B., Helm, R. F., and Scharf, B. E. (2020). An updated perspective on *Sinorhizobium meliloti* chemotaxis to alfalfa flavonoids. *Front. Microbiol.* 11:581482. doi: 10.3389/fmicb.2020.581482

Compton, K. K., and Scharf, B. E. (2021). Rhizobial chemoattractants, the taste and preferences of legume symbionts. *Front. Plant Sci.* 12:686465. doi: 10.3389/fpls.2021.686465

Chaulagain, D., and Frugoli, J. (2021). The regulation of nodule number in legumes is a balance of three signal transduction pathways. *Int. J. Mol. Sci.* 22:1117. doi: 10.3390/ijms22031117

Chung, J. H., Song, G. C., and Ryu, C. M. (2016). Sweet scents from good bacteria: case studies on bacterial volatile compounds for plant growth and immunity. *Plant Mol. Biol.* 90, 677–687. doi: 10.1007/s11103-015-0344-8

Ferguson, B. J., and Mathesius, U. (2014). Phytohormone regulation of legume-rhizobia interactions. *J. Chem. Ecol.* 40, 770–790. doi: 10.1007/s10886-014-0472-7

Gao, M., Teplitski, M., Robinson, J. B., and Bauer, W. D. (2003). Production of substances by *Medicago truncatula* that affect bacterial quorum sensing. *Mol. Plant-Microbe Interact.* 16, 827–834. doi: 10.1094/MPMI.2003.16.9.827

Garbeva, P., and Weisskopf, L. (2020). Airborne medicine: bacterial volatiles and their influence on plant health. *New Phytol.* 226, 32–43. doi: 10.1111/nph.16282

Hernández-Calderón, E., Aviles-Garcia, M. E., Castulo-Rubio, D. Y., Macías-Rodríguez, L., Montejano Ramírez, V., Santoyo, G., et al. (2018). Volatile compounds from beneficial or pathogenic bacteria differentially regulate root exudation, transcription of iron transporters, and defense signaling pathways in *Sorghum bicolor*. *Plant Mol. Biol.* 96, 291–304. doi: 10.1007/s11103-017-0694-5

Jones, J. D., and Dangl, J. L. (2006). The plant immune system. *Nature* 444, 323–329. doi: 10.1038/nature05286

Kai, M., Effmert, U., and Piechulla, B. (2016). Bacterial-plant-interactions: approaches to unravel the biological function of bacterial volatiles in the rhizosphere. *Front. Microbiol.* 7:108. doi: 10.3389/fmicb.2016.00108

Kanchiswamy, C. N., Malnoy, M., and Maffei, M. E. (2015). Bioprospecting bacterial and fungal volatiles for sustainable agriculture. *Trends Plant Sci.* 20, 206–211. doi: 10.1016/j.tplants.2015.01.004

Koen, E., Trapet, P., Brule, D., Kulik, A., Klinguer, A., Atauri-Miranda, L., et al. (2014). Beta-aminobutyric acid (BABA)-induced resistance in *Arabidopsis thaliana*: link with iron homeostasis. *Mol. Plant-Microbe Interact.* 27, 1226–1240. doi: 10.1094/MPMI-05-14-0142-R

Lemfack, M. C., Gohlke, B. O., Toguem, S. M. T., Preissner, S., Piechulla, B., and Preissner, R. (2018). mVOC 2.0: a database of microbial volatiles. *Nucleic Acids Res.* 46, D1261–D1265. doi: 10.1093/nar/gkx1016

López-Lara, I. M., Nogales, J., Pech-Canul, A., Calatrava-Morales, N., Bernabéu-Roda, L. M., Durán, P., et al. (2018). 2-tridecanone impacts surface-associated bacterial behaviours and hinders plant-bacteria interactions. *Environ. Microbiol.* 20, 2049–2065. doi: 10.1111/1462-2920.14083

López-Ráez, J. A., Shirasu, K., and Foo, E. (2017). Strigolactones in plant interactions with beneficial and detrimental organisms: the yin and yang. *Trends Plant Sci.* 22, 527–537. doi: 10.1016/j.tplants.2017.03.011

Mathesius, U., Mulders, S., Gao, M., Teplitski, M., Caetano-Anollés, G., Rolfe, B. G., et al. (2003). Extensive and specific responses of a eukaryote to bacterial quorum-sensing signals. *Proc. Natl. Acad. Sci. U. S. A.* 100, 1444–1449. doi: 10.1073/pnas.262672599

McAdam, E. L., Hugill, C., Fort, S., Samain, E., Cottaz, S., Davies, N. W., et al. (2017). Determining the site of action of strigolactones during nodulation. *Plant Physiol.* 175, 529–542. doi: 10.1104/pp.17.00741

Meldau, D. G., Meldau, S., Hoang, L. H., Underberg, S., Wunsche, H., and Baldwin, I. T. (2013). Dimethyl disulfide produced by the naturally associated bacterium *Bacillus* sp B55 promotes *Nicotiana attenuata* growth by enhancing sulfur nutrition. *Plant Cell* 25, 2731–2747. doi: 10.1105/tpc.113.114744

Misztal, P. K., Lymperopoulou, D. S., Adams, R. I., Scott, R. A., Lindow, S. E., Bruns, T., et al. (2018). Emission factors of microbial volatile organic compounds from environmental bacteria and fungi. *Environ. Sci. Technol.* 52, 8272–8282. doi: 10.1021/acs.est.8b00806

Montejano-Ramírez, V., García-Pineda, E., and Valencia-Cantero, E. (2020). Bacterial compound *N,N*-dimethylhexadecylamine modulates expression of iron deficiency and defense response genes in *Medicago truncatula* independently of the jasmonic acid pathway. *Plants* 9:624. doi: 10.3390/plants9050624

Morcillo, R. J., Singh, S. K., He, D., An, G., Vilchez, J. I., Tang, K., et al. (2020). Rhizobacterium-derived diacetyl modulates plant immunity in a phosphate-dependent manner. *EMBO J.* 39:e102602. doi: 10.15252/embj.2019102602

Oldroyd, G. E. (2013). Speak, friend, and enter: signalling systems that promote beneficial symbiotic associations in plants. *Nat. Rev. Microbiol.* 11, 252–263. doi: 10.1038/nrmicro2990

Orozco-Mosqueda, M. C., Macías-Rodríguez, L. I., Santoyo, G., Farías-Rodríguez, R., and Valencia-Cantero, E. (2013). *Medicago truncatula* increases its iron-uptake mechanisms in response to volatile organic compounds produced by *Sinorhizobium meliloti*. *Folia Microbiol.* 58, 579–585. doi: 10.1007/s12223-013-0243-9

Peláez-Vico, M. A., Bernabéu-Roda, L., Kohlen, W., Soto, M. J., and López-Ráez, J. A. (2016). Strigolactones in the *Rhizobium*-legume symbiosis: stimulatory effect on bacterial surface motility and down-regulation of their levels in nodulated plants. *Plant Sci.* 245, 119–127. doi: 10.1016/j.plantsci.2016.01.012

Poole, P., Ramachandran, V., and Terpolilli, J. (2018). Rhizobia: from saprophytes to endosymbionts. *Nat. Rev. Microbiol.* 16, 291–303. doi: 10.1038/nrmicro.2017.171

Romera, F. J., García, M. J., Lucena, C., Martínez-Medina, A., Aparicio, M. A., Ramos, J., et al. (2019). Induced systemic resistance (ISR) and Fe deficiency responses in dicot plants. *Front. Plant Sci.* 10:287. doi: 10.3389/fpls.2019.00287

Roy, S., Liu, W., Nandety, R. S., Crook, A., Mysore, K. S., Pislariu, C. I., et al. (2020). Celebrating 20 years of genetic discoveries in legume nodulation and symbiotic nitrogen fixation. *Plant Cell* 32, 15–41. doi: 10.1105/tpc.19.00279

Ryu, C. M., Farag, M. A., Hu, C. H., Reddy, M. S., Wei, H. X., Pare, P. W., et al. (2003). Bacterial volatiles promote growth in *Arabidopsis*. *Proc. Natl. Acad. Sci. U. S. A.* 100, 4927–4932. doi: 10.1073/pnas.0730845100

Sánchez-López, A. M., and Baslam, M., De Diego,N., Muñoz, F. J., Bahaji, A., Almagro, G., et al. (2016). Volatile compounds emitted by diverse phytopathogenic microorganisms promote plant growth and flowering through cytokinin action. *Plant Cell Environ.* 39, 2592–2608. doi:10.1111/pce.12759

Scharf, B. E., Hynes, M. F., and Alexandre, G. M. (2016). Chemotaxis signaling systems in model beneficial plant-bacteria associations. *Plant Mol. Biol.* 90, 549–559. doi: 10.1007/s11103-016-0432-4

Schmidt, R., Cordovez, V., de Boer, W., Raaijmakers, J., and Garbeva, P. (2015). Volatile affairs in microbial interactions. *ISME J.* 9, 2329–2335. doi: 10.1038/ismej.2015.42

Schmidt, R., Jager, V., Zuhlke, D., Wolff, C., Bernhardt, J., Cankar, K., et al. (2017). Fungal volatile compounds induce production of the secondary metabolite sodorifen in *Serratia plymuthica* PRI-2C. *Sci. Rep.* 7:862. doi: 10.1038/s41598-017-00893-3

Schulz-Bohm, K., Gerards, S., Hundscheid, M., Melenhorst, J., de Boer, W., and Garbeva, P. (2018). Calling from distance: attraction of soil bacteria by plant root volatiles. *ISME J.* 12, 1252–1262. doi: 10.1038/s41396-017-0035-3

Schulz-Bohm, K., Martin-Sanchez, L., and Garbeva, P. (2017). Microbial volatiles: small molecules with an important role in intra- and inter-kingdom interactions. *Front. Microbiol.* 8:2484. doi: 10.3389/fmicb.2017.02484

Schulz, S., and Dickschat, J. S. (2007). Bacterial volatiles: the smell of small organisms. *Nat. Prod. Rep.* 24, 814–842. doi: 10.1039/b507392h

Sharifi, R., and Ryu, C. M. (2018). Sniffing bacterial volatile compounds for healthier plants. *Curr. Opin. Plant Biol.* 44, 88–97. doi: 10.1016/j.pbi.2018.03.004

Soto, M. J., Fernández-Aparicio, M., Castellanos-Morales, V., García-Garrido, J. M., Ocampo, J. A., Delgado, M. J., et al. (2010). First indications for the involvement of strigolactones on nodule formation in alfalfa (*Medicago sativa*). *Soil Biol. Biochem.* 42, 383–385. doi: 10.1016/j.soilbio.2009.11.007

Streeter, J., and Wong, P. P. (1988). Inhibition of legume nodule formation and N_2 fixation by nitrate. *Crit. Rev. Plant Sci.* 7, 1–23. doi: 10.1080/07352688809382257

Thomas, G., Withall, D., and Birkett, M. (2020). Harnessing microbial volatiles to replace pesticides and fertilizers. *Microb. Biotechnol.* 13, 1366–1376. doi: 10.1111/1751-7915.13645

Tyagi, S., Mulla, S. I., Lee, K. J., Chae, J. C., and Shukla, P. (2018). VOCs-mediated hormonal signaling and crosstalk with plant growth promoting microbes. *Crit. Rev. Biotechnol.* 38, 1277–1296. doi: 10.1080/07388551.2018.1472551

Tyc, O., Song, C., Dickschat, J. S., Vos, M., and Garbeva, P. (2017). The ecological role of volatile and soluble secondary metabolites produced by soil bacteria. *Trends Microbiol.* 25, 280–292. doi: 10.1016/j.tim.2016.12.002

Veliz-Vallejos, D. F., Kawasaki, A., and Mathesius, U. (2020). The presence of plant-associated bacteria alters responses to *N*-acyl homoserine lactone quorum sensing signals that modulate nodulation in *Medicago truncatula*. *Plants* 9:777. doi: 10.3390/plants9060777

Veliz-Vallejos, D. F., van Noorden, G. E., Yuan, M., and Mathesius, U. (2014). A *Sinorhizobium meliloti*-specific *N*-acyl homoserine lactone quorum-sensing signal increases nodule numbers in *Medicago truncatula* independent of autoregulation. *Front. Plant Sci.* 5:551. doi: 10.3389/fpls.2014.00551

Weisskopf, L., Schulz, S., and Garbeva, P. (2021). Microbial volatile organic compounds in intra-kingdom and inter-kingdom interactions. *Nat. Rev. Microbiol.* 19, 391–404. doi: 10.1038/s41579-020-00508-1

Williams, W. G., Kennedy, G. G., Yamamoto, R. T., Thacker, J. D., and Bordner, J. (1980). 2-tridecanone: a naturally occurring insecticide from the wild tomato *Lycopersicon hirsutum* f. *glabratum*. *Science* 207, 888–889. doi: 10.1126/science.207.4433.888

Zamioudis, C., Korteland, J., Van Pelt, J. A., van Hamersveld, M., Dombrowski, N., Bai, Y., et al. (2015). Rhizobacterial volatiles and photosynthesis-related signals coordinate MYB72 expression in *Arabidopsis* roots during onset of induced systemic resistance and iron-deficiency responses. *Plant J.* 84, 309–322. doi: 10.1111/tpj.12995

Zhang, H., Sun, Y., Xie, X., Kim, M. S., Dowd, S. E., and Pare, P. W. (2009). A soil bacterium regulates plant acquisition of iron *via* deficiency-inducible mechanisms. *Plant J.* 58, 568–577. doi: 10.1111/j.1365-313X.2009.03803.x

Zhang, H., Xie, X., Kim, M. S., Kornyeyev, D. A., Holaday, S., and Pare, P. W. (2008). Soil bacteria augment *Arabidopsis* photosynthesis by decreasing glucose sensing and abscisic acid levels in planta. *Plant J.* 56, 264–273. doi: 10.1111/j.1365-313X.2008.03593.x

Zipfel, C., and Oldroyd, G. E. D. (2017). Plant signalling in symbiosis and immunity. *Nature* 543, 328–336. doi: 10.1038/nature22009

Conflict of Interest: The authors declare that the research was conducted in the absence of any commercial or financial relationships that could be construed as a potential conflict of interest.

frontiers in Plant Science

ORIGINAL RESEARCH
published: 23 July 2021
doi: 10.3389/fpls.2021.678976

ExoS/ChvI Two-Component Signal-Transduction System Activated in the Absence of Bacterial Phosphatidylcholine

Otto Geiger[1], Christian Sohlenkamp[1], Diana Vera-Cruz[1], Daniela B. Medeot[1], Lourdes Martínez-Aguilar[1], Diana X. Sahonero-Canavesi[1], Stefan Weidner[2†], Alfred Pühler[2] and Isabel M. López-Lara[1]*

[1] Centro de Ciencias Genómicas, Universidad Nacional Autónoma de México, Cuernavaca, Mexico, [2] Institut für Genomforschung und Systembiologie, Centrum für Biotechnologie (CeBiTec), Universität Bielefeld, Bielefeld, Germany

OPEN ACCESS

Edited by:
Benjamin Gourion, UMR 2594 Laboratoire Interactions Plantes-Microorganismes (LIPM), France

Reviewed by:
Birgit Edeltraud Scharf, Virginia Tech, United States
Franz Narberhaus, Ruhr University Bochum, Germany

***Correspondence:**
Otto Geiger
otto@ccg.unam.mx

† Deceased

Specialty section:
This article was submitted to Plant Symbiotic Interactions, a section of the journal Frontiers in Plant Science

Received: *10 March 2021*
Accepted: *24 June 2021*
Published: *23 July 2021*

Citation:
Geiger O, Sohlenkamp C, Vera-Cruz D, Medeot DB, Martínez-Aguilar L, Sahonero-Canavesi DX, Weidner S, Pühler A and López-Lara IM (2021) ExoS/ChvI Two-Component Signal-Transduction System Activated in the Absence of Bacterial Phosphatidylcholine. Front. Plant Sci. 12:678976. doi: 10.3389/fpls.2021.678976

Sinorhizobium meliloti contains the negatively charged phosphatidylglycerol and cardiolipin as well as the zwitterionic phosphatidylethanolamine (PE) and phosphatidylcholine (PC) as major membrane phospholipids. In previous studies we had isolated *S. meliloti* mutants that lack PE or PC. Although mutants deficient in PE are able to form nitrogen-fixing nodules on alfalfa host plants, mutants lacking PC cannot sustain development of any nodules on host roots. Transcript profiles of mutants unable to form PE or PC are distinct; they differ from each other and they are different from the wild type profile. For example, a PC-deficient mutant of *S. meliloti* shows an increase of transcripts that encode enzymes required for succinoglycan biosynthesis and a decrease of transcripts required for flagellum formation. Indeed, a PC-deficient mutant is unable to swim and overproduces succinoglycan. Some suppressor mutants, that regain swimming and form normal levels of succinoglycan, are altered in the ExoS sensor. Our findings suggest that the lack of PC in the sinorhizobial membrane activates the ExoS/ChvI two-component regulatory system. ExoS/ChvI constitute a molecular switch in *S. meliloti* for changing from a free-living to a symbiotic life style. The periplasmic repressor protein ExoR controls ExoS/ChvI function and it is thought that proteolytic ExoR degradation would relieve repression of ExoS/ChvI thereby switching on this system. However, as ExoR levels are similar in wild type, PC-deficient mutant and suppressor mutants, we propose that lack of PC in the bacterial membrane provokes directly a conformational change of the ExoS sensor and thereby activation of the ExoS/ChvI two-component system.

Keywords: *Sinorhizobium meliloti*, membrane lipid, symbiosis, phosphatidylethanolamine, succinoglycan, motility

INTRODUCTION

For the establishment of a nitrogen-fixing root nodule symbiosis between legume plants and rhizobial bacteria, a precise temporary sequence of mutual signaling and recognition events is required in order to guarantee a successful outcome for this symbiosis (Gibson et al., 2008). The early events in nodulation are relatively well understood. Plant flavonoids induce nodulation (*nod*)

genes most of which are involved in the production of lipochitin oligosaccharide signal molecules (nodulation factors). Nodulation factors are able to induce nodule primordia on respective host plants and thereby trigger the developmental process resulting in nodule formation. Rhizobial exopolysaccharides (EPS), K-like capsular polysaccharides, and cyclic glucans are important secreted compounds required for the infection process by rhizobia as they modulate the host defense response during bacterial invasion of the plant. Subsequently, rhizobial lipopolysaccharides are required for intracellular colonization and for establishing a chronic host infection (Gibson et al., 2008). However, many rhizobial factors, required especially for the late stages of symbiotic development, may still be unrecognized.

In the specific case of *S. meliloti* 1021, which can form a symbiosis with *Medicago sativa* (alfalfa), the synthesis of exopolysaccharide I (EPSI; succinoglycan) or exopolysaccharide II (EPSII; galactoglucan) is required for bacterial advancement in the infection thread and for invasion of the nodule (Cheng and Walker, 1998b). A number of regulatory systems control the formation of EPSI and EPSII (Janczarek, 2011), among them a two-component signal-transduction system that consists of the integral membrane histidine kinase ExoS and the associated cytoplasmic response regulator ChvI (Cheng and Walker, 1998a). The enzymatic activities of the ExoS/ChvI system are controlled by the periplasmic regulator protein ExoR, through direct interaction with ExoS (Wells et al., 2007). Three distinct forms of ExoR are known, the precursor version of ExoR, $ExoR_p$, the mature form of ExoR, $ExoR_m$, and a shorter, inactive 20 kD form of ExoR, $ExoR_{c20}$ (Lu et al., 2012). During synthesis of $ExoR_p$, the N-terminus is recognized by the type II secretion system, followed by cleavage of the N-terminal signal sequence and transport of the mature $ExoR_m$ to the periplasm (Wiech et al., 2015). The model for the ExoR-ExoS/ChvI signaling pathway suggests that the ExoS/ChvI system is turned off when the periplasmic domain of ExoS forms a protein complex with the mature periplasmic form $ExoR_m$. In the $ExoR_m$-ExoS complex, ExoS acts as a phosphatase and keeps ChvI dephosphorylated and inactive. Upon disruption of the $ExoR_m$-ExoS interaction, for example, through the proteolytic degradation of $ExoR_m$ to $ExoR_{c20}$, the ExoS/ChvI system becomes derepressed. Signaling by the derepressed ExoS/ChvI system involves autophosphorylation of the transmembrane histidine kinase sensor ExoS, transphosphorylation to the transcriptional regulator ChvI and activation or inhibition of *chvI* box-preceded genes by the phosphorylated ChvI regulator, resulting in upregulation of succinoglycan biosynthesis, repression of flagellum biosynthesis, and altered expression of more than 100 genes, allowing the cells to switch from a free-living to a host-invading form (Yao et al., 2004; Wells et al., 2007; Lu et al., 2012). An extensive list of target genes regulated by ChvI and a consensus sequence for ChvI binding has been identified (Chen et al., 2009; Ratib et al., 2018). The two-component system ExoS/ChvI has not only important roles in succinoglycan production and motility, but also in biofilm formation, nutrient utilization and growth of free-living bacteria (Chen et al., 2009). Mutations in *exoR* or *exoS* that permanently switch on signaling through the ExoS/ChvI system demonstrate reduced efficiency of root hair colonization and a reduction in symbiotic performance, overproduction of succinoglycan, and suppression of flagellum synthesis (Yao et al., 2004). Notably, whereas the *exoS* mutant reported by Yao et al. (2004) is constitutively activated, an *exoS* null mutant has a phenotype similar to a *chvI* mutant, cannot establish an effective symbiosis with *M. sativa* either, and exhibits a pleiotropic phenotype (Bélanger et al., 2009). The mutant deleted in *chvI* failed to grow on complex medium, exhibited lower tolerance to acidic conditions, did not produce EPS or smooth LPS, was hypermotile and symbiotically defective (Wang et al., 2010).

The Gram-negative model bacterium *Escherichia coli* has phosphatidylglycerol (PG), cardiolipin (CL), and phosphatidylethanolamine (PE) as major membrane phospholipids. Although phosphatidylcholine (PC) is ubiquitous in eukaryotes, only about 15% of the bacteria are able to synthesize PC for their membranes (Sohlenkamp et al., 2003; Geiger et al., 2013). In *S. meliloti*, both zwitterionic lipids (PE and PC) are major components of the membrane. The only difference between the two types of molecules is that the primary amino group of PE is substituted with three additional methyl groups in the case of PC (**Figure 1**). In *S. meliloti* and most other bacteria, CDP-diacylglycerol (CDP-DAG) is the central activated lipid precursor for the diversification of membrane lipids with different phosphoalcohol head groups (**Figure 1**). For example, condensation of serine with CDP-DAG is catalyzed by phosphatidylserine synthase (PssA) and leads to the formation of phosphatidylserine (PS) and CMP (Sohlenkamp et al., 2004). In a second step, phosphatidylserine decarboxylase (Psd) converts PS into PE and CO_2 (Vences-Guzmán et al., 2008). In *S. meliloti*, PE can be further converted into PC by phospholipid *N*-methyltransferase (PmtA) by triple methylation using *S*-adenosylmethionine as methyl donor and forming *S*-adenosylhomocysteine (de Rudder et al., 2000). *S. meliloti* and many PC-containing bacteria have a second PE-independent pathway for PC formation, the phosphatidylcholine synthase (Pcs) pathway (de Rudder et al., 1999; Sohlenkamp et al., 2000). Pcs catalyzes the condensation of choline with CDP-DAG and forms PC and CMP in one step. In a previous study, we had constructed a double mutant (OG10017) that was deficient in PmtA and Pcs and therefore was unable to form PC (de Rudder et al., 2000; **Figure 1**). In another study, a mutant (CS111) was constructed that was deficient in PssA and therefore could not form PE (Sohlenkamp et al., 2004). However, CS111 could form PC via the Pcs pathway when cultivated in choline-containing growth media such as complex media containing tryptone and yeast extract (**Figure 1**). Although the PE-deficient mutant CS111 forms less nodules on legume host plants than the wild type, the mutant was symbiotically effective (Vences-Guzmán et al., 2008). PC occurs in a subset of bacteria many of which are known to interact as pathogens or symbionts with eukaryotic hosts and there has been speculation that bacterial PC might be a requirement for this interaction (de Rudder et al., 1997; Sohlenkamp et al., 2003).

Here we report that a PC-deficient mutant of *S. meliloti* is unable to form a nitrogen-fixing symbiosis with its host plant

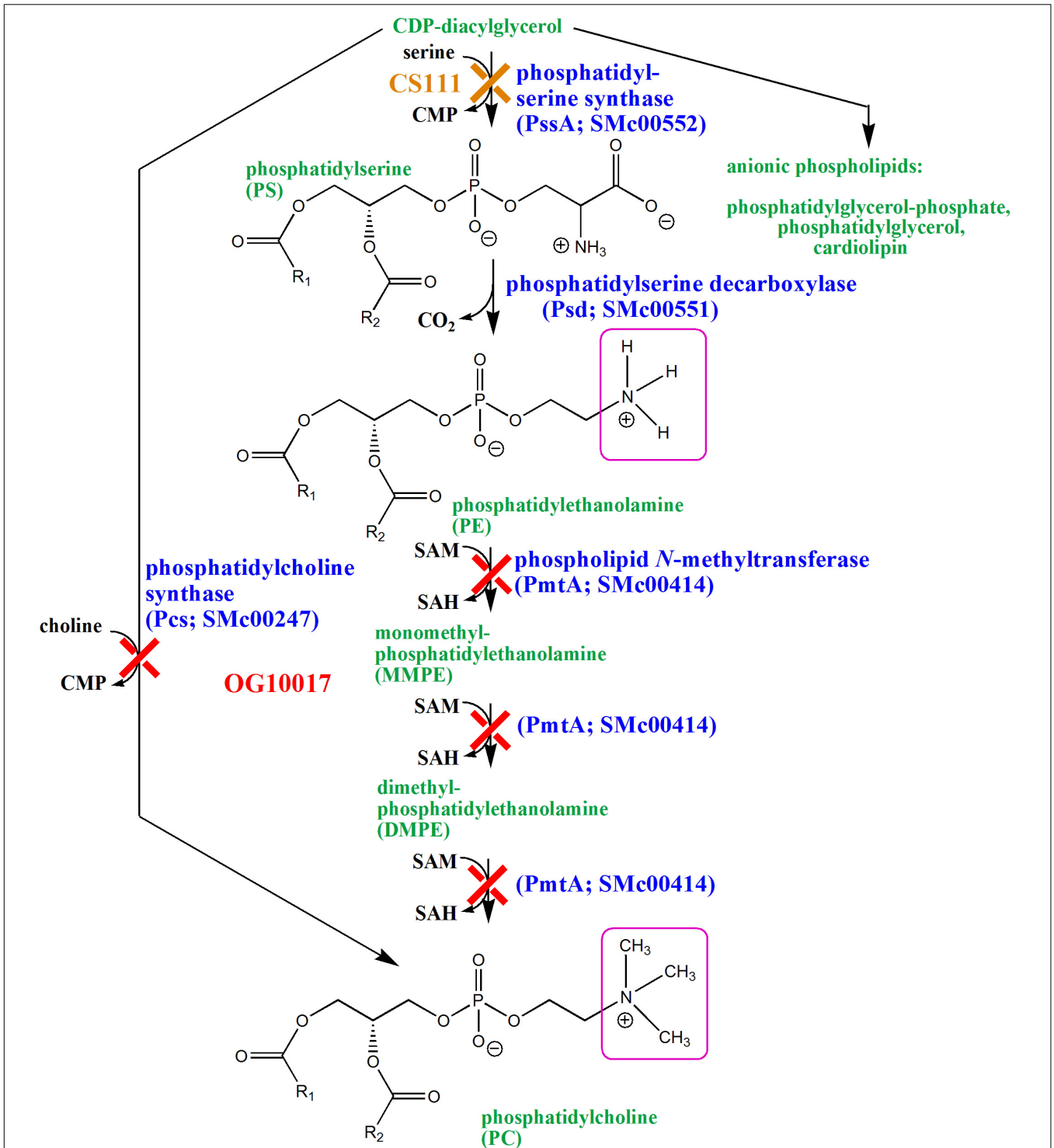

FIGURE 1 | Biosynthesis of phospholipids in *Sinorhizobium meliloti* wild type and in mutants deficient in PE (CS111) or PC (OG10017) formation. Cytidine monophosphate (CMP), cytidine diphosphate (CDP), inorganic phosphate (P_i), *S*-adenosylmethionine (SAM), *S*-adenosylhomocysteine (SAH). Structural differences between PE and PC are highlighted by pink squares.

alfalfa. We show that transcript profiles of mutants deficient in PE or PC differ from each other and are different from the profile of the wild type. Finally, we suggest that the lack of PC in *S. meliloti* activates the ExoR/ExoS/ChvI three-component system which might explain a symbiosis-deficient phenotype of a PC-deficient mutant.

RESULTS

PC-Deficient Mutant of *S. meliloti* Cannot Form Nitrogen-Fixing Root Nodules on Alfalfa

In order to study whether bacterial PC was required for the symbiotic interaction of *S. meliloti* with its alfalfa (*M. sativa*) host plant, aseptically grown alfalfa seedlings were inoculated with *S. meliloti* wild type, the *pmtA*-deficient mutant KDR516, the *pcs*-deficient mutant KDR568, the PC-deficient mutant OG10017, OG10017 expressing *pmtA* from plasmid pTB2042, OG10017 expressing *pcs* from plasmid pTB2532, or OG10017 harboring the empty broad host range plasmid pRK404. Of all the strains tested, only the PC-deficient mutant OG10017, which lacks both pathways for PC formation, and OG10017 harboring the empty broad host range plasmid pRK404 were unable to form any nodules on alfalfa host plants (**Figure 2A**). In contrast, strains with the ability to form PC (wild type, KDR516, KDR568, OG10017 expressing *pmtA*, or OG10017 expressing *pcs*) were able to form pink, nitrogen-fixing root nodules on alfalfa (**Figure 2A**). A lack of host plant nodulation is often due to a deficient formation and secretion of lipochitin oligosaccharide nodulation factors by the rhizobial microsymbiont (Gibson et al., 2008). However, when analyzing spent culture media we found that *S. meliloti* wild type, the *pmtA*-deficient mutant KDR516, the *pcs*-deficient mutant KDR568, and the PC-deficient mutant OG10017 were able to form several distinct nodulation factors in the typical flavonoid-dependent way (**Figure 2B**), that were previously shown to constitute a family of structurally related nodulation factors (Schultze et al., 1992). The fact that KDR516 ($pmtA^-$) and OG10017 (PC^-) seem to produce less nodulation factors (**Figure 2B**), is probably due to the reduced growth of both strains on the minimal medium employed. Microscopic analysis of plantlets inoculated either with the wild type or the PC-deficient mutant OG10017, shows that in the case of wild type a typical nodule structure is formed (**Figure 2C**), whereas in the case of the PC-deficient mutant only an initiating meristem (**Figure 2D**), that is distinct from side root meristems, is formed. Initiating meristems on alfalfa roots are another indication that the PC-deficient mutant OG10017 can form and secrete nodulation factors in an adequate way.

Growth Analysis of *S. meliloti* Wild Type and Phospholipid-Deficient Mutants

Our previous results indicated that the PC-deficient mutant OG10017 grew poorly in low osmolarity media such as TY (de Rudder et al., 2000) whereas the PE-deficient mutant CS111 was unable to grow on all the minimal media we tested (Sohlenkamp et al., 2004). In order to get hints why the PC-deficient mutant was symbiotically impaired, we decided to analyze transcript profiles of *S. meliloti* wild type and mutants CS111 ($pssA^-$; PE^-) and OG10017 ($pmtA^-/pcs^-$; PC^-). Bacterial strains were cultivated on LB/MC+ medium in which they showed similar rates during the exponential phase of growth (**Figure 3**) following the increase of OD_{600} (**Figure 3A**) or of colony-forming units (CFU) (**Figure 3B**) over time. In LB/MC+ medium, the PE-deficient mutant CS111 and the PC-deficient mutant OG10017 showed only slightly reduced growth rates when compared to the wild type and when cultures reached an OD_{600} of 0.8, RNA was isolated and transcriptional profiles established as described in Materials and Methods and in more detail by Hellweg and collaborators (Hellweg et al., 2009). Lipid composition of all three strains after growth on LB/MC+ medium was determined and at those conditions PE is absent in CS111 ($pssA^-$) and PC is absent in OG10017 ($pmtA^-/pcs^-$) (**Table 1**).

Transcriptional and Physiological Differences Between Wild Type and PE-Deficient Mutant Cells

Several differences were observed when the expression profiles of the PE-deficient mutant CS111 and the wild type were compared. In the PE-deficient mutant, transcripts for 11 genes were increased (M-value > 1) and transcripts for 12 genes were reduced (M-value < -1) (**Table 2** and **Supplementary Table 1**). In CS111, transcripts for the putative quinoprotein methanol dehydrogenase MxaF (SMb20173), cytochromes C (SMb20172, SMb20174), a methanol oxidation protein (SMb20175), and transcripts (SMb20204, SMb20207) required for the formation of the pyrroloquinoline (PQQ) cofactor of bacterial methanol dehydrogenases are increased which would be in agreement with an increased capability of the PE-deficient mutant CS111 to convert methanol to formaldehyde (**Figure 4**). Also, transcripts for enzymes of the glutathione (GSH)-dependent formaldehyde oxidation (glutathione-dependent formaldehyde-activating enzyme Gfa SMb20186, glutathione-dependent formaldehyde dehydrogenase Fdh SMb20170, *S*-formyl glutathione hydrolase Fgh SMb20171) (Goenrich et al., 2002) are increased in CS111 suggesting an efficient conversion of formaldehyde to formic acid. In this context it is interesting to note that also transcripts for genes (*fdoG*, *fdsG*) of the two functional formate dehydrogenase systems (Pickering and Oresnik, 2008) are slightly increased in CS111 (M-value < 1) (**Supplementary Table 1**) suggesting an increment in the conversion of formic acid to CO_2. Therefore, the PE-deficient mutant CS111 shows increased transcripts for proteins that might be involved in the degradation of C1 compounds such as methanol or formaldehyde (**Figure 4**). Presently, we do not know why transcripts for C1 catabolism are increased in the PE-deficient mutant.

In contrast, several transcripts that might encode proteins required for efficient iron uptake by the hemin or rhizobactin systems are reduced in the PE-deficient mutant CS111 (**Figure 4**). For example, transcripts for the TonB-dependent, hemin-binding outer membrane protein receptor ShmR (SMc02726), the putative hemin transport protein HmuS (SMc01513) and a gene transcribed in opposite direction encoding the hypothetical protein SMc01514 are reduced (**Table 2**) which could be explained by an altered regulation through the HmuP regulatory protein (SMc01747)(Amarelle et al., 2010). Also, transcripts for the rhizobactin siderophore biosynthesis proteins RhbABCDEF (SMa2400, SMa2402, SMa2404, SMa2406, SMa2408, SMa2410) (**Table 2** and **Supplementary Table 1**),

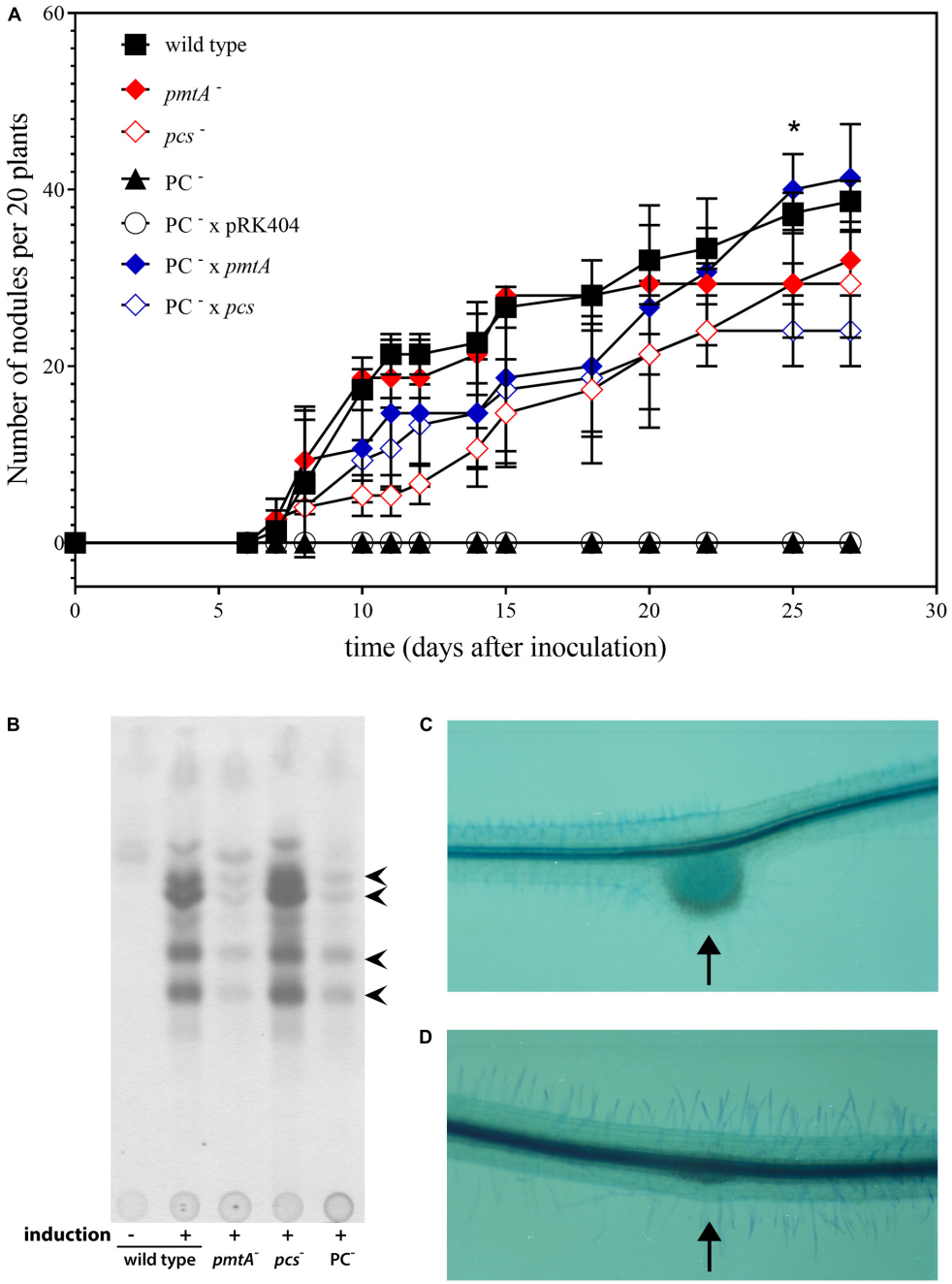

FIGURE 2 | Symbiotic performance of *Sinorhizbium meliloti* strains affected in PC biosynthesis. **(A)** Nodulation kinetics of *S. meliloti* wild type and mutant strains on alfalfa plants. Results for *S. meliloti* wild type strain 1021 (■), *pmtA*-deficient mutant KDR516 (♦), *pcs*-deficient mutant KDR568 (◊), PC-deficient mutant OG10017 (▲),PC-deficient mutant OG10017 harboring the empty plasmid pRK404 (○),PC-deficient mutant OG10017 complemented with *pmtA*-expressing plasmid pTB2042 (♦), and PC-deficient mutant OG10017 complemented with *pcs*-expressing plasmid pTB2532 (◊). The symbols of ▲ and ○ overlap. Values represent means of three independent experiments and standard deviation is shown. Statistical analysis was performed by a two-way ANOVA with Tukey's multiple comparisons test as described in Materials and Methods. As an example, comparisons at 25 d after inoculation reveal that nodule numbers of all PC-deficient strains (PC^-, PC^- x pRK404) are significantly different (*$p < 0.05$) from PC-containing strains (wild type, *pmtA*$^-$, *pcs*$^-$, PC^- x *pmtA*), except *pcs*$^-$ versus PC^- or *pcs*$^-$ versus PC^- x pRK404 ($p < 0.0557$). **(B)** PC-deficient *S. meliloti* mutant can form nodulation (Nod) factors. Thin-layer chromatographic analysis of Nod factor formation when *S. meliloti* wild type 1021 was not induced (lane 1) or induced with the flavonoid naringenin (lane 2), or when *pmtA*-deficient mutant KDR516 (lane 3), *pcs*-deficient mutant KDR568 (lane 4), or PC-deficient mutant OG10017 (lane 5) were induced with naringenin. All strains carried plasmid pMP280 for an increased production of Nod factors (Spaink et al., 1987). Arrowheads mark different Nod factors formed by *S. meliloti*. **(C,D)** PC-deficient *S. meliloti* mutant triggers initiation of nodule meristems on alfalfa roots. Arrows indicate a nodule induced by *S. meliloti* wild type (C), or a typical nodule meristem induced by the PC-deficient mutant OG10017 (D), respectively, 10 d after inoculation. For **(C)** and **(D)**, roots were cleared with hypochlorite and stained with methylene blue as described by Truchet and collaborators (Truchet et al., 1989).

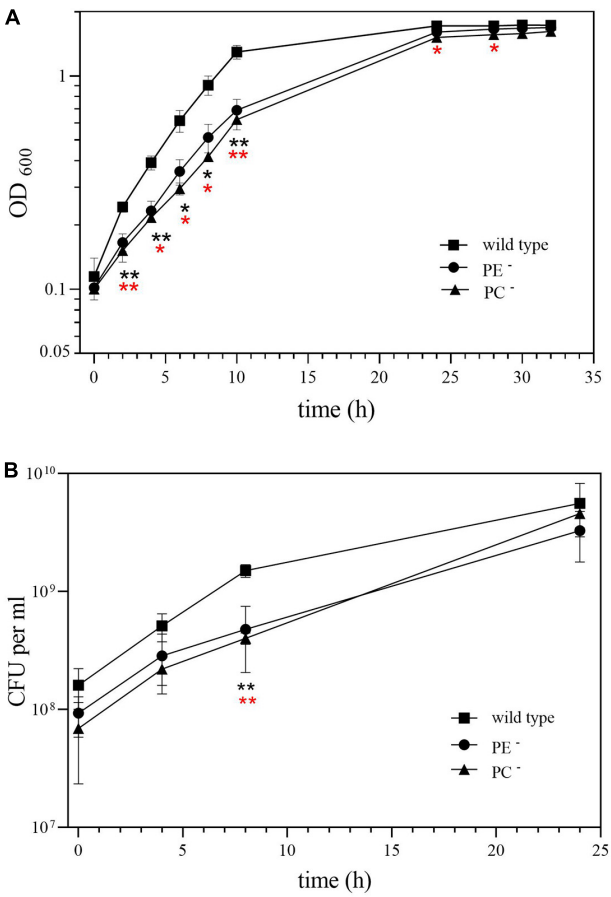

FIGURE 3 | Growth of *Sinorhizobium meliloti* wild type (■), PE-deficient mutant CS111 (●), and PC-deficient mutant OG10017 (▲) on LB/MC+ medium. Growth was recorded by measuring **(A)** the optical density of cultures at 600 nm (OD_{600}) or by determining **(B)** the concentration of viable cells as colony-forming units (CFU) per ml. Values represent means of three independent experiments and standard deviation is shown. Statistical analysis was performed by a two-way ANOVA with Tukey's multiple comparisons test as described in Materials and Methods. Comparisons of the PE-deficient (black asterisks) or the PC-deficient (red asterisks) mutant to wild type are indicated. Statistical significance is shown (*$p < 0.05$; **$p < 0.01$).

TABLE 1 | Membrane lipid composition of *Sinorhizobium meliloti* wild type 1021, phosphatidylethanolamine-deficient (*pssA*$^-$) mutant CS111, phosphatidylcholine-deficient (*pmtA*$^-$/*pcs*$^-$) mutant OG10017 after *in vivo* labeling for 24 h during growth on complex LB/MC+ medium.

strain	wild type	*pssA*$^-$	*pmtA*$^-$/*pcs*$^-$
PC	75.2 ± 7.6	44.9 ± 3.8	n.d.
PE + (MMPE)	10.2 ± 4.8	n.d.	80.9 ± 5.6
CL	1.4 ± 0.3	16.2 ± 2.7	3.6 ± 2.7
PG	7.1 ± 3.2	33.6 ± 4.8	12.0 ± 2.4
OL	4.1 ± 1.0	1.7 ± 0.8	2.7 ± 0.2
SL	1.2 ± 0.7	3.5 ± 2.1	2.6 ± 1.4
DMPE	0.9 ± 0.5	n.d.	0.5 ± 0.1

n.d., Not detected; PC, phosphatidylcholine; PE, phosphatidylethanolamine; MMPE, monomethyl-phosphatidylethanolamine; CL, cardiolipin; PG, phosphatidylglycerol; OL, ornithine-containing lipid; SL, sulfolipid; DMPE, dimethyl-phosphatidylethanolamine. Numbers are the mean of three independent experiments ± standard deviation.

a TonB-dependent siderophore receptor SMc01658, and a periplasmic component of a high affinity iron transport system (SMc01659) (**Supplementary Table 1**) seem to be reduced in the PE-deficient mutant CS111 (**Figure 4**). We therefore speculated that the PE-deficient mutant might suffer from an iron deficiency.

In previous attempts we were unable to obtain sustained growth for the PE-deficient mutant on defined minimal media (Sohlenkamp et al., 2004). We now used a modified MOPS minimal medium in which Ca^{2+} concentration was increased 4-fold, whereas phosphate concentration was reduced 10-fold, and which permitted sustained growth of the PE-deficient mutant CS111 in subcultivations. In earlier experiments we showed that choline contributes to growth of CS111 (Sohlenkamp et al., 2004) and we now show that the addition of Fe^{2+} further stimulates growth of both, the PE-deficient mutant CS111 and the wild type (**Supplementary Figure 1**). In modified MOPS minimal medium supplemented with choline and Fe^{2+}, the time of duplication for the PE-deficient mutant CS111 is maintained at distinct subcultivations (**Supplementary Figure 1**).

Also, transcripts in rhizopine or inositol catabolism are reduced (**Figure 4**), among them transcripts for a periplasmic rhizopine-binding protein (SMb20072), a *scyllo*-inositol oxidase IolY (SMc01163), a *myo*-inositol transporter (SMb20713), and *myo*-inositol catabolism proteins IolBCD (SMc00432, SMc01165, SMc01166), suggesting that regulation involving the IolR repressor (SMc01164) (Kohler et al., 2011) is altered in the PE-deficient mutant CS111. Although some *S. meliloti* wild type strains are able to degrade rhizopine, *S. meliloti* 1021 is not (Rossbach et al., 1995). However, *S. meliloti* 1021 can use *myo*-inositol as carbon source. When cultivating *S. meliloti* 1021 on 1/20 LB/MC+ media, the addition of *myo*-inositol clearly stimulates growth and final cell yield of *S. meliloti* 1021 wild type (**Supplementary Figure 2**) which is also the case for the PC-deficient mutant OG10017 (**Supplementary Figure 2**). Surprisingly, for the PE-deficient mutant CS111, after initial growth stimulation by *myo*-insitol, growth suddenly stops (**Supplementary Figure 2**). Determination of colony-forming units after different times clarifies that CS111 is not killed by the presence of *myo*-inositol (data not shown); CS111 rather seems to enter a dormant state when *myo*-inositol is present. Presently we do not know the reason for the *myo*-inositol-provoked growth arrest in the PE-deficient mutant CS111.

Transcriptional Differences Between Wild Type and PC-Deficient Mutant Cells

Several differences were observed when the expression profiles of the PC-deficient mutant and the wild type were compared. In the PC-deficient mutant, 21 genes were induced (M-value > 1) and 11 genes were repressed (M-value < -1) (**Table 3**). The most strongly increased transcript in the PC-deficient mutant OG10017, when compared with wild type, is SMb21440 encoding for a conserved hypothetical protein. Other strongly induced transcripts encode for a putative membrane-bound

TABLE 2 | Partial list of *S. meliloti* genes differently expressed in the phosphatidylethanolamine-deficient mutant CS111 (M > 1 or M < −1).

Gene	Description	*M*-value
SMb20186 *(gfa)*	glutathione-dependent formaldehyde-activating enzyme	3.58
SMb20204 *(pqqA)*	putative pyrroloquinoline quinone synthesis protein A (PqqA)	3.17
SMb20173 *(mxaF)*	putative methanol dehydrogenase, large subunit	2.20
SMb20171 *(fgh)*	putative *S*-formylglutathione hydrolase	1.45
SMb20325 *(thuE)*	probable trehalose/maltose-binding protein	1.43
SMc02156	conserved hypothetical protein	1.39
SMb20174 *(cytC1)*	putative cytochrome C	1.38
SMc02689	probable aldehyde dehydrogenase	1.33
SMb20172 *(cytC2)*	putative cytochrome C alcohol dehydrogenase subunit	1.24
SMb20175 *(mxaJ)*	putative methanol oxidation protein	1.22
SMa1450	probable thiolase	1.02
SMc01659	putative ATP transporter periplasmic component of high affinity iron transport system	−1.02
SMc00432 *(iolB)*	putative *myo*-inositol catabolism protein	−1.06
SMc01513 (*hmuS*)	putative hemin transport protein	−1.08
SMa2410 (*rhbF*)	rhizobactin siderophore biosynthesis protein RhsF	−1.09
SMc01514	conserved hypothetical protein	−1.11
SMc01163 (*iolY*)	putative bacterial glucose/fructose oxidoreductase	−1.16
SMc01165 (*iolC*)	putative sugar kinase	−1.19
SMc01166 (*iolD*)	putative malonic semialdehyde oxidative decarboxylase	−1.19
SMb20713 *(iatA)*	putative *myo*-inositol transporter, ATP-binding protein	−1.20
SMa2408 *(rhbE)*	rhizobactin siderophore biosynthesis protein	−1.33
SMb20072	putative rhizopine binding protein	−1.62
SMc02726 *(shmR)*	hemin-binding outer membrane receptor	−1.92

M-values describe the log_2 ratio between mutant signal/wild type signal as described in section "Materials and Methods."

lytic transglycosylase (SMc01855), for enzymes (UDP-glucose pyrophosphorylase ExoN, galactosyltransferase ExoY) required for the biosynthesis of succinoglycan (exopolysaccharide I) (**Figure 4**), for the heat shock protein HspQ (SMc00949) and an Hsp20-like heat shock protein (SMb21295), for the symbiotically induced protein Nex18 (SMa1077), and others (**Table 3**). It is remarkable that many of the induced transcripts encode for small proteins that possess a transmembrane alpha-helix or proteins that have an N-terminal signal sequence destining them for transport by the type II secretion system across the cytoplasmic membrane. In contrast, transcripts encoding proteins required for flagella formation (SMc03038, SMc03037, SMc03049, SMc03027, SMc03046, SMc03051) or pili (SMc04114) are reduced in the PC-deficient mutant OG10017 and therefore the transcriptional activation cascade for flagellar synthesis is expected to be reduced in its function in this mutant (**Figure 4**). Similarly as noted for the PE-deficient mutant CS111 (**Table 2**), in the PC-deficient mutant OG10017, a reduction for transcripts encoding for proteins required for *myo*-inositol catabolism (IolD, IatA, IolA) (**Figure 4**) is observed (**Table 3**). The complete set of differentially expressed genes for the PC-deficient mutant OG10017 is available (**Supplementary Table 2**).

PC-Deficient Mutant Is Impaired for Swimming and Overproduces Succinoglycan

Sinorhizobium meliloti wild type, the PE-deficient mutant CS111, and the PC-deficient mutant OG10017 were analyzed for their ability to swim on soft agar plates. Whereas *S. meliloti* wild type and to some lesser extent the PE-deficient mutant exhibited their ability to swim in soft agar (**Figure 5A**), the PC-deficient mutant did not show any migration away from the initial spot of inoculation (**Figure 5**). When OG10017 was complemented with the phospholipid *N*-methyltransferase (*pmtA*)-expressing plasmid or with the phosphatidylcholine synthase (*pcs*)-expressing plasmid, swimming was regained which was not the case when an empty broad host range plasmid was employed instead (**Figure 5B**). As wild type levels of PC can be recuperated in the PC-deficient mutant OG10017 by expressing either *pmtA* or *pcs* (de Rudder et al., 2000), there is a strict correlation between PC formation and the ability to swim in *S. meliloti*.

Sinorhizobium meliloti wild type, the PE-deficient mutant CS111, and the PC-deficient mutant OG10017 were analyzed for their ability to produce succinoglycan (exopolysaccharide I) on Calcofluor-containing agar plates. Of the three strains only OG10017 provoked a strong fluorescence (**Figure 6**), indicating that only the PC-deficient mutant OG10017 overproduced succinoglycan while the *S. meliloti* wild type or the PE-deficient mutant CS111 did not. When OG10017 was complemented with the phospholipid *N*-methyltransferase (*pmtA*)-expressing plasmid or with the phosphatidylcholine synthase (*pcs*)-expressing plasmid, succinoglycan was hardly formed as indicated by the lack of fluorescence (**Supplementary Figure 3**), however, fluorescence was maintained when an empty broad host range plasmid was employed instead (**Supplementary Figure 3**). Again, as PC formation is recuperated in the PC-deficient mutant OG10017 by expressing either *pmtA* or *pcs*, repression of succinoglycan formation in *S. meliloti* is observed and there is a strict correlation between the presence of PC and reduced formation of succinoglycan in *S. meliloti*.

PC-Deficient Mutant Is Impaired for Growth at Slightly Acidic pH

Interestingly, a shift of *S. meliloti* wild type to slightly acidic pH provokes transcriptomic changes when compared to the transcriptome at neutral pH (Hellweg et al., 2009), that resemble the alterations observed in the PC-deficient mutant when compared with wild type at neutral pH. We analyzed growth of *S. meliloti* wild type, the PE-deficient mutant CS111, and the PC-deficient mutant OG10017. As reported previously (Hellweg et al., 2009), growth of the wild type on buffered

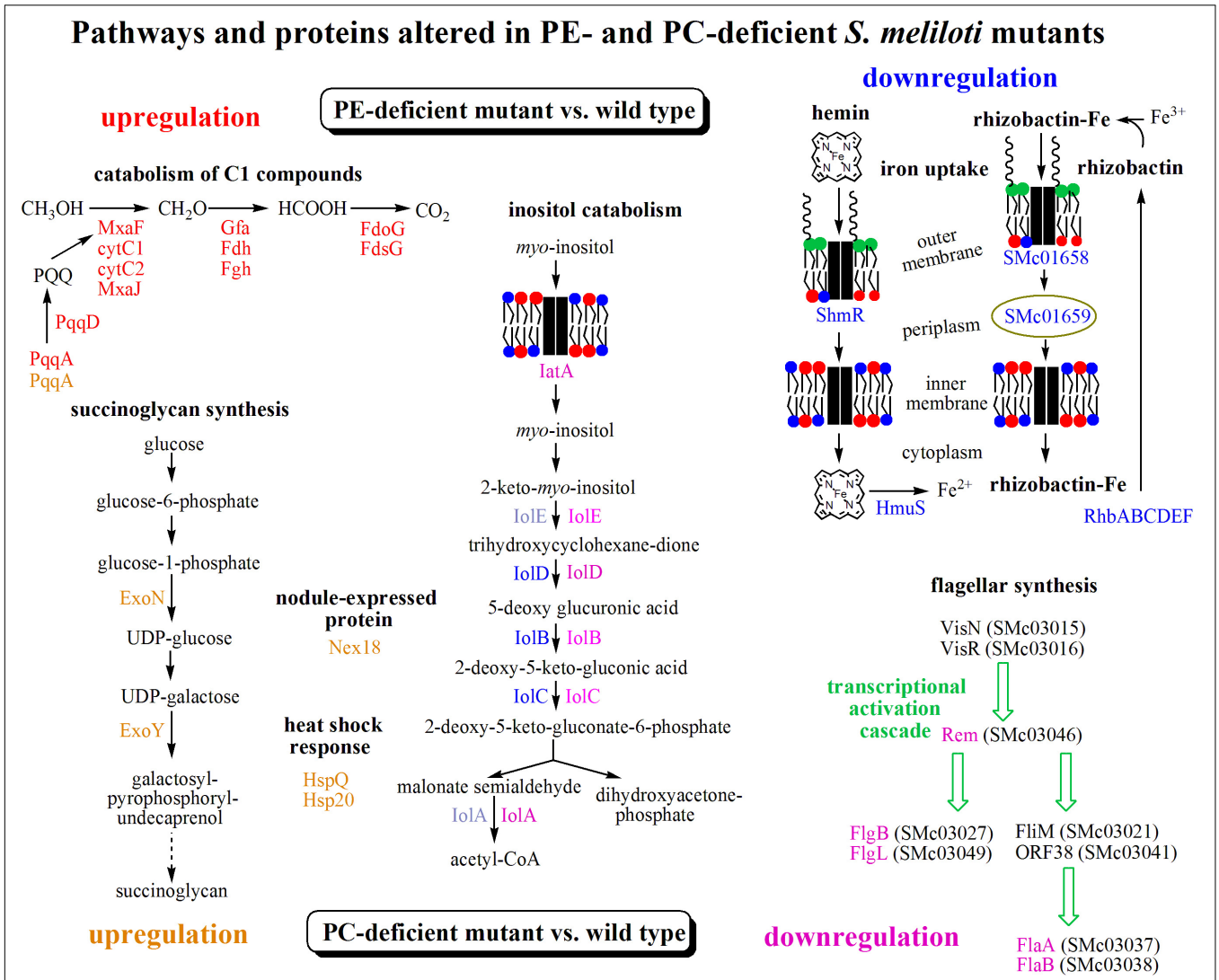

FIGURE 4 | Transcriptomic results suggest differently altered pathways in PE- and PC-deficient mutants of *S. meliloti*. Comparison of transcript profiles of phospholipid-deficient mutants with *S. meliloti* wild type suggests that a pathway for C1 catabolism is upregulated (red) and pathways for inositol catabolism and iron uptake are downregulated (blue) in the PE-deficient mutant CS111 and that the pathway for succinoglycan biosynthesis and heat shock response are upregulated (orange) and pathways for inositol catabolism and flagellar synthesis are downregulated (pink) in the PC-deficient mutant OG10017. Proteins from altered transcripts are highlighted with the respective colors. For details see text, **Tables 2**, **3**, **Supplementary Tables 1, 2**.

LB/MC+ medium at acidic pH 5.75 is only slightly reduced when compared to growth at neutral (pH 7.0) conditions (**Figure 7**) which holds true for the PE-deficient mutant as well. The PC-deficient mutant OG10017 grows at a similar rate as wild type or PE-deficient mutant at neutral pH (**Figure 7A**). However, at slightly acidic conditions of pH 5.75, growth of the PC-deficient mutant OG10017 is severely affected (**Figure 7B**). The lack of PC in mutant OG10017 is in large compensated by PE (**Table 1**), a lipid with a small head group (**Figure 1**) causing more negative curvature in each lipid monolayer. PE has a tendency to form the hexagonal II (H_{II}) phase and is less prone to form bilayers (Dowhan et al., 2008). Therefore, PC-deficient membranes might be less compact, more permeable for ions and especially for protons.

Some Mutants Altered in the ExoR/ExoS/ChvI Signal Transduction System Resemble the PC-Deficient Mutant

In trying to understand how PC deficiency is connected on a molecular level to the observed macroscopic and transcriptomic phenotypes, we searched for transcriptome profiles of mutants in the literature that were similarly altered as the one of a PC-deficient mutant. A strain of *S. meliloti* containing a *chvI(D52E)* mutant version in addition to the wild type copy of *chvI* is thought to produce a more active version of ChvI and displays a transcript profile (Chen et al., 2009) that is quite similar to the one we report here for the

TABLE 3 | Partial list of *Sinorhizobium meliloti* genes differently expressed in the phosphatidylcholine-deficient mutant OG10017 (M > 1 or M < −1).

Gene	Description	*M*-value
SMb21440	conserved hypothetical protein*	2.52
SMc01855	putative lytic transmembrane transglycosylase*	2.06
SMc02156	conserved hypothetical protein*	2.01
SMa1246	conserved hypothetical protein DUF88	1.70
SMa0994	conserved hypothetical protein	1.65
SMa1077 (*nex18*)	symbiotically induced conserved protein*	1.57
SMc00949 (*hspQ*)	heat shock protein	1.53
SMb20204 *(pqqA)*	putative pyrroloquinoline quinone synthesis protein A (PqqA)	1.52
SMb20960 (*exoN*)	UDP-glucose pyrophosphorylase	1.46
SMc03999	hypothetical protein DUF465	1.39
SMb20902	putative sugar uptake ABC transporter, periplasmic solute binding protein precursor*	1.38
SMc02900	conserved hypothetical protein DUF1137	1.35
SMc02051	conserved hypothetical protein DUF1137	1.32
SMc01465 (*creA*)	putative CreA protein*	1.28
SMc02052	conserved hypothetical protein DUF1137	1.27
SMc01580	conserved hypothetical protein*	1.25
SMa1831 (*ureF*)	putative urease accessory protein*	1.24
SMb21295 *(hsp20)*	putative small heat shock protein, hsp20 family	1.14
SMc02266	conserved hypothetical protein	1.11
SMb20946 *(exoY)*	galactosyltransferase	1.06
SMb21337	carbon monoxide dehydrogenase (acceptor part of multienzyme complex, twin-arginine translocation pathway signal)	1.03
SMc00781 *(iolA)*	putative methylmalonate-semialdehyde dehydrogenase	−1.04
SMc20072	putative rhizopine binding protein*	−1.11
SMb20713 *(iatA)*	putative *myo*-inositol ABC transporter, ATP-binding protein	−1.11
SMc04114 (*pilA1*)	putative pilin subunit protein*	−1.16
SMc01166 (*iolD*)	putative malonic semialdehyde oxidative decarboxylase	−1.20
SMc03051 (*flbT*)	putative flagellin synthesis repressor protein	−1.32
SMc03046 (*rem*)	transcriptional regulator of exponential growth motility	−1.36
SMc03027 *(flgB)*	flagellar basal body rod protein	−1.56
SMc03049 *(flgL)*	putative flagellar hook-associated protein	−1.56
SMc03037 *(flaA)*	flagellin A	−2.51
SMc03038 (*flaB*)	flagellin B	−2.79

**indicates a predicted N-terminal signal sequence destining the respective protein for transport and processing by the type II secretion system. M-values describe the log_2 ratio between mutant signal/wild type signal as described in section "Materials and Methods." As of March 22, 2020 the record for DUF1137 domain-containing proteins was discontinued at the NCBI database.*

PC-deficient mutant OG10017 (**Table 3** and **Supplementary Table 2**). From these data one might speculate that, in the absence of PC in sinorhizobial membranes, one or several components of the ExoR/ExoS/ChvI three-component regulatory system are altered resulting in a more active ChvI regulator and the ensuing phenotypes such as increased formation of succinoglycan as well as the absence of flagella and swimming capability.

Isolation of PC-Deficient Suppressor Mutants That Regain Capacity to Swim and Produce Less Succinoglycan

In order to identify additional elements that might define how PC deficiency causes the loss of swimming and the overproduction of succinoglycan, distinct individual colonies of the PC-deficient mutant OG10017 were used to inoculate each on a swim plate (LB/MC+ medium with 0.3% agar). Though no swimming was observed after 8 d of incubation, possible suppressor mutants for swimming recuperation were sampled with a toothpick from an area that seemed devoid of bacteria and reinoculated on fresh swimming plates. Of about 40 initial isolates, some 30 had regained the capacity to swim after two rounds of selection for swimming. Of these 30 suppressor mutants that regained the capacity to swim, none could form PC, and 5 of these mutants also showed a reduced wild type-like formation of succinoglycan (EPSI). These 5 suppressor mutants (M15, M16, M22, M33, M36) that had regained swimming and formed reduced levels of succinoglycan we named correlated mutants. As mutants altered in components of the ExoR/ExoS/ChvI system usually affect both, swimming and succinoglycan synthesis in a correlated but inverse way, we expected that suppressor mutations in the correlated mutants might map in any of the genes encoding for the three component system ExoR/ExoS/ChvI. The *exoR*, *exoS*, and *chvI* genes as well as their upstream and downstream regions were amplified by PCR from genomic DNA of the 5 respective suppressor mutants and sequenced. Correlated suppressor mutants M15, M33, and M36 displayed *exoR*, *exoS*, and *chvI* genes identical to the wild type. In contrast, M16 had a point mutation T944 to C resulting in an I315T mutation in ExoS and M22 had a mutation G1423 to A resulting in a G475S mutation in ExoS. ExoS contains 595 amino acid residues and the mutation I315T in M16 is located in the HAMP domain, just downstream of the second transmembrane domain/helix of ExoS whereas G475S in M22 is located early in the N box (Cheng and Walker, 1998a) of ExoS. If M16 or M22 were complemented with a wild type version of *exoS*, swimming was suppressed (**Figure 8A**) and succinoglycan overproduction was recuperated (**Figure 8B**) which was not the case if an empty broad host range plasmid was present in M16 or M22 (**Figure 8**). Therefore, the expression of an intact *exoS* gene in M16 or in M22 again reversed the correlated phenotype observed in M16 and M22 and led to similar phenotypes as detected in the PC-deficient mutant OG10017.

S. meliloti Suppressor Mutants M16 and M22 Carry Reduced Function ExoS Mutations

When comparing wild type and PC-deficient mutant in our microarray studies (**Table 3** and **Supplementary Table 2**), we found that transcripts for SMb21440, SMc01855, *exoN*, and *exoY* were increased in the mutant whereas transcripts for *visN*, *rem*, *flgB*, and *flaA* were reduced. Determination of the

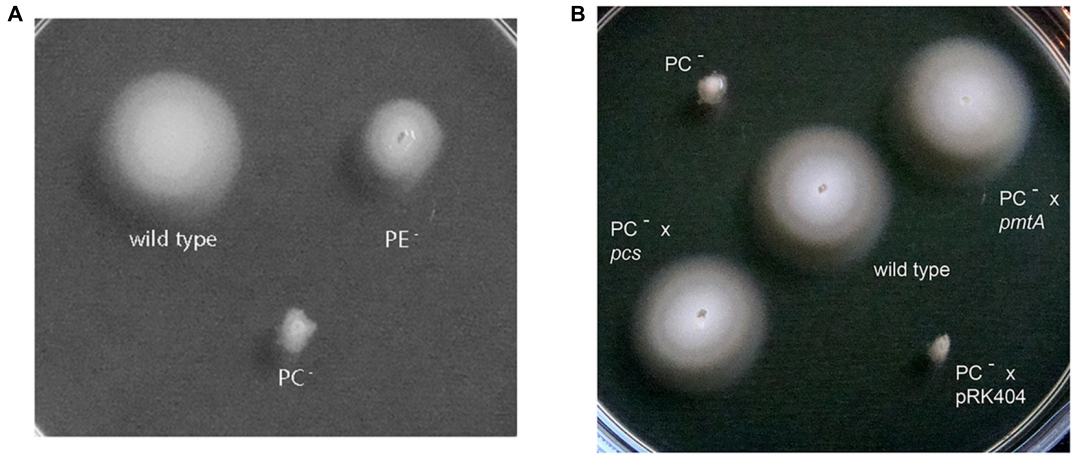

FIGURE 5 | Swimming motility of *Sinorhizobium meliloti* 1021 strains. The assay was performed at 28°C on LB/MC+-containing swim plates (0.3% agar) and analyzed after 2 days. **(A)** *S. meliloti* 1021 (wild type), PC-deficient mutant OG10017, PE-deficient mutant CS111. **(B)** *S. meliloti* 1021 (wild type), PC-deficient mutant OG10017, OG10017 complemented with *pmtA*-expressing plasmid pTB2042, OG10017 complemented with *pcs*-expressing plasmid pTB2532, and OG10017 harboring the empty broad host range plasmid pRK404.

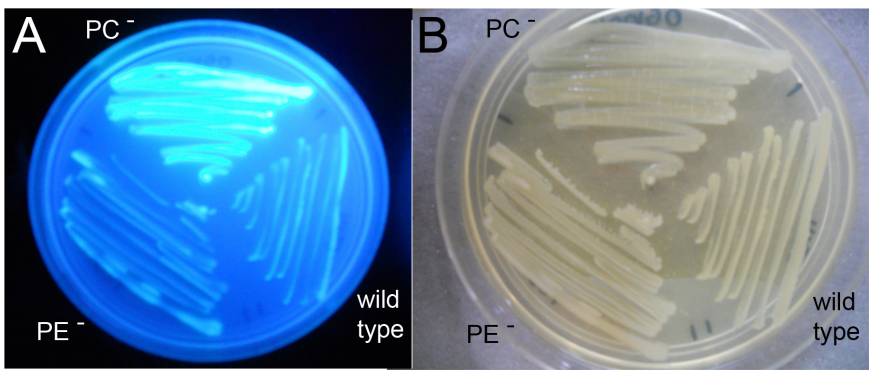

FIGURE 6 | Phosphatidylcholine (PC)-deficient mutant OG10017 shows increased succinoglycan (exopolysaccharide I) formation. *S. meliloti* 1021 (wild type), PC-deficient mutant OG10017, and the PE-deficient mutant CS111 were cultivated for 72 h on LB/MC+-containing agar in the presence of Calcofluor. Upon UV excitation, only the PC-deficient mutant showed much fluorescence indicating overproduction of succinoglycan **(A)**, whereas growth was similar for all three strains **(B)**.

relative expression of these genes by RT-PCR (**Supplementary Figure 4**) using specific oligonucleotides (**Supplementary Table 3**), confirms our previous results that mRNA levels of SMb21440, SMc01855, *exoN*, and *exoY* were increased in PC-deficient mutant OG10017 whereas transcripts for *visN*, *rem*, *flgB*, an d *flaA* were reduced. Expression levels of these target genes in M16 or M22 suppressor mutants were at (SMb21440, SMc01855, and *rem*) or close to (*exoN*, *exoY, visN, flgB,* and *flaA*) wild type levels (**Supplementary Figure 4**), emphasizing that in the ExoS-altered mutants M16 and M22, well-known ExoS-controlled genes are altered like in ExoS reduced function mutants. Recent studies suggest that ChvI negatively regulates transcription of *rem* directly (Ratib et al., 2018), thereby reducing the transcriptional regulator Rem required for the expression *flgB*, *flaA* and other flagellar genes.

In order to show that reduced function mutations of *exoS* in M16 and M22 were linked to an increased swimming phenotype, we introduced a gentamicin resistance-conferring cassette at a distance of 15 kb from the *exoS* gene. Transduction of gentamicin resistance from M16 or M22 to wild type or PC-deficient mutant OG10017 led to the isolation of transductants. Some of these transductants showed increased swimming when compared to their respective parent strains (**Figure 9** and **Supplementary Figure 5**). Sequencing of the *exoS* genes in improved swimming transductants of wild type or OG10017 showed that they carried the *exoS* mutant alleles of M16 or M22, respectively (**Figure 9**). It is especially remarkable that the *exoS* mutant alleles of M16 or M22 in a PC-replete wild type background display even larger swimming diameter than the *S. meliloti* wild type (**Figure 9A**), suggesting that both, the presence of PC as well as the presence of the M16 or M22 mutant alleles contribute to obtain an even more inactive ExoS sensor. These data strongly suggest that the reduced function point mutations detected in M16 or

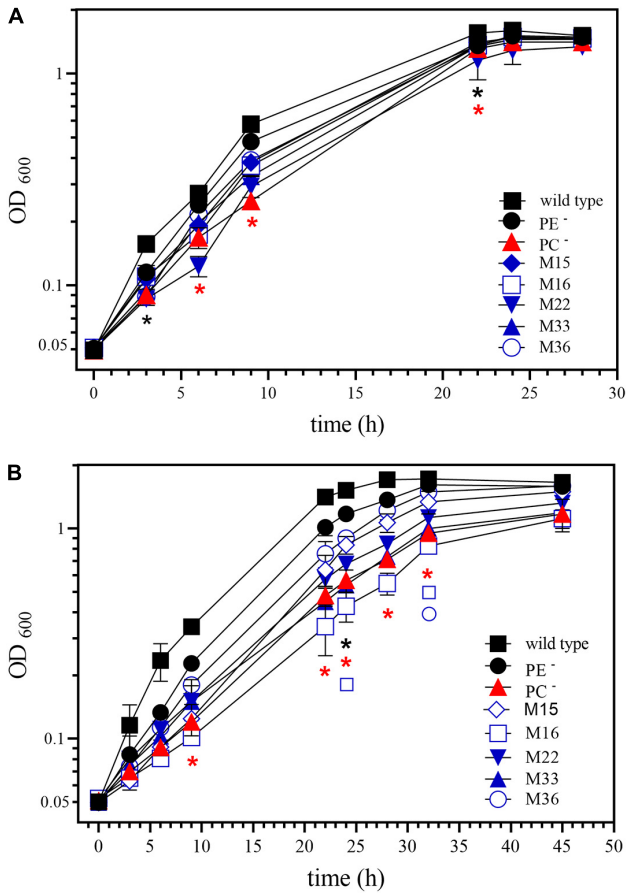

FIGURE 7 | Phosphatidylcholine (PC)-deficient mutant OG10017 is severely impaired in growth on slightly acidic media. Growth of *S. meliloti* wild type strain 1021 (■), phosphatidylethanolamine (PE)-deficient mutant CS111. (●), PC-deficient mutant OG10017 (▲), and the correlated suppressor mutants M15 (◊), M16 (□), M22 (▼), M33 (▲), M36 (○) was recorded on LB/MC+ medium containing 20 mM Bis-Tris methane, pH 7.0 **(A)** or on LB/MC+ medium containing 20 mM Bis-Tris methane, pH 5.75 **(B)** by measuring the optical density of cultures at 600 nm (OD_{600}). Values represent means of three independent experiments and standard deviation is shown. Statistical analysis was performed by a two-way ANOVA with Tukey's multiple comparisons test as described in Materials and Methods. Comparisons of the PE-deficient (black asterisks) or the PC-deficient (red asterisks) mutant to wild type are indicated. Statistical significance is shown (*$p < 0.05$). Also indicated are statistically significant comparisons between the PC-deficient mutant and correlated suppressor mutants M16 (□) and M36 (○).

M22 can be cotransduced with the gentamicin resistance-conferring cassette and are the cause for the improved swimming phenotypes, respectively.

Restoration of PC biosynthesis in the PC-deficient mutant OG10017 restored the ability to swim (**Figure 5** and **Supplementary Figure 6**). Also in suppressor mutants M16 and M22 swimming behavior is further increased when PC biosynthesis is restored by the action of PmtA or Pcs, which is not the case when M16 or M22 harbored an empty vector (**Supplementary Figure 6**). Again these data suggest that both, the presence of PC and the presence of the M16 or M22 mutant alleles contribute to reduce ExoS signaling activity in an additive way.

Expression of distinct *exoS* versions in sinorhizobial strains revealed swimming was suppressed slightly in wild type and strongly in M22 when the M16 version of *exoS* was expressed *in trans* (**Supplementary Figure 7**). Also, when the M16 version of *exoS* was expressed in wild type or M16, exopolysaccharide production was clearly reduced. In contrast, expression of wild type or the M22 versions of *exoS*, did not cause major alterations in swimming behavior or exopolysaccharide production (**Supplementary Figure 7**). As ExoS can display three distinct enzymatic activities, i.e., autophosphorylation, phosphorylation of ChvI and phosphatase activity on ChvI, it will require future studies of the individual enzyme-catalyzed steps in order to resolve which of the steps might be affected in the respective mutants.

The point mutations encountered in M16 and M22 are both reduced function *exoS* mutations. It is worth noting that while the *exoS* point mutations in M16 and M22 restored wild type-like swimming behavior or exopolysaccharide production, they did not restore wild type-like growth at acidic conditions (pH 5.75). Whereas M22 grows similarly bad as OG10017, M16 grows even worse (**Figure 7B**). Other, so far uncharacterized, correlated suppressor mutants grew similarly (M33), slightly better (M15), or much better (M36) than OG10017 at acidic conditions (pH 5.75) (**Figure 7B**). In the future, whole genome sequencing of the DNA from M15, M33, M36 will identify the mutation(s) responsible for the correlated suppressor phenotypes in those mutants.

ExoR Levels Are Similar in Wild Type, PC-Deficient Mutant and Suppressor Mutants

In PC-deficient mutants of *S. meliloti*, the ExoS/ChvI two-component regulatory system seems to be activated. This regulatory system is usually switched on when the mature and functional form of the periplasmic ExoR regulator protein, $ExoR_m$, is proteolytically degraded at acidic conditions (Wu et al., 2012; Wiech et al., 2015). Western blot analyses (**Figure 10**) indicate that the amounts of $ExoR_m$ are similar in *S. meliloti* wild type, the PC-deficient mutant OG 10017 and the correlated suppressor mutants M16 or M22 (**Figure 10**). We therefore conclude that there is no major alteration of $ExoR_m$ levels in *S. meliloti* strains that lack PC. Thus it is unlikely that PC deficiency is mediated through $ExoR_m$ and that reduced $ExoR_m$ levels in the PC-deficient mutant would activate the ExoS/ChvI two-component regulatory system. We therefore assume that the lack of PC in the cytoplasmic membrane of *S. meliloti* and the concomitant increase of PE directly affect the protein parts of ExoS which are in contact with the membrane, i.e., the two transmembrane helices. We postulate that the orientation of the two ExoS transmembrane helices is altered in a PC-deficient mutant and that these alterations provoke

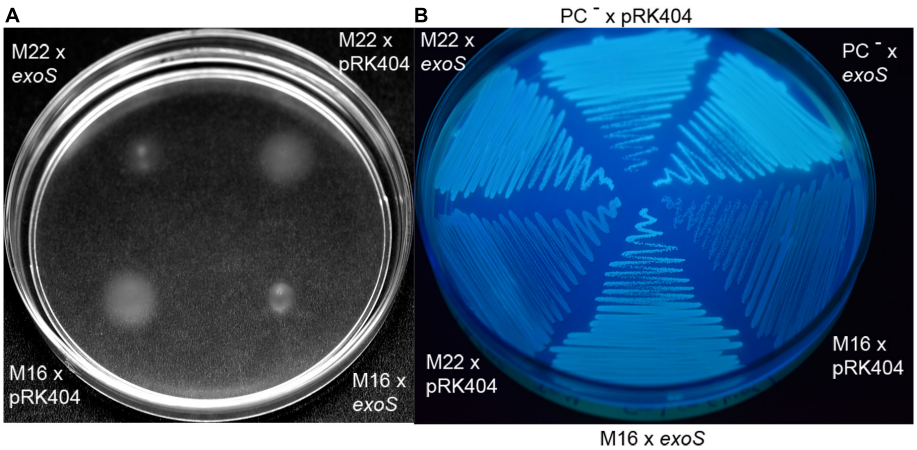

FIGURE 8 | Intact ExoS suppresses swimming and increases exopolysaccharide formation in ExoS-impaired correlated suppressor mutants M16 and M22. **(A)** Swimming of ExoS-impaired correlated suppressor mutants M16 and M22 harboring a plasmid with the wild type version of *exoS* or harboring the empty plasmid pRK404 after 4 d of incubation on LB/MC+-containing swim plates (0.3% agar) in the presence of 4 μg/ml tetracycline. **(B)** Exopolysaccharide production of ExoS-impaired correlated suppressor mutants M16 and M22 harboring a plasmid with the wild type version of *exoS* or harboring the empty plasmid pRK404 after 3 days of incubation.

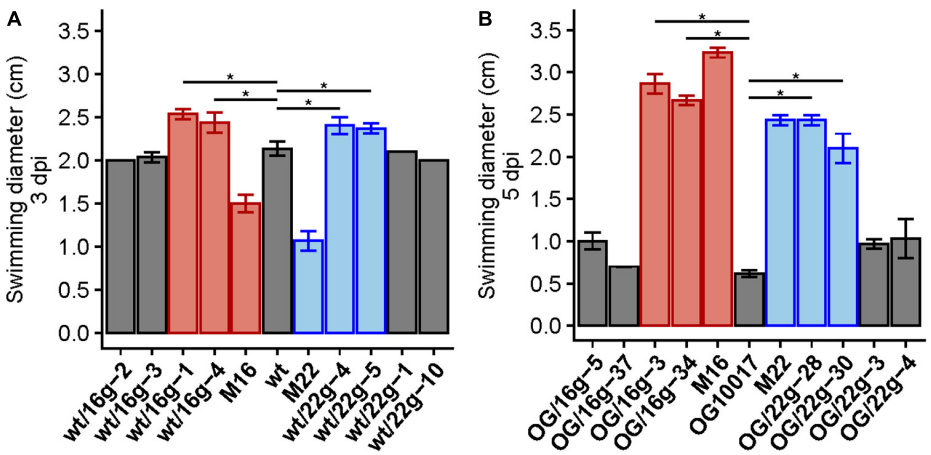

FIGURE 9 | Transduction of M16 and M22 versions of *exoS* increase swimming behavior in wild type and OG10017 backgrounds. Swimming diameters of wild type (wt), correlated suppressor mutants M16 and M22 and some gentamicin-resistant wild type transductants (wt/16g or wt/22g) 3 days post inoculation (3 dpi) **(A)**, as well as swimming behavior of OG10017 (OG), correlated suppressor mutants M16 and M22 and some gentamicin-resistant OG10017 transductants (OG/16g or OG/22g) 5 days post inoculation (5 dpi) **(B)**. Colors indicate the *exoS* version of strains: wt (gray), M16 (red), M22 (blue). The assays were performed at 28°C on LB/MC+-containing swim plates (0.3% agar). Values represent means of three independent experiments and standard deviation is shown. Pairwise comparisons were done using a Wilcox test and denoted by horizontal lines between the compared groups. Statistical significance is shown (*$p < 0.05$).

conformational changes that lead to the activation of the ExoS cytoplasmic domain.

DISCUSSION

Model for the Regulation of the ExoR/ExoS/ChvI Signal Transduction System

Our results demonstrate that a PC-deficient mutant of *S. meliloti* is unable to form a nitrogen-fixing root nodule symbiosis with its host plant *M. sativa*, overproduces genes for succinoglycan production and represses genes for flagellum formation. The PC-deficient mutant is indeed unable to swim and overproduces succinoglycan. The transcriptomic phenotype of a PC-deficient mutant resembles that of a strain which is activated in the ExoS/ChvI two-component regulatory system leading to the hypothesis that the absence of PC in *S. meliloti* leads to the activation of ExoS/ChvI. It is generally thought that for the activation of ExoS/ChvI, the inhibition of ExoS by ExoR must be eliminated (**Figure 11**), probably through proteolytic degradation of the periplasmic $ExoR_m$ inhibitor, resulting in activation of the ExoS/ChvI signal transduction system. However, as $ExoR_m$ levels in the PC-deficient mutant are essentially on the same level as

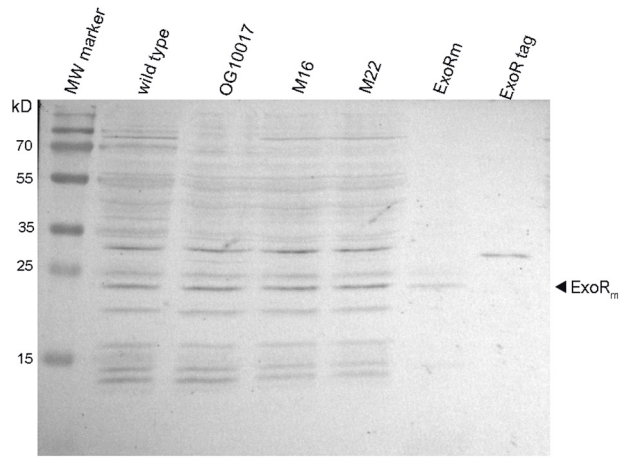

FIGURE 10 | Levels of mature $ExoR_m$ are similar in *Sinorhizobium meliloti* wild type and in PC-deficient mutants. Western blot detection of ExoR protein after electrophoretic separation of extracts from *S. meliloti* wild type, OG10017, M16, M22 strains, an extract of *E. coli* BL21(DE3) strain overexpressing $ExoR_m$ (ExoRm), and purified $ExoR_p$ with an N-terminal His-tag (ExoR tag). For estimation of molecular weights for distinct ExoR versions, a molecular weight (MW) marker (PageRuler Prestained Protein Ladder, Thermo Fisher Scientific) was used.

in wild type, we suggest that PC-deficiency is not transmitted to ExoS via $ExoR_m$ but in a more direct way. We propose that the lack of PC in the cytoplasmic membrane of *S. meliloti* and the concomitant relative increase of PE cause negative curvature in both monolayers of the cytoplasmic membrane and suggest that this directly affects interactions with the protein parts of ExoS that are in contact with the membrane, i.e., the two transmembrane helices. We postulate that the orientation of the two ExoS transmembrane helices is altered in a PC-deficient mutant and that these alterations provoke conformational changes that lead to the activation of the ExoS cytoplasmic domain, autophosphorylation of ExoS, transphosphorylation to ChvI and alteration of ChvI-controlled gene expression (**Figure 11**). In the course of this work we have isolated spontaneous suppressor mutants of the PC-deficient mutant OG10017, that had regained swimming and formed reduced levels of succinoglycan. Two of those mutants had distinct point mutations in the *exoS* gene. Mutant M16 had a point mutation T944 to C resulting in an I315T mutation in ExoS and M22 had a mutation G1423 to A resulting in a G475S mutation in ExoS. ExoS contains 595 amino acid residues and the mutation I315T in M16 is located in a domain, present in histidine kinases, adenyl cyclases, methyl-accepting proteins, and phosphatases (HAMP), just downstream of the second transmembrane domain/helix of ExoS. The HAMP domain is critical for dimerization of ExoS monomers and dimerization is a requisite for phosphorylation of the conserved H residue in the H box of one monomer by the phosphorylation domain of the other monomer. In contrast, G475S in M22 is located early in the N box (Cheng and Walker, 1998a) of ExoS. The N box of two-component sensor proteins is part of the nucleotide binding cleft, required for ATP binding and therefore critical for their kinase activity (**Figure 11**). Transduction of the suppressor point mutations to the PC-deficient mutant OG10017 yielded transductants that regained swimming, suggesting that in these transductants, even in the absence of PC, ExoS signaling is silenced, ChvI remains inactive, and flagellar target genes are expressed. Therefore, the lack of PC in mutant OG10017 must have been transmitted via the ExoS sensor to the genes of the ChvI regulon. Our proposal that membrane composition and properties affect the functioning of two-component system sensors might constitute a more common feature, as also in *E. coli* mutant strains that lack PE, the CpxA/CpxR two-component signal transduction pathway is activated (Mileykovskaya and Dowhan, 1997) and it has been suggested that this activation might occur by envelope stress exerted in the cytoplasmic membrane.

ExoR/ExoS/ChvI Orthologs and PC Co-occur in the *Rhizobiales*

Orthologs of *S. meliloti* ExoS and ChvI play important roles in other *Rhizobiales* known for their symbiosis with other legumes or for causing plant or animal pathogenesis. The orthologous ChvG/ChvI system of *Rhizobium leguminosarum* is important for successful nodule formation on peas, lentils, and vetch (Vanderlinde and Yost, 2012). The *Agrobacterium tumefaciens* ChvG/ChvI two-component regulatory system controls the expression of acid-inducible genes, bacterial virulence regulation via the VirA/VirG two-component regulatory system, as well as succinoglycan production, and motility (Heckel et al., 2014). The orthologous two-component regulatory system in *Brucella abortus* is BvrS/BvrR; it controls expression of the *Brucella* type IV secretion system and is essential for virulence (Martínez-Nuñez et al., 2010). In the causative agent of cat-scratch disease *Bartonella henselae*, the orthologous BatS/BatR two-component regulatory system controls the adaptive response during infection of human endothelial cells (Quebatte et al., 2010). Whereas ExoS/ChvI orthologs are more widespread in alpha-proteobacteria, orthologs of ExoR seem to be limited to the *Rhizobiales* (Wiech et al., 2015; Heavner et al., 2015) and most of them interact with eukaryotic hosts in a symbiotic or pathogenic way. All the bacteria mentioned above possess PC as a major membrane lipid (Martínez-Morales et al., 2003) and our own analysis (**Supplementary Table 4**) shows that at least one probable PC biosynthesis pathway exists in all the *Rhizobiales* analyzed, but also in some other alpha-proteobacteria, such as members of the *Acetobacteraceae* (*Gluconobacter*), the *Rhodobacterales* (*Rhodobacter*), or the *Sphingomonadales* (*Sphingomonas, Zymomonas*). Therefore, in all cases where a complete ExoR/ExoS/ChvI (RSI) invasion switch is present, the capability to form PC exists, suggesting that PC is generally required for the proper functioning of the ExoR/ExoS/ChvI system.

Diverse Roles for PC in Bacteria

The lack of PC in distinct bacteria has phenotypic consequences of varying severity (Geiger et al., 2013). Pcs-deficient mutants of different *Pseudomonas aeruginosa* strains did not produce

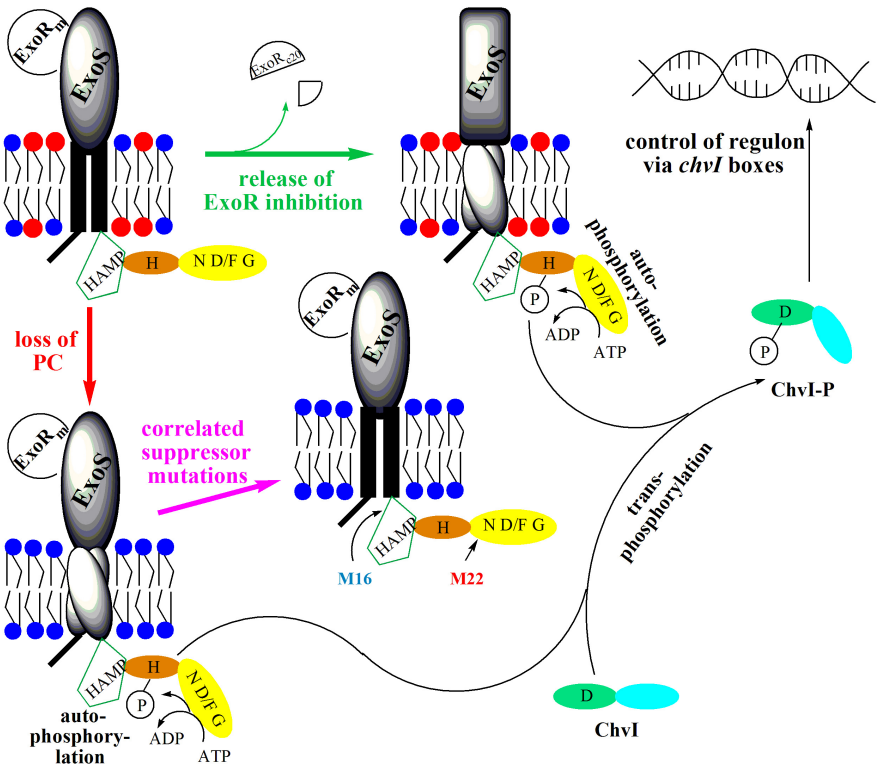

FIGURE 11 | Model for the activation of sensor kinase ExoS by release of ExoR inhibition or by loss of PC from the membrane. In free-living *S. meliloti* bacteria, the two-component regulatory system ExoS/ChvI, remains inactive due to binding of the periplasmic inhibitor protein ExoR$_m$ to the ExoS sensor kinase. Upon contact of *S. meliloti* with its legume host, ExoR$_m$ is proteolytically degraded, forming ExoR$_{c20}$, thereby eliminating the inhibition of ExoS and triggering autophosphorylation of ExoS on the conserved H368 residue. Subsequently, the ExoS transphosphorylation activity phosphorylates the conserved D52 residue of the ChvI response regulator. Phosphorylated ChvI-P alters transcription of more than 100 genes, leading for example to the formation of more succinoglycan, less flagellar proteins and to reduced swimming capability. Loss of PC from the membrane probably provokes rearrangement of transmembrane helices 1 and 2 of ExoS, thereby triggering conformational change and activation of the cytoplasmic domain of ExoS. Autophosphosphorylation of ExoS followed by transphosphorylation to ChvI results also in production of more succinoglycan and reduced swimming. Correlated suppressor mutations in M16 (I315T) or M22 (G475S) render the cytoplasmic ExoS domain into a more inactive conformation avoiding autophosphorylation of ExoS, transphosphorylation to ChvI and formation of phosphorylated ChvI-P. Therefore, correlated suppressor mutants M16 and M22 display wild type-like succinoglycan production and swimming behavior. The ExoS protein from *S. meliloti* comprises 595 amino acid residues and contains an N-terminal cytoplasmic domain (residues 1-47), transmembrane helix 1 (residues 48-68), a periplasmic domain (residues 69-278), transmembrane helix 2 (residues 279-299), and a C-terminal cytoplasmic domain (residues 300-595). Within the cytoplasmic domain, a HAMP-domain (residues 301-357) and a histidine kinase domain (residues 365-593) can be distinguished. The HAMP domain is considered crucial for dimerization of sensor kinase monomers and for functionality of the sensor. The histidine kinase domain comprises the conserved H368-containing H box (residues 361-380), as well as the nucleotide binding cleft defined by several conserved amino acids motifs, the N box (residues 473-494), the D/F box (residues 513-540), and the G box (residues 549-567). PC is highlighted by a red circle for its head group, whereas head groups for PE and other membrane lipids are represented by a blue circle.

detectable amounts of PC and behaved like their respective wild types when assayed for many phenotypes, among them motility, biofilm formation, colonization, or virulence (Malek et al., 2012). In the causative agent of Legionnaires' disease, *Legionella pneumophila*, PC is required for proper functioning of a type IVB secretion system, for cytotoxicity and full virulence, but also for the specific attachment of *L. pneumophila* to macrophages via the platelet-activating receptor (Conover et al., 2008) before entering the host cell. Also, for the animal pathogen *Brucella abortus*, PC is required for full virulence (Comerci et al., 2006; Conde-Alvarez et al., 2006). A PmtA-deficient mutant of *Bradyrhizobium japonicum* showed reduced levels of PC in its membranes, affected nodule development, diminished nitrogen fixation activity and did therefore not form a fully functional symbiosis with its host plant soybean (Minder et al., 2001). Surprisingly, a *B. japonicum* mutant deficient in a toxin-antitoxin-like module was unable to produce any PC and formed less nodules on soybean than the wild type (Miclea et al., 2010). Nevertheless, nitrogen fixation by this PC-deficient strain apparently occurred and therefore there seems to be no absolute requirement of bacterial PC for nitrogen fixation by *B. japonicum* (Miclea et al., 2010). *Agrobacterium tumefaciens* is a tumor-inducing plant pathogen and agrobacterial PC is required for the formation of a type IV secretion system essential for tumorgenesis (Wessel et al., 2006). A proteomic and transcriptomic characterization of a PC-deficient mutant of *A. tumefaciens* indicated that expression of virulence genes in this mutant is dramatically (several hundred-fold) reduced when compared to the wild type, whereas the majority of differentially expressed genes, not related to virulence, was

altered only several-fold (Klüsener et al., 2010). Expression of the virulence-related genes is controlled by the two-component regulatory system VirA/VirG and it has been suggested that the VirA/VirG system might not function properly in the PC-deficient mutant of *A. tumefaciens* (Klüsener et al., 2010). We now show that a PC-deficient mutant of *S. meliloti* is unable to form a nitrogen-fixing symbiosis with its host plant alfalfa and we suggest that the lack of PC in *S. meliloti* leads to an activation of the ExoR/ExoS/ChvI three-component. Signaling through ExoR/ExoS/ChvI in *S. meliloti* wild type is normally switched on when the bacterium changes from a free-living life style to a symbiotic one. In contrast, in the PC-deficient mutant this system is already switched on and active when the bacterium gets in contact with the host plant. This premature signaling through ExoS/ChvI might be one reason for the symbiotic deficiency of the PC-deficient mutant.

MATERIALS AND METHODS

Bacterial Strains, Media and Growth Conditions

The bacterial strains and plasmids used and their relevant characteristics are shown in **Table 4**. *S. meliloti* strains were usually grown at 30°C either in complex LB/MC+ medium, which contained 10 mM of $CaCl_2$ instead of 2.5 mM as described previously for LB/MC medium (Glazebrook and Walker, 1991). As PE-deficient mutants require elevated concentrations of bivalent cations for good growth (Sohlenkamp et al., 2004), we used 10 mM $CaCl_2$ in culture media in order to obtain similar growth for *S. meliloti* wild type, the PE-deficient mutant CS111, and the PC-deficient mutant OG10017. For cultivation of strains at different pH-values, Bis-tris methane/HCl of different pH-values was added to LB/MC+ medium to a final concentration of 20 mM. Utilization of compounds as carbon or energy sources

TABLE 4 | Bacterial strains and plasmids used in this study.

Strain or plasmid	Relevant characteristics	References
S. meliloti 1021our	SU47rfr-21	López-Lara et al., 2005
Sm1021our derivatives		
CS111	*pssA* gene replaced with gentamicin resistance cassette, cannot form PE	Sohlenkamp et al., 2004
KDR516	*pmtA::kan,* Nm^R	de Rudder et al., 2000
KDR568	*pcs::aadA,* Spc^R	Sohlenkamp et al., 2000
OG10017	*pmtA::kan, pcs::aadA,* cannot form PC	de Rudder et al., 2000
M16	OG10017 derivative carrying a mutated *exoS* (T944C) gene	This work
M22	OG10017 derivative carrying a mutated *exoS* (G1423A) gene	This work
Sm1021g	*S. meliloti* 1021our derivative harboring a gentamicin resistance cassette between SMc02762 and SMc02761 gene	This work
M16g	M16 derivative harboring a gentamicin resistance cassette between SMc02762 and SMc02761 gene	This work
M22g	M22 derivative harboring a gentamicin resistance cassette between SMc02762 and SMc02761 gene	This work
E. coli		
DH5α	*recA*l Φ80 *lacZ*Δ*M15;* cloning strain	Hanahan, 1983
S17-1	*thi, pro*, recA, *hsdR, hsdM*+, RP4Tc::Mu, Km::Tn7;Tp^R, Sm^R, Spc^R,	Simon et al., 1983
BL21(DE3)	Expression strain	Studier et al., 1990
Plasmids		
pUC19	Cloning vector, Cb^R	Yanisch-Perron et al., 1985
pLysS	Production of lysozyme for repression of T7 polymerase, Cm^R	Studier et al., 1990
pMP280	IncP broad-host range vector, carrying *nodD* promoter and *nodD* gene from *Rhizobium leguminosarum*, Tc^R	Spaink et al., 1987
pMP3510	Broad-host range vector, Tc^R	Spaink et al., 1995
pRK404	Broad-host range vector, Tc^R	Ditta et al., 1985
pTB2042	*pmtA*-containing 2.9 kb *Pst*I/*Pst*I insert in pRK404	de Rudder et al., 2000
pTB2532	*pcs*-containing 4.6 kb *Hin*dIII/*Hin*dIII insert in pRK404	Sohlenkamp et al., 2000
pJMV01	*exoS* gene of *S. meliloti* including 412 b upstream and 29 b downstream, cloned as *Bam*HI fragment in pRK404	This work
pLMA16	mutated *exoS* (T944C) gene of *S. meliloti* including 412 b upstream and 29 b downstream, cloned as *Bam*HI fragment in pRK404	This work
pLMA22	mutated *exoS* (G1423A) gene of *S. meliloti* including 412 b upstream and 29 b downstream, cloned as *Bam*HI fragment in pRK404	This work
pLMA38R	$exoR_p$, cloned as *Nde*I/*Bam*HI fragment in pET16b	This work
pLMA92R	$exoR_m$, cloned as *Nde*I/*Bam*HI fragment in pET9a	This work

Cb^R, Nm^R, Sm^R, Spc^R, Cm^R and Tp^R: carbenicillin, neomycin, streptomycin, spectinomycin, chloramphenicol, and trimethoprim resistance, respectively.

was evaluated using 1/20 LB/MC+ medium containing reduced concentrations of tryptone (0.5 g/l) and yeast extract (0.25 g/l), normal concentrations of NaCl (5 g/l), $MgSO_4$ (2.5 mM) and $CaCl_2$ (10 mM), the compound to be evaluated and determining final growth yields (OD_{600}). Growth of *S. meliloti* strains on defined media was performed on MOPS minimal medium (Bardin et al., 1996) or, for growth experiments with the PE-deficient mutant CS111, on a modified version of MOPS minimal medium containing 40 mM 4-morpholinepropanesulfonic acid (MOPS), 20 mM KOH, 20 mM NH_4Cl, 100 mM NaCl, 2 mM $MgSO_4$, 5 mM $CaCl_2$, 0.3 mg biotin/l, 15 mM succinate, 0.1 mM potassium phosphate buffer, pH 7. *E. coli* strains were grown on Luria-Bertani medium (Miller, 1972) at 37°C. Antibiotics were added to the medium in the following concentrations when required (in μg per ml): 200 for neomycin, 400 for spectinomycin, 40 for gentamicin, 30 for nalidixic acid, 4 for tetracycline for *S. meliloti* and 100 for carbenicillin, 50 for kanamycin, and 20 for tetracycline for *E. coli*.

Broad host range plasmids, such as pRK404 derivatives were mobilized into *S. meliloti* strains by diparental mating using the *E. coli* S17-1 donor strain as described by Simon et al. (1983).

Detection of Lipochitin Oligosaccharide Nodulation Factors by Thin-Layer Chromatography

Cultures of *S. meliloti* harboring plasmid pMP280 were grown on MOPS minimal medium (Bardin et al., 1996) at 30°C on a gyratory shaker in the presence of 2 μg/ml tetracycline. *In vivo* labeling of lipochitin oligosaccharides (LCOs) was carried out in 1 ml cultures at an initial cell density of OD_{600} = 0.06, in the presence of 0.4 μCi of D-[1-^{14}C]glucosamine (54 mCi/mmol; Amersham), and in the cases of induction, naringenin (2 μg/ml final concentration) was added. After overnight growth, the LCOs were isolated from the cultures by n-butanol extraction. Samples were concentrated by evaporation and chromatographed on reversed phase C_{18}-coated silica plates (Sigma) using acetonitrile/water (1:1; vol/vol) as mobile phase similarly as described (López-Lara et al., 1995). The developed chromatogram was subjected to autoradiography by exposure to a Kodak X-OMAT XK1 film.

Transcriptional Profiling Using the SM14kOligo Whole Genome Microarray

For microarray hybridization two independent bacterial cultures from each *S. meliloti* strain were grown in LB/MC+ medium to an OD_{600} of 0.8. RNA isolation was performed according to the protocol published by Rüberg et al. (2003) using the RNeasy mini kit (QIAGEN, Hildesheim, Germany). Total RNA (10 μg) was used for the preparation of Cy3 and Cy5 labeled cDNAs. To each SM14kOligo microarray slide (Krol and Becker, 2004) the cDNA of the two respective *S. meliloti* strains were mixed and hybridized. Analysis of microarray images was carried out applying the ImaGen 5.0 software (Biodiscovery Inc., Los Angeles, CA, United States) as described previously (Hellweg et al., 2009). Normalization and significance tests were performed with the EMMA software (Dondrup et al., 2003). *M*-values ($\log_2$ ratio between both channels), *P*-values (*t*-test) and *A*-values ($\log_2$ of combined intensity of both channels) were also calculated with EMMA. Detailed protocols and raw data resulting from the microarray experiments have been deposited in the ArrayExpress database with the accession number E-MTAB-3676.

Reverse Transcription Quantitative Real-Time PCR

Reverse transcription quantitative real-time PCR (RT-qPCR) was essentially performed as described (Nogales et al., 2010). In short, total RNA (1 μg) treated with RNase-free DNase I (Thermo Scientific) was transcribed reversely using Superscript II reverse transcriptase (Thermo Scientific) and random hexamers (Thermo Scientific) as primers. Quantitative real-time PCR was performed on a StepOnePlus (Applied Biosystems). Each 25 μl reaction contained 1 μl of the cDNA, 200 nM of each primer and iQ SyBrGreen Supermix (Thermo Scientific). In order to confirm the absence of contaminating genomic DNA, control PCR reactions of the RNA samples not treated with reverse transcriptase were also performed. By heating at 95°C for 3 min, samples were initially denatured and a 35-cycle amplification and quantification program (95°C for 30 s, 55°C for 45 s, and 72°C for 45 s) followed. The oligonucleotide sequences for qPCR are listed in **Supplementary Table 3**. The expression levels of selected genes in the mutants were normalized to the expression levels in the wild type strain. The fold change in gene expression was calculated using the comparative critical threshold ($\Delta\Delta C_T$) method (Schmittgen and Livak, 2008).

Motility Assays

Swim plates (LB/MC+ medium with 0.3% agar) were point-inoculated with a toothpick and usually incubated for 48 h at 28°C similarly as described (Medeot et al., 2010). Swimming was assessed qualitatively by examining the circular turbid zone formed by the bacterial cells migrating away from the point of inoculation.

Exopolysaccharide Production

Calcofluor white M2R (fluorescent brightener 28, Sigma) was added to a final concentration of 0.02% in LB/MC+ agar media and production of succinoglycan (exopolysaccharide I) was evaluated based on fluorescence intensity using a hand-held long-wave UV lamp (Leigh et al., 1985).

DNA Manipulations

Recombinant DNA techniques were performed following standard protocols (Sambrook and Russell, 2001). Commercial sequencing of amplified genes was performed by Eurofins Medigenomix (Martinsried, Germany).

Cloning and Expression of *exoS* and *exoR* Genes From *S. meliloti*

Using PCR and specific oligonucleotides (AAAGGATCCGGCGTCGGCTATCGCTTCCGCG and AAAGGATCCGGTCCCGTGGACATTGACGAAGG), the genes coding for *exoS* wild type as well as the M16 and

M22 mutant versions, including 412 bp upstream and 29 bp downstream, were amplified from the respective genomic DNAs. Suitable restriction sites (underlined) for cloning of the genes were introduced by PCR with the oligonucleotides. After restriction with *Bam*HI, the PCR-amplified DNA fragments were cloned into pUC19 for DNA sequencing. The *Bam*HI-restricted fragments of the wild type *exoS* or the M16 or M22 mutant versions were recloned into a pRK404 vector to obtain pJMV01, pLMA16 or pLMA22, respectively, for expression of the *exoS* wild type gene or the altered M16 or M22 versions in *S. meliloti*.

In order to clone genes coding for $ExoR_m$ or for a His-tagged version of $ExoR_p$, PCR and specific oligonucleotides (GGAATTCCATATGTTCGATCCCGGAGCCGGCGT and GGGGATCCTATCAATCGTCGTCGTTCTGC for $ExoR_m$ or GGAATTCCATATGATGCGCGCGGGTGAATTGAAGTC and CCGGATCCTCAATCGTCGTCGTTCTGCAGATGCA for His-tagged $ExoR_p$) were employed. Suitable restriction sites (underlined) for cloning of the genes were introduced by PCR with the oligonucleotides. After restriction with *Nde*I/*Bam*HI, the PCR-amplified DNA fragments were cloned into pET9a (for $ExoR_m$) yielding plasmid pLMA92R or pET16b (for $ExoR_p$) yielding plasmid pLMA38R and the correct sequences for cloned DNA fragments were corroborated. After transformation of these plasmid constructs to *E. coli* BL21(DE3) x pLysS, transformed strains were cultivated at 29°C and genes were expressed with 0.1 mM IPTG. Cell suspensions of *E. coli* BL21(DE3) x pLysS x pLMA92R were prepared for Western blot analysis, whereas His-tagged $ExoR_p$ was purified from cell-free extracts of *E. coli* BL21(DE3) x pLysS x pLMA38R by Ni affinity chromatography before being analyzed in Western blots.

Insertion of a Gentamicin Resistance-Conferring Cassette Into the Genome of *S. meliloti* at a Distance of 15 kb From *exoS*

In order to insert a gentamicin resistance-conferring cassette into the genome of *S. meliloti*, first genomic fragments involving the end of the TRm22 (SMc02762) gene or the end of the *trxA* (SMc02761) gene were amplified by PCR from genomic DNA of *S. meliloti* using specific pair of oligonucleotide primers. Amplification with primers AAATCTAGACGCTGGGTAAGCTGTACGATTG and ACTGGATCCAGACCATTTGGTTTGGGATG yielded a 771 bp fragment, containing part of TRm22, and introduced an *Xba*I and *Bam*HI site, respectively, whereas amplification with primers ACTGGATCCCCGCTATGCATGAATTTTCC and ACTGAATTCACGATCGCCGATACAAGAC produced a 776 bp fragment, containing part of *trxA*, and introducing an *Bam*HI and *Eco*RI site, respectively. After digesting both fragments with the restriction enzymes mentioned, they were cloned into plasmid pK18*mobsacB* (Schäfer et al., 1994). Subsequently, a gentamicin cassette derived from pACΩ-Gm (Schweizer, 1993) was obtained and cloned into the *Bam*HI site of the previous plasmid yielding plasmid pLMA71. The suicide vector pLMA71 was introduced into wild type *S. meliloti* 1021, and double recombinants in which the gentamicin resistance-conferring cassette had been inserted between *trxA* and TRm22 at a distance of about 15 kb from the *exoS* gene were obtained following a procedure described previously (Sohlenkamp et al., 2004). Double recombinants, i.e., Sm1021g, were confirmed by PCR. General transduction employing the phage M12 (Finan et al., 1984) was used to move the gentamicin resistance-conferring cassette from the *S. meliloti* wild type background to M16 and M22. Gentamicin-resistant derivatives of M16 and M22 were isolated and when they resembled M16 or M22 in their swimming behavior, the maintenance of the altered *exoS* genes of M16 or M22, i.e., in M16g or in M22g, respectively, was confirmed by sequencing of the PCR-amplified *exoS* gene. Subsequently, the gentamicin resistance was transduced from the M16g or M22g to the *S. meliloti* wild type or the PC-deficient mutant OG10017 and transductants were isolated. For some of the transductants, the *exoS* gene was PCR-amplified and sequenced and transductants were identified which harbored wild type or M16 versions of *exoS* when M16g was employed as donor or wild type or M22 versions of *exoS* with M22g as donor.

In vivo Labeling of *Sinorhizobium meliloti* With [^{14}C]Acetate and Quantitative Analysis of Lipid Extracts

The lipid compositions of *S. meliloti* 1021 wild type and mutant strains were determined following labeling with [1-^{14}C]acetate (55 mCi/mmol; Perkin Elmer). Cultures (1 ml) of wild type and mutant strains in LB/MC+ medium were inoculated from precultures grown in the same medium. After addition of 0.5 μCi [^{14}C]acetate to each culture, the cultures were incubated for 24 h. The cells were harvested by centrifugation, washed with 500 μl of phosphate-buffered saline (PBS)(Sambrook and Russell, 2001) and resuspended in 100 μl of PBS. The lipids were extracted according to Bligh and Dyer (Bligh and Dyer, 1959) substituting water with PBS. The chloroform phase was used for lipid analysis on thin-layer chromatography (TLC) plates (HPTLC aluminum sheets, silica gel 60, Merck) and after one-dimensional or two-dimensional separation using the solvent systems described (de Rudder et al., 1997), the individual lipids were quantified using a phosphorimager (Storm 820, Molecular Dynamics).

Preparation of ExoR Antibodies and Their Purification

His-tagged $ExoR_p$ (ExoR tag) was purified from cell-free extracts of *E. coli* BL21(DE3) x pLysS x pLMA38R by Ni affinity chromatography as described above and 400 μg of the purified protein were injected into a rabbit on four occasions, respectively, at intervals described previously (Cooper and Paterson, 2008). The serum of the rabbit contained antibodies against the ExoR tag protein as determined by testing serial dilutions on immunoblots.

Purification of the ExoR antibody was performed with the ExoR tag protein essentially as described (Scharf et al., 2001). Only during the washing steps of the filter chips, 0.5% BSA and 0.5% Nonidet P40 was used instead of 0.1% BSA and 0.1% Nonidet P40.

Detection of Different Forms of ExoR by Western Blot Analysis

Cultures of *S. meliloti* strains were grown in LB/MC+ medium to an OD_{600} of 0.8. Aliquots (500 μl) of cultures were quickly harvested for 2 min at 10000 rpm in an Eppendorf centrifuge and resuspended in 50 μl of 50 mM Tris/HCl buffer, pH 7.4 containing 100 mM KCl. An equal volume of 2 × treatment buffer was added to the resuspended cells and the mixture was boiled for 10 min. Protein samples, usually corresponding to 100 μl of the liquid cell cultures, were analyzed by SDS-containing polyacrylamide gel electrophoresis (15%). Separated proteins were transferred to a polyvinylidene difluoride membrane and blots were incubated with ExoR-specific purified antibodies in a 1:300 dilution, as primary antibody and anti-rabbit serum (1:4000 dilution) coupled with alkaline phosphatase as secondary antibody. Blots were developed by treatment with nitro-blue tetrazolium and 5-bromo-4-chloro-3′-indolylphosphate (Sigma).

Plant Assays

Alfalfa (*Medicago sativa* L.) plants were grown hydroponically on a nitrogen-free medium as described by Olivares and associates (Olivares et al., 1980), which contained about 0.7 mM phosphate. To test the infectivity of the rhizobial strains, 30 individual plants were inoculated with 10^5 cells. After inoculation the number of nodulated plants and the number of nodules per plant were recorded every three days until no more changes in the total nodule numbers were observed. Plants were incubated in a plant growth chamber at 22°C using a 12-/12-h day/night cycle.

Statistical Analysis

A two-way ANOVA with Tukey's multiple comparisons test was conducted on the mean of each OD/CFU/nodule value measured by triplicate to evaluate that observed changes were statistically significant. A p-value < 0.05 was considered statistically significant. Data are presented as mean ± standard error of the mean. The analysis was conducted using Graphpad Prism Software version 9.02 (GraphPad Software, San Diego, CA, United States)[1].

[1] www.graphpad.com

DATA AVAILABILITY STATEMENT

The datasets presented in this study can be found in the ArrayExpress database (www.ebi.ac.uk/arrayexpress) with the accession number E-MTAB-3676 and as **Supplementary Tables S1, S2**.

AUTHOR CONTRIBUTIONS

OG, CS, SW, AP, and IL-L designed the study. OG, CS, DV-C, DM, LM-A, and IL-L carried out the experiments. OG, CS, DV-C, DM, LM-A, DS-C, SW, AP, and IL-L carried out the data analysis and discussed the results. OG, AP, and IL-L were involved in drafting the manuscript and all authors, except SW who passed away, read and approved the final manuscript.

FUNDING

This work was supported by grants from DGAPA/UNAM (203612 and 218009) and the Consejo Nacional de Ciencia y Tecnología de México (CONACyT 178359 and 253549). We acknowledge the financial support of the German Research Foundation (DFG) and the Open Access Publication Fund of Bielefeld University for the article processing charge.

ACKNOWLEDGMENTS

We would like to thank José Miguel Villarreal Ascencio for the construction of plasmid pJMV01 and Angeles Moreno as well as Gabriela Guerrero for skillful technical assistance. This article is dedicated to the memory of the late Eugene P. Kennedy.

SUPPLEMENTARY MATERIAL

The Supplementary Material for this article can be found online at: https://www.frontiersin.org/articles/10.3389/fpls.2021.678976/full#supplementary-material

REFERENCES

Amarelle, V., Koziol, U., Rosconi, F., Noya, F., O'Brian, M. R., and Fabiano, E. (2010). A new small regulatory protein, HmuP, modulates haemin acquisition in *Sinorhizobium meliloti*. *Microbiology* 156, 1873–1882. doi: 10.1099/mic.0.037713-0

Bardin, S., Dan, S., Osteras, M., and Finan, T. M. (1996). A phosphate transport system is required for symbiotic nitrogen fixation by *Rhizobium meliloti*. *J. Bacteriol.* 178, 4540–4547. doi: 10.1128/jb.178.15.4540-4547.1996

Bélanger, L., Dimmick, K. A., Fleming, J. S., and Charles, T. C. (2009). Null mutations in *Sinorhizobium meliloti exoS* and *chvI* demonstrate the importance of this two-component regulatory system for symbiosis. *Mol. Microbiol.* 74, 1223–1237. doi: 10.1111/j.1365-2958.2009.06931.x

Bligh, E. G., and Dyer, W. J. (1959). A rapid method of total lipid extraction and purification. *Can. J. Biochem. Physiol.* 37, 911–917. doi: 10.1139/o59-099

Chen, E. J., Fisher, R. F., Perovich, V. M., Sabio, E. A., and Long, S. R. (2009). Identification of direct transcriptional target genes of ExoS/ChvI two-component signaling in *Sinorhizobium meliloti*. *J. Bacteriol.* 191, 6833–6842. doi: 10.1128/JB.00734-09

Cheng, H. P., and Walker, G. C. (1998a). Succinoglycan production by *Rhizobium meliloti* is regulated through the ExoS-ChvI two-component regulatory system. *J. Bacteriol.* 180, 20–26. doi: 10.1128/JB.180.1.20-26.1998

Cheng, H. P., and Walker, G. C. (1998b). Succinoglycan production is required for initiation and elongation of infection threads during nodulation of alfalfa by *Rhizobium meliloti*. *J. Bacteriol.* 180, 5183–5191. doi: 10.1128/JB.180.19.5183-5191.1998

Comerci, D. J., Altabe, S., de Mendoza, D., and Ugalde, R. A. (2006). *Brucella abortus* synthesizes phosphatidylcholine from choline provided by the host. *J. Bacteriol.* 188, 1929–1934. doi: 10.1128/JB.188.5.1929-1934.2006

Conde-Alvarez, R., Grilló, M. J., Salcedo, S. P., de Miguel, M. J., Fugier, E., Gorvel, J. P., et al. (2006). Synthesis of phosphatidylcholine, a typical eukaryotic

phospholipid, is necessary for full virulence of the intracellular bacterial parasite *Brucella abortus*. *Cell. Microbiol.* 8, 1322–1335. doi: 10.1111/j.1462-5822.2006.00712.x

Conover, G., Martínez-Morales, F., Heidtman, M. I., Luo, Z. Q., Tang, M., Chen, C., et al. (2008). Phosphatidylcholine synthesis is required for optimal function of *Legionella pneumophila* virulence determinants. *Cell. Microbiol.* 10, 514–528. doi: 10.1111/j.1462-5822.2007.01066.x

Cooper, H. M., and Paterson, Y. (2008). Production of polyclonal antisera. *Curr. Protoc. Mol. Biol.* Chapter 2:Unit 2.4.1–2.4.10. doi: 10.1002/0471142735.im0204s82

de Rudder, K. E. E., López-Lara, I. M., and Geiger, O. (2000). Inactivation of the gene for phospholipid *N*-methyltransferase in *Sinorhizobium meliloti*: phosphatidylcholine is required for normal growth. *Mol. Microbiol.* 37, 763–772. doi: 10.1046/j.1365-2958.2000.02032.x

de Rudder, K. E. E., Sohlenkamp, C., and Geiger, O. (1999). Plant-exuded choline is used for rhizobial membrane lipid biosynthesis by phosphatidylcholine synthase. *J. Biol. Chem.* 274, 20011–20016. doi: 10.1074/jbc.274.28.20011

de Rudder, K. E. E., Thomas-Oates, J. E., and Geiger, O. (1997). *Rhizobium meliloti* mutants deficient in phospholipid *N*-methyltransferase still contain phosphatidylcholine. *J. Bacteriol.* 179, 6921–6928. doi: 10.1128/jb.179.22.6921-6928.1997

Ditta, G., Schmidhauser, T., Yakobson, E., Lu, P., Liang, X. W., Finlay, D. R., et al. (1985). Plasmids related to the broad host range vector, pRK290, useful for gene cloning and for monitoring expression. *Plasmid* 13, 149–153. doi: 10.1016/0147-619x(85)90068-x

Dondrup, M., Goesmann, A., Bartels, D., Kalinowski, J., Krause, L., Linke, B., et al. (2003). EMMA: a platform for consistent storage and efficient analysis of microarray data. *J. Biotechnol.* 106, 135–146. doi: 10.1016/j.jbiotec.2003.08.010

Dowhan, W., Bogdanov, M., and Mileykovskaya, E. (2008). "Functional roles of lipids in membranes," in *Biochemistry of Lipids, Lipoproteins and Membranes*, 5th Edn, eds D. E. Vance and J. E. Vance (Amsterdam: Elsevier), 1–37.

Finan, T. M., Hartwieg, E., LeMieux, K., Bergman, K., Walker, G. C., and Signer, E. R. (1984). General transduction in *Rhizobium meliloti*. *J. Bacteriol.* 159, 120–124. doi: 10.1128/JB.159.1.120-124.1984

Geiger, O., López-Lara, I. M., and Sohlenkamp, C. (2013). Phosphatidylcholine biosynthesis and function in bacteria. *Biochim. Biophys. Acta* 1831, 503–513. doi: 10.1016/j.bbalip.2012.08.009

Gibson, K. E., Kobayashi, H., and Walker, G. C. (2008). Molecular determinants of a symbiotic chronic infection. *Annu. Rev. Genet.* 42, 413–441. doi: 10.1146/annurev.genet.42.110807.091427

Glazebrook, J., and Walker, G. C. (1991). Genetic techniques in *Rhizobium meliloti*. *Methods Enzymol.* 204, 398–418. doi: 10.1016/0076-6879(91)04021-f

Goenrich, M., Bartoschek, S., Hagemeier, C. H., Griesinger, C., and Vorholt, J. A. (2002). A glutathione-dependent formaldehyde-activating enzyme (Gfa) from *Paracoccus denitrificans* detected and purified via two-dimensional proton exchange NMR spectroscopy. *J. Biol. Chem.* 277, 3069–3072. doi: 10.1074/jbc.C100579200

Hanahan, D. (1983). Studies on transformation of *Escherichia coli* with plasmids. *J. Mol. Biol.* 166, 557–580. doi: 10.1016/s0022-2836(83)80284-8

Heavner, M. E., Qiu, W.-G., and Cheng, H.-P. (2015). Phylogenetic co-occurrence of ExoR, ExoS, and ChvI, components of the RSI bacterial invasion switch, suggests a key adaptive mechanism regulating the transition between free-living and host-invading phases in Rhizobiales. *PLoS One* 10:e0135655. doi: 10.1371/journal.pone.0135655

Heckel, B. C., Tomlinson, A. D., Morton, E. R., Choi, J. H., and Fuqua, C. (2014). *Agrobacterium tumefaciens exoR* controls acid response genes and impacts exopolysaccharide synthesis, horizontal gene transfer, and virulence gene expression. *J. Bacteriol.* 196, 3221–3233. doi: 10.1128/JB.01751-14

Hellweg, C., Pühler, A., and Weidner, S. (2009). The time course of the transcriptomic response of *Sinorhizobium meliloti* 1021 following a shift to acidic pH. *BMC Microbiol.* 9:37. doi: 10.1186/1471-2180-9-37

Janczarek, M. (2011). Environmental signals and regulatory pathways that influence exopolysaccharide production in rhizobia. *Int. J. Mol. Sci.* 12, 7898–7933. doi: 10.3390/ijms12117898

Klüsener, S., Hacker, S., Tsai, Y. L., Bandow, J. E., Gust, R., Lai, E. M., et al. (2010). Proteomic and transcriptomic characterization of a virulence-deficient phosphatidylcholine-negative *Agrobacterium tumefaciens* mutant. *Mol. Genet. Genomics* 283, 575–589. doi: 10.1007/s00438-010-0542-7

Kohler, P. R. A., Choong, E. L., and Rossbach, S. (2011). The RpiR-like repressor IolR regulates inositol catabolism in *Sinorhizobium meliloti*. *J. Bacteriol.* 193, 5155–5163. doi: 10.1128/JB.05371-11

Krol, E., and Becker, A. (2004). Global transcriptional analysis of the phosphate starvation response in *Sinorhizobium meliloti* strains 1021 and 2011. *Mol. Genet. Genomics* 272, 1–17. doi: 10.1007/s00438-004-1030-8

Leigh, J. A., Signer, E. R., and Walker, G. C. (1985). Exopolysaccharide-deficient mutants of *Rhizobium meliloti* that form ineffective nodules. *Proc. Natl. Acad. Sci. U.S.A.* 82, 6231–6235. doi: 10.1073/pnas.82.18.6231

López-Lara, I. M., Gao, J. L., Soto, M. J., Solares-Pérez, A., Weissenmayer, B., Sohlenkamp, C., et al. (2005). Phosphorus-free membrane lipids of *Sinorhizobium meliloti* are not required for the symbiosis with alfalfa but contribute to increased cell yields under phosphorus-limiting conditions of growth. *Mol. Plant Microbe Interact.* 18, 973–982. doi: 10.1094/MPMI-18-0973

López-Lara, I. M., van den Berg, J. D. J., Thomas-Oates, J. E., Glushka, J., Lugtenberg, B. J. J., and Spaink, H. P. (1995). Structural identification of the lipo-chitin oligosaccharide nodulation signals of *Rhizobium loti*. *Mol. Microbiol.* 15, 627–638. doi: 10.1111/j.1365-2958.1995.tb02372.x

Lu, H. Y., Luo, L., Yang, M. H., and Cheng, H. P. (2012). *Sinorhizobium meliloti* ExoR is the target of periplasmic proteolysis. *J. Bacteriol.* 194, 4029–4040. doi: 10.1128/JB.00313-12

Malek, A. A., Wargo, M. J., and Hogan, D. A. (2012). Absence of membrane phosphatidylcholine does not affect virulence and stress tolerance phenotypes in the opportunistic pathogen *Pseudomonas aeruginosa*. *PLoS One* 7:e30829. doi: 10.1371/journal.pone.0030829

Martínez-Morales, F., Schobert, M., López-Lara, I. M., and Geiger, O. (2003). Pathways for phosphatidylcholine biosynthesis in bacteria. *Microbiology* 149, 3461–3471. doi: 10.1099/mic.0.26522-0

Martínez-Nuñez, C., Altamirano-Silva, P., Alvarado-Guillén, F., Moreno, E., Guzmán-Verri, C., and Chaves-Olarte, E. (2010). The two-component sytem BvrR/BvrS regulates the expression of the type IV secretion system VirB in *Brucella abortus*. *J. Bacteriol.* 192, 5603–5608. doi: 10.1128/JB.00567-10

Medeot, D. B., Sohlenkamp, C., Dardanelli, M. S., Geiger, O., Garcia de Lema, M., and López-Lara, I. M. (2010). Phosphatidylcholine levels of peanut-nodulating *Bradyrhizobium* sp. SEMIA 6144 affect cell size and motility. *FEMS Microbiol. Lett.* 303, 123–131. doi: 10.1111/j.1574-6968.2009.01873.x

Miclea, P. S., Peter, M., Végh, G., Cinege, G., Kiss, E., Váró, G., et al. (2010). Atypical transcriptional regulation of a new toxin-antitoxin-like module and its effect on the lipid composition of *Bradyrhizobium japonicum*. *Mol. Plant Microbe Interact.* 23, 638–650. doi: 10.1094/MPMI-23-5-0638

Mileykovskaya, E. I., and Dowhan, W. (1997). The Cpx two-component signal transduction pathway is activated in *Escherichia coli* mutant strains lacking phosphatidylethanolamine. *J. Bacteriol.* 179, 1029–1034. doi: 10.1128/jb.179.4.1029-1034.1997

Miller, J. H. (1972). *Experiments in Molecular Genetics*. Plainview, NY: Cold Spring Harbor Laboratory Press.

Minder, A. C., de Rudder, K. E. E., Narberhaus, F., Fischer, H. M., Hennecke, H., and Geiger, O. (2001). Phosphatidylcholine levels in *Bradyrhizobium japonicum* are critical for an efficient symbiosis with the soybean host plant. *Mol. Microbiol.* 39, 1186–1198. doi: 10.1111/j.1365-2958.2001.02325.x

Nogales, J., Domínguez-Ferreras, A., Amaya-Gómez, C. V., van Dillewijn, P., Cuéllar, V., Sanjuán, J., et al. (2010). Transcriptome profiling of a *Sinorhizobium meliloti fadD* mutant reveals the role of rhizobactin 1021 biosynthesis and regulation genes in the control of swarming. *BMC Genomics* 11:157. doi: 10.1186/1471-2164-11-157

Olivares, J., Casadesús, J., and Bedmar, E. J. (1980). Method for testing degree of infectivity of *Rhizobium meliloti* strains. *Appl. Environ. Microbiol.* 39, 967–970. doi: 10.1128/AEM.39.5.967-970.1980

Pickering, B. S., and Oresnik, I. J. (2008). Formate-dependent autotrophic growth in *Sinorhizobium meliloti*. *J. Bacteriol.* 190, 6409–6418. doi: 10.1128/JB.00757-08

Quebatte, M., Dehio, M., Tropel, D., Basler, A., Toller, I., Raddatz, G., et al. (2010). The BatR/BatS two-component regulatory system controls the adaptive response of *Bartonella henselae* during human endothelial cell infection. *J. Bacteriol.* 192, 3352–3367. doi: 10.1128/JB.01676-09

Ratib, N. R., Sabio, E. Y., Mendoza, C., Barnett, M. J., Clover, S. B., Ortega, J. A., et al. (2018). Genome-wide identification of genes directly regulated by ChvI

and a consensus sequence for ChvI binding in *Sinorhizobium meliloti*. *Mol. Microbiol.* 110, 596–615. doi: 10.1111/mmi.14119

Rossbach, S., Rasul, G., Schneider, M., Eardly, B., and de Bruijn, F. J. (1995). Structural and functional conservation of the rhizopine catabolism locus is limited to selected *Rhizobium meliloti* strains and unrelated to their geographical origin. *Mol. Plant Microbe Interact.* 8, 549–559. doi: 10.1094/mpmi-8-0549

Rüberg, S., Tian, Z. X., Krol, E., Linke, B., Meyer, F., Wang, Y., et al. (2003). Construction and validation of a *Sinorhizobium meliloti* whole genome DNA microarray: genome-wide profiling of osmoadaptive gene expression. *J. Biotechnol.* 106, 255–268. doi: 10.1016/j.jbiotec.2003.08.005

Sambrook, J., and Russell, D. R. (2001). *Molecular Cloning: A Laboratory Manual*. Cold Spring Harbor, NY: Cold Spring Harbor Press.

Schäfer, A., Tauch, A., Jäger, W., Kalinowski, J., Thierbach, G., and Pühler, A. (1994). Small mobilizable multi-purpose cloning vectors derived from the *Escherichia coli* plasmids pK18 and pK19: selection of defined deletions in the chromosome of *Corynebacterium glutamicum*. *Gene* 145, 69–73. doi: 10.1016/0378-1119(94)90324-7

Scharf, B., Schuster-Wolff-Bühring, H., Rachel, L., and Schmitt, R. (2001). Mutational analysis of the *Rhizobium lupini* H13-3 and *Sinorhizobium meliloti* flagellin genes: importance of flagellin A for flagellar filament structure and transcriptional regulation. *J. Bacteriol.* 183, 5334–5342. doi: 10.1128/JB.183.18.5334-5342.2001

Schmittgen, T. D., and Livak, K. J. (2008). Analyzing real-time PCR data by the comparative CT method. *Nat. Protoc.* 3, 1101–1108. doi: 10.1038/nprot.2008.73

Schultze, M., Quiclet-Sire, B., Kondorosi, E., Virelizier, H., Glushka, J. N., Endre, G., et al. (1992). *Rhizobium meliloti* produces a family of sulfated lipo-oligosaccharides exhibiting different degrees of plant host specificity. *Proc. Natl. Acad. Sci. U.S.A.* 89, 192–196. doi: 10.1073/pnas.89.1.192

Schweizer, H. D. (1993). Small broad-host-range gentamycin resistance gene cassettes for site-specific insertion and deletion mutagenesis. *BioTechniques* 15, 831–834.

Simon, R., Priefer, U., and Pühler, A. (1983). A broad host range mobilization system for in vivo genetic engineering: transposon mutagenesis in gram-negative bacteria. *Bio Technol.* 1, 784–791.

Sohlenkamp, C., de Rudder, K. E. E., and Geiger, O. (2004). Phosphatidylethanolamine is not essential for growth of *Sinorhizobium meliloti* on complex culture media. *J. Bacteriol.* 186, 1667–1677. doi: 10.1128/jb.186.6.1667-1677.2004

Sohlenkamp, C., de Rudder, K. E. E., Röhrs, V., López-Lara, I. M., and Geiger, O. (2000). Cloning and characterization of the gene for phosphatidylcholine synthase. *J. Biol. Chem.* 275, 18919–18925. doi: 10.1074/jbc.M000844200

Sohlenkamp, C., López-Lara, I. M., and Geiger, O. (2003). Biosynthesis of phosphatidylcholine in bacteria. *Prog. Lipid Res.* 42, 115–162. doi: 10.1016/s0163-7827(02)00050-4

Spaink, H. P., Wijffelman, C. A., Pee, S. E., Okker, R. J. H., and Lugtenberg, B. J. J. (1987). *Rhizobium* nodulation gene *nodD* as a determinant of host specificity. *Nature* 328, 337–340.

Spaink, H. P., Wijfjes, A. H. M., and Lugtenberg, B. J. J. (1995). Rhizobium NodI and NodJ proteins play a role in the efficiency of secretion of lipochitin oligosaccharides. *J. Bacteriol.* 177, 6276–6281. doi: 10.1128/jb.177.21.6276-6281.1995

Studier, F. W., Rosenberg, A. H., Dunn, J. J., and Dubendorff, J. W. (1990). Use of T7 RNA polymerase to direct expression of cloned genes. *Methods Enzymol.* 185, 60–89. doi: 10.1016/0076-6879(90)85008-c

Truchet, G., Camut, S., de Billy, F., Odorico, R., and Vasse, J. (1989). The *Rhizobium*-legume symbiosis. Two methods to discriminate between nodules and other root derived structures. *Protoplasma* 149, 82–88.

Vanderlinde, E. M., and Yost, C. K. (2012). Mutation of the sensor kinase *chvG* in *Rhizobium leguminosarum* negatively impacts cellular metabolism, outer membrane stability, and symbiosis. *J. Bacteriol.* 194, 768–777. doi: 10.1128/JB.01140-09

Vences-Guzmán, M. A., Geiger, O., and Sohlenkamp, C. (2008). *Sinorhizobium meliloti* mutants deficient in phosphatidylserine decarboxylase accumulate phosphatidylserine and are strongly affected during symbiosis with alfalfa. *J. Bacteriol.* 190, 6846–6856. doi: 10.1128/JB.00610-08

Wang, C., Kemp, J., Da Fonseca, I. O., Equi, R. C., Sheng, X., Charles, T. C., et al. (2010). *Sinorhizobium meliloti* 1021 loss-of-function deletion mutation in *chvI* and its phenotypic characteristics. *Mol. Plant Microbe Interact.* 23, 153–160. doi: 10.1094/MPMI-23-2-0153

Wells, D. H., Chen, E. J., Fisher, R. F., and Long, S. R. (2007). ExoR is genetically coupled to the ExoS-ChvI two-component system and located in the periplasm of *Sinorhizobium meliloti*. *Mol. Microbiol.* 64, 647–664. doi: 10.1111/j.1365-2958.2007.05680.x

Wessel, M., Klüsener, S., Gödeke, J., Fritz, C., Hacker, S., and Narberhaus, F. (2006). Virulence of *Agrobacterium tumefaciens* requires phosphatidylcholine in the bacterial membrane. *Mol. Microbiol.* 62, 906–915. doi: 10.1111/j.1365-2958.2006.05425.x

Wiech, E. M., Cheng, H. P., and Singh, S. M. (2015). Molecular modeling and computational analyses suggests that the *Sinorhizobium meliloti* periplasmic regulator protein ExoR adopts a superhelical fold and is controlled by a unique mechanism of proteolysis. *Protein Sci.* 24, 319–327. doi: 10.1002/pro.2616

Wu, C. F., Lin, Y. S., Shaw, G. C., and Lai, E. M. (2012). Acid-induced type VI secretion system is regulated by ExoR-ChvG/ChvI signaling cascade in *Agrobacterium tumefaciens*. *PLoS Pathog.* 8:e1002938. doi: 10.1371/journal.ppat.1002938

Yanisch-Perron, C., Viera, J., and Messing, J. (1985). Improved M13 phage cloning vectors and host strains: nucleotide sequences of the M13mp18 and pUC19 vectors. *Gene* 33, 103–119. doi: 10.1016/0378-1119(85)90120-9

Yao, S. Y., Luo, L., Har, K. J., Becker, A., Rüberg, S., Yu, G. Q., et al. (2004). *Sinorhizobium meliloti* ExoR and ExoS proteins regulate both succinoglycan and flagellum production. *J. Bacteriol.* 186, 6042–6049. doi: 10.1128/JB.186.18.6042-6049.2004

Conflict of Interest: The authors declare that the research was conducted in the absence of any commercial or financial relationships that could be construed as a potential conflict of interest.

Publisher's Note: All claims expressed in this article are solely those of the authors and do not necessarily represent those of their affiliated organizations, or those of the publisher, the editors and the reviewers. Any product that may be evaluated in this article, or claim that may be made by its manufacturer, is not guaranteed or endorsed by the publisher.

frontiers in Plant Science

ORIGINAL RESEARCH
published: 28 July 2021
doi: 10.3389/fpls.2021.699590

Differential Expression of *Paraburkholderia phymatum* Type VI Secretion Systems (T6SS) Suggests a Role of T6SS-b in Early Symbiotic Interaction

*Sebastian Hug[1], Yilei Liu[1], Benjamin Heiniger[2], Aurélien Bailly[1], Christian H. Ahrens[2], Leo Eberl[1] and Gabriella Pessi[1]**

[1] Department of Plant and Microbial Biology, University of Zurich, Zurich, Switzerland, [2] Agroscope, Research Group Molecular Diagnostics, Genomics and Bioinformatics, Swiss Institute of Bioinformatics, Wädenswil, Switzerland

OPEN ACCESS

Edited by:
Jose María Vinardell,
University of Seville, Spain

Reviewed by:
Luis Rey,
Polytechnic University of Madrid, Spain
Euan James,
The James Hutton Institute, United Kingdom

***Correspondence:**
Gabriella Pessi
gabriella.pessi@botinst.uzh.ch

Specialty section:
This article was submitted to Plant Symbiotic Interactions, a section of the journal Frontiers in Plant Science

Received: 23 April 2021
Accepted: 28 June 2021
Published: 28 July 2021

Citation:
Hug S, Liu Y, Heiniger B, Bailly A, Ahrens CH, Eberl L and Pessi G (2021) Differential Expression of Paraburkholderia phymatum Type VI Secretion Systems (T6SS) Suggests a Role of T6SS-b in Early Symbiotic Interaction. Front. Plant Sci. 12:699590. doi: 10.3389/fpls.2021.699590

Paraburkholderia phymatum STM815, a rhizobial strain of the *Burkholderiaceae* family, is able to nodulate a broad range of legumes including the agriculturally important *Phaseolus vulgaris* (common bean). *P. phymatum* harbors two type VI Secretion Systems (T6SS-b and T6SS-3) in its genome that contribute to its high interbacterial competitiveness *in vitro* and in infecting the roots of several legumes. In this study, we show that *P. phymatum* T6SS-b is found in the genomes of several soil-dwelling plant symbionts and that its expression is induced by the presence of citrate and is higher at 20/28°C compared to 37°C. Conversely, T6SS-3 shows homologies to T6SS clusters found in several pathogenic *Burkholderia* strains, is more prominently expressed with succinate during stationary phase and at 37°C. In addition, T6SS-b expression was activated in the presence of germinated seeds as well as in *P. vulgaris* and *Mimosa pudica* root nodules. Phenotypic analysis of selected deletion mutant strains suggested a role of T6SS-b in motility but not at later stages of the interaction with legumes. In contrast, the T6SS-3 mutant was not affected in any of the free-living and symbiotic phenotypes examined. Thus, *P. phymatum* T6SS-b is potentially important for the early infection step in the symbiosis with legumes.

Keywords: root nodule, legume, rhizobium, T6SS, competition, temperature regulation, citrate, C4-dicarboxylates

INTRODUCTION

Crop production is often limited by nitrogen supply, even though nitrogen gas (N_2) makes up 78% of the Earth's atmosphere (Fields, 2004). A specialized group of prokaryotes, the diazotrophic bacteria, is able to convert inert atmospheric nitrogen into biologically available ammonium (NH_4) by a process called biological N_2 fixation (BNF), which plays an important role for sustainable food production by contributing up to 65% of nitrogen used in agriculture (Vance and Graham, 1995; Udvardi and Poole, 2013; Lindström and Mousavi, 2020). BNF by rhizobia involves the establishment of a symbiotic relationship, which leads to the formation of a specialized plant organ on the root or on the stem, the nodule (Masson-Boivin et al., 2009; Oldroyd et al., 2011;

Wheatley et al., 2020). Upon sensing plant signal molecules produced by the roots (flavonoids), rhizobia produce lipochitooligosaccharides, called Nod factors (NFs), which modulate the growth of the root tip and induce root hair curling (Gage and Margolin, 2000; Cooper, 2007). A rhizobial microcolony grows in the curl and finally enters the root hair by hydrolysing the plant cell wall and inducing an invagination of the plasma membrane (Ibáñez et al., 2017). This invagination leads to the creation of a so called infection thread (IT) inside the root hair, in which the bacteria continue to grow (Gage and Margolin, 2000). The IT grows toward the base of root hair cells, ramifies within the root cortical tissue and releases the rhizobia within the cytoplasm of cortical cells via endocytosis, leading to an intracellular rhizobia-legume symbiosis. The rhizobia are then surrounded by a plant membrane forming an organelle like structure called a symbiosome. Within these symbiosomes, the bacteria differentiate into nitrogen-fixing bacteroids (Udvardi and Poole, 2013; Clarke et al., 2014; Ledermann et al., 2021). The rhizobial enzyme nitrogenase, a complex two-component metalloenzyme that consists of a homodimeric reductase (the Fe protein, encoded by *nifH*) and of a heterotetrameric dinitrogenase (the MoFe protein, encoded by *nifD* and *nifK*), reduces N_2 into a plant usable nitrogen form (Halbleib and Ludden, 2000; Dixon and Kahn, 2004). Typical carbon sources delivered by the plant as energy source to the symbiont are C4-dicarboxylates such as succinate, malate and fumarate, which are transported by the dicarboxylate transporter A (DctA) inside bacterial cells (Janausch et al., 2002; Yurgel and Kahn, 2004). DctA is a secondary active symporter belonging to the glutamate transporter family and is known to be important for rhizobia to differentiate into nitrogen-fixing bacteroids (Ronson et al., 1981; Finan et al., 1983; Yurgel and Kahn, 2004). Thus, rhizobia are able to adapt to different lifestyles ranging from free-living growth in the soil to biofilm growth when colonizing the root, through stressful growth conditions inside the IT and finally as N_2-fixing bacteroids inside the cells. Rhizobia are polyphyletic and include members of two classes of proteobacteria, the alpha-proteobacteria and since 2001 the beta-proteobacteria from the family *Burkholderiaceae* (Chen et al., 2001; Moulin et al., 2001; Masson-Boivin et al., 2009; Bontemps et al., 2010; Gyaneshwar et al., 2011). *Paraburkholderia phymatum* STM815, previously called *Burkholderia phymatum*, was isolated from root nodules in 2001 (Moulin et al., 2001, 2014; Gyaneshwar et al., 2011; Mishra et al., 2012) and was subsequently shown to have an exceptionally broad host range by nodulating over 40 different *Mimosa* species from South America, Asia, Africa and even papilionoid legumes such as the agriculturally important *Phaseolus vulgaris* (common bean) (Elliott et al., 2007; dos Reis et al., 2010; Talbi et al., 2010; Moulin et al., 2014; Lemaire et al., 2016). Competition experiments revealed that *P. phymatum* STM815 was more competitive than other alpha- and beta-rhizobia in infecting and nodulating the root of several legumes (Elliott et al., 2009; Melkonian et al., 2014; Lardi et al., 2017; Klonowska et al., 2018). This high competitiveness mainly depends on environmental conditions (nitrogen limitation as well as low pH favors *P. phymatum* dominance) and on host and symbiont genotype (Elliott et al., 2009; Garau et al., 2009). In other rhizobia, lipopolysaccharides (LPS), exopolysaccharides (EPS), antibiotic production (Bhagwat et al., 1991; Zdor and Pueppke, 1991; Robleto et al., 1998; Geddes et al., 2014), motility (Mellor et al., 1987), and catabolism of certain compounds (Kohler et al., 2010; Ding et al., 2012; Wheatley et al., 2020) have been shown to be important for high competitiveness. However, the factors that are important for competitiveness and promiscuity of *P. phymatum* are still largely unknown. However, in *P. phymatum* large genome two *P. phymatum* Type VI Secretion Systems (T6SSs) located on plasmid pBPHY01 (T6SS-b and T6SS-3) were shown to play a role in inter-bacterial competition (de Campos et al., 2017). The T6SS was first described in the human pathogens *Vibrio cholerae* and *Pseudomonas aeruginosa* and was later found in numerous other Gram-negative bacteria (Mougous et al., 2006; Pukatzki et al., 2006; Boyer et al., 2009). Interestingly, the T6SS was originally discovered in the rhizobium *Rhizobium leguminosarum* bv. *trifolii*, but not recognized as part of a secretion system at that time. The locus "*imp*" (for impaired in nodulation, now called *tssK*), was responsible for the impaired ability of this vetch-nodulating strain to infect pea (Roest et al., 1997; Bladergroen et al., 2003). The number of genes encoded within a T6SS cluster can vary between 16 and 38, although only 13 genes encode the core components needed for a fully functional T6SS (Boyer et al., 2009). The core system is composed of a membrane complex (TssJLM), a baseplate (TssAEFGK), a tail tube (TssD or Hcp), a tail tip (TssI or VgrG), and a contractile sheath (TssBC) (Cianfanelli et al., 2016). The membrane complex forms a channel through the cytoplasm membrane and the peptidoglycan layer and the baseplate is important for tube and sheath assembly (Zoued et al., 2014). The tube is composed of hexametric rings of hemolysin-coregulated proteins (Hcp) that assemble into a channel like structure and is covered by a valine-glycine repeat protein G (VgrG), which acts as a spike to penetrate the target cell. This VgrG can be topped again by proteins from the proline-alanine-alanine-arginine (PAAR) repeat superfamily to which effector proteins can be attached (Shneider et al., 2013). The purpose of the T6SS is to puncture and transport effector proteins into a eukaryotic or prokaryotic target cell. The T6SS effector proteins are often encoded within the T6SS gene cluster and usually located downstream of *vgrG* but can also be found outside of T6SS clusters, forming small clusters including effector and immunity genes (Zoued et al., 2014; Alcoforado Diniz et al., 2015; Santos et al., 2019). The effectors can be divided in three classes: cell wall degrading enzymes (e.g., muramidase and amidase), DNA or RNA targeting nucleases (e.g., AHH nuclease and pyocinS/colicin/Tde DNase), and membrane targeting (e.g., lipase) (Durand et al., 2014; Kapitein and Mogk, 2014; Ma et al., 2014; Salomon et al., 2014). These effectors can kill the target cells if the required immunity protein is missing (Dong et al., 2013; Yang et al., 2018). Only recently, a study reported for the first time a positive role for T6SS in rhizobial symbiosis. Three different *Rhizobium etli* Mim1 T6SS mutants deficient in *tssD*, *tssM* or lacking the whole structural gene cluster (*tssA* – *tagE*) led to the formation of smaller nodules in symbiosis with *P. vulgaris* (Salinero-Lanzarote et al., 2019). However, nitrogenase activity and symbiotic efficiency was

not affected in nodules occupied by these mutants, potentially indicating that earlier steps of the symbiosis could be affected.

In this study, we first evaluated the phylogenetic conservation and expression of the two *P. phymatum* T6SS-b and T6SS-3 clusters *in vitro* in response to different carbon sources and temperatures. Furthermore, we explored the expression and role of the T6SS clusters during symbiosis, in the presence of germinated seeds and within root nodules. We show that T6SS-b is also present in other soil bacteria and its expression is elevated at lower temperature and in the presence of citrate as carbon source. In contrast, T6SS-3 is also found in pathogenic *Burkholderia* strains (*Burkholderia pseudomallei* and *Burkholderia mallei*), which may explain its higher expression at 37°C and in stationary phase. Moreover, T6SS-b was also expressed in the presence of germinated seedlings and in *P. vulgaris* and *Mimosa pudica* root nodules. Phenotypical analysis indicated a role of T6SS-b in motility, suggesting that this cluster may play a role in the early step of plant infection.

MATERIALS AND METHODS

Bacterial Strains, Media, and Cultivation

The strains, plasmids and primers used in this study are listed in the **Supplementary Table 1**. All *Paraburkholderia* strains were grown in Luria-Bertani (LB) medium without salt at 28°C and 180 rpm (Liu et al., 2020). All other strains were grown in LB medium (Miller, 1972). If needed, the media were supplemented with the appropriate concentrations of antibiotics: chloramphenicol (Cm, 20 μg/ml for *Escherichia coli* and 80 μg/ml for *P. phymatum*), kanamycin (Km, 25 μg/ml for *E. coli* and 50 μg/ml for *P. phymatum*), tetracycline (Tc, 15 μg/ml for *E. coli* and 30 μg/ml for *P. phymatum*), trimethoprim (Trp, 50 μg/ml for *E. coli* and 100 μg/ml for *P. phymatum*). For the induction of the promotors fusions in AB minimal medium (Clark and Maaløe, 1967), the bacteria were grown with different carbon source: 10 mM citrate (ABC), 10 mM glucose (ABG), 12.5 mM glutamate (ABGlu), 15 mM succinate (ABS) / fumarate (ABF) / malate (ABM) / aspartate (ABA). The concentration of the carbon source was adjusted to the number of C-atoms in the molecule. For the plant infection tests, the cultures were washed with AB minimal medium without nitrogen [(A)B medium] (Liu et al., 2020).

Construction of GFP Reporter Strains and Mutant Strains

The two promotor fusions p5978 (upstream of *tssB* in T6SS-b) and p6115 (upstream of *tssH* in T6SS-3) were constructed using the vector pPROBE-NT as previously described (Lardi et al., 2020). The promotors of Bphy_6116 (gene coding for a hypothetical protein in the second half of T6SS-3), Bphy_7722 (*nodB*), were PCR amplified by using *phymatum* STM815 genomic DNA (gDNA) (Moulin et al., 2014) with primer pairs: p6115_EcoRI_For and p6115_SalI_Rev, p7722_Sal1_For and p7722_EcoR1_Rev, respectively. The amplified fragments were digested and cloned into the vector pPROBE-NT in front of the gene coding for a green fluorescent protein (GFP) (Miller et al., 2000). The cloned sequences were confirmed by sequencing at Microsynth (Balgach, St. Gallen, Switzerland). All constructed plasmids were transferred into *P. phymatum* STM815 by triparental mating. Deletion mutants of T6SSs were constructed by cloning two pieces of DNA sequence flanking the region to be deleted, together with an antibiotic resistance gene in the middle, into a suicide plasmid. The plasmid was then transconjugated into *P. phymatum* STM815 wild-type and plated on selective medium. To construct *P. phymatum* ΔT6SS-b, Bphy_5978 *(tssB)* and Bphy_5979 (*tssC*), which builds the sheath of the T6SS-b, were deleted. The primers Bphy_5978_up_F_NotI and Bphy_5978_up_R_MfeI were used to amplify the upstream fragment and the primers Bphy_5979_dn_F_NdeI and Bphy_5979_dn_R_NotI for the downstream fragment. In between the two fragments, was cloned a trimethoprim resistance cassette *dhfr* with a transcription terminator which was amplified from plasmid p34E-TpTer (Shastri et al., 2017) with the primers Trim_stop_F_NdeI and Trim_stop_R_NdeI. The resulting sequence was then cloned into pSHAFT resulting in pSHAFT::ΔT6SS-b plasmid and the correct construct was confirmed by sequencing. After transconjugation, clones that were chloramphenicol sensitive and trimethoprim resistant were selected as the deletion mutant ΔT6SS-b. In the same way, two ΔT6SS-3 deletion mutants were constructed, where the genes coding for the sheath tssBC (Bphy_6113 and Bphy_6114) were replaced with a trimethoprim cassette (*dhfr*) or a chloramphenicol cassette (*catA2*) cloned from plasmid pSHAFT with the primers catA1_F_EcoR1 and catA2_R_NdeI. The Bphy_6113 upstream fragment was amplified with the primers Bphy_6114_up_F_XbaI and Bphy_6114_up_R_MfeI. The Bphy_6114 downstream fragment was amplified from the gDNA with the primers Bphy_6113_dn_F_NdeI and Bphy_6113_dn_R_XbaI. The ligated inserts were cloned into suicide plasmids pSHAFT and pEX18-Tc, respectively, resulting in constructs pSHAFT::ΔT6SS-3 and pEX18-Tc::ΔT6SS-3. The deletion mutant STM815-ΔT6SS-3 (*dhfr*) was chloramphenicol sensitive and trimethoprim resistant, mutant STM815-ΔT6SS-3 (*catA2*) was tetracycline sensitive and chloramphenicol resistant. To construct a Δ Δ *T6SS* mutant, the plasmid pEX18-Tc::ΔT6SS-3 (*dhfr*) was transferred by triparental mating in *P. phymatum* ΔT6SS-b. The resulting mutant strain was named *P. phymatum* STM815 Δ ΔT6SS.

Expression Analysis

The GFP expression of the promoter reporter strains that were grown in liquid cultures was measured by a plate reader (Tecan Infinite M200 Pro, Tecan Trading AG, Switzerland) with excitation at 488 nm and emission at 520 nm, recording fluorescence in relative fluorescence units (RFU) and the cell density (OD_{600}). The GFP expression of bacteria in solid media were visualized by a digital camera (Infinity 3 camera, Lumenera) with GFP filter. The different T6SS reporter constructs (empty pPROBE, p5978, p6115, and p6116) were grown with different carbon sources in 96-well plates (Falcon, Corning, United States) at 30°C for 48 h. Two biological replicates of each strain were tested. To observe the temperature dependent GFP expression of each promoter

reporter, bacteria were grown in 50 ml LB-NaCl in 250 ml Erlenmeyer flasks (starting OD_{600} = 0.05) at 180 rpm at different temperatures (20, 28, and 37°C). To visualize the GFP expression responding to the roots of bean germinated seedlings, a suspension of the *P. phymatum* reporter strains (pPROBE, p5978, p6115, p6116, and p7722 at a final OD of OD_{600} = 0.05) was mixed with melted soft agar (0.8%) ABS medium. A germinated bean was placed in the middle of the plate with root tip stabbed into the soft agar medium. After 3 days of incubation at 30°C, the primary roots were inspected under a Leica M165 FC fluorescent stereo microscope, and their relative fluorescent signal acquired through a GFP2 filter set (480/40 nm excitation, 520/10 nm emission) at constant focal distance and acquisition settings (7.3× magnification, 1 s exposure, 1.5× gain). The green channel of resulting RGB images was separated in FiJi and the mean gray signal, 1 mm around each root apex was quantified. The expression of GFP in the nodules of bean and mimosa inoculated with the *P. phymatum* reporter strains (WT-pPROBE, WT-pPROBE-p5978, WT-pPROBE-p6115, WT-pPROBE-p6116) was quantified by using a Leica SPE DM5500Q confocal LASER scanning microscope with an ACS APO 40.0× 1.15 oil objective and the images were analyzed with Fiji (Schindelin et al., 2012). In short, fresh nodule transversal sections were imaged throughout the sample at constant acquisition settings in serial 1 µm optical z-sections from the section plan until the GFP signal was lost. Intact colonized cells were extracted from maximum z-stack projections of the fluorescence channel using the FiJi manual selection tool. Mean gray values were measured for the given number of cells from three discrete plants; 1–2 nodules per plant were examined.

Phenotypic Analysis

The swimming motility assay was carried out as previously described (Lardi et al., 2020) in a different medium, which was LB plates without salt (0.2% agar). EPS production assay was done as previously described (Liu et al., 2020). Images were taken after 72 h incubation at 28°C. To compare the resistance to H_2O_2 and antibiotics of wild-type and mutant strains, soft agar plates were inoculated at a bacterial concentration of OD_{600} = 0.05 in ABS medium. The antibiotic discs (Becton, Dickinson and Company, REF: 231264, 231344, 231299, and 231301) and discs containing 10M, 5M, 1M H_2O_2, and H_2O were placed on the plate and images were taken after 24 h incubation.

Plant Infection Test

The bean seeds (*P. vulgaris*, cv. Negro Jamapa) and mimosa seeds (*M. pudica*) were surface sterilized as previously described (Talbi et al., 2010; Mishra et al., 2012). Seeds were germinated on 0.8% agarose plates at 28°C. Germinated seeds were planted into yogurt-jars filled with sterile vermiculite (VTT-Group, Muttenz, Switzerland) and Jensen medium (Hahn and Hennecke, 1984). One ml of bacterial cells at an OD_{600} = 0.025 (10^7 cells pro ml) were inoculated onto each seed and the plants were incubated for 21 (bean) or 28 (mimosa) days in the green house (25°C during day, 22°C at night, 60% humidity, 16 h light per day). The colony forming units (CFU) of each inoculum was determined on LB-NaCl plates. The plants were watered twice a week with autoclaved deionized H_2O. Symbiotic properties (nodule number, nodule dry weight, and nitrogenase activity) were determined as previously described (Göttfert et al., 1990; Lardi et al., 2017, 2018). Root attachment assay was done as previously described using about 10^7 cells and a 2-days old germinated seed (Liu et al., 2020).

Bioinformatics and Statistical Analysis

To find homologs in other bacteria, the *P. phymatum* T6SS-b and T6SS-3 clusters were searched with blastn 2.9.0+ (Camacho et al., 2009) against the NCBI nt database[1] in megablast mode using default parameters, a max_target_seq value of 100 and an e-value threshold of 1e-10. For T6SS-b, the nucleotide sequence of the whole cluster (Bphy_5978 to Bphy_5997, NC_010625.1:510771–535444) was searched and sequences of the retrieved homologous clusters were searched again to identify additional, more distantly related clusters. Since the T6SS-3 cluster consisted of two operons pointing in opposite directions (**Figure 1B**), the sequence of each operon (NC_010625.1:654424–668524 and NC_010625.1:668949–683600) was blasted separately. For strains identified in both Blast searches, the genomic positions of the two operons were visualized in R and strains where matches of both operons co-localized were selected. The identified homologous T6SS-b and T6SS-3 cluster sequences were manually assessed with CLC Genomics Workbench v11.0 (QIAGEN CLC bio, Aarhus, Denmark) to verify that they contained the same core genes as *P. phymatum* and in the same order. ClustalX2 (Larkin et al., 2007) was used to align the manually verified cluster sequences (T6SS-b: *tssB – tssA;* T6SS-3: *tssL – tssH*, and Bhy_6116 – *tssA*) and MEGA X was used to construct a maximum likelihood phylogenetic tree with a Tamura-Nei parameter (discrete gamma distribution, five rate categories, bootstrap = 100) (Tamura and Nei, 1993; Kumar et al., 2018). Putative operons were predicted with OperonBD[2]. For the statistical analysis, ANOVA with Tukey's multiple comparison was performed using GraphPad Prism 7.0 ($^*p \leq 0.05$, $^{**}p \leq 0.01$, $^{***}p \leq 0.001$, $^{****}p \leq 0.0001$).

RESULTS

Genomic Analysis of the Two T6SSs Clusters in *P. phymatum* STM815

Two T6SSs clusters have been identified in the *P. phymatum* STM815 genome (Moulin et al., 2014), which consists of two chromosomes and two megaplasmids, with one of them (pBPHY02) containing the symbiotic genes. Both clusters, T6SS-b and T6SS-3, contain all 13 core genes required for the assembly of a fully functional T6SS complex and are located on plasmid pBPHY01 (**Figures 1A,B**; de Campos et al., 2017). According to the SecReT6 database, these two clusters were assigned to the T6SS-families i4a (T6SS-b) and 3 (T6SS-3) (Barret et al., 2013; Li et al., 2015). While cluster T6SS-b is predicted to be

[1]https://ftp.ncbi.nlm.nih.gov/blast/db/, downloaded on January 28, 2020.
[2]http://operondb.ccb.jhu.edu/cgi-bin/operons.cgi

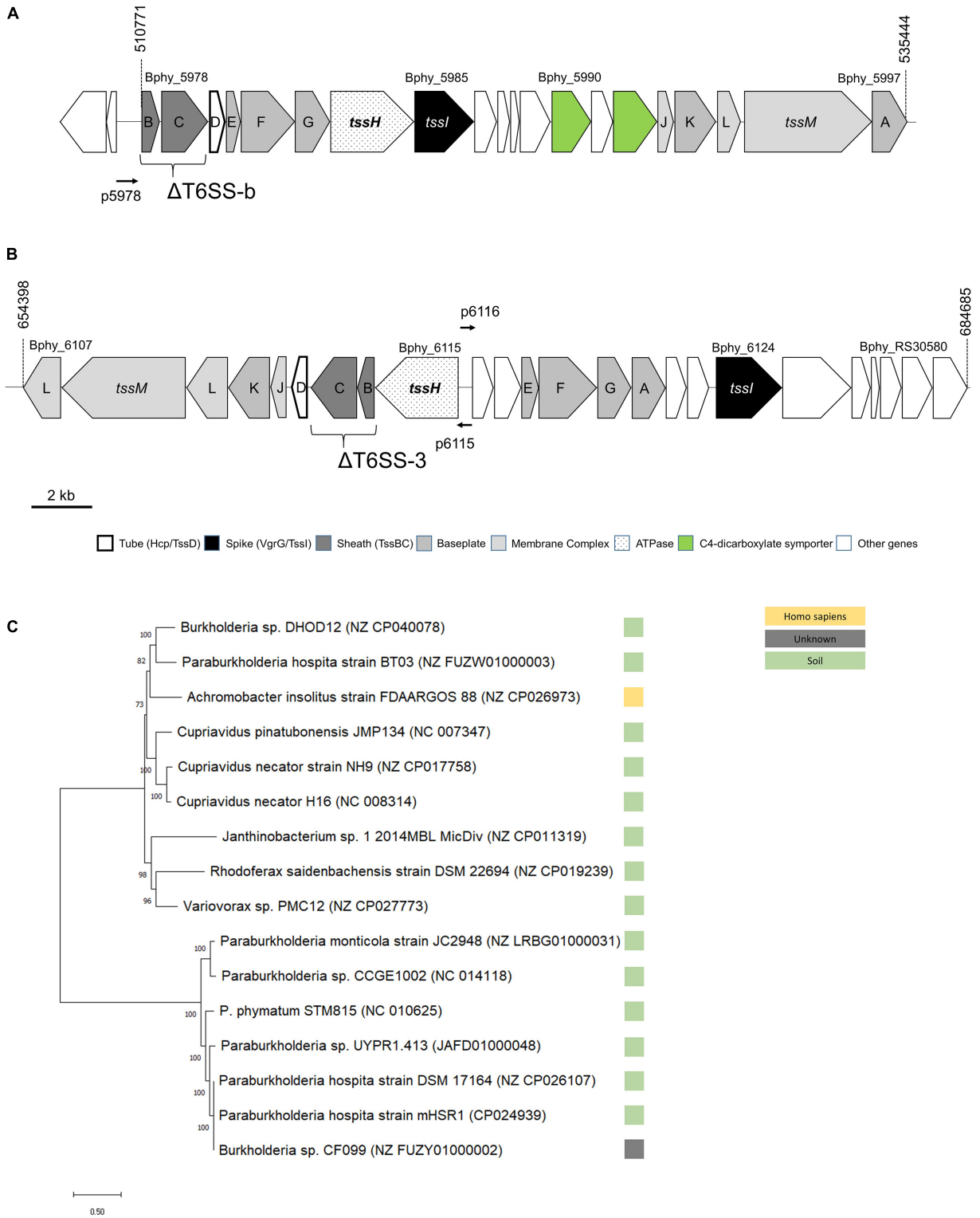

FIGURE 1 | Physical map of the two T6SS loci, **(A)** T6SS-b, **(B)** T6SS-3, and **(C)** unrooted maximum likelihood phylogenetic tree for T6SS-b. In **(A,B)**, numbers on top refer to nucleotide positions according to NCBI. The *tssBC* genes mutated to obtain the T6SS deletion (Δ) mutants are shown. TheT6SS promoters cloned in vector pPROBE are also displayed with a horizontal thin arrow (p5978 with upstream region of Bphy_5978, p6115 with the promoter of Bphy_6115, and p6116 contains the promoter region of Bphy_6116). The phylogenetic tree of T6SS-b **(C)** is based on the DNA sequence as described in section "Materials and Methods". The reference sequence accession numbers of the NCBI database is shown in brackets and the bootstrap values are shown left of the respective branches. The bar at the bottom left indicates the distance.

organized as a single operon, T6SS-3 is arranged in two operons facing in opposite direction, one (from Bphy_6107 to 6115) containing *tssHBCDIKLMI* and the other (from Bphy_6116 to Bphy_RS30580) carrying *tssEFGA* and *tssI* (**Figure 1B**). Each cluster also contains a *vgrG* gene, which codes for a VgrG. Downstream of *vgrG* (Bphy_5985) in the T6SS-b cluster, we found eight genes coding for putative proteins: an YwqK family antitoxin (Bphy_5986), a PAAR-like protein (Bphy_5987), a hypothetical protein (HP) (Bphy_5988), an amino acid ABC transporter (Bphy_5989), a sodium:dicarboxylate symporter (Bphy_5990), an aspartate/glutamate racemase (Bphy_5991) and a second sodium:dicarboxylate symporter (Bphy_5992) (**Figure 1A**). The presence of two sodium:dicarboxylate symporters in a rhizobial T6SS is intriguing and may suggest a role of T6SS-b during symbiosis, where dicarboxylates are an important source of energy provided by the legume. However, a global search for dicarboxylate transporters in the *P. phymatum* genome revealed the presence of three additional transporters on plasmid pBPHY01 and two genes coding for C4-dicarboxylate transporters similar to DctA encoded on chromosome 1 (Bphy_0225 and Bphy_2596). An alignment of the protein sequences of these different dicarboxylate symporters suggests that the symporters located in T6SS-b likely transport a different substrate compared to that of the known DctA transporters (**Supplementary Figure 1**; Yurgel and Kahn, 2004). Downstream of *vgrG* (Bphy_6124) located in the T6SS-3 cluster, five genes potentially coding for effectors were identified: two M23 family metallopeptidases (Bphy_6125 and Bphy_RS30575), Bphy_6126 and Bphy_6128 both coding for a HP and Bphy_6127 coding for a PAAR-like protein (**Figure 1B**). As in many other bacteria, in *P. phymatum*, *vgrG* genes are also found outside of the T6SS-b and T6SS-3 clusters, often containing effector and immunity genes (Santos et al., 2019). *P. phymatum* STM815 contains six orphan *vgrG* copies outside of the T6SS clusters distributed over the genome (Bphy_0023, Bphy_1932, Bphy_3640, Bphy_5197, Bphy_5744, and Bphy_7022). We next looked for the presence of similar T6SS clusters in other strains by blasting the DNA sequence of either the entire cluster for T66S-b, i.e., from Bphy_5978 (*tssB*) to Bphy_5997 (*tssA*), and of the two operons of T6SS-3, i.e., from Bphy_6107 (*tssL*) to Bphy_5107 (*tssH*) and Bphy_6116 to Bphy_RS30575 against the NCBI nt database[3] (see section "Materials and Methods"). Fifteen strains were found to contain a T6SS-b cluster similar to that of *P. phymatum* STM815. These strains exclusively represent beneficial bacteria occurring in the soil; they include six *Paraburkholderia* strains (*Paraburkholderia monticola* JC2948, *Paraburkholderia atlantica* CCGE1002, *Paraburkholderia* sp. UYPR1.413, *Paraburkholderia hospita* mHSR1 DSM17164 and BT03, two *Burkholderia* strains (*Burkholderia* sp. DHOD12 and sp. CF099), three *Cupriavidus* strains (*Cupriavidus pinatubonensis* JMP134, *Cupriavidus necator* H16 and NH9), *Achromobacter insolitus* FDAARGOS 88, *Variovorax* sp. PMC12, and *Rhodoferax saidenbachensis* DSM22694. One strain (*Janthinobacterium* sp. 1-2014MBL) had three additional genes downstream of *vgrG*, one coding for a GIY-YIG nuclease family protein and two encoding HPs. Moreover, the T6SS-b cluster in *Janthinobacterium* sp. 1-2014MBL did not contain the racemase encoding gene between the two sodium:dicarboxylate symporters. A phylogenetic analysis based on the DNA sequence of the clusters grouped the T6SS-b clusters of these bacteria in two clades (**Figure 1C**). In contrast, 44 strains were identified (see section "Materials and Methods") that harbored a cluster similar to T6SS-3 (from Bphy_6107 to Bphy_RS30580), which all belong to different *B. mallei* strains or *B. pseudomallei* strains (**Supplementary Figure 2**). In order to investigate the expression levels of the T6SSs under different environmental conditions, for each operon, a promotor fusion to the reporter gene *gfp* was constructed (p5978 for T6SS-b, p6115 and p6116 for T6SS-3; **Figures 1A,B**). While the promoter in p6115 drives expression of the T6SS structural genes, p6116 is the promoter of the operon containing *tssEF* and *vgrG* (*tssI*) together with potential effector genes.

T6SS-b Is Highly Expressed in Presence of Citrate and T6SS-3 Expression Is Maximal in the Stationary Phase When Succinate Is Used as Carbon Source

As mentioned above, the T6SS-b cluster contains two sodium:dicarboxylate symporters downstream of *vgrG*. To investigate if these transporters (Bphy_5990 and Bphy_5992) are involved in induction of T6SS-b expression, the reporter constructs for T6SS-b (p5978) and T6SS-3 (p6115 and p6116) (**Figures 1A,B**) were grown in AB minimal media with different C4-dicarboxylates as carbon sources (succinate, malate, fumarate, and aspartate). Additionally, T6SS expression in presence of a C5-dicarboxylate (glutamate), a C6-tricarboxylate (citrate), glucose (C6) as well as in complex medium (LB without salt) was investigated at different time points. The expression levels of the three T6SS reporter constructs at the end of the exponential and in the stationary phase are shown in **Figure 2**. While in LB without salt all *P. phymatum* strains reached the stationary phase after 11 h of growth, the growth rates in minimal media depended on the available carbon source. *P. phymatum* reached the stationary phase after 11, 12, and 14 h with glutamate, succinate, and malate, respectively. With other carbon sources the stationary phase was reached later: glucose (21 h), fumarate (26 h), citrate (36 h), and aspartate (38 h). T6SS-b (p5978) and T6SS-3 (p6115 and p6116) expression was followed for 48 h and in **Figure 2** we show the normalized values taken at the end of the exponential phase (E) and in the stationary phase after 48 h (S). In complex medium, T6SS-b showed high levels of expression in both the exponential and the stationary phase, while T6SS-3 was highly expressed only in the stationary phase (**Figure 2A**). However, the background fluorescence measured in complex medium was very high. When grown in minimal medium, T6SS-b showed the highest expression levels with citrate independent of the growth phase (**Figure 2B**), a 1.6-fold increase compared to cells grown with malate as carbon source (**Figure 2C**). The expression of both T6SS-3 operons (p6115 and p6116) in citrate, malate, and fumarate was low and was not induced when the cells grew to the stationary phase. The level of

[3] ftp://ftp.ncbi.nlm.nih.gov/blast/db/

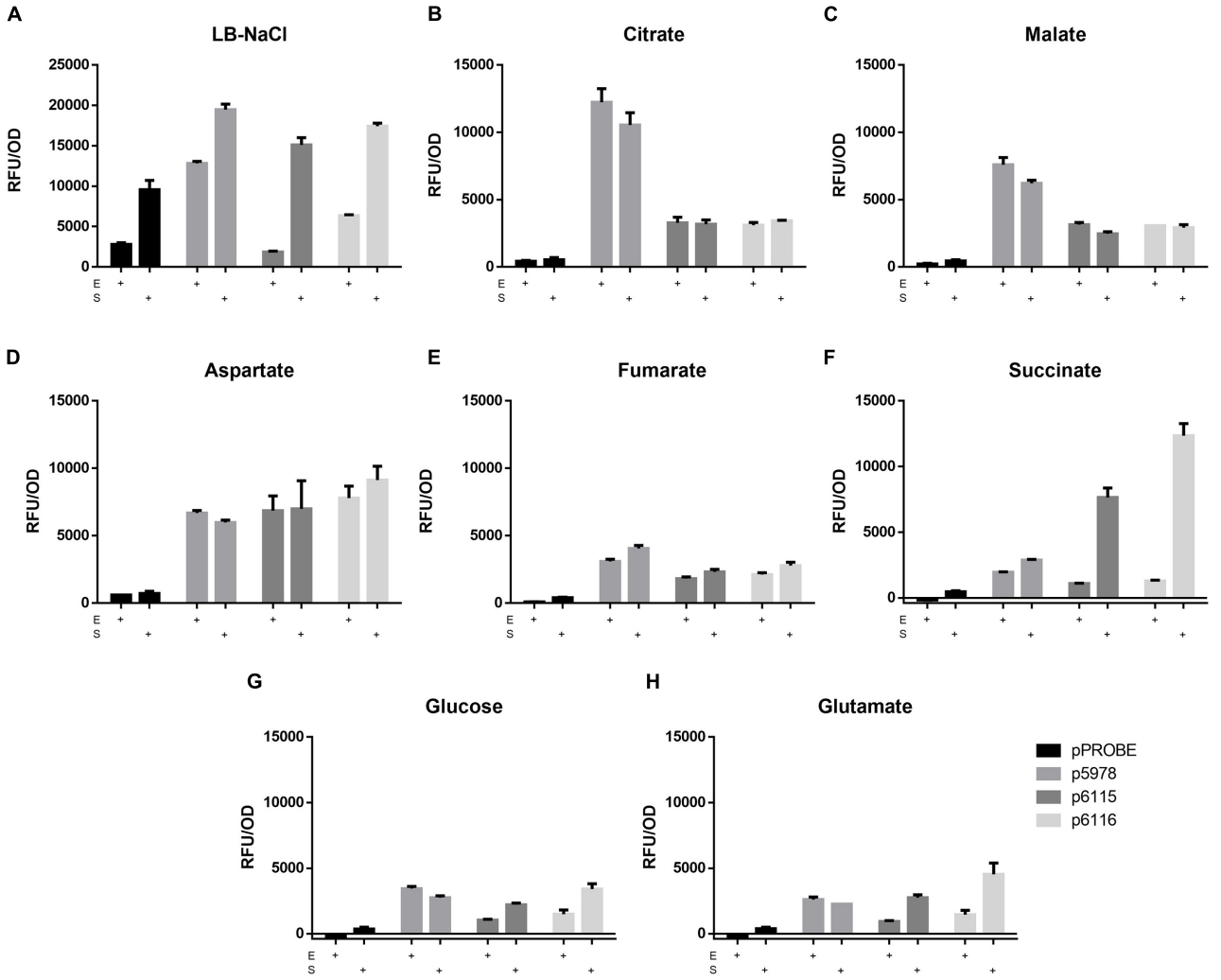

FIGURE 2 | The expression of the promotor fusions (p5978 for T6SS-b and p6115 and p6116 for T6SS-3) in LB-NaCl **(A)** and minimal media [**(B)** citrate, **(C)** malate, **(D)** aspartate, **(E)** fumarate, **(F)** succinate, **(G)** glucose, **(H)** glutamate] with different carbon sources. The expression (GFP) and the growth (OD_{600}) were recorded at the end of the exponential phase (E) and the stationary phase (S). A one-way ANOVA with Tukey's multiple comparisons test was used to analyze the biological duplicates.

T6SS-b and T6SS-3 expression in a medium containing aspartate was comparable at the end of exponential phase (**Figure 2D**). When the reporter strains were grown with fumarate, expression of both clusters was low (**Figure 2E**). While T6SS-b expression remained low in the presence of succinate, expression of T6SS-3 was 9.5-fold upregulated in the stationary phase compared to the end of the exponential phase, showing the highest expression levels for p6116 (**Figure 2F**). Phase-dependent expression levels were also observed for both T6SS-3 reporters (p6115 and p6116) in minimal medium containing glucose and glutamate (**Figures 2G,H**, respectively). Conversely, T6SS-b expression remained low in both glucose and glutamate-containing media. Finally, a significant difference in the expression of these two operons (p6115/p6116) was observed in LB-NaCl at the end of the exponential phase. Together, these findings suggested that both T6SS clusters were differentially expressed depending on the available carbon source. T6SS-b showed maximal expression in the presence of citrate independent of the growth phase and highest expression of T6SS-3 was observed in the presence of succinate in the stationary phase.

Thermoregulation of T6SS Expression

Since the entire T6SS-b operon is found in selected other soil bacteria (**Figure 1C**), while the T6SS-3 cluster is more similar to T6SS from pathogenic *Burkholderia* such as *B. pseudomallei* and *B. mallei* strains (**Supplementary Figure 2**), we measured expression of both *P. phymatum* T6SS clusters at three different temperatures in LB-NaCl, which mimics soil and host environments. Importantly, the expression was followed over time and the values measured in the exponential phase are shown in **Figure 3**. Expression of the entire T6SS-b was found to be significantly ($p \leq 0.0001$) up-regulated when *P. phymatum* was

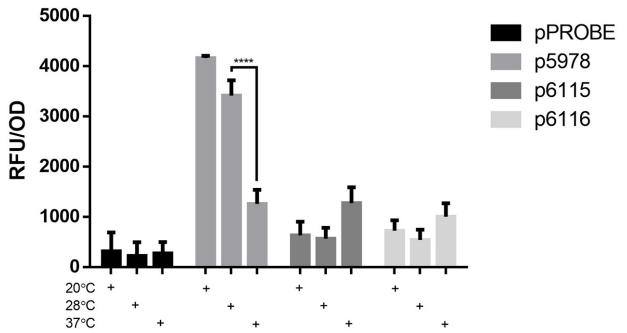

FIGURE 3 | Expression of the T6SS GFP reporter fusion strains (p5978, p6115, and p6116) and a control strain (pPROBE) in LB-NaCl at 180 rpm and 20, 28, or 37°C at the end of exponential phase. The means of biological triplicates are shown with error bars representing the standard deviation. A one-way ANOVA with Tukey's multiple comparisons test was used to analyze the biological triplicate (****$p \leq 0.0001$).

grown at lower temperatures (20 and 28°C). T6SS-b expression increased about 3.3-fold at 20°C compared to 37°C. In contrast, higher T6SS-3 expression levels were determined at 37 vs 28°C (p6115: 2.3-fold and p6116: 1.9-fold; $p = 0.066$ and $p = 0.42$, respectively). Thus, it appears that both systems are subjected to temperature-dependent regulation, which seems to be in line with the different origin of both gene clusters (**Figure 1C** and **Supplementary Figure 2**).

The Presence of a Germinated Seed Induced T6SS-b Expression

To assess the expression of *P. phymatum* T6SS during the early steps of the symbiotic process, soft-agar plates containing an OD_{600} = 0.05 of the T6SS reporter constructs p5978, p6115, and p6116 were prepared. The reporter construct p7722, which contains the promotor of Bphy_7722 (*nodB*) fused to *gfp* was used as a positive control. The gene *nodB* is involved in the biosynthesis of the backbone of the NF which is produced in response to flavonoids secreted by the root. Next, a 2 days-old germinated bean seed was added on the plate and the expression was analyzed under a fluorescence stereomicroscope after 3 days of incubation at 28°C. While the T6SS-b cluster (p5978) was expressed, at the tip of the root, both T6SS-3 reporter constructs p6115 and p6116 showed low expression in the presence of the germinated bean seed (**Figure 4A**). The GFP expression of the reporter constructs was quantified 1 mm around each root apex (**Figure 4B**). As expected, *nodB* (p7722) was highly expressed displaying a diffused signal around the root, confirming the well-known induction of *nodB* expression by root exudates. Since T6SS-b expression was localized on the root, we suggest that T6SS-b expression is induced by a component present on the tip of the root.

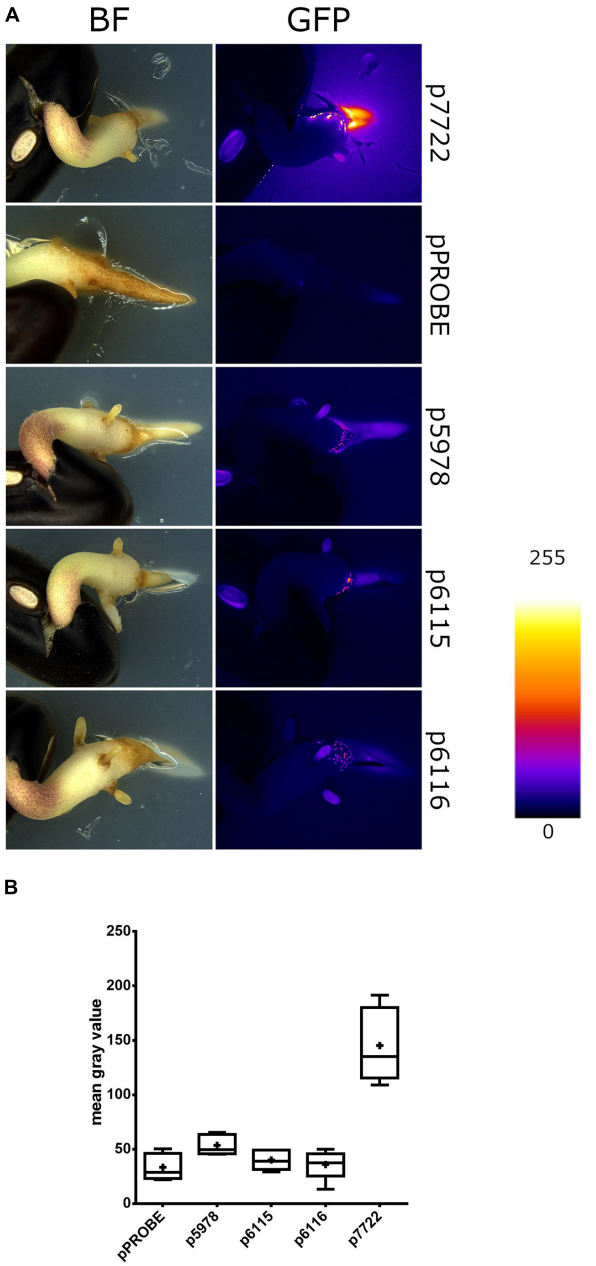

FIGURE 4 | The *gfp* expression of T6SS-b (p5978) and T6SS-3 (p6115 and p6116) clusters on bean roots. **(A)** Representative stereomicrographs. The empty pPROBE vector samples only display plant autofluorescence. All samples were imaged in the same conditions. Fire LUT indicates fluorescent signal intensity. **(B)** Semiquantitative analysis of GFP expression near *P. vulgaris* root tips. Plus signs indicate the arithmetic mean, whiskers minimum to maximum values and black dots outliers according to Tukey's test. Significant differences between samples were analyzed in a one-way ANOVA with Tukey's *post hoc* test. Only p7722 values were found statistically different from others (p-value < 0.0001).

T6SS-b and T6SS-3 Are Expressed in Plant Root Nodules

The expression of both *P. phymatum* T6SSs clusters during symbiosis in root nodules was analyzed using *P. vulgaris* and *M. pudica* as host plants. The plants were infected with the *P. phymatum* T6SS-b (p5978) and T6SS-3 (p6115 and p6116) reporter strains and the root nodules analyzed 21 or

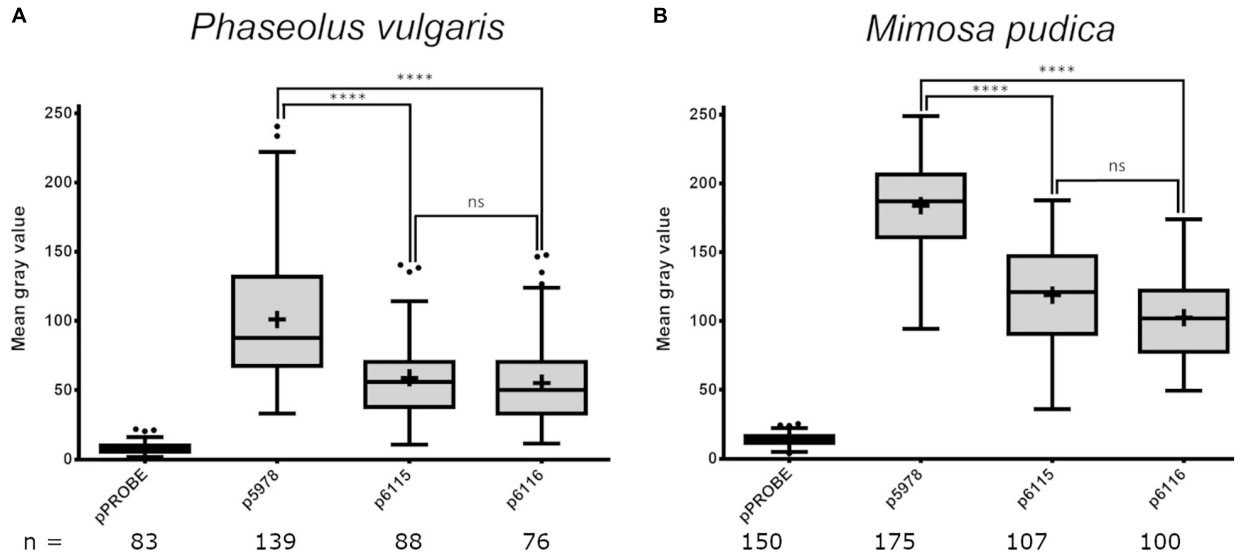

FIGURE 5 | Expression of *P. phymatum* wild-type GFP reporter constructs (pPROBE, p5978, p6115, and p6116) in nodules of *Phaseolus vulgaris* **(A)** and *Mimosa pudica* **(B)**. The pPROBE was used as negative control. Images were acquired with a confocal laser scanning microscope (DM5500Q; Leica) and single cells specific fluorescence quantified with Fiji. Plus signs indicate the arithmetic mean, whiskers minimum to maximum values and black dots outliers according to Tukey's test. Significant differences between samples were analyzed in a one-way ANOVA with Tukey's *post hoc* test (****p-value < 0.0001, ns, not significant). All T6SS reporter constructs values were found statistically different from pPROBE values.

28 dpi. The T6SS-b (p5978) was expressed at a higher level than T6SS-3 (p6115 and p6116) in *P. vulgaris* and *M. pudica* (**Figure 5**). In the papilionoid plant *P. vulgaris* (**Figure 5A** and **Supplementary Figure 3**), T6SS-b and T6SS-3 were expressed at a lower level compared to expression in *M. pudica* nodules (**Figure 5B**). Both operons of the T6SS-3 cluster (p6115 and p6116) showed a similar expression in *P. vulgaris* and *M. pudica* (**Figure 5**).

T6SS-b Is Involved in *P. phymatum* Motility

To further investigate the role of both T6SSs in *P. phymatum* STM815 during the different steps of the symbiotic interaction with the plants, we deleted the sheath genes (*tssB* and *tssC*) in each T6SS cluster (ΔTssBC-b and ΔTssBC-3) and we constructed a T6SS double mutant strain (ΔΔTssBC). The growth profile of all T6SS mutants in LB without NaCl showed a slightly faster growth of the ΔΔT6SS, while the growth of the ΔT6SS-b and ΔT6SS-3 strains was similar to the growth of the wild-type. We tested phenotypes relevant in different steps of the rhizobium-legume symbiosis such as exopolysaccharide (EPS) production, motility, root attachment, and sensitivity to H_2O_2 and antibiotics (Gage and Margolin, 2000; Downie, 2010). While the formation of EPS was not influenced by the T6SS mutant strains (data not shown), the ability to swim was significantly reduced in the ΔT6SS-b and ΔΔT6SS strains (**Figure 6**). In fact, the ΔT6SS-b and ΔΔT6SS strains showed a 29 and 21% reduced swimming diameter compared to the wild-type strain, respectively. The ability to attach to the roots was tested in a root attachment assay (Liu et al., 2020), revealing no differences between wild-type and mutants (**Supplementary Figure 4**). Moreover, the three T6SS

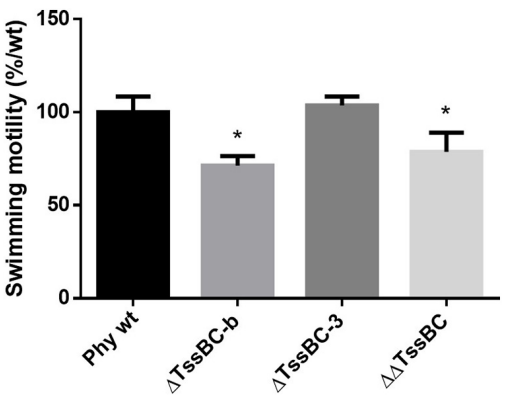

FIGURE 6 | Swimming motility of *P phymatum* wild-type, and the three deletions strains ΔT6SS-b, ΔT6SS-3, and ΔΔT6SS was tested on LB media without salt. The diameter of the halo was measured after 4 days incubation at 28°C. Three biological replicates were analyzed using a one-way ANOVA (*p-value ≤ 0.05), respectively, and bars represent the standard deviation.

mutants displayed a similar sensitivity to hydrogen peroxide (H_2O_2) and to different antibiotics (gentamycin, kanamycin, and tetracycline) compared to the wild-type (**Supplementary Table 2**) and the reporter constructs were not activated by the presence of 1 mM H_2O_2 (data not shown). Next, the symbiotic properties of ΔT6SS-b, ΔT6SS-3, and ΔΔT6SS strains (nodule numbers, nodule weight, weight per nodule, and normalized nitrogenase activity) were analyzed during symbiosis with *P. vulgaris* and *M. pudica* as host plants and compared with plants infected with *P. phymatum* wild-type (**Table 1**). While all deletion

TABLE 1 | The symbiotic properties (nodules per plant, weight per nodule, and nitrogenase activity) of *P. vulgaris* and *M. pudica* nodules infected by *P. phymatum* wild-type, ΔT6SS-b, ΔT6SS-3, and ΔΔT6SS.

Strain	Plant	Number of nodules	Nodule dry weight (mg)	Weight per nodule (mg)	Nitrogen fixation (%/g/min)
WT	*P. vulgaris*	109 ± 38	11.96 ± 3.25	0.11 ± 0.02	0.06 ± 0.04
ΔTssBC-3	*P. vulgaris*	82 ± 29	8.74 ± 2.37	0.12 ± 0.05	0.13 ± 0.06
ΔTssBC-b	*P. vulgaris*	110 ± 11	12.85 ± 1.85	0.12 ± 0.01	0.09 ± 0.04
ΔΔTssBC	*P. vulgaris*	103 ± 38	10.28 ± 3.64	0.09 ± 0.03	0.07 ± 0.06
WT	*M. pudica*	5 ± 2	0.48 ± 0.13	0.13 ± 0.08	1.34 ± 0.30
ΔTssBC-3	*M. pudica*	5 ± 2	0.45 ± 0.09	0.10 ± 0.03	1.43 ± 0.38
ΔTssBC-b	*M. pudica*	6 ± 2	0.47 ± 0.19	0.09 ± 0.02	1.25 ± 0.32
ΔΔTssBC	*M. pudica*	6 ± 1	0.53 ± 0.05	0.09 ± 0.02	1.29 ± 0.26

Two biological replicates, consisting of five plants per replicate, were used (n = 10) for each strain. Values indicate the average and the standard deviation.

mutants exhibited no significant differences in the symbiotic properties in either host plant, the ΔT6SS-3 strain showed a 27% lower nodule dry weight in *P. vulgaris* compared to wild-type nodules (**Table 1**). Further, ΔT6SS-3 infected nodules showed higher nitrogenase activity in *P. vulgaris* and *M. pudica* nodules. However, these tendencies were not statistically significant. In summary, our *in vitro* and *in planta* phenotypic analyses suggested that T6SS-b plays a role in the control of motility and that neither of the T6SSs is required for a functional symbiosis with *P. vulgaris* and *M. pudica*.

DISCUSSION

The role of T6SS during the symbiosis between rhizobia and legumes is still poorly understood. Before T6SS were officially discovered in 2006, the *impJ* gene (later known as *tssK*) of *R. leguminosarum* was shown to be required to extend the host range of this rhizobium (Roest et al., 1997; Bladergroen et al., 2003). Two secreted proteins in this T6SS cluster showed homologies to ribose binding proteins (RbsB) found in *Bacillus subtilis* and *V. cholerae*. These RbsB were shown to be responsible for the blocking of effective nodulation in pea plants (Bladergroen et al., 2003). The exact molecular mechanisms underlying *R. leguminosarum* RbsB function is still unknown. Interestingly, the secretion of these proteins has been shown to be dependent on the environmental temperature and accordingly the effect on the host was stronger when the plants were grown at 24°C compared to 20°C. We report here that the expression of both T6SS in *P. phymatum* is thermoregulated with T6SS-b being expressed at higher levels at 20/28 vs 37°C and T6SS-3 showing the opposite behavior i.e., higher expression at 37°C. While temperatures between 20 and 28°C are typical for the soil environment, temperatures around 37°C are often a signal for the bacterium to be within a mammalian infection host (Cornelis, 2006; Fang et al., 2016). In contrast to most beneficial environmental strains, *P. phymatum* is able to grow well at 37°C, demonstrating that it can adapt to different environmental niches. Until 2014, *P. phymatum* belonged to the highly versatile *Burkholderia* genus, before it was divided into two genera: *Burkholderia* and *Paraburkholderia*, containing pathogenic and non-pathogenic species, respectively (Sawana et al., 2014). This phylogenetic division was used for a first approximation of the pathogenicity of the different strains (Eberl and Vandamme, 2016). In 2016, *Caballeronia* was proposed as a third genus, containing 12 *Burkholderia* and *Paraburkholderia* species (Dobritsa and Samadpour, 2016). *Burkholderia andropogonis* was reclassified in a new fourth genus named *Robbsia* (Lopes-Santos et al., 2017) and two additional genera were recently described (*Mycetohabitans* and *Trinickia*) (Beukes et al., 2017; Estrada-de Los Santos et al., 2018; Mannaa et al., 2018). Interestingly, our study shows that the entire *P. phymatum* T6SS-b cluster also occurs in 15 other environmental strains (**Figure 1C**), 14 of which were isolated from soil samples. Some of the soil isolates containing T6SS-b are root nodulating bacteria (*Paraburkholderia* sp. UYPR1.413 isolated from *Parapiptadenia rigida* and *Paraburkholderia* sp. CCGE1002 from *Mimosa occidentalis*) or bacteria found in the root endosphere (*P. hospita* BT03 was found in *Populus deltoides*) (Gottel et al., 2011; Ormeño-Orrillo et al., 2012; Taulé et al., 2012). *P. hospita* mHSR1 is a root-associated strain, which induces a systemic resistance against the leaf pathogen *Xanthomonas campestris* in *Brassica oleracea,* and *Variovorax* PMC12 promotes growth of *Solanum lycopersicum* under abiotic stress conditions as well as induces resistance to wilt disease caused by *Ralstonia solanacearum* (Lee et al., 2018; Jeon et al., 2021). Interestingly, downstream of *P. phymatum* VgrG (Bphy_5985) within the T6SS-b cluster, where usually effectors are located, we found two genes coding for potential sodium:dicarboxylate symporters (Bphy_5990 and Bphy_5992; **Figure 1A**). These transporters are only found in bacteria and belong to the C4-dicarboxylate transporters, a subfamily of the glutamate transporter family that uses C4-dicarboxylates like succinate, fumarate, orotate, aspartate, or malate as substrate (Slotboom et al., 1999). The presence of two putative sodium:dicarboxylate symporters inside a T6SS is intriguing and has to our knowledge not been reported before. Sodium:dicarboxylate symporters are usually located in the inner membrane and may sense the presence of dicarboxylates, i.e., the main carbon source delivered by the plant to the bacteria, leading to an activation of T6SS-b during symbiosis. In *P. aeruginosa*, it has been shown that membrane proteins present in the H1-T6SS cluster are involved in trans-membrane signaling leading to T6SS post-transcriptional activation under optimal environmental conditions (Casabona

et al., 2013). To explore the possibility that C4-dicarboxylates activate the expression of *P. phymatum* T6SS-b, we fused the T6SS-b promoter to the reporter *gfp* gene and investigated its expression. Most recently, a study on the opportunistic pathogen *Klebsiella pneumoniae* serotype ST258, pointed to the C4-dicarboxylates itaconate, succinate and fumarate as being inducers of T6SS expression (Wong et al., 2020). While *P. phymatum* T6SS-b was constitutively expressed when cells were grown with the C4-dicarboxylates malate and aspartate as carbon sources, the highest expression of T6SS-b was observed in the presence of the C6 compound citrate. Citrate is known to be exudated by *P. vulgaris* roots under phosphate limited conditions or as part of the aluminum resistance mechanisms of the plant (Shen et al., 2002; Rangel et al., 2010). In case of citrate exudation in response to aluminum resistance, the position of exudation has been shown to be located at the root apices (Rangel et al., 2010). The fact that we found T6SS-b to be expressed to at the root apices (**Figure 4**), suggests that secretion of citrate from the roots induces T6SS-b expression. A role of T6SS-b during the symbiotic interaction was also suggested by our previous work, which showed that the key symbiotic sigma factor σ^{54} (RpoN) positively controls expression of T6SS-b under nitrogen limiting conditions (Lardi et al., 2020). Although we did not observe any obvious symbiotic phenotype of the T6SS-b mutant, T6SS-b was expressed at the root apices (**Figure 4**) and in *P. vulgaris* and *M. pudica* root nodules (**Figure 5**). This suggests that T6SS-b is playing a role during the early symbiotic process. Indeed, a motility test confirmed that a T6SS-b mutant was significantly affected in swimming motility, an important competitive trait for the plant infection process (**Figure 6**). The involvement of T6SS in motility was already reported in previous studies performed with *P. aeruginosa*, *V. cholera*, and *Pseudomonas fluorescens* (Decoin et al., 2015; Chen et al., 2020; Frederick et al., 2020). A BLAST analysis of the second T6SS cluster in *P. phymatum*, T6SS-3, indicated that the entire cluster is found in the primary pathogens *B. mallei* and *B. pseudomallei* (**Supplementary Figure 2**). More precisely, *P. phymatum* T6SS-3 is similar to one of the six T6SSs present in the genome of *B. pseudomallei* (T6SS-3; **Supplementary Figure 2**; Shalom et al., 2007). Although *B. pseudomallei* T6SS-5 has been shown to be a major virulence determinant in animal models (Pilatz et al., 2006; Schell et al., 2007; Schwarz et al., 2014), to our knowledge nothing is known about the function and regulation of T6SS-3. Bioinformatics analysis showed that two putative effector genes found downstream of *vgrG* in this cluster had homology with metallopeptidases that may target cell wall peptidoglycan. The fact that T6SS-3 is more prominently expressed at higher temperatures such as 37°C compared to 28 and 20°C may reflect the environmental condition where this cluster could be used to interact with other prokaryotes or with eukaryotic hosts. Interestingly, in the pathogen *Yersinia pestis* a temperature increase from 28 to 37°C has been shown to induce secretion of proteins required for a functional type III secretion system (T3SS) and for virulence (Cornelis, 2006). Analysis of the expression kinetics of T6SS-b and T6SS-3 indicated that in complex and ABS media, T6SS-b was constitutively expressed, while the T6SS-3 expression increased over time and was maximal at the end of the stationary phase (**Figure 2**). Constitutive T6SS expression was previously observed in the pathogen *V. cholerae* O37 serogroup strain V52 and suggested to contribute to its fitness in the natural environment (Unterweger et al., 2012). In contrast, regulation of T6SS in *V. cholerae* strain O1 was shown to be cell density dependent with *hcp* expression reacting to environmental factors such as high temperature (37°C) or high osmolarity (340 mM NaCl) (Liu et al., 2008; Ishikawa et al., 2009, 2012). Further stress factors such as acidity, H_2O_2 and ethanol also activated expression of T6SS in *Vibrio anguillarum* (Weber et al., 2009). In *P. aeruginosa* T6SS has been shown to react to stress induced by subinhibitory concentrations of antibiotics such as kanamycin or polymyxins (Jones et al., 2013; Vitale et al., 2020). Additionally, *P. aeruginosa* T6SS facilitates the uptake of molybdate and increases its competitiveness (Wang et al., 2021). Our results showed that the expression of *P. phymatum* T6SS was not influenced by the presence of subinhibitory and inhibitory concentrations of several tested antibiotics, at least not at the transcriptional level (data not shown). We also tested if a decrease in pH would affect T6SS expression but could not see a difference when *P. phymatum* was grown at pH 5.5 or 7, suggesting that pH and acidity do not affect T6SS expression (data not shown). Temperature and growth-phase-dependent expression of T6SSs is reminiscent of regulation of virulence factor production in bacterial pathogens, which can involve various regulatory mechanisms such as the stationary phase sigma factor RpoS, different quorum sensing systems or the secondary messenger c-di-GMP (Rossi et al., 2018). *P. phymatum*'s genome contains *rpoS* (Bphy_0962) and the *cepRI* quorum sensing system (Bphy_4439-Bphy_4437), as well as several genes involved in c-di-GMP metabolism. Additional work will be required to unravel the molecular basis of the stationary phase induction of T6SS-3.

Under our experimental settings, we did not identify a role for T6SS-3 in free-living or symbiotic growth conditions. We cannot, however, exclude that in symbiosis with other plants or other host organisms, T6SS-b or T6SS-3 are playing a role or even that the T6SS may have bearing on the exceptional promiscuity of *P. phymatum*. Finally, our study suggests that *P. phymatum* seemingly activates its T6SS copies depending on the environmental niche it is currently occupying, responding to environmental cues such as carbon sources and temperature. We showed that T6SS-b is occurring in other soil-dwelling bacteria and is activated at temperatures found in the soil and in the rhizosphere, which possibly contains citrate, another inducer of T6SS-b expression. In contrast, T6SS-3 is found mostly in pathogenic *Burkholderia* strains and is expressed at highest levels at temperatures usually found in animal hosts (37°C) and in an environment containing succinate or aspartate as a carbon source. The identification of T6SS-b and T6SS-3 effector proteins following induction of each T6SS using the corresponding external clues and analyzing the secretome with proteomics represent important follow-up studies that aim at achieving a better molecular understanding of the respective function(s) of these systems that co-occur in genomes of this versatile group of bacteria.

DATA AVAILABILITY STATEMENT

The original contributions presented in the study are included in the article/**Supplementary Material**, further inquiries can be directed to the corresponding author/s.

AUTHOR CONTRIBUTIONS

SH and GP conceived and designed the experiments and wrote the manuscript. SH, YL, and AB performed the experiments. SH, BH, AB, CA, LE, and GP analyzed the data. All authors contributed to the article and approved the submitted version.

FUNDING

This work was supported by the Swiss National Science Foundation (grant 31003A_179322 to GP).

ACKNOWLEDGMENTS

We thank Samanta Bolzan de Campos for helping in constructing reporter construct p7722, Karl Huwiler for help in the greenhouse, and Paula Bellés Sancho, Daphné Golaz, and Simona Huwiler for precious advice and help in the lab. We acknowledge the two reviewers for their insightful comments.

SUPPLEMENTARY MATERIAL

The Supplementary Material for this article can be found online at: https://www.frontiersin.org/articles/10.3389/fpls.2021.699590/full#supplementary-material

Supplementary Figure 1 | Alignment of all C4-dicarboxylate transporter found in *P. phymatum* which are similar to Bphy_5990 compared with other C4-dicarboxylate transporter from Yurgel and Kahn (2004). Glutamate transporter family proteins show eight conserved domains and four conserved motifs. Motif A is the most conserved motif and is hypothesized to correspond to the substrate-binding site.

Supplementary Figure 2 | (A) The maximum likelihood phylogenetic tree of T6SS-3 was constructed as described in methods based on the DNA sequences of the identified clusters. The reference sequence accession numbers of the NCBI database is shown in brackets and the bootstrap values are shown left of the respective branches. The bar at the bottom left indicates the distance. **(B)** Comparison of the gene arrangement of the two T6SS-3 clusters in *P. phymatum* STM815 and *B. pseudomallei* K96243. NC_006351 from the NCBI database, visualized with CLC Genomics Workbench 11.0.

Supplementary Figure 3 | Expression of *P. phymatum* wild-type GFP reporter constructs (pPROBE, p5978, p6115, and p6116) in nodules of *Phaseolus vulgaris*. The pPROBE was used as negative controls. Images were taken with a confocal laser scanning microscope (DM5500Q; Leica). LUT Fire was used to color-code the expression.

Supplementary Figure 4 | Root attachment assay with wild-type and T6SS mutants. No significant difference in the root attachment ability was observed between the strains. Three independent experiments were performed with nine biological replicates per strain ($n = 9$). A one way-ANOVA showed no significant difference between the strains. Error bars indicate the standard deviation.

REFERENCES

Alcoforado Diniz, J., Liu, Y.-C., and Coulthurst, S. J. (2015). Molecular weaponry: diverse effectors delivered by the type VI secretion system. *Cell. Microbiol.* 17, 1742–1751. doi: 10.1111/cmi.12532

Barret, M., Egan, F., and O'Gara, F. (2013). Distribution and diversity of bacterial secretion systems across metagenomic datasets. *Environ. Microbiol. Rep.* 5, 117–126. doi: 10.1111/j.1758-2229.2012.00394.x

Beukes, C. W., Palmer, M., Manyaka, P., Chan, W. Y., Avontuur, J. R., van Zyl, E., et al. (2017). Genome data provides high support for generic boundaries in *Burkholderia* Sensu Lato. *Front. Microbiol.* 8:1154. doi: 10.3389/fmicb.2017.01154

Bhagwat, A. A., Tully, R. E., and Keister, D. L. (1991). Isolation and characterization of a competition-defective *Bradyrhizobium japonicum* mutant. *Appl. Environ. Microbiol.* 57, 3496–3501. doi: 10.1128/aem.57.12.3496-3501.1991

Bladergroen, M. R., Badelt, K., and Spaink, H. P. (2003). Infection-blocking genes of a symbiotic *Rhizobium leguminosarum* strain that are involved in temperature-dependent protein secretion. *Mol. Plant. Microbe. Interact.* 16, 53–64. doi: 10.1094/MPMI.2003.16.1.53

Bontemps, C., Elliott, G. N., Simon, M. F., Dos Reis Júnior, F. B., Gross, E., Lawton, R. C., et al. (2010). *Burkholderia* species are ancient symbionts of legumes. *Mol. Ecol.* 19, 44–52. doi: 10.1111/j.1365-294X.2009.04458.x

Boyer, F., Fichant, G., Berthod, J., Vandenbrouck, Y., and Attree, I. (2009). Dissecting the bacterial type VI secretion system by a genome wide *in silico* analysis: what can be learned from available microbial genomic resources? *BMC Genom.* 10:104. doi: 10.1186/1471-2164.10-104

Camacho, C., Coulouris, G., Avagyan, V., Ma, N., Papadopoulos, J., Bealer, K., et al. (2009). BLAST+: architecture and applications. *BMC Bioinform.* 10:421. doi: 10.1186/1471-2105-10-421

Casabona, M. G., Silverman, J. M., Sall, K. M., Boyer, F., Couté, Y., Poirel, J., et al. (2013). An ABC transporter and an outer membrane lipoprotein participate in posttranslational activation of type VI secretion in *Pseudomonas aeruginosa*. *Environ. Microbiol.* 15, 471–486. doi: 10.1111/j.1462-2920.2012.02816.x

Chen, L., Zou, Y., Kronfl, A. A., and Wu, Y. (2020). Type VI secretion system of Pseudomonas aeruginosa is associated with biofilm formation but not environmental adaptation. *MicrobiologyOpen* 9:e991. doi: 10.1002/mbo3.991

Chen, W. M., Laevens, S., Lee, T. M., Coenye, T., deVos, P., Mergeay, M., et al. (2001). *Ralstonia taiwanensis* sp. nov., isolated from root nodules of *Mimosa* species and sputum of a cystic fibrosis patient. *Int. J. Syst. Evol. Microbiol.* 51, 1729–1735. doi: 10.1099/00207713-51-5-1729

Cianfanelli, F. R., Monlezun, L., and Coulthurst, S. J. (2016). Aim, load, fire: The type VI secretion system, a bacterial nanoweapon. *Trends Microbiol.* 24, 51–62. doi: 10.1016/j.tim.2015.10.005

Clark, D. J., and Maaløe, O. (1967). DNA replication and the division cycle in *Escherichia coli*. *J. Mol. Biol.* 23, 99–112. doi: 10.1016/S0022-2836(67)80070-6

Clarke, V. C., Loughlin, P. C., Day, D. A., and Smith, P. M. C. (2014). Transport processes of the legume symbiosome membrane. *Front. Plant. Sci.* 5:699. doi: 10.3389/fpls.2014.00699

Cooper, J. E. (2007). Early interactions between legumes and rhizobia: disclosing complexity in a molecular dialogue. *J. Appl. Microbiol.* 103, 1355–1365. doi: 10.1111/j.1365-2672.2007.03366.x

Cornelis, G. R. (2006). The type III secretion injectisome. *Nat. Rev. Microbiol.* 4, 811–825. doi: 10.1038/nrmicro1526

de Campos, S. B., Lardi, M., Gandolfi, A., Eberl, L., and Pessi, G. (2017). Mutations in two *Paraburkholderia phymatum* type VI secretion systems cause reduced fitness in interbacterial competition. *Front. Microbiol.* 8:2473. doi: 10.3389/fmicb.2017.02473

Decoin, V., Gallique, M., Barbey, C., Le Mauff, F., Poc, C. D., Feuilloley, M. G. J., et al. (2015). A *Pseudomonas* fluorescens type 6 secretion system is related to mucoidy, motility and bacterial competition. *BMC Microbiol.* 15:72. doi: 10.1186/s12866-015-0405-9

Ding, H., Yip, C. B., Geddes, B. A., Oresnik, I. J., and Hynes, M. F. (2012). Glycerol utilization by *Rhizobium leguminosarum* requires an ABC transporter and affects competition for nodulation. *Microbiology* 158, 1369–1378. doi: 10.1099/mic.0.057281-0

Dixon, R., and Kahn, D. (2004). Genetic regulation of biological nitrogen fixation. *Nat. Rev. Microbiol.* 2, 621–631. doi: 10.1038/nrmicro954

Dobritsa, A. P., and Samadpour, M. (2016). Transfer of eleven species of the genus *Burkholderia* to the genus *Paraburkholderia* and proposal of *Caballeronia* gen. nov. to accommodate twelve species of the genera *Burkholderia* and *Paraburkholderia*. *Int. J. Syst. Evol. Microbiol.* 66, 2836–2846. doi: 10.1099/ijsem.0.001065

Dong, T. G., Ho, B. T., Yoder-Himes, D. R., and Mekalanos, J. J. (2013). Identification of T6SS-dependent effector and immunity proteins by Tn-seq in *Vibrio cholerae*. *Proc. Natl. Acad. Sci. U.S.A.* 110, 2623–2628. doi: 10.1073/pnas.1222783110

dos Reis, F. B., Simon, M. F., Gross, E., Boddey, R. M., Elliott, G. N., Neto, N. E., et al. (2010). Nodulation and nitrogen fixation by *Mimosa* spp. in the Cerrado and Caatinga biomes of Brazil. *New Phytol.* 186, 934–946. doi: 10.1111/j.1469-8137.2010.03267.x

Downie, J. A. (2010). The roles of extracellular proteins, polysaccharides and signals in the interactions of rhizobia with legume roots. *FEMS Microbiol. Rev.* 34, 150–170. doi: 10.1111/j.1574-6976.2009.00205.x

Durand, E., Cambillau, C., Cascales, E., and Journet, L. (2014). VgrG, Tae, Tle, and beyond: the versatile arsenal of Type VI secretion effectors. *Trends Microbiol.* 22, 498–507. doi: 10.1016/j.tim.2014.06.004

Eberl, L., and Vandamme, P. (2016). Members of the genus *Burkholderia*: good and bad guys. *F1000Res* 5:F1000. doi: 10.12688/f1000research.8221.1

Elliott, G. N., Chen, W.-M., Chou, J.-H., Wang, H.-C., Sheu, S.-Y., Perin, L., et al. (2007). *Burkholderia phymatum* is a highly effective nitrogen-fixing symbiont of *Mimosa* spp. and fixes nitrogen *ex planta*. *New Phytol.* 173, 168–180. doi: 10.1111/j.1469-8137.2006.01894.x

Elliott, G. N., Chou, J.-H., Chen, W.-M., Bloemberg, G. V., Bontemps, C., Martínez-Romero, E., et al. (2009). *Burkholderia* spp. are the most competitive symbionts of *Mimosa*, particularly under N-limited conditions. *Environ. Microbiol.* 11, 762–778. doi: 10.1111/j.1462-2920.2008.01799.x

Estrada-de Los Santos, P., Palmer, M., Chávez-Ramírez, B., Beukes, C., Steenkamp, E. T., Briscoe, L., et al. (2018). Whole genome analyses suggests that *Burkholderia* sensu lato contains two additional novel genera (*Mycetohabitans* gen. nov., and *Trinickia* gen. nov.): implications for the evolution of diazotrophy and nodulation in the *Burkholderiaceae*. *Genes (Basel)* 9:389. doi: 10.3390/genes9080389

Fang, F. C., Frawley, E. R., Tapscott, T., and Vázquez-Torres, A. (2016). Bacterial stress responses during host infection. *Cell. Host. Microbe.* 20, 133–143. doi: 10.1016/j.chom.2016.07.009

Fields, S. (2004). Global nitrogen: cycling out of control. *Environ. Health Perspect.* 112, A556–A563. doi: 10.1289/ehp.112-a556

Finan, T. M., Wood, J. M., and Jordan, D. C. (1983). Symbiotic properties of C4-dicarboxylic acid transport mutants of *Rhizobium leguminosarum*. *J. Bacteriol.* 154, 1403–1413. doi: 10.1128/jb.154.3.1403-1413.1983

Frederick, A., Huang, Y., Pu, M., and Rowe-Magnus, D. A. (2020). *Vibrio cholerae* type VI activity alters motility behavior in mucin. *J. Bacteriol.* 202:e00261–20. doi: 10.1128/JB.00261-20

Gage, D. J., and Margolin, W. (2000). Hanging by a thread: invasion of legume plants by rhizobia. *Curr. Opin. Microbiol.* 3, 613–617. doi: 10.1016/S1369-5274(00)00149-1

Garau, G., Yates, R. J., Deiana, P., and Howieson, J. G. (2009). Novel strains of nodulating *Burkholderia* have a role in nitrogen fixation with papilionoid herbaceous legumes adapted to acid, infertile soils. *Soil Biol. Biochem.* 41, 125–134. doi: 10.1016/j.soilbio.2008.10.011

Geddes, B. A., González, J. E., and Oresnik, I. J. (2014). Exopolysaccharide production in response to medium acidification is correlated with an increase in competition for nodule occupancy. *Mol. Plant. Microbe. Interact.* 27, 1307–1317. doi: 10.1094/MPMI-06-14-0168-R

Gottel, N. R., Castro, H. F., Kerley, M., Yang, Z., Pelletier, D. A., Podar, M., et al. (2011). Distinct microbial communities within the endosphere and rhizosphere of *Populus deltoides* roots across contrasting soil types. *Appl. Environ. Microbiol.* 77, 5934–5944. doi: 10.1128/AEM.05255-11

Göttfert, M., Hitz, S., and Hennecke, H. (1990). Identification of *nodS* and *nodU*, two inducible genes inserted between the *Bradyrhizobium japonicum nodYABC* and *nodIJ* genes. *Mol. Plant. Microbe. Interact.* 3, 308–316. doi: 10.1094/mpmi-3-308

Gyaneshwar, P., Hirsch, A. M., Moulin, L., Chen, W.-M., Elliott, G. N., Bontemps, C., et al. (2011). Legume-nodulating Betaproteobacteria: diversity, host range, and future prospects. *Mol. Plant. Microbe. Interact.* 24, 1276–1288. doi: 10.1094/MPMI-06-11-0172

Hahn, M., and Hennecke, H. (1984). Localized mutagenesis in *Rhizobium japonicum*. *Molec. Gen. Genet.* 193, 46–52. doi: 10.1007/BF00327412

Halbleib, C. M., and Ludden, P. W. (2000). Regulation of biological nitrogen fixation. *J. Nutr.* 130, 1081–1084. doi: 10.1093/jn/130.5.1081

Ibáñez, F., Wall, L., and Fabra, A. (2017). Starting points in plant-bacteria nitrogen-fixing symbioses: intercellular invasion of the roots. *J. Exp. Bot.* 68, 1905–1918. doi: 10.1093/jxb/erw387

Ishikawa, T., Rompikuntal, P. K., Lindmark, B., Milton, D. L., and Wai, S. N. (2009). Quorum sensing regulation of the two *hcp* alleles in *Vibrio cholerae* O1 strains. *PLoS One* 4:e6734. doi: 10.1371/journal.pone.0006734

Ishikawa, T., Sabharwal, D., Bröms, J., Milton, D. L., Sjöstedt, A., Uhlin, B. E., et al. (2012). Pathoadaptive conditional regulation of the type VI secretion system in *Vibrio cholerae* O1 strains. *Infect. Immun.* 80, 575–584. doi: 10.1128/IAI.05510-11

Janausch, I., Zientz, E., Tran, Q., Kröger, A., and Unden, G. (2002). C4-dicarboxylate carriers and sensors in bacteria. *Biochim. Biophys. Acta* 1553, 39–56. doi: 10.1016/s0005-2728(01)00233-x

Jeon, J.-S., Carreno-Quintero, N., van Eekelen, H. D. L. M., de Vos, R. C. H., Raaijmakers, J. M., and Etalo, D. W. (2021). Impact of root-associated strains of three *Paraburkholderia* species on primary and secondary metabolism of *Brassica oleracea*. *Sci. Rep.* 11:2781. doi: 10.1038/s41598-021-82238-9

Jones, C., Allsopp, L., Horlick, J., Kulasekara, H., and Filloux, A. (2013). Subinhibitory concentration of kanamycin induces the *Pseudomonas aeruginosa* type VI secretion system. *PLoS One* 8:e81132. doi: 10.1371/journal.pone.0081132

Kapitein, N., and Mogk, A. (2014). Type VI secretion system helps find a niche. *Cell. Host. Microbe.* 16, 5–6. doi: 10.1016/j.chom.2014.06.012

Klonowska, A., Melkonian, R., Miché, L., Tisseyre, P., and Moulin, L. (2018). Transcriptomic profiling of *Burkholderia phymatum* STM815, *Cupriavidus taiwanensis* LMG19424 and *Rhizobium mesoamericanum* STM3625 in response to *Mimosa pudica* root exudates illuminates the molecular basis of their nodulation competitiveness and symbiotic evolutionary history. *BMC Genom.* 19:105. doi: 10.1186/s12864-018-4487-2

Kohler, P. R. A., Zheng, J. Y., Schoffers, E., and Rossbach, S. (2010). Inositol catabolism, a key pathway in *Sinorhizobium meliloti* for competitive host nodulation. *Appl. Environ. Microbiol.* 76, 7972–7980. doi: 10.1128/Aem.01972-10

Kumar, S., Stecher, G., Li, M., Knyaz, C., and Tamura, K. (2018). MEGA X: molecular evolutionary genetics analysis across computing platforms. *Mol. Biol. Evol.* 35, 1547–1549. doi: 10.1093/molbev/msy096

Lardi, M., de Campos, S. B., Purtschert, G., Eberl, L., and Pessi, G. (2017). Competition experiments for legume infection identify *Burkholderia phymatum* as a highly competitive β-rhizobium. *Front. Microbiol.* 8:1527. doi: 10.3389/fmicb.2017.01527

Lardi, M., Liu, Y., Giudice, G., Ahrens, C. H., Zamboni, N., and Pessi, G. (2018). Metabolomics and transcriptomics identify multiple downstream targets of *Paraburkholderia phymatum* σ^{54} during symbiosis with *Phaseolus vulgaris*. *Int. J. Mol. Sci.* 19:1049. doi: 10.3390/ijms19041049

Lardi, M., Liu, Y., Hug, S., Bolzan de Campos, S., Eberl, L., and Pessi, G. (2020). *Paraburkholderia phymatum* STM815 σ^{54} controls utilization of dicarboxylates, motility, and T6SS-b expression. *Nitrogen* 1, 81–98. doi: 10.3390/nitrogen1020008

Larkin, M. A., Blackshields, G., Brown, N. P., Chenna, R., McGettigan, P. A., McWilliam, H., et al. (2007). Clustal W and Clustal X version 2.0. *Bioinformatics* 23, 2947–2948. doi: 10.1093/bioinformatics/btm404

Ledermann, R., Schulte, C. C. M., and Poole, P. S. (2021). How Rhizobia adapt to the nodule environment. *J. Bacteriol.* doi: 10.1128/JB.00539-20

Lee, S. A., Kim, H. S., Kim, Y., Sang, M. K., Song, J., and Weon, H.-Y. (2018). Complete genome sequence of *Variovorax* sp. PMC12, a plant growth-promoting bacterium conferring multiple stress resistance in plant. *Korean J. Microbiol.* 54, 471–473. doi: 10.7845/kjm.2018.8075

Lemaire, B., Chimphango, S. B. M., Stirton, C., Rafudeen, S., Honnay, O., Smets, E., et al. (2016). Biogeographical patterns of legume-nodulating *Burkholderia*

spp. from African Fynbos to continental scales. *Appl. Environ. Microbiol.* 82, 5099–5115. doi: 10.1128/AEM.00591-16

Li, J., Yao, Y., Xu, H. H., Hao, L., Deng, Z., Rajakumar, K., et al. (2015). SecReT6: a web-based resource for type VI secretion systems found in bacteria. *Environ. Microbiol.* 17, 2196–2202. doi: 10.1111/1462-2920.12794

Lindström, K., and Mousavi, S. A. (2020). Effectiveness of nitrogen fixation in rhizobia. *Microb. Biotechnol.* 13, 1314–1335. doi: 10.1111/1751-7915.13517

Liu, H., Coulthurst, S. J., Pritchard, L., Hedley, P. E., Ravensdale, M., Humphris, S., et al. (2008). Quorum sensing coordinates brute force and stealth modes of infection in the plant pathogen *Pectobacterium atrosepticum*. *PLoS Pathog.* 4:e1000093. doi: 10.1371/journal.ppat.1000093

Liu, Y., Bellich, B., Hug, S., Eberl, L., Cescutti, P., and Pessi, G. (2020). The exopolysaccharide cepacian plays a role in the establishment of the *Paraburkholderia phymatum – Phaseolus vulgaris* symbiosis. *Front. Microbiol.* 11:1600. doi: 10.3389/fmicb.2020.01600

Lopes-Santos, L., Castro, D. B. A., Ferreira-Tonin, M., Corrêa, D. B. A., Weir, B. S., Park, D., et al. (2017). Reassessment of the taxonomic position of *Burkholderia andropogonis* and description of *Robbsia andropogonis* gen. nov., comb. nov. *Antonie Van Leeuwenhoek* 110, 727–736. doi: 10.1007/s10482-017-0842-6

Ma, L.-S., Hachani, A., Lin, J.-S., Filloux, A., and Lai, E.-M. (2014). *Agrobacterium tumefaciens* deploys a superfamily of type VI secretion DNase effectors as weapons for interbacterial competition *in planta*. *Cell. Host. Microbe.* 16, 94–104. doi: 10.1016/j.chom.2014.06.002

Mannaa, M., Park, I., and Seo, Y.-S. (2018). Genomic features and insights into the taxonomy, virulence, and benevolence of plant-associated *Burkholderia* species. *Int. J. Mol. Sci.* 20:121. doi: 10.3390/ijms20010121

Masson-Boivin, C., Giraud, E., Perret, X., and Batut, J. (2009). Establishing nitrogen-fixing symbiosis with legumes: how many rhizobium recipes? *Trends Microbiol.* 17, 458–466. doi: 10.1016/j.tim.2009.07.004

Melkonian, R., Moulin, L., Béna, G., Tisseyre, P., Chaintreuil, C., Heulin, K., et al. (2014). The geographical patterns of symbiont diversity in the invasive legume *Mimosa pudica* can be explained by the competitiveness of its symbionts and by the host genotype. *Environ. Microbiol.* 16, 2099–2111. doi: 10.1111/1462-2920.12286

Mellor, H. Y., Glenn, A. R., Arwas, R., and Dilworth, M. J. (1987). Symbiotic and competitive properties of motility mutants of *Rhizobium trifolii* TA1. *Arch. Microbiol.* 148, 34–39. doi: 10.1007/BF00429644

Miller, J. H. (1972). *Experiments in molecular genetics*. New York: Cold Spring Harbor.

Miller, W. G., Leveau, J. H. J., and Lindow, S. E. (2000). Improved *gfp* and *inaZ* broad-host-range promoter-probe vectors. *Mol. Plant. Microbe. Interact.* 13, 1243–1250. doi: 10.1094/MPMI.2000.13.11.1243

Mishra, R. P. N., Tisseyre, P., Melkonian, R., Chaintreuil, C., Miché, L., Klonowska, A., et al. (2012). Genetic diversity of *Mimosa pudica* rhizobial symbionts in soils of French Guiana: investigating the origin and diversity of *Burkholderia phymatum* and other beta-rhizobia. *FEMS Microbiol. Ecol.* 79, 487–503. doi: 10.1111/j.1574-6941.2011.01235.x

Mougous, J. D., Cuff, M. E., Raunser, S., Shen, A., Zhou, M., Gifford, C. A., et al. (2006). A virulence locus of *Pseudomonas aeruginosa* encodes a protein secretion apparatus. *Science* 312, 1526–1530. doi: 10.1126/science.1128393

Moulin, L., Klonowska, A., Caroline, B., Booth, K., Vriezen, J. A. C., Melkonian, R., et al. (2014). Complete genome sequence of *Burkholderia phymatum* STM815(T), a broad host range and efficient nitrogen-fixing symbiont of *Mimosa* species. *Stand. Genom. Sci.* 9, 763–774. doi: 10.4056/sigs.4861021

Moulin, L., Munive, A., Dreyfus, B., and Boivin-Masson, C. (2001). Nodulation of legumes by members of the beta-subclass of *Proteobacteria*. *Nature* 411, 948–950. doi: 10.1038/35082070

Oldroyd, G. E. D., Murray, J. D., Poole, P. S., and Downie, J. A. (2011). The rules of engagement in the legume-rhizobial symbiosis. *Annu. Rev. Genet.* 45, 119–144. doi: 10.1146/annurev-genet-110410-132549

Ormeño-Orrillo, E., Rogel, M. A., Chueire, L. M. O., Tiedje, J. M., Martínez-Romero, E., and Hungria, M. (2012). Genome sequences of *Burkholderia* sp. strains CCGE1002 and H160, isolated from legume nodules in Mexico and Brazil. *J. Bacteriol.* 194:6927. doi: 10.1128/JB.01756-12

Pilatz, S., Breitbach, K., Hein, N., Fehlhaber, B., Schulze, J., Brenneke, B., et al. (2006). Identification of *Burkholderia pseudomallei* genes required for the intracellular life cycle and *in vivo* virulence. *Infect. Immun.* 74, 3576–3586. doi: 10.1128/IAI.01262-05

Pukatzki, S., Ma, A. T., Sturtevant, D., Krastins, B., Sarracino, D., Nelson, W. C., et al. (2006). Identification of a conserved bacterial protein secretion system in *Vibrio cholerae* using the *Dictyostelium* host model system. *Proc. Natl. Acad. Sci. U.S.A.* 103, 1528–1533. doi: 10.1073/pnas.0510322103

Rangel, A. F., Rao, I. M., Braun, H.-P., and Horst, W. J. (2010). Aluminum resistance in common bean *(Phaseolus vulgaris)* involves induction and maintenance of citrate exudation from root apices. *Physiol. Plant* 138, 176–190. doi: 10.1111/j.1399-3054.2009.01303.x

Robleto, E. A., Kmiecik, K., Oplinger, E. S., Nienhuis, J., and Triplett, E. W. (1998). Trifolitoxin production increases nodulation competitiveness of *Rhizobium etli* CE3 under agricultural conditions. *Appl. Environ. Microbiol.* 64, 2630–2633. doi: 10.1128/aem.64.7.2630-2633.1998

Roest, H. P., Mulders, I. H., Spaink, H. P., Wijffelman, C. A., and Lugtenberg, B. J. (1997). A *Rhizobium leguminosarum* biovar *trifolii* locus not localized on the sym plasmid hinders effective nodulation on plants of the pea cross-inoculation group. *Mol. Plant. Microbe. Interact.* 10, 938–941. doi: 10.1094/MPMI.1997.10.7.938

Ronson, C. W., Lyttleton, P., and Robertson, J. G. (1981). C(4)-dicarboxylate transport mutants of *Rhizobium trifolii* form ineffective nodules on *Trifolium repens*. *Proc. Natl. Acad. Sci. U.S.A.* 78, 4284–4288. doi: 10.1073/pnas.78.7.4284

Rossi, E., Paroni, M., and Landini, P. (2018). Biofilm and motility in response to environmental and host-related signals in Gram negative opportunistic pathogens. *J. Appl. Microbiol.* doi: 10.1111/jam.14089

Salinero-Lanzarote, A., Pacheco-Moreno, A., Domingo-Serrano, L., Durán, D., Ormeño-Orrillo, E., Martínez-Romero, E., et al. (2019). The type VI secretion system of *Rhizobium etli* Mim1 has a positive effect in symbiosis. *FEMS Microbiol. Ecol.* 95:fiz054. doi: 10.1093/femsec/fiz054

Salomon, D., Kinch, L. N., Trudgian, D. C., Guo, X., Klimko, J. A., Grishin, N. V., et al. (2014). Marker for type VI secretion system effectors. *Proc. Natl. Acad. Sci. U.S.A.* 111, 9271–9276. doi: 10.1073/pnas.1406110111

Santos, M. N. M., Cho, S.-T., Wu, C.-F., Chang, C.-J., Kuo, C.-H., and Lai, E.-M. (2019). Redundancy and specificity of type VI secretion *vgrG* loci in antibacterial activity of *Agrobacterium tumefaciens* 1D1609 strain. *Front. Microbiol.* 10:3004. doi: 10.3389/fmicb.2019.03004

Sawana, A., Adeolu, M., and Gupta, R. S. (2014). Molecular signatures and phylogenomic analysis of the genus *Burkholderia*: proposal for division of this genus into the emended genus *Burkholderia* containing pathogenic organisms and a new genus *Paraburkholderia* gen. nov. harboring environmental species. *Front. Genet.* 5:429. doi: 10.3389/fgene.2014.00429

Schell, M. A., Ulrich, R. L., Ribot, W. J., Brueggemann, E. E., Hines, H. B., Chen, D., et al. (2007). Type VI secretion is a major virulence determinant in *Burkholderia mallei*. *Mol. Microbiol.* 64, 1466–1485. doi: 10.1111/j.1365-2958.2007.05734.x

Schindelin, J., Arganda-Carreras, I., Frise, E., Kaynig, V., Longair, M., Pietzsch, T., et al. (2012). Fiji: an open-source platform for biological-image analysis. *Nat. Methods* 9, 676–682. doi: 10.1038/nmeth.2019

Schwarz, S., Singh, P., Robertson, J. D., LeRoux, M., Skerrett, S. J., Goodlett, D. R., et al. (2014). VgrG-5 is a *Burkholderia* type VI secretion system-exported protein required for multinucleated giant cell formation and virulence. *Infect. Immun.* 82, 1445–1452. doi: 10.1128/IAI.01368-13

Shalom, G., Shaw, J. G., and Thomas, M. S. (2007). In vivo expression technology identifies a type VI secretion system locus in *Burkholderia pseudomallei* that is induced upon invasion of macrophages. *Microbiology* 153, 2689–2699. doi: 10.1099/mic.0.2007/006585-0

Shastri, S., Spiewak, H. L., Sofoluwe, A., Eidsvaag, V. A., Asghar, A. H., Pereira, T., et al. (2017). An efficient system for the generation of marked genetic mutants in members of the genus *Burkholderia*. *Plasmid* 89, 49–56. doi: 10.1016/j.plasmid.2016.11.002

Shen, H., Yan, X., Zhao, M., Zheng, S., and Wang, X. (2002). Exudation of organic acids in common bean as related to mobilization of aluminum- and iron-bound phosphates. *Environ. Exper. Bot.* 48, 1–9. doi: 10.1016/S0098-8472(02)00009-6

Shneider, M. M., Buth, S. A., Ho, B. T., Basler, M., Mekalanos, J. J., and Leiman, P. G. (2013). PAAR-repeat proteins sharpen and diversify the type VI secretion system spike. *Nature* 500, 350–353. doi: 10.1038/nature12453

Slotboom, D. J., Konings, W. N., and Lolkema, J. S. (1999). Structural features of the glutamate transporter family. *Microbiol. Mol. Biol. Rev.* 63, 293–307. doi: 10.1128/mmbr.63.2.293-307.1999

Talbi, C., Delgado, M. J., Girard, L., Ramírez-Trujillo, A., Caballero-Mellado, J., and Bedmar, E. J. (2010). *Burkholderia phymatum* strains capable of nodulating *Phaseolus vulgaris* are present in Moroccan soils. *Appl. Environ. Microbiol.* 76, 4587–4591. doi: 10.1128/AEM.02886-09

Tamura, K., and Nei, M. (1993). Estimation of the number of nucleotide substitutions in the control region of mitochondrial DNA in humans and chimpanzees. *Mol. Biol. Evol.* 10, 512–526. doi: 10.1093/oxfordjournals.molbev.a040023

Taulé, C., Zabaleta, M., Mareque, C., Platero, R., Sanjurjo, L., Sicardi, M., et al. (2012). New betaproteobacterial *Rhizobium* strains able to efficiently nodulate *Parapiptadenia rigida* (Benth.) Brenan. *Appl. Environ. Microbiol.* 78, 1692–1700. doi: 10.1128/aem.06215-11

Udvardi, M., and Poole, P. S. (2013). Transport and metabolism in legume-rhizobia symbioses. *Annu. Rev. Plant Biol.* 64, 781–805. doi: 10.1146/annurev-arplant-050312-120235

Unterweger, D., Kitaoka, M., Miyata, S. T., Bachmann, V., Brooks, T. M., Moloney, J., et al. (2012). Constitutive type VI secretion system expression gives *Vibrio cholerae* intra- and interspecific competitive advantages. *PLoS One* 7:e48320. doi: 10.1371/journal.pone.0048320

Vance, C. P., and Graham, P. H. (1995). "Nitrogen Fixation in Agriculture: Application and Perspectives," in *Nitrogen Fixation: Fundamentals and Applications: Proceedings of the 10th International Congress on Nitrogen Fixation, St. Petersburg, Russia, May 28–June 3, 1995*, eds I. A. Tikhonovich, N. A. Provorov, V. I. Romanov, and W. E. Newton (Dordrecht: Springer), 77–86. doi: 10.1007/978-94-011-0379-4_10

Vitale, A., Pessi, G., Urfer, M., Locher, H. H., Zerbe, K., Obrecht, D., et al. (2020). Identification of genes required for resistance to peptidomimetic antibiotics by transposon sequencing. *Front. Microbiol.* 11:1681. doi: 10.3389/fmicb.2020.01681

Wang, T., Du, X., Ji, L., Han, Y., Dang, J., Wen, J., et al. (2021). *Pseudomonas aeruginosa* T6SS-mediated molybdate transport contributes to bacterial competition during anaerobiosis. *Cell. Rep.* 35:108957. doi: 10.1016/j.celrep.2021.108957

Weber, B., Hasic, M., Chen, C., Wai, S. N., and Milton, D. L. (2009). Type VI secretion modulates quorum sensing and stress response in *Vibrio anguillarum*. *Environ. Microbiol.* 11, 3018–3028. doi: 10.1111/j.1462-2920.2009.02005.x

Wheatley, R. M., Ford, B. L., Li, L., Aroney, S. T. N., Knights, H. E., Ledermann, R., et al. (2020). Lifestyle adaptations of *Rhizobium* from rhizosphere to symbiosis. *Proc. Natl. Acad. Sci. U.S.A.* 117, 23823–23834. doi: 10.1073/pnas.2009094117

Wong, T., Shi, W., Urso, A., Annavajhala, M., Uhlemann, A.-C., and Prince, A. S. (2020). Carbapenemase-producing *Klebsiella pneumoniae* ST258 activates the T6SS in response to the host metabolite itaconate to promote bacterial adaptation to the lung," in D102. BACTERIAL INFECTIONS: IMMUNITY AND BASIC MECHANISMS. Philadelphia, PA: American Thoracic Society, A7735–A7735.

Yang, X., Long, M., and Shen, X. (2018). Effector Immunity pairs provide the T6SS nanomachine its offensive and defensive capabilities. *Molecules* 23:1009. doi: 10.3390/molecules23051009

Yurgel, S. N., and Kahn, M. L. (2004). Dicarboxylate transport by rhizobia. *FEMS Microbiol. Rev.* 28, 489–501. doi: 10.1016/j.femsre.2004.04.002

Zdor, R. E., and Pueppke, S. G. (1991). Nodulation competitiveness of Tn*5*-induced mutants of *Rhizobium fredii* USDA208 that are altered in motility and extracellular polysaccharide production. *Can. J. Microbiol.* 37, 52–58. doi: 10.1139/m91-008

Zoued, A., Brunet, Y. R., Durand, E., Aschtgen, M.-S., Logger, L., Douzi, B., et al. (2014). Architecture and assembly of the type VI secretion system. *Biochim. Biophys. Acta* 1843, 1664–1673. doi: 10.1016/j.bbamcr.2014.03.018

Conflict of Interest: The authors declare that the research was conducted in the absence of any commercial or financial relationships that could be construed as a potential conflict of interest.

Publisher's Note: All claims expressed in this article are solely those of the authors and do not necessarily represent those of their affiliated organizations, or those of the publisher, the editors and the reviewers. Any product that may be evaluated in this article, or claim that may be made by its manufacturer, is not guaranteed or endorsed by the publisher.

frontiers in Plant Science

REVIEW
published: 27 August 2021
doi: 10.3389/fpls.2021.725338

Rhizobial Chemotaxis and Motility Systems at Work in the Soil

*Samuel T. N. Aroney, Philip S. Poole and Carmen Sánchez-Cañizares**

Department of Plant Sciences, University of Oxford, Oxford, United Kingdom

Bacteria navigate their way often as individual cells through their chemical and biological environment in aqueous medium or across solid surfaces. They swim when starved or in response to physical and chemical stimuli. Flagella-driven chemotaxis in bacteria has emerged as a paradigm for both signal transduction and cellular decision-making. By altering motility, bacteria swim toward nutrient-rich environments, movement modulated by their chemotaxis systems with the addition of pili for surface movement. The numbers and types of chemoreceptors reflect the bacterial niche and lifestyle, with those adapted to complex environments having diverse metabolic capabilities, encoding far more chemoreceptors in their genomes. The Alpha-proteobacteria typify the latter case, with soil bacteria such as rhizobia, endosymbionts of legume plants, where motility and chemotaxis are essential for competitive symbiosis initiation, among other processes. This review describes the current knowledge of motility and chemotaxis in six model soil bacteria: *Sinorhizobium meliloti*, *Agrobacterium fabacearum*, *Rhizobium leguminosarum*, *Azorhizobium caulinodans*, *Azospirillum brasilense*, and *Bradyrhizobium diazoefficiens*. Although motility and chemotaxis systems have a conserved core, rhizobia possess several modifications that optimize their movements in soil and root surface environments. The soil provides a unique challenge for microbial mobility, since water pathways through particles are not always continuous, especially in drier conditions. The effectiveness of symbiont inoculants in a field context relies on their mobility and dispersal through the soil, often assisted by water percolation or macroorganism movement or networks. Thus, this review summarizes the factors that make it essential to consider and test rhizobial motility and chemotaxis for any potential inoculant.

Keywords: rhizobia, *Rhizobium leguminosarum*, *Sinorhizobium meliloti*, *Azospirillum brasilense*, *Bradyrhizobium diazoefficiens*, motility, chemotaxis, soil

OPEN ACCESS

Edited by:
Maria Jose Soto, Estación Experimental de Zaidín, Consejo Superior de Investigaciones Científicas (CSIC), Spain

Reviewed by:
Anibal Roberto Lodeiro, CONICET Instituto de Biotecnologia y Biologia Molecular (IBBM), Argentina
Ivan John Oresnik, University of Manitoba, Canada

****Correspondence:***
Carmen Sánchez-Cañizares
carmen.sanchez-canizares@plants.ox.ac.uk

Specialty section:
This article was submitted to Plant Symbiotic Interactions, a section of the journal Frontiers in Plant Science

Received: *15 June 2021*
Accepted: *06 August 2021*
Published: *27 August 2021*

Citation:
Aroney STN, Poole PS and Sánchez-Cañizares C (2021) Rhizobial Chemotaxis and Motility Systems at Work in the Soil. Front. Plant Sci. 12:725338. doi: 10.3389/fpls.2021.725338

INTRODUCTION

There are several strategies bacteria use to actively navigate their environment, motile forces produced either through pili retraction or flagella rotation. Pili drive twitching motility across surfaces by extending, adhering and retracting to pull the bacterium forward (Mattick, 2002), whereas flagella are rigid helical structures, anchored to the cell wall and rotated by a protein motor to produce thrust (Macnab and Aizawa, 1984). This enables the bacteria to move sporadically as individuals (swimming) or continuously as an organized group (swarming) (reviewed by Henrichsen, 1972). Alternatively, organized and continuous movement can be driven by motor proteins anchored to a surface or nearby bacterium, moving along helical tracks in the inner membrane and pushing the cell forwards (gliding) (Nan and Zusman, 2016). Other, passive

strategies have also been described that are driven by the expansion of a growing culture, with the bacteria either producing substances to reduce friction and enable mass movement (sliding) or producing an aggregate capsule from which cells are ejected (darting) (Henrichsen, 1972; Pollitt and Diggle, 2017).

Active bacterial motility tends to be controlled by chemotaxis systems that respond to different stimuli, allowing bacteria to migrate to optimal environments. This occurs through sensing the binding of a ligand to its cognate chemoreceptors (methyl accepting chemotaxis proteins, MCPs). In response to signal transduction, motility systems produce runs, tumbles, reverses, pauses and other phenomena that together form a biased three-dimensional walk. Although tumbles, reverses and pauses are random reorientation events, the movement of bacteria is biased by controlling the frequency of these events. Some bacterial flagella rotate bidirectionally, others unidirectionally, to bias stopping and starting (Kearns, 2010).

An impressive diversity of motility mechanisms has evolved in prokaryotes. Among Gram-negative bacteria, *Escherichia coli* is the best understood model of flagella-based swimming. Also belonging to this group are a variety of nitrogen-fixing soil bacteria, known as rhizobia, that have evolved several differences from the *E. coli* model and are compared in this review. These include *Sinorhizobium meliloti* RU11 (also *Ensifer meliloti*), which nodulates alfalfa (*Medicago sativa*) and *Medicago truncatula* (Meade et al., 1982); *Agrobacterium fabacearum* H13-3 (formerly *R. lupini* H13-3), which nodulates *Lupinus luteus*, the European yellow lupin (Delamuta et al., 2020); *Rhizobium leguminosarum* bv. *viciae* 3841, which nodulates pea (*Pisum sativum*), various *Vicia*, lentils (*Lens culinaris*), grass peas and sweet peas (various *Lathyrus*) (Young et al., 2006); *Azorhizobium caulinodans* ORS571, which nodulates *Sesbania rostrata* (Lee et al., 2008); *Azospirillum brasilense* Sp7, a non-endosymbiote but a microaerobic diazotroph that colonizes the rhizospheres of grasses (Zhulin and Armitage, 1993); and finally, *Bradyrhizobium diazoefficiens* USDA110 (formerly *B. japonicum*), which nodulates soybean (*Glycine max*) (Kaneko et al., 2002). The relevance of motility and chemotaxis for rhizobia, both as free-living bacteria in the soil and as symbiotic cells inside plant nodules, is then discussed in the context of rhizobial inoculants and the importance of evaluating the chemotaxis and motility properties of strains used in the field.

The *Escherichia coli* Motility Model and Marine Bacteria Motility

E. coli typically have 5–10 flagella protruding from various points around the cell body (peritrichous flagellation) that form an integrated bundle oriented in the same direction (Macnab and Aizawa, 1984). Each flagellum consists of a basal body, hook and filament (see **Figure 1A**). The basal body is made up of a central hollow rod surrounded by anchoring stacks of rings (Wang et al., 2012). At the base of the basal body is the motor, where torque is produced via transmembrane gradients of H^+ ions, and in other bacterial species, also of Na^+ or K^+ ions (Hirota and Imae, 1983; Armitage and Schmitt, 1997; Kojima and Blair, 2001; Terahara et al., 2012). This motor is further subdivided into the rotor, the proteins that rotate with the flagella, and the stator, the proteins driving rotation. The hook is a highly curved helix; a flexible coupling that connects the central rod to the filament. The filament is a left-handed helix consisting of a single protein, flagellin. When rotated in a counterclockwise (CCW) manner, the flagella provide a powerful forward thrust. However, if the rotary direction is flipped to a clockwise (CW) direction, a polymorphic change is induced that causes a right-angled bend in the filament to propagate along the flagella. This compels the bundle of flagella to separate, causing a period of rotational movement due to the low impact of inertia at microbial scales. This process is called a tumble and allows bacteria to change their direction of movement (Macnab and Aizawa, 1984; Armitage and Schmitt, 1997; Berg, 2003; Stock et al., 2012; Wang et al., 2012). The "run and tumble" mechanism produces a movement called a "biased random walk," with the rate of tumbles being random but biased by the chemotaxis system (Sourjik and Wingreen, 2012).

In contrast, marine bacteria such as *Vibrio alginolyticus* tend to reverse their swimming direction instead of tumbling, by stably rotating their polar or subpolar flagella in the opposite direction and dragging the cell body. This "run and reverse" mechanism can also produce a "biased random walk" by controlling the frequency of reversal movements, although it is reliant on Brownian motion to reorient the cell body (Mitchell et al., 1996). *Vibrio* spp. (including *V. alginolyticus*) were recently discovered to also 'flick' the cell body after a reversal, caused by buckling of the hook adapter, and resulting in a tumble-like random reorientation of the cell (Xie et al., 2011; Son et al., 2013; Taktikos et al., 2013). Indeed, up to 60% of marine bacteria may actually be performing "run, reverse, and flick" motility (Son et al., 2013).

The Complex Flagella of *Sinorhizobium meliloti* and *Agrobacterium fabacearum*

S. meliloti and *A. fabacearum* are both well-studied Gram-negative swimming bacteria. Although their flagella are built in a similar fashion to those in *E. coli* and in similar numbers, there are several important differences (see **Figure 1B**). The main difference is the shape of the filament; *S. meliloti* and *A. fabacearum*'s filaments are formed by right-handed helices and as such forward thrust is produced by CW rotation (Gotz et al., 1982; Armitage and Schmitt, 1997; Sourjik and Schmitt, 1998). They also have increased rigidity, likely due to the use of several distinct flagellin proteins. Half of the flagella mass consists of the FlaA protein which forms heterodimers with two or three other proteins: FlaB, FlaD and, in *S. meliloti*, FlaC (Scharf et al., 2001). The rigid *S. meliloti* and *A. fabacearum* flagella may be adapted for use in the relatively viscous medium of soil, compared to the native habitat of *E. coli*, the human gut (Armitage and Schmitt, 1997; Attmannspacher et al., 2005). In addition, they are unable to switch the rotary direction of the motor. Instead, they modulate the speed of rotation through an extra stator protein, MotC, that binds MotB in the periplasm and may, thus, regulate the speed of the motor. A further

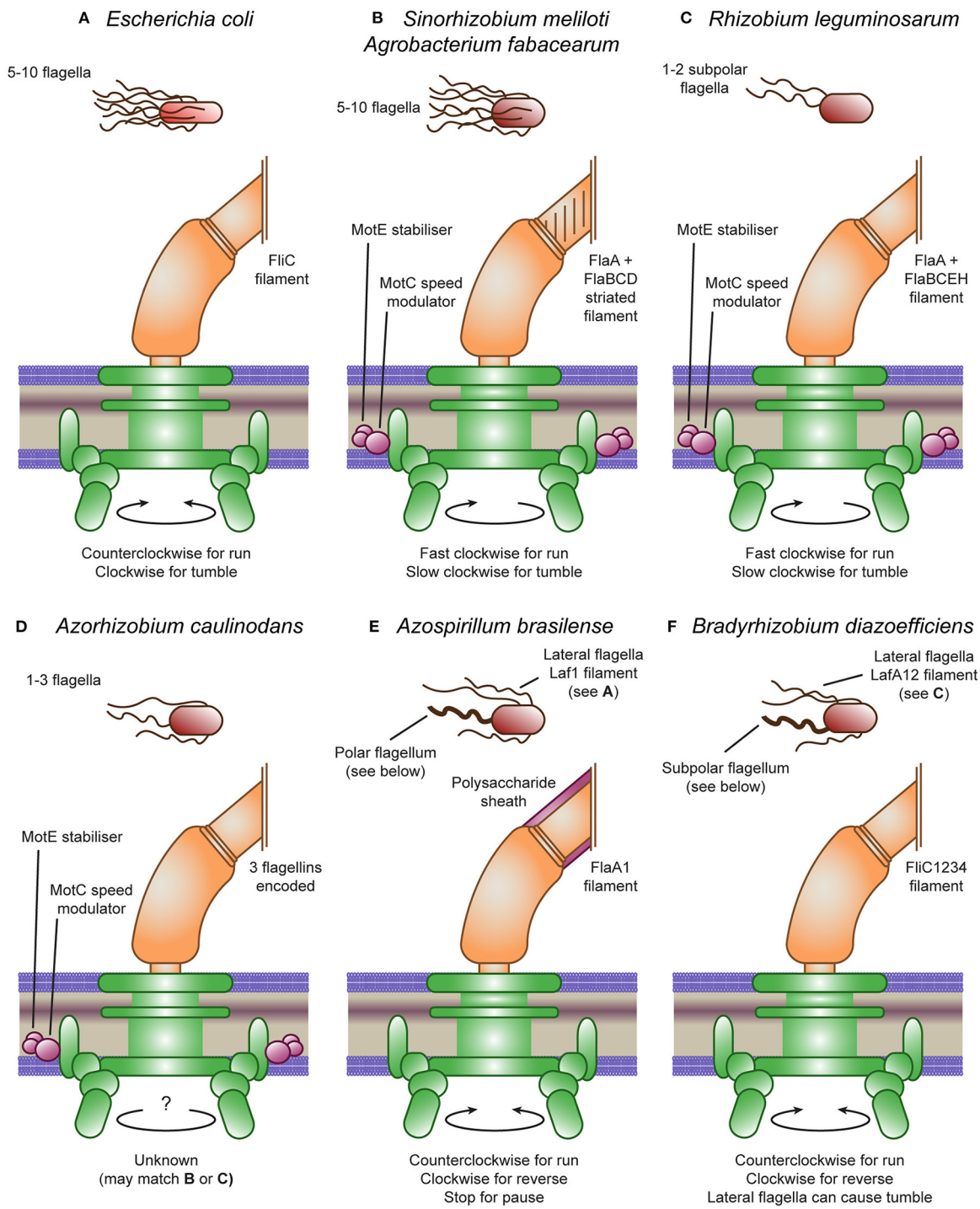

FIGURE 1 | *Escherichia coli* and rhizobial motility models. **(A)** The *E. coli* peritrichous flagella provides thrust through counterclockwise rotation and tumbles through clockwise rotation causing the flagella bundle to dissociate. **(B)** The *Sinorhizobium meliloti* and *Agrobacterium fabacearum* peritrichous flagella provide thrust through clockwise rotation and tumbles through speed modulation causing the flagella bundle to dissociate. This speed modulation is controlled by MotC, stabilized by MotE. The reversed direction is due to the heterogeneous filament proteins producing a right-handed striated filament. **(C)** The *Rhizobium leguminosarum* subpolar flagella also provide thrust through clockwise rotation and tumbles through speed modulation, although they do not form a flagella bundle. The *R. leguminosarum* flagella also have heterogeneous filaments, although they are not visibly striated. **(D)** The *Azorhizobium caulinodans* flagella are not well-studied but may match either **(B)** or **(C)**, having the MotC and MotE accessory proteins. **(E)** *Azospirillum brasilense* produces two flagella types: a polar flagellum covered by a polysaccharide sheath that provides thrust through counterclockwise rotation, reverses through clockwise rotation and can pause by stopping the motor; and lateral flagella matching **(A)**. **(F)** *Bradyrhizobium diazoefficiens* produces two flagella types: a subpolar flagellum that provides thrust through counterclockwise rotation and reverses through clockwise rotation; and lateral flagella matching **(C)** that can cause tumbles.

additional protein, MotE, stabilizes MotC and may target the protein to the flagellar motor (Eggenhofer et al., 2004). The product of another nearby gene was originally designated as the novel motor protein MotD; however, mutational analysis revealed its function to be that of FliK, the flagellar hook length regulator that controls the switch from secretion of hook-type substrates to filament-type substrates (Eggenhofer et al., 2006).

Despite being unable to cause a tumble in the same way as *E. coli* due to their unidirectional flagella, *S. meliloti* and *A. fabacearum* can still tumble. The bacteria achieve this by asynchronously modulating the rotational speed of their flagella, causing their bundle of flagella to disassociate, causing a tumble (Armitage and Schmitt, 1997; Attmannspacher et al., 2005). The ability to modulate the speed of their flagella also enables the bacteria to increase cell velocity in addition to reducing tumbling in response to high attractant concentrations (Meier et al., 2007).

The Smooth Flagella of *Rhizobium leguminosarum* and *Azorhizobium caulinodans*

Motility in *R. leguminosarum* and *A. caulinodans* appears to be closely related to that in *S. meliloti*, containing all the accessory genes (see **Figures 1C,D**). *R. leguminosarum* appear to only have 1-2 subpolar flagella with a smooth surface, lacking the helical perturbations found in *S. meliloti* (Tambalo et al., 2010a). *A. caulinodans* also have 1–3 smooth flagella, although they are arranged around the cell in a peritrichous arrangement (Liu et al., 2018a). The protein structure of the *R. leguminosarum* filament is closely related to *S. meliloti*, again consisting of heterologous pairs of a main flagellin (FlaA) and multiple secondary flagellin (FlaB, FlaC, FlaE, and FlaH) (Scharf et al., 2001; Tambalo et al., 2010a). Indeed, this bacterium is also unable to change the direction of rotation, so directional changes are driven by modulating the rotational speed of a single or pair of flagella, although the mechanism is currently unknown (Miller et al., 2007). However, *R. leguminosarum* still appears to tumble approximately every 3 s under homogeneous conditions, while it swims at approximately 38 μm/s (Miller et al., 2007). The protein structure of the *A. caulinodans* filament is unknown, but it does encode three flagellin copies. In addition, although the rotation direction of the flagella of *A. caulinodans* is unknown, since it encodes both *motC* and *motE*, it likely also modulates the speed of rotation (Lee et al., 2008).

The Composite Flagellar Systems of *Azospirillum brasilense* and *Bradyrhizobium diazoefficiens*

Both *A. brasilense* and *B. diazoefficiens* encode two flagella systems, one producing a single polar or subpolar flagellum and the other producing multiple lateral flagella (see **Figures 1E,F** (Zhulin and Armitage, 1993; Kaneko et al., 2002). The flagellins forming the lateral flagella are encoded by *laf1* in *A. brasilense* and, *lafA1* and *lafA2* in *B. diazoefficiens* and are all 300–400 amino acids long, similar in size to other rhizobia (Moens et al., 1995a,b; Kanbe et al., 2007). In contrast, the flagellins forming the polar flagella are encoded by *fla1* in *A. brasilense* and, *fliC1*, *fliC2*, *fliC3*, and *fliC4* in *B. diazoefficiens* and are all 600–800 amino acids long, producing thicker filaments with bidirectional rotation (Zhulin and Armitage, 1993; Quelas et al., 2016). In addition, the lateral flagella of *B. diazoefficiens* were found to be more closely related to the flagella of other rhizobia than the divergent polar flagellum (Garrido-Sanz et al., 2019). Indeed, the *B. diazoefficiens* lateral flagella can only rotate in a single direction and their cluster also encodes *motC* and *motE* (Kanbe et al., 2007). The rotation direction of the *A. brasilense* lateral flagella is unknown but the cluster does not encode *motC* and *motE*. A further difference is that the polar flagellum of *A. brasilense* is covered with a polysaccharide sheath not found in other rhizobia (Moens et al., 1995b; Burygin et al., 2007; Belyakov et al., 2012). Glycosylation of flagella has been linked to avoiding plant immunity in *Pseudomonas syringae* (Takeuchi et al., 2003; Taguchi et al., 2009; Iwashkiw et al., 2013). In contrast, other rhizobial flagellin are sufficiently divergent from pathogenic flagellins to avoid a plant response (Felix et al., 1999). Perhaps the polar flagellum of *A. brasilense* requires glycosylation to prevent plant detection, in which case, the subpolar flagellum of *B. diazoefficiens* may be similarly glycosylated. Two flagellin modification genes, *flmA* and *flmB*, were found to be essential for the formation of the *A. brasilense* polar flagellum (Rossi et al., 2016). In addition to having a similar composite system, the physical properties of the *A. brasilense* and *B. diazoefficiens* lateral flagella and separately their polar flagella were found to be nearly identical and were classified into the same groups (Fujii et al., 2008). In contrast, the *S. meliloti* flagella were divergent from these groups, potentially due to their complex, striated structure (Fujii et al., 2008).

The swarming motility of both *A. brasilense* and *B. diazoefficiens* are driven mainly by the lateral flagella, with *A. brasilense* only producing lateral flagella on solid or semi-solid surfaces (Zhulin and Armitage, 1993; Covelli et al., 2013). The swimming motility of *A. brasilense* is mixed, following mainly "run and reverse" and "run, reverse, and flick" motility with occasional pauses and reduced swimming speed in response to attractants (chemokinesis) driven mainly by the polar flagellum (Zhulin and Armitage, 1993; Mukherjee et al., 2019). The swimming motility of *B. diazoefficiens* is similarly mixed, following 50% "run and reverse," 30% "run, reverse, and flick" and, interestingly, 20% "run and tumble" (Quelas et al., 2016). The reversals and flicks were driven by the polar flagellum, whereas the tumbles were produced by the lateral flagella. The composite flagellar systems of *B. diazoefficiens* thus produce a composite motility performance.

Rhizobial Pili Systems

In addition to flagella, *S. meliloti*, *A. fabacearum*, *R. leguminosarum*, *A. brasilense* and *B. diazoefficiens* encode type IV pili on their chromosomes, with *S. meliloti* and *B. diazoefficiens* encoding additional, truncated clusters (Krehenbrink and Downie, 2008; Wibberg et al., 2011; Wisniewski-Dye et al., 2011; Zatakia et al., 2014; Mongiardini et al., 2016). The main cluster of *B. diazoefficiens* is split with the *tadE*, *tadF*, and *tadG* genes located almost 3 Mb away from the remaining genes

(Mongiardini et al., 2016). *A. caulinodans* does not encode a pili system (Lee et al., 2008). Each species' main cluster displays high homology to the *tad* systems of *Aggregatibacter actinomycetemcomitans* and *Caulobacter crescentus* (Tomich et al., 2007; Clock et al., 2008; Imam et al., 2011). Beyond bioinformatic characterization, very little research has been conducted on rhizobial pili systems. *A. brasilense* was found to form polar pili bundles that are required for biofilm formation (Shelud'ko and Katsy, 2001; Wisniewski-Dye et al., 2011). Interestingly, deletion of *pilA1*, the integral pilin subunit of the chromosomal cluster of *S. meliloti*, was found to reduce competitive nodulation of *Medicago sativa* plants (Zatakia et al., 2014). In addition, the TadG protein of *B. diazoefficiens* has some sequence similarity to *Bradyrhizobium* lectin BJ38, which is important for soybean root adhesion (Loh et al., 1993; Ho et al., 1994; Mongiardini et al., 2016). This indicates that there is a role for pili in legume symbiosis, perhaps during root colonization.

The *Escherichia coli* Chemotaxis Model

Chemotaxis involves regulating motility through variations in the concentration of metabolically-relevant chemicals, being either attractants (compounds which benefit the bacteria) or repellents (those compounds with negative effects). Bacterial size is insufficient to spatially sense concentration gradients at swimming speeds so, instead, concentrations are compared temporally (Porter et al., 2011). Bacteria bias their movements toward high concentrations of attractants by reducing their tumbles, and away either from low concentrations of attractants or high concentrations of repellents by increasing their tumbles.

The core of the chemotaxis response in *E. coli* is the phosphorylation of the response regulator CheY by the histidine kinase CheA in response to negative signal transduction from the chemoreceptor proteins. The chemoreceptors tend to sense in the periplasm and form a coiled coil of about 30–40 heptads (7 amino acid repeats) in the cytoplasm (forming the categories 34H, 36H, 38H, and 40H) and bind CheA at the base (**Figure 2A**) (Wuichet and Zhulin, 2010). The length of the coiled coil determines the association between chemoreceptors, with those of the same length forming hexagonal arrays (Jones and Armitage, 2015). The binding of CheA to the chemoreceptors within these hexagonal arrays is stabilized by CheW. Phosphorylated CheY binds the motor protein FliM, reducing rotary speed and inducing a tumble (Sourjik and Schmitt, 1998). In addition, the chemotaxis proteins CheR and phosphorylated CheB methylate and demethylate chemoreceptors, reducing and increasing their signal sensitivity, respectively (Rice and Dahlquist, 1991; Armitage and Schmitt, 1997; Porter et al., 2011). *E. coli* encodes an additional chemotaxis protein, CheZ, which interacts with CheY to remove phosphorylation, enabling the cell to quickly adapt to new conditions.

Chemotaxis Systems in Symbiotic Bacteria

In contrast to *E. coli*, most of the rhizobia encode multiple chemotaxis systems. The rhizobia also encode a diversity of chemoreceptors divergent from the 5 chemoreceptors encoded by *E. coli* K12, with the motility model strain *S. meliloti* RU11 encoding 8 chemoreceptors, *A. fabacearum* H13-3 encoding 22, *R. leguminosarum* biovar *viciae* 3841 encoding 26, *A. caulinodans* ORS571 encoding 43, *A. brasilense* Sp7 encoding 41, and *B. diazoefficiens* USDA110 encoding 36 (Rebbapragada et al., 1997; Yost et al., 2004; Jiang et al., 2016; Scharf et al., 2016; Zatakia et al., 2017). However, the main chemotactic systems of *S. meliloti*, *A. fabacearum*, and *R. leguminosarum* have a similar core system to that of *E. coli*, belonging to class F7 and being associated with chemoreceptors of type 36H (Sourjik and Schmitt, 1998; Miller et al., 2007; Tambalo et al., 2010a,b; Wibberg et al., 2011) (see **Figures 2A,B**). These species do not encode CheZ, instead they encode two copies of CheY, with CheY2 propagating the signal and CheY1 acting as a phosphate sink, increasing the rate at which CheY2 returns to its unphosphorylated state (Sourjik and Schmitt, 1998). A further rhizobial protein, CheS, forms a dimer that binds CheA and CheY1, increasing phosphate transfer and thus CheY2 dephosphorylation (Dogra et al., 2012; Arapov et al., 2020). The rhizobia also encode two uncharacterized chemotaxis proteins: CheD and CheT. In the case of CheD, this protein has homology to *Bacillus subtilis* CheD protein which was found to deamidate chemoreceptors, a role served by CheB in *E. coli* (Kristich and Ordal, 2002; Rao et al., 2008). In *S. meliloti*, *cheT* mutants have a chemotaxis defect, indicating that it is likely to have some relevant, although currently unknown, chemotactic role (Arapov et al., 2020).

A. caulinodans, in contrast, only encodes a single chemotaxis system belonging to class F5 and being associated with chemoreceptors of type 38H. This bacterium encodes a cluster with *cheY*, *cheA*, *cheR*, *cheB*, *cheW* and two chemoreceptors (Jiang et al., 2016). In addition, it has a separate cluster located 37 kb upstream and encoding a second copy of the *cheY* gene and a *cheZ* gene. CheZ appears to be a functional protein with a conserved phosphatase motif critical for chemotactic activity (Liu et al., 2018b). Both of the CheY proteins appear to be active, with the main operon *cheY1* mutant displaying a reduced tumble rate, causing a 40% reduction in the chemotaxis swimming halo on semi-solid media, and a *cheY2* mutant displaying an increased tumble rate with a 90% reduction in the chemotaxis swimming halo (Liu et al., 2020).

In addition to the main systems described above, both *A. fabacearum* and *R. leguminosarum* encode accessory chemotaxis systems. These systems are F8-class chromosomal clusters encoding *cheY*, *cheA*, *cheR*, *cheB*, two *cheW* genes with one chemoreceptor (*mcpB*) in *A. fabacearum* and three in *R. leguminosarum*. These three chemoreceptors of *R. leguminosarum* (*mcrA*, *mcrB*, and *mcrC*) are of type 34H, indicating that it is an independent sensory system to the 36H chemoreceptors of Che1 (see **Figure 2A**). The class of the chemoreceptor encoded by *A. fabacearum* has not been determined, although this protein is likely to match *mcrA*, *mcrB*, and *mcrC* of *R. leguminosarum* due to the chemotaxis cluster arrangements. The *R. leguminosarum* Che2 cluster has a minor role in chemotaxis in free-living conditions (Miller et al., 2007). However, a recent insertion sequencing experiment in *R. leguminosarum* bv. *viciae* 3841 found that insertions in any of the *che2* cluster genes were over-represented in nodule bacteria samples, suggesting a role in symbiosis (Wheatley et al., 2020).

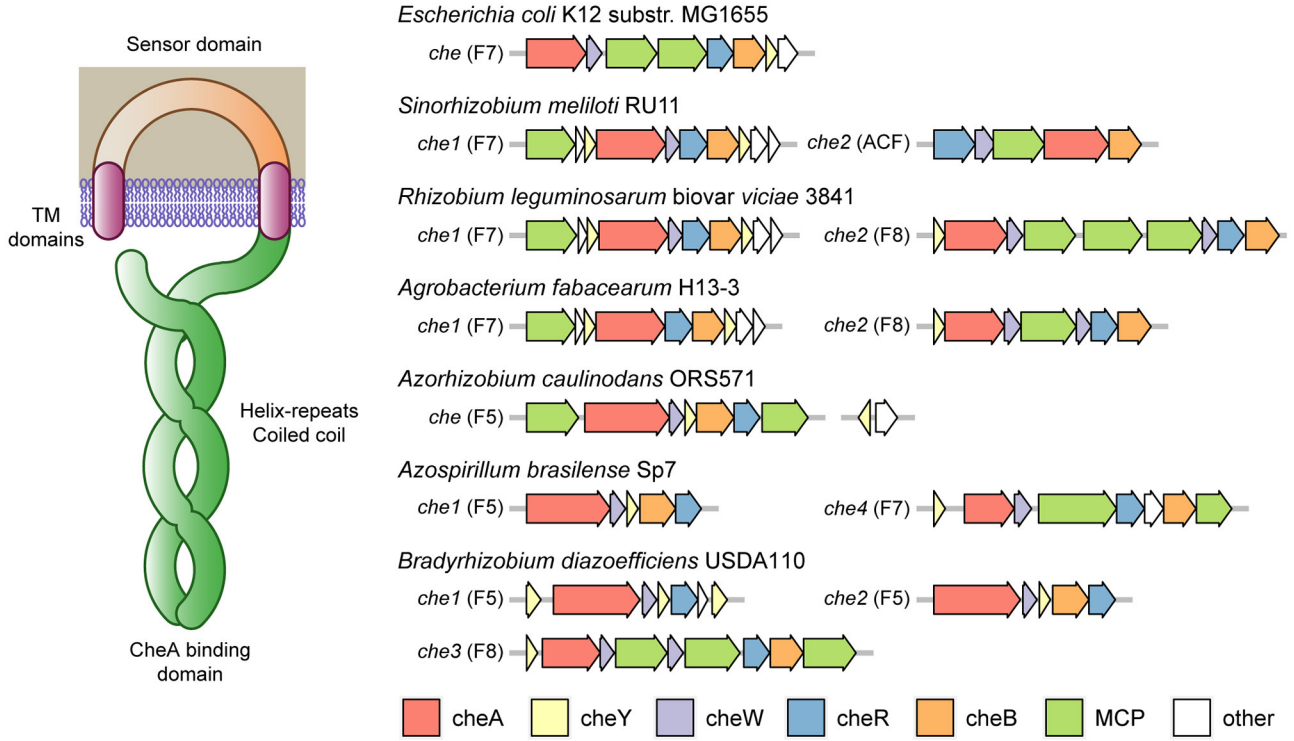

FIGURE 2 | *Escherichia coli* and rhizobial chemotaxis systems. **(A)** Typical MCP (methyl-accepting chemotaxis protein) chemoreceptor domain structure including transmembrane domains flanking a periplasmic sensor domain. In the cytoplasm, the receptors form a coiled coil of alpha helices down to the CheA binding domain and returning to the plasma membrane to complete the coiled coil. Methylation and demethylation occur at sites along the coiled coil. The number of helix repeats varies, with some MCPs containing 34, 36, 38 or 40 repeats (classes 34H, 36H, 38H, and 40H, respectively). **(B)** The chemotaxis clusters of *Escherichia coli* and various rhizobia. Most clusters consist of the *che* genes *A*, *Y*, *W*, *R*, and *B*. *E. coli* K12 substr. MG1655 has one cluster of class F7 containing an extra *cheZ* gene and two MCP genes. *Sinorhizobium meliloti* RU11 has two clusters: one of class F7 containing extra *che* genes *Y*, *S*, *D*, and *T* and one MCP gene; and one of class ACF containing the standard genes except an altered *cheA*-REC, missing *cheY* and one MCP gene. *Rhizobium leguminosarum* biovar *viciae* 3841 has two clusters: one of class F7 containing extra *che* genes *Y*, *S*, *D*, and *T* and one MCP gene; and one of class F8 containing an extra *cheW* and three MCP genes. *Agrobacterium fabacearum* H13-3 has two clusters: one of class F7 containing extra *che* genes *Y*, *S*, *D*, and *T* and one MCP gene but missing *cheW*; and one of class F8 containing an extra *cheW* and one MCP gene. *Azorhizobium caulinodans* ORS571 has one cluster of class F5 containing the standard genes and one MCP gene; and 37 kb upstream the *che* genes *Y* and *Z*. *Azospirillum brasilense* Sp7 has four clusters: one of class F5 containing the standard genes; and one of class F7 containing the standard genes, *cheD* and two MCP genes. The two clusters not shown have not been linked to chemotaxis. *Bradyrhizobium diazoefficiens* USDA110 has three clusters: one of class F5 containing two extra *cheY* genes and one operon reading frame but missing *cheB*; one of class F5 containing the standard genes; and one of class F8 containing an extra *cheW* gene and three MCP genes.

S. meliloti also encodes an accessory chemotaxis system located on its pSymA plasmid, which belongs to the alternative cellular function (ACF) class and encodes only *cheR*, *cheB*, *cheW*, a chemoreceptor (*mcpS*) and a *cheA* gene fused with a response-regulator (REC) domain (Wuichet and Zhulin, 2010; Scharf et al., 2016). This cluster is associated with a chemoreceptor of type 40H, *mcpS*, which is divergent from the other *S. meliloti* chemoreceptors of type 36H (see **Figure 2A**). The *mcpS* gene was not expressed in free-living cells, indicating that this chemotaxis operon is not active under those conditions (Meier and Scharf, 2009; Scharf et al., 2016). In addition, the absence of a *cheY* gene indicates that the system does not control flagella; instead, it is likely that the modified CheA-REC protein regulates downstream effectors.

Chemotaxis Systems Controlling "Run and Reverse" Motility

In addition to multiple flagellar systems, *A. brasilense* has four chemotaxis clusters and *B. diazoefficiens* has three (see **Figure 2B**). Three of the four chemotaxis systems of *A. brasilense* (*che1*, *che2*, and *che4*) include the core *cheY*, *cheA*, *cheR*, *cheB*, and *cheW* genes. The *che1* system of *A. brasilense* is an F5-class cluster associated with chemoreceptors of type 38H (of which there are 33 in the genome), harboring the core genes above, including a *cheA* gene fused with a response-regulator (REC) domain (Wuichet and Zhulin, 2010). The *che2* system is an F9-class cluster containing the core genes mentioned above, including a fragmented *cheA* in addition to another *cheY* and a *cheC* phosphatase gene. The *che3* system is an ACF-class

cluster only encoding a fragmented *cheA*, *cheB*, *cheW* genes, one chemoreceptor and a putative histidine-kinase response-regulator pair. Finally, the *che4* system is an F7-class cluster associated with chemoreceptors of type 36H (of which there are 8 in the genome), encoding the core genes and a *cheD* gene. *A. brasilense* has been observed to react with reverses and pauses and to modulate speed in response to chemical gradients (Zhulin and Armitage, 1993; Mukherjee et al., 2019). Numerous studies have revealed that the Che4 system modulates reversals by changing the rotation direction of the polar flagellum, while the Che1 system modulates swimming speed (Zhulin and Armitage, 1993; Bible et al., 2012; Mukherjee et al., 2016; Ganusova et al., 2021). In addition, the Che4 system, in concert with two orphan CheY proteins (CheY6 and CheY7), also modulates the pausing behavior, aerotaxis and the induction of swarming motility (Mukherjee et al., 2019; Ganusova et al., 2021). The Che2 and Che3 systems do not appear to be involved in chemotaxis. Regarding the three *B. diazoefficiens* chemotaxis clusters (*che1*, *che2*, and *che3*), they include the core *cheY*, *cheA*, *cheR*, *cheB*, and *cheW* genes, except the *che1* F5-class system, which does not contain a *cheB* gene but an additional two *cheY* genes. The *che2* system is also an F5-class cluster including the core genes. The *che3* system is an F8-class cluster associated with chemoreceptors of type 34H and encodes an additional *cheW* gene with three chemoreceptors (Kaneko et al., 2002; Wuichet and Zhulin, 2010). The involvement of these systems on chemotaxis is currently unknown, although it was found that only the subpolar flagellum of *B. diazoefficiens* responds chemotactically to glutamate and succinate (Quelas et al., 2016). This indicates that the primary chemotactic response is via the subpolar flagellum, similar to *A. brasilense*.

Regulation of Motility and Chemotaxis

S. meliloti, *A. fabacearum*, and *R. leguminosarum* all have the same transcriptional activation system for flagellar and chemotaxis genes. Regulation of flagella in bacteria typically follows a hierarchical class system: regulatory class I genes control the transcription of class II genes required to initiate flagellar assembly and which, in turn, regulate class III genes to complete assembly and perform chemotaxis (McCarter, 2006). This class system ensures that each gene is active only when its product is useful. In the above rhizobia, the class I heterodimer VisNR is induced by some unknown effector to activate both promoters of *rem* and negatively regulate *visN* (Rotter et al., 2006). In turn, Rem activates the transcription of class IIA downstream regulators *fliM* (encoding a motor protein) and *orf38* (encoding a potential basal body protein) in addition to flagellar assembly and motor genes (class IIB) (Tambalo et al., 2010b). Presumably activated through some signal of basal body completion, FliM and Orf38 then activate flagellin and chemotaxis genes (class III), to produce functional flagella with chemotactic ability. Mutants in *visN*, *visR*, and *rem* are nonmotile and non-flagellated, indicating that they form the master regulators for flagella in *S. meliloti* and *R. leguminosarum* (Sourjik et al., 2000; Rotter et al., 2006; Tambalo et al., 2010b). Although all of these genes are encoded by *A. fabacearum*, their function has not yet been confirmed. In *R. leguminosarum*, VisNR and Rem are expressed throughout exponential growth phase, but their expression drops sharply during stationary phase; although the cells are still motile, likely retaining their flagella due to the stability of the filament (McCarter, 2006; Tambalo et al., 2010b; Zhuang and Lo, 2020; Nedeljkovia et al., 2021). The only motility and chemotaxis genes in *R. leguminosarum* that are independent of VisNR are scattered chemoreceptors and, notably, the *che2* cluster (Scharf et al., 2016). This possibly allows the bacteria to target the expression of *che2* genes independently of that of motility genes and indicates that the role of the Che2 cluster may not be linked to flagella.

Neither *A. caulinodans* nor *B. diazoefficiens* encode *visNR*, although both encode homologs of *rem* (Lee et al., 2008; Mongiardini et al., 2017). The *B. diazoefficiens* Rem-homolog LafR was recently found to control transcriptional regulation of its lateral flagella but not its polar flagellum. The orphan response regulator did not require phosphorylation for its effect although it was activated by arabinose and oxidative stress while being repressed by mannitol, oxygen limitation, and iron deficiency (Mongiardini et al., 2017). LafR was found to activate genes across multiple operons, including *flbT*, the gene product of which translationally induces the LafA1 and LafA2 lateral flagellins (Mongiardini et al., 2017). Although the role of *rem* in *A. caulinodans* is unknown, some recent work has indicated that the flagella and chemotaxis genes have increased transcription in the presence of the amino acids histidine, arginine and aspartate (Liu et al., 2019). *A. caulinodans* displays chemotaxis toward these amino acids, that are sensed by the chemoreceptor TlpH, although the *tlpH* mutant did not remove the transcriptional effect (Liu et al., 2019). The mechanistic link between the amino acids and flagellar transcriptional regulation remains unknown. In contrast to the other rhizobia, *A. brasilense* does not encode *visNR* or *rem*. Instead, it appears that the nitrogen regulator NtrA controls flagellar gene transcription via a σ^{54} box. Indeed, a *ntrA* mutant was found to be non-flagellated (Moens et al., 1995a).

Importance of Chemotaxis and Motility Systems for Rhizobia as Free-Living Bacteria in Soil Conditions

Bacterial movement through soil depends on continuous water pathways with their inability to traverse air pockets (Griffin and Quail, 1968) (see **Figure 3**). Overall, with insufficient soil water content, microbial mobility is limited, whereas overloaded soil has greatly reduced oxygen concentrations (Tecon and Or, 2017). The water content in the soil has been described by different measures including matric potential, moisture content and percentage field capacity which all increase with increasing water content. For example, the swarming motility of various *Pseudomonas* species was found to be restricted to high matric potential agar with very high moisture content, showing a fast transition to non-motility upon drying (Dechesne and Smets, 2012). The soil bacterium *Pseudomonas aeruginosa* displayed reduced motility with decreases in soil water content (increased matric suction), to the point of non-motility (Griffin and Quail, 1968). *Rhizobium trifolii* motility also slowed with increasing water tension and was halted by discontinuity; conversely, the mean radius of the bacterial motility area increased with

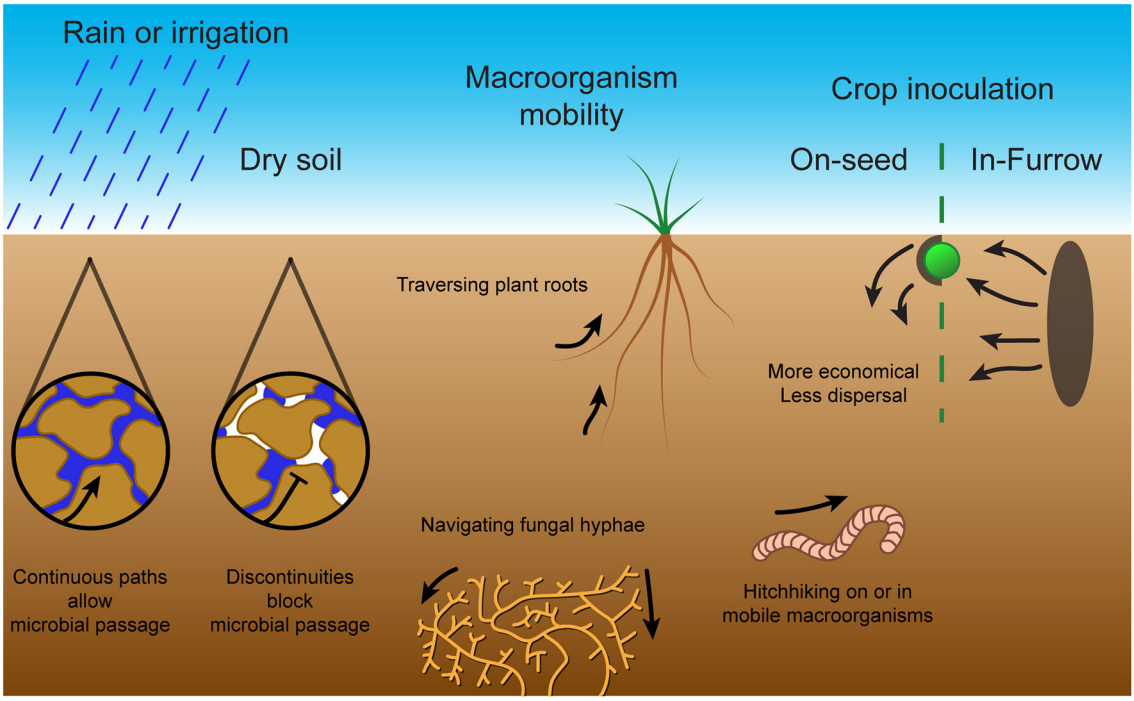

FIGURE 3 | Bacterial mobility methods and challenges in soil. Microbial passage through the soil is dependent on sufficient moisture content to produce continuous pathways through water. Without rain or irrigation, air pockets form within the soil and prevent microbial passage. To combat this, microbes can exploit macroorganisms through methods including traversal along plant roots, navigation of fungal hyphae or hitching a ride on or in mobile macroorganisms. These mobility methods and challenges in soil are important for symbiont inoculation of crop plants. The two main inoculation techniques are on-seed, which although economical does not provide much dispersal, and in-furrow, which requires large amounts of inoculated soil but provides extensive dispersal.

increased water content (Hamdi, 1971). The bean symbiont *Rhizobium leguminosarum* bv. *phaseoli* displayed a reduction in travel distance in soil with reduced moisture content such that it resembled a non-flagellated, non-motile mutant strain (Issa et al., 1993). The soil bacterium *Pseudomonas fluorescens* had reduced horizontal and vertical migration with decreased water irrigation flow rate (Singh et al., 2002). In addition, soil bacteria *A. brasilense* and *P. fluorescens* displayed increased migration in soil with large continuous pores (sand) over soil with narrow water channels (clay or loamy soils) (Bashan, 1986; Singh et al., 2002). The reduction in microbial dispersal with reduced soil water content implies that the usual state of soil bacteria is sessility imposed by the ubiquitous unsaturated state of soils (Tecon and Or, 2017). Thus, motility is limited in importance to temporary flooded states of soil formed immediately after rainfall or irrigation.

An effective rhizobial inoculant must survive in the competitive environment of the soil (Atieno and Lesueur, 2018). Water content was again found to be a key determinant for survival in the soil. Soil with higher moisture content and soil types with high field capacity (total water capacity of the soil) were found to support larger populations of *B. japonicum* and *R. leguminosarum* (Mahler and Wollum, 1981). *P. fluorescens* also had increased survival in soil with increased moisture content (van Elsas et al., 1991). At microbial scale, however, the soil is dynamic and fragmented with changes in soil hydration and pore-spaces dramatically influencing their dispersion and fluctuating nutrient gradients attracting them down fleeting paths. This produces a heterogeneity in microsites that is averaged out by macro studies at the cm^3 scale (Tecon and Or, 2017). For instance, motile *E. coli* was found to accumulate within funnel-shaped microsites; thus, porous wet soil could cause heterogenous arrangements of bacteria simply by their shapes (Galajda et al., 2007). Theoretical models have indicated that in heterogeneous environments, a more motile bacteria can outgrow a metabolically superior species (Lauffenburger et al., 1982). Therefore, an elite inoculant would need to have powerful but adaptable motility and chemotaxis systems.

There are additional complications to chemotaxis control of motility in the soil. The control exerted by chemotaxis systems on bacterial motility does provide an improvement over random cell motility, with chemotactic strains having 10 times faster predicted soil dispersal rates (Ebrahimi and Or, 2014). Indeed, *P. fluorescens* was found to migrate further in soil irrigated by chemoattractant-rich fungal exudates when compared to sterile water (Singh et al., 2002). The soil bacteria *A. brasilense* and *P. fluorescens* migrate toward roots guided by chemotaxis at increased rates with increased water content up to the water capacity of the soil (Bashan, 1986). In contrast, the symbiont *B. diazoefficiens* was found to swarm quickly through wet

soil with no supplemented chemoattractants (Covelli et al., 2013). Chemotactic detection of nutrients in soil is limited by fragmentation of water pockets due to drainage, plant uptake and evaporation, factors limiting nutrient diffusion and gradient establishment. Thus, reduction in soil matric potential—reducing moisture content—exponentially decreases chemotactic movement (Ebrahimi and Or, 2014).

Since active movement through dry soil is severely limited, other passive forms of movement dominate (see **Figure 3**). These include environmental forces, such as water percolation or wind dispersal of soil particles on the surface, in addition to "hitchhiking" on larger organisms such as earthworms, nematodes, protozoa, soil fungal networks or plant roots (Yang and van Elsas, 2018; King and Bell, 2021). This "hitchhiking" occurs through either adhesion to macroorganism surfaces, or through consumption and survival in the gut with subsequent release into the soil by expulsion or death of the macroorganism. For instance, *S. meliloti* migration through sterile soil was improved by the presence of *Caenorhabditis elegans* nematode worms, and migration of *B. japonicum* and *Pseudomonas putida* was improved by the presence of burrowing earthworms (Madsen and Alexander, 1982; Horiuchi et al., 2005). On the other hand, excessive adhesion may reduce dispersal, as *E. coli*, *Rhodococcus erythropolis* and *P. putida* species were found to be retained more in more adhesive soils with reduced vertical dispersal by water percolation (Jimenez-Sanchez et al., 2015; Sepehrnia et al., 2019). In addition, migration along hyphal networks or across plant roots enables mobility despite discontinuities in the surrounding soil pores (Yang and van Elsas, 2018). *Rhizobium leguminosarum* bv. *trifolii* was found to migrate further in presence of clover plant roots and *P. fluorescens* displayed greatly increased depth and magnitude of soil colonization in the presence of wheat plant roots (van Elsas et al., 1991; Worrall and Roughley, 1991). The range and depth of *A. brasilense* soil colonization was also increased by the presence of both wheat and weed roots (Bashan and Levanony, 1987). Thus, the importance of bacterial motility and chemotaxis in the soil is reliant on favorable environmental factors.

Importance of Chemotaxis and Motility Systems for Plant Colonization and in Symbiosis

Motility and chemotaxis also appear to be crucial for competitive root surface colonization and for the establishment of a successful symbiosis (Catlow et al., 1990; Yost et al., 1998; Miller et al., 2007; Scharf et al., 2016). Indeed, most symbionts of eukaryotes have flagellar and chemotaxis capabilities (Raina et al., 2019). However, experiments were performed in well-watered pots that may not truly reflect the field environments in which these symbionts are applied as inoculants. There have been hints that macro-scale mechanisms, such as water percolation, are required to enable bacterial mobility and for effective colonization and nodulation. For example, in low-moisture soil, the symbiont *R. trifolii* inoculated on the seed displayed delayed infection thread formation and nodulation of *Trifolium subterraneum* plants that was partially recovered by watering (Worrall and Roughley, 1976). Vertical transportation of the symbiont *B. japonicum* and the soil bacterium *P. putida* in soil was found to be limited even in the presence of developing soybean and bean plant roots with the absence of percolating water or burrowing earthworms (Madsen and Alexander, 1982). The colonization and nodulation competitiveness of *R. leguminosarum* bv. *viciae* on lentil plants was also found to decrease with depth in non-sterile soil but to partially recover with increased soil moisture content (Karmakar and Chandra, 2012). Finally, various motile *B. diazoefficiens* strains (LP3001 and LP3008) out-competed their non-motile derivatives at soybean plant nodulation under flooded conditions but not when merely at field capacity (Althabegoiti et al., 2011).

A bacterium can achieve a growth advantage by arriving and establishing itself at the root surface before competing bacteria. In addition, flagella-based swarming motility enables movement along the surface of the root for more effective colonization (Simons et al., 1996; Gao et al., 2016). Indeed, motility and chemotaxis mutants of the soil bacterium *B. subtilis* display greatly reduced colonization on *Arabidopsis thaliana* roots after 4 h and on tomato roots after 2 weeks (Allard-massicotte et al., 2016; Gao et al., 2016). In addition, a *P. fluorescens* motile strain out-competed a non-motile strain in root colonization and attachment in sterile soil, whereas transfer of *A. brasilense* through sand from wheat to soybean roots was only observed with the motile strain (Bashan and Holguin, 1994; Turnbull et al., 2001). In contrast, *P. fluorescens* 2-79 RN10 was also found to traverse further along wheat plant roots when inoculated at the root apex rather than the seed, indicating that the bacteria moved with root growth (Parke et al., 1986). Thus, while motility and chemotaxis are integral systems for a competitively colonizing inoculant, they are not the sole mechanism for soil dispersal.

Dispersal of Symbionts as Crop Inoculants in Field Conditions

Farming techniques alter soil microbial diversity and abundance by changing soil composition through crop cultivation or fertilizer application or by disrupting aggregate structures through tillage (Tecon and Or, 2017). Thus, it is important that any inoculants used are tested in real-world field use and are applied in an efficient and effective manner. Current inoculants tend to be applied either on-seed as a coating or in-furrow within the soil. Seed inoculation is more economical, so it has been used more extensively, although some studies indicate that in-furrow inoculation provides improved dispersal of the inoculant (Deaker et al., 2012; Iturralde et al., 2019). For instance, in field soil multiple symbiotic *B. japonicum* strains inoculated on-seed were found to have reduced nodule occupancy compared to in-furrow inoculation, particularly at depth and on lateral roots (McDermott and Graham, 1989; Wadisirisuk et al., 1989; Bogino et al., 2011). In addition, *B. japonicum* LP3001 established in vermiculite soil greatly out-competed (in soybean root nodulation) the equally competitive *B. japonicum* LP3004 inoculated on the seed (Lopez-Garcia et al., 2002). Interestingly, the seed-inoculated *Bradyrhizobium*

had 50% reduced colonization in the mid root and apical root sections, such that slow vertical displacement of the seed-inoculated strain was identified as a major factor in the relative competitiveness of the strains (Lopez-Garcia et al., 2002). In further experiments with a hyper-motile strain, it was found that in-furrow inoculation of *B. japonicum* LP3008 could also considerably improve soybean root nodulation competitiveness compared to seed inoculation in field soil conditions (Lopez-Garcia et al., 2009). In addition, although on-seed inoculation of *R. leguminosarum* bv. *viciae* on faba bean and *Bradyrhizobium lupini* on lupin produced more and larger nodules than in-furrow inoculation at more than half of the field sites tested, potentially these nodules were larger because they were taproot nodules initiated earlier (Denton et al., 2017). Denton et al. (2017) also found that, in general, rhizobial inoculation improved taproot nodulation, whereas only improved lateral root nodulation in sites with reduced native rhizobia. Thus, the effectiveness of these two application techniques may depend on both the field conditions and the native rhizobial population. To improve the competitiveness of inoculants, other strategies include in-field dispersal in porous bags filled with inoculated soil which enable multiple establishment attempts or by leveraging interactions with motile organisms or fungal hyphal networks to promote dispersal (King and Bell, 2021). However, selecting for excess dispersal could actually be counterproductive by diluting inoculants away from the intended targets.

DISCUSSION

Regardless of the complexity and importance of motility and chemotaxis in the soil environment, there is a clear selection for chemotaxis genes in wildtype rhizobia. Analysis of 264 completed bacterial genomes gave an average chemoreceptor gene count of 14, which was found to be increased in species with high metabolic diversity, low stability of habitat and those with interactions with other living species (Lacal et al., 2010). The category with the highest number of chemoreceptors included soil-dwelling organisms such as *Azospirillum lipoferum* or *Bradyrhizobium* sp. strain BTAi1 encoding 63 and 60 predicted chemoreceptors, respectively, and several plant-interacting bacteria, including *A. caulinodans* ORS571 encoding 43 genes, *R. leguminosarum* bv. *viciae* 3841 encoding 26 genes and *B. diazoefficiens* USDA110 encoding 36 genes (Scharf et al., 2016). In contrast, *E. coli*, a human gut microbe, has only 5 chemoreceptor genes. A mutant of *Azorhizobium caulinodans* ORS571 with the chemotaxis cluster deleted was defective in *Sesbania rostrata* root surface colonization and competitive nodulation (Liu et al., 2018a). In *R. leguminosarum* biovar *viciae* VF39SM, deletion of the chemotaxis receptors *mcpB* or *mcpC* resulted in a significant reduction of nodulation competitiveness on pea plants, although the ability to nodulate was not affected (Yost et al., 1998). Importantly, the VF39SM *mcpC* mutant does not have a competitiveness disadvantage in symbiosis with other plants, indicating that plant specificity is based on the perception of the different exudates each plant secretes and which accordingly drive a defined chemotaxis response (Scharf et al., 2016). In the case of *S. meliloti* RU11, the chemoreceptors McpU and McpX have been found to target amino acids and quaternary ammonium compounds, respectively, being both present in the alfalfa host seed exudate (Webb et al., 2016, 2017a,b). Once inside the plant root, *S. meliloti* motility genes still appear to be expressed in bacteria in the infection thread channel but are completely down-regulated in bacteroids inside mature nodules (Yost, 1998). Interestingly, in other eukaryote-microbe symbioses, similar channels are generated to select for and guide their symbionts through generated gradients, via chemotaxis, toward the symbiosis space (e.g., the slime cavities of Hornwort or the ducts of the bobtail squid) (Raina et al., 2019). However, once inside the nodule, motility and chemotaxis are unnecessary for the now sessile bacteroids. This has been observed in *R. leguminosarum*, with down-regulation of chemoreceptors during bacteroid differentiation to undetectable amounts of expression in bacteroids (Yost et al., 2004; Karunakaran et al., 2009; Tambalo et al., 2010b). This regulation appears unrelated to the low oxygen conditions and organic acid availability inside the nodule (Yost et al., 2004; Tambalo et al., 2010b; Scharf et al., 2016). Thus, both motility and chemotaxis as dispersal strategies and competitive advantages are important aspects of symbiotic rhizobia.

As we have seen, chemotaxis and motility systems in rhizobia have a clear role both in free-living cells in soil and in symbiotic lifestyles, as indicated by their prevalence and the average number of receptor genes (Lacal et al., 2010; Scharf et al., 2016). However, bacterial movement through soil depends on continuous water pathways with their inability to traverse air pockets and, thus, the role of motility is limited to the temporary flooded states of soil formed immediately after rainfall or irrigation (Griffin and Quail, 1968). In addition, reduction in moisture content also decreases exponentially chemotactic movement by preventing the dispersal of chemoattractants and the formation of gradients (Ebrahimi and Or, 2014). Alternatively, environmental forces such as water percolation and the movement of larger organisms such as earthworms provide some degree of microbial dispersal, bypassing discontinuities in water channels (Yang and van Elsas, 2018; King and Bell, 2021). Another method used to bypass air pockets is traveling along eukaryotic pathways such as fungal hyphal networks and plant roots. Colonization of these networks can provide growth and settlement advantages, with chemotaxis and motility systems enabling the bacterium to arrive and establish before competing bacteria. Thus, although bacterial motility and chemotaxis are clearly important for soil competition, their importance is reliant on the favorable state of environmental factors.

The importance of motility and chemotaxis for elite inoculants—based on competitive and effective strains—is equally complex. Although motility and chemotaxis are integral systems for a competitively colonizing inoculant, their shortcomings mentioned above mean that they are not the sole mechanism for soil dispersal. It is thus important for any inoculant strain to be tested in field conditions and applied through efficient and effective methods. Of the two main techniques, it appears that on-seed inoculation is more economical but provides reduced dispersal opportunities, whereas in-furrow inoculation requires a larger quantity of

the inoculant but provides superior dispersal along crop root systems (Deaker et al., 2012; Tecon and Or, 2017). The effectiveness of both application techniques also seems to depend on both the field conditions and the native rhizobial population. Therefore, both motility and chemotaxis should be considered factors in the selection of elite inoculants, together with other dispersal strategies.

CONCLUSIONS

Improvements in symbiont inoculants depend on improvements in (1) understanding of motility and chemotaxis systems in rhizobia, (2) observations of motility and chemotaxis processes in the soil and (3) fast-throughput assays for individual inoculant selection. Firstly, more detailed knowledge of the chemotaxis and motility systems in rhizobia could determine the applicability of studies in other bacteria, such as *E. coli*, and enable mobility improvements to existing symbiont inoculants. For instance, improved knowledge of the many chemoreceptors with uncharacterized sensor domains could provide critical knowledge of the chemotactic signals that are critical for effective soil motility (Compton and Scharf, 2021). Additionally, assays that emulate field conditions, such as capillary and microfluidic assays, could be used to discover the decision-making logic of soil chemotaxis to allow targeted mimicry in engineered inoculants (Mao et al., 2003; Walsh et al., 2017; Lopez-Farfan et al., 2019). Secondly, improved observations of motility and chemotaxis processes in the soil would provide more detailed information about the heterogeneity of movement in the soil and rhizobial motility at the micro-scale. The micro-scale control of motility in the soil has not previously been directly observed. Potentially, transparent pseudo-soils could enable visual tracking of mobility and dispersal from different inoculation techniques toward crop plants (Bhattacharjee and Datta, 2019; Ma et al., 2019). Finally, inoculant selection could be improved by the development of fast-throughput assays that could assess the dispersal effectiveness of an inoculant. For example, the work by Mendoza-Suarez et al. (2020) describes a fast-throughput assay to test the competitiveness and effectiveness of strains in a particular soil. Similar experiments could be devised to measure the field dispersal properties of candidate strains for inoculant formulations. In addition, they could enable more precise testing of other inoculation strategies, such as porous bag embedding or interactions with motile macroorganisms (King and Bell, 2021). These improvements could enable a faster and more effective generation work-flow for selecting or engineering symbiont inoculants by clarifying the importance of effective soil dispersal and dynamic chemotaxis and motility systems.

AUTHOR CONTRIBUTIONS

SA, CS-C, and PP conceived the project and wrote and edited the manuscript. All authors contributed to the article and approved the submitted version.

FUNDING

This work was supported by Biotechnology and Biological Sciences Research Council [grant BB/M011224/1] and The Leverhulme Trust [grant RPG-2019-246].

REFERENCES

Allard-massicotte, R., Tessier, L., Lecuyer, F., Lakshmanan, V., and Lucier, J. (2016). *Bacillus subtilis* early colonization of *Arabidopsis thaliana* roots. *mBio* 7, e01664-16. doi: 10.1128/mBio.01664-16

Althabegoiti, M. J., Covelli, J. M., Pérez-Giménez, J., Quelas, J. I., Mongiardini, E. J., López, M. F., López-Garcia, S. L., and Lodeiro, A. R. (2011). Analysis of the role of the two flagella of *Bradyrhizobium japonicum* in competition for nodulation of soybean. *FEMS Microbiol. Lett.* 319, 133–139. doi: 10.1111/j.1574-6968.2011.02280.x

Arapov, T. D., Saldaña, R. C., Sebastian, A. L., Ray, W. K., Helm, R. F., and Scharf, B. E. (2020). Cellular stoichiometry of chemotaxis proteins in *Sinorhizobium meliloti*. *J. Bacteriol.* 202:e00141-20. doi: 10.1128/JB.00141-20

Armitage, J. P., and Schmitt, R. (1997). Bacterial chemotaxis: *Rhodobacter sphaeroide* and *Sinorhizobium meliloti* - variations on a theme? *Microbiology* 143, 3671–3682. doi: 10.1099/00221287-143-12-3671

Atieno, M., and Lesueur, D. (2018). Opportunities for improved legume inoculants: enhanced stress tolerance of rhizobia and benefits to agroecosystems. *Symbiosis* 77, 191–205. doi: 10.1007/s13199-018-0585-9

Attmannspacher, U., Scharf, B., and Schmitt, R. (2005). Control of speed modulation (chemokinesis) in the unidirectional rotary motor of *Sinorhizobium meliloti*. *Mol. Microbiol.* 56, 708–718. doi: 10.1111/j.1365-2958.2005.04565.x

Bashan, Y. (1986). Migration of the rhizosphere bacteria *Azospirillum brasilense* and *Pseudomonas fluorescens* towards wheat roots in the soil. *J. Gen. Microbiol.* 132, 3407–3414.

Bashan, Y., and Holguin, G. (1994). Root-to-root travel of the beneficial bacterium *Azospirillum brasilense*. *Appl. Environ. Microbiol.* 60, 2120–2131.

Bashan, Y., and Levanony, H. (1987). Horizontal and vertical movement of *Azospirillum brasilense* Cd in the soil and along the rhizosphere of wheat and weeds in controlled and field environments. *Microbiology* 133, 3473–3480. doi: 10.1099/00221287-133-12-3473

Belyakov, A. Y., Burygin, G. L., Arbatsky, N. P., Shashkov, A. S., Selivanov, N. Y., Matora, L. Y., et al. (2012). Identification of an O-linked repetitive glycan chain of the polar flagellum flagellin of *Azospirillum brasilense* Sp7. *Carbohydr. Res.* 361, 127–132. doi: 10.1016/j.carres.2012.08.019

Berg, H. C. (2003). The rotary motor of bacterial flagella. *Annu. Rev. Biochem.* 72, 19–54. doi: 10.1146/annurev.biochem.72.121801.161737

Bhattacharjee, T., and Datta, S. S. (2019). Bacterial hopping and trapping in porous media. *Nat. Commun.* 10:2075. doi: 10.1038/s41467-019-10115-1

Bible, A., Russell, M. H., and Alexandre, G. (2012). The *Azospirillum brasilense* Che1 chemotaxis pathway controls swimming velocity, which affects transient cell-to-cell clumping. *J. Bacteriol.* 194, 3343–3355. doi: 10.1128/JB.00310-12

Bogino, P., Nievas, F., Banchio, E., and Giordano, W. (2011). Increased competitiveness and efficiency of biological nitrogen fixation in peanut via in-furrow inoculation of rhizobia. *Eur. J. Soil Biol.* 47, 188–193. doi: 10.1016/j.ejsobi.2011.01.005

Burygin, G. L., Shirokov, A. A., Sheluď ko, A. V., Katsy, E. I., Shchygolev, S. Yu., and Mato, L. Yu. (2007). Detection of a sheath on *Azospirillum brasilense* polar flagellum. *Microbiology* 76, 728–734. doi: 10.1134/S0026261707060124

Catlow, H. Y., Glenn, A. R., and Dilworth, M. J. (1990). Does rhizobial motility affect its ability to colonize along the legume root? *Soil Biol. Biochem.* 22, 573–575. doi: 10.1016/0038-0717(90)90196-7

Clock, S. A., Planet, P. J., Perez, B. A., and Figurski, D. H. (2008). Outer membrane components of the tad (tight adherence) secreton of *Aggregatibacter actinomycetemcomitans*. *J. Bacteriol.* 190, 980–990. doi: 10.1128/JB.01347-07

Compton, K. K., and Scharf, B. E. (2021). Rhizobial chemoattractants, the taste and preferences of legume symbionts. *Front. Plant Sci.* 12:686465. doi: 10.3389/fpls.2021.686465

Covelli, J. M., Althabegoiti, M. J., López, M. F., and Lodeiro, A. R. (2013). Swarming motility in *Bradyrhizobium japonicum*. *Res. Microbiol.* 164, 136–144. doi: 10.1016/j.resmic.2012.10.014

Deaker, R., Hartley, E., and Gemell, G. (2012). Conditions affecting shelf-life of inoculated legume seed. *Agriculture* 2, 38–51. doi: 10.3390/agriculture2010038

Dechesne, A., and Smets, B. F. (2012). Pseudomonad swarming motility is restricted to a narrow range of high matric water potentials. *Appl. Environ. Microbiol.* 78, 2936–2940. doi: 10.1128/AEM.06833-11

Delamuta, J. R. M., Scherer, A. J., Ribeiro, R. A., and Hungria, M. (2020). Genetic diversity of *Agrobacterium* species isolated from nodules of common bean and soybean in Brazil, Mexico, Ecuador and Mozambique, and description of the new species *Agrobacterium fabacearum* sp. nov. *Int. J. Syst. Evol. Microbiol.* 70, 4233–4244. doi: 10.1099/ijsem.0.004278

Denton, M. D., Phillips, L. A., Peoples, M. B., Pearce, D. J., Swan, A. D., Mele, P. M., et al. (2017). Legume inoculant application methods: Effects on nodulation patterns, nitrogen fixation, crop growth and yield in narrow-leaf lupin and faba bean. *Plant Soil* 419, 25–39. doi: 10.1007/s11104-017-3317-7

Dogra, G., Purschke, F. G., Wagner, V., Haslbeck, M., Kriehuber, T., Hughes, J. G., et al. (2012). *Sinorhizobium meliloti* CheA complexed with CheS exhibits enhanced binding to CheY1, resulting in accelerated CheY1 dephosphorylation. *J. Bacteriol.* 194, 1075–1087. doi: 10.1128/JB.06505-11

Ebrahimi, A. N., and Or, D. (2014). Microbial dispersal in unsaturated porous media: Characteristics of motile bacterial cell motions in unsaturated angular pore networks. *Water Resour. Res.* 50, 7406–7429. doi: 10.1002/2014wr015897

Eggenhofer, E., Haslbeck, M., and Scharf, B. (2004). MotE serves as a new chaperone specific for the periplasmic motility protein, MotC, in *Sinorhizobium meliloti*. *Mol. Microbiol.* 52, 701–712. doi: 10.1111/j.1365-2958.2004.04022.x

Eggenhofer, E., Rachel, R., Haslbeck, M., and Scharf, B. (2006). MotD of *Sinorhizobium meliloti* and related -proteobacteria is the flagellar-hook-length regulator and therefore reassigned as FliK. *J. Bacteriol.* 188, 2144–2153. doi: 10.1128/JB.188.6.2144-2153.2006

Felix, G., Duran, J. D., Volko, S., and Boller, T. (1999). Plants have a sensitive perception system for the most conserved domain of bacterial flagellin. *Plant J.* 18, 265–276. doi: 10.1046/j.1365-313X.1999.00265.x

Fujii, M., Shibata, S., and Aizawa, S.-I. (2008). Polar, peritrichous, and lateral flagella belong to three distinguishable flagellar families. *J. Mol. Biol.* 379, 273–283. doi: 10.1016/j.jmb.2008.04.012

Galajda, P., Keymer, J., Chaikin, P., and Austin, R. (2007). A wall of funnels concentrates swimming bacteria. *J. Bacteriol.* 189, 8704–8707. doi: 10.1128/JB.01033-07

Ganusova, E. E., Vo, L. T., Mukherjee, T., and Alexandre, G. (2021). Multiple CheY proteins control surface-associated lifestyles of *Azospirillum brasilense*. *Front. Microbiol.* 12:664826. doi: 10.3389/fmicb.2021.664826

Gao, S., Wu, H., Yu, X., Qian, L., and Gao, X. (2016). Swarming motility plays the major role in migration during tomato root colonization by *Bacillus subtilis* SWR01. *Biol. Control* 98, 11–17. doi: 10.1016/j.biocontrol.2016.03.011

Garrido-Sanz, D., Redondo-Nieto, M., Mongiardini, E., Blanco-Romero, E., Duron, D., Quelas, J. I., et al. (2019). Phylogenomic analyses of *Bradyrhizobium* reveal uneven distribution of the lateral and subpolar flagellar systems, which extends to rhizobiales. *Microorganisms* 7:50. doi: 10.3390/microorganisms7020050

Gotz, R., Limmer, N., Ober, K., and Schmitt, R. (1982). Motility and chemotaxis in two strains of *Rhizobium* with complex flagella. *Microbiology* 128, 789–798. doi: 10.1099/00221287-128-4-789

Griffin, D. M., and Quail, G. (1968). Movement of bacteria in moist particulate systems. *Aust. Jnl. Of Bio. Sci.* 21, 579–582. doi: 10.1071/bi9680579

Hamdi, Y. A. (1971). Soil-water tension and the movement of rhizobia. *Soil Biol. Biochem.* 3, 121–126. doi: 10.1016/0038-0717(71)90004-6

Henrichsen, J. (1972). Bacterial surface translocation: a survey and a classification. *Bacteriol. Rev.* 36, 478–503. doi: 10.1128/br.36.4.478-503.1972

Hirota, N., and Imae, Y. (1983). Na+-driven flagellar motors of an alkalophilic *Bacillus* strain YN-1. *J. Biol. Chem.* 258, 10577–10581.

Ho, S.-C., Wang, J. L., Schindler, M., and Loh, J. T. (1994). Carbohydrate binding activities of *Bradyrhizobium japonicum* III. Lectin expression, bacterial binding, and nodulation efficiency. *Plant J.* 5, 873–884. doi: 10.1046/j.1365-313X.1994.5060873.x

Horiuchi, J., Prithiviraj, B., Bais, H. P., Kimball, B. A., and Vivanco, J. M. (2005). Soil nematodes mediate positive interactions between legume plants and rhizobium bacteria. *Planta* 222, 848–857. doi: 10.1007/s00425-005-0025-y

Imam, S., Chen, Z., Roos, D. S., and Pohlschroder, M. (2011). Identification of surprisingly diverse type IV pili, across a broad range of gram-positive bacteria. *PLoS ONE* 6:e28919. doi: 10.1371/journal.pone.0028919

Issa, S., Wood, M., and Simmonds, L. P. (1993). Active movement of chickpea and bean rhizobia in dry soil. *Soil Biol. Biochem.* 25, 951–958. doi: 10.1016/0038-0717(93)90098-V

Iturralde, E. T., Covelli, J. M., Alvarez, F., Perez-Gimenez, J., Arrese-Igor, C., and Lodeiro, A. R. (2019). Soybean-nodulating strains with low intrinsic competitiveness for nodulation, good symbiotic performance, and stress-tolerance isolated from soybean-cropped soils in Argentina. *Front. Microbiol.* 10:1061. doi: 10.3389/fmicb.2019.01061

Iwashkiw, J. A., Vozza, N. F., Kinsella, R. L., and Feldman, M. F. (2013). Pour some sugar on it: the expanding world of bacterial protein O-linked glycosylation. *Mol. Microbiol.* 89, 14–28. doi: 10.1111/mmi.12265

Jiang, N., Liu, W., Li, Y., and Xie, Z. (2016). Comparative genomic and protein sequence analyses of the chemotaxis system of *Azorhizobium caulinodans*. *Acta Microbiol. Sin.* 56, 1256–1265. doi: 10.13343/j.cnki.wsxb.20150500

Jimenez-Sanchez, C., Wick, L. Y., Cantos, M., and Ortega-Calvo, J.-J. (2015). Impact of dissolved organic matter on bacterial tactic motility, attachment, and transport. *Environ. Sci. Technol.* 49, 4498–4505. doi: 10.1021/es5056484

Jones, C. W., and Armitage, J. P. (2015). Positioning of bacterial chemoreceptors. *Trends Microbiol.* doi: 10.1016/j.tim.2015.03.004

Kanbe, M., Yagasaki, J., Zehner, S., Gottfert, M., and Aizawa, S.-I. (2007). Characterization of two sets of subpolar flagella in *Bradyrhizobium japonicum*. *J. Bacteriol.* 189, 1083–1089. doi: 10.1128/JB.01405-06

Kaneko, T., Nakamura, Y., Sato, S., Minamisawa, K., Uchiumi, T., Sasamoto, S., et al. (2002). Complete genomic sequence of nitrogen-fixing symbiotic bacterium *Bradyrhizobium japonicum* USDA110. *DNA Res.* 9, 189–197. doi: 10.1093/dnares/9.6.189

Karmakar, R., and Chandra, R. (2012). Effect of soil type and moisture content on survival, mobility, nodule occupancy of inoculated *Rhizobium leguminosarum* bv. *viciae* and lentil growth. *Int. J. Agric. Environ. Biotechnol.* 5, 7–12. Available online at: https://www.indianjournals.com/ijor.aspx?target=ijor:ijaeb&volume=5&issue=1&article=002

Karunakaran, R., Ramachandran, V. K., Seaman, J. C., East, A. K., Mouhsine, B., Mauchline, T. H., et al. (2009). Transcriptomic analysis of *Rhizobium leguminosarum* biovar *viciae* in symbiosis with host plants *Pisum sativum* and *Vicia cracca*. *J. Bacteriol.* 191, 4002–4014. doi: 10.1128/JB.00165-09

Kearns, D. B. (2010). A field guide to bacterial swarming motility. *Nat. Rev. Microbiol.* 8, 634–644. doi: 10.1038/nrmicro2405

King, W. L., and Bell, T. H. (2021). Can dispersal be leveraged to improve microbial inoculant success? *Trends Biotechnol.* doi: 10.1016/j.tibtech.2021.04.008. [EPub ahead of print].

Kojima, S., and Blair, D. F. (2001). Conformational change in the stator of the bacterial flagellar motor. *Biochemistry* 40, 13041–13050. doi: 10.1021/bi011263o

Krehenbrink, M., and Downie, J. A. (2008). Identification of protein secretion systems and novel secreted proteins in *Rhizobium leguminosarum* bv. *viciae*. *BMC Genomics* 9:55. doi: 10.1186/1471-2164-9-55

Kristich, C. J., and Ordal, G. W. (2002). *Bacillus subtilis* CheD is a chemoreceptor modification enzyme required for chemotaxis. *J. Biol. Chem.* 277, 25356–25362. doi: 10.1074/jbc.M201334200

Lacal, J., Garcia-Fontana, C., Munoz-Martinez, F., Ramos, J. L., and Krell, T. (2010). Sensing of environmental signals: Classification of chemoreceptors according to the size of their ligand binding regions. *Environ. Microbiol.* 12, 2873–2884. doi: 10.1111/j.1462-2920.2010.02325.x

Lauffenburger, D., Aris, R., and Keller, K. (1982). Effects of cell motility and chemotaxis on microbial population growth. *Biophys. J.* 40, 209–219. doi: 10.1016/S0006-3495(82)84476-7

Lee, K.-B., De Backer, P., Aono, T., Liu, C.-T., Suzuki, S., Suzuki, T., et al. (2008). The genome of the versatile nitrogen fixer *Azorhizobium caulinodans* ORS571. *BMC Genomics* 9:271. doi: 10.1186/1471-2164-9-271

Liu, W., Bai, X., Li, Y., Min, J., Kong, Y., and Hu, X. (2020). CheY1 and CheY2 of *Azorhizobium caulinodans* ORS571 regulate chemotaxis and competitive colonization with the host plant. *Appl. Environ. Microbiol.* 86:e00599-20. doi: 10.1128/AEM.00599-20

Liu, W., Sun, Y., Shen, R., Dang, X., Liu, X., Sui, F., et al. (2018a). A chemotaxis-like pathway of *Azorhizobium caulinodans* controls flagella-driven motility, which regulates biofilm formation, exopolysaccharide biosynthesis, and competitive nodulation. *Mol. Plant. Microbe Interact.* 31, 737–749. doi: 10.1094/MPMI-12-17-0290-R

Liu, X., Liu, W., Sun, Y., Xia, C., Elmerich, C., and Xie, Z. (2018b). A *cheZ*-like gene in *Azorhizobium caulinodans* is a key gene in the control of chemotaxis and colonization of the host plant. *Appl. Environ. Microbiol.* 84:e01827-17. doi: 10.1128/AEM.01827-17

Liu, X., Xie, Z., Wang, Y., Sun, Y., Dang, X., and Sun, H. (2019). A dual role of amino acids from *Sesbania rostrata* seed exudates in the chemotaxis response of *Azorhizobium caulinodans* ORS571. *Mol. Plant. Microbe Interact.* 32, 1134–1147. doi: 10.1094/MPMI-03-19-0059-R

Loh, J. T., Ho, S. C., de Feijter, A. W., Wang, J. L., and Schindler, M. (1993). Carbohydrate binding activities of *Bradyrhizobium japonicum*: unipolar localization of the lectin BJ38 on the bacterial cell surface. *Proc. Natl. Acad. Sci. U.S.A.* 90, 3033–3037. doi: 10.1073/pnas.90.7.3033

Lopez-Farfan, D., Reyes-Darias, J. A., Matilla, M. A., and Krell, T. (2019). Concentration dependent effect of plant root exudates on the chemosensory systems of *Pseudomonas putida* KT2440. *Front. Microbiol.* 10:78. doi: 10.3389/fmicb.2019.00078

Lopez-Garcia, S. L., Perticari, A., Piccinetti, C., Ventimiglia, L., Arias, N., Battista, J. J. D., et al. (2009). In-furrow inoculation and selection for higher motility enhances the efficacy of *Bradyrhizobium japonicum* nodulation. *Agron. J.* 101, 357–363. doi: 10.2134/agronj2008.0155x

Lopez-Garcia, S. L., Vezquez, T. E. E., Favelukes, G., and Lodeir, A. R. (2002). Rhizobial position as a main determinant in the problem of competition for nodulation in soybean. *Environ. Microbiol.* 4, 216–224. doi: 10.1046/j.1462-2920.2002.00287.x

Ma, L., Shi, Y., Siemianowski, O., Yuan, B., Egner, T. K., Mirnezami, S. V., et al. (2019). Hydrogel-based transparent soils for root phenotyping *in vivo*. *Proc. Natl. Acad. Sci. U.S.A.* 116, 11063–11068. doi: 10.1073/pnas.1820334116

Macnab, R. M., and Aizawa, S. I. (1984). Bacterial motility and the bacterial flagellar motor. *Annu. Rev. Biophys. Bioeng.* 13, 51–83. 10.1146/annurev.bb.13.060184.000411.

Madsen, E. L., and Alexander, M. (1982). Transport of rhizobium and pseudomonas through soil. *Soil Sci. Soc. Am. J.* 46, 557–560. doi: 10.2136/sssaj1982.03615995004600030023x

Mahler, R. L., and Wollum, A. G. (1981). The influence of soil water potential and soil texture on the survival of *Rhizobium japonicum* and *Rhizobium leguminosarum* isolates in the soil. *Soil Sci. Soc. Am. J.* 45, 761–766. doi: 10.2136/sssaj1981.03615995004500040017x

Mao, H., Cremer, P. S., and Manson, M. D. (2003). A sensitive, versatile microfluidic assay for bacterial chemotaxis. *Proc. Natl. Acad. Sci. U.S.A.* 100, 5449–5454. doi: 10.1073/pnas.0931258100

Mattick, J. S. (2002). Type IV pili and twitching motility. *Annu. Rev. Microbiol.* 56, 289–314. doi: 10.1146/annurev.micro.56.012302.160938

McCarter, L. L. (2006). Regulation of flagella. *Curr. Opin. Microbiol.* 9, 180–186. doi: 10.1016/j.mib.2006.02.001

McDermott, T. R., and Graham, P. H. (1989). *Bradyrhizobium japonicum* inoculant mobility, nodule occupancy, and acetylene reduction in the soybean root system. *Appl. Environ. Microbiol.* 55, 2493–2498.

Meade, H. M., Long, S. R., Ruvkun, G. B., Brown, S. E., and Ausubel, F. M. (1982). Physical and genetic characterization of symbiotic and auxotrophic mutants of *Rhizobium meliloti* induced by transposon Tn5 mutagenesis. *J. Bacteriol.* 149, 114–122. doi: 10.1128/jb.149.1.114-122.1982

Meier, V. M., Muschler, P., and Scharf, B. E. (2007). Functional analysis of nine putative chemoreceptor proteins in *Sinorhizobium meliloti*. *J. Bacteriol.* 189, 1816–1826. doi: 10.1128/JB.00883-06

Meier, V. M., and Scharf, B. E. (2009). Cellular localization of predicted transmembrane and soluble chemoreceptors in *Sinorhizobium meliloti*. *J. Bacteriol.* 191, 5724–5733. doi: 10.1128/JB.01286-08

Mendoza-Suarez, M. A., Geddes, B. A., Sanchez-Canizares, C., Ramarez-Gonzalez, R. H., Kirchhelle, C., Jorrin, B., and Poole, P. S. (2020). Optimizing Rhizobium-legume symbioses by simultaneous measurement of rhizobial competitiveness and N2 fixation in nodules. *Proc. Natl. Acad. Sci. U.S.A.* 117, 9822–9831. doi: 10.1073/pnas.1921225117

Miller, L. D., Yost, C. K., Hynes, M. F., and Alexandre, G. (2007). The major chemotaxis gene cluster of *Rhizobium leguminosarum* bv. *viciae* is essential for competitive nodulation. *Mol. Microbiol.* 63, 348–362. doi: 10.1111/j.1365-2958.2006.05515.x

Mitchell, J. G., Pearson, L., and Dillon, S. (1996). Clustering of marine bacteria in seawater enrichments. *Appl. Environ. Microbiol.* 62, 3716–3721. doi: 10.1128/aem.62.10.3716-3721.1996

Moens, S., Michiels, K., Keijers, V., Van Leuven, F., and Vanderleyden, J. (1995a). Cloning, sequencing, and phenotypic analysis of Laf1, encoding the flagellin of the lateral flagella of *Azospirillum brasilense* Sp7. *J. Bacteriol.* 177, 5419–5426.

Moens, S., Michiels, K., and Vanderleyden, J. (1995b). Glycosylation of the flagellin of the polar flagellum of *Azospirillum brasilense*, a Gram-negative nitrogen-fixing bacterium. *Microbiology* 141, 2651–2657. doi: 10.1099/13500872-141-10-2651

Mongiardini, E. J., Parisi, G. D., Quelas, J. I., and Lodeiro, A. R. (2016). The tight-adhesion proteins TadGEF of *Bradyrhizobium diazoefficiens* USDA 110 are involved in cell adhesion and infectivity on soybean roots. *Microbiol. Res.* 182, 80–88. doi: 10.1016/j.micres.2015.10.001

Mongiardini, E. J., Quelas, J. I., Dardis, C., Althabegoiti, M. J., and Lodeiro, A. R. (2017). Transcriptional control of the lateral-flagellar genes of *Bradyrhizobium diazoefficiens*. *J. Bacteriol.* 199, e00253-17. doi: 10.1128/JB.00253-17

Mukherjee, T., Elmas, M., Vo, L., Alexiades, V., Hong, T., and Alexandre, G. (2019). Multiple CheY homologs control swimming reversals and transient pauses in *Azospirillum brasilense*. *Biophys. J.* 116, 1527–1537. doi: 10.1016/j.bpj.2019.03.006

Mukherjee, T., Kumar, D., Burriss, N., Xie, Z., and Alexandre, G. (2016). *Azospirillum brasilense* chemotaxis depends on two signaling pathways regulating distinct motility parameters. *J. Bacteriol.* 198, 1764–1772. doi: 10.1128/JB.00020-16

Nan, B., and Zusman, D. R. (2016). Novel mechanisms power bacterial gliding motility. *Mol. Microbiol.* 101, 186–193. doi: 10.1111/mmi.13389

Nedeljkovia, M., Sastre, D. E., and Sundbe, E. J. (2021). Bacterial flagellar filament: a supramolecular multifunctional nanostructure. *Int. J. Mol. Sci.* 22:7521. doi: 10.3390/ijms22147521

Parke, J. L., Moen, R., Rovira, A. D., and Bowen, G. D. (1986). Soil water flow affects the rhizosphere distribution of a seed-borne biological control agent, *Pseudomonas fluorescens*. *Soil Biol. Biochem.* 18, 583–588. doi: 10.1016/0038-0717(86)90079-9

Pollitt, E. J. G., and Diggle, S. P. (2017). Defining motility in the *Staphylococci*. *Cell. Mol. Life Sci.* 74, 2943–2958. doi: 10.1007/s00018-017-2507-z

Porter, S. L., Wadhams, G. H., and Armitage, J. P. (2011). Signal processing in complex chemotaxis pathways. *Nat. Rev. Microbiol.* 9, 153–165. doi: 10.1038/nrmicro2505

Quelas, J. I., Althabegoiti, M. J., Jimenez-Sanchez, C., Melgarejo, A. A., Marconi, V. I., Mongiardini, E. J., et al. (2016). Swimming performance of *Bradyrhizobium diazoefficiens* is an emergent property of its two flagellar systems. *Sci. Rep.* 6:23841. doi: 10.1038/srep23841

Raina, J.-B., Fernandez, V., Lambert, B., Stocker, R., and Seymour, J. R. (2019). The role of microbial motility and chemotaxis in symbiosis. *Nat. Rev. Microbiol.* 17, 284–294. doi: 10.1038/s41579-019-0182-9

Rao, C. V., Glekas, G. D., and Ordal, G. W. (2008). The three adaptation systems of *Bacillus subtilis* chemotaxis. *Trends Microbiol.* 16, 480–487. doi: 10.1016/j.tim.2008.07.003

Rebbapragada, A., Johnson, M. S., Harding, G. P., Zuccarelli, A. J., Fletcher, H. M., Zhulin, I. B., et al. (1997). The Aer protein and the serine chemoreceptor Tsr independently sense intracellular energy levels and transduce oxygen, redox, and energy signals for *Escherichia coli* behavior. *Proc. Natl. Acad. Sci. U.S.A.* 94, 10541–10546. doi: 10.1073/pnas.94.20.10541

Rice, M. S., and Dahlquist, F. W. (1991). Sites of deamidation and methylation in Tsr, a bacterial chemotaxis sensory transducer. *J. Biol. Chem.* 266, 9746–9753. doi: 10.1007/s00249-007-0247-y

Rossi, F. A., Medeot, D. B., Liaudat, J. P., Pistorio, M., and Jofre, E. (2016). In *Azospirillum brasilense*, mutations in *flmA* or *flmB* genes affect polar flagellum assembly, surface polysaccharides, and attachment to maize roots. *Microbiol. Res.* 190, 55–62. doi: 10.1016/j.micres.2016.05.006

Rotter, C., Muhlbacher, S., Salamon, D., Schmitt, R., and Scharf, B. (2006). Rem, a new transcriptional activator of motility and chemotaxis in *Sinorhizobium meliloti*. *J. Bacteriol.* 188, 6932–6942. doi: 10.1128/JB.01902-05

Scharf, B., Schuster-Wolff-Bhring, H., Rachel, R., and Schmitt, R. (2001). Mutational analysis of the *Rhizobium lupini* H13-3 and *Sinorhizobium meliloti* flagellin genes: Importance of flagellin A for flagellar filament structure and transcriptional regulation. *J. Bacteriol.* 183, 5334–5342. doi: 10.1128/JB.183.18.5334-5342.2001

Scharf, B. E., Hynes, M. F., and Alexandre, G. M. (2016). Chemotaxis signaling systems in model beneficial plant-bacteria associations. *Plant Mol. Biol.* 90, 549–559. doi: 10.1007/s11103-016-0432-4

Sepehrnia, N., Bachmann, J., Hajabbasi, M. A., Rezanezhad, F., Lichner, L., Hallett, P. D., et al. (2019). Transport, retention, and release of *Escherichia coli* and *Rhodococcus erythropolis* through dry natural soils as affected by water repellency. *Sci. Total Environ.* 694:133666. doi: 10.1016/j.scitotenv.2019.133666

Shelud'ko, A. V., and Katsy, E. I. (2001). Formation of polar bundles of pili and the behavior of *Azospirillum brasilense* cells in a semiliquid Agar. *Microbiology* 70, 570–575. doi: 10.1023/A:1012364323315

Simons, M., van der Bij, A. J., Brand, I., de Weger, L. A., Wijffelman, C. A., and Lugtenberg, B. J. J. (1996). Gnotobiotic system for studying rhizosphere colonization by plant growth-promoting *Pseudomonas* bacteria. *Mol. Plant Microbe Interact.* 9, 600–607. doi: 10.1094/mpmi-9-0600

Singh, T., Srivastava, A. K., and Arora, D. K. (2002). Horizontal and vertical movement of *Pseudomonas fluorescens* toward exudate of *Macrophomina phaseolina* in soil: influence of motility and soil properties. *Microbiol. Res.* 157, 139–148. doi: 10.1078/0944-5013-00142

Son, K., Guasto, J. S., and Stocker, R. (2013). Bacteria can exploit a flagellar buckling instability to change direction. *Nat. Phys.* 9, 494–498. doi: 10.1038/nphys2676

Sourjik, V., Muschler, P., Scharf, B., and Schmitt, R. (2000). VisN and VisR are global regulators of chemotaxis, flagellar, and motility genes in *Sinorhizobium* (*Rhizobium*) *meliloti*. *J. Bacteriol.* 182, 782–788. doi: 10.1128/JB.182.3.782-788.2000

Sourjik, V., and Schmitt, R. (1998). Phosphotransfer between CheA, CheY1, and CheY2 in the chemotaxis signal transduction chain of *Rhizobium meliloti*. *Biochemistry* 37, 2327–2335. doi: 10.1021/bi972330a

Sourjik, V., and Wingreen, N. S. (2012). Responding to chemical gradients: Bacterial chemotaxis. *Curr. Opin. Cell Biol.* 24, 262–268. doi: 10.1016/j.ceb.2011.11.008

Stock, D., Namba, K., and Lee, L. K. (2012). Nanorotors and self-assembling macromolecular machines: The torque ring of the bacterial flagellar motor. *Curr. Opin. Biotechnol.* 23, 545–554. doi: 10.1016/j.copbio.2012.01.008

Taguchi, F., Suzuki, T., Takeuchi, K., Inagaki, Y., Toyoda, K., Shiraishi, T., and Ichinose, Y. (2009). Glycosylation of flagellin from *Pseudomonas syringae* pv. *tabaci* 6605 contributes to evasion of host tobacco plant surveillance system. *Physiol. Mol. Plant Pathol.* 74, 11–17. doi: 10.1016/j.pmpp.2009.08.001

Takeuchi, K., Taguchi, F., Inagaki, Y., Toyoda, K., Shiraishi, T., and Ichinose, Y. (2003). Flagellin glycosylation island in *Pseudomonas syringae* pv. *glycinea* and its role in host specificity. *J. Bacteriol.* 185, 6658–6665. doi: 10.1128/JB.185.22.6658-6665.2003

Taktikos, J., Stark, H., and Zaburdaev, V. (2013). How the Motility Pattern of Bacteria Affects Their Dispersal and Chemotaxis. *PLoS ONE* 8:e81936. doi: 10.1371/journal.pone.0081936

Tambalo, D. D., Bustard, D. E., Del Bel, K. L., Koval, S. F., Khan, M. F., and Hynes, M. F. (2010a). Characterization and functional analysis of seven flagellin genes in *Rhizobium leguminosarum* bv. *viciae*. *BMC Microbiol.* 10:219. doi: 10.1186/1471-2180-10-219

Tambalo, D. D., Del Bel, K. L., Bustard, D. E., Greenwood, P. R., Steedman, A. E., and Hynes, M. F. (2010b). Regulation of flagellar, motility and chemotaxis genes in *Rhizobium leguminosarum* by the VisN/R-Rem cascade. *Microbiology* 156, 1673–1685. doi: 10.1099/mic.0.035386-0

Tecon, R., and Or, D. (2017). Biophysical processes supporting the diversity of microbial life in soil. *FEMS Microbiol. Rev.* 41, 599–623. doi: 10.1093/femsre/fux039

Terahara, N., Sano, M., and Ito, M. (2012). A *Bacillus* flagellar motor that can use both Na+ and K+ as a coupling ion is converted by a single mutation to use only Na+. *PLoS ONE* 7:e46248. doi: 10.1371/journal.pone.0046248

Tomich, M., Planet, P. J., and Figurski, D. H. (2007). The *Tad* locus: postcards from the widespread colonization island. *Nat. Rev. Microbiol.* 5, 363–375. doi: 10.1038/nrmicro1636

Turnbull, G. A., Morgan, J. A. W., Whipps, J. M., and Saunders, J. R. (2001). The role of bacterial motility in the survival and spread of *Pseudomonas fluorescens* in soil and in the attachment and colonisation of wheat roots. *FEMS Microbiol. Ecol.* 36, 21–31. doi: 10.1111/j.1574-6941.2001.tb00822.x

van Elsas, J. D., Trevors, J. T., and van Overbeek, L. S. (1991). Influence of soil properties on the vertical movement of genetically-marked *Pseudomonas fluorescens* through large soil microcosms. *Biol. Fert. Soils* 10, 249–255. doi: 10.1007/BF00337375

Wadisirisuk, P., Danso, S. K. A., Hardarson, G., and Bowen, G. D. (1989). Influence of *Bradyrhizobium japonicum* location and movement on nodulation and nitrogen fixation in soybeans. *Appl. Environ. Microbiol.* 55, 1711–1716.

Walsh, E. J., Feuerborn, A., Wheeler, J. H. R., Tan, A. N., Durham, W. M., Foster, K. R., and Cook, P. R. (2017). Microfluidics with fluid walls. *Nat. Commun.* 8:816. doi: 10.1038/s41467-017-00846-4

Wang, W., Jiang, Z., Westermann, M., and Ping, L. (2012). Three mutations in *Escherichia coli* that generate transformable functional flagella. *J. Bacteriol.* 194, 5856–5863. doi: 10.1128/JB.01102-12

Webb, B. A., Compton, K. K., del Campo, J. S. M., Taylor, D., Sobrado, P., and Scharf, B. E. (2017a). *Sinorhizobium meliloti* chemotaxis to multiple amino acids is mediated by the chemoreceptor McpU. *Mol. Plant Microbe Interact.* 30, 770–777. doi: 10.1094/MPMI-04-17-0096-R

Webb, B. A., Helm, R. F., and Scharf, B. E. (2016). Contribution of individual chemoreceptors to *Sinorhizobium meliloti* chemotaxis towards amino acids of host and nonhost seed exudates. *Mol. Plant Microbe Interact.* 29, 231–239. doi: 10.1094/MPMI-12-15-0264-R

Webb, B. A., Karl Compton, K., Castaneda Saldana, R., Arapov, T. D., Keith Ray, W., Helm, R. F., et al. (2017b). *Sinorhizobium meliloti* chemotaxis to quaternary ammonium compounds is mediated by the chemoreceptor McpX. *Mol. Microbiol.* 103, 333–346. doi: 10.1111/mmi.13561

Wheatley, R. M., Ford, B. L., Li, L., Aroney, S. T. N., Knights, H. E., Ledermann, R., et al. (2020). Lifestyle adaptations of *Rhizobium* from rhizosphere to symbiosis. *Proc. Natl. Acad. Sci. U.S.A.* 117, 23823–23834. doi: 10.1073/pnas.2009094117

Wibberg, D., Blom, J., Jaenicke, S., Kollin, F., Rupp, O., Scharf, B., et al. (2011). Complete genome sequencing of *Agrobacterium* sp. H13-3, the former *Rhizobium lupini* H13-3, reveals a tripartite genome consisting of a circular and a linear chromosome and an accessory plasmid but lacking a tumor-inducing Ti-plasmid. *J. Biotechnol.* 155, 50–62. doi: 10.1016/j.jbiotec.2011.01.010

Wisniewski-Dye, F., Borziak, K., Khalsa-Moyers, G., Alexandre, G., Sukharnikov, L. O., Wuichet, K., et al. (2011). *Azospirillum* genomes reveal transition of bacteria from aquatic to terrestrial environments. *PLoS Genet.* 7:e1002430. doi: 10.1371/journal.pgen.1002430

Worrall, V., and Roughley, R. J. (1991). Vertical movement of *Rhizobium leguminosarum* bv. *trifolii* in soil as influenced by soil water potential and water flow. *Soil Biol. Biochem.* 23, 485–486. doi: 10.1016/0038-0717(91)90014-B

Worrall, V. S., and Roughley, R. J. (1976). The effect of moisture stress on infection of *Trifolium subterraneum* L. By *Rhizobium trifolii* Dang. *J. Exp. Bot.* 27, 1233–1241. doi: 10.1093/jxb/27.6.1233

Wuichet, K., and Zhulin, I. B. (2010). Origins and diversification of a complex signal transduction system in prokaryotes. *Sci. Signal.* 3, 1–14. doi: 10.1126/scisignal.2000724

Xie, L., Altindal, T., Chattopadhyay, S., and Wu, X.-L. (2011). Bacterial flagellum as a propeller and as a rudder for efficient chemotaxis. *Proc. Natl. Acad. Sci. U.S.A.* 108, 2246–2251. doi: 10.1073/pnas.1011953108

Yang, P., and van Elsas, J. D. (2018). Mechanisms and ecological implications of the movement of bacteria in soil. *Appl. Soil Ecol.* 129, 112–120. doi: 10.1016/j.apsoil.2018.04.014

Yost, C. K. (1998). Characterization of *Rhizobium leguminosarum* genes homologous to chemotaxis chemoreceptors.

Yost, C. K., Del Bel, K. L., Quandt, J., and Hynes, M. F. (2004). *Rhizobium leguminosarum* methyl-accepting chemotaxis protein genes are down-regulated in the pea nodule. *Arch. Microbiol.* 182, 505–513. doi: 10.1007/s00203-004-0736-7

Yost, C. K., Rochepeau, P., and Hynes, M. F. (1998). *Rhizobium leguminosarum* contains a group of genes that appear to code for methyl-accepting chemotaxis proteins. *Microbiology* 144, 1945–1956. doi: 10.1099/00221287-144-7-1945

Young, J. P. W., Crossman, L. C., Johnston, A. W. B., Thomson, N. R., Ghazoui, Z. F., Hull, K. H., et al. (2006). The genome of *Rhizobium leguminosarum* has recognizable core and accessory components. *Genome Biol.* 7. doi: 10.1186/gb-2006-7-4-r34

Zatakia, H. M., Arapov, T. D., Meier, V. M., and Scharf, B. E. (2017). Cellular stoichiometry of methyl-accepting chemotaxis proteins inx *Sinorhizobium meliloti*. *J. Bacteriol.* 200:e00614-17. doi: 10.1128/JB.00614-17

Zatakia, H. M., Nelson, C. E., Syed, U. J., and Scharf, B. E. (2014). ExpR coordinates the expression of symbiotically important, bundle-forming Flp pili with quorum sensing in *Sinorhizobium meliloti*. *Appl. Environ. Microbiol.* 80, 2429–2439. doi: 10.1128/AEM.04088-13

Zhuang, X.-Y., and Lo, C.-J. (2020). Construction and loss of bacterial flagellar filaments. *Biomolecules* 10:1528. doi: 10.3390/biom10111528

Zhulin, I. B., and Armitage, J. P. (1993). Motility, chemokinesis, and methylation-independent chemotaxis in *Azospirillum brasilense*. *J. Bacteriol.* 175, 952–958.

Conflict of Interest: The authors declare that the research was conducted in the absence of any commercial or financial relationships that could be construed as a potential conflict of interest.

Publisher's Note: All claims expressed in this article are solely those of the authors and do not necessarily represent those of their affiliated organizations, or those of the publisher, the editors and the reviewers. Any product that may be evaluated in this article, or claim that may be made by its manufacturer, is not guaranteed or endorsed by the publisher.

frontiers in Plant Science

ORIGINAL RESEARCH
published: 12 November 2021
doi: 10.3389/fpls.2021.696450

The *Lotus japonicus* ROP3 Is Involved in the Establishment of the Nitrogen-Fixing Symbiosis but Not of the Arbuscular Mycorrhizal Symbiosis

Ivette García-Soto[1,2], Raphael Boussageon[3], Yareni Marlene Cruz-Farfán[1], Jesus Daniel Castro-Chilpa[1], Liz Xochiquetzal Hernández-Cerezo[1], Victor Bustos-Zagal[1], Alfonso Leija-Salas[1], Georgina Hernández[1], Martha Torres[1], Damien Formey[1], Pierre-Emmanuel Courty[3], Daniel Wipf[3], Mario Serrano[1]* and Alexandre Tromas[1,4]**

[1] Centro de Ciencias Genómicas, Universidad Nacional Autónoma de México, Cuernavaca, Mexico, [2] Programa de Doctorado en Ciencias Bioquímicas, Centro de Ciencias Genómicas, Universidad Nacional Autónoma de México, Cuernavaca, Mexico, [3] Agroécologie, AgroSup Dijon, CNRS, Université de Bourgogne, INRAE, Université Bourgogne Franche-Comté, Dijon, France, [4] La Cité College, Bureau de la Recherche et de l'Innovation, Ottawa, ON, Canada

OPEN ACCESS

Edited by:
Christian Staehelin,
Sun Yat-sen University, China

Reviewed by:
Viktor E. Tsyganov,
All-Russian Research Institute of Agricultural Microbiology of the Russian Academy of Agricultural Sciences, Russia
Danxia Ke,
Xinyang Normal University, China

***Correspondence:**
Ivette García-Soto
ivette.garcia@ibt.unam.mx
Mario Serrano
serrano@ccg.unam.mx
Alexandre Tromas
ATroma@lacitec.on.ca

Specialty section:
This article was submitted to Plant Symbiotic Interactions, a section of the journal Frontiers in Plant Science

Received: 16 April 2021
Accepted: 25 October 2021
Published: 12 November 2021

Citation:
García-Soto I, Boussageon R, Cruz-Farfán YM, Castro-Chilpa JD, Hernández-Cerezo LX, Bustos-Zagal V, Leija-Salas A, Hernández G, Torres M, Formey D, Courty P-E, Wipf D, Serrano M and Tromas A (2021) The Lotus japonicus ROP3 Is Involved in the Establishment of the Nitrogen-Fixing Symbiosis but Not of the Arbuscular Mycorrhizal Symbiosis. Front. Plant Sci. 12:696450. doi: 10.3389/fpls.2021.696450

Legumes form root mutualistic symbioses with some soil microbes promoting their growth, rhizobia, and arbuscular mycorrhizal fungi (AMF). A conserved set of plant proteins rules the transduction of symbiotic signals from rhizobia and AMF in a so-called common symbiotic signaling pathway (CSSP). Despite considerable efforts and advances over the past 20 years, there are still key elements to be discovered about the establishment of these root symbioses. Rhizobia and AMF root colonization are possible after a deep cell reorganization. In the interaction between the model legume *Lotus japonicus* and *Mesorhizobium loti*, this reorganization has been shown to be dependent on a SCAR/Wave-like signaling module, including Rho-GTPase (ROP in plants). Here, we studied the potential role of ROP3 in the nitrogen-fixing symbiosis (NFS) as well as in the arbuscular mycorrhizal symbiosis (AMS). We performed a detailed phenotypic study on the effects of the loss of a single ROP on the establishment of both root symbioses. Moreover, we evaluated the expression of key genes related to CSSP and to the rhizobial-specific pathway. Under our experimental conditions, *rop3* mutant showed less nodule formation at 7- and 21-days post inoculation as well as less microcolonies and a higher frequency of epidermal infection threads. However, AMF root colonization was not affected. These results suggest a role of ROP3 as a positive regulator of infection thread formation and nodulation in *L. japonicus*. In addition, CSSP gene expression was neither affected in NFS nor in AMS condition in *rop3* mutant. whereas the expression level of some genes belonging to the rhizobial-specific pathway, like *RACK1*, decreased in the NFS. In conclusion, ROP3 appears to be involved in the NFS, but is neither required for intra-radical growth of AMF nor arbuscule formation.

Keywords: symbiotic nitrogen fixation, ROP, rho-GTPase, *Lotus japonicus*, arbuscular mycorrhizal symbiosis

Abbreviations: NFS, nitrogen-fixing symbiosis; AMS, arbuscular mycorrhizal symbiosis; AMF, arbuscular mycorrhizal fungi; DAI, days after inoculation; ROPs, rho of plants; IT, infection thread; RH, root hair; NFs, nodulation factors; CSSP, common symbiosis signaling pathway; RSP, rhizobial signaling pathway; GEF, guanine nucleotide exchange factor; GAP, GTPase-activating proteins; GDI, guanine nucleotide dissociation inhibitor.

INTRODUCTION

Roots of legumes interact with multiple soil beneficial microorganisms, including bacteria and fungi. Legumes can form two main root symbioses: the nitrogen-fixing symbiosis (NFS) and the arbuscular-mycorrhizal symbiosis (AMS). In NFS, plants offer an anoxic environment, nutrients and organic acids to the diazotrophic bacteria, which in exchange provide fixed atmospheric nitrogen to the host plant. This process occurs in the nodule, a root structure derived from inner or outer cortical cells, depending on whether the organ belongs to the indeterminate or determinate type, respectively (Roy et al., 2020). In AMS, hyphae of arbuscular mycorrhizal fungi (AMF) penetrate root epidermis, colonize cortical cells and form highly branched structures called arbuscules. This ancestral interaction allows plants to improve the use of natural soil resources including macronutrients (e.g., phosphorus and nitrogen) and water, and to better respond to abiotic and biotic stresses (Gianinazzi et al., 2010; Wipf et al., 2019).

The legume-rhizobia symbiosis is initiated by a molecular dialogue. Plant roots exude flavonoids and betaines that induce the expression of bacterial *nod* genes (Peters et al., 1986; Redmond et al., 1986; Dénarié and Cullimore, 1993). *nod* genes encode nodulation factors (NFs) that trigger several molecular responses in legumes, including intracellular Ca^{2+} oscillation (Charpentier and Oldroyd, 2013), root hair (RH) deformation, and NF-induced signaling genes (Geurts et al., 2005).

A conceptual signaling cascade, the so-called '*common symbiosis signaling pathway*' (CSSP), is shared between the NFS and AMS (Oldroyd, 2013). The CSSP signaling is triggered by the perception of NFs (rhizobia) and Myc (mycorrhizal fungus) factors at the plasma membrane, leading to nuclear calcium spiking. In the model legume *Lotus japonicus*, this pathway includes genes such as the *SYMRK* receptor-like kinase, the nucleoporins *NUP85*, *NUP133* and *NENA*, cationic channels *CASTOR* and *POLLUX*, located on the nuclear envelope and a nuclear calcium- and calmodulin-dependent kinase, *CCaMK* and its substrate *CYCLOPS* (Genre and Russo, 2016; Roy et al., 2020). SYMRK interacts with the NF receptors in Lotus and is required for the Myc Factor induced calcium spiking. CCaMK interprets the rhythmic nuclear calcium elevations and interacts with the transcription factor CYCLOPS. In the NFS, CYCLOPS activates NIN and ERN1 that trigger expression of genes required for formation of an infection thread (IT) and nodule organogenesis. In the AMS, CYCLOPS activates RAM1, one of the best characterized mycorrhizal-induced TF, that is essential for the development of the highly branched arbuscular form of the inner cortex. RAM1 is thus involved in both nutrient uptake from, as well as carbon supply to, the fungus (Rich et al., 2017; Pimprikar and Gutjahr, 2018).

Recent evidence has raised the importance of the cytoskeleton during the formation of both symbiosis (Liu et al., 2020; Roy et al., 2020). In the NFS, reorganization of actin filaments has been related to several events, including IT formation, cell membrane remodeling, and nucleus relocation (Timmers, 2008). Additionally, it has been reported that the presence of NFs induces RH deformation as a consequence of actin filament remodeling (Cárdenas et al., 1998). Progression of the IT is directed by bacterial growth and division of the cell wall, as well as by extracellular matrix deposition and actin remodeling (Timmers, 2008). Interestingly, mutations in genes coding for proteins belonging to SCAR/WAVE complex, that regulates the actin remodeling complex, result in defects in rhizobial infection and nodule colonization (Yokota et al., 2009). In AMS, host cells undergo a drastic reorganization of cellular organelles, including the nucleus and endoplasmic reticulum (ER), as well as changes in the membrane and cell wall that allow hyphal progression through plant tissues. Actin filaments and microtubules form a dense network in arbuscule-containing cells involved in vesicle trafficking and membrane protein localization. Interestingly, the cytoskeleton is also actively reorganized in adjacent cells and in cells contacting the intercellular hyphae (Genre and Bonfante, 1998).

In the past years, the importance of Rho GTPases as key elements for the rearrangement of the cytoskeleton during symbiotic interactions was demonstrated (Yalovsky et al., 2008; Fu, 2010). GTPases hydrolyze nucleotide guanosine triphosphate (GTP) to guanosine diphosphate (GDP) and are functioning as a molecular switch in various signaling pathways (Yang, 2002). In beans, GTPases were demonstrated to participate in vesicle trafficking involved in polar growth of RHs (Blanco et al., 2009). Another group of small GTPase proteins called ROPs (rho of plants) have been described to regulate several biological processes such as endocytosis, exocytosis, auxin response, secondary cell wall, response to oxidative stress, and response to bacteria and fungi (Rivero et al., 2019).

Rho of plants belong to a highly conserved multigenic family and act as molecular switches, oscillating between an active state (bound to GTP) and inactive state (bound to GDP). Activation induces a conformational change that allows interaction with their molecular effectors. ROPs are regulated by other protein families such as the activators ROPGEF (GDP/GTP Exchange Factors), the inactivators ROPGAP (GTPase Activating Proteins) and the chaperon proteins ROPGDI (GDP Dissociation Inhibitors) (Rivero et al., 2019). ROPGEFs catalyze GDP/GTP exchange and activate ROPs, while ROPGAPs increase ROP-GTP hydrolysis. Additionally, GDIs participate in determining ROP subcellular localization and protein half-life (Feiguelman et al., 2018). From a structural point of view, ROPs contain a catalytic N-terminal domain, where GTP, GDP, and effectors interact. The C-terminal domain is a hypervariable region containing prenylation or geranylation sites. These post-translational modifications depend on the hypervariable sequence and are used to classify ROPs as ROP type I or ROP type II proteins (Feiguelman et al., 2018).

It has been proposed that ROPs are involved in the establishment of legume-rhizobia interactions (Ke et al., 2012, 2016; Liu et al., 2020). During the NFS, MtROP10 from *Medicago truncatula* and ROP6 from *L. japonicus* interact directly with NF receptors, suggesting a possible participation of ROPs in the NFS signaling pathway (Ke et al., 2012; Lei et al., 2015). Additionally, it was recently reported that ROP6, one of the 10 ROP members in *L. japonicus,* is important for the formation and maintenance of the IT through its activation by the GEF

protein SPIKE1. ROP6 is also related to the NFS *via* its interaction with the clathrin heavy chain 1 (CHC1) protein, stimulating the early nodulation gene expression and rhizobial infection (Wang et al., 2015). Recently, two studies showed that GEF2, phosphorylated by NFR1/LYK3, controls the NFS in soybean and *M. truncatula* through the activation of ROP9 (Wang et al., 2021). In soybean, this regulation occurs through the association of ROP9 with a scaffold protein Receptor for Activated C Kinase (RACK1), which plays a pivotal role in *Phaseolus vulgaris* NFS (Islas-Flores et al., 2012).

However, no evidence for the role of ROPs in the AMS has been described to date, suggesting that ROPs act independently of CSSP. To investigate whether other ROP family members could be part of the NFS regulation and to better understand the role of ROPs in mutualistic symbioses, we decided to further study the potential role of *ROP1*, *ROP3,* and *ROP10* during the NFS and the role of *ROP3* during AMS in *L. japonicus*. We found that *ROP3* is involved in the establishment of the NFS and that this gene is not required for the AMS in *L. japonicus*.

MATERIALS AND METHODS

Biological Material

Lotus japonicus mutant lines were obtained from the LORE1 mutant database[1] (Małolepszy et al., 2016). *rop1, rop3,* and *rop10* ID mutant lines were 30000786, 30000537, and 30058643, respectively. Wild-type Gifu wild-type seeds and *Mesorhizobium loti* (strain MAFF303099) were kindly provided by Krzysztof Szczyglowski's laboratory. The mycorrhizal fungus *Rhizophagus irregularis* DAOM 197198 was obtained from Agronutrition (Carbonne, France).

Genotyping

To confirm the genotype of LORE1 insertion mutants, genomic DNA from each mutant was extracted and amplified by PCR using specific primers (**Supplementary Table 1**) as previously described (Urbański et al., 2012). Genomic DNA was extracted from each mutant and Gifu wild-type young trifoliate leaves according to Alonso and Stepanova (2015). DNA concentration was evaluated by UV spectrophotometry (NanoDrop™, Thermo Fisher Scientific™, United States).

Construction of Binary Vectors for Plant Transformation

For functional complementation, a 2,000 bp fragment, located prior to the start codon of the *ROP3* promoter, was amplified from genomic DNA using primers described in the **Supplementary Table 1**. The amplicon was then purified, digested with restriction enzymes *Aat*II and *Sal*I, and inserted into the binary vector PC-GW (Dalal et al., 2015) using DNA ligase (#EL0011). The coding sequence of *ROP3* was synthesized by GenScript[2], digested with *Aat*II and *Xba*I, and ligated into the binary vector PC-GW mCherry (Dalal et al., 2015).

[1]https://lotus.au.dk/

[2]https://www.genscript.com/

Plant Transformation and Functional Complementation

Agrobacterium rhizogenesis AR10 strains containing the binary vectors were used to transform *L. japonicus* roots. Seeds were germinated for a week in B&D medium (Broughton and Dilworth, 1971) supplemented with 1.2% agar and were kept in the dark to elongate hypocotyls. After 2 days, hypocotyls were punched with a needle covered with *A. rhizogenesis* AR10. Plants were transferred to a new B&D plate and kept in the dark for 24 h, and then transferred to a growth chamber for 2 weeks (28% humidity, 22°C and 16/8 h photoperiod). Transformed roots were selected using mCherry fluorescence and transferred to vermiculite.

To perform functional complementation, Gifu wild-type, and *rop3* plants were transformed with the empty vector and the binary vector containing the promoter and the coding region of *ROP3* (*pROP3:ROP3*). Plants were inoculated with *M. loti* 7 days after being transferred to vermiculite to count the nodules. Results were obtained from 3 independent experiments ($n > 15$ roots).

Plant Growth Conditions

Seeds were surface sterilized in a solution containing 75% ethanol and 0.1% SDS for 5 min. The solution was then discarded and seeds were treated with a 20% bleach + 0.1% SDS solution for 2 min and rinsed 10 times with sterile water. Afterward, seeds were incubated at room temperature under continuous shaking overnight. Seeds were then placed on Petri dishes containing wet Whatman manuscript and incubated for 1 week in a growth chamber at 21–25°C and 16/8 h photoperiod. Seedlings were transferred to pots containing vermiculite supplemented with either B&D medium (Broughton and Dilworth, 1971) with minimal nitrogen concentration (0.5 mM) for inoculated plants or B&D medium supplemented with 1 mM nitrogen for non-inoculated plants. During the first week, pots were covered with a plastic bag and gradually opened to allow proper acclimation of the plants.

Mesorhizobium loti Inoculation

Lotus japonicus plants were inoculated with *M. loti* 7 days after transfer to pots, by pipetting 1 mL of bacteria grown 2 days in TY medium at 28°C until reaching a OD of 0.8 at 600 nm and resuspended in tap water as previously described (Pajuelo and Stougaard, 2005).

Characterization of Symbiosis-Related Phenotypes

Infections threads (ITs), nodulation events (number of nodules and nodule primordia), microcolonies and percentage of deformed RHs were determined 7 or 21 days after inoculation (DAI). Visualization of the symbiotic bacteria was achieved through LacZ staining of the *M. loti* MAFF303099 carrying the *hemA:lacZ* reporter gene (Wopereis et al., 2000). *LacZ* staining was performed as previously described (Díaz et al., 2005). Roots were mounted in water and observed under a 20x objective on a Zeiss Axioskop 2 (Zeiss™, Germany)

coupled to a Zeiss AxioCam MRc camera. IT and nodulation events were determined by counting total IT or nodulation events divided by the length of the primary root. All values correspond to $n > 15$ roots per line and are derived from three independent experiments.

Gene Expression Analysis

Total RNA was isolated from roots at 7 DAI for the *M. loti* interaction and 2 month post inoculation (MPI) for the *R. irregularis* interaction. RNA was isolated using the Plant/Fungi Total RNA Purification Kit according to the manufacturer's instructions (NORGEN BIOTEK CORP., Canada) and treated with RNase free DNase I, (Thermo Fisher Scientific™, United States). The concentration of purified total RNAs were estimated using a UV spectrophotometer (NanoDrop™, Thermo Fisher Scientific™, United States). First-strand cDNA was synthesized using 1 μg of total RNAs and SCRIPT cDNA Synthesis Kit according to the manufacturer's instructions (Jena Bioscience, Germany). Real-time quantitative PCR was conducted with Maxima SYBR Green/ROX qPCR Master Mix (2X) (Thermo Fisher Scientific™, United States) and 10 μM gene-specific primers (**Supplementary Table 1**). Each PCR (10 μL final volume) contained 4 μL of cDNA, 1 μl of primers mixture, and 5 μL of Maxima SYBR Green/ROX qPCR Master Mix. Thermocycling conditions were as follows: an initial holding stage of 2 min at 50°C, followed by 15 min at 95°C, then 40 cycles of denaturation for 15 s at 95°C, annealing for 30 s at 62°C and extension for 30 s at 72°C, with a final melt gradient starting from 60°C and heating to 95°C at a rate of 0.3°C s^{-1}. The real-time PCRs were carried out in the StepOnePlus™ Real-Time PCR System (Applied Biosystems™, United States). The PCR efficiency was confirmed by establishment of a standard curve. The *PROTEIN PHOSPHATASE 2A* (*PP2A*), UBIQUITIN (*UBC*), and *ATP SYNTHASE* (*ATPs*) genes served as internal controls. Three independent experiments each with 3 biological replicates were performed for each tested condition.

Rhizophagus irregularis Inoculation

Lotus japonicus seeds were surface-sterilized (2.5% KClO, 10 min), then rinsed with sterile deionized water several times and soaked in sterile deionized water overnight. Seeds were pre-germinated on autoclaved sand (121°C, 30 min) at 25°C for 24 h and then grown in the dark at room temperature for 72 h. One plantlet was transplanted per 1.5-L pot filled with an autoclaved (121°C, 30 min) quartz sand (diameter < 4 mm, Kaltenhouse, France): zeolithe (diameter 1– 2.5 mm, Symbiom, Czechia) mixture (1:1, *v:v*). To establish mycorrhizal and rhizobial symbioses, plantlets were individually inoculated with the arbuscular mycorrhizal fungus (AMF) *R. irregularis* DAOM 197198 (1 ml of a suspension of 100 spores/mL). For the controls (non-inoculated plantlets), the same amount of autoclaved inoculum was added to the mixture. Plants were grown under controlled conditions (12 h of light at 24°C and 12 h of dark at 22°C) and weekly fertilized with a modified Hoagland solution (P concentration: 0.5 mM; N concentration: 6 mM) (Calabrese et al., 2019). After 2 months of growth post-inoculation (vegetative state), plants were gently dug out. Roots were divided into two subsamples; one of 100 mg was snap-frozen in liquid nitrogen and stored at −80°C for gene expression analysis and one was used to determine the degree of AMF root colonization. Remaining root samples and shoot materials were dried at 60°C for 48 h and weighed. Root subsamples were immersed in 10% KOH and stored in 20-ml glass tubes at 4°C overnight. Roots were rinsed under tap water and immersed in 2% HCl at room temperature for 1 h. Roots were rinsed under tap water, immersed in 0.05% trypan blue and stored at 4°C overnight. Roots were rinsed again under tap water and destained in lactic acid glycerol (3:1). Total root colonization was measured using the method described by Trouvelot et al. (1986).

Phosphorus, Nitrogen, and Carbon Quantification

To measure N uptake by plants, 15N-enriched ammonium nitrate was applied once in each pot at 1 month post-inoculation ($15NH_4 15NO_3$, > 98% 15N; Sigma Aldrich, St. Louis, United States) to reach δ 15N = + 4450, corresponding to an enrichment of 2% (calculated value using isotopic abundance of the unlabeled and 15N-enriched ammonium nitrate and their molar ratio in the liquid fertilizer). Dry shoot and root materials were ground separately in tungsten tubes using tungsten carbide balls in a Retch MM301 vortexer (Retch GmbH & Co., Haan, Germany). Total N, 15N and C aliquots of 2 mg were weighed for elemental analyses, and their concentrations were determined using an ANCA elemental analyzer/mass spectrometer (Wellience, Dijon, France). To measure phosphorus (P) content of plants, dry leaf material (20 mg) was ashed at 550°C for 8 h. The residue was dissolved in 2 ml H_2O and 100 μl HCl (32%). One ml of the solution was then transferred to a 2-ml Eppendorf tube and centrifuged at 12,000 rpm for 10 min in a benchtop centrifuge. One hundred μl of the supernatant were transferred into a well of a 96-wells microtiter plate. Phosphorus concentration was then measured by the malachite green method (Ohno and Zibilske, 1991).

Statistical Analyses

All graphs and statistical analysis were performed on GraphPad Prism 9. An analysis of variance (ANOVA) was performed on the normalized gene expressions, followed by Tukey's HSD test for separating the means. Differences between means of variables were analyzed by Kruskal-wallis test, followed by *post hoc* Dunn's Multiple Comparison Test. A probability of $P \leq 0.05$ was considered as significant.

RESULTS

The *rop3* Mutant Shows Defects in the *Lotus japonicus- Mesorhizobium loti* Symbiosis but Not in Root Growth

The genome of *L. japonicus* contains 10 *ROP* genes and, to date, few insertional mutants have been generated for these genes, including mutants in *ROP1*, *ROP3*, *ROP6,* and *ROP10*. To assess a potential role of ROPs other than *ROP6* (Ke et al., 2012, 2016)

during the NFS between *L. japonicus* and *M. loti*, we quantified the infection events in *rop1*, *rop3,* and *rop10* mutants. Seven DAI, *rop3* showed a reduction of about 40% in nodules number compared to the wild-type plant (Gifu wild-type), while *rop1* and *rop10* were not different from wild type plants (**Figure 1A** and **Supplementary Figure 1**). These results indicate that from the *ROP* gene mutants analyzed, only *rop3* presented defects in the NFS. To assess the effect of a delay or a real defect in nodule formation, we counted the number of nodules per cm of primary root at 21 DAI. We observed significantly reduced nodulation in *rop3* compared to Gifu wild-type plants, suggesting a strong effect on nodule formation (**Figure 1A**). The insertion in the *rop3* mutant line is located in the 5′UTR region (**Supplementary Figure 2A**). In order to confirm that the transposon insertion in *ROP3′s* 5′UTR altered its expression, we first compared *ROP3* transcript accumulation by qRT-PCR in Gifu wild-type and the *rop3* mutant line. Almost no accumulation of transcript was observed in the insertional mutant as compared to Gifu wild-type, confirming that the insertion impairs *ROP3* expression (**Supplementary Figure 2B**). Additionally, as those insertions lines contained more than one insertion and to ensure that the observed phenotype was due only to the loss of *ROP3* expression, we performed a functional complementation assay. A native copy of *ROP3* was reinserted into the *rop3* background and the complemented *rop3* plants regained the ability to produce a number of nodules similar to Gifu wild-type plants transformed with an empty vector (**Supplementary Figure 2C**). This confirmed that the observed phenotype is associated with the lack of *ROP3* expression.

Rho of plants are known to regulate multiple biological processes (Rivero et al., 2019). Before further characterization of the role of *rop3* during NFS, we wanted to ensure that it would not cause any defect in plant root development. *L. japonicus* Gifu wild-type and *rop3* mutant lines were grown under optimal conditions (soil supplemented with nitrogen) and their primary root length was measured. No significant differences were observed between Gifu wild-type and *rop3* plants (**Figure 1B**). These results suggest that *ROP3* may not be involved in root development but rather during the symbiotic interaction.

Bacterial Infection and Progression Within the Plant Is Hindered in *rop3*

Rhizobial microcolonies in the infection chamber of RH curls, ITs as well as their progressions, were quantified and compared

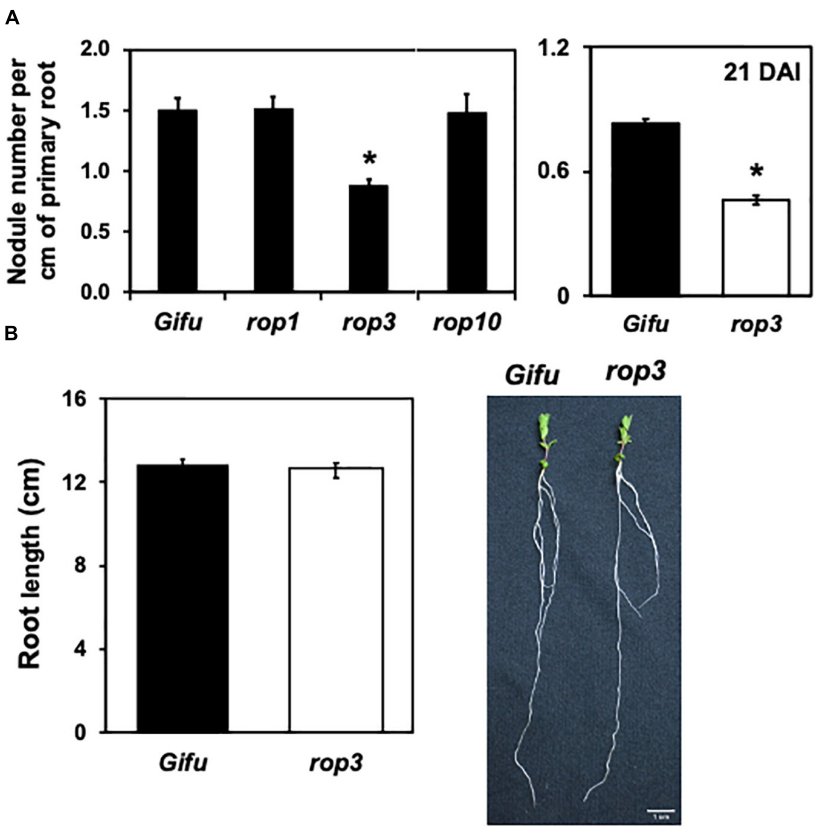

FIGURE 1 | *rop3* mutant presents defects in the *L. japonicus-M. loti* symbiosis. *Lotus japonicus* Gifu wild-type and the indicated mutant lines were inoculated with *M. loti* and **(A)** number of nodules were quantified at 7 DAI (left) and at 21 DAI (right). **(B)** Primary root length of *L. japonicus* plants grown under optimal conditions were measured, and pictures of representative Gifu wild-type and *rop3* plants are shown. Bars represent mean values (± SD) of 3 independent experiments ($n > 15$). The asterisk indicates statistical significance between the indicated mutant and Gifu wild-type according to one way ANOVA test and a *post hoc* analysis ($p < 0.05$).

between Gifu wild-type and *rop3* plants at 7 DAI with *M. loti*. We measured a reduction of about 50% of the number of microcolonies in *rop3* plants compared to Gifu wild-type (**Figure 2A** and **Supplementary Figure 3**). Additionally, *rop3* showed a significant reduction in IT number per cm of root (**Figure 2B**). Moreover, *rop3* produced less cortical IT than Gifu wild-type and exhibited abnormal IT growth arrest in the epidermis and thus not reaching cortical cells (**Figure 2C** and **Supplementary Figure 3**). These results indicate that ROP3 play an important role in the entry and progression of the bacteria into the plant roots.

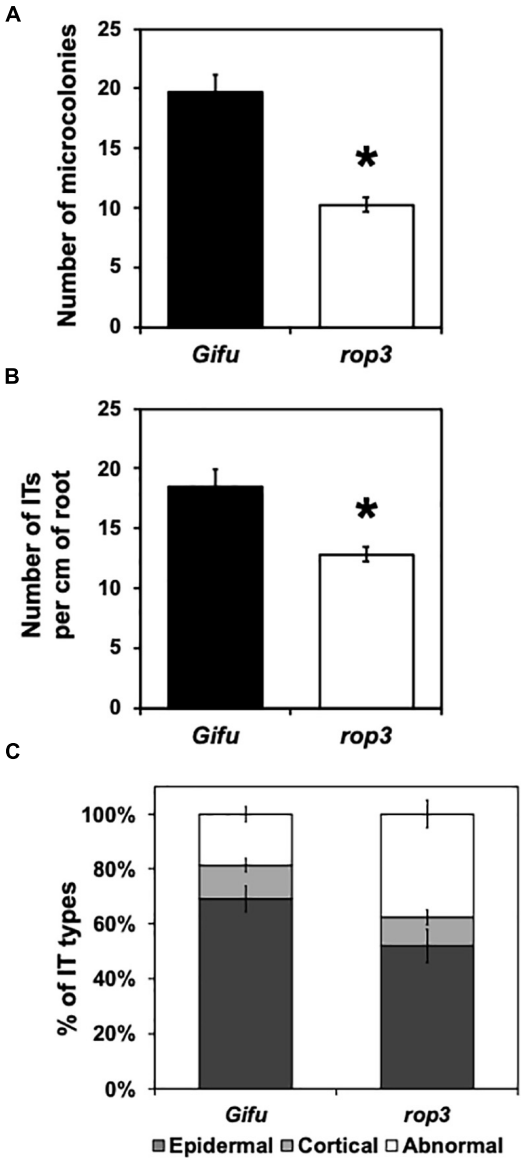

FIGURE 2 | Infection thread progression are modified in the *rop3* mutant. Number of microcolonies **(A)**, infection thread per cm of root **(B),** and Infection thread types **(C)** were quantified on Gifu wild-type and *rop3* plants at 7 DAI with *M. loti*. Bars represent mean values (± SD) of 3 independent experiments ($n > 15$). The asterisk indicates statistical significance between *rop3* and Gifu wild-type according to one way ANOVA test and a *post hoc* analysis ($p < 0.05$).

Root Hair Deformation in Response to Symbiotic Bacteria Is Misregulated in *rop3* Mutant

To further characterize the phenotypic alterations observed in *rop3,* we compared RHs deformation in *rop3* and Gifu wild-type plants (**Figure 3A**), with and without rhizobial inoculation. In non-inoculated plants, *rop3* and Gifu wild-type shared the same low percentage of deformed RHs (**Figure 3B**). However, at 7 DAI, a fraction of Gifu wild-type RHs was deformed in response to the bacteria, but the majority was not deformed and conserved their normal shape. In contrast, *rop3* exhibited a greater number of

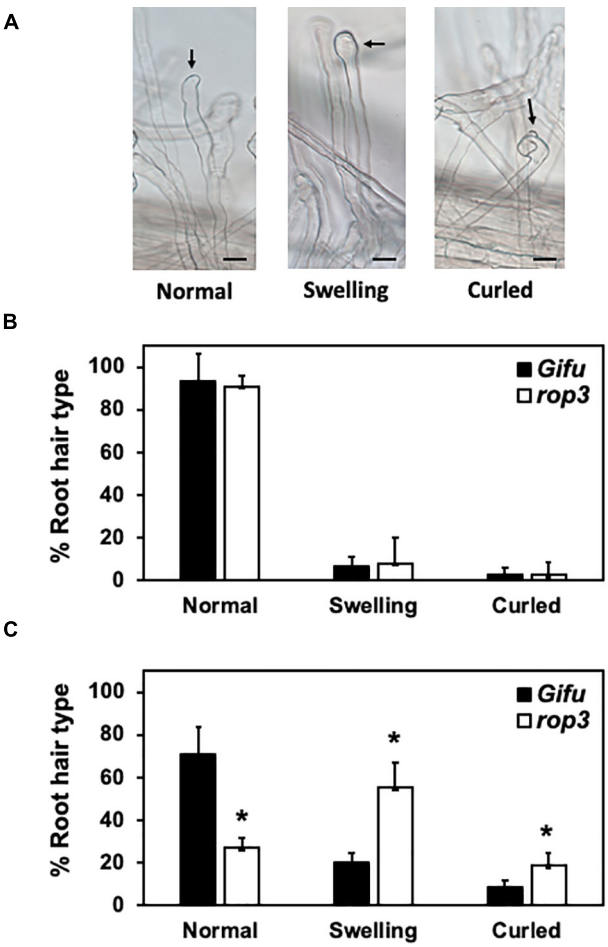

FIGURE 3 | *rop3* plants showed a misregulation of RH deformation after interaction with *M. loti*. RHs deformation types were counted in *rop3* and Gifu wild-type plants. Representative pictures of RH types evaluated in Gifu wild-type and *rop3* plants, arrows point the site of interest, black bar = 40 μm **(A).** RH deformation types without bacteria inoculation **(B)** and at 7 DAI with *M. loti* **(C)**. Bars represent mean values (± SD) of 3 independent experiments ($n > 15$). The asterisk indicates statistical significance between *rop3* and Gifu wild-type according to one way ANOVA test and a *post hoc* analysis ($p < 0.05$).

deformed RHs, both swollen and curled (**Figure 3C**). The absence of ROP3 did not seem to impede RH deformation in response to symbiotic bacteria but rather increased its frequency and extent. These results indicate that ROP3 does not take part in normal RH formation or growth but might be involved in regulating RH deformation responses.

The Benefits of Arbuscular Mycorrhizal Symbiosis Are Not Altered in *rop3* Mutant

Based on the role of *ROP3* in nodulation, we hypothesized that the mutation should also impact the AMS. Shoot and root dry weight were significantly increased when both Gifu wild-type and *rop3* plants were inoculated with *R. irregularis* (**Figures 4A,B**). Frequencies of mycorrhization (F%) and arbuscule abundance (A%) in the root system were similar in Gifu wild-type and *rop3* plants (**Figures 5A,B**). To assess the efficiency of the mycorrhizal symbiosis, P elemental analysis was performed. P contents and P concentrations in shoots and roots were significantly higher in mycorrhizal plants compared to non-mycorrhizal plants in both genotypes (**Figures 5C–F**). We analyzed the expression of three plant mycorrhizal marker genes *AMT2.2, PT4,* and *PT8* genes (Guether et al., 2009; Casieri et al., 2013). Marker genes were induced by the infection with *R. irregularis*, without significant difference between Gifu wild-type and *rop3* (**Supplementary Figure 4**). In both Gifu wild-type and *rop3* plants, inoculation with *R. irregularis* increases N and P content in plant tissues and increased C assimilation compared to control plants (**Supplementary Figure 5**). However, no significant differences were observed between Gifu wild-type and *rop3* plants.

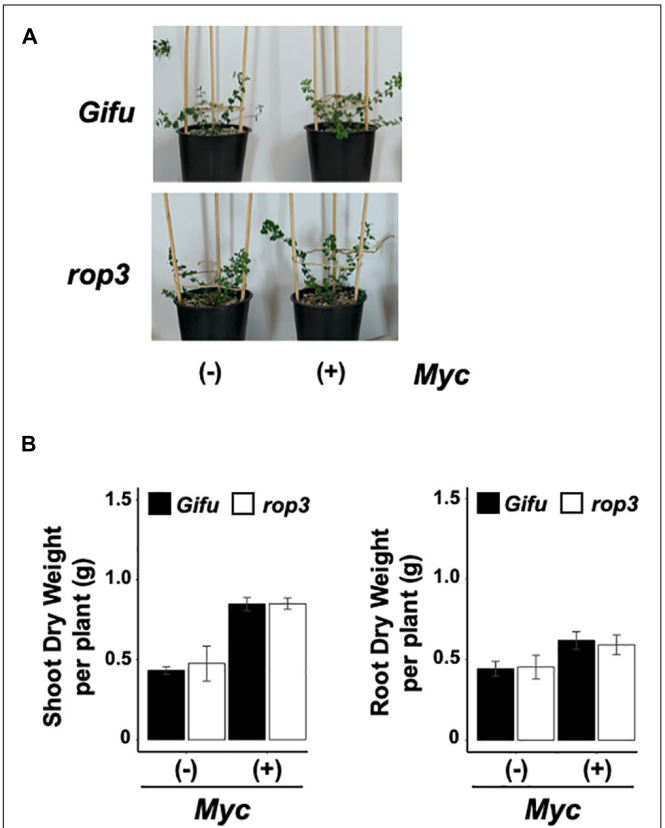

FIGURE 4 | ROP3 does not play a role in AM symbiosis in *L. japonicus*. **(A)** Development of Gifu wild-type and *rop3* plants inoculated with *R. irregularis*. Pictures of representative plants are shown. **(B)** Shoot and root dry weight were determined for Gifu wild-type and *rop3* plants with and without inoculation. Bars represent mean values (± SD) of 3 independent experiments ($n = > 15$).

Expression of Nodulation Signaling Pathway Genes Is Altered in *rop3* Mutant

In legumes, nodule formation is regulated by a complex signaling pathway, including genes from the CSSP and genes specific to the rhizobial signaling pathway (RSP) (Roy et al., 2020). We hypothesized that the expression of some of these genes might be altered in *rop3*, revealing possible explanations for the different phenotypes observed between NFS and AMS. Therefore, we analyzed the relative expression of representative genes of RSP and CSSP in Gifu wild-type and *rop3* plants during both symbioses (**Figure 6**). As expected, *SYMRK*, *CYCLOPS,* and *CCAMK* expression was not impacted by both plants and interactions, which suggests that the reduced number of nodules in *rop3* is not due to an alteration of CSSP gene expression. In contrast, expression of RSP-related genes (*NFR1, NFR5, RACK1*, and *NIN*) was altered in *rop3* compared to Gifu wild-type plants. Particularly, the expression of *RACK1* is highly reduced in *rop3* during the NFS and not in the AMS. The expression of two other RSP genes, *NFR5* and *NIN*, was also altered in *rop3* compared to Gifu wild-type, but in a similar way in both interactions. Hence, the symbiotic phenotype of *rop3* could be due to a functional CSSP but an altered RSP.

DISCUSSION

Biological nitrogen fixation in legumes is regulated by a set of well-described genes, from NF perception to nodule senescence (Roy et al., 2020). One of the first step of rhizobial root infection is the deformation of RHs that allows symbiont penetration in the roots. Recently, Liu et al. (2020) revealed that the absence of ROP6 leads to a reduction of infection events and IT progression in the root. In soybean and *M. truncatula*, ROP9 has also been reported to be a key player of the RSP (Gao et al., 2021; Wang et al., 2021). Here, we show that ROP3, in contrast to ROP1 and ROP10, whose corresponding mutants did not display an altered symbiotic phenotype, takes part in the *L. japonicus-M. loti* symbiosis. ROP3 may play a role in the bacterial infection and then progression within the root. However, in contrast to ROP6, ROP9 and homologs, ROP3 does not seem to play a role in RH formation or growth, but seems to participate in RH deformation in response to rhizobia. The lower number of ITs able to reach the root cortex in *rop3* mutant plants also indicates that ROP3 might be involved in the polarized growth of ITs following rhizobial infection. Additionally, *rop3* mutant shows a reduction in the number of detectable microcolonies trapped in the RH curl that could be due to a modification of the infection

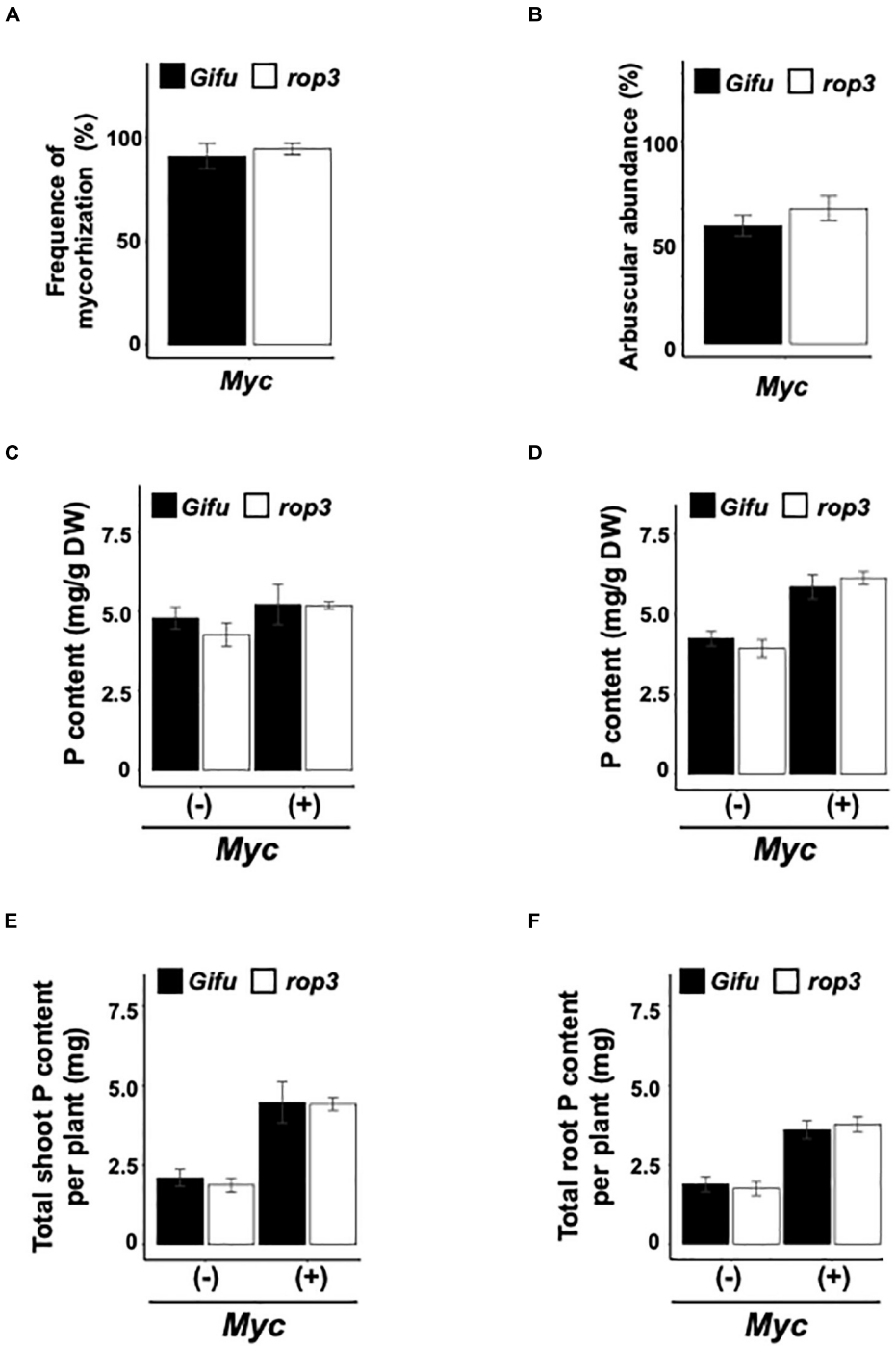

FIGURE 5 | Arbuscular mycorrhizal symbiosis is not altered in the *rop3* mutant. **(A)** Frequency of mycorrhization, **(B)** arbuscular abundance, **(C)** phosphate contents in dried shoots, **(D)** roots, **(E)** total phosphate contents of shoots, and **(F)** roots were determined in Gifu wild-type and *rop3* plants inoculated with *R. irregularis*. Bars represent mean values (± SD) of 3 independent experiments ($n = > 15$).

chamber conditions, a consequence of altered RH deformation, or inhibition of bacterial growth and/or division. The increased RH deformation may be link to a compensatory mechanism, as previously observed in other symbiosis-deficient mutants such as *ccamk* (Maekawa-Yoshikawa and Murooka, 2009).

In this context, we evaluated whether ROP3 might be involved in the signaling pathway in response to the rhizobial NFs. We showed that alteration of *ROP3* accumulation does not affect transcript accumulation of representative CSSP genes (Roy et al., 2020), suggesting that ROP3 is not involved in the CSSP. This

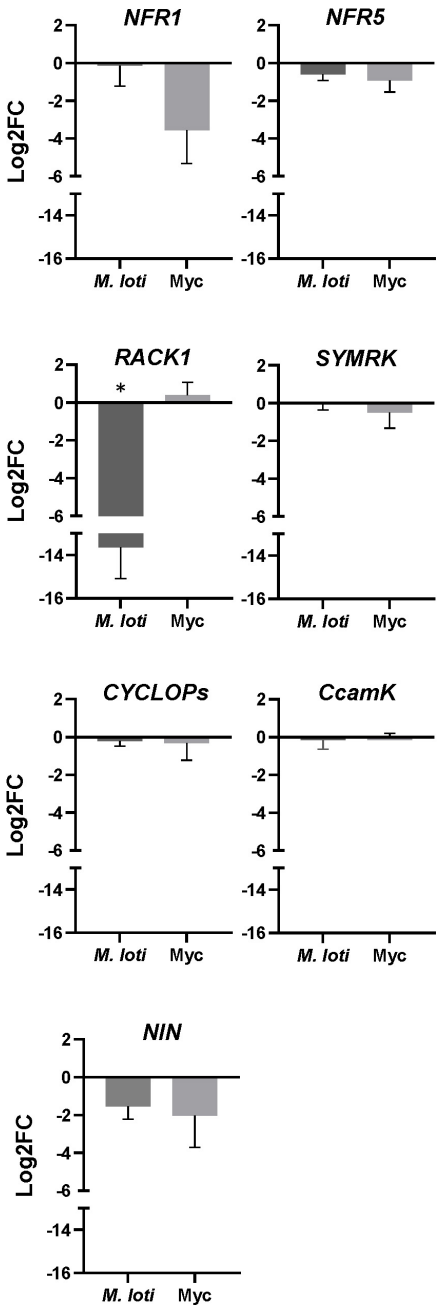

FIGURE 6 | RSP but not CSSP gene expression is altered in the *rop3* mutant. Expression analysis of indicated symbiotic genes was performed by qRT-PCR for Gifu wild-type and *rop3* mutant plants inoculated either with *M. loti* (at 7 DPI) or with *R. irregularis* (at 2 MPI). Data show the ratio of Log2FC values obtained from *rop3* vs. Gifu wild type plants. Three independent experiments each with 3 biological replicates were performed. The asterisk indicates statistical significance between *rop3* and Gifu wild-type according to one way ANOVA and a *post hoc* analysis ($p < 0.05$).

result is congruent with the lack of an altered AMS phenotype in *rop3* mutant. Furthermore, we analyzed the expression profile of RSP genes in the two genotypes and symbioses. The gene most differentially expressed in *rop3* during the NFS and AMS was *RACK1*. During NFS, RACK1 has been identified as an interactor of GmROP9 in soybean, depending on the activation by the NFR1/NFR5/GEF2 complex (Gao et al., 2021), and it has been shown to be an important element of the signal transduction pathway downstream of NF detection in common bean (Islas-Flores et al., 2012). Up to date, there is no report on the implication of RACK1 in the AMS. In our study, the drastic low accumulation of *RACK1* transcripts in *rop3* is specific to the NFS, and was not found during the AMS. This phenomenon could be due to an indirect regulation of *RACK1* transcription in consequence of a misactivation by the NFR1/NFR5/GEF2 complex, and a regulation loop after NF perception, but not after Myc factor perception by the corresponding receptor complex. Like GmROP9, ROP3 could be an interactor of RACK1, and this could explain the partial nodulation in *rop3* mutant plants. We suggest that ROP3 can be compensated by other ROPs such as ROP9. In parallel, the decrease of *NFR5* and *NIN* expression may explain the reduced number of nodule formation, probably by limiting the signal transduction to SYMRK and the proper transcriptomic response, downstream NF signaling.

Rho of plants GTPases are known to be involved in vesicle trafficking, actin organization and maintenance of reactive oxygen species (ROS) as well as Ca^{2+} signaling (Bloch et al., 2011), which are essential for the NFS or the AMS (Roy et al., 2020). ROP6 interacts with the NF receptor NFR5 and is involved in the establishment of the rhizobial symbiosis (Ke et al., 2012). We could assume that ROP3, like ROP6, might also directly associate with NFR5 to initiate the NFS signaling pathway. The control of polar growth of both the RH as well as the IT by ROP3 might also be achieved through its interaction with SPIKE1, a GEF protein known to activate ROPs, similarly to what was observed with ROP6 (Liu et al., 2020). ROP6 and ROP3 might share the same activator, SPIKE1, but might trigger a different downstream response by interacting with different effectors. Alternatively, ROP3 could be associated with other receptor-like kinases involved in the perception of rhizobia, like the exopolysaccharide receptor, EPR3 (Kawaharada et al., 2015). This hypothesis would explain why *rop3* plants can still form nodules and grow like the wild type. ROPs regulate cell growth and shape by reorganizing the actin filaments that direct cytoplasmic stream and vesicle trafficking. We suggest that ROP3 might participate in this process and that its absence impairs proper RH deformation in response to rhizobia and/or the invagination of the plant plasma membrane. It will be important to assess if ROP3 plays a role in the reorganization of actin filaments in response to rhizobia or NFs, known to be regulated by the SCAR/WAVE-ARP2-3 complex (Yokota et al., 2009; Hossain et al., 2012; Qiu et al., 2015).

Additionally, spatiotemporal regulation of ROS was shown to be indispensable to the proper establishment of the NFS, as the decrease of ROS level prevents RH curling as well as formation and progression of ITs (Cárdenas et al., 2008; Damiani et al., 2016; Engelhardt et al., 2020). ROS are transiently produced during rhizobial infection in legumes. Various NADPH oxidases, also named respiratory burst oxidase homologs (Rbohs), have been associated with ROS generation (Damiani et al., 2016). Some ROPs like OsRAC1 have been demonstrated to directly

interact with RbohB proteins like OsRbohB (Engelhardt et al., 2020). This interaction, which supports NADPH oxidase enzyme activity, demonstrates the regulatory role that ROPs play in the production of ROS (Engelhardt et al., 2020).

Even though ROPs have been associated with several characterized signaling proteins involved in symbioses, our knowledge is still fragmentary, and we are far from assembling all the pieces of the puzzle. Various genes coding for ROPs have been conserved during evolution (10 in *L. japonicus*) and this raises the question of their specialization or functional redundancy. It is likely that some might have evolved to perform specific tasks, and this would explain why some ROP genes could play such a pleiotropic role in plant development. Each ROP might have a different affinity for their multiple regulators like ROPGEFs, GAPs or GDIs as well as with their upstream and downstream interactors (Engelhardt et al., 2020).

Our results confirm that ROP3 is involved in the establishment of the NFS but not of the AMS, and therefore does not play a role in the CSSP. P analysis revealed that *rop3* mutation does not functionally impact the AMS (**Figure 6**). In the AMS, ROP3 or others ROPs might have a specialized function not yet highlighted. Kiirika et al. (2012) showed that silencing *ROP9* in *M. truncatula* results in a stimulation of the infection by AM fungus and a fungal pathogen but has a negative effect on the rhizobial symbiosis (Kiirika et al., 2012). The defect of ROS signaling and defense mechanisms enhanced fungal colonization in roots but not arbuscular frequency (Nath et al., 2016). In our study, we investigated a plant-AMF interaction under undisturbed conditions during inoculation that may lead to the establishment of compensation mechanisms by both the plant and fungus. A more complex system involving stress conditions or double inoculation with *Sinorhizobium* or even a rhizobial community would be suitable to explore the role of ROP3 in plant-microorganism interactions. However, *rop3* mutant plants exhibited a strong phenotype during the NFS suggesting that ROP3 is related to the specific RH rearrangements during rhizobial infection. It is tempting to speculate that the AMS is not affected in *rop3* mutant plants because ROP3 perhaps preferentially acts in RHs and AMF do not colonize roots via this cell type.

CONCLUSION

In this study, we showed that ROP3 specifically plays a role in the establishment of the NFS, but not during the AMS. ROP3 seems to impact the RH rearrangement during NFS, controlling the formation of a functional infection chamber, and then allowing an efficient microcolony capture leading to the formation of a complete IT. ROP3 seems to be involved in RH rearrangement by impacting the proper accumulation of RACK1, an essential component of the NF signaling pathway.

DATA AVAILABILITY STATEMENT

The original contributions presented in the study are included in the article/**Supplementary Material**, further inquiries can be directed to the corresponding authors.

AUTHOR CONTRIBUTIONS

IG-S, RB, YC-F, JC-C, LH-C, VB-Z, AL-S, and MT performed the experiments. GH, P-EC, DW, DF, MS, and AT conceived and designed the experiments. IG-S, RB, P-EC, DW, DF, MS, and AT wrote and revised the manuscript. All authors contributed to the article and approved the submitted version.

FUNDING

IG-S, YC-F, and LH-C acknowledge fellowships Nos. 856458, 929222, and 957577 from Consejo Nacional de Ciencia y Tecnología (CONACYT), Mexico. This work was supported by funds from Dirección General de Asuntos del Personal Académico-UNAM (PAPIIT), grants IA202620, IN203720, and IA200816 to DF, MS, and AT, respectively, as well as the Ciencias Básicas grant from CONACYT Nos. 253494 and A1-S-16129 to AT and DF, respectively.

ACKNOWLEDGMENTS

We would like to thank Michael F. Dunn for critical reading and comments of the manuscript. We would also like to thank Krzysztof Szczyglowski 's group for providing *L. japonicus* Gifu wild-type seeds and the *M. loti* bacterial strains.

SUPPLEMENTARY MATERIAL

The Supplementary Material for this article can be found online at: https://www.frontiersin.org/articles/10.3389/fpls.2021.696450/full#supplementary-material

Supplementary Table 1 | List of used primers.

REFERENCES

Alonso, J. M., and Stepanova, A. N. (2015). *Plant Functional Genomics. Methods and Protocols*. 2nd Edn. 1284, 1–526. doi: 10.1007/978-1-4939-2444-8

Blanco, F. A., Peltzer Meschini, E., Zanetti, M. E., and Aguilar, O. M. (2009). A Small GTPase of the Rab Family Is Required for Root Hair Formation and Preinfection Stages of the Common Bean–*Rhizobium* Symbiotic Association. *Plant Cell* 21:2797. doi: 10.1105/tpc.108.063420

Bloch, D., Monshausen, G., Singer, M., Gilroy, S., and Yalovsky, S. (2011). Nitrogen source interacts with ROP signalling in root hair tip-growth. *Plant Cell Environ.* 34, 76–88. doi: 10.1111/j.1365-3040.2010.02227.x

Broughton, W. J., and Dilworth, M. J. (1971). Control of leghaemoglobin synthesis in snake beans. *Biochem. J.* 125, 1075–1080. doi: 10.1042/bj1251075

Calabrese, S., Cusant, L., Sarazin, A., Niehl, A., Erban, A., Brulé, D., et al. (2019). Imbalanced Regulation of Fungal Nutrient Transports According to Phosphate Availability in a Symbiocosm Formed by Poplar, Sorghum, and *Rhizophagus irregularis*. *Front. Plant Sci.* 10:1617. doi: 10.3389/fpls.2019.01617

Cárdenas, L., Martínez, A., Sánchez, F., and Quinto, C. (2008). Fast, transient and specific intracellular ROS changes in living root hair cells responding to Nod factors (NFs). *Plant J.* 56, 802–813. doi: 10.1111/j.1365-313X.2008.03644.x

Cárdenas, L., Vidali, L., Domínguez, J., Pérez, H., Sánchez, F., Hepler, P. K., et al. (1998). Rearrangement of Actin Microfilaments in Plant Root Hairs Responding to *Rhizobium etli* Nodulation Signals. *Plant Physiol.* 116:871. doi: 10.1104/pp.116.3.871

Casieri, L., Ait Lahmidi, N., Doidy, J., Veneault-Fourrey, C., Migeon, A., Bonneau, L., et al. (2013). Biotrophic transportome in mutualistic plant-fungal interactions. *Mycorrhiza* 23, 597–625. doi: 10.1007/s00572-013-0496-9

Charpentier, M., and Oldroyd, G. E. (2013). Nuclear calcium signaling in plants. *Plant Physiol.* 163, 496–503. doi: 10.1104/pp.113.220863

Dalal, J., Yalamanchili, R., La Hovary, C., Ji, M., Rodriguez-Welsh, M., Aslett, D., et al. (2015). A novel gateway-compatible binary vector series (PC-GW) for flexible cloning of multiple genes for genetic transformation of plants. *Plasmid* 81, 55–62. doi: 10.1016/j.plasmid.2015.06.003

Damiani, I., Pauly, N., Puppo, A., Brouquisse, R., and Boscari, A. (2016). Reactive Oxygen Species and Nitric Oxide Control Early Steps of the Legume - *Rhizobium* Symbiotic Interaction. *Front. Plant Sci.* 7:454. doi: 10.3389/fpls.2016.00454

Dénarié, J., and Cullimore, J. (1993). Lipo-oligosaccharide nodulation factors: a new class of signaling molecules mediating recognition and morphogenesis. *Cell* 74, 951–954. doi: 10.1016/0092-8674(93)90717-5

Díaz, C. L., Schlaman, H. R. M., and Spaink, H. P. (2005). "Concurrent visualization of *gusA* and *lacZ* reporter gene expression," in *Lotus japonicus Handbook*, ed. A. J. Márquez (Dordrecht: Springer), 99–109.

Engelhardt, S., Trutzenberg, A., and Hückelhoven, R. (2020). Regulation and Functions of ROP GTPases in Plant-Microbe Interactions. *Cells* 9:2016. doi: 10.3390/cells9092016

Feiguelman, G., Fu, Y., and Yalovsky, S. (2018). ROP GTPases Structure-Function and Signaling Pathways. *Plant Physiol.* 176, 57–79. doi: 10.1104/pp.17.01415

Fu, Y. (2010). "ROP GTPases and the Cytoskeleton," in *Integrated G Proteins Signaling in Plants*, eds S. Yalovsky, F. Baluška, and A. Jones (Berlin: Springer), 91–104.

Gao, J.-P., Xu, P., Wang, M., Zhang, X., Yang, J., Zhou, Y., et al. (2021). Nod factor receptor complex phosphorylates GmGEF2 to stimulate ROP signaling during nodulation. *Curr. Biol.* 31, 3538–3550.e5. doi: 10.1016/j.cub.2021.06.011

Genre, A., and Bonfante, P. (1998). Actin versus tubulin configuration in arbuscule-containing cells from mycorrhizal tobacco roots. *New Phytol.* 140, 745–752. doi: 10.1046/j.1469-8137.1998.00314.x

Genre, A., and Russo, G. (2016). Does a Common Pathway Transduce Symbiotic Signals in Plant–Microbe Interactions?. *Front. Plant Sci.* 7:96. doi: 10.3389/fpls.2016.00096

Geurts, R., Fedorova, E., and Bisseling, T. (2005). Nod factor signaling genes and their function in the early stages of *Rhizobium* infection. *Curr. Opin. Plant Biol.* 8, 346–352. doi: 10.1016/j.pbi.2005.05.013

Gianinazzi, S., Gollotte, A., Binet, M.-N., van Tuinen, D., Redecker, D., and Wipf, D. (2010). Agroecology: the key role of arbuscular mycorrhizas in ecosystem services. *Mycorrhiza* 20, 519–530. doi: 10.1007/s00572-010-0333-3

Guether, M., Neuhäuser, B., Balestrini, R., Dynowski, M., Ludewig, U., and Bonfante, P. (2009). A Mycorrhizal-Specific Ammonium Transporter from *Lotus japonicus* Acquires Nitrogen Released by Arbuscular Mycorrhizal Fungi. *Plant Physiol.* 150:73. doi: 10.1104/pp.109.136390

Hossain, M. S., Liao, J., James, E. K., Sato, S., Tabata, S., Jurkiewicz, A., et al. (2012). *Lotus japonicus* ARPC1 is required for rhizobial infection. *Plant Physiol.* 160, 917–928. doi: 10.1104/pp.112.202572

Islas-Flores, T., Guillén, G., Sánchez, F., and Villanueva, M. A. (2012). Changes in RACK1 expression induce defects in nodulation and development in *Phaseolus vulgaris*. *Plant Signal. Behav.* 7, 132–134. doi: 10.4161/psb.7.1.18485

Kawaharada, Y., Kelly, S., Nielsen, M. W., Hjuler, C. T., Gysel, K., Muszyński, A., et al. (2015). Receptor-mediated exopolysaccharide perception controls bacterial infection. *Nature* 523, 308–312. doi: 10.1038/nature14611

Ke, D., Fang, Q., Chen, C., Zhu, H., Chen, T., Chang, X., et al. (2012). The small GTPase ROP6 interacts with NFR5 and is involved in nodule formation in *Lotus japonicus*. *Plant Physiol.* 159, 131–143. doi: 10.1104/pp.112.197269

Ke, D., Li, X., Han, Y., Cheng, L., Yuan, H., and Wang, L. (2016). ROP6 is involved in root hair deformation induced by Nod factors in *Lotus japonicus*. *Plant Physiol. Biochem.* 108, 488–498. doi: 10.1016/j.plaphy.2016.08.015

Kiirika, L. M., Bergmann, H. F., Schikowsky, C., Wimmer, D., Korte, J., Schmitz, U., et al. (2012). Silencing of the Rac1 GTPase *MtROP9* in *Medicago truncatula* Stimulates Early Mycorrhizal and Oomycete Root Colonizations But Negatively Affects Rhizobial Infection. *Plant Physiol.* 159:501. doi: 10.1104/pp.112.193706

Lei, M.-J., Wang, Q., Li, X., Chen, A., Luo, L., Xie, Y., et al. (2015). The Small GTPase ROP10 of Medicago truncatula Is Required for Both Tip Growth of Root Hairs and Nod Factor-Induced Root Hair Deformation. *Plant Cell* 27, 806–822. doi: 10.1105/tpc.114.135210

Liu, J., Liu, M. X., Qiu, L. P., and Xie, F. (2020). SPIKE1 Activates the GTPase ROP6 to Guide the Polarized Growth of Infection Threads in *Lotus japonicus*. *Plant Cell* 32:3774. doi: 10.1105/tpc.20.00109

Maekawa-Yoshikawa, M., and Murooka, Y. (2009). Root hair deformation of symbiosis-deficient mutants of *Lotus japonicus* by application of Nod factor from *Mesorhizobium loti*. *Microbes Environ.* 24, 128–134. doi: 10.1264/jsme2.me09103

Małolepszy, A., Mun, T., Sandal, N., Gupta, V., Dubin, M., Urbański, D., et al. (2016). The LORE1 insertion mutant resource. *Plant J.* 88, 306–317. doi: 10.1111/tpj.13243

Nath, M., Bhatt, D., Prasad, R., Gill, S. S., Anjum, N. A., and Tuteja, N. (2016). Reactive Oxygen Species Generation-Scavenging and Signaling during Plant-Arbuscular Mycorrhizal and Piriformospora indica Interaction under Stress Condition. *Front. Plant Sci.* 7:1574. doi: 10.3389/fpls.2016.01574

Ohno, T., and Zibilske, L. M. (1991). Determination of Low Concentrations of Phosphorus in Soil Extracts Using Malachite Green. *Soil Sci. Soc. Am. J.* 55, 892–895. doi: 10.2136/sssaj1991.03615995005500030046x

Oldroyd, G. E. (2013). Speak, friend, and enter: signalling systems that promote beneficial symbiotic associations in plants. *Nat. Rev. Microbiol.* 11, 252–263. doi: 10.1038/nrmicro2990

Pajuelo, E., and Stougaard, J. (2005). "*Lotus japonicus*'s a model system," in *Lotus japonicus Handbook*, ed. A. J. Márquez (Dordrecht: Springer), 3–24.

Peters, N. K., Frost John, W., and Long Sharon, R. (1986). A Plant Flavone, Luteolin, Induces Expression of *Rhizobium meliloti* Nodulation Genes. *Science* 233, 977–980. doi: 10.1126/science.3738520

Pimprikar, P., and Gutjahr, C. (2018). Transcriptional Regulation of Arbuscular *Mycorrhiza* Development. *Plant Cell Physiol.* 59, 678–695. doi: 10.1093/pcp/pcy024

Qiu, L., Lin, J. S., Xu, J., Sato, S., Parniske, M., Wang, T. L., et al. (2015). SCARN a Novel Class of SCAR Protein That Is Required for Root-Hair Infection during Legume Nodulation. *PLoS Genet.* 11:e1005623. doi: 10.1371/journal.pgen.1005623

Redmond, J. W., Batley, M., Djordjevic, M. A., Innes, R. W., Kuempel, P. L., and Rolfe, B. G. (1986). Flavones induce expression of nodulation genes in *Rhizobium*. *Nature* 323, 632–635. doi: 10.1038/323632a0

Rich, M. K., Courty, P.-E., Roux, C., and Reinhardt, D. (2017). Role of the GRAS transcription factor ATA/RAM1 in the transcriptional reprogramming of arbuscular mycorrhiza in *Petunia hybrida*. *BMC Genomics* 18:589. doi: 10.1186/s12864-017-3988-8

Rivero, C., Traubenik, S., Zanetti, M. E., and Blanco, F. A. (2019). Small GTPases in plant biotic interactions. *Small GTPases* 10, 350–360. doi: 10.1080/21541248.2017.1333557

Roy, S., Liu, W., Nandety, R. S., Crook, A., Mysore, K. S., Pislariu, C. I., et al. (2020). Celebrating 20 Years of Genetic Discoveries in Legume Nodulation and Symbiotic Nitrogen Fixation. *Plant Cell* 32:15. doi: 10.1105/tpc.19.00279

Timmers, A. C. J. (2008). The role of the plant cytoskeleton in the interaction between legumes and *rhizobia*. *J. Microsc.* 231, 247–256. doi: 10.1111/j.1365-2818.2008.02040.x

Trouvelot, A., Kough, J. L., and Gianinazzi-Pearson, V. (1986). "Mesure du taux de mycorhization VA d'un système radiculaire. Recherche de méthodes d'estimation ayant une signification fonctionnelle," in *Physiological And Genetical Aspects Of Mycorrhizae*, eds V. Gianinazzi-Pearson and S. Gianinazzi (Paris: INRA edition).

Urbański, D. F., Małolepszy, A., Stougaard, J., and Andersen, S. U. (2012). Genome-wide LORE1 retrotransposon mutagenesis and high-throughput insertion detection in *Lotus japonicus*. *Plant J.* 69, 731–741. doi: 10.1111/j.1365-313X.2011.04827.x

Wang, C., Zhu, M., Duan, L., Yu, H., Chang, X., Li, L., et al. (2015). *Lotus japonicus* Clathrin Heavy Chain1 Is Associated with Rho-Like GTPase ROP6 and Involved in Nodule Formation. *Plant Physiol.* 167, 1497–1510. doi: 10.1104/pp.114.256107

Wang, M., Feng, H., Xu, P., Xie, Q., Gao, J., Wang, Y., et al. (2021). Phosphorylation of MtRopGEF2 by LYK3 mediates MtROP activity to regulate rhizobial infection in *Medicago truncatula*. *J. Integr. Plant Biol.* 63, 1787–1800. doi: 10.1111/jipb.13148

Wipf, D., Krajinski, F., van Tuinen, D., Recorbet, G., and Courty, P.-E. (2019). Trading on the arbuscular mycorrhiza market: from arbuscules to common mycorrhizal networks. *New Phytol.* 223, 1127–1142. doi: 10.1111/nph.15775

Wopereis, J., Pajuelo, E., Dazzo, F. B., Jiang, Q., Gresshoff, P. M., De Bruijn, F. J., et al. (2000). Short root mutant of *Lotus japonicus* with a dramatically altered symbiotic phenotype. *Plant J.* 23, 97–114. doi: 10.1046/j.1365-313x.2000.00799.x

Yalovsky, S., Bloch, D., Sorek, N., and Kost, B. (2008). Regulation of membrane trafficking, cytoskeleton dynamics, and cell polarity by ROP/RAC GTPases. *Plant Physiol.* 147, 1527–1543. doi: 10.1104/pp.108.122150

Yang, Z. (2002). Small GTPases: versatile signaling switches in plants. *Plant Cell* 14, S375–S388. doi: 10.1105/tpc.001065

Yokota, K., Fukai, E., Madsen, L. H., Jurkiewicz, A., Rueda, P., Radutoiu, S., et al. (2009). Rearrangement of actin cytoskeleton mediates invasion of *Lotus japonicus* roots by *Mesorhizobium loti*. *Plant Cell* 21, 267–284. doi: 10.1105/tpc.108.063693

Conflict of Interest: The authors declare that the research was conducted in the absence of any commercial or financial relationships that could be construed as a potential conflict of interest.

Publisher's Note: All claims expressed in this article are solely those of the authors and do not necessarily represent those of their affiliated organizations, or those of the publisher, the editors and the reviewers. Any product that may be evaluated in this article, or claim that may be made by its manufacturer, is not guaranteed or endorsed by the publisher.

frontiers in Plant Science

ORIGINAL RESEARCH
published: 13 December 2021
doi: 10.3389/fpls.2021.709857

Amino Acid Polymorphisms in the VHIID Conserved Motif of Nodulation Signaling Pathways 2 Distinctly Modulate Symbiotic Signaling and Nodule Morphogenesis in *Medicago truncatula*

Szilárd Kovacs[1†], Lili Fodor[2†], Agota Domonkos[2], Ferhan Ayaydin[3,4], Krisztián Laczi[1,5], Gábor Rákhely[5,6] and Péter Kalo[1,2]*

[1] Institute of Plant Biology, Biological Research Center, Eötvös Lóránd Research Network, Szeged, Hungary, [2] Institute of Genetics and Biotechnology, Hungarian University of Agriculture and Life Sciences, Gödöllő, Hungary, [3] Hungarian Centre of Excellence for Molecular Medicine (HCEMM) Nonprofit Ltd., Szeged, Hungary, [4] Cellular Imaging Laboratory, Biological Research Center, Eötvös Lóránd Research Network, Szeged, Hungary, [5] Department of Biotechnology, University of Szeged, Szeged, Hungary, [6] Institute of Biophysics, Biological Research Center, Eötvös Lóránd Research Network, Szeged, Hungary

Legumes establish an endosymbiotic association with nitrogen-fixing soil bacteria. Following the mutual recognition of the symbiotic partner, the infection process is controlled by the induction of the signaling pathway and subsequent activation of symbiosis-related host genes. One of the protein complexes regulating nitrogen-fixing root nodule symbiosis is formed by GRAS domain regulatory proteins Nodulation Signaling Pathways 1 and 2 (NSP1 and NSP2) that control the expression of several early nodulation genes. Here, we report on a novel point mutant allele (*nsp2-6*) affecting the function of the *NSP2* gene and compared the mutant with the formerly identified *nsp2-3* mutant. Both mutants carry a single amino acid substitution in the VHIID motif of the NSP2 protein. We found that the two mutant alleles show dissimilar root hair response to bacterial infection. Although the *nsp2-3* mutant developed aberrant infection threads, rhizobia were able to colonize nodule cells in this mutant. The encoded NSP2 proteins of the *nsp2-3* and the novel *nsp2* mutants interact with NSP1 diversely and, as a consequence, the activation of early nodulin genes and nodule organogenesis are arrested in the new *nsp2* allele. The novel mutant with amino acid substitution D244H in NSP2 shows similar defects in symbiotic responses as a formerly identified *nsp2-2* mutant carrying a deletion in the *NSP2* gene. Additionally, we found that rhizobial strains induce delayed nodule formation on the roots of the *ns2-3* weak allele. Our study highlights the importance of a conserved Asp residue in the VHIID motif of NSP2 that is required for the formation of a functional NSP1-NSP2 signaling module. Furthermore, our results imply the involvement of NSP2 during differentiation of symbiotic nodule cells.

Keywords: root nodule symbiosis, nitrogen fixation, Nod-factor signaling, *Medicago*, rhizobia, GRAS transcription factors, NSP1, NSP2

OPEN ACCESS

Edited by:
Christian Staehelin, Sun Yat-sen University, China

Reviewed by:
Songli Yuan, Oil Crops Research Institute, Chinese Academy of Agricultural Sciences (CAAS), China
Weijun Dai, South China Agricultural University, China

****Correspondence:***
Péter Kalo
kalo.peter@brc.hu

† These authors have contributed equally to this work

Specialty section:
This article was submitted to Plant Symbiotic Interactions, a section of the journal Frontiers in Plant Science

Received: *14 May 2021*
Accepted: *11 October 2021*
Published: *13 December 2021*

Citation:
Kovacs S, Fodor L, Domonkos A, Ayaydin F, Laczi K, Rákhely G and Kalo P (2021) Amino Acid Polymorphisms in the VHIID Conserved Motif of Nodulation Signaling Pathways 2 Distinctly Modulate Symbiotic Signaling and Nodule Morphogenesis in Medicago truncatula. Front. Plant Sci. 12:709857. doi: 10.3389/fpls.2021.709857

INTRODUCTION

The restricted availability of nitrogen extremely restrains plant development. *Medicago truncatula* and other leguminous plants can overcome this limitation because of their capability to establish nitrogen-fixing symbiotic associations with soil bacteria collectively termed as rhizobia. Symbiotic nodules are specialized organs that formed on legume roots, which provide a microaerobic environment for endosymbiotic rhizobia. Within the nodules, rhizobia reduce atmospheric nitrogen to ammonia that is utilized by the host plant in return to carbon sources (Gibson et al., 2008). Nodule formation is a result of several consecutive communication steps between the two organisms. The bacterially derived lipochitooligosaccharides called Nod factors (NFs) are key signaling molecules for the early stages of nitrogen-fixing symbiotic interactions [reviewed in references (Jones et al., 2007; Oldroyd and Downie, 2008)].

The perception of NFs induces a signaling pathway that activates many early symbiotic responses in the symbiosis sensitive region of the host root. NFs trigger root hair deformation, oscillations in cytosolic calcium levels (Ca-spiking) in root hair cells, and induction of symbiosis specific gene expression (epidermal responses). NFs also induce mitotic activation of inner cortical cells that leads to the formation of nodule primordia (cortical response) (Oldroyd and Downie, 2008). Genetic mutants of the model legumes *M. truncatula* and *Lotus japonicus* defective in the transduction of the rhizobial symbiotic signal were used to identify the components of the NF signaling pathway, such as receptors, signal-transmitting kinases such as DMI2 (Endre et al., 2002) [SymRK in *L. japonicus* (Stracke et al., 2002)], ion-channel proteins, and transcription factors (Oldroyd, 2013; Kang et al., 2016). A calcium/calmodulin-dependent protein kinase (CCaMK) interacting with the IPD3 (CYCLOPS in *L. japonicus*) transcriptional activator (Singh et al., 2014) decodes the calcium signal and regulates both epidermal and cortical responses (Oldroyd and Downie, 2008), which are mediated by GRAS proteins, Nodulation Signaling Pathways 1 and 2 (NSP1 and NSP2) (Kalo et al., 2005; Smit et al., 2005; Heckmann et al., 2006) and other transcriptional regulators [e.g., NIN, ERNs, and NF-YA (Schauser et al., 1999; Andriankaja et al., 2007; Middleton et al., 2007; Laporte et al., 2014)]. The NSP1–NSP2 complex interacts with IPD3 and CCaMK through DELLA proteins (Jin et al., 2016).

Nodulation Signaling Pathways 1 and 2 are GRAS-type transcription regulators named after the first three discovered members, *GIBBERELLIN-INSENSITIVE* (*GAI*), repressor of *ga1-3* (*RGA*), and *SCARECROW* (*SCR*) (Pysh et al., 1999), and are essential for most rhizobium-induced symbiotic responses. Mutant plants defective in NSP1 or NSP2 show altered root-hair deformation and are blocked in NF-induced gene expression, infection thread (IT) initiation, and cortical cell division (Catoira et al., 2000; Oldroyd and Long, 2003). The NSP2 protein plays a critical role in the activation of early nodulin gene expressions, such as *MtENOD11* expression, in the epidermis through NF signaling (Gleason et al., 2006). NSP2 is also essential for the CCaMK-activated cytokinin signaling pathway *via* the cytokinin receptor CRE1 leading to cortical cell division and nodule organogenesis (Tirichine et al., 2007; Ariel et al., 2012). NSP2 forms a heterodimer with NSP1, and the complex of NSP2 and NSP1 directly binds to promoters of early nodulin genes, such as *ENOD11*, *ERN1*, and *NIN* (Hirsch et al., 2009). The GRAS domains of NSP1 and NSP2 contain two leucine heptad repeat motifs (LHRI and LHRII) and have three additional motifs, VHIID, PFYRE, and SAW named after the most prominent residues, which are all of them characteristic for GRAS proteins (Bolle, 2004). An analysis of deletion mutants of *NSP1* and *NSP2* revealed that several domains of NSP1 are required for the interaction with NSP2, and also showed that the LHR1 and VHIID of NSP2 domains have a prominent function in the association with NSP1 (Hirsch et al., 2009). The *nsp2-3* point mutant allele carrying the nonconservative substitution E232K develops small white nodules, indicating that the nodule developmental program is not completely blocked in this mutant (Kalo et al., 2005). The mutation of E232K abolishes the autoactivation of NSP2 but does not negatively affect the formation of the NSP1-NSP2 complex (Hirsch et al., 2009).

Bacterial infection is associated with root hair curling and formation of tubular structures called ITs in root hairs that guide rhizobia into the root cortex where bacteria invade cells of nodule primordia through an endocytosis-like process (Gage, 2002, 2004). Rhizobia are surrounded by plant–derived membranes forming a cytoplasmic structure referred to as symbiosomes (Brewin, 2004; Jones et al., 2007). Bacteria undergo morphological changes and metabolomic transition within symbiosomes (Pfau et al., 2018). Differentiated rhizobia termed bacteroids convert the atmospheric nitrogen in nodule cells into ammonia that can be assimilated by the host plant. The symbiotic interaction between *Sinorhizobium* (*Ensifer*) sp. and *M. truncatula* leads to the formation of cylindrical-shaped indeterminate nodules. The persistent meristem (zone I) of indeterminate nodules produces a developmental gradient of cells from the apex of nodules toward the senescent cells proximal to the root (Vasse et al., 1990). The subsequent zone to the meristematic region is the infection zone (zone II) wherein bacteria are released from ITs and internalized in symbiosomes that multiply, thereby filling up the colonized cells. Both rhizobia and infected nodule cells undergo differentiation in the interzone (zones II–III), resulting in enlarged infected cells containing elongated polyploid bacteroids. The nitrogen fixation zone (zone III) is composed of the central tissue of the indeterminate nodules. Zone III consists of small noninfected cells and large infected cells with differentiated bacteroids, which convert atmospheric nitrogen to ammonia. In the basal part of older nodules, bacteroids and plant cells are disintegrated and collapse in the senescence zone (zone IV) proximal to zone III.

The activity of the NF signaling pathway is not restricted to the initiation of infection and nodule organogenesis but also plays a role in later stages of nodule development. It was found that at least two NF signaling genes, *DMI2,* coding for a leucine-rich-repeat-containing receptor kinase (Endre et al., 2002), and *NIN*, coding for a transcription factor (Schauser et al., 1999), are expressed in the distal part of symbiotic nodules (Limpens et al., 2005; Liu et al., 2021). *DMI2* transcripts are abundant in few cell layers adjacent to the meristem, and *NIN* is highly

expressed in the infection zone. It was demonstrated that the partial reduction of *DMI2* expression in wild-type plants or the misregulation of *DMI2* in *dmi2* background caused extensive IT formation and defects in symbiosome formation (Limpens et al., 2005). In two *nin* alleles of *M. truncatula*, *NIN* mRNA levels were greatly reduced but not abolished completely. In these *nin* mutants, nodule development was not blocked fully, which is in contrast with the non-nodulation phenotype of *nin* alleles wherein *NIN* transcripts were completely abolished. The mutant alleles that expressed the *NIN* gene at a low level developed white nonfunctional nodules showing early senescence, incomplete rhizobial differentiation, and defects in symbiosome formation (Liu et al., 2021). These findings indicated that some alleles of genes involved in the NF signaling pathway could reveal the function of these components in later stages of nodule development.

Several mutant alleles of *NSP2* were found previously in genetic screens of *M. truncatula* targeting the identification of symbiotic nitrogen-fixing mutants impaired in bacterial signal perception and transduction. The *nsp2* mutants were identified in mutant collections generated by either fast neutron (FN) bombardment [*nsp2-1*, *nsp2-2,* and *nsp2-5* alleles (Oldroyd and Long, 2003; Domonkos et al., 2013) or retrotransposon insertion (*nsp2-4* and several other insertions alleles (Rakocevic et al., 2009; Pislariu et al., 2012)] that generally generate knockout (null) mutants. The formerly identified *nsp2-3* mutant is able to form functional nodules with a symbiotically effective strain of rhizobia, and these nodules display unusual nodule colonization with a reduced number of uninfected cells.

In this study, we have analyzed two-point mutant *nsp2* alleles that carry substitutions in the VHIID motif of NSP2. The early steps of nodule development are completely blocked, and the interaction with NSP1, which is required for NF inducible gene activation, is abolished in the novel *nsp2-6* allele, supporting that the substitution in a conserved residue of the VHIID domain is essential for NSP2 function. We also report on a strain-dependent nodulation phenotype of the weak *nsp2-3* allele.

MATERIALS AND METHODS

Plant Material, Bacterial Strains, and Growth Conditions

The *M. truncatula* Jemalong A17 genotype was used as a wild-type (wt) control in all of the experiments. The NF-FN9199 mutant line was identified in a former genetic screen (Kontra-Kováts et al., 2019). The *Mtnsp2-2* and *nsp2-3* mutant lines used in this study have been described previously (Kalo et al., 2005). Seeds were germinated as described in the *M. truncatula* handbook (Garcia et al., 2006). Seedlings were grown under symbiotic conditions in a zeolite substrate (Geoproduct Kft., Mád, Hungary) in growth chambers and kept under a photoperiod of 16 h of light and 8 h of darkness at 24°C. Five-day old seedlings were inoculated with a suspension of rhizobia diluted to OD_{600} 0.1 *Sinorhizobium* (*Ensifer*) *medicae* WSM419 carrying the pMEpTrpGFPGUS plasmid expressing the β-glucuronidase-GFP fusion protein (Auriac and Timmers, 2007), and strains *Sinorhizobium* (*Ensifer*) *meliloti* 1021 and *S. medicae* WSM419 carrying the pXLGD4 plasmid expressing the *lacZ* reporter gene under the control of the *hemA* promoter were used for inoculation of plants.

In hairy root transformation and *Nicotiana benthamiana* infiltration experiments, *Agrobacterium rhizogenes* ARqua1, and *Agrobacterium tumefaciens* C58C1 strains carrying appropriate constructs were used. All the bacterial strains were grown for 48–72 h at 30°C in a complete TA medium supplemented with appropriate antibiotics.

Generation of Constructs

The constructs used in this study were generated with Gateway Technology (Invitrogen, Life Technologies, Carlsbad, CA, United States) according to the protocol of the manufacturer.

The mutant *NSP2* alleles were amplified from the genomic DNA of *nsp2-3* and *nsp2-6* using Q5High Fidelity DNA Polymerase (NEB, Ipswich, MA, United States) with the primers listed in **Supplementary Material**. An additional A nucleotide was added to the 3′ end by incubation with DreamTaq polymerase (Thermo Fisher Scientific, Waltham, MA, United States). A-tailed PCR fragments were then cloned into a pCR™8/GW/TOPO® (Invitrogen, Carlsbad, CA, United States) vector and verified by sequencing. Destination clones were generated by LR clonase II- (Invitrogen) mediated recombination using the entry constructs. For yeast two-hybrid (Y2H) experiments, destination vectors pDEST-GBKT7 and pDEST-GADT7 (Clontech Laboratories, Inc., Takara Bio Europe, Saint-Germain-en-Laye, France), and pUBN-cYFP-DEST (Grefen et al., 2010) plasmids were used for bimolecular fluorescence complementation (BiFC) assays. For genetic complementation experiments, a previously described construct consisting of the *NSP2* coding sequence under the control of the 35S constitutive promoter was used (Kalo et al., 2005).

The *NSP1* and *NSP2* expression clones (either for BiFC or Y2H) and the autoactive CRE1 clone were kindly provided by Giles Oldroyd (Cambridge University, United Kingdom) and Erik Limpens (Wageningen University, Netherlands).

Yeast Two-Hybrid Experiments

Bait and prey plasmids were transformed into *Saccharomyces cerevisiae* PJ-69-4A cells as recommended by the manufacturer (Clontech Laboratories, Inc., Protocol No. *PT3247-1*. 2.) using the original components and salmon sperm DNA (Sigma) as carrier. Transformed PJ-69-4A yeast strains were selected on plates containing synthetic-defined (SD) minimal yeast media [SD (dropout)/without Leu and Trp (-LW)]. Expression of the *HIS3* reporter gene were tested using a spot assay. PJ-69-4A yeasts containing the appropriate constructs were grown in SD-LW medium with shaking at 30°C for 16 h. The diluted cultures (OD_{600} 0.1) were spotted to SD-LW with or without histidine (SD-HLW) containing 10 or 40 mM 3-amino-1,2,4-triazole (3-AT) plates for monitoring of the growth of yeast colonies. The liquid β-galactosidase assay was performed according to the Yeast Protocols Handbook (PT3024-1, Clontech). The immunoblot experiment was carried out to detect the stability of wild-type and mutant NSP2 proteins fused to the HA-tagged activation domain

in yeast using an *a*-HA antibody according to the protocol of the manufacturer (Invitrogen, cat. 26183).

Complementation and Bimolecular Fluorescence Complementation Experiments

The constructs generated for plant transformation experiments were introduced into *A. tumefaciens* C58C1 or *A. rhizogenes* ARqua1 strains by electroporation.

The hairy root transformation was carried out as described in The *Medicago truncatula* Handbook (Chabaud et al., 2006), and transgenic roots were selected based on the fluorescent signals of the DsRED marker protein.

For the infiltration of *N. benthamiana* leaves, two to three colonies of *A. tumefaciens* carrying paired vector combinations for the BiFC experiments and of the strain carrying the p19 silencing suppressor construct (Silhavy et al., 2002; Voinnet et al., 2003) were inoculated into 10 ml of TA medium and grown at 28°C with shaking for 16 h, and 1 ml of overnight bacterial culture was transferred into 20 ml fresh TA medium containing 10 mM MES (pH 5.6), 20 μM acetosyringone (Merck KGaA, Darmstadt, Germany), and appropriate antibiotics. After growth for 16 h at 28°C, the bacterial cultures were centrifuged at 4,000 rpm for 15 min. The pellet was resuspended in sterile water containing 10 mM MES (pH 5.6), 10 mM $MgCl_2$, and 150 μM acetosyringone (MMA solution) diluted to OD_{600} 0.3 and incubated for 3 h at room temperature in the dark. The prepared *Agrobacterium* dilutions were mixed and infiltrated into the top leaves of 6-week-old *N. benthamiana* plants. Infiltration of the fully expanded leaves was performed with a 1-ml syringe, and the plants were kept in the dark overnight to enhance the efficiency of transformation. YFP fluorescence was observed 3 days after the infiltration by confocal laser scanning microscopy (see below).

Histochemical Staining and Imaging

The nodule and root samples were harvested at indicated time points upon inoculation with rhizobia. For GUS staining, the nodules were embedded in 5% agarose, and 70 μm sections were prepared using a MICROM HM 650 V vibratome. Nodule sections or whole roots were vacuum-infiltrated for 30 min, and then incubated in a GUS staining solution [2 mM 5-bromo-4-chloro-3-indolyl β-D-glucuronide (X-Gluc; Duchefa Biochemie, Haarlem, The Netherlands), 1 mM EDTA, 0.1% Triton X-100, 0.1% Sarcosyl, 0.05% SDS, 1 mM potassium ferricyanide, and 1 mM ferrocyanide in phosphate buffered saline (PBS) (pH 7.4)] for 1–3 h at 37°C.

For β-galactosidase and SYTO13 (Invitrogen) staining, the nodule samples were vacuum-fixed in 4% paraformaldehyde three times for 30 s, post-fixed for 30 min on ice, and then washed 3 × 5 min in PBS (pH 7.4). The fixed samples were embedded in 5% (w/v) agarose, and 70 μm sections were prepared using a MICROM HM 650 V vibratome. To assay β-galactosidase activity, the sections were stained with 0.1% X-Gal in PBS (pH 7.4) supplemented with 5 mM potassium ferricyanide and 5 mM potassium ferrocyanide for 1–3 h at 37°C. The GUS and X-gal-stained samples were analyzed using DM LB2 Light Microscope (Leica), and images were captured using a QImaging MicroPublisher 3.3 RTV camera. For SYTO13-staining, the nodule sections were incubated in 1 × PBS (pH 7.4) containing 5 μM SYTO13 for 20 min at room temperature in the dark and then rinsed with 1 × PBS. Images were captured by confocal laser scanning microscopy.

Confocal Laser Scanning Microscopy and Image Analysis

The samples were analyzed using an Olympus Fluoview FV1000 confocal laser scanning microscope (Olympus Life Science Europa GmbH, Hamburg, Germany). The microscope configuration was as follows: Objectives: UPLSAPO 10× dry (N.A. 0.4), UPFLN 40× Oil (N.A. 1.3), LUMPFLF 40× Water (N.A. 0.8); sampling speed: 8 μs/pixel; line averaging: 2; laser excitation: 405 (cell wall autofluorescence, pseudocolored red), 488 (SYTO 13, green), and 515 nm (YFP/BiFC, green). Autofluorescence was detected between 425 and 475 nm, and SYTO13 and YFP emissions were detected between 500 and 600, and 530 and 630 nm, respectively, using spectral detectors. Brightfield images were captured on a transmitted light detector by either 405- or 515-nm laser excitation.

To quantify the degree of nodule colonization, the FIJI software (ver. 1.53c) was used (Schindelin et al., 2012). Green colored SYTO13 images were converted to 8-bit black and white images. The perimeter of the nodules was traced manually using a freehand selection tool. Regions of interest were cut out and pasted as a new image to obtain a clean image while excluding any debris or non-cellular area around the nodules. To eliminate bias, the images were auto-thresholded to isolate and highlight highly fluorescent, infected cell-containing regions. Using the "Find connected regions" plugin of the FIJI program, the size and number of connected regions larger than 70 pixels were quantified. (Plugin was written by Mark Longair; for details of the FIJI plugin, visit: https://github.com/fiji/VIB/blob/master/src/main/java/util/Find_Connected_Regions.java).

A lower limit of 70 pixels was selected to include the smallest infected cells while excluding small fluorescent objects and image noise. Results displaying "the total number and size of the connected areas" were exported to Microsoft Excel to plot the charts after sorting areas from lowest to highest. Large connected areas (which were less in number) were considered as an indicator of more densely infected nodules, whereas smaller sized connected areas, which were also more frequent, were considered as an indicator of less frequently infected cells within the nodule.

Acetylene Reduction Assay

The activity of bacterial nitrogenase was measured by acetylene reduction assay (ARA). Nodulated root sections of the mutant and wild-type plants were harvested 21 days after inoculation with either strain *S. meliloti* 1021 or strain *S. medicae* WSM419. Five to six nodules and root samples as negative control were enclosed in 1.8-ml glass vials sealed with rubber stoppers. Promptly, 180 μl acetylene (Linde Gas Hungary Co., Ltd., Répcelak, Hungary) was injected into the vials, the samples were incubated for 2 h in the dark, and then 100 μl gas was injected into an Agilent 6890 (Agilent Technologies Inc., Santa Clara, CA, United States) gas chromatograph equipped with a split/splitless

injector and a Flame Ionization Detector to measure the amount of ethylene. The analytical column was HP-PLOT/Q+PT Cat No. 19095P-QO4PT (Agilent Technologies Inc.) with dimensions of 30 m × 0.53 mm × 40 μm. The carrier gas was hydrogen with a purity of 5.0 (Messer Hungarogáz Ltd., Budapest, Hungary). The column flow was 4.5 ml/min, and the split ratio was set to 9:1. The oven temperature was constant 50°C. The samples were injected manually with a 250-μl Hamilton syringe 1725 RN (Hamilton Company, Bonaduz, Switzerland) equipped with a ga22s pt5 needle. The effectiveness of acetylene reduction was calculated in ARA units (nmol of ethylene per mg nodule per hour). The ARA was carried out with four biological replicates. For ethylene calibration, ethylene gas (Linde Gas Hungary Co., Ltd.) with a purity of 3 was used. The molarity of ethylene was calculated with the van der Waals equation.

Gene Expression Analysis

For real-time RT-PCR, root segments susceptible to rhizobia were harvested in liquid nitrogen at 4 days post inoculation (dpi) with *S. medicae* strain WSM19. RNA was extracted with TRI Reagent (Merck KGaA, Darmstadt, Germany) and Direct-zol RNA MiniPrep Kit (Zymo Research, Irvine, CA, United States). RNA samples were treated with DNaseI on columns according to the instructions of the manufacturer to remove the residual genomic DNA. Total RNA was quantified using a spectrophotometer (Nanodrop-1000; NanoDrop Technologies, Thermo Fisher Scienific, Waltham, MA, United States), and the quality was checked by gel electrophoresis. Complementary DNA was prepared from 1 μg total RNA with SuperScript IV First-Strand Synthesis System (Life Technologies, Invitrogen, Carlsbad, CA, United States) using oligo-dT primers according to the instructions of the manufacturer. Quantitative PCR (qPCR) was performed with LightCycler 96 (Roche, Mannheim, Germany) using qPCRBIOSyGreen Mix (PCR Biosystems, London, United Kingdom) according to the protocol of the manufacturer. Cycle threshold values were obtained and data were analyzed with the LightCycler 96 SW1.1 software. Relative expression levels were calculated by normalization against the expression of an ubiquitin-like gene (see **Supplementary Table 1**; Kakar et al., 2008). Values of relative transcript levels were the mean of five or six biological replicates. Fold induction was calculated by normalizing the data to the wild-type samples (A17 4 dpi). The primers used for qPCR are listed in **Supplementary Table 1**.

RESULTS

The Conserved VHIID Motif Is Affected in Point Mutant Alleles of *NSP2*

Nodulation Signaling Pathway 2 is an essential component of the NF signaling pathway (Oldroyd and Long, 2003). In order to investigate the altered activity and function of the NSP2 protein, formerly identified point mutant alleles of *NSP2* were analyzed in this study. The previously described point mutant allele *nsp2-3* containing a non-conservative E232K change forms small white nodules following inoculation with *S. meliloti* strain 1021 (Kalo et al., 2005), indicating impaired symbiosis. Another mutant, NF-FN9199, was identified in a forward genetic screen and was found to be completely deficient in nodule formation (Nod-) (Kontra-Kováts et al., 2019). The position of the nodulation defective locus and the sequence analysis of *NSP*2 in mutant NF-FN9199 suggested that this mutant is a novel *nsp2* allele. In order to confirm that the mutation in *NSP2* caused the nodulation deficient phenotype of NF-FN9199, genetic complementation experiments were carried out. The coding sequence of *NSP2* under the control of the 35S promoter was introduced into the NF-FN9199 roots by *A. rhizogenes*-mediated hairy root transformation. Transformed roots were detected by the DsRed fluorescent marker. The growth habit and formation of nodules on the transformed roots were assessed 3 weeks post inoculation (wpi) with *S. medicae* strain WSM419 (pXLGD4) (SmWSM419). NF-FN9199 mutant plants transformed with the *NSP2* gene showed improved growth rate and developed dark green leaves compared with empty vector-transformed mutant plants, indicating the recovery of mutant plants from nitrogen starvation (**Figure 1E**). Moreover, pinkish nodules that formed on the NF-FN9199 roots and transformed with *p35S::NSP2* also confirmed the function of symbiotic interaction with rhizobia (**Figures 1A,B,E**). Although nodules on the NF-FN9199 roots were less elongated compared with the nodules that formed on wild-type roots transformed with empty vector (**Figures 1C,D**), they were pink because of the presence of leghemoglobin, indicating the establishment of an efficient symbiotic interaction to some degree. However, the lower ratio of the pink nodules that formed on the NF-FN9199 roots transformed with the construct *p35S::NSP2* was observed compared with the empty vector-transformed wild-type roots (**Figure 1E**), indicating that the *NSP2* gene controlled by the 35S constitutive promoter was able to restore the nodule development of *nsp2* mutants, whereas not all the nodules were completely functional. The genetic complementation of the mutant with *NSP2* confirmed that the point mutation in *NSP2* caused the nodulation deficiency of NF-FN9199; therefore, this mutant was termed *nsp2-6* hereafter. The sequence analysis of the *NSP2* gene amplified from *nsp2-6* revealed a point mutation at nucleotide position 730 in the coding sequence of *NSP2*. The single base-pair change from G to C caused an amino acid substitution of Asp to His (D244H) in VHIID, one of the five motifs of the GRAS domain of the NSP2 protein (**Figure 2**; Kontra-Kováts et al., 2019). The mutation in *nsp2-6* led to amino-acid change in one of the prominent residues in the so-called VHIID motif. It has been reported previously that the mutation in *nsp2-3* causes a nonconservative E232K substitution in the VHIID motif, and that a 435-bp deletion in *nsp2-2* eliminates the major part of the GRAS domain of NSP2 (Kalo et al., 2005).

Point Mutant Alleles of *NSP2* Show Distinct Root Hair and Infection Phenotypes

Root hair deformation and curling are the first morphological responses to rhizobial infection. The *nsp2-1* and *nsp2-2*

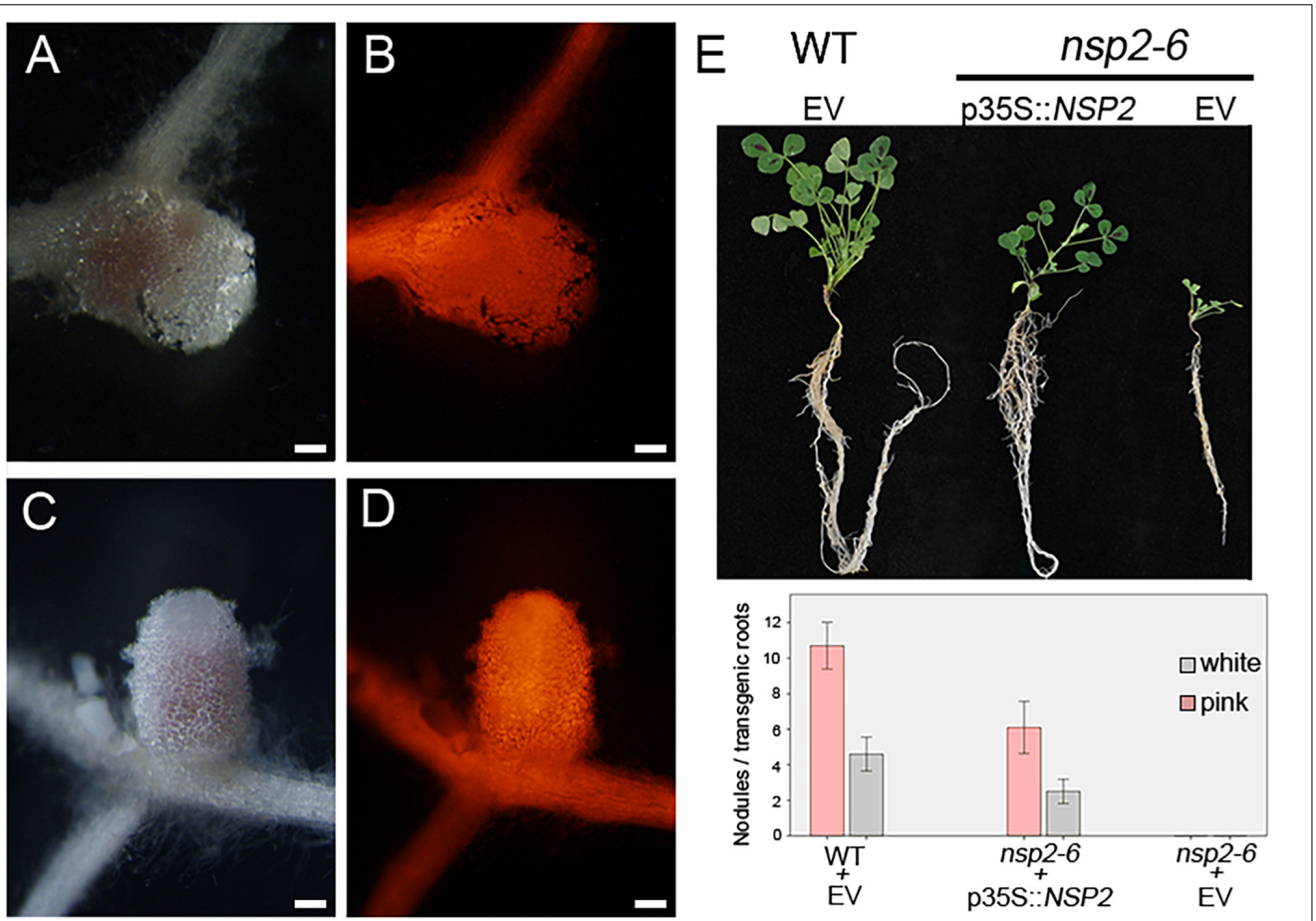

FIGURE 1 | *NSP2* restores the nodulation phenotype of the *nsp2-6* allele. The *NSP2* gene driven by the constitutive 35S promoter (*p35S::NSP2*) was introduced into the *nsp2-6* roots by *Agrobacterium rhizogenes*-mediated hairy root transformation. Transformed roots were inoculated with *Sinorhizobium medicae* WSM419. Bright field stereomicroscope images of nodules **(A,C)** developed on transgenic roots identified by DsRed fluorescence **(B,D)** were analyzed at 21 days post inoculation with rhizobia. Nodules formed on the *nsp2-6* roots transformed with the *p35S::NSP2* construct **(A,B)**. Pink and nitrogen-fixing nodules were formed on wild-type (WT) *Medicago truncatula* A17 roots transformed with empty vector (EV) **(C,D)**. Retarded shoot growth of *nsp2-6* is partially restored with *p35S::NSP2* **(E)**. Average number of pink and white nodules detected on transgenic roots (WT n = 14, *nsp2-6* n = 18 and 22 transformed with *p35S::NSP2* and empty vector, respectively **(E)**. Error bars represent standard errors. Scale bars, 200 μm **(A–D)**.

deletion mutant alleles showed root hair deformation with imperfect curling at 3 dpi with compatible rhizobia (Oldroyd and Long, 2003). To analyze the root hair responses of the point mutant alleles of *NSP2*, *nsp2-2*, *nsp2-3*, *nsp2-6* mutant, and wild-type plants were inoculated with SmWSM419 carrying the constitutively expressed *GUS* reporter gene. We monitored the root hair responses and, in addition, the roots were stained for GUS activity to visualize rhizobia in ITs at 3 and 14 dpi. Rhizobia triggered the formation of tightly curled root hairs called shepherd's crooks and ITs containing rhizobia on the wild-type roots (**Figures 3A,B,I**). The most advanced morphological alteration in the *nsp2-2* deletion mutant was the incomplete curling of root hairs without entrapped bacteria, although rhizobia were found on the surface of the root hairs (**Figures 3C,I**). Similar to *nsp2-2*, only imperfect curling of the root hairs could be detected in *nsp2-6* at 3 dpi (**Figures 3D,I**), and the monitoring of the root hairs at 14 dpi did not identify any progression in root hair responses (**Figure 3E**). Entrapped bacteria formed by the complete curling of root hairs on *nsp2-3* mutant roots that led to the initiation of IT growth were found in the infection chamber (**Figures 3F,I**). Although these ITs were often discontinuous or showed abnormal development with outgrowths and the occurrence of aggregated bacteria (**Figure 3G**), several ITs reached the dividing cortical cells where rhizobia were released, resulting in infected nodule primordia at 4 dpi (**Figures 3H,I**).

Substitution D244H in the VHIID Motif of Nodulation Signaling Pathways 2 Impairs the Nod Factor Signaling Pathway and Blocks Nodule Organogenesis

The common symbiotic signaling pathway downstream of the CCaMK protein splits into root nodule and mycorrhiza-specific branching. NSP2 is primarily required for transmitting

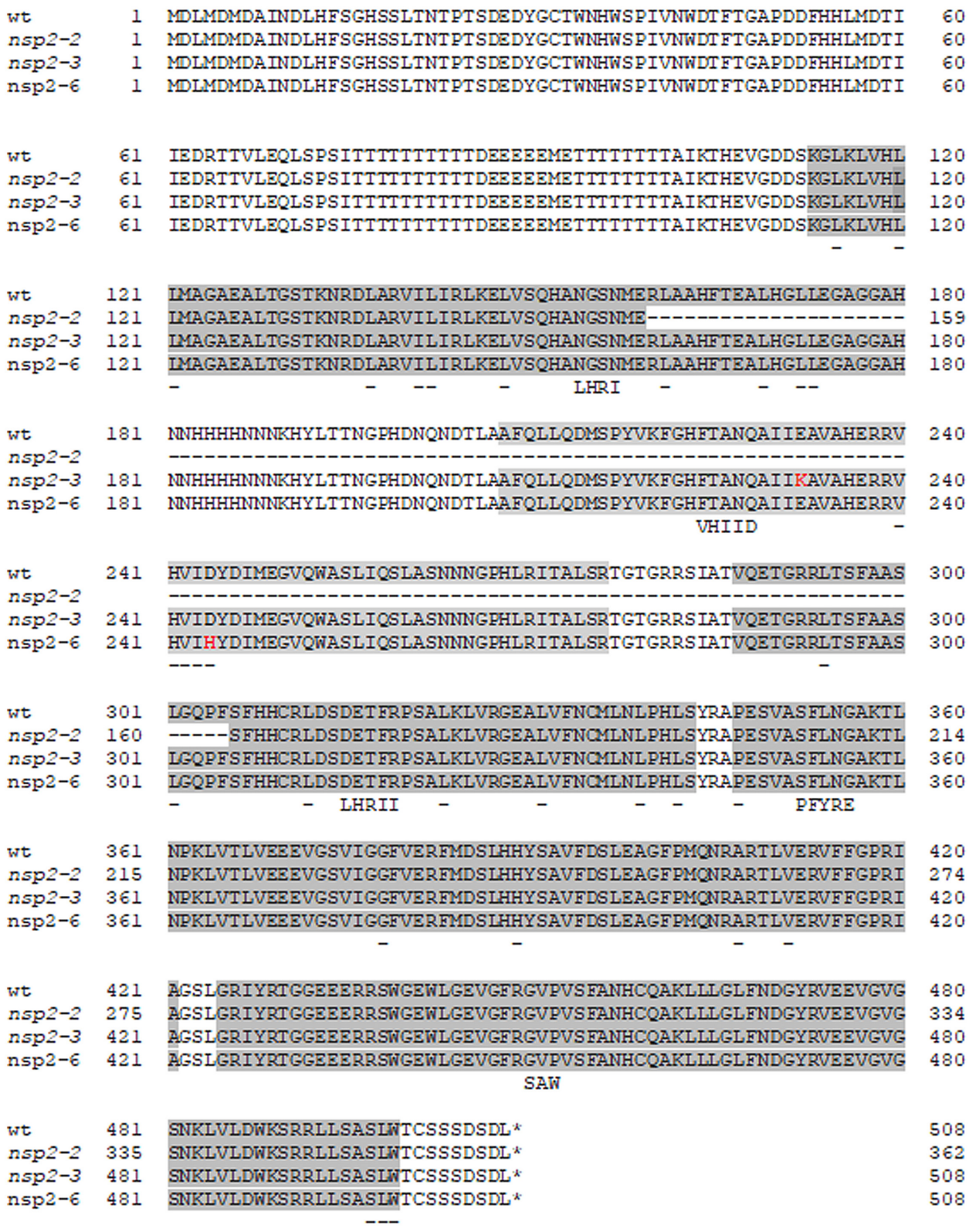

FIGURE 2 | Alignment of the amino acid sequences of wild-type and Nodulation Signaling Pathway 2 (NSP2) mutant alleles. Single amino acid substitutions in the *nsp2-3* (E232K) and *nsp2-6* (NF-FN9199) (D244H) mutants are highlighted with red characters. The conserved LHRI, VHIID, LHRII, PFYRE, and SAW motifs of the GRAS domain are highlighted with gray background. Conserved residues of the subdomains are underlined. Deletion in *nsp2-2* allele affects the motifs LHRI, VHIID, and LHRII.

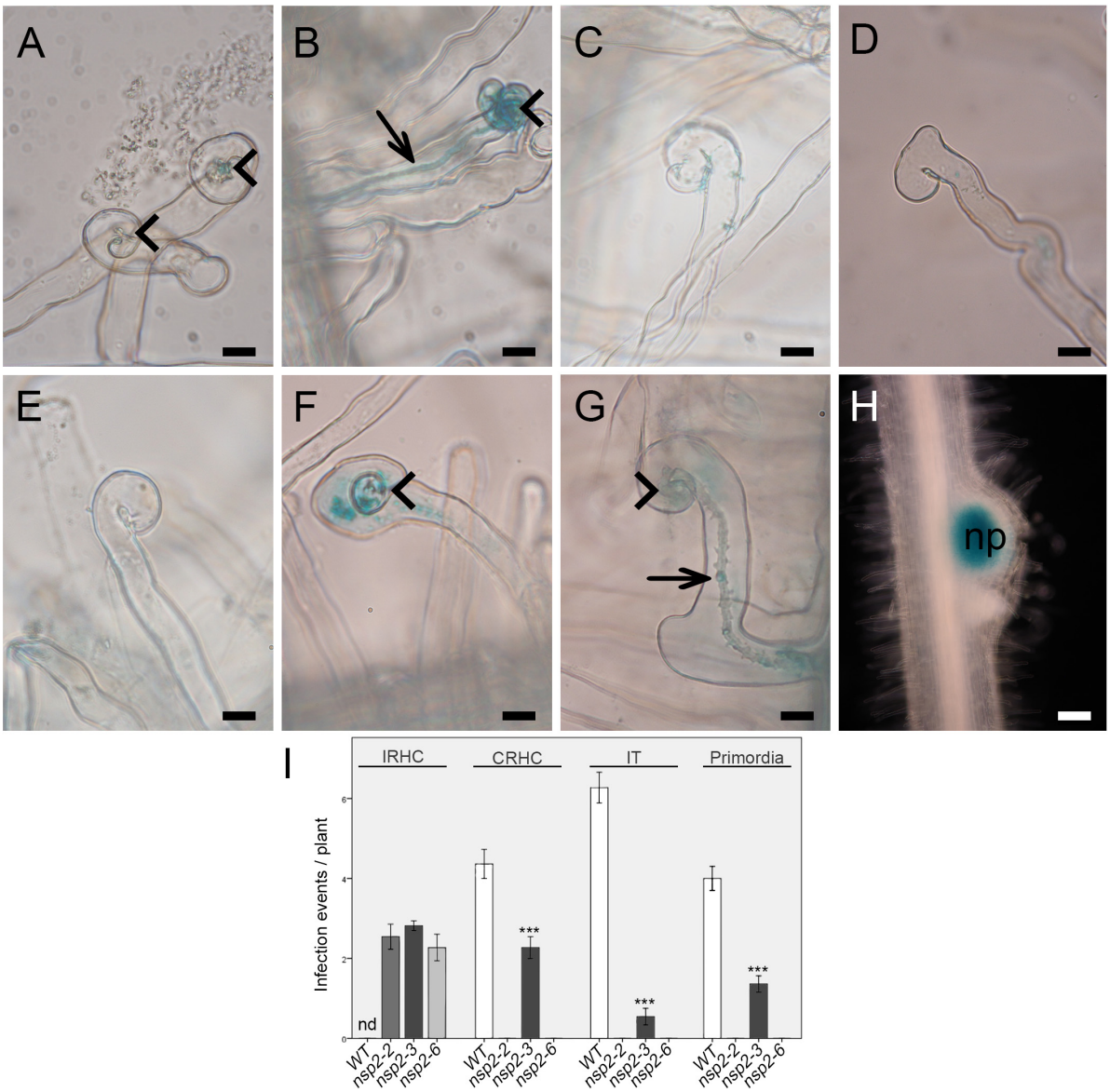

FIGURE 3 | Early infection phenotype of different *nsp2* alleles. **(A)** Root hair curling at 2 days post inoculation (dpi) and **(B)** initiation of infection thread (IT) development on wild-type roots at 3 dpi with *S. medicae* strain WSM419 constitutively expressing the *gusA* gene. Rhizobia triggered merely incomplete root hair curling (IRHC) on *nsp2-2* and *nsp2-6* mutant roots at 3 dpi **(C,D)** and even at 14 dpi on *nsp2-6* roots **(E)**. Rhizobial inoculation induced complete root hair curling (CRHC) **(F)** and infection thread growth with abnormal morphology **(G)** on *nsp2-3* roots at 3 dpi and formation of nodule primordia **(H)** with infected cells at 4 dpi. Arrowhead, root hair curling; arrow, infection thread; np, nodule primordium. Scale bars: 50 μm **(A–G)** and 25 μm **(H)**. Average number of infection events detected on WT (n = 13) and *nsp2* mutant roots (*nsp2-2* n = 11, *nsp2-3* n = 15, and *nsp2-6* n = 11) at 3 dpi and average number of nodule primordia on WT (n = 16) and *nsp2-3* (n = 16) mutant roots at 4 dpi with *S. medicae* strain WSM419 **(I)**. IRHC, incomplete root hair curling; CRHC, complete root hair curling; IT, infection thread; nd, not determined. Error bars represent standard errors. Asterisks indicate significant differences by Student's t-test: $^{***}P \leq 0.001$.

NF signaling to induce nodulation-specific gene expression leading to nodule organogenesis and rhizobial infection (Oldroyd and Long, 2003). To assess how point mutant alleles of NSP2 modulate the induction of root nodule-specific signaling pathway, the expression of *ENOD11*, *NIN*, *ERN1*, and *NF-YA1* (also termed Heme Activator Protein 2 gene, *HAP2*) acting downstream of the CCaMK/IPD3 and the NSP1/NSP2 regulatory complexes was monitored 4 dpi with SmWSM419 by qPCR (Oldroyd and Long, 2003; Kalo et al., 2005; Horvath et al., 2011). A severe reduction in the relative transcript level of *ENOD11*, *NIN*, and *NF-YA1* was detected in *nsp2* mutants, but the expression of these marker genes was always higher in *nsp2-3* compared with *nsp2-2* and *nsp2-6,* indicating a partial activity of $NSP2_{E232K}$ in symbiosis-specific gene induction (**Figure 4A**). Although the relative expression level of *ERN1* was reduced, it did not show significant variation among the different *nsp2*

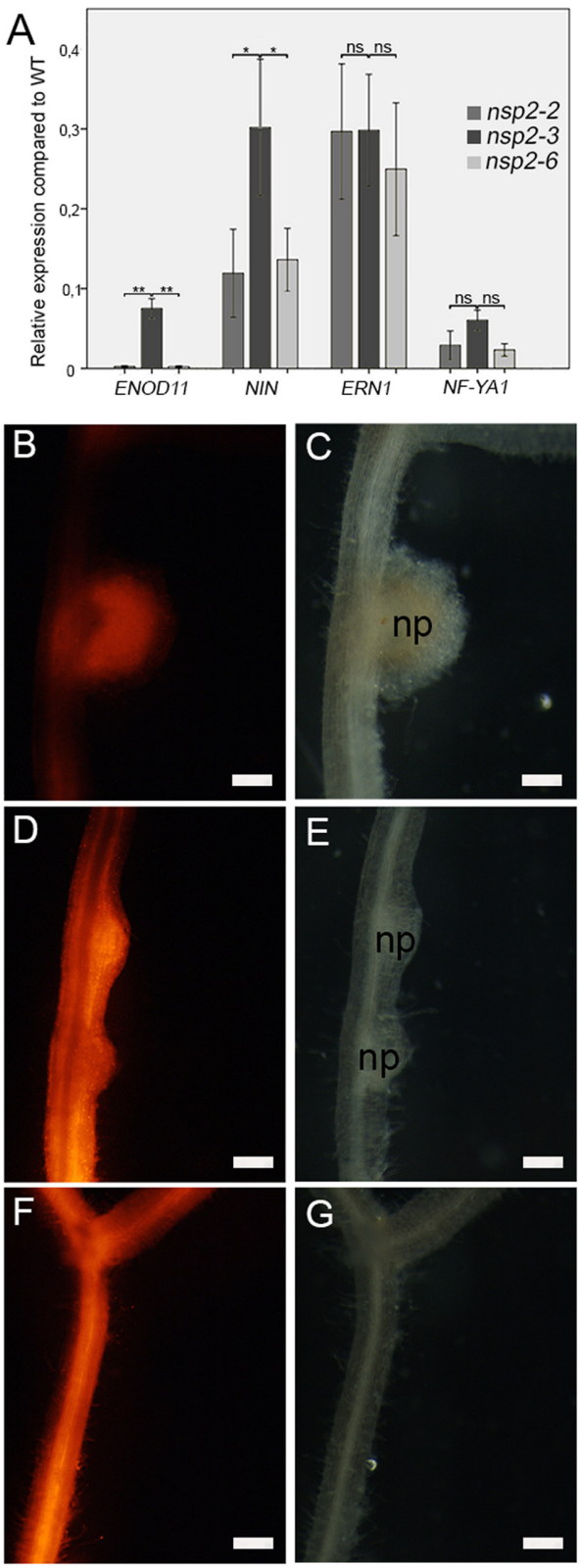

FIGURE 4 | Mutant alleles of NSP2 show distinct symbiotic signaling responses. Relative transcript levels of the symbiotic marker genes *ENOD11*, *(Continued)*

FIGURE 4 | *NIN*, *ERN1*, and *NF-YA1* in the *nsp2-2*, *nsp2-3*, and *nsp2-6* mutant plants were calculated in relation to those of the WT plants following inoculation with *S. medicae* strain WSM419 at 4 dpi **(A)**. Spontaneous nodule formation was induced on roots transformed with the construct of the autoactive CRE1* protein. Spontaneous nodules that developed on WT **(B,C)** transgenic roots confirmed the activity of CRE1*. The formation of nodule primordia on the *nsp2-3* **(D,E)** roots indicated that the nonconservative substitution E232K of NSP2 did not block but delayed nodule formation. Lack of spontaneous nodules on the *nsp2-6* transgenic roots **(F,G)** revealed that the substitution D244H blocked nodule organogenesis. Transgenic roots were identified by DsRed fluorescence. Values of the transcript levels are the mean of five biological replicates. Error bars represent standard errors. Asterisks indicate significant differences as determined by Student's *t*-test: ns $P \geq 0.05$, $^{*}P \leq 0.05$, and $^{**}P \leq 0.01$. Scale bars, 200 μm **(B–G)**.

alleles, suggesting a possible indirect effect of NSP2 on *ERN1* gene expression.

The formation of symbiotic nodules is the result of two coordinated developmental programs, rhizobial infection and nodule formation, and the arrest in either process blocks the progress of the other one. We demonstrated that $NSP2_{D244H}$ blocks the infection in root hairs, but it was still in question whether the non-nodulation phenotype of *nsp2-6* was the result of the arrest of the rhizobial infection or whether the D244H substitution abolished nodule organogenesis, too. *CCaMK*, encoding a calcium- and calmodulin-dependent kinase, and the cytokinin receptor gene *CRE1* are both essential for nodule organogenesis. The activation of CCaMK and CRE1 initiates root cortical cell division and downstream signaling components, such as NSP2, which is required for the formation of nodule primordia (Gleason et al., 2006; Plet et al., 2011). The gain-of-function variants of CCAMK and CRE1 are able to induce spontaneous nodule formation (Gleason et al., 2006; Gonzalez-Rizzo et al., 2006; Tirichine et al., 2007). To test the requirements of the Asp residue at position 244 in NSP2 for nodule organogenesis, we introduced the gain-of-function version of CRE1 [CRE1* (L267F); Ovchinnikova et al., 2011]; into the roots of the wild-type (**Figures 4B,C**) and *nsp2* mutant plants (**Figures 4D–G**) by *A. rhizogenes*-mediated hairy root transformation. Transformed plants were grown in the absence of rhizobia and scored for spontaneous nodule formation 8 weeks post transformation. Primordia of spontaneous nodules formed on *nsp2-3* transgenic roots (**Figures 4D,E**), indicating that the mutation in *nsp2-3* is neutral for nodule induction although the $NSP2_{E232K}$ protein variant appears to cause delayed formation of spontaneous nodules (**Figures 4D,E**). In contrast, no nodules could be detected on *nsp2-6* transgenic roots (**Figures 4F,G**), indicating that the variant $NSP2_{D244H}$ abolishes nodule formation.

Substitution of D244H in the VHIID Motif of Nodulation Signaling Pathways 2 Abolishes the Interaction With Nodulation Signaling Pathways 1

It was previously demonstrated in yeast and *in planta* by two-hybrid experiments and BiFC assay that NSP1 and NSP2 form heterodimers, and that this complex interact with the promoter

of NF inducible genes *ENOD11*, *ERN1*, and *NIN* (Hirsch et al., 2009). It was found that the amino acid change $NSP2_{E232K}$ in the VHIID domain in *nsp2-3* abolished the autoactivation capacity of NSP2 but did not inhibit the interaction with NSP1 (Hirsch et al., 2009). To test how the substitution in mutant *nsp2-6* affects the interaction with NSP1, we tested the capability of $NSP2_{D244H}$ to form a complex with NSP1 along with wild-type NSP2 and mutant $NSP2_{E232K}$ in *S. cerevisiae* using a yeast-two hybrid (Y2H) system.

Nodulation Signaling Pathway 2 showed strong autoactivation in the Y2H experiments when fused to the Gal4 DNA binding domain (Hirsch et al., 2009). To improve the stringency of the interaction, we raised the amount of supplemented 3-aminotriazole (3-AT) to a relatively high concentration that abolished the autoactivation activity of NSP2 (**Figure 5A**), allowing us to use it in the Y2H assay. Yeast strains containing $NSP2_{E232K}$ or $NSP2_{D244H}$ fused to the Gal4 DNA binding domain could grow in -HLT plates, indicating the reduced capability of these proteins to autoactivate the Gal4 system (data not shown). Both wild-type NSP2 and $NSP2_{E232K}$ interacted with NSP1, when fused either to the Gal4 DNA binding domain or to the activation domain (**Figure 5A**). These results are consistent with previous studies showing that $NSP2_{E232K}$ does not affect the complex formation between NSP1 and NSP2 (Hirsch et al., 2009). However, the mutation in $NSP2_{D244H}$ inhibited the interaction with NSP1 in yeast, indicating that the Asp residue in the VHIID motif of NSP2 was essential for the interaction with NSP1. The interaction between $NSP2_{E232K}$ or $NSP2_{D244H}$ with NSP1 was quantified by measuring β-galactosidase activity. The results showed a significant reduction in yeast containing $NSP2_{E232K}$ and NSP1 (**Supplementary Figure 1A**) compared with the interaction between wild-type NSP2 and NSP1, although the yeast strain producing $NSP2_{E232K}$ and NSP1 proteins could grow in the spot assay (**Figure 5A**). We detected low levels of β-galactosidase activity in *S. cerevisiae* producing $NSP2_{D244H}$ and NSP1, but this activity probably did not exceed the threshold to allow the growth of yeast expressing these proteins. Control immunoblotting with anti-HA was performed to show the stability of the mutant versions of NSP2 (**Supplementary Figure 2B**), and that the absence of interaction between $NSP2_{D244H}$ and NSP1 was not due to lack of the mutant NSP2 protein.

To validate the differential interaction of $NSP2_{E232K}$ and $NSP2_{D244H}$ with NSP1 observed in the Y2H experiment, we analyzed their association in *N. benthamiana* leaves by BiFC assay. We fused NSP1 to the N-terminal part of the yellow fluorescent protein (N-YFP) and NSP2, and $NSP2_{E232K}$ and $NSP2_{D244H}$ to the C-terminal part of the yellow fluorescent protein (C-YFP). We co-infiltrated the constructs of NSP1 with the different version of NSP2 into *N. benthamiana* leaf epidermal cells using *A. tumefaciens*. Previously, nuclear localization of NSP1 and NSP2 has been observed (Kalo et al., 2005; Smit et al., 2005). The nuclear signal of YFP was detected when we transiently expressed the nuclear localized NSP1 with either NSP2 or $NSP2_{E232K}$, indicating an *in planta* interaction between these proteins (**Figure 5B**). No nuclear signal of YFP was detected when NSP1 was co-infiltrated with $NSP2_{D244H}$, confirming the eliminated interaction between these proteins that has been found in Y2H previously. These results highlight the requirement of a conserved residue in the VHIID motif of NSP2 that is essential for the interaction between NSP1 and NSP2 and required for both nodule formation and rhizobial infection.

Medicago truncatula nsp2-3 Shows a Strain-Dependent Nodulation Phenotype

The emergence of nodule primordia at 4 dpi with SmWSM419 (**Figure 3H**) did not correspond completely to the previously reported nodulation phenotype of *nsp2-3*. The former study found no nodule primordium development on *nsp2-3* roots at 4 dpi with *S. meliloti* strain 1021 (Sm1021) although small white nodules could be detected at later time points (Kalo et al., 2005). To characterize the strain-dependent nodulation phenotype of *nsp2-3*, the kinetics of nodule development were monitored on wild-type and *nsp2-3* plants inoculated with the rhizobial strains *S. meliloti* 1021 (pXLGD4) and *S. medicae* WSM419 (pXLGD4) constitutively expressing the *lacZ* reporter gene. Nodule primordia were formed on wild-type roots at 4 dpi with both rhizobial strains and on *nsp2-3* roots inoculated with SmWSM419 (**Figures 6A,D,G**), but no primordia were visible on Sm1021-inoculated mutant roots at this time point (**Figure 6J**). Round-shaped young nodules containing invaded cells were formed on wild-type roots inoculated with both rhizobial strains and on *nsp2-3* roots (**Figures 6B,E,H**) at 10 dpi, but only nodule primordia were visible at this time point on *nsp2-3* roots elicited with Sm1021 (**Figure 6K**). Fully developed pink nodules expressing leghemoglobin and showing characteristic zonation of indeterminate nodules were found on the wild-type roots at 18 dpi with both strains (**Figures 6C,I**). White or occasionally slightly pinkish nodules developed on *nsp2-3* roots inoculated with SmWSM419 at 18 dpi, which were less elongated compared with wild-type nodules (**Figure 6F**). However, the formation of spherical undeveloped nodules on the *nsp2-3* roots at 18 dpi with Sm1021 indicated that the nodule development program was merely delayed and not blocked in the *nsp2-3* roots (**Figure 6L**). Infrequently, we observed pink nodules elicited by Sm1021 on the *nsp2-3* roots at 18 dpi. We counted the number of nodule primordia, and non-fixing white and nitrogen-fixing pink nodules on the wild-type and *nsp2-3* plants at 18 dpi with both rhizobial strains (**Figure 7C**). The wild-type plants developed a slightly higher number of functional pink nodules with SmWSM419 compared with Sm1021, confirming that *M. truncatula* genotype A17 has a better symbiotic performance with strain SmWSM419 compared with strain Sm1021 as reported previously (Terpolilli et al., 2008). The higher ratio of nodule primordia and a lower percentage of white nodules detected on the *nsp2-3* roots with Sm1021 compared with SmWSM419 indicated delayed nodule development with strain Sm1021. Although there was a difference in the percentage of leghemoglobin expressing pink nodules between the two bacterial strains, the morphology and colonization of these nodules looked similar (**Figures 7A,B**). To further investigate the strain-dependent nodule development and symbiotic effectiveness, the activity of bacterial nitrogenase

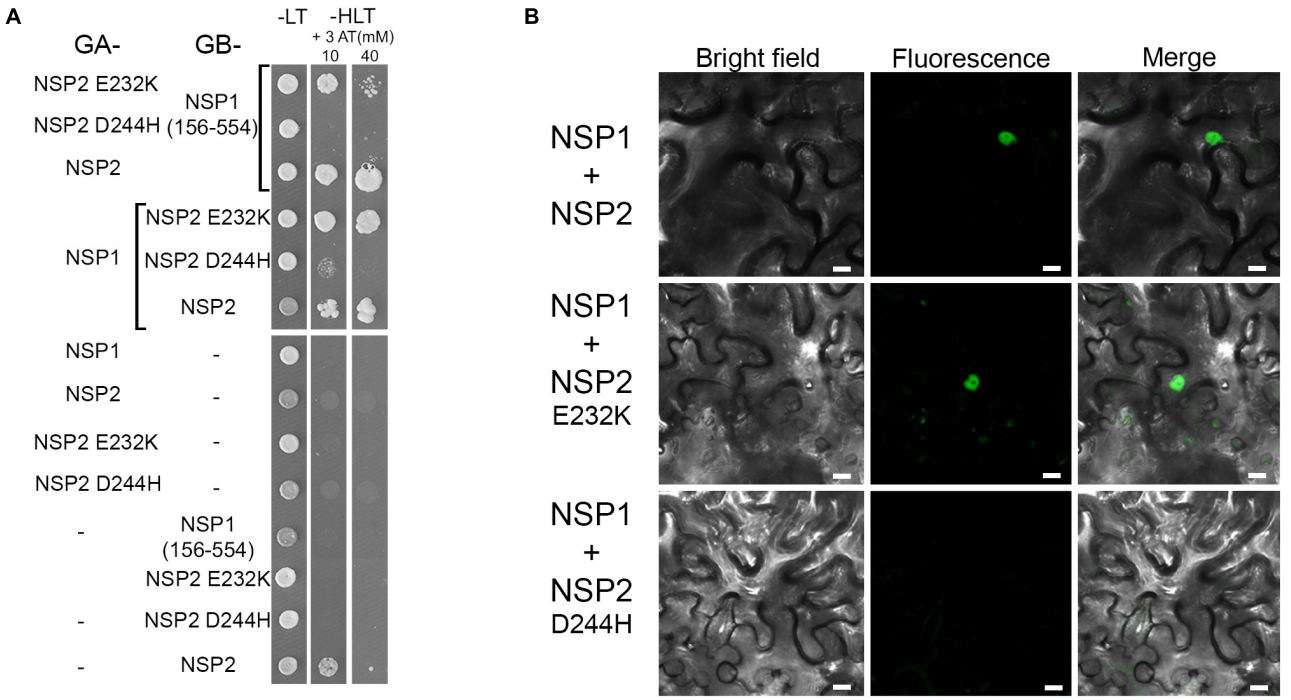

FIGURE 5 | Interaction between the NSP1 and NSP2 derivatives. Interactions were tested in yeast-two-hybrid (Y2H) **(A)** and in bimolecular fluorescence complementation (BiFC) **(B)** assays. **(A)** NSP1 and NSP2 derivatives were fused either to the yeast Gal4 activation (GA) domain or the Gal4 DNA binding (GB) domain and transformed into *Saccharomyces cerevisiae* strain PJ69-4A. To test the direct interactions between NSP1 and NSP2, the growth of yeast colonies was compared in the presence (-LT) and absence [-HLT supplemented with 3-amino-1,2,4-triazole (3-AT)] of histidine. Y2H assay showed that NSP2-D244H does not interact with NSP1. In order to test the interaction between NSP1 and WT or mutant versions of NSP2 that were fused to the yeast Gal4 activation, the non-autoactive deletion version of NSP1 (156-554) fused to GB was used. **(B)** Constructs encoding for the N-terminal or C-terminal parts of the YFP fused to the N-terminal part of the NSP1 and NSP2 derivatives, respectively, were co-transformed transiently into *Nicotiana benthamiana* leaves. Interactions of the proteins in leaf epidermal cells were observed by confocal microscopy 3 days after transformation. Scale bars, 10 μm.

of pink nodules that developed on the *nsp2-3* and wild-type roots was measured with the help of ARA at 3 wpi. The acetylene reduction rate of *nsp2-3* pink nodules was higher with SmWSM419 compared with Sm1021 (**Figure 7D**), suggesting better nitrogen fixation capacity of the interaction with strain SmWSM419. Shoot dry weight measurements of the *nsp2* mutant alleles and wild-type plants at 8 wpi with SmWSM419 showed that *nsp2-3* had significantly higher biomass than *nsp2-2* and *nsp2-6* alleles under symbiotic growth conditions (**Figure 7E**), indicating a weak effect of the nonconservative substitution E232K on the symbiotic function of NSP2.

Substitution E232K in the VHIID Motif of Nodulation Signaling Pathways 2 Affects Nodule Invasion

The pink nodules of the *nsp2-3* mutant inoculated with SmWSM419 showed similar rhizobial colonization and nitrogen fixation capacity compared with the wild-type plants at 18 dpi, although the *nsp2-3* nodules were less elongated. The analysis of nodule morphology and rhizobial invasion at 4 wpi with SmWSM419 carrying the *GUS* reporter gene revealed that the *nsp2-3* pink nodules were thicker, and that their colonization was more extensive compared with the wild-type ones (**Figures 8A,B**). The structure and colonization of the *nsp2-3* pink nodules were further analyzed following staining with the nucleic acid-binding dye SYTO13 and investigation by confocal laser scanning microscopy. The autofluorescent property of cell walls was used to visualize the outline of the nodules. The analysis of the SYTO13-stained longitudinal (**Figures 8C–H**) and cross (**Figures 8I,L**) sections of 28 dpi wild-type and *nsp2-3* mutant nodules showed cells that were similarly colonized by bacteria, although some remarkable differences were observed. Similar to the GUS staining, a higher number of green fluorescent infected cells were found in the *nsp2-3* nodules (**Figures 8F,L**) compared with wild-type plants (**Figures 8C,I**), and uninfected cells displaying autofluorescence could hardly ever be observed in the *nsp2-3* nodules (**Figures 8G,H,L**). Higher magnification of nodule cross-sections prepared from the distal part of the nitrogen fixation zone showed infected cells containing elongated bacteroids that were orientated toward the central vacuole in the wild-type nodules (see inset images on **Figure 8J,K,M,N**). In the *nsp2-3* nodules, densely located infected cells with hardly visible or contracted vacuoles, disorganized symbiosomes, and tens of starch granules were detected (**Figures 8M,N**). The lack of autofluorescent cells in the inner cortical cell layer and uninfected cells in the central nodule tissue was also apparent in these mutant sections. The *nsp2-3* mutant nodules were extensively

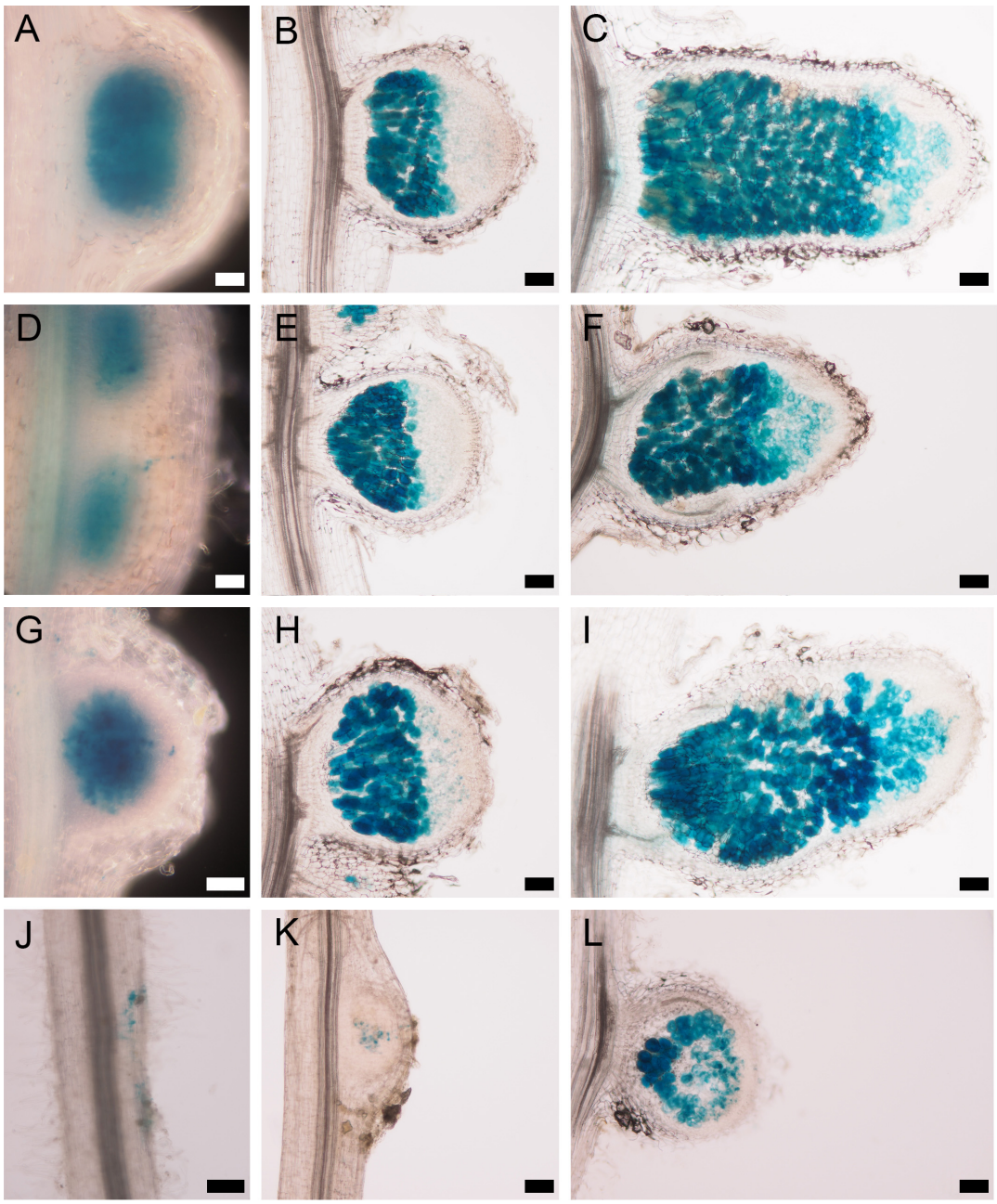

FIGURE 6 | Strain-dependent nodulation kinetics of the *nsp2-3* mutant. WT *Medicago truncatula* A17 plants inoculated with either the **(A–C)** *S. medicae* strain WSM419 or with the **(G–I)** *S. meliloti* strain 1021 expressing the *lacZ* gene show similar nodulation phenotypes at **(A,G)** 4 dpi, **(B,H)** 10 dpi, and **(C,I)** 18 dpi. *nsp2-3* mutant inoculated with the *S. medicae* strain WSM419 at **(D)** 4 and **(E)** 10 dpi displayed similar nodule morphology and rhizobial colonization as WT nodules. Slightly delayed development could be detected in the *nsp2-3* nodules at **(F)** 18 dpi. *nsp2-3* mutant showed remarkable delayed nodule development at **(J)** 4 dpi, **(K)** 10 dpi, and **(L)** 18 dpi with strain *S. meliloti* 1021. Scale bars, 100 μm.

filled up with colonized cells but also possessed a reduced number of small uninfected cells, indicating a function of NSP2 in controlling the balance between the infected and uninfected cells. Nodule sections analyzed at higher magnification showed mostly fluorescence signals of rhizobia when analyzed in the green channel. In order to quantify the infected cells in the wild-type and *nsp2-3* mutant nodules, we measured the area of colonized cells on SYTO13-stained nodules of the *nsp2-3* and wild-type plants. Sections were analyzed using the image-analysis software FIJI (Schindelin et al., 2012) to determine the number and area of connected fluorescent regions. The analysis revealed a higher number of smaller areas of fluorescence in sections of the wild-type plants as compared with the mutant (**Supplementary Figure 2**) plants, indicating that the infected

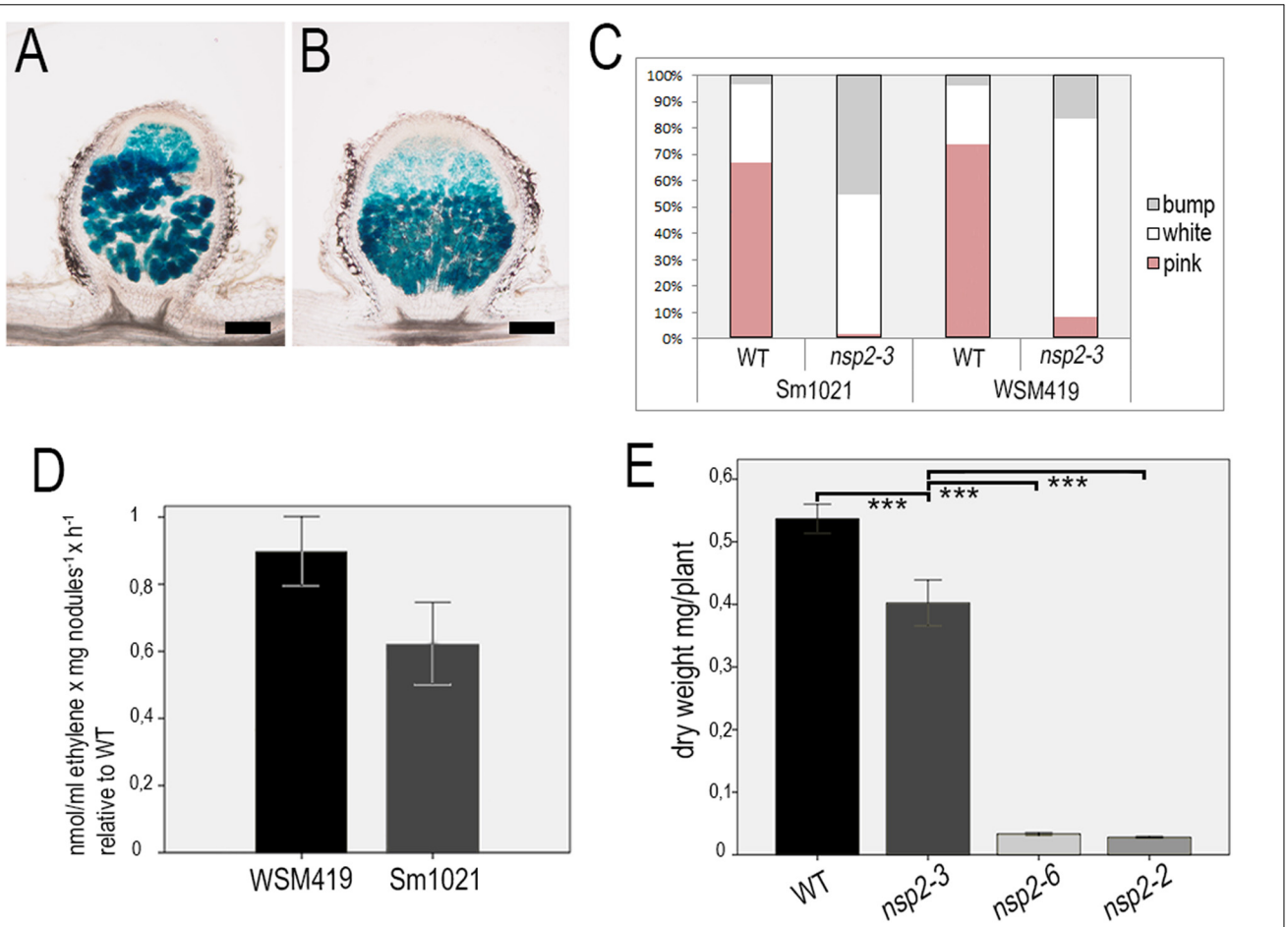

FIGURE 7 | Pink nodules of the *nsp2-3* mutant plants display better symbiotic performance with SmWSM419. Colonization of the pink nodules occasionally formed on *nsp2-3* roots at 18 dpi with strains **(A)** Sm1021 or **(B)** SmWSM419 is similar. Distribution of pink (fixing) nodules, white spherical (non-fixing) nodules, and bumps (nodule primordia) that formed on WT and *nsp2-3* roots at 18 dpi **(C)**. Relative ethylene production measured by the ARA of pink nodules harvested from the *nsp2-3* and WT roots. Values represent the mean ± SE of three replicates **(D)**. Shoot dry weight of the WT and different *nsp2* mutant plants at 8 wpi with SmWSM419. Values represent the mean ± SE of 20 plants **(E)**. Asterisks indicate significant differences determined by Student's *t*-test: ***$P \leq .001$. Scale bars, 200 μm.

cells in the wild-type sections are more frequently surrounded by uninfected cells and that the mutant nodules contained more densely infected cells.

DISCUSSION

Two GRAS-type transcription regulators, NSP1 and NSP2, form a complex that binds to the promoters of early nodulin genes and induce their transcriptional activity (Hirsch et al., 2009). The appropriate activity of the NSP1–NSP2 complex is required for synchronized processes of IT formation and invasion of roots by nitrogen-fixing rhizobia and the induction of cortical cell divisions essential for nodule organogenesis (Catoira et al., 2000; Oldroyd and Long, 2003; Kalo et al., 2005; Smit et al., 2005).

Here, we report that two-point mutant alleles of *NSP2* containing mutation in the VHIID conserved region of the GRAS domain show distinct early responses to rhizobial inoculation. The *nsp2-6* mutant allele was identified in a screen of FN-mutagenized *M. truncatula* population (Kontra-Kováts et al., 2019). Fast neutron bombardment (FNB) is a promising source to induce smaller and larger deletions for gene disruptions. Although single base pair substitutions were detected in FN-mutagenized *Arabidopsis thaliana* populations (Belfield et al., 2012), to our knowledge, no FNB-induced single nucleotide exchange has been reported in FN-mutagenized *M. truncatula*. However, we cannot exclude that spontaneous mutation generated the nucleotide exchange in this *nsp2* allele. The mutation in *nsp2-6* caused the change in one of the conservative residues of the VHIID motif of NSP2 ($NSP2_{D244H}$), and this mutation phenocopies the *nsp2-2* null allele identified earlier (Oldroyd and Long, 2003). Both the *nsp2-2* and *nsp2-6* alleles showed root hair deformation, but entrapped bacteria forming microcolonies were not observed when inoculated with rhizobia. These mutant alleles were similarly blocked for NF-induced gene expression. The substitution of $NSP2_{D244H}$ abolished the interaction with NSP1 in yeast and *N. benthamiana* like the

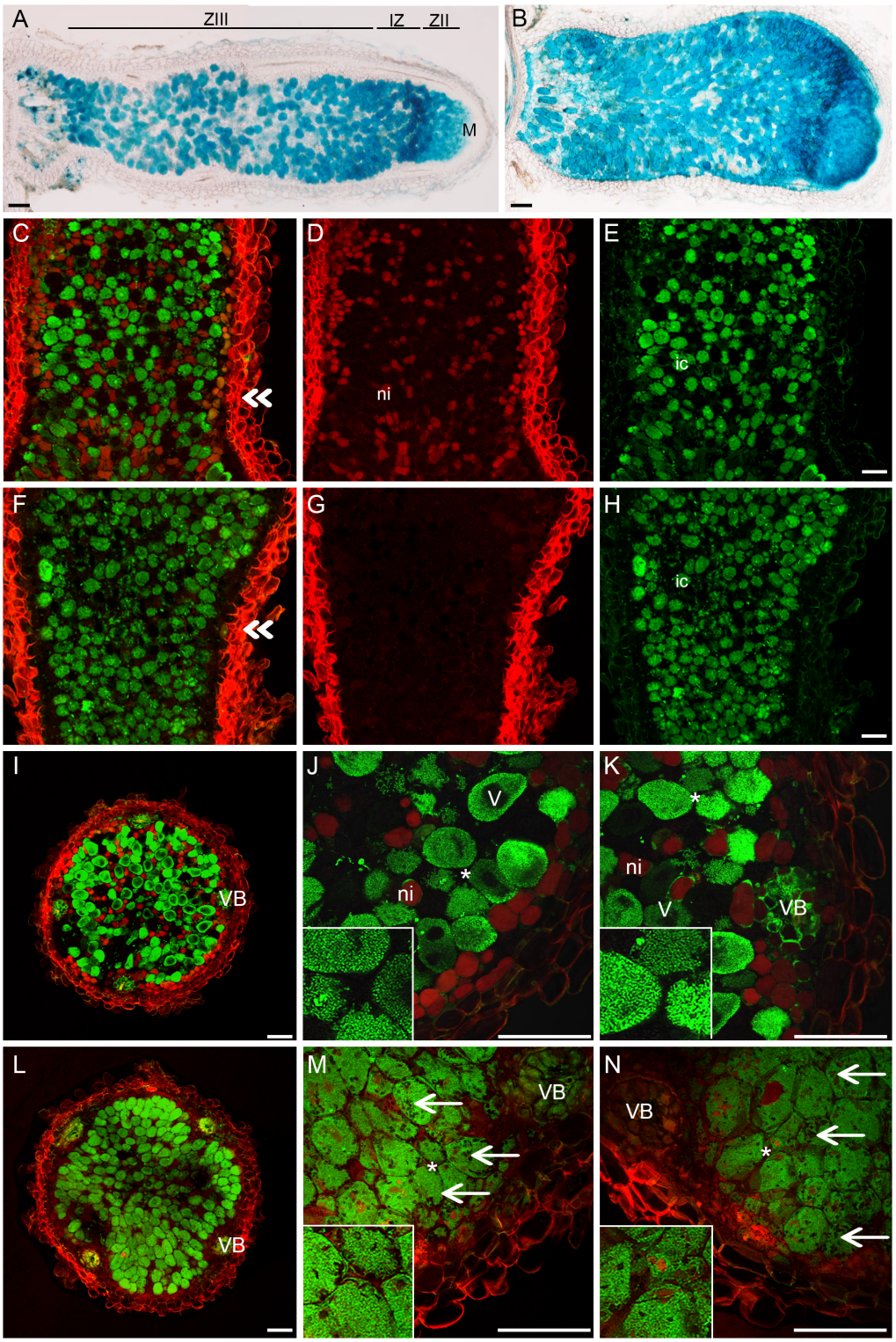

FIGURE 8 | *nsp2-3* nodules contain colonized cells more densely. **(A)** WT and **(B)** *nsp2-3* plants were inoculated with SmWSM419 with the *gusA* marker gene. Pink nodules were harvested at 4 wpi, and sections were GUS-stained to detect infected cells. Sections of pink WT and *nsp2-3* mutant nodules were stained with SYTO13 and analyzed by confocal microscopy. **(C–E)** Longitudinal and cross- **(I–K)** sections from the fixation zone of WT and **(F–H)** longitudinal and cross- **(L–N)** sections from the fixation zone of *nsp2-3* nodules are shown. **(E,H)** Bacterial DNA and plant nuclei showed green fluorescence after SYTO13 staining. Outline of the nodules showed autofluorescence of the cell wall and is shown in red **(D,G)**. Panels **(C,F)** show overlay images of **(D,E)** and **(G,H)**, respectively. Panels **(J,K)** and **(M,N)** show higher magnification of cross-sections **(I,L)**. ZIII, fixation zone; IZ, interzone; ZII, invasion zone; M, meristem. Double arrowheads show the position of the cross sections, ni, non-infected cells; ic, infected cells; VB, vascular bundle; V, vacuole; arrow, starch granules in *nsp2-3* nodule cells. Asterisks indicate cells shown in insets in higher magnification. Scale bar, 100 μm.

deletion derivatives of the GRAS domain of NSP2 detected previously (Hirsch et al., 2009). In addition to the deficiency in the infection process, the nodule development program was also blocked in the *nsp2-6* mutant. These phenotypes suggest that *nsp2-6* is a strong point mutant allele of *NSP2*. The VHIID motif is presumed to mediate DNA-protein interactions (Pysh et al., 1999) and maintain the structural integrity and conformation of the GRAS domain (Li et al., 2016). The symbiotic phenotype of *nsp2-6* and the abolished interaction between NSP1 and $NSP2_{D244H}$ demonstrated the requirement of D244 in the domain of VHIID for the function of the NSP2 protein.

We also report in our study that the mutants $NSP2_{E232K}$ and $NSP2_{D244H}$ interact diversely with NSP1. This finding provides an explanation for the observed changes in NF-induced gene expression and distinct nodulation phenotype of *nsp2-3* and *nsp2-6*. The two point mutations occurred in the VHIID motif suggest different relevance of the residues of E232 and D244 for the function of NSP2. NSP2 and other family members of GRAS proteins contain a conserved GRAS domain that contains five motifs (LHR1, VHIID, LHRII, PFYRE, and SAW) named after their conserved residues. The analysis of the crystal structure of the GRAS domains of SCR and a SCR-LIKE protein (SCL7) (Li et al., 2016; Hakoshima, 2018) revealed that each GRAS domain comprises an α-helical cap and an α/β core subdomain; the latter contains 10 α-helices and nine β-strands (β1–β9). *nsp2-6* contains a D244H mutation in the VHIID motif, which, alone, forms the β1 strand that appears to be important for stabilizing the overall structure of the GRAS domain (Li et al., 2016; Hakoshima, 2018). The E232K mutation in *nsp2-3* is located in the α-helix A5, one of the six α-helices flanking the central β-sheet. Based on the distinct interaction of $NSP2_{E232K}$ and $NSP2_{D244H}$ with NSP1, we suggest that the D244H mutation affects the structure of NSP2 more seriously as compared with the E232K mutation.

In contrast to *nsp2-6*, the *nsp2-3* allele encoding NSP2 with a E232K substitution was reported to form small white nodules, although the infection and nodulation phenotype of this mutant allele has not been studied in detail (Kalo et al., 2005). Complete root hair curling and entrapment of bacteria were detected on the *nsp2-3* roots inoculated with *S. medicae* WSM419. ITs in the root hairs showed thick abnormal morphology with edgy protrusions resembling the ITs found in the root hairs of a *vapyrin* (*vpy*) mutant (Murray et al., 2011) but dissimilar to the swollen, blister-like and bulbous formations observed in *nf-ya-1* mutant root hairs (Laporte et al., 2014) or within the elongated-type nodules of *ipd3-1* (Horvath et al., 2011). However, in contrast to the mutants *vpy* and *nf-ya-1*, ITs in *nsp2-3* penetrated into the cortical cells and released bacteria, which colonized nodule primordia. Because we noticed that the development of nodule primordia was more progressed on the *nsp2-3* roots inoculated with SmWSM419 compared with the nodulation phenotype inoculated with Sm1021 (Kalo et al., 2005), the kinetics of nodule development was analyzed using a less effective (Sm1021) and a highly compatible (SmWSM419) strain (Terpolilli et al., 2008). The difference between wild-type and *nsp2-3* nodule development was not evident until 10 dpi with SmWSM419, and the reduced number of functional pink nodules at a later time point indicated the delay in nodule development. In order to analyze the performance of the pink nodules on *nsp2-3* roots elicited by SmWSM419, nitrogen fixation capacity was assayed, and dry weight measurements were conducted. The symbiotic performance of the pink nodules on the *nsp2-3* roots with SmWSM419 was nearly identical to that of the nodules of the wild-type plants, providing evidence that $NSP2_{E232K}$ was still functioning. However, the tardy nodule differentiation, lower ratio of uninfected cells, and accumulation of starch granules in the *nsp2-3* pink nodules suggest an inaccurate action of $NSP2_{E232K}$.

The delayed nodule development was more striking with the strain Sm1021, indicating a strain-dependent symbiotic phenotype of *nsp2-3*. The suboptimal compatibility of Sm1021 with wild-type *M. truncatula* A17 has been reported previously (Terpolilli et al., 2008; Kazmierczak et al., 2017), and the better-performing microsymbiont SmWSM419 was suggested to be used in symbiotic tests. It was found that Sm1021 efficiently induces nodule organogenesis, but that the complete differentiation of symbiotic nodule cells does not take place (Kazmierczak et al., 2017). Although the genetic basis of the reduced effectiveness of *M. truncatula* A17 with Sm1021 is still unclear, our results suggest that the strain-dependent symbiotic performance is probably already manifested in the NF signaling pathway and that an incomplete differentiation of symbiotic nodule cells or a different nitrogen-fixation capacity of these strains cannot provide explanations per se. Our results also imply the function of NF signaling components during the differentiation of nodule cells at late stages of nodulation.

The analysis of the RNA sequencing data obtained from laser-capture microdissected nodule zones (Roux et al., 2014) revealed that both *NSP1* and *NSP2* are active in the apex of mature nodule. About 70 and 90% of the *NSP1* and *NSP2* transcripts, respectively, were located in the nodule meristem and in the distal part of the infection zone (zone II), supporting a function of *NSP2* in nodule differentiation. The involvement of components of the NF signaling pathway in the late stages of the nitrogen-fixing interaction was reported earlier for *DMI2* and *NIN* (Limpens et al., 2005; Liu et al., 2021). The partial activity of both genes causes defects in symbiosome formation. Our results provide evidence that NSP2 also has a function during IT development and in mature nodules.

CONCLUSION

In summary, we showed here the requirement of a conserved residue in the GRAS domain of NSP2 and the function of NSP2 during early and late stages of nodule symbiosis. Point mutations often induce a partial suppression of gene function and enable the mapping of essential residues for the activity of proteins. Our results also elucidated the benefit of studying weak alleles of symbiotic genes that can be used to define gene functions at later stages of nodule symbiosis. This study also underscores the importance of studying strain-dependent effects of early symbiotic genes.

DATA AVAILABILITY STATEMENT

The original contributions presented in the study are included in the article/**Supplementary Material**, further inquiries can be directed to the corresponding author.

AUTHOR CONTRIBUTIONS

SK, AD, and PK designed the research and analyzed and interpreted the data. SK, LF, and AD performed the experiments. FA contributed to microscopy analysis. KL and GR conducted the acetylene reduction measurements. PK wrote the manuscript. All authors contributed to the article and approved the submitted version.

FUNDING

This study was supported by the Hungarian National Research, Development and Innovation Office (K-119652, KH-129547 and K-120300), ICGEB Research Grant Programme (CRP/HUN17-03), and the Hungarian Ministry for National Economy GINOP-2.3.2-15-2016-00001 (PK). SK received a Young Researcher Fellowship from the Eötvös Lóránd Research Network and his work supported by the Dr. Rollin D. Hotchkiss Foundation. FA received funding from H2020 (SGA No. 739593).

ACKNOWLEDGMENTS

We would like to thank Sándor Jenei, Zsuzsa Liptay, and Hajnalka Tolnainé Csákány for their valuable laboratory assistance during this project. We also thank Erik Limpens (Wageningen University, Netherlands) and Giles Oldroyd (Cambridge University, United Kingdom) for providing the autoactive CRE* and *NSP1* and *NSP2* expression clones for the BiFC and Y2H experiments, respectively.

SUPPLEMENTARY MATERIAL

The Supplementary Material for this article can be found online at: https://www.frontiersin.org/articles/10.3389/fpls.2021.709857/full#supplementary-material

REFERENCES

Andriankaja, A., Boisson-Dernier, A., Frances, L., Sauviac, L., Jauneau, A., Barker, D. G., et al. (2007). AP2-ERF transcription factors mediate nod factor dependent Mt ENOD11 activation in root hairs via a novel cis-regulatory motif. *Plant Cell* 19, 2866–2885. doi: 10.1105/tpc.107.052944

Ariel, F., Brault-Hernandez, M., Laffont, C., Huault, E., Brault, M., Plet, J., et al. (2012). Two direct targets of cytokinin signaling regulate symbiotic nodulation in medicago truncatula. *Plant Cell* 24, 3838–3852. doi: 10.1105/tpc.112.103267

Auriac, M. C., and Timmers, A. C. (2007). Nodulation studies in the model legume medicago truncatula: advantages of using the constitutive EF1alpha promoter and limitations in detecting fluorescent reporter proteins in nodule tissues. *Mol. Plant Microbe. Interact.* 20, 1040–1047. doi: 10.1094/MPMI-20-9-1040

Belfield, E. J., Gan, X., Mithani, A., Brown, C., Jiang, C., Franklin, K., et al. (2012). Genome-wide analysis of mutations in mutant lineages selected following fast-neutron irradiation mutagenesis of *Arabidopsis thaliana*. *Genome Res* 22, 1306–1315. doi: 10.1101/gr.131474.111

Bolle, C. (2004). The role of GRAS proteins in plant signal transduction and development. *Planta* 218, 683–692. doi: 10.1007/s00425-004-1203-z

Brewin, N. J. (2004). Plant cell wall remodelling in the rhizobium-legume symbiosis. *Crit. Rev. Plant Sci.* 23, 293–316. doi: 10.1080/07352680490480734

Catoira, R., Galera, C., De Billy, F., Penmetsa, R. V., Journet, E. P., Maillet, F., et al. (2000). Four genes of medicago truncatula controlling components of a nod factor transduction pathway. *Plant Cell* 12, 1647–1666. doi: 10.1105/tpc.12.9.1647

Chabaud, M., Boisson-Dernier, A., Zhang, J., Taylor, C. G., Yu, O., and Barker, D. G. (2006). Agrobacterium rhizogenes-mediated root transformation of chickpea: a rapid and efficient method for reverse genetics studies. *Plant Methods* 14:55.

Domonkos, A., Horvath, B., Marsh, J. F., Halasz, G., Ayaydin, F., Oldroyd, G. E., et al. (2013). The identification of novel loci required for appropriate nodule development in medicago truncatula. *BMC Plant Biol.* 13:157. doi: 10.1186/1471-2229-13-157

Endre, G., Kereszt, A., Kevei, Z., Mihacea, S., Kalo, P., and Kiss, G. B. (2002). A receptor kinase gene regulating symbiotic nodule development. *Nature* 417, 962–966. doi: 10.1038/nature00842

Gage, D. J. (2002). Analysis of infection thread development using Gfp- and Dsred-expressing sinorhizobium meliloti. *J. Bacteriol.* 184, 7042–7046. doi: 10.1128/JB.184.24.7042-7046.2002

Gage, D. J. (2004). Infection and invasion of roots by symbiotic, nitrogen-fixing rhizobia during nodulation of temperate legumes. *Microbiol. Mol. Biol. Rev.* 68:280. doi: 10.1128/Mmbr.68.2.280-300.2004

Garcia, J., Barker, D. G., and Journet, E. P. (2006). *Seed Storage and Germination. Medicago Truncatula Handbook*. Available online at: http://www.noble.org/MedicagoHandbook/

Gibson, K. E., Kobayashi, H., and Walker, G. C. (2008). Molecular determinants of a symbiotic chronic infection. *Ann. Rev. Genet.* 42, 413–441. doi: 10.1146/annurev.genet.42.110807.091427

Gleason, C., Chaudhuri, S., Yang, T. B., Munoz, A., Poovaiah, B. W., and Oldroyd, G. E. D. (2006). Nodulation independent of rhizobia induced by a calcium-activated kinase lacking autoinhibition. *Nature* 441, 1149–1152. doi: 10.1038/nature04812

Gonzalez-Rizzo, S., Crespi, M., and Frugier, F. (2006). The medicago truncatula CRE1 cytokinin receptor regulates lateral root development and early symbiotic interaction with *Sinorhizobium meliloti*. *Plant Cell* 18, 2680–2693. doi: 10.1105/tpc.106.043778

Grefen, C., Donald, N., Hashimoto, K., Kudla, J., Schumacher, K., and Blatt, M. R. (2010). A ubiquitin-10 promoter-based vector set for fluorescent protein tagging facilitates temporal stability and native protein distribution in transient and stable expression studies. *Plant J.* 64, 355–365. doi: 10.1111/j.1365-313X.2010.04322.x

Hakoshima, T. (2018). Structural basis of the specific interactions of GRAS family proteins. *FEBS Lett.* 592, 489–501. doi: 10.1002/1873-3468.12987

Heckmann, A. B., Lombardo, F., Miwa, H., Perry, J. A., Bunnewell, S., Parniske, M., et al. (2006). Lotus japonicus nodulation requires two GRAS domain regulators, one of which is functionally conserved in a non-legume. *Plant Physiol.* 142, 1739–1750. doi: 10.1104/pp.106.089508

Hirsch, S., Kim, J., Munoz, A., Heckmann, A. B., Downie, J. A., and Oldroyd, G. E. D. (2009). GRAS proteins form a DNA binding complex to induce gene expression during nodulation signaling in medicago truncatula. *Plant Cell* 21, 545–557. doi: 10.1105/tpc.108.064501

Horvath, B., Yeun, L. H., Domonkos, A., Halasz, G., Gobbato, E., Ayaydin, F., et al. (2011). Medicago truncatula IPD3 Is a member of the common symbiotic signaling pathway required for rhizobial and mycorrhizal symbioses. *Mol. Plant Microbe Interact.* 24, 1345–1358. doi: 10.1094/Mpmi-01-11-0015

Jin, Y., Liu, H., Luo, D., Yu, N., Dong, W., Wang, C., et al. (2016). DELLA proteins are common components of symbiotic rhizobial and mycorrhizal signalling pathways. *Nat. Commun.* 7:12433. doi: 10.1038/ncomms12433

Jones, K. M., Kobayashi, H., Davies, B. W., Taga, M. E., and Walker, G. C. (2007). How rhizobial symbionts invade plants: the *Sinorhizobium*-medicago model. *Nat. Rev. Microbiol.* 5, 619–633. doi: 10.1038/nrmicro1705

Kakar, K., Wandrey, M., Czechowski, T., Gaertner, T., Scheible, W. R., Stitt, M., et al. (2008). A community resource for high-throughput quantitative RT-PCR analysis of transcription factor gene expression in medicago truncatula. *Plant Methods* 4:18. doi: 10.1186/1746-4811-4-18

Kalo, P., Gleason, C., Edwards, A., Marsh, J., Mitra, R. M., Hirsch, S., et al. (2005). Nodulation signaling in legumes requires NSP2, a member of the GRAS family of transcriptional regulators. *Science* 308, 1786–1789. doi: 10.1126/science.1110951

Kang, Y., Li, M., Sinharoy, S., and Verdier, J. (2016). A snapshot of functional genetic studies in medicago truncatula. *Front. Plant Sci.* 7:1175. doi: 10.3389/fpls.2016.01175

Kazmierczak, T., Nagymihaly, M., Lamouche, F., Barriere, Q., Guefrachi, I., Alunni, B., et al. (2017). Specific host-responsive associations between medicago truncatula accessions and sinorhizobium strains. *Mol. Plant Microbe Interact.* 30, 399–409. doi: 10.1094/MPMI-01-17-0009-R

Kontra-Kováts, G. Z., Fodor, L., Horváth, B., Domonkos, A., Iski, G., Chen, Y., et al. (2019). *Isolation and Characterization of Non-Transposon Symbiotic Nitrogen Fixing Mutants of Medicago Truncatula. The Model Legume Medicago Truncatula*. Hoboken, NJ: John Wiley & Sonspp, 1006–1014.

Laporte, P., Lepage, A., Fournier, J., Catrice, O., Moreau, S., Jardinaud, M. F., et al. (2014). The CCAAT box-binding transcription factor NF-YA1 controls rhizobial infection. *J. Exp. Bot.* 65, 481–494. doi: 10.1093/jxb/ert392

Li, S., Zhao, Y., Zhao, Z., Wu, X., Sun, L., Liu, Q., et al. (2016). Crystal structure of the gras domain of scarecrow-LIKE7 in oryza sativa. *Plant Cell* 28, 1025–1034. doi: 10.1105/tpc.16.00018

Limpens, E., Mirabella, R., Fedorova, E., Franken, C., Franssen, H., Bisseling, T., et al. (2005). Formation of organelle-like N2-fixing symbiosomes in legume root nodules is controlled by DMI2. *Proc. Natl. Acad. Sci. U.S.A.* 102, 10375–10380. doi: 10.1073/pnas.0504284102

Liu, J. Y., Rasing, M., Zeng, T., Klein, J., Kulikova, O., and Bisseling, T. (2021). NIN is essential for development of symbiosomes, suppression of defence and premature senescence in medicago truncatula nodules. *New Phytol.* 230, 290–303. doi: 10.1111/nph.17215

Middleton, P. H., Jakab, J., Penmetsa, R. V., Starker, C. G., Doll, J., Kalo, P., et al. (2007). An ERF transcription factor in medicago truncatula that is essential for nod factor signal transduction. *Plant Cell* 19, 1221–1234. doi: 10.1105/tpc.106.048264

Murray, J. D., Muni, R. R. D., Torres-Jerez, I., Tang, Y. H., Allen, S., Andriankaja, M., et al. (2011). Vapyrin, a gene essential for intracellular progression of arbuscular mycorrhizal symbiosis, is also essential for infection by rhizobia in the nodule symbiosis of medicago truncatula. *Plant J.* 65, 244–252. doi: 10.1111/j.1365-313X.2010.04415.x

Oldroyd, G. E. (2013). Speak, friend, and enter: signalling systems that promote beneficial symbiotic associations in plants. *Nat. Rev. Microbiol.* 11, 252–263. doi: 10.1038/nrmicro2990

Oldroyd, G. E., and Downie, J. A. (2008). Coordinating nodule morphogenesis with rhizobial infection in legumes. *Annu Rev. Plant Biol.* 59, 519–546. doi: 10.1146/annurev.arplant.59.032607.092839

Oldroyd, G. E., and Long, S. R. (2003). Identification and characterization of nodulation-signaling pathway 2, a gene of medicago truncatula involved in nod actor signaling. *Plant Physiol.* 131, 1027–1032. doi: 10.1104/pp.102.010710

Ovchinnikova, E., Journet, E. P., Chabaud, M., Cosson, V., Ratet, P., Duc, G., et al. (2011). IPD3 controls the formation of nitrogen-fixing symbiosomes in pea and medicago Spp. *Mol. Plant Microbe Interact.* 24, 1333–1344. doi: 10.1094/MPMI-01-11-0013

Pfau, T., Christian, N., Masakapalli, S. K., Sweetlove, L. J., Poolman, M. G., and Ebenhoh, O. (2018). The intertwined metabolism during symbiotic nitrogen fixation elucidated by metabolic modelling. *Sci. Rep.* 8:12504. doi: 10.1038/s41598-018-30884-x

Pislariu, C. I., Murray, J. D., Wen, J., Cosson, V., Muni, R. R., Wang, M., et al. (2012). A medicago truncatula tobacco retrotransposon insertion mutant collection with defects in nodule development and symbiotic nitrogen fixation. *Plant Physiol.* 159, 1686–1699. doi: 10.1104/pp.112.197061

Plet, J., Wasson, A., Ariel, F., Le Signor, C., Baker, D., Mathesius, U., et al. (2011). MtCRE1-dependent cytokinin signaling integrates bacterial and plant cues to coordinate symbiotic nodule organogenesis in Medicago truncatula. *Plant J.* 65, 622–633. doi: 10.1111/j.1365-313X.2010.04447.x

Pysh, L. D., Wysocka-Diller, J. W., Camilleri, C., Bouchez, D., and Benfey, P. N. (1999). The GRAS gene family in arabidopsis: sequence characterization and basic expression analysis of the scarecrow-like genes. *Plant J.* 18, 111–119. doi: 10.1046/j.1365-313x.1999.00431.x

Rakocevic, A., Mondy, S., Tirichine, L., Cosson, V., Brocard, L., Iantcheva, A., et al. (2009). MERE1, a low-copy-number copia-type retroelement in medicago truncatula active during tissue culture. *Plant Physiol.* 151, 1250–1263. doi: 10.1104/pp.109.138024

Roux, B., Rodde, N., Jardinaud, M. F., Timmers, T., Sauviac, L., Cottret, L., et al. (2014). An integrated analysis of plant and bacterial gene expression in symbiotic root nodules using laser-capture microdissection coupled to RNA sequencing. *Plant J.* 77, 817–837. doi: 10.1111/tpj.12442

Schauser, L., Roussis, A., Stiller, J., and Stougaard, J. (1999). A plant regulator controlling development of symbiotic root nodules. *Nature* 402, 191–195. doi: 10.1038/46058

Schindelin, J., Arganda-Carreras, I., Frise, E., Kaynig, V., Longair, M., Pietzsch, T., et al. (2012). Fiji: an open-source platform for biological-image analysis. *Nat. Methods* 9, 676–682. doi: 10.1038/nmeth.2019

Silhavy, D., Molnar, A., Lucioli, A., Szittya, G., Hornyik, C., Tavazza, M., et al. (2002). A viral protein suppresses RNA silencing and binds silencing-generated, 21-to 25-nucleotide double-stranded RNAs. *Embo J.* 21, 3070–3080. doi: 10.1093/emboj/cdf312

Singh, S., Katzer, K., Lambert, J., Cerri, M., and Parniske, M. (2014). CYCLOPS, a DNA-binding transcriptional activator, orchestrates symbiotic root nodule development. *Cell Host Microbe* 15, 139–152. doi: 10.1016/j.chom.2014.01.011

Smit, P., Raedts, J., Portyanko, V., Debelle, F., Gough, C., Bisseling, T., et al. (2005). NSP1 of the GRAS protein family is essential for rhizobial nod factor-induced transcription. *Science* 308, 1789–1791. doi: 10.1126/science.1111025

Stracke, S., Kistner, C., Yoshida, S., Mulder, L., Sato, S., Kaneko, T., et al. (2002). A plant receptor-like kinase required for both bacterial and fungal symbiosis. *Nature* 417, 959–962. doi: 10.1038/nature00841

Terpolilli, J. J., O'hara, G. W., Tiwari, R. P., Dilworth, M. J., and Howieson, J. G. (2008). The model legume medicago truncatula A17 is poorly matched for N2 fixation with the sequenced microsymbiont *Sinorhizobium meliloti* 1021. *New Phytol.* 179, 62–66. doi: 10.1111/j.1469-8137.2008.02464.x

Tirichine, L., Sandal, N., Madsen, L. H., Radutoiu, S., Albrektsen, A. S., Sato, S., et al. (2007). A gain-of-function mutation in a cytokinin receptor triggers spontaneous root nodule organogenesis. *Science* 315, 104–107. doi: 10.1126/science.1132397

Vasse, J., De Billy, F., Camut, S., and Truchet, G. (1990). Correlation between ultrastructural differentiation of bacteroids and nitrogen fixation in alfalfa nodules. *J. Bacteriol.* 172, 4295–4306. doi: 10.1128/jb.172.8.4295-4306.1990

Voinnet, O., Rivas, S., Mestre, P., and Baulcombe, D. (2003). An enhanced transient expression system in plants based on suppression of gene silencing by the p19 protein of tomato bushy stunt virus. *Plant J.* 33, 949–956. doi: 10.1046/j.1365-313X.2003.01676.x

Conflict of Interest: The authors declare that the research was conducted in the absence of any commercial or financial relationships that could be construed as a potential conflict of interest.

Publisher's Note: All claims expressed in this article are solely those of the authors and do not necessarily represent those of their affiliated organizations, or those of the publisher, the editors and the reviewers. Any product that may be evaluated in this article, or claim that may be made by its manufacturer, is not guaranteed or endorsed by the publisher.

Advantages of publishing in Frontiers

OPEN ACCESS
Articles are free to read for greatest visibility and readership

FAST PUBLICATION
Around 90 days from submission to decision

HIGH QUALITY PEER-REVIEW
Rigorous, collaborative, and constructive peer-review

TRANSPARENT PEER-REVIEW
Editors and reviewers acknowledged by name on published articles

Frontiers
Avenue du Tribunal-Fédéral 34
1005 Lausanne | Switzerland

Visit us: www.frontiersin.org
Contact us: frontiersin.org/about/contact

REPRODUCIBILITY OF RESEARCH
Support open data and methods to enhance research reproducibility

DIGITAL PUBLISHING
Articles designed for optimal readership across devices

FOLLOW US
@frontiersin

IMPACT METRICS
Advanced article metrics track visibility across digital media

EXTENSIVE PROMOTION
Marketing and promotion of impactful research

LOOP RESEARCH NETWORK
Our network increases your article's readership